ADVANCED OXIDATION PROCESSES IN WASTEWATER TREATMENT: INVESTIGATIONS ON THE PHENOMENON OF OSCILLATION IN THE CONCENTRATION OF CONCURRENTLY FORMED H_2O_2 IN SONO, PHOTO AND SONOPHOTO CATALYTIC SYSTEMS

Thesis submitted to

Cochin University of Science and Technology

in partial fulfillment of the requirements

for the award of the degree of

Doctor of Philosophy

in

Environmental Technology

Under the faculty of Environmental Studies

By

Jyothi K. P.

(Reg. No. 4124)

SCHOOL OF ENVIRONMENTAL STUDIES

COCHIN UNIVERSITY OF SCIENCE AND TECHNOLOGY

KOCHI - 682 022

December **2016**

Advanced oxidation processes in wastewater treatment: Investigations on the phenomenon of oscillation in the concentration of concurrently formed H_2O_2 in sono, photo and sonophoto catalytic systems

Ph.D. Thesis under the Faculty of Environmental Studies

Author

Jyothi K. P.
Research Scholar
School of Environmental Studies
Cochin University of Science and Technology
Kochi – 682 022
Kerala, India

Supervising Guide

Dr. E. P. Yesodharan
Professor (Emeritus)
School of Environmental Studies,
Cochin University of Science and Technology
Kochi – 682 022
Kerala, India

School of Environmental Studies
Cochin University of Science and Technology
Kochi, Kerala, India 682 022

December 2016

SCHOOL OF ENVIRONMENTAL STUDIES
COCHIN UNIVERSITY OF SCIENCE AND TECHNOLOGY
KOCHI - 682 022

Dr. E. P. Yesodharan
Professor (Emeritus)

Certificate

This is to certify that this thesis entitled **"Advanced Oxidation Processes in Wastewater Treatment: Investigations on the Phenomenon of Oscillation in the Concentration of Concurrently Formed H_2O_2 in Sono, Photo and Sonophoto Catalytic Systems"** is an authentic record of the research work carried out by **Smt. Jyothi K. P.**, Full-Time Research Scholar (Reg. No. 4124) under my guidance at the School of Environmental Studies, Cochin University of Science and Technology in partial fulfillment of the requirements for the award of the degree of Doctor of Philosophy in Environmental Technology and no part of this work has previously formed the basis for the award of any other degree, diploma, associateship, fellowship or any other similar title or recognition. All the relevant corrections and modifications suggested by the audience during the pre-synopsis seminar and recommended by the Doctoral committee have been incorporated in the thesis.

Kochi - 22
Date: /12/2016

Dr. E. P. Yesodharan
(Supervising Guide)

Declaration

I do hereby declare that the work presented in the thesis entitled **"Advanced Oxidation Processes in Wastewater Treatment: Investigations on the Phenomenon of Oscillation in the Concentration of Concurrently Formed H_2O_2 in Sono, Photo and Sonophoto Catalytic Systems"** is based on the authentic record of the original work done by me, for my Doctoral Degree under the guidance of **Dr. E. P. Yesodharan**, Professor (Emeritus), School of Environmental Studies, Cochin University of Science and Technology in partial fulfillment of the requirements for the award of the degree of Doctor of Philosophy in Environmental Technology and no part of this work has previously formed the basis for the award of any other degree, diploma, associateship, fellowship or any other similar title or recognition.

Kochi – 22 **Jyothi K. P.**

Date: /12/2016

Acknowledgements

It gives me immense pleasure to acknowledge all the people who have helped me in different ways for completing this work successfully. I humbly dedicate this work to all those who have helped me in exploring the vast expanses of knowledge.

I take immense pleasure to express my sincere thanks and deep sense of gratitude to my supervising guide, Dr. E. P. Yesodharan, Professor (Emeritus), School of Environmental Studies (SES), Cochin University of Science and Technology (CUSAT) for his inspiring guidance, heartfelt support and affection. His deep knowledge level, dedication, keen interest and above all his overwhelming attitude to help his students is the primary reason for the timely completion of this work. His timely advice, meticulous scrutiny, scholarly interventions and scientific approach have helped me to a very great extent to accomplish this task.

I find no words to express my intense gratitude and respect to Dr. Suguna Yesodharan, Professor (Emeritus), SES, CUSAT who gave me motivation to venture into the world of Advanced Oxidation Processes. I was fortunate to have her presence and guidance throughout my research career. The high level of encouragement and personal guidance from her laid the strong foundation for this work.

I offer my gratitude to the present Director, SES, Dr. S. Rajathy Sivalingam as well as previous Directors Prof. Suguna Yesodharan, Prof. Ammini Joseph and Dr. Harindranathan Nair for providing all the facilities of the school for the smooth conduct of my research. I also wish to place on record my thanks to Prof. I. S. Bright Singh, Dr. Sivanandan Achari and Mr. M. Anand, faculty members of the school, for all their suggestions, help, support and encouragement throughout the period of research. I also thank the non-teaching staff of the school for their help and assistance.

I would like to express my sincere and heartfelt gratitude to all the research scholars of our laboratory, Dr. Anju, Mr. Shibin, Ms. Sindhu, Ms. Phonsy, Mr. Rajeev, Mr. Hariprasad, Ms. Veena, Ms. Gayathri, Ms. Vidya and Ms. Deepthi and all other research scholars in SES for their timely advice, help and affection, which made my stay in the laboratory a pleasant one.

I would like to extend my sincere gratitude to UGC for awarding me the Research Fellowship and to the CUSAT for providing me the facility to conduct my research work.

Finally I thank my parents, my in-laws and above all my husband and son for providing me continuous support and inspiration to carry on with my research.

Above all, this piece of work is accomplished with the blessings and powers that work within me and also the people in my life. I bow before GOD for all with a sense of humility and gratitude.....

Jyothi K P

Preface

Water pollution is a major concern in today's world. Main causes of water pollution include population growth, increased industrialization, urbanization, use of non-biodegradable pesticides/herbicides/fungicides, changing life styles etc. Conventional wastewater treatment methods are unable to remove these pollutants completely and irreversibly. In this context, an innovative wastewater treatment method known as Advanced Oxidation Process (AOP) is being developed and widely investigated for the complete removal of trace amount of pollutants.

AOP is an aqueous phase process based on the production and utilization of $^{\bullet}OH$ radicals for the degradation and eventual removal of mainly organic pollutants from water. Some of the major AOPs are wet-air oxidation, radiolysis, cavitation, photolysis, photocatalysis, fenton oxidation, microwave catalysis and electrochemical oxidation. They can be used either independently or in combination with other techniques in order to enhance efficacy, economy and safety of the process. The advantage of AOP is that it does not produce hazardous byproducts or sludge which requires further treatment. Reactive Oxygen Species (ROS) such as $^{\bullet}OH$, $HO_2^{\bullet}$, $O_2^{-\bullet}$ and H_2O_2 produced in the process interact with the pollutants and degrade them. H_2O_2 is the most stable ROS and its concentration in the system is closely related to other ROS. However, in the pursuit of developing suitable systems for the complete mineralisation of pollutants, the fate of concurrently formed H_2O_2 was often overlooked.

The current study is the first major attempt focusing on the fate and role of H_2O_2 formed insitu in sono, photo and sonophoto catalytic processes. The main objectives of the study are:

- To compare the efficiency of the three AOPs, i.e., sono, photo and sonophoto catalysis for the removal of trace organic pollutants in water.
- To investigate the fate of concurrently formed H_2O_2 which plays a crucial role in the mineralization process.
- To throw more light on the influence of naturally occurring contaminants on the efficiency of the process.

The thesis provides detailed report on the findings aimed at achieving the above objectives and critical analysis of the observations.

The thesis is presented in seven chapters and four annexures as follows:

Chapter 1- Introduction: Background literature.

Chapter 2- Objectives of the study, Materials used and Plan of the thesis.

Chapter 3- Investigations on the photocatalytic degradation of phenol and the fate of H_2O_2 formed insitu.

Chapter 4- Investigations on the sonocatalytic degradation of phenol and the fate of H_2O_2 formed insitu.

Chapter 5- Investigations on the sonophotocatalytic degradation of phenol and the fate of H_2O_2 formed insitu.

Chapter 6- Effect of inorganic salts/ions on the photo, sono and sonophoto catalytic degradation of phenol and oscillation in the concentration of H_2O_2 formed insitu.

Chapter 7- Summary and Conclusion.

Annexures:

Annexure I Abbreviations used.

Annexure II List of original research papers based on the results of the current study, published in peer reviewed journals and presented in conferences.

Annexure III Reprints of papers published in peer reviewed journals.

Annexure IV Awards/Recognitions conferred based on the current study

Contents

List of Tables

List of Figures

Chapter 1

INTRODUCTION: BACKGROUND LITERATURE

Contents

1.1 General

Water is the driving force for all forms of life. It is the most abundant and the most important boon which nature bestowed on earth to sustain life of plants and animals. Water has been used since antiquity as a symbol to express devotion and purity. Two thirds of the earth's surface is covered by water (figure 1.1) and 75% of human body weight is made up of it. Water circulates through land as it does through the human body, transporting, dissolving and replenishing nutrients and organic matter, while carrying away the waste material. Water shortage has become the most serious political and social issue that humanity faces today due to various factors such as rapid population growth, booming industrialization activities and climate change. Huge quantity of organic and inorganic substances such as dyes, phenols, pesticides, fertilizers, detergents, etc. are introduced into water bodies from various sources such as industrial effluents, agricultural runoff and chemical spills. Their toxicity, unrelenting stability to natural decomposition and persistence in environment have been the cause of much concern to societies, countries and regulatory authorities around the world.

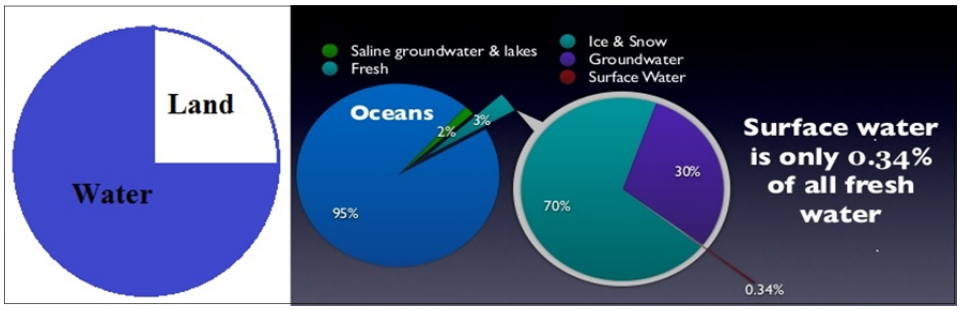

Fig. 1.1: Distribution of water on earth's surface

Water must be purified and disinfected suitably so that it can be used in daily life without any fear of contamination. Three basic considerations of water treatment are:

1) It must be safe for human consumption
2) It must be appealing to the consumer
3) It must provide quality water at reasonable cost

Accordingly, the objectives of water treatment must be:

- Improving the organoleptic properties of water (clarification, decolourization, deodourization)
- Enhancing the epidemiological safety (chlorination, ozonization, ultraviolet irradiation)
- Conditioning of the mineral composition of water (fluorination or de-fluorination, de-ironing, de-manganisation, softening, desalination, etc.)

1.1.1 Classification of wastewater treatment

Conventionally, the treatment of wastewater so that it can be safely discharged into the environment, consists of three stages; namely primary, secondary and tertiary.

1.1.1.1 Primary treatment

It is employed for the removal of suspended solids and floating materials and also for conditioning the waste water for either discharge to a receiving body of water or a secondary treatment (by neutralization and/or equalization) facility. The process involves screening, sedimentation, floatation, oil separation, equalization, neutralization, etc.

1.1.1.2 Secondary treatment

This consists mainly of conventional biological treatment processes. The process involves removing the suspended solids that did not settle in the primary tank and the dissolved Biological Oxygen Demand (BOD) that is unaffected by physical treatment methods. The treatment techniques include activated sludge process, extended aeration, contact stabilization, trickling filters, anaerobic treatment, etc.

1.1.1.3 Tertiary treatment

It is intended primarily for the elimination of pollutants not removed by conventional biological treatment. Secondary treatment can remove up to 85-95% BOD and Total Suspended solid (TSS) in raw sanitary sewage. This leaves part of BOD and TSS still in the effluent. Main tertiary treatment processes are micro screening, precipitation and coagulation, adsorption, ion exchange, reverse osmosis, electro dialysis, etc.

Generally these traditional methods of treatment are non-destructive, slow at high concentration and rather ineffective at low contaminant levels. For e.g. activated carbon adsorption involves just

phase transfer of pollutants without decomposition and thus induces another pollution problem. Chemical oxidation is unable to mineralize all organic substances and is economically suitable only for the removal of pollutants at high concentrations. For biological treatment, the main drawbacks are: slow reaction rates, problem of disposal of sludge and the need for strict control of proper pH and temperature [1].

Recent developments in water decontamination processes focus on the oxidation of bio-recalcitrant organic compounds. These methods rely on the formation of highly reactive oxygen species that degrade more number of recalcitrant molecules into biodegradable compounds. The techniques are generally known as Advanced Oxidation Processes (AOP).

1.2 Advanced Oxidation Process (AOP)

AOP which involves the insitu generation of highly potent chemical oxidants such as the hydroxyl radical ($^{\bullet}OH$), has emerged as an important class of technology for accelerating the oxidation and destruction of a wide range of organic contaminants in polluted water. The advantage of AOP is that it does not produce hazardous byproducts or sludge which require further handling [2-7]. When applied appropriately, AOP reduces the contaminant concentration from several hundred 'parts per million' (ppm) to less than 5 'parts per billion' (ppb). Other advantages of the AOPs include relatively mild reaction conditions and proven ability to degrade several toxic refractory pollutants.

AOP can be divided mainly into two types based on the nature of the medium in which the processes take place i.e. Homogeneous and Heterogeneous AOP.

Figure 1.2 provides a general schematic presentation of the two types of processes.

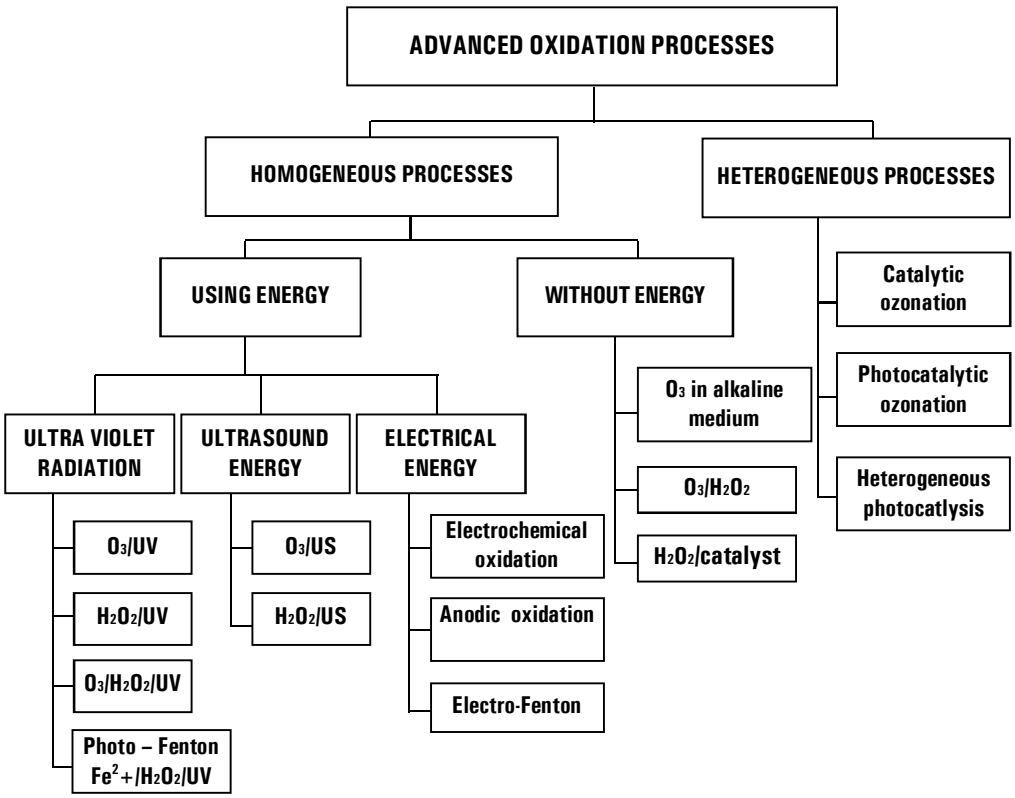

Fig. 1.2: Classification of Advanced Oxidation Processes [8]

1.2.1 Homogeneous AOP

Homogeneous AOPs using ultraviolet (UV) radiation are generally employed for the degradation of compounds that absorb UV radiation. Processes based on this include UV/Photolysis, UV/H_2O_2, O_3/UV, Photo Fenton, etc. Other sources of radiation such as ultrasound (US), electrical energy, microwave (MW), etc. are also being investigated. Instances of 'no irradiation' with H_2O_2, O_3, homogeneous catalysts, etc. as the initiator have also been reported.

1.2.2 Heterogeneous AOP

Heterogeneous AOPs generally use catalysts to enhance the degradation of compounds. The term heterogeneous refers to the fact that the contaminants are present in the aqueous phase, while the catalyst is in the solid phase. The catalyst accelerates the chemical reaction through a process involving the formation of electron-hole pairs on irradiation with an appropriate energy source. The AOP-generated holes and electrons lead to oxidation and reduction processes respectively.

1.2.3 General mechanism of AOP

Oxidation is a process by which transfer of one or more electrons from an electron donor (reductant) to an electron acceptor (oxidant), which has a higher affinity for electron, takes place. As a result of this, chemical transformation takes place in both oxidant and reductant.

In some cases odd electron species known as radicals are produced during this process which are highly unstable and highly reactive. Oxidation reactions that produce radicals tend to be followed by additional oxidation reactions between the radical oxidants and other reactants (both organic and inorganic) until thermodynamically stable oxidation products are formed. The ability of the oxidant to initiate chemical reactions is measured in terms of its oxidation potential. The oxidation potential of some of the common oxidizer species is given in table 1.1.

Table 1.1: Oxidation potential of common oxidizing agents.

Sl. No.	Oxidation species	Oxidation potential, eV
1	Fluorine	3.06
2	Hydroxyl radical	2.80
3	Sulphate radical	2.60
4	Atomic oxygen	2.42
5	Nascent oxygen	2.42
6	Ozone	2.07
7	Persulphate	2.01
8	Hydrogen peroxide	1.77
9	Perhydroxyl radical	1.70
10	Permanganate	1.68
11	Hypobromous acid	1.59
12	Hypochlorous Acid	1.49
13	Hypochlorite	1.49
14	Hypoiodous acid	1.45
15	Chlorine	1.36
16	Chlorine dioxide	1.27
17	Oxygen(molecular)	1.23
18	Bromine	1.09
19	Iodine	0.54

General mechanism of AOP involves generation of highly reactive free radicals viz. hydroxyl radicals ($^{\bullet}OH$), which are very effective in destroying organic chemicals. They are reactive electrophiles (electron preferring) that react rapidly and nonselectively with nearly all electron-rich organic compounds. They have an oxidation potential of 2.8 eV and exhibit faster rates of oxidation reactions compared to conventional oxidants such as H_2O_2 and $KMnO_4$.

Once generated, the hydroxyl radicals can attack organic chemicals by radical addition, hydrogen abstraction and electron transfer. In the following reactions, R represents the reacting organic compound.

$R + {}^{\bullet}OH \rightarrow ROH$: Addition ..... (1)

$R + {}^{\bullet}OH \rightarrow R^{\bullet} + H_2O$: Abstraction ..... (2)

$R + {}^{\bullet}OH \rightarrow R^{+} + OH^{-}$: Electron transfer ..... (3)

In view of the importance of the role played by $^{\bullet}OH$ radicals in AOP, depending on the mode of generation of the radical, the process is classified as photochemical and non-photochemical.

Table 1.2: Photochemical and Non-photochemical AOPs.

Photochemical	**Non-photochemical**
H_2O_2/UV	$O_3/{}^{\bullet}OH$
O_3/UV	O_3/H_2O_2
O_3/ H_2O_2/UV	O_3/ Ultrasound (US)
Fe^{2+}/ H_2O_2/UV (Photo Fenton)	O_3 /GAC*
TiO_2/UV, ZnO/UV	Fe^{2+}/H_2O_2(Fenton system)
H_2O_2/TiO_2/UV	Electro-Fenton
O_2/ TiO_2/UV	Electron beam irradiation
UV/US	US
	H_2O_2/US

*GAC- Granulated Activated Carbon

Various steps involved in AOPs can be summarized as follows:

1) Formation of strong oxidants (e.g. hydroxyl radicals).
2) Reaction of these oxidants with organic compounds in water producing biodegradable intermediates.
3) Reaction of biodegradable intermediates with oxidants referred to as mineralization (i.e., production of water, carbon dioxide and inorganic salts).

The steps are schematically presented in figure 1.3.

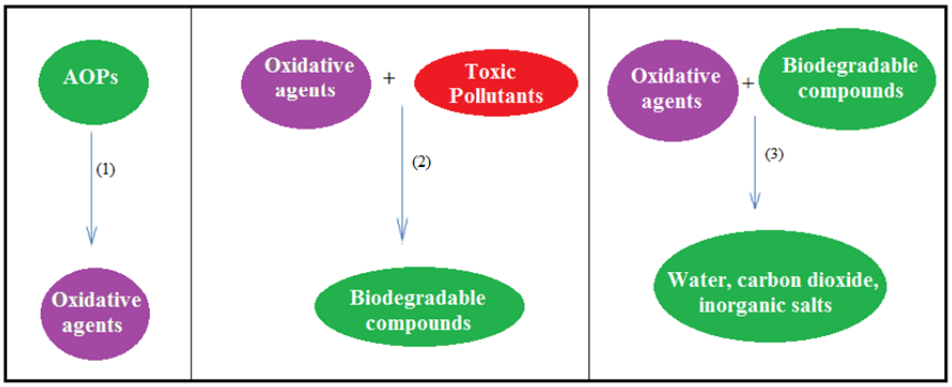

Fig. 1.3: Different steps involved in AOP

1.2.4 Advantages of AOP

The advantages of AOP are in general:

1) Rapid reaction rate
2) Small footprint
3) Potential to reduce toxicity and possibly complete mineralization of the organics treated
4) Does not concentrate waste requiring further treatment as in the case of methods such as membrane filtration, absorption, adsorption, etc.
5) Does not create sludge as in the case of physicochemical processes or biological processes

1.2.5 Disadvantages of AOP

Generally cited disadvantages of AOP are:

1) High treatment cost
2) Must be tailored to suit specific application

3) For some applications, quenching is needed because of the use of very reactive chemicals

1.2.6 Photocatalysis

The word photocatalysis is of Greek origin and composes of two parts: The prefix 'Photo' (Phos: light) and the word catalysis (Katalyo: break apart, decompose). Photocatalysis is used to describe a process in which light is used to activate a substance i.e., the photocatalyst which modifies the rate of a chemical reaction without itself being involved in the chemical transformation. Photocatalytic reaction may occur homogeneously or heterogeneously.

The photochemical/photocatalytic reactions take place at different wavelengths depending on the processes and the photochemical characteristics of the components. The wavelength range for various photo-based AOPs may be generally presented as in figure 1.4.

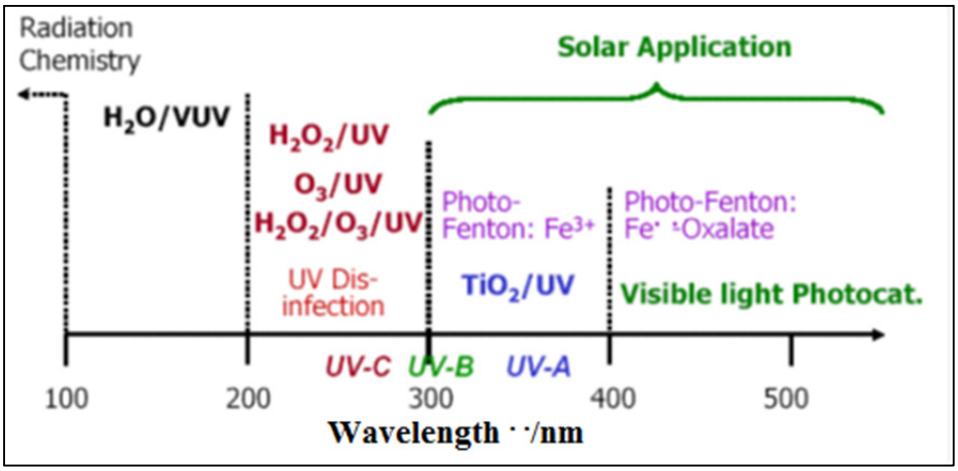

Fig. 1.4: Wavelength range of photochemical degradation

Depending on the characteristics of the reaction medium, i.e., homogenous or heterogeneous, the photocatalysis can be classified into homogenous photocatalysis and heterogeneous photocatalysis.

1.2.6.1 Homogenous photocatalysis

Here the reactants and the photocatalyst exist in the same phase. The most commonly used homogeneous photocatalytic processes include O_3/UV, H_2O_2/UV, O_3/H_2O_2/UV and Photo Fenton. The chemical H_2O_2 has very low oxidizing strength. Irradiation by UV light enhances the rate and strength of the oxidation process through production of increased amounts of $^{\bullet}OH$ radicals.

1.2.6.1.1 *UV/H_2O_2*

This process involves the formation of hydroxyl radicals by the photolysis of H_2O_2 and subsequent propagation reactions. The photolysis of hydrogen peroxide occurs when UV radiation (hv) with wavelength of less than 400 nm is applied. The process requires relatively high dose of H_2O_2 and longer UV-exposure time.

The main reactions taking place in the system are given below:

$H_2O_2 + hv$	$\leftrightarrow$	$2^{\bullet}OH$	Initial reaction	..... (4)
H_2O_2	$\rightarrow$	$H_2O + ½O_2$		..... (5)
$^{\bullet}OH + H_2O_2$	$\rightarrow$	$HO_2^{\bullet} + H_2O$	Propagation	..... (6)
$HO_2^{\bullet} + H_2O_2$	$\rightarrow$	$^{\bullet}OH + H_2O + O_2$		..... (7)
$HO_2^{\bullet} + HO_2^{-}$	$\rightarrow$	$^{\bullet}OH + HO^{-} + O_2$		..... (8)
$^{\bullet}OH + {}^{\bullet}OH$	$\rightarrow$	H_2O_2	Recombination	..... (9)

Advantages of UV/H_2O_2 homogeneous photocatalysis include:

- Commercial availability of the oxidant
- Thermal stability and storage on-site
- Infinite solubility in water
- No mass transfer problems associated with gases
- Two hydroxyl radicals are formed for each molecule of H_2O_2
- Photolysed peroxyl radicals are generated after $^{\bullet}OH$ attack on most organic substrates, leading to subsequent thermal oxidation reactions
- Minimal capital investment
- Cost-effective source of hydroxyl radicals
- Simple operation procedure

Disadvantages include:

- The presence of residual hydrogen peroxide in the treated effluent will promote biological re-growth in the distribution system
- The rate of chemical oxidation of the contaminant is limited by the rate of formation of hydroxyl radicals, and the rather small absorption coefficient of H_2O_2 at 254 nm

1.2.6.1.2 *O_3/UV*

Light induced decomposition of ozone involves its homolysis and subsequent production of $^{\bullet}OH$ radicals by the reaction of O with water [2, 9]

$O_3 + h\nu \rightarrow O_2 + O$ ..... (10)

$O + H_2O \rightarrow {}^{\bullet}OH + {}^{\bullet}OH$ ..... (11)

However, it has been observed that photolysis of ozone dissolved in water leads to the production of hydrogen peroxide in a sequence of reactions.

$O_3 + H_2O \rightarrow H_2O_2 + O_2$ ..... (12)

If at all hydroxyl radicals are formed they do not escape from the solvent cage.

Advantages are:

- The removal efficiency of the combined O_3/UV process is typically higher than the additive removal efficiencies of ozone or UV alone
- Higher amount of hydroxyl radicals are generated during this process

Disadvantages are:

- Solubility of ozone in water is low compared to H_2O_2
- The process is less energy efficient

1.2.6.1.3 *O_3/UV/H_2O_2*

When H_2O_2 is added to the O_3/UV process the decomposition of ozone is accelerated, which results in increased rate of formation of ${}^{\bullet}OH$ radicals. The reaction pathways leading to the formation of ${}^{\bullet}OH$ radicals are summarized below [9]:

$H_2O_2 + H_2O \leftrightarrow H_3O^+ + HO_2^-$ ..... (13)

$O_3 + H_2O_2 \rightarrow O_2 + {}^{\bullet}OH + HO_2^{\bullet}$ (Very slow) ..... (14)

$O_3 + HO_2^- \rightarrow {}^{\bullet}OH + O_2^{-\bullet} + O_2$ ..... (15)

$O_3 + O_2^{-\bullet} \rightarrow O_3^{-\bullet} + O_2$ ..... (16)

$O_3^{-\bullet} + H_2O \rightarrow {}^{\bullet}OH + OH^- + O_2$ ..... (17)

Reaction pathways involving O_3/UV and O_3/H_2O_2 are schematically presented in figure 1.5.

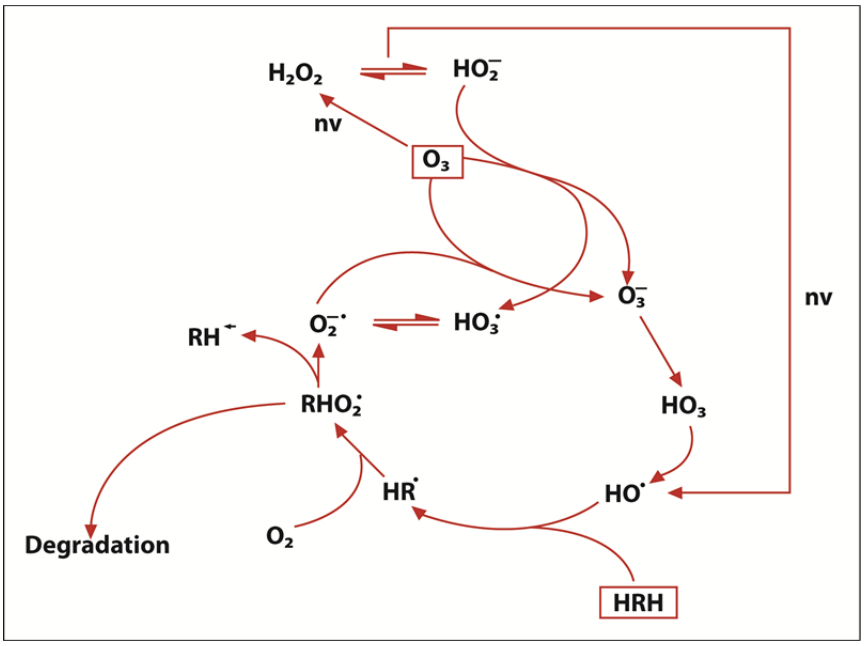

Fig. 1.5: Reaction pathways in the O_3/UV and O_3/H_2O_2 systems [9]

1.2.6.1.4 *Fenton's reactions*

Fenton's reagent, a mixture of ferrous iron (catalyst) and hydrogen peroxide (oxidizing agent) was discovered by Henry J.H. Fenton. The mechanism of the Fenton process is as below [10, 11]:

$$Fe^{2+} + H_2O_2 \rightarrow Fe^{3+} + OH^- + {}^{\bullet}OH \quad \text{..... (18)}$$

$$Fe^{2+} + {}^{\bullet}OH \rightarrow Fe^{3+} + OH^- \quad \text{..... (19)}$$

$${}^{\bullet}OH + RH \rightarrow H_2O + R^{\bullet} \quad \text{..... (20)}$$

$$R^{\bullet} + Fe^{3+} \rightarrow R^+ + Fe^{2+} \quad \text{..... (21)}$$

In dark condition the reaction stops when the Fe^{2+} is completely converted to Fe^{3+}. The photo Fenton process ($H_2O_2/Fe^{2+}/UV$) involves the ${}^{\bullet}OH$ formation through photolysis of hydrogen peroxide (H_2O_2/UV) and Fenton as reagent (H_2O_2/Fe^{2+}). In the presence of UV irradiation, the ferric ions (Fe^{3+}) formed in reaction (18) are photocatalytically converted back to ferrous ions (Fe^{2+}) as in reaction (22) with formation of an additional equivalent of hydroxyl radical [12].

$$Fe^{3+} + H_2O \rightarrow Fe^{2+} + H^+ + {}^{\bullet}OH \quad \text{..... (22)}$$

The hydroxyl radicals formed react with organic species, promoting their oxidation.

Advantages of Fenton Process are:

1) Complete mineralization of organic matter
2) Very fast reaction; takes only minutes or at the most hours depending on the concentration of H_2O_2

Disadvantages are:

1) Fenton reaction requires low pH
2) Formation of ferric oxide sludge, which requires continuous removal

1.2.6.2 Heterogeneous photocatalysis

Here the catalyst is in a different phase from the reactant. Heterogeneous photocatalysis can be carried out in various media: gas phase, pure organic liquid phases or aqueous solutions. According to Jean-Marie Hermaan [13], heterogeneous photocatalytic processes occur in 5 steps.

1) Transfer of reactants to the surface
2) Adsorption of at least one of the reactants
3) Reactions of the reactants in the adsorbed phase
4) Desorption of the products
5) Diffusion of the products from the surface

Most common heterogeneous photocatalysts are transition metal oxides and semiconductors which have unique characteristics.

1.2.6.2.1 *Semiconductors as photocatalysts*

Semiconductors are electronic conductors with electric resistivity values generally in the range of 10^{-2} to 10^{9} ohm-cm at room temperature, intermediate between conductors (10^{-6} ohms-cm) and insulators (10^{14} to 10^{22} ohm-cm) [14]. At absolute zero temperature, pure and perfect crystals of most semiconductors will be insulators. In the semiconductor, the highest occupied energy band is called the valence band (VB) and lowest empty energy band is called the conduction band (CB). These two bands are separated by an energy gap called band gap. Figure 1.6 shows the band structure and band filling in insulator, conductors and semiconductor.

A semiconductor by definition is non-conducting in its undoped ground state because an energy gap, the band gap, exists between the top of the filled valence band and the bottom of the vacant conduction band.

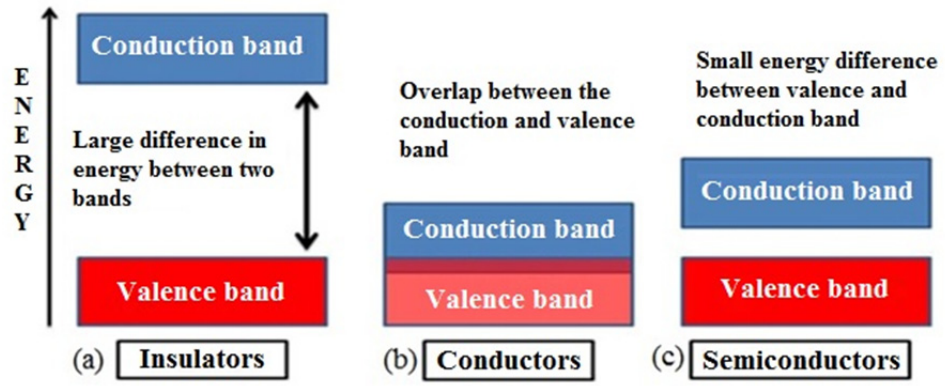

Fig. 1.6: Difference between energy bands of (a) insulators, (b) conductors and (c) semiconductors.

There are two types of semiconductors - n-type, in which majority charge carriers are electrons and p-type in which majority charge carriers are holes. Semiconductors can be made conductive by either putting extra electrons into the conduction bands or by removal of an electron from the valence band that creates a positively charged hole. The hole can be regarded as the mobility entity because annihilation of a hole by a nearby electron effectively moves the hole over in space. The energy of the most energetic electrons in the partially filled band is called Fermi level. In a p-type semiconductor, Fermi level lies just above the valence band edge, and in an n-type semiconductor, it lies just below the conduction band.

In semiconductors, mobile charge carrier can be generated by three different mechanisms:

1) Thermal excitation: If the band gap energy is sufficiently small (less than half electron volt) thermal excitation can promote electron from valence band to the conduction band

2) Photoexcitation: In this case, an electron can be promoted from the valence band to the conduction band upon absorption of a photon of light, provided that the photon energy is greater or equal to the band gap energy

3) Doping: It is a process of introducing new level into the band gap. There are two types of doping. For n-type doping (with group III elements like B, Al, Ga and In), occupied donor levels are created near the conduction band edge where conduction is done mainly by negative charge carriers. Likewise, p-type doping (with group V elements like P, As, Sb and Bi) corresponds to the formation of empty acceptor levels near the valence band, creating positive charge carriers where conduction is done mainly by positive charges. The surface defects and impurities in n-type or p-type semiconductors are responsible for the change in band gap of the semiconductor

Metal oxides and sulphides represent a large class of semiconductor materials suitable for photocatalysis [15, 16, 17]. Semiconductor must exhibit certain characteristics such as suitable band-gap energies, stability toward photo-corrosion, nontoxic nature, low cost and physical characteristics that enable them to act as catalysts. Many materials such as TiO_2, ZnO, ZrO_2, CdS, MoS_2, Fe_2O_3, WO_3 and their various combinations have been examined as photocatalysts for the degradation of organic and inorganic pollutants [18]. Figure 1.7 lists the energy levels of some selected semiconductor materials, which are used for photocatalytic reactions.

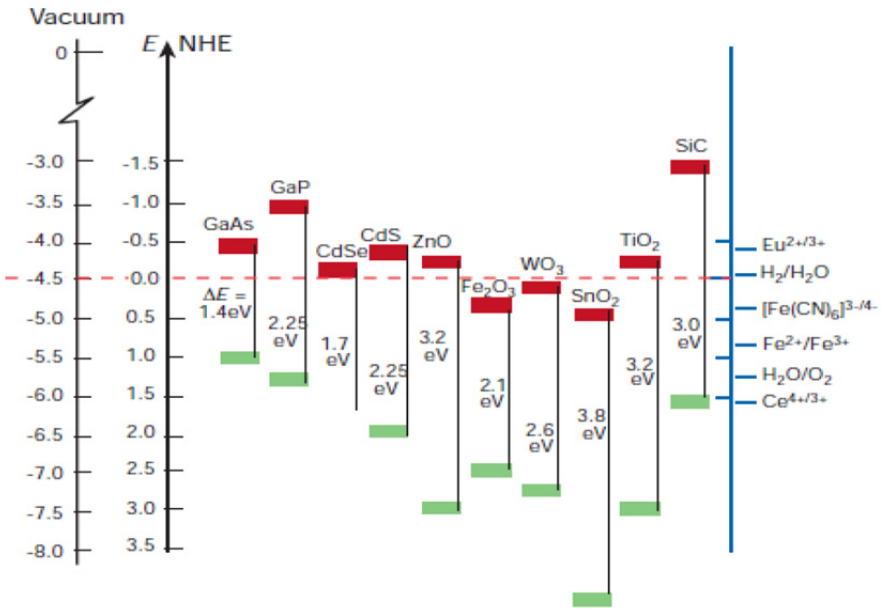

Fig. 1.7: Energy levels of various semiconductors [19]

When a photon with energy equal to or greater than the band gap is absorbed by the semiconductor, an electron is excited from the valence band to the conduction band generating positive hole in the valence band and electron in the conduction band. The excited electron and hole can recombine and release the energy gained from the excitation of the electron as heat. Recombination is undesirable and leads to an inefficient photocatalyst. The lifetime of an e^--h^+ pair is a few nanoseconds, but this is still long enough for promoting redox reactions in the solution or gas phase in contact with the semiconductor. The transfer of electrons to and from a substrate adsorbed on to the light-activated semiconductor is probably the most critical step in photocatalysis. The excited electrons react with the oxidant to generate a reduced product while reaction between the generated holes with a reductant results in an oxidized product. Due to the generation of

positive holes and electrons, oxidation-reduction reactions take place at the surface of the semiconductors. In the oxidative reaction, positive holes react with the moisture present on the surface and produce a hydroxyl radical. Typical schematic diagram of semiconductor photocatalysis is shown in figure 1.8.

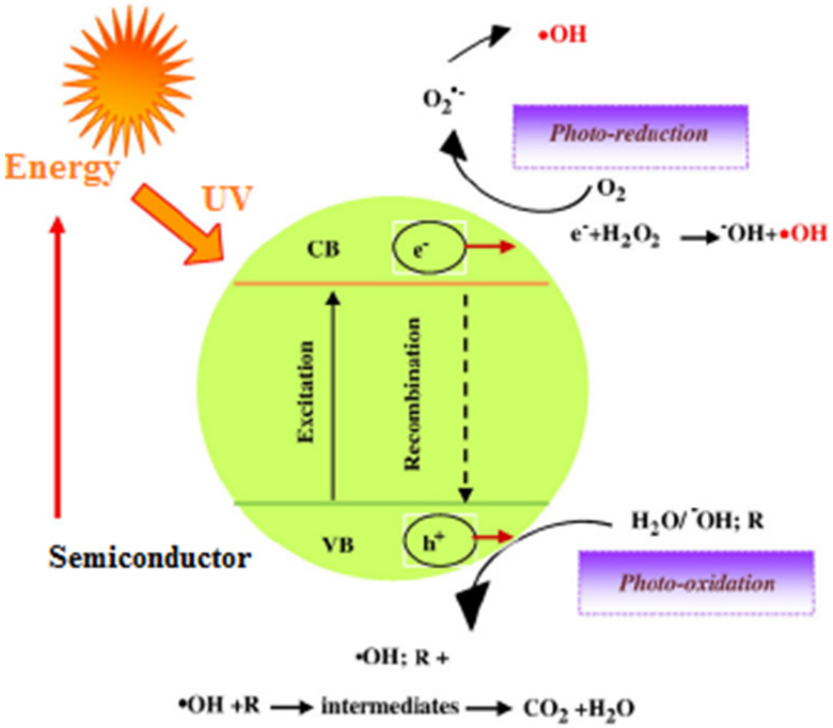

Fig. 1.8: Schematic diagram illustrating the principle of semiconductor photocatalysis [20]

The basic reactions taking place are:

$$h\nu + \text{semiconductor} \rightarrow h^+ + e^- \quad \text{..... (23)}$$

$$h^+ + H_2O \rightarrow H^+ + {}^{\bullet}OH \quad \text{..... (24)}$$

$$2h^+ + 2H_2O \rightarrow 2H^+ + H_2O_2 \quad \text{..... (25)}$$

$$H_2O_2 \rightarrow {}^{\bullet}OH + {}^{\bullet}OH \quad \text{..... (26)}$$

The reductive reaction due to photocatalytic effect

$e^- + O_2 \rightarrow O_2^{-\bullet}$ ..... (27)

$O_2^{-\bullet} + HO_2^{\bullet} + H^+ \rightarrow H_2O_2 + O_2$ ..... (28)

$H_2O_2 \rightarrow {}^{\bullet}OH + {}^{\bullet}OH$ ..... (29)

h: hole e: electron

Ultimately the hydroxyl radicals are generated in the reactions. These hydroxyl radicals are very oxidative in nature and non-selective with redox potential $E_0 \sim 2.8$ eV. Hydroxyl radical ($^{\bullet}OH$) and superoxide radical anion ($O_2^{-\bullet}$) are the primary oxidizing species in the photocatalytic oxidation processes. They have the power to oxidize the organic compounds adsorbed on the surface of semiconductor as well as in the liquid bulk and convert them completely to stable intermediates or mineralize to CO_2 and H_2O.

1.2.6.2.2 ***Some typical photocatalytic studies***

A number of investigations have been carried out on photocatalytic reactions mediated by semiconductors. Most of these are aimed at degradation and eventual mineralization of the organics. However photocatalysis can also be used for the synthesis of new molecules. These investigations are summarized in many excellent reviews [1, 3, 9, 16]. Some of the recent studies relevant in the present context are briefly discussed below.

Turchi and Ollis [21] investigated the degradation of organic water pollutants in illuminated TiO_2 photocatalyst slurries. They proposed that the hydroxyl radical, $^{\bullet}OH$, is the primary oxidant in photocatalytic system. Four possible mechanisms are suggested; all based on $^{\bullet}OH$ attack of the

organic reactant. The kinetic parameters for the photocatalytic degradation are estimated from data on the physical properties of the catalyst, the electron-hole recombination, trapping rates, etc.

Abdullah et al. [22] investigated the effects of pH and common inorganic anions on the rates of photocatalytic oxidation of salicylic acid, aniline and ethanol to CO_2 over near-UV illuminated glass-supported TiO_2**.** The rate of oxidation decreased with increasing concentration of Cl^-. They also observed that ClO_4^- and NO_3^- have very little effect on oxidation. SO_4^{2-} or PO_4^{3-} even at millimolar concentrations are rapidly adsorbed by the catalyst and reduce the rates of oxidation by 20-70%. They explained the inhibitory effect of ions by assuming that inorganic anions may compete with organic solutes for oxidizing sites on the surface to form oxidizing inorganic radical anions. Some of these radical anions also react with surface-adsorbed organics to give CO_2 but at decreased rates.

Minero et al. [23] investigated the photocatalytic transformation of phenol on naked TiO_2 and on TiO_2/F (0.01 M F^-) at pH 3.6 in the presence of different alcohols (tert-butyl alcohol, 2-propanol and furfuryl alcohol). F^- ions displace surficial hydroxyl groups and coordinate surface-bound titanium atoms directly. For 0.01 M F^- concentration and 0.10 g/L of TiO_2 in the range pH 2 to 6, the degradation rate of phenol is up to 3 times more than that in the absence of F^- ions. They suggested that on TiO_2/F the reaction proceeds almost entirely in the homogeneous medium with the hydroxyl radicals in the bulk because of the unavailability of surface-bound hydroxyl in the presence of F^- ions. The decrease in the degradation rate of phenol at a high concentration (over

0.01 M) in the presence of naked TiO_2 is largely diminished in the presence of F^- ions. It was also proposed that under a helium atmosphere and in the presence of F^- ions, phenol is slowly but significantly degraded, although total organic carbon does not decrease, suggesting the occurrence of a photocatalytically induced hydrolysis.

Calza and Pelizzetti [24] investigated the influence of halide ions on the photocatalytic processes on titanium dioxide. Cl^- and Br^- ions deeply inhibit the degradation rate of chloroform and tetrachloromethane. F^- ions, unlike in the case of other halides, cannot be oxidized by the valence band hole. They also suggested that this difference may be used as a diagnostic tool in mechanistic studies.

Sakthivel et al. [25] investigated the photocatalytic activity of commercial ZnO powder and compared it with Degussa P-25 TiO_2. Laboratory experiments with Acid Brown 14 as the model pollutant were carried out to evaluate the performance of both ZnO and TiO_2 catalysts. Solar light was used as the energy source. Highest photo degradation rates were observed for ZnO, suggesting that it absorbs wider range of the solar spectrum and more light quanta than TiO_2.

The photocatalytic degradation of small concentration of an organo-phosphorous insecticide phosphamidon, in water, on ZnO and TiO_2 was investigated by Sandhya et al. [26]. TiO_2 was found to be more effective as a photocatalyst for this reaction. There is simultaneous formation and decomposition of H_2O_2 in the system, resulting in periodic increase and decrease in its concentration.

Hua et al. [27] studied the effect of acidity and inorganic ions that are common in industrial effluent on the photocatalytic degradation of azo dyes in UV illuminated TiO_2 dispersions. They demonstrated that inorganic anions affect the photodegradation of dyes by adsorption onto the surface of TiO_2 and trapping positive hole (h^+) and $^{\bullet}OH$.

Sivalingam et al. [28] studied the photocatalytic degradation of various chlorophenols and methylphenols using nano-sized, high surface area pure anatase TiO_2 synthesized by the solution combustion method. The degradation rates of o-chlorophenol, p-chlorophenol, dichlorophenol, trichlorophenol, pentachlorophenol, o- and m-methylphenol (cresol) under UV exposure were determined and the results were compared with the degradation rates in presence of commercial Degussa P-25. The chlorophenols degraded much faster than the methylphenols, which degraded faster than phenol. The photocatalytic activity of combustion synthesized TiO_2 was significantly higher than that of Degussa P-25 under similar conditions. No intermediates were observed when combustion synthesized TiO_2 catalyst was used for the photocatalytic degradation of the phenols, while several intermediates were observed for the same reactions catalyzed by Degussa P-25. Some of the intermediates are toxic and hence combustion synthesized TiO_2 may be more beneficial in environmental catalysis.

The physicochemical properties and photocatalytic activity of transition metal-loaded TiO_2 catalysts were studied by Wu et al. [29]. Pd, Cr and Ag were deposited on TiO_2 via post-hydrothermal synthesis and photo-assisted reduction/impregnation. Under the irradiation of visible

light, the Pd and Cr loaded TiO_2 showed higher photocatalytic activity for salicylic acid degradation compared to pristine TiO_2. Si-W loaded TiO_2 had no catalytic activity, although the threshold absorptions of all metal loaded TiO_2 is similar to that of pure TiO_2. They found that the crystallinity of TiO_2, the absorption threshold, the interaction between metal ions and TiO_2, oxidation state, the concentration of the metal and the irradiation source have an impact on the catalytic activity of metal-loaded TiO_2 photo catalysts. Under the irradiation by visible light, Pd–TiO_2 has the highest activity amongst all the metal-loaded TiO_2 reported in the article. This may be due to the fact that Pd ion has the strongest interaction with TiO_2.

Han et al. [30] studied the photocatalytic decomposition and mineralization of 4-chlorophenol, hydroquinone and 4-nitrophenol in an aqueous solution using two kinds of low-pressure mercury lamps: an ultraviolet lamp emitting at 254 nm and a vacuum ultraviolet lamp emitting at both 254 and 185 nm. The catalyst was TiO_2. Different mechanisms of photocatalysis and photolysis under vacuum ultraviolet irradiation were proposed. The degradation rate was correlated to the molecular structures of the substrates. Chlorophenol was easy to be decomposed, while hydroquinone was easy to be mineralized. However nitrophenol was difficult to be decomposed or mineralized. Vacuum UV was efficient for decomposition of refractory compounds, such as nitrophenols and the catalyst was efficient for Total Organic Carbon (TOC) removal.

Zhang et al. [31] studied the effects of various anions, Cl^-, ClO_4^-, SO_4^{2-}, NO_3^-, HCO_3^-, $H_2PO_4^-$ and $C_2O_4^{2-}$, on the photocatalytic and photoelectrocatalytic degradation of reactive brilliant orange K-R and

found that the nature and concentrations of these inorganic anions significantly affected the photocatalytic and photoelectrocatalytic degradation performance of the reactive dye. Almost all these ions inhibit the photocatalytic degradation and strongest inhibition effect on photocatalytic and photoelectrocatalytic degradation of the dye was observed in the presence of HCO_3^- ions.

By taking methylene blue (MB) as a model molecule, Guillard et al. [32] evaluated the impact of inorganic salts, present in textile waste waters, on the adsorption properties and on the photocatalytic efficiency of TiO_2. Anions such as NO_3^-, Cl^-, SO_4^{2-}, PO_4^{3-} and CO_3^{2-} do not scavenge the $^{\bullet}OH$ radicals at neutral and basic pH. The decrease in the rate of MB photocatalytic degradation in the presence of inorganic salts was shown to be due to the formation of an inorganic salt layer at the surface of TiO_2, which inhibits the approach of MB molecules.

Barka et al. [33] studied the effect of various inorganic ions on the photocatalytic degradation of rhodamine B (RhB) over TiO_2-coated non-woven paper. They studied the influence of various factors that affect the photocatalytic degradation, such as adsorption, initial concentration of dye solution, temperature and some inorganic anions commonly present in wastewater such as Cl^-, NO_3^-, SO_4^{2-}, CH_3COO^- and HPO_4^{2-}. The experimental results show that adsorption is an important parameter that controls the apparent kinetic order of the degradation. The photocatalytic reaction is favoured by high concentration of the substrate in accordance with Langmuir–Hinshelwood model. It was found that photodegradation is temperature-dependent and high rate of degradation was obtained at high

temperature. Inorganic ions such as Cl^-, CH_3COO^- and HPO_4^{2-} decrease the effectiveness of photodegradation whereas SO_4^{2-} increases the rate of the degradation. The inhibition by Cl^- ion is due to the competition with RhB for adsorption on TiO_2 surface and the scavenging of photo-produced $^{\bullet}OH$ by Cl^-.

$$^{\bullet}OH + Cl^- \rightarrow Cl^{\bullet} + OH^- \quad \text{..... (30)}$$

The $Cl^{\bullet}$ radicals are also capable of oxidizing pollutants, but at lower rates than the $^{\bullet}OH$ radicals because of their lower oxidation power.

HPO_4^{2-} also inhibits the adsorption of RhB on TiO_2 surface and scavenges the $^{\bullet}OH$ radicals.

Acetate and sulphate ions react with holes as follows:

$$CH_3COO^- + h^+ \rightarrow {}^{\bullet}CH_3 + CO_2 \quad \text{..... (31)}$$
$$h^+ + H_2O \rightarrow {}^{\bullet}OH + H^+ \quad \text{..... (32)}$$
$$h^+ + OH^- \rightarrow {}^{\bullet}OH \quad \text{..... (33)}$$
$$h^+ + SO_4^{2-} \rightarrow SO_4^{-\bullet} \quad \text{..... (34)}$$

Sulphur is a strong oxidizing agent and hence $SO_4^{-\bullet}$ can actively participate in the degradation reaction.

Parag and Giridhar [34] synthesized base metal (Cr, Mn, Fe, Ni, Cu) substituted $CeVO_4$ compounds which were used for photocatalytic degradation of phenol. They compared the degradation rates in the presence of these compounds vis a vis commercial Degussa P-25 TiO_2 catalyst. Fe and Cr substituted $CeVO_4$ showed photocatalytic activity comparable to Degussa P-25 TiO_2. The major intermediates identified

during phenol degradation over Degussa P-25 TiO_2 were catechol, hydroquinone and pyrogallol. However their concentrations were negligible when phenol was degraded over combustion synthesized catalyst. Fe-substituted orthovanadates showed high catalytic activity which increased with increase in the amount of Fe up to the optimum of 1% Fe-substituted $CeVO_4$. Thereafter the activity showed gradual decline.

Leticia et al. [35] investigated porous carbon both as a photocatalyst and as a catalyst support (in the carbon/titania composite) for the photodegradation of phenol and compared the results with those in presence of bare titanium oxide. The immobilization of titania on the activated carbon provoked acceleration of the degradation rate under UV irradiation, which can be attributed to the porosity of the carbon support.

Mangrulkar et al. [36] studied the photo-oxidation properties of N-doped mesoporous titania in photodegradation of phenolics under visible light. The rate of photocatalytic degradation was observed to be higher for o-chlorophenol than for phenol. The effect of various operating parameters such as catalyst loading, pH, initial concentration and the effect of co-existing ions on the rate of photocatalytic degradation were studied in detail. It was seen that initial pH and co-existing ions have significant influence on the photocatalytic degradation rates. Maximum degradation was observed at neutral pH while the presence of co-ions has a detrimental effect on the degradation rates in case of both phenol and o-chlorophenol.

Lu et al. [37] suggested that $NaBiO_3$ photocatalysis could be an effective technique for the destruction of acridine orange (AO) in aqueous solutions. It is found that the solution pH, catalyst dosage, initial dye

concentration and the presence of anions can affect the photocatalytic performance. About 99% AO (0.1 g/L) was decomposed under visible light over $NaBiO_3$ (1 g/L) in 160 minutes. In this respect $NaBiO_3$ is more efficient than TiO_2 (P-25, 1 g/L) under identical conditions. Low TOC removal or mineralization yield while the AO removal was high indicated the formation of intermediate products. Five N-demethylated intermediates of AO were identified during the photooxidative reaction, and the successive appearance of the maximum of each intermediate reveals that the N-demethylation of AO is a stepwise process. The methyl groups are removed one by one, as confirmed by the gradual wavelength shifts of the maximum-peaks toward the blue region. From the stable values of TOC, it is inferred that at least some of the intermediates are stable which do not get mineralized under the reaction condition.

Ameta a et al. [38] investigated the photocatalytic degradation of methylene blue over ferric tungstate. The effect of some parameters affecting the rate of reaction, such as pH, dye concentration, amount of semiconductor, light intensity, etc. has been studied. The optimum pH at which maximum degradation of the dye was obtained was 9.5 and the optimum catalyst dosage was 0.06 g/50 ml. Kinetic studies showed that this reaction follows pseudo-first order kinetics.

Benhebal et al. [39] investigated the photocatalytic degradation of phenol and benzoic acid in aqueous solution using ZnO powder synthesized by sol–gel process. The catalyst was characterized by X-ray diffraction and Transmission Electron Microscopy (TEM). The Brunauer–Emmett–Teller (BET) surface area and the band gap of the catalyst samples were also

measured. The influence of various key parameters such as amount of photocatalyst, initial solution pH and the initial concentration of the organics was also investigated. It was found that at ZnO concentration of 1.5 g/L, initial phenol concentration of 0.20 g/L and pH 2.5, the degradation of phenol is ~ 60% in 120 minutes.

Jallouli et al. [40] studied the photocatalytic degradation of acetaminophen ((N-(4-hydroxyphenyl) acetamide)), an analgesic drug using TiO_2 P-25 as a photocatalyst. TiO_2 (P-25 Degussa) /UV and TiO_2 films/solar light systems were tested to assess the suitability of these processes to promote the degradation and mineralization of paracetamol. Using TiO_2 P-25 nanoparticles, much faster photodegradation of paracetamol [> 90% of 2.65×10^{-4} M] and effective mineralization occurred under UV irradiation. Changes in pH values affected the adsorption and the photodegradation of paracetamol. The optimum pH for the photodegradation was found to be 9.0. Hydroquinone, benzoquinone, p-nitrophenol and 1, 2, 4-trihydroxybenzene were detected as intermediates. It was observed that TiO_2 suspension/UV system is more efficient than the TiO_2/cellulosic fiber/sunlight for the photocatalytic degradation. Reusability and mechanical integrity of the TiO_2/cellulosic fiber were also investigated. The final degradation efficiency decreased by only 17% after five repetitive experiments under sunlight irradiation, indicating that the TiO_2 film has very good stability and can be reused several times.

Dalbhanjan et al. [41] investigated the treatment of patent blue V dye-containing wastewater using modified photocatalytic reactor with

special focus on the effect of various process parameters and additives. Comparison of results with natural (solar radiation) and artificial light (fluorescent lamp, 11 W) sources confirmed that the treatment is more efficient using the artificial source. Significant degradation was obtained from the use of solar light also. Modifications by glass coating at the interior of the polyacrylic reactor for possible enhanced utilization of the incident energy showed better degradation efficiency. The removal efficiency was also observed to be dependent on the operating parameters viz. initial concentration and pH, with maximum degradation at 10 ppm and pH of 2.5. Using optimized conditions, in presence of various additives, the maximum degradation obtained is in the order UV/H_2O_2 (92.8%) > UV/TiO_2 (86.4%) > UV/Ferrous sulphate (81.56%) > Solar/H_2O_2 (72.1%) > UV/ZnO (68.4%) > Solar/TiO_2 (64.7%) > Solar/ZnO (59.0%).

Rathore et al. [42] studied the photocatalytic degradation of azure A in the presence of N-doped zinc oxide which was prepared by doping pure ZnO with urea by precipitation method. The effect of different parameters like pH, dye concentrations, catalyst amount and light intensity were studied. The observations revealed that azure A dye could be degraded successfully by using N-doped ZnO under visible light. In comparative evaluation, N-doped ZnO has shown six times better photocatalytic activity than pure ZnO.

1.2.7 Sonocatalysis

The concept of ultrasound was known as far back as 1880 with the discovery of the piezoelectric effect by the Curies [43]. Ultrasound has

been investigated as a potential activation source in AOP for wastewater treatment because of its ability for the production of $^{\bullet}OH$ in aqueous solution and subsequent oxidation of pollutants [44].

$$H_2O \rightarrow H^{\bullet} + {}^{\bullet}OH \quad \text{.....(35)}$$

$$H^{\bullet} + O_2 \rightarrow HOO^{\bullet} \quad \text{.....(36)}$$

$$\text{Pollutants} + {}^{\bullet}OH \rightarrow \text{Degradation products} \quad \text{.....(37)}$$

$$\text{Pollutants} + HOO^{\bullet} \rightarrow \text{Degradation products} \quad \text{.....(38)}$$

The formation of $^{\bullet}OH$ radicals by ultrasonic decomposition of water was first proposed by Weiss [45] and later confirmed by Makino et al. [46].

Ultrasound is defined as any wave frequency that is greater than the upper limit of human hearing ability i.e. at frequencies above 16 kHz (16,000 cycles/s) [47]. The frequency range of ultrasound is shown in figure 1.9.

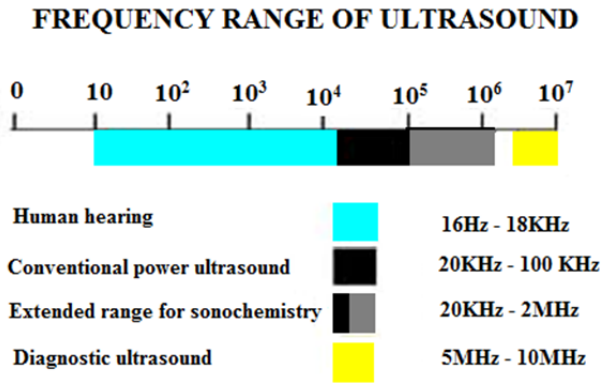

Fig. 1.9: Frequency range of ultrasound [48]

Ultrasonic waves consist of compression and expansion (rarefaction) cycles [49]. During compression cycle a positive pressure is created on liquid which pushes the molecules together. In rarefaction cycle a

negative pressure is created which pull the molecules apart. In an expansion sound wave cycle with sufficient intensity, when the distance between molecules exceeds the specific molecular distance required to hold the liquid together (for water molecules the critical molecular distance R is 10^{-8} m) [50] cavities/voids can be generated. Intensity of the sound wave needed for cavitation depends on the type and purity of liquid. Through repetitive compression & rarefaction cycles, cavitation bubble will grow in size by entrapping most of the vapor from the medium and reach a critical size before the implosion of the bubbles occurs.

Schematic presentation of the formation and growth of cavitation bubbles is shown in figure 1.10.

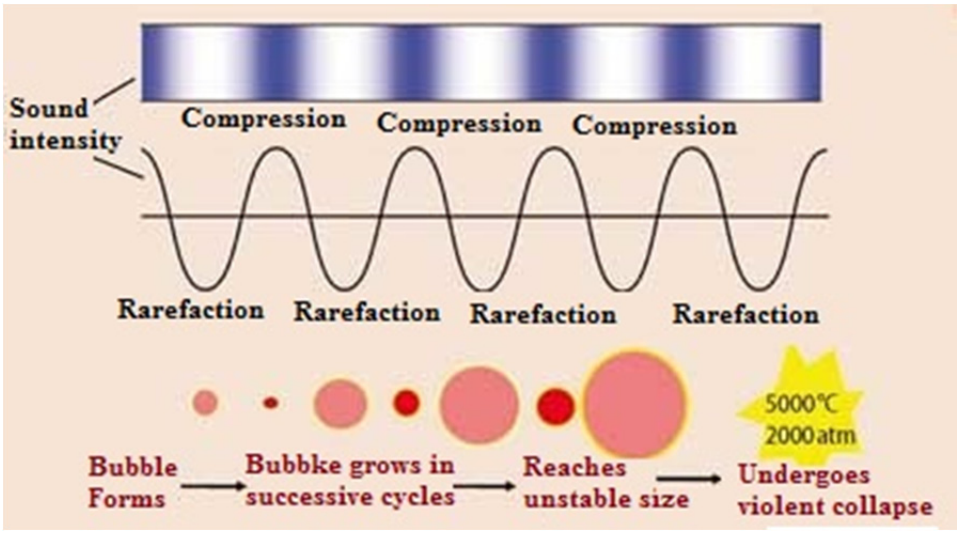

Fig. 1.10: Schematic representation of the growth of bubble [51]

The radius of the bubble before collapsing when irradiated at 20 kHz is estimated to be in the order of several hundred micrometers. The time scale for the collapse of bubbles is less than 100 nanoseconds

[52]. The effective lifetime is less than 2 microseconds after which they start to collapse [53]. In addition, the critical size of cavitation bubbles formed in water is inversely proportional to the frequency of the ultrasound. For instance, it was reported that the size of the cavities was within 100 to 170 μm when 20 kHz of ultrasonic irradiation was used while at 1 MHz, it was about 3.3 μm [50, 54].

In summary, the phenomenon of cavitation consists of three repetitive and distinct steps. i.e., Formation (nucleation), rapid growth (expansion) during the compression/ rarefaction cycles until they finally reach a critical size which leads to the third step of violent collapse (implosion) in the liquid [53].

1.2.7.1 Bubble cavitation

There are three potential reaction zones in sonochemistry [54] i.e. inside of the cavitation bubble, at the interfacial liquid region between cavitation bubbles and bulk liquid, and in the bulk solution. The temperatures of interior and interfacial regions of the cavitation bubbles in alkanes as determined by Suslick et al. [55] were 5200 K and 1900 K, respectively. These bubbles' temperature values range from 750 to 6000 K, depending on the technique used and experimental conditions [56]. Gogate et al. [49] reported that the temperature of the interfacial region of cavitation bubbles in the water supercritical phase is only 647 K. The collapse of cavitation bubbles near the micro-particle surface will generate high-speed microjets of liquid having a speed of the order of several hundred meters/s [57]. This will subsequently produce ultrasonic asymmetric shock wave upon implosion of cavitation bubbles which may

cause direct erosion (damage) on the particle's surface and de-aggregation of particles. Consequently, it will experience a decrease in particle size and an increase in reactive surface area available for subsequent reaction. The severity of the cavitation erosion that causes pitting and cracking of the particle surface is strongly influenced by the solid particle size [47, 58].

1.2.7.2 Mechanism of sonochemical process

It is reported that the efficiency of sonochemical reactions improve in presence of dissolved oxygen. However, it is not necessary in water sonolysis because sonochemical oxidation can proceed in the presence of any gas such as air, nitrogen, argon and hydrogen [54]. Ultrasound will induce the splitting of water molecules in the presence of dissolved oxygen and causes reactions (39)–(51) [54, 59].

$H_2O + >>> \rightarrow {}^{\bullet}OH + {}^{\bullet}H$ ..... (39)

$O_2 + >>> \rightarrow 2{}^{\bullet}O$ ..... (40)

${}^{\bullet}OH + {}^{\bullet}O \rightarrow {}^{\bullet}OOH$ ..... (41)

${}^{\bullet}O + H_2O \rightarrow 2{}^{\bullet}OH$ ..... (42)

${}^{\bullet}H + O_2 \rightarrow {}^{\bullet}OOH$ ..... (43)

${}^{\bullet}OH + {}^{\bullet}H \rightarrow H_2O$ ..... (44)

$2{}^{\bullet}OH \rightarrow H_2O + {}^{\bullet}O$ ..... (45)

${}^{\bullet}OOH + {}^{\bullet}OH \rightarrow O_2 + H_2O$ ..... (46)

$2{}^{\bullet}OH \rightarrow H_2O_2$ ..... (47)

$2{}^{\bullet}OOH \rightarrow H_2O_2 + O_2$ ..... (48)

${}^{\bullet}H + H_2O_2 \rightarrow {}^{\bullet}OH + H_2O$ ..... (49)

${}^{\bullet}OH + H_2O_2 \rightarrow {}^{\bullet}OOH + H_2O$ ..... (50)

$2{}^{\bullet}H \rightarrow H_2$ ..... (51)

'>>>' denotes the ultrasonic irradiation.

Thermal dissociation of water and dissolved oxygen molecules in the cavities will form reactive species such as $^{\bullet}OH$, hydrogen atoms ($^{\bullet}H$), $^{\bullet}O$ atoms and hydroperoxyl radicals ($^{\bullet}OOH$) {reactions (39)–(43)}. These reactive radicals can enter into a variety of chemical reactions in the cavitation bubble and/or in the bulk solution. In the absence of any solutes, these primary radicals could recombine to form H_2O and oxygen (O_2) which are released into the bulk solution {reactions (44)–(46)}.

Schematic presentation of the formation of cavitation bubbles and subsequent catalytic processes at the interfacial region are given in figure 1.11.

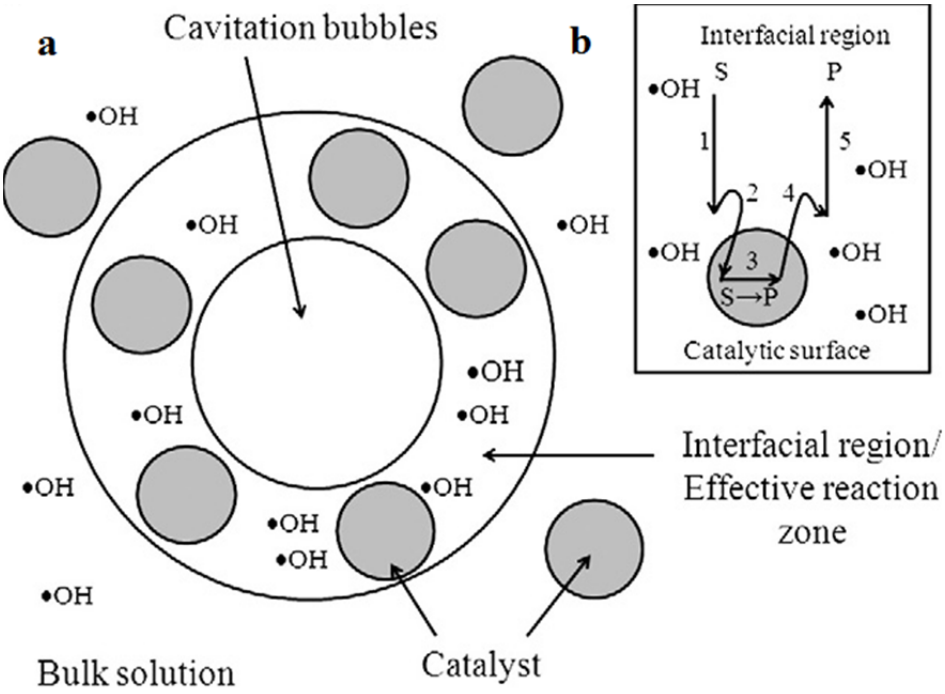

Fig. 1.11: Schematic representations of (a) Effective reaction zone in cavitation bubbles and (b) 5 steps in heterogeneous catalytic reaction in the interfacial region [60]

H_2O_2 will be formed outside the hot bubbles or at the cooler interface as a consequence of $^{\bullet}OH$ and $^{\bullet}OOH$ recombination (reactions (47) and (48)). On the other hand, the $^{\bullet}H$ and $^{\bullet}OH$ species may further react with H_2O_2 as shown in reactions (49)–(50). The radicals ($^{\bullet}OH$ and $^{\bullet}OOH$) may also reach the liquid–bubble interface and may pass into bulk solution where they can react with solutes.

1.2.7.3 Some typical sonocatalytic studies

One of the earliest studies in sonochemistry was by Kotronarou et al. [61] who studied the kinetics and mechanism of the sonochemical reactions of p-nitrophenol in oxygenated aqueous solutions. In the presence of ultrasound (20 kHz, 84 W) p-nitrophenol degraded primarily by denitration to yield NO_2^-, NO_3^-, benzoquinone, hydroquinone, 4-nitro catechol, $HCOO^-$ and $C_2O_4^{2-}$.

Lin et al. [62] investigated the sonochemical degradation of 2-chlorophenol using hydrogen peroxide. Effect of different operating parameters including concentration of hydrogen peroxide was studied. The decomposition of 2-chlorophenol was more effective at increased amplitude of ultrasound, higher concentration of H_2O_2 and smaller operating pH. They also reported that use of $FeSO_4$ as a catalyst was not as effective as direct addition of hydrogen peroxide, indicating that quantum of hydrogen peroxide generated insitu (by recombination reaction of hydroxyl radicals generated during the cavity collapse) is not sufficient to drive a Fenton-like mechanism.

Jiang et al. [63] investigated the effect of pH on the degradation of ionic aromatic compounds. They concluded that, pH, which results in

modification of the physical properties (including charge) of molecules with ionisable functional groups, plays an important role in the sonochemical degradation of many chemical contaminants. For hydrophilic substrates, the neutral species diffuse to and accumulate at the hydrophobic interface of liquid–gas bubbles more easily in comparison with their corresponding ionic forms.

Svitelska et al. [64] investigated sonolytic degradation of polyphenolic compound in presence of H_2O_2 in a sonochemical reactor operated at 20 kHz and a maximum input power of 250 W in basic medium. The removal efficiency reached its maximum (94%) at pH 11.4 and 49 ± 2 °C in the presence of 0.05 M of H_2O_2. However, only 15% degradation was achieved in the absence of H_2O_2. Role of other parameters such as pH and temperatures on the removal efficiency of phenolic compounds was also studied. They observed that pH and temperature also have significant effect on removal efficiency in the presence of H_2O_2, both with and without sonication.

Mahamuni and Pandit [65] studied the effect of NaCl addition on the sono degradation of phenol. Compared to the experimental runs without NaCl, the addition of NaCl at 2% and 8% (wt/vol) increased the reaction rate by 1.1 and 1.5 times, respectively. Higher amount of Cl^- created more salting out effects to cause phenol molecules to move towards the interface of the cavities. This would increase the possibility of $^{\bullet}OH$ attack on phenol molecules.

Shimizu et al. [66] studied the degradation of methylene blue by the irradiation of ultrasound in presence of TiO_2. Addition of H_2O_2

accelerated the degradation of the dye in TiO_2 containing system. The radical scavengers dimethyl sulfoxide (DMSO), methanol and mannitol reduced the degradation process. They also reported that the addition of 50 mM Cl^-, SO_4^{2-} and CO_3^{2-} could suppress ultrasonic degradation of methylene blue when operated at 39 kHz and 200 W. Addition of Na_2CO_3 to aqueous solution would produce both CO_3^{2-} and HCO_3^- ions which are known to be effective $^{\bullet}OH$ scavengers. Moreover, Cl^- and SO_4^{2-} ions could also suppress the reaction by trapping the oxidizing radicals.

Sun et al. [67] used a combination of ultrasound and low concentration iron (< 3 mg/L) (US/Fenton) to treat wastewater containing acid black 1 (AB1). They observed that the oxidation power of low concentration iron in Fenton could be significantly enhanced by ultrasonic irradiation. The degradation of AB1 in aqueous solution by US/Fenton is more compared to either Fenton oxidation or ultrasound alone. Many operational parameters, such as ultrasonic power density, pH, Fe^{2+} dosage, H_2O_2 dosage, AB1 concentration and temperature affect the degradation efficiency. It was also observed that inhibitory effect of various inorganic anions on the degradation of AB1 is in the following decreasing order: $SO_3^{2-} > CH_3COO^- > Cl^- > CO_3^{2-} > HCO_3^- > SO_4^{2-} > NO_3^-$. The drastic inhibition by SO_3^{2-} on the degradation of AB1 is due to its reaction with H_2O_2 which decreases the production of $^{\bullet}OH$. It may also quench $^{\bullet}OH$ directly.

Findik and Gunduk [68] investigated the ultrasonic degradation of acetic acid. The effects of several parameters such as: ultrasonic power, initial concentration, addition of Cl^- and several oxides to the solution etc.

were investigated. It was observed that degree of degradation of acetic acid increased with decreasing power and initial concentration of acetic acid. Increase in power at the same reactor area increases the ultrasound intensity. But the magnitude of the pressure pulse generated due to the collapse of a single cavity is inversely proportional to the operating intensity. So with increase in the operating intensity, cavitation events become less violent resulting in lower extent of degradation. Addition of Cl^- (0.37–1.5 M NaCl) to the acetic acid solution caused an enhancement in the degradation. The addition of natural zeolite and silicon dioxide (SiO_2) during the sonolysis of acetic acid at an ultrasound frequency of 40 kHz and 84 W has a positive effect on the initial degradation rate.

Nakui et al. [69] investigated the influence of coal ash (53–106 μm in particle size and concentrations of 0.0-1.5 wt %) on the degradation of small concentration of (10 mg/l) phenol in water. When sonicated at 200 kHz and 200 W, sonochemical degradation of phenol was enhanced in the presence of coal ash and the optimum amount of coal ash was between 0.4 and 0.6 wt %. However, at higher concentration of coal ash, ultrasonic wave could be scattered or absorbed thereby reducing the enhancing effect. They also observed that the phenol degradation did not occur by the addition of hydrogen peroxide or nitric acid (used to adjust the pH) under conventional stirring conditions. The sonochemical degradation with coal ash was depressed by the addition of tertiary butyl alcohol as a radical scavenger.

Hartmann et al. [70] studied the degradation of diclofenac in water under ultrasound irradiation. They used TiO_2 as the catalyst and concluded

that sonolysis in water could be a useful method to degrade pharmaceuticals like diclofenac into smaller, more polar compounds. Chlorinated anilines, phenols and carboxylic acid derivatives were identified as intermediates during sonolysis of diclofenac. About 35% of organic chlorine is transformed into inorganic chloride.

Li et al. [71] studied the decolorisation of azo dyes under ultrasound in presence of exfoliated graphite. Coupled ultrasound/exfoliated graphite-H_2O_2 process appears to have a positive synergistic effect on the decolourisation of some azo dyes such as reactive red 2, methyl orange, acid red 1, acid red 73, acid red 249, acid orange 7, acid blue 113, acid brown 75, acid green 20, acid yellow 42, acid mordant brown 33, acid mordant yellow 10 and direct green 1.

Ghodbane and Hamdaoui [72] found that acid blue 25 (AB 25) can be degraded by high frequency ultrasonic irradiation (1700 kHz) in aqueous solutions. The rate of AB25 degradation is dependent on initial dye concentration, pH and temperature. Addition of salts such as NaCl, $CaCl_2$, $NaHCO_3$ and KI to the aqueous solution pushes AB25 molecules from the bulk aqueous phase to the bulk–bubble interface and thus increased the degradation rate. Ultrasonic degradation of AB25 conducted in natural water showed that the rate of degradation was higher than that obtained in distilled water. The initial rate of dye degradation was significantly enhanced by the addition of Fe (II). Addition of H_2O_2 to the ultrasound system substantially enhanced the degradation efficiency.

Xie et al. [73] studied the ultrasonic degradation of m-xylene in aqueous solution and concluded that the degradation was rapid and

efficient at very high frequency (806.3 kHz) with about 93% degradation in 1 hour time. Simple additives such as Mn^{4+}, Cu^{2+}, Fe^{2+} and H_2O_2 cannot enhance the ultrasonic degradation effect. Adding Fenton reagent can promote the removal of m-xylene slightly. Presence of radical scavengers such as Na_2CO_3 and t-butyl alcohol could not affect the removal of m-xylene suggesting that ultrasonic degradation of m-xylene takes place predominantly inside the bubbles by direct pyrolysis. The sono degradation of m-xylene was found to follow pseudo-first-order kinetics.

Guzman-Duque et al. [74] showed that ultrasonic degradation of crystal violet in water occurs mainly through reactions with hydroxyl radicals. Reaction rates are strongly affected by pollutant concentration, gas saturation, applied ultrasonic power and anions (Cl^-, SO_4^{2-} and HCO_3^-) as well as cations (Fe^{2+}) in the water matrix. Significant differences in pollutant degradation were not observed in the presence of Cl^- and SO_4^{2-}. However, HCO_3^- at higher concentration showed a detrimental effect when the pollutant concentration was relatively lower (2.45 μmol/L). Under same conditions, lower concentration of HCO_3^- has positive effect. The presence of Fe^{2+}also increased the dye degradation by 32% after 180 minutes.

Moumeni et al. [75] showed that sonochemical degradation of malachite green (MG) was considerably intensified in the presence of Br^-. The promoting effect increases with increasing Br^- level and decreasing MG concentration. The improvement of the destruction rates may be due to the dibromine radical anion ($^{\bullet}Br_2^-$) produced by the reaction of Br^- with $^{\bullet}OH$ ejected from the bubble of cavitation which is likely to migrate towards the bulk of the solution. They also observed that in the presence

of Br^-, addition of Cl^- had practically no impact on the removal of dye. Addition of HCO_3^- ion had a negative effect on the elimination kinetics of MG in presence of Br^- ion.

Hoseini et al. [76] demonstrated that US treatment alone may not be an efficient method for the removal of tetracycline (TC) antibiotics from aqueous solution. Removal efficiency of TC was improved by the addition of TiO_2 nano-particles and H_2O_2 under US process which resulted in the complete removal of TC after 75 minutes of reaction time. It was found that decreasing the initial TC concentration caused an increase in the % degradation. The optimum conditions for TC removal in US/TiO_2/H_2O_2 process was achieved at TiO_2 concentration of 250 mg/L and H_2O_2 concentration of 100 mg/L at acidic pH.

Zhao et al. [77] studied the catalytic ultrasonic degradation of aqueous methyl orange using MnO_2/CeO_2. Results showed that ultrasonic process could remove 3.5% of methyl orange while catalytic ultrasonic process could remove 85% of methyl orange in 10 minutes. They also studied the effects of free radical scavengers to determine the role of hydroxyl free radical in catalytic ultrasonic process. It was observed that methyl orange degradation efficiency declined after adding free radical scavengers, illustrating that hydroxyl free radical played an important role in the degradation. They also studied the effects of pre-adsorption of dye (methyl orange) on catalytic ultrasonic process and concluded that the process significantly improved the dye removal.

Cai et al. [78] observed that the decolorization of azo dye orange G in aqueous solution can be achieved in an aluminum powder-acid system

irradiated by ultrasound. They concluded that the decolorization rate was dependent on the operating parameters including the initial pH, initial dye concentration, aluminium powder dosage and ultrasound power. The decolorization rate is enhanced significantly by the addition of hydrogen peroxide due to the additional hydroxyl radicals.

Khataee et al. [79] studied the sonocatalytic performance of the synthesized TiO_2/Montmorillonite K10 (TiO_2/MMT) nanocomposite for the removal of basic blue 3 (BB3) from water. They observed that immobilizing the TiO_2 nanoparticles on the surface of MMT led to decrease in size of nanoparticles and increase its sonocatalytic performance. The decolourisation efficiency of BB3 solution increased with the increasing TiO_2/MMT nanocomposite dose and power of ultrasonic generator and decrease in initial BB3 concentration. The optimal pH value of the solutions was observed to be 7.0. The inhibitory effect of inorganic anions on the decolourisation of BB3 is in the following decreasing order: $Cl^- > CO_3^{2-} > SO_4^{2-}$.

1.2.8 Sonophotocatalysis

In sonophotocatalytic process, photocatalyst (usually a semiconductor powder such as TiO_2 or ZnO) is irradiated with ultraviolet radiation in the presence of ultrasonic sound waves. The basic reaction mechanism for both ultrasound initiated degradation process and photocatalytic oxidation (either using UV light or solar energy) is the generation of free radicals and their subsequent attack on the pollutant organic species.

The general mechanism of semiconductor mediated sonophotocatalytic degradation is shown in figure 1.12.

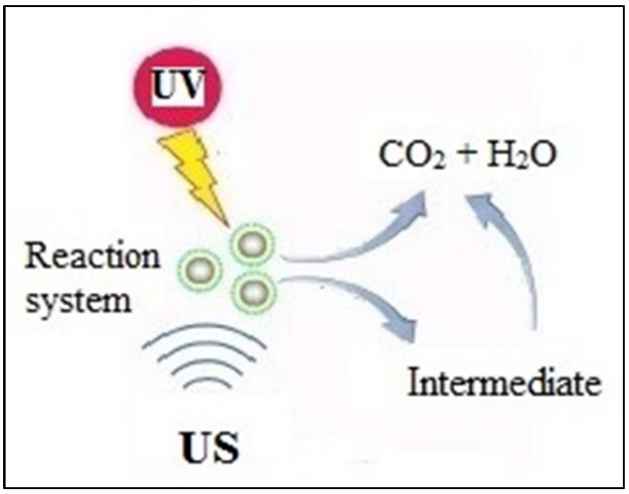

Fig. 1.12: General mechanism of sonophotocatalysis

If the two modes of irradiations (UV and US) are operated in combination, more number of free radicals will be available for the reaction thereby increasing the rates of reaction. Thus the combination provides an additive or synergistic effect which can enhance the degradation of pollutants.

The most common problem associated with photocatalysis is the reduced efficiency of photocatalyst with continuous operation possibly due to the adsorption of contaminants at the surface and blocking of the sites, which makes them unavailable for adsorption by fresh molecules or generation of active species. Photocatalysis is also affected by severe mass transfer limitations especially in the case of immobilized catalyst type reactors, which are generally preferred over slurry reactors to avoid problem of solid catalyst separation. The turbulence induced by the cavitation phenomenon can aid in eliminating the drawbacks of blocking the surface sites by reactant/intermediates/products associated with

photocatalysis. Although photocatalysis and sonolysis have been extensively employed individually for the degradation of several organic species in water, their combined use (i.e. sonophotocatalysis) has received much less attention. Process integration may be favorable in eliminating the disadvantages associated with individual processes, thus increasing the degradation rates. For instance, in heterogeneous catalytic systems, the use of ultrasound creates conditions of increased turbulence in the liquid, thus decreasing mass transfer limitations and increasing the surface area available by catalyst fragmentation and de-agglomeration [80].

1.2.8.1 Some typical studies in sonophotocatalysis

Sonophotocatalysis has been studied for the degradation of compounds such as salicylic acid [81], 1,4- dioxane [82], 2- (butylamino) ethanethiol [83], 2-chlorophenol [84, 85] dyes, methyl *tert*-butyl ether (MTBE) [86], phenol [87] etc.

Wu et al. [88] observed that the percentage of phenol degradation under the combined effect of UV and US was larger compared to the respective individual effects. Based on the results of TOC removal, synergistic action of US and UV light was established. Fe^{2+} present in the aqueous phenol solution enhanced TOC removal. They also observed that rate of phenol degradation increased with decreasing solution pH and increasing dissolved oxygen in the aqueous solutions.

Davydov et al. [81] investigated the effect of ultrasound on the photo degradation of salicylic acid using commercially available TiO_2 powder. The combination of the action of ultrasound and UV-assisted photocatalysis yielded synergistic effects for catalysts with smaller particle

size, while negligible enhancement was observed for photocatalysis with large particle size.

Harada [89] showed that sonophotocatalysis is able to decompose water in to hydrogen and oxygen stoichiometrically and continuously, which was impossible by sonocatalysis or photocatalysis alone.

Chen et al. [90] investigated the photocatalytic oxidation of dimethyl methyl phosphonate (DMMP) in presence of low frequency ultrasonic irradiation. They concluded that low frequency ultrasonic irradiation increases the rate of DMMP photocatalytic oxidation due to enhanced mass transport. They also found that sonophotocatalytic oxidation of DMMP generates the same set of intermediate products as the photocatalytic oxidation.

Silva et al. [91] studied the efficiency of photocatalysis and sonolysis individually and in combination in the presence and absence of H_2O_2 for the treatment of a complex synthetic solution containing 13 compounds typically found in olive mill waters. They found that combined process was considerably more effective than the respective individual treatments, i.e. sonolysis and photocatalysis. The degradation was further enhanced in the presence of H_2O_2 acting as hydroxyl radical source.

Vinu and Giridhar [92] also confirmed the synergistic effect of sonophotocatalysis using various anionic dyes, viz., orange G, remazol brilliant blue R, alizarin red S, methyl blue, and indigo carmine, with solution combustion synthesized TiO_2 and commercial Degussa P-25 TiO_2. They also proposed a dual-pathway network mechanism for

sonophotocatalytic degradation and the rate equations were modeled using the network reduction technique.

Park [93] investigated the degradation and the relative toxicity reduction of agricultural wastewater system containing methyl 1-[(butylamino)carbonyl]-1H-benzimidazol-2-ylcarbamate (benomyl) by sonophotocatalysis. It was found that the degradation rate with a sonication/UV/TiO_2 system was about 1.5 times higher than that with a UV/TiO_2 system. Sonication/UV/TiO_2/H_2O_2 system was about 1.3 times more efficient than the UV/TiO_2/H_2O_2 system. It was also observed that under optimal conditions, the relative toxicity of a sonophotocatalytic system was about 10 to 18% lower than corresponding photocatalytic system, the reduction being dependent on the duration of operation.

Madhavan et al. [94] studied the sonolytic, photocatalytic and sonophotocatalytic degradation of monocrotophos in the presence of homogeneous (Fe^{3+}) and heterogeneous photocatalysts (TiO_2). The photocatalytic degradation rate of monocrotophos using TiO_2 was lower than that of sonolysis due to the interference by PO_4^{3-} ions formed as an intermediate. The sonophotocatalytic degradation rate also was lower than the sum of the individual sonolysis and photocatalysis. But the mineralization due to TiO_2 or Fe^{3+} sonophotocatalysis was additive.

Sekiguchi et al. [95] investigated the synergistic effects of US and UV/TiO_2 for degradation of formaldehyde and benzaldehyde. They found that at high concentration, the removal rate of formaldehyde, using US/UV/TiO_2, was much more compared to the addition of US and UV/TiO_2 individually. However, the removal rate of benzaldehyde was

not improved much by US/UV/TiO_2 compared to the addition of US and UV/TiO_2. At low concentrations, all processes (US, UV/TiO_2 and US/UV/TiO_2) followed pseudo-first-order kinetics. Synergy was observed for the degradation of formaldehyde and benzaldehyde under US/UV/TiO_2 conditions.

Kavitha and Palanisami [96] reported that the degradation of dye over TiO_2 under visible light is accelerated by ultrasound. They also proposed that photo degradation kinetics follows the Langmuir–Hinshelwood model and depends on the TiO_2 concentration and pH.

Anoop et al. [97] studied the photocatalytic, sonolytic and sonophotocatalytic degradation of 4-chloro-2-nitrophenol (4C2NP) using TiO_2 catalyst. They optimized the catalyst concentration at 1.5 g/L, pH at 7 and oxidant (H_2O_2) concentration at 1.5 g/L. They obtained almost 80% degradation for photocatalytic treatment in 120 minutes whereas combination with ultrasound imparted synergistic effect which could achieve 96% degradation in 90 minutes. The degradation follows the trend sonophotocatalysis > photocatalysis > sonocatalysis > sonolysis.

Durán et al. [98] studied the mineralization of antipyrine using an innovative sonophotocatalytic oxidation process (H_2O_2/UV/Fe/Ultrasound). TOC removal was significantly increased when compared with each individual process. The synergism between the sonolysis and photo fenton process was also observed.

Talebian et al. [99] studied the effects of sonolysis, sonocatalysis, photocatalysis and sonophotocatalysis on the degradation of chrome intra orange G by varying the initial dye concentration, pH, catalyst morphology

and loading to ascertain the synergistic effect on the degradation process. ZnO sonophotocatalysis was always faster than the respective individual processes. Ultrasound may be modifying the rate of photocatalytic degradation by promoting the deaggregation of the catalyst, increase of its active surface area and increasing the amount of reactive radical species through cavitation resulting in water splitting and formation of H_2O_2.

Nileema et al. [100] studied the sonocatalytic and sonophotocatalytic degradation of rhodamine 6G (Rh 6G) using cupric oxide (CuO) and TiO_2 as catalysts. They concluded that combined processes give higher extent of degradation as compared to the individual processes based on US or UV irradiations. They also studied effect of radical scavengers such as methanol (CH_3OH) and n-butanol (C_4H_9OH) on the extent of degradation and confirmed the dominance of radical mechanism.

Ahmad et al., [101] studied the degradation of RhB in the presence of pristine ZnO nanoparticles and ZnO/Carbon nanotube composites using photocatalysis and sonocatalysis systems separately and simultaneously. Pseudo - first order kinetics was observed in photocatalytic, sonocatalytic and sonophotocatalytic processes but the rate constant of sonophotocatalysis is higher than the sum of photocatalytic and sonocatalytic rate constants. The sonophotocatalysis was faster than the respective individual processes due to the formation of more reactive radicals as well as the increase of the active surface area of ZnO/CNTs photocatalyst. Chemical oxygen demand (COD) reduction of textile wastewater containing RhB confirmed the destruction of the organic molecules.

Zaviska et al. [102] studied the effect of nitrate ion on the photosonochemical (US/UV) process for phenol degradation. They concluded that concentration of hydroxyl radical is directly proportional to the initial nitrate concentration. However, the degradation of organic compound such as phenol is not improved in presence of NO_3^- probably because of the UV filter effect of aqueous anions. The NO_3^- ion also inhibits the sonochemical degradation of organic contaminants due to the $^{\bullet}OH$ scavenging effect.

As may be seen, the emphasis in all these investigations is to achieve maximum degradation efficiency for various pollutant molecules. The concurrently formed H_2O_2 was given only secondary treatment. Its contribution to the efficiency of the process and its fate were mostly neglected. The present study, among other findings, is the first major attempt, to the best of our knowledge, focussing on the hitherto ignored role and fate of H_2O_2 in sono, photo and sonophoto catalytic systems using phenol as test substrate and ZnO as the catalyst.

Chapter 2

OBJECTIVES OF THE STUDY, MATERIALS USED AND PLAN OF THE THESIS

Contents

2.1 Objectives

As mentioned in Chapter 1, semiconductor mediated sonocatalysis, photocatalysis and sonophotocatalysis are promising AOPs for the degradation/mineralisation of a variety of pollutant molecules in water. AOPs are based on the generation of highly reactive $^{\bullet}OH$ radicals which attack the target molecules, degrade them and eventually mineralise into harmless CO_2, water and salts. H_2O_2 is the most stable Reactive Oxygen Species (ROS) and its net concentration in the system is closely related to other ROS. H_2O_2 functions as a reactant, intermediate and end product in AOPs. It is formed by a number of reactions involving various free radicals formed during the AOP. These include mainly:

$$2^{\bullet}OH \rightarrow H_2O_2 \quad \text{.....(52)}$$

$$\text{ROS } (^{\bullet}OH, HO_2^{\bullet}\text{etc}) + \text{Phenol} \rightarrow \text{Intermediates} + H_2O_2 \rightarrow H_2O_2 + H_2O + CO_2 \quad \text{.....(53)}$$

The H_2O_2 can also undergo concurrent decomposition resulting in the formation of $^{\bullet}OH$ and/or $(H_2O + O_2)$.

$H_2O_2 \rightarrow 2^{\bullet}OH$ .....(54)

$2H_2O_2 \rightarrow 2H_2O + O_2$ .....(55)

This concurrent formation and decomposition of H_2O_2 makes its role in many AOPs inconsistent and unpredictable.

The fate of H_2O_2 in AOPs has not received due attention as the focus has always been on the removal of the pollutant and purification of water. At the same time, the study is especially relevant in view of the fact that H_2O_2 is an important water soluble trace gas species in the atmosphere which can act as a precursor for highly reactive free radicals $^{\bullet}OH$ and $HO_2^{\bullet}$. In the presence of suspended particulate matter including solar active materials, these free radicals can lead to the formation of a variety of chemical species with short and long term impact on atmospheric chemistry and climate change.

The current study is the first major attempt focusing on the fate and role of H_2O_2 formed insitu in sono, photo and sonophoto catalysis. Thus the main objectives are:

- To compare the efficiency of the three AOPs, i.e., sono, photo and sonophoto catalysis for the removal of trace organic pollutants in water.
- To investigate the fate of concurrently formed H_2O_2 which plays a crucial role in the mineralization process.
- To throw more light on the influence of naturally occurring contaminants on the efficiency of the process.

Phenol is chosen as the model pollutant in view of its presence in a wide variety of industrial wastewater. ZnO is selected as the catalyst in view of its availability, efficiency, safety and extended absorption in the

visible range of solar spectrum. Since the study was mostly focused on the removal of pollutants from wastewater under neutral pH (around neutral range), the corrosion of ZnO under extreme acidic condition and photo corrosion are not expected to be of any concern.

Specific activities to achieve the objectives include:

- Characterization of the selected commercially available semiconductor oxide catalyst, i.e., in this case ZnO
- Laboratory testing of the above catalyst for the possible removal of selected chemical pollutant (Phenol in this case) under different conditions using sono, photo and sonophoto catalysis
- Optimization of various reaction parameters such as catalyst dosage, particle size, pH, pollutant concentration, O_2 etc., for the degradation of the pollutant under each of the three AOPs
- Investigations on the effect of various contaminant anions and cations in water on the efficiency of degradation and the fate of insitu formed H_2O_2
- In-depth investigations on the fate of the insitu formed H_2O_2 under various reaction conditions and
- Elucidation of a suitable mechanism for the degradation of the pollutant and the behavior of H_2O_2

2.2 Materials used

2.2.1 Zinc oxide

ZnO has been proven to be a good photocatalyst for a number of reactions. It has a band-gap energy of ~ 3.4 eV. ZnO is capable of absorbing a relatively larger fraction of the solar spectrum [25] and hence

is more active in the visible region for the photocatalytic decontamination of water [103-106]. It is for this reason that ZnO is investigated more extensively in recent years as a photocatalyst compared to TiO_2, even though the former has the disadvantage of getting corroded at extreme pH as well as under UV light. The comparatively lower light-scattering effect of ZnO due to its lower refractive index (ZnO: 2.0, TiO_2: 2.5–2.7) also favours better photocatalytic efficiency.

ZnO is an n-type semiconductor. It is a white powder. It is present in earth's crust as zincite. ZnO possesses transparency, high electron mobility and strong room-temperature luminescence. Zinc oxide crystallizes mainly in two forms, wurtzite (hexagonal) and zinc blende (cubic). The most common and most stable form of ZnO at ambient temperature is wurtzite. Figure 2.1 shows the wurtzite structure of ZnO.

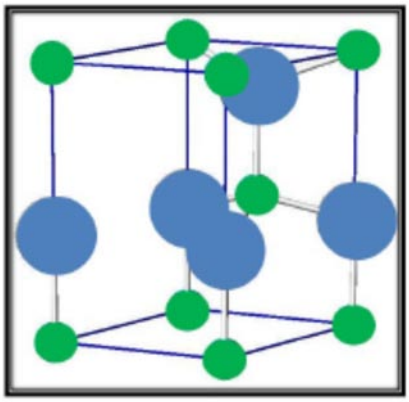

Fig. 2.1: Wurtzite structure of ZnO (green balls are Zn^{2+} and blue balls O^{2-} showing tetrahedral coordination) [107]

In both cases, the zinc and oxide centers are tetrahedral, the most characteristic geometry for Zn (II). Crystalline zinc oxide is thermochromic i.e., its colour changes from white to yellow on heating in air and revert to

white on cooling. This colour change is due to the loss of oxygen to the environment at high temperatures to form the non-stoichiometric $Zn_{1+x}O$, where x = 0.00007 at 800°C.

Zinc oxide is amphoteric in nature. It is nearly insoluble in water, but it is soluble in (degraded by) most acids, such as hydrochloric acid.

$$ZnO + 2\ HCl \rightarrow ZnCl_2 + H_2O \quad \text{.....(56)}$$

ZnO decomposes into zinc vapor and oxygen at around 1975°C. In a carbothermic reaction, heating with carbon converts the oxide into zinc vapor at a much lower temperature (around 950°C).

$$ZnO + C \rightarrow Zn\ (Vapor) + CO \quad \text{.....(57)}$$

It reacts with hydrogen sulfide to give zinc sulfide. This reaction is used commercially for the removal of H_2S.

$$ZnO + H_2S \rightarrow ZnS + H_2O \quad \text{.....(58)}$$

Physical characteristics of ZnO are shown in table 2.1

Table 2.1: Physical properties of ZnO

Property	**Value**
Molecular mass	81.37 g/mol
Crystal structure	Wurtzite
Density	5.606 g/cm^3
Melting point	1975^{0}C
Boiling point	2360^{0}C
Solubility in water	0.16g/100 ml
Thermal conductivity	0.6, 1-1.2 Wcm^{-1} K^{-1}
Energy gap	3.4 eV
Excitation binding energy	60 mV
Static dielectric constant	8.656
Refractive index	2.008,2.029

ZnO is an inexpensive, moisture stable, reusable and commercially available catalyst [108-111]. The powder is widely used as an additive for numerous materials and products including plastics, ceramics, glass, cement, rubber (e.g. car tyres), lubricants, paints, ointments, adhesives, sealants, pigments, foods (sources of Zn nutrient), batteries, ferrites, fire retardants, first-aid tapes, etc. Commercial ZnO is produced synthetically. In the laboratory, ZnO is prepared by electrolyzing a solution of sodium bicarbonate with a zinc anode. Zinc hydroxide and hydrogen gas are produced. The zinc hydroxide upon heating decomposes to zinc oxide.

$$Zn + 2\ H_2O \rightarrow Zn(OH)_2 + H_2 \quad \text{.....(59)}$$

$$Zn(OH)_2 \rightarrow ZnO + H_2O \quad \text{.....(60)}$$

ZnO has a relatively large direct band gap of ~ 3.4 eV at room temperature. Advantages of this include higher breakdown voltages, ability to sustain large electric fields, lower electronic noise, as well as high-temperature and high-power operation. The bandgap of ZnO can be further modified by doping it with magnesium oxide or cadmium oxide.

ZnO is also known as II-VI semiconductor because zinc and oxygen belong to the 2^{nd} and 6^{th} groups of the periodic table, respectively. Its stability, non-toxicity, high catalytic efficiency, low cost and abundance in nature also make it a favourable catalyst [112-114].

2.2.2 Phenol

Phenol, the test pollutant used in this study, is an aromatic organic compound with molecular formula C_6H_5OH. It is also known as carbolic acid. Structure of phenol is shown in figure 2.2.

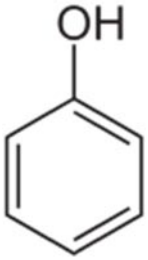

Fig. 2.2: Structure of Phenol

It is one of the most common pollutants found in effluents from industries such as petrochemicals, pharmaceuticals, pesticides, paints, dyes, organic chemicals, etc. Presence of minute quantity of phenol in water results in a high level of toxicity. It is listed as a priority pollutant in the list of 129 toxic pollutants by the US Environmental Protection Agency (EPA). According to Environment Protection Rules of Central Pollution Control Board, India (1992), the discharge limit of phenols in land water is less than 1 ppm.

Table 2.2 shows some of the physical properties of phenol.

Table 2.2: Physical properties of phenol

Molecular formula	**C_6H_5OH**
Molar mass	94.11 g/mol
Appearance	Transparent crystalline solid
Stability	Stable, Flammable
Odour	Sweet and tarry
Density	1.07 g/cm^3
Melting point	40.5^{o}C
Boiling point	181.7^{o}C
Solubility in water	8.3 g/ 100 mL
UV- Vis (λ_{max})	270.75 nm
Dipole moment	1.224 D
Acidity (pK_a)	9.95 (in water)

Phenol is weakly acidic and gives phenoxide ions at high pH.

$$C_6H_5OH \rightleftharpoons C_6H_5O^- + H^+ \quad \text{.....(61)}$$

Major use of phenol includes its conversion to plastics and related materials. It also has medicinal value as antiseptic. Inhalation of phenol and dermal exposure results in high irritation to the skin, eyes and mucous membranes. Acute toxicity in humans includes symptoms such as irregular breathing, muscle weakness and tremors, loss of coordination, convulsions, coma and respiratory arrest at lethal doses. Phenol used in the current study is of AnalaR Grade supplied by Qualigen (India) and purity is 99.5%.

2.2.3 Hydrogen peroxide (H_2O_2)

H_2O_2 is a colourless liquid with viscosity slightly greater than that of water. It is used as an oxidizer, bleaching agent and disinfectant. Structure of H_2O_2 is shown in figure 2.3.

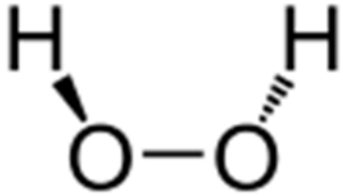

Fig. 2.3: Structure of H_2O_2

Aqueous solution of H_2O_2 differs in its properties from pure H_2O_2 due to the presence of hydrogen bonding. It is thermodynamically unstable and decompose into water and oxygen as in reaction (5).

Major properties of H_2O_2 are summarized in table 2.3.

Table 2.3: Physical properties of H_2O_2

Molecular formula	**H_2O_2**
Molecular mass	34.0147 g/mol
Density	1.1 g/cm^3
Melting point	-0.43^{0}C
Boiling point	150.2^{0}C
Solubility in water	Miscible
Acidity (pKa)	11.75
Viscosity	1.245 cP
Dipole moment	2.26 D

2.2.4 Miscellaneous materials

Details of various other materials used in the study are provided in respective chapters.

2.3 Experimental set up

The experimental set up and the procedures are described in respective chapters.

2.4 Analytical procedures

The analytical procedures adopted in this study include chromatography, spectroscopy, microscopy as well as conventional wet methods. These are appropriately described in the respective chapters.

2.5 Plan of the thesis

The current thesis is divided into seven chapters. Each chapter has its own specific objectives, experimental procedures, results, discussion and conclusions.

Chapter 1 entitled "**Introduction: Background literature**" gives an overview of the recent relevant literature and discussion on various types of AOPs with special focus on the application of sonocatalysis, photocatalysis and sonophotocatalysis in pollution control and water treatment.

Chapter 2 entitled "**Objectives of the study, Materials used and Plan of the thesis**" describes the main objectives of the study, specific activities undertaken to accomplish the objectives and characteristics of the main materials used in the study, namely ZnO, phenol and H_2O_2. The chapter also provides the general layout of the thesis.

Chapter 3 entitled **"Investigations on the photocatalytic degradation of phenol and the fate of H_2O_2 formed insitu"** deals with studies on the photocatalytic degradation of phenol and the fate of insitu formed H_2O_2 in presence ZnO catalyst under different conditions. Detailed experimental procedures followed, reaction details, analytical procedures, etc., are also provided. This chapter clearly illustrates that the lack of correlation observed between the phenol degraded and the concentration of concurrently formed H_2O_2 is due to the simultaneous formation and decomposition (oscillation) of H_2O_2. Various parameters influencing the oscillation in the concentration of H_2O_2 are also investigated and presented in this chapter.

Parts of the major findings reported in this chapter were published in journals/presented as original research papers in conferences as below:

Paper 1. "Semiconductor mediated photocatalytic degradation of plastics and recalcitrant organic pollutants in water: Effect of additives and fate of insitu formed H_2O_2", ***J. Adv. Oxid. Technol.***, 18, 85-97 (2015).

Paper 2. "Sono, photo and sonophotocatalytic decontamination of organic pollutants in water : Studies on the lack of correlation between pollutant degradation and concurrently formed H_2O_2", ***Current Science,*** 109, 189–195 (2015).

Paper 3. "Ultrasound (US), Ultraviolet light (UV) and combination (US + UV) assisted semiconductor catalysed degradation of organic pollutants in water: Oscillation in the concentration of hydrogen peroxide formed in situ", ***Ultrason. Sonochem.***, 21, 1787-1796 (2014).

Paper 4. "Influence of reaction intermediates on the oscillation in the concentration of insitu formed hydrogen peroxide during the photocatalytic degradation of phenol pollutant in water on semiconductor oxides", ***Res. J .Recent. Sci.,*** 2, 82-89 (2013).

Paper 5. "Role and fate of hydrogen peroxide in the sono and photocatalytic transformation of organic pollutants in water"; Paper presented in the '***National Conference on Climate Change: Challenges and Strategies***' held at Newman college, Thodupuzha in Feb. 2012; Proceedings of the conference, p 19.

Paper 6. "Unusual behavior of insitu formed H_2O_2 during the sono, photo and sonophotocatalytic transformation of organic pollutants in water" Paper presented in the **25th *Kerala Science Congress***, held at Thiruvananthapuram in Jan. 2013; Proceedings of the conference, pp 306-308.

Paper 7. "What happens to the H_2O_2 formed during the photocatalytic degradation of organic pollutants in water? An investigation",

Paper presented in the **26th *Kerala Science Congress*,** held at Wayanad in Jan. 2014; Proceedings of the conference**,** p. 128.

Paper 8. "Investigations on resolving the inconsistency in insitu formed H_2O_2 during advanced oxidation processes: Clear evidence for the phenomenon of oscillation" Paper presented in the **27th *Kerala Science Congress***, held at Alapuzha in Jan. 2015; Proceedings of the conference, p. 49.

Chapter 4 entitled "**Investigations on the sonocatalytic degradation of phenol and the fate of H_2O_2 formed insitu"** deals with the sonocatalytic degradation of phenol and the fate of concurrently formed H_2O_2 in presence of ZnO under different conditions. Relevant experimental procedures and analytical techniques are also described. Some of the results which are presented in this chapter together with those described in Chapter 3 are published/presented in conferences as described above in papers 2, 3, 5, 6 and 8. Additionally, the following research paper is published based on the results in this chapter.

Paper 9. "Periodic change in the concentration of hydrogen peroxide formed during the semiconductor mediated sonocatalytic treatment of wastewater: Investigations on pH effect and other operational variables", ***Res. J. Recent. Sci.,*** 1, 191-201 (2012).

Chapter 5 entitled "**Investigations on the sonophotocatalytic degradation of phenol and the fate of H_2O_2 formed insitu**" deals with the simultaneous utilization of light and sound in presence of semiconductor oxide for the degradation of phenol in water. The fate of concurrently formed H_2O_2 also is closely monitored. The chapter confirms the synergy of sonophotocatalysis

in which the efficiency of the process is more than that of the individual sono or photocatalysis or their additive effect. Some of the results from this chapter together with those described in Chapter 3 and 4 were incorporated and published/presented in conferences as given under papers 2, 3, 6 and 8 above.

Chapter 6 entitled "**Effect of inorganic salts/ions on the photo, sono and sonophoto catalytic degradation of phenol and oscillation in the concentration of H_2O_2 formed insitu**" deals with the effect of various salts and the respective anions and cations which are likely to be present naturally in water on the photo, sono and sonophoto catalytic degradation of phenol. Contrary to many earlier reports in literature, according to which the salts function as inhibitors, most of the ions enhance the photo, sono and sonophoto catalytic degradation of phenol in the current instance. Various parameters such as concentration of the ions and time of reaction, competitive adsorption by the anions, etc. which influence the efficiency of the phenol degradation, are also investigated in detail. Fate of insitu formed H_2O_2 in presence of these ions is also studied and presented in detail in this chapter.

Some of the findings reported in this chapter were published/ presented as original research papers as follows:

Paper 10. "Influence of commonly occurring cations on the sono, photo and sonophoto catalytic decontamination of water", ***IOSR J. Appl. Chem.***, Special issue, ICETEM 16, 15-24 (2016).

Paper 11. "Effect of anionic contaminants on the sonocatalytic degradation of phenol and concurrently formed H_2O_2" Paper presented in

the ***3rd International Conference on Advanced Oxidation Process,*** held at Munnar, in September, 2014; Proceedings of the conference, p. 47.

Paper 12. "Effect of Anions on the Oscillation in the Concentration of Hydrogen Peroxide formed insitu in Sonocatalytic Systems" Paper presented in the **2nd *Asia-Oceania Sonochemical Society Conference (AOSS-2)***, held at Kuala Lumpur, Malaysia in July 2015; Proceedings of the conference, p. 60.

Paper 13. "Natural contaminants as facilitators in wastewater treatment: reversal of role from inhibition to enhancement in photocatalysis" Paper presented in the **28th *Kerala Science Congress*** held at Kozhikode in Jan. 2016; Proceedings of the conference, p. 2661-2669.

Chapter 7 entitled "**Summary and Conclusion**" summarizes the findings of the study and highlights the conclusions.

Annexure I lists the abbreviations used in the thesis. Expansions of respective abbreviation are shown in the text also in the first place where they appear in the thesis.

Annexure II provides the list of original research papers based on the results of this study published in peer reviewed journals and/or presented in conferences.

Annexure III compiles the reprints of the papers already published.

Annexure IV Lists major awards conferred based on the contributions from the current study

Chapter 3

INVESTIGATIONS ON THE PHOTOCATALYTIC DEGRADATION OF PHENOL AND THE FATE OF H_2O_2 FORMED INSITU

Contents

3.1 Introduction

Phenol and its derivatives are widely reported chemical pollutants in industrial wastewaters. Due to its relative stability in the environment, solubility in water, high toxicity and associated health problems, removal of phenol from industrial wastewater is important. Semiconductor mediated photocatalysis is one of the major AOPs being investigated for the complete mineralization of phenol to CO_2 and water. One of the end-products of the AOP-promoted degradation of organic pollutants in water is H_2O_2 which also functions as a reactant as well as intermediate. However, the fate of H_2O_2 has not received due attention since the focus has always been on the removal of the pollutant and purification of water. This gap is addressed to some extent in the current study. The findings on the fate of H_2O_2 formed during the photocatalytic degradation of phenol in water are presented and discussed in this chapter.

3.2 Experimental details

3.2.1 Materials used

ZnO (99.5%) used in the study was supplied by Merck India Limited. The surface area, as determined by the BET method is ~ 12 m^2/g. The physicochemical characteristics of ZnO used in the study were confirmed by X-ray diffraction (XRD), Transmission Electron Microscopy (TEM), Scanning Electron Microscopy (SEM), particle size and adsorption measurements. The average particle size, determined by SEM was 10×10^{-2} μm. Phenol AnalaR Grade (99.5% purity) and H_2O_2 (30.0% w/v) from Qualigen (India) were used as such without further purification. All other chemicals used were of AnalaR Grade or equivalent unless indicated otherwise. Twice distilled water was used in all the experiments.

3.2.2 Analytical procedures

3.2.2.1 Phenol

The concentration of phenol in routine experiments was measured by spectrophotometry. At periodic intervals, samples were drawn from the reactor, centrifuged and the centrifugate was analysed for the concentration of phenol left behind. The analysis is based on the reaction of phenolic compounds with 4-amino antipyrine at pH 7.9 ± 0.1 in presence of potassium ferricyanide to form a coloured antipyrine dye. The absorbance of this dye solution is measured at 500 nm using a spectrophotometer (Varian UV-VIS spectrophotometer). A similar reaction system kept in the dark under exactly identical conditions but without UV irradiation was used as the reference. The major intermediates of phenol degradation before ultimate mineralization were verified by High Performance Liquid

Chromatography (HPLC) {micro Bondapack C18 column of 36 cm length, eluting solvent is water-acetonitrile in the ratio 80:20 and UV detector}. The identified intermediates are catechol, hydroquinone and benzoquinone. However, they are not consistently detected quantitatively or are detected in only negligible quantities, indicating that they undergo faster/ comparable degradation in relation to the parent compound. Hence, they are not expected to interfere in the spectrophotometric analysis of phenol.

3.2.2.2 H_2O_2

H_2O_2 was analyzed by standard iodometry. The oxidation of iodide ions by H_2O_2 was carried out in 1N sulphuric acid in presence of a few drops of saturated ammonium molybdate solution, which acts as a catalyst. The reaction was allowed to go to completion (5 minutes) in the dark. The liberated iodine was then titrated against a standard solution of sodium thiosulphate, (usually of 5×10^{-3} N) prepared freshly from 10^{-1} N stock solution. Freshly prepared starch was used as the indicator. Mineralization was verified from the evolution of CO_2 after prolonged irradiation. CO_2 was detected by the precipitation of $BaCO_3$ when the gas phase above the reaction suspension was flushed with O_2 and passed through Ba $(OH)_2$ solution. In addition, TOC content of reaction solution was recorded using the TOC Analyzer Vario TOC CUBE (Elementer Analysen systeme make).

3.2.2.3 Chemical Oxygen Demand (COD)

COD of the samples were determined using open reflux method [115]. 50 ml of the sample was pipetted into a refluxing flask. $HgSO_4$ (1 g) was added along with several glass beads. Added 5 ml of sulfuric acid reagent (5.5g Ag_2SO_4 + 543 ml Conc. H_2SO_4) slowly with mixing to

dissolve $HgSO_4$. The sample was cooled while mixing to avoid the possible loss of volatile material. 25 ml of 0.05 N $K_2Cr_2O_7$ solution was also added and mixed well. Remaining (70 ml) sulfuric acid reagent was added through the open end of the condenser. The whole mixture was refluxed for 2 hours and cooled thereafter to room temperature. The mixture was diluted to 150 ml and the excess $K_2Cr_2O_7$ was titrated against 0.05 N ferrous ammonium sulphate (FAS) solution. The end point was sharp change of color from blue-green to reddish brown. A blank was also carried out under identical conditions using the reagents and distilled water in place of the sample.

COD is calculated from the following equation:

$$\text{COD as mg } O_2/L = \frac{(A-B) \times M \times 8000}{\text{mL Sample}} \quad \text{.....(62)}$$

A = ml FAS used for blank

B = ml FAS used for sample

M = molarity of FAS

8000 = milliequivalent weight of oxygen × 1000 ml/L

3.2.2.4 Phosphate

Phosphate phosphorus was determined using 'ascorbic acid' method [116]. A standard solution of KH_2PO_4 (5 µg PO_4^{3-} phosphorous) was prepared. Pipetted out 0.2, 0.4, 0.6, 0.8 and 1 ml of this standard into separate tubes and added distilled water to make up to a total volume of 10 ml and mixed well. 10 ml of distilled water in a tube served as the reference. To each of these tubes 1 ml of combined reagent (5 N H_2SO_4 + 0.008 M Potassium antimony (III) oxide tartrate + 0.3 M Ammonium molybdate + 0.1 M Ascorbic acid) was added, mixed well and allowed to stand for 10 minutes.

The absorbance was then measured at 880 nm versus the reference. A calibration graph was plotted with absorbance against concentration of the respective standards. The test sample also was prepared similarly and its absorbance was measured. The phosphate phosphorous concentration of the sample corresponding to the measured absorbance was determined from the graph.

Surface area of the catalysts was measured using BET method using Micrometrics TriStar surface and porosity analyser. The XRD measurements were made using Rigaku X-ray diffractometer with Cu-Kα radiation. SEM measurements were performed using JEOL Model JSM-6390 LV. TEM was done using Joel/JEM 2100 with source LaB6.

3.2.3 Adsorption

A fixed amount (0.1 g) of the catalyst was introduced into 50 ml of the phenol solution of required concentration in a 100 ml beaker and the pH was adjusted as required. The suspension was agitated continuously at a constant temperature of 29 ± 1^oC for 2 hours to achieve equilibrium. This was then centrifuged at 3000 rpm for 10 minutes. After centrifugation, the concentration of phenol in the centrifugate was determined spectrophotometrically. The adsorbate uptake was calculated from the relation:

$$q_e = (C_0 - C_e)\, V / W \qquad \text{.....(63)}$$

Where C_0 is the initial adsorbate concentration (mg/L), C_e is the equilibrium adsorbate concentration in solution (mg/L), V is the volume of the solution in litre, W is the mass of the adsorbent in gram and q_e is the amount adsorbed in mg per gram of the adsorbent at equilibrium.

3.2.4 Detection of hydroxyl radicals

The formation of hydroxyl radicals in the presence of ZnO during UV irradiation is tested by the photoluminescence (PL) technique using terephthalic acid (TPA) as the probe molecule [117, 118]. The hydroxyl radicals formed insitu in the system reacts with TPA and form 2-hydroxy terephthalic acid (HTPA), which is a fluorescent molecule. The intensity of its PL is proportional to the formation of $^{\bullet}OH$ radicals in the system. In this method, ZnO (0.1 g) is suspended in a mixed aqueous solution of TPA ($2x10^{-4}$ M) and NaOH ($2x10^{-3}$ M) and irradiated by UV. The PL spectrum of the product HTPA is recorded in the range of 400 to 450 nm in 5 and 10 minutes of irradiation. The excitation wavelength was 315 nm. The PL intensity at 425 nm corresponds to the concentration of HTPA and hence of the $^{\bullet}OH$ radicals formed in the system. Shimadzu model RF-5301 PC fluorescence spectrophotometer is used for recording the spectrum.

3.2.5 Photocatalytic experimental set up

In a typical experiment, required amount of the catalyst is suspended in an aqueous solution of phenol of desired concentration in the reactor. Simple glass beakers (250 ml) were used as rectors in routine experiments. The beakers were placed in a water bath through which water at the required temperature (29 ± 1^{o}C unless mentioned otherwise) is circulated. The reaction suspension was continuously mixed using a magnetic stirrer. The suspension was illuminated with a 400W high-pressure mercury lamp mounted above the system (figure 3.1a). For specific experiments specially designed jacketed reactor (figure 3.1b) was used. This reactor has provision for circulation of water in the jacket and to bubble gas through the suspension.

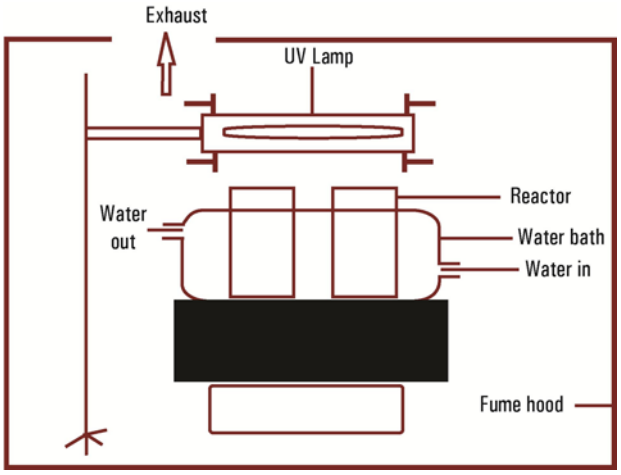

Fig. 3.1a: Schematic diagram of the photocatalytic experimental set up

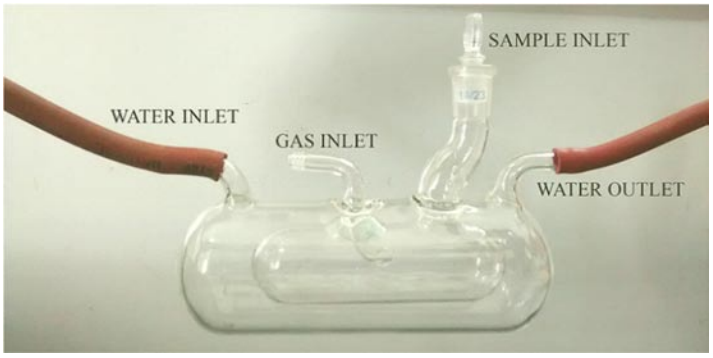

Fig. 3.1b: Special photoreactor used in the study

At periodic intervals, samples were drawn, the suspended catalyst particles were removed by centrifugation and the concentration of phenol left behind was analyzed as explained under analytical procedure in section 3.2.2. In this case also a similar reaction system kept in the dark under exactly identical conditions was used as the reference. The samples were also analysed for determining the amount of H_2O_2 present in the system at various time intervals. For the identification of intermediates

higher concentration of phenol (50 ppm) and higher loading of catalyst in the optimized ratio were used in the experiments. The irradiation is done upto ~ 50% degradation of phenol and the solution was analysed by HPLC for the intermediates. The identity of the intermediates was confirmed by using standard reference samples of respective components.

3.3 Results and discussion

3.3.1 Catalyst characterization

The catalyst ZnO used in the study was characterized by surface area, particle size analysis, pore size distribution, adsorption, XRD, SEM and TEM. The pore size distribution is shown in figure 3.2.

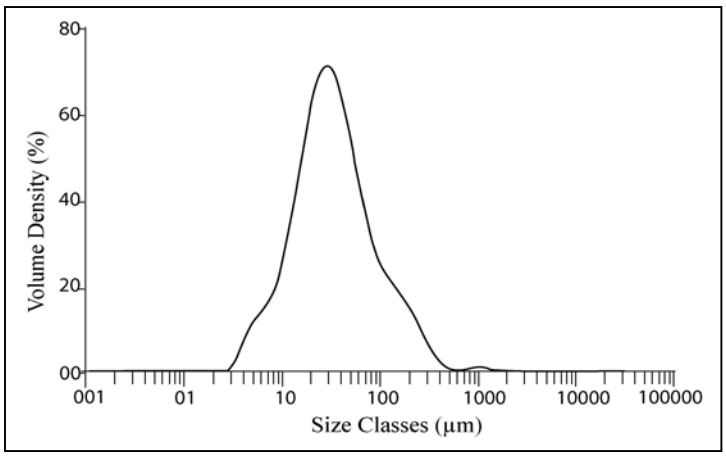

Fig. 3.2: Pore size distribution of ZnO

Pore size analysis using Micrometrics Tristar surface area and porosity analyser showed that more than 70% of the pores in ZnO were < 250 Å. The average pore width is 123 Å and size distribution is approximately; < 250 Å (70.1%), 250 to 500 Å (11.3%) and > 500 Å (17.8%).

The XRD pattern of ZnO is shown in figure 3.3.

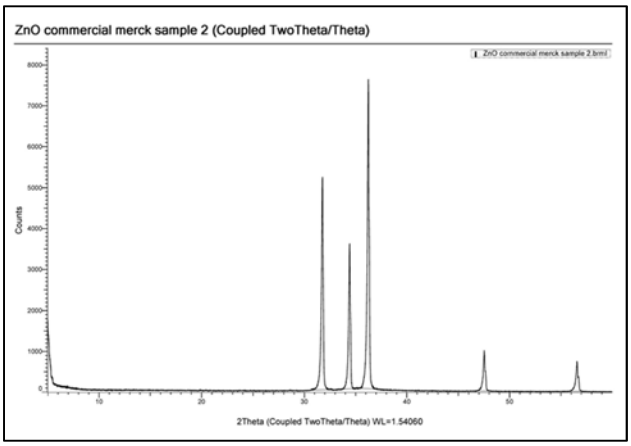

Fig. 3.3: XRD pattern of ZnO

XRD shows three sharp peaks from 30 to 40° with very high intensity which is typical of ZnO.

Figure 3.4 gives the SEM image of ZnO. The particles were rod shaped with average particle size in the range of ~ 0.1 μm.

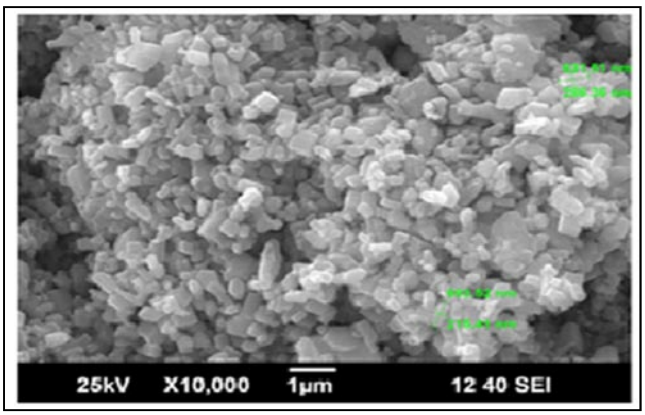

Fig. 3.4: SEM image of ZnO

The morphology, size distribution and surface characterization of ZnO were further verified by TEM. Figure 3.5 gives the TEM image of ZnO used.

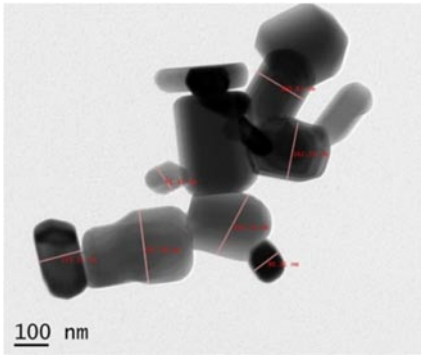

Fig. 3.5: TEM image of ZnO

The particles are of rod shape with an average particle size of 0.09 to 0.2 μm.

In general, the particle size was in the range of 0.1 to 0.2 μm.

3.3.2 Preliminary results

Preliminary studies on the photocatalytic degradation of phenol in the presence and absence of ultraviolet light revealed that both catalyst and light are essential for reasonable degradation (figure 3.6).

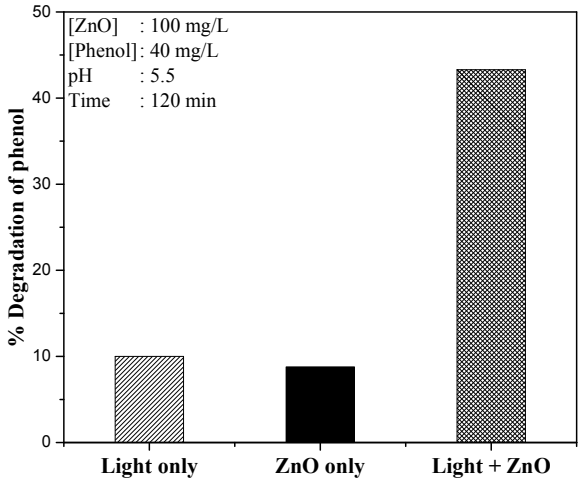

Fig. 3.6: Degradation of phenol under various conditions

This can be explained based on the general mechanism of photocatalysis. When semiconductor oxides such as TiO_2, ZnO, etc. are irradiated by UV, electrons get promoted from the valence band to the conduction band creating holes in the valence band. The OH^- ions that are adsorbed on the surface of the catalyst get oxidized to $^{\bullet}OH$ radicals by the holes in the valence band. The electron in the conduction band is donated to oxygen generating superoxide radical anion $^{\bullet}O_2^-$which eventually gives rise to more reactive species such as $HO_2^{\bullet}$, $^{\bullet}OH$, H_2O_2 etc. These species are involved in photooxidation reactions resulting in the degradation and eventual mineralization of phenol and formation of H_2O_2 as follows:

ROS ($^{\bullet}OH$, $HO_2^{\bullet}$ etc) + phenol → Intermediates +
H_2O_2 →→ $H_2O_2 + H_2O + CO_2$ .....(64)

$2^{\bullet}OH \rightarrow H_2O_2$ .....(65)

$HO_2^{\bullet} + HO_2^{\bullet} \rightarrow H_2O_2 + O_2$ .....(66)

The percentage degradation of phenol with time is shown in figure 3.7

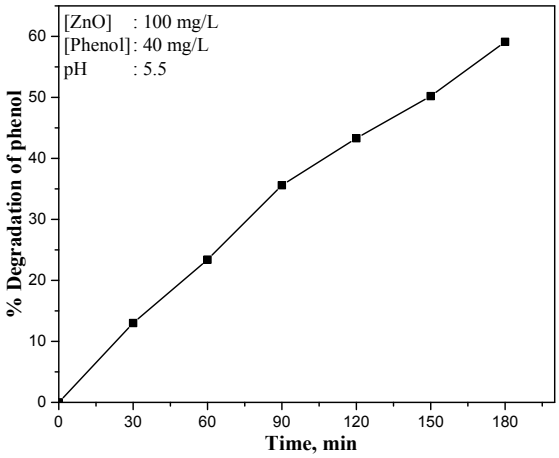

Fig. 3.7: Photocatalytic degradation of phenol

As expected the % degradation of phenol increases with increase in reaction time.

The concentration of concurrently formed H_2O_2 during the degradation of phenol with time in presence of ZnO is shown in figure 3.8

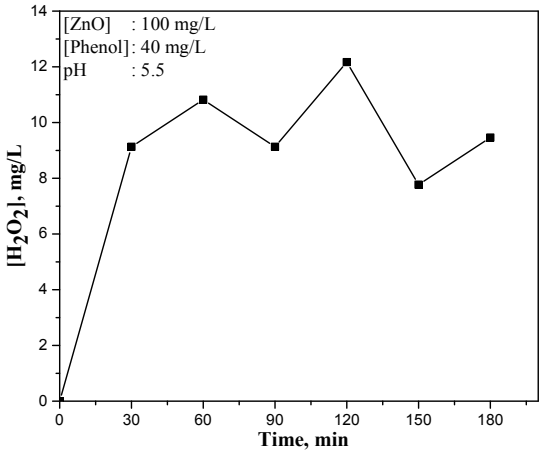

Fig. 3.8: Concentration of H_2O_2 during the photocatalytic degradation of phenol

The concentration of H_2O_2 increases and then decreases with time in a wave-like fashion (oscillation) resulting in periodic crests and troughs. Since H_2O_2 is an essential byproduct of phenol degradation, its concentration was expected to increase with the degradation of phenol and ultimately stabilize when the phenol degradation is complete. The oscillation in the concentration shows that H_2O_2 is generated and decomposed/consumed simultaneously depending on the reaction conditions, in particular its concentration. When the concentration of H_2O_2 reaches a particular maximum, the decomposition dominates bringing its net concentration down. Similarly when the concentration reaches a critical minimum, the formation process gets precedence. This process happens many times

repeatedly. The degradation of phenol continues unabated even when the concurrently formed H_2O_2 shows oscillation.

3.3.3 Effect of catalyst dosage

The catalyst dosage for optimum degradation of phenol is experimentally checked in the range of 10 to 250 mg/L and the result is shown in figure 3.9

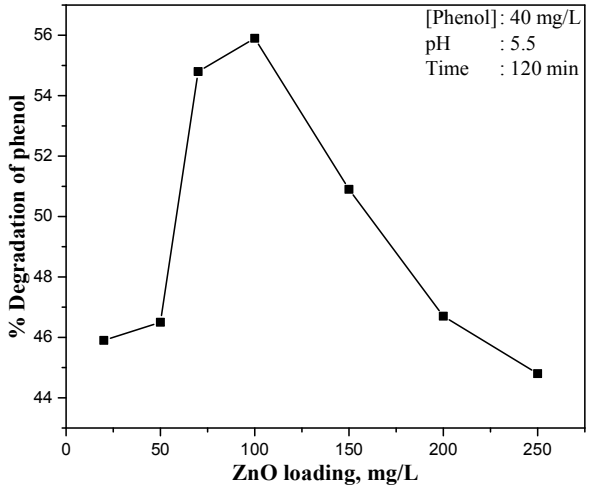

Fig. 3.9: Effect of catalyst loading on the photocatalytic degradation of phenol

Phenol degradation increases with increase in catalyst loading, reaches an optimum and then decreases. Better adsorption of the reactant molecules due to increased availability of catalyst sites, better absorption of radiation and generation of reactive free radicals and their interactions are the attributable reasons for this enhanced degradation efficiency. However, it should be noted that increased catalyst concentration beyond optimal limits can cause shrinkage in photo activated volume of suspension. This will result in light scattering and reduced passage of light through

the sample. Aggregation of catalyst particles causing decrease in number of exposed active surface sites may be another reason for the reduced rate. In any particular reactor, particles cannot be fully and effectively suspended beyond a particular loading. This causes suboptimal penetration of light and reduced adsorption of substrates on the surface. The optimum range of ZnO for photocatalysis under the current reaction condition is 75 to 100 mg/L.

Since the concentration of H_2O_2 does not increase corresponding to the degradation of phenol and it stabilizes or fluctuates, possibly due to concurrent formation and decomposition, the optimum catalyst loading for phenol degradation need not necessarily hold good for optimum H_2O_2 at any point of time. The effect of catalyst dosage on the formation and fate of H_2O_2 during ZnO mediated photocatalytic degradation of phenol is presented in figure 3.10.

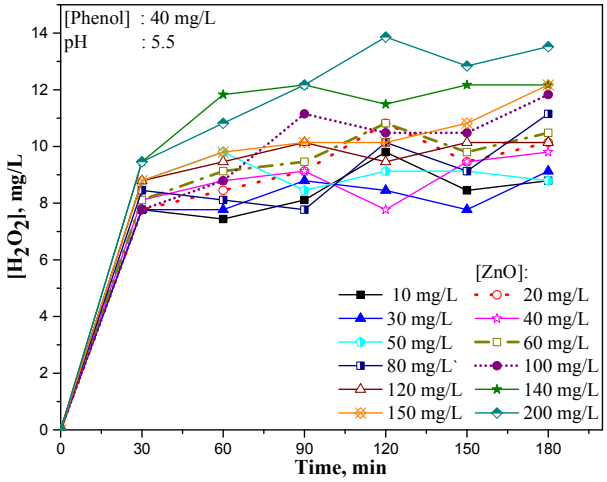

Fig. 3.10: Effect of catalyst loading on the oscillation in the concentration of H_2O_2 under photocatalysis. (*Also see Fig. 3.10.1 and 3.10.2*)

Since the data and the curves are too crowded in the figure 3.10, they are split into two as figures 3.10.1 and 3.10.2 for convenience and better clarity.

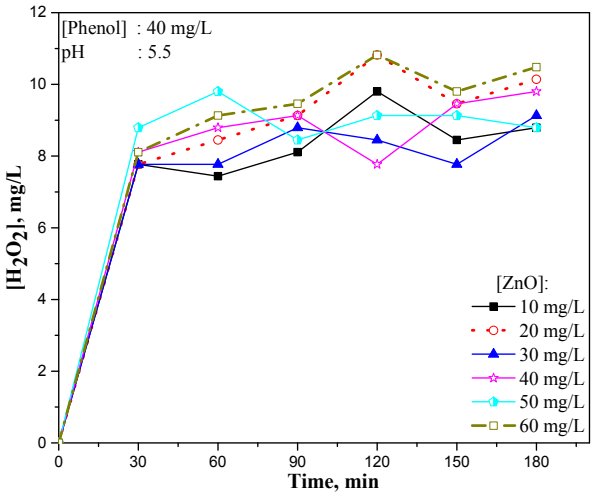

Fig. 3.10.1: Effect of catalyst loading (10 to 60 mg/L) on the oscillation in the concentration of H_2O_2 under photocatalysis

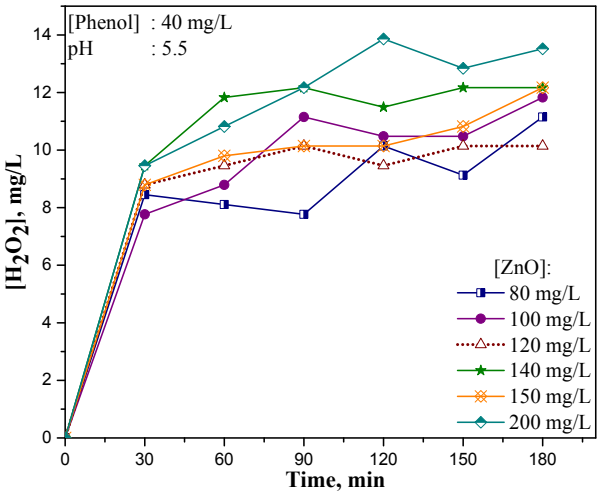

Fig. 3.10.2: Effect of catalyst loading (80 to 200 mg/L) on the oscillation in the concentration of H_2O_2 under photocatalysis

As the catalyst loading increases the phenol degradation also increases. Correspondingly, the quantity of H_2O_2 also increases though there are some exceptions. Even though the phenomenon of oscillation is there at all catalyst dosages, there is no direct correlation between the maxima/minima and the catalyst loading. The highest maximum in the concentration of H_2O_2 in the oscillation curve also increases with loading, though exceptions are there in this case too. The exceptions are mainly due to the inconsistent nature of concurrent formation and decomposition of H_2O_2 which depends on a number of factors, the catalyst dosage being one of them. Eventually the concentration of H_2O_2 tends to level off, especially at higher catalyst dosage, indicating comparable rates of formation and decomposition.

The oscillatory behavior is seen even in the net initial rate of formation of H_2O_2 before it reaches the first maximum in the oscillation curve as seen in the results plotted in figure 3.11.

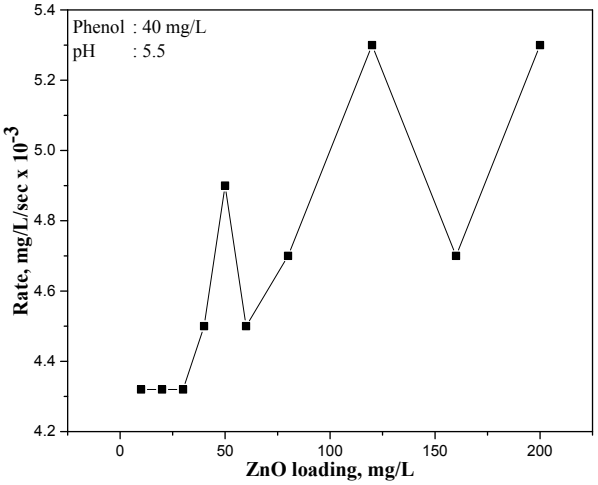

Fig. 3.11: Effect of catalyst loading on the net initial rate of formation of H_2O_2 under photocatalysis

The net initial rate of formation of H_2O_2 increases slowly with increase in catalyst loading and reaches the first maximum at 50 mg/L. Then the rate decreases, reaches a minimum and then increases sharply. After reaching a sharp maximum at ZnO loading of 125 mg/L, the net rate decreases sharply probably because the decomposition becomes more prominent. This formation/decomposition process cycle of H_2O_2 continues and a clear oscillatory pattern is obtained.

3.3.4 Effect of pH

The UV-induced degradation of organic pollutants in water is reported to be dependent on the pH of the solution [87]. Hence after optimizing catalyst loading, the effect of pH on the photocatalytic degradation of phenol is investigated in the range 3 to 11. The pH of the suspension was adjusted before irradiation and it was not controlled thereafter. The results are presented in figure 3.12.

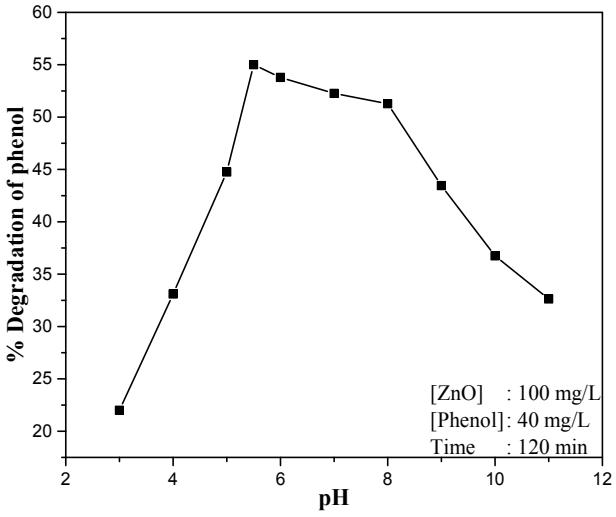

Fig. 3.12: Effect of pH on the photocatalytic degradation of phenol

The degradation is more efficient in the pH range of 5 to 8, which peaks at pH 5.5. This observation is similar to that of Wu et al. [88] who reported 98% degradation of phenol in presence of TiO_2 in the acidic range which decreases progressively in the alkaline conditions. Higher degradation efficiency in the acidic range has been reported by other authors also [119-121] with different types of phenol using TiO_2 as the catalyst. In the present study, the relatively lower degradation rate below pH 4 is probably because ZnO is corroding more in this acidic range resulting in decreased concentration of catalyst and consequently reduced catalytic activity.

pH effect can be explained at least partially based on the amphoteric behaviour and surface charge of ZnO. The Point of Zero Charge (PZC) of ZnO is ~ 9 ± 0.3 [25]. So the ZnO surface is positively charged when the pH is lower than this value and negatively charged when the pH is higher. pH of the solution influences the ionisation state of ZnO surface as follows:

$$\ldots Zn\text{-}OH + H^+ \leftrightarrow ZnOH_2^+ \quad \ldots\ldots\ldots\ldots\ldots (67)$$

$$\ldots Zn\text{-}OH + OH^- \leftrightarrow ZnO^- + H_2O \quad \ldots\ldots\ldots\ldots\ldots (68)$$

pKa of phenol is ~ 10 and in the alkaline pH range, where phenol is expected to be in the ionised form, the adsorption on ZnO which is negatively charged will be weaker. So the surface mediated degradation will be less. However under acidic conditions, phenol which remains mainly in the neutral form can get adsorbed or come closer to the catalyst surface, resulting in its degradation via active surface species and/or bulk hydroxyl radicals produced in the aqueous media [122]. Further, the

presence of more protons can facilitate the formation of reactive $^{\bullet}OH$ radicals from the available OH ions. However, in the alkaline range where repulsion between like charges of the substrate and the catalyst particles occurs, the degradation is much lower.

The effect of pH on the fate of H_2O_2, especially the oscillation resulting from simultaneous formation and decomposition, has not been reported so far. Figure 3.13 shows the concentration of H_2O_2 in the system at different times during the photocatalytic degradation of phenol on ZnO at different pH values.

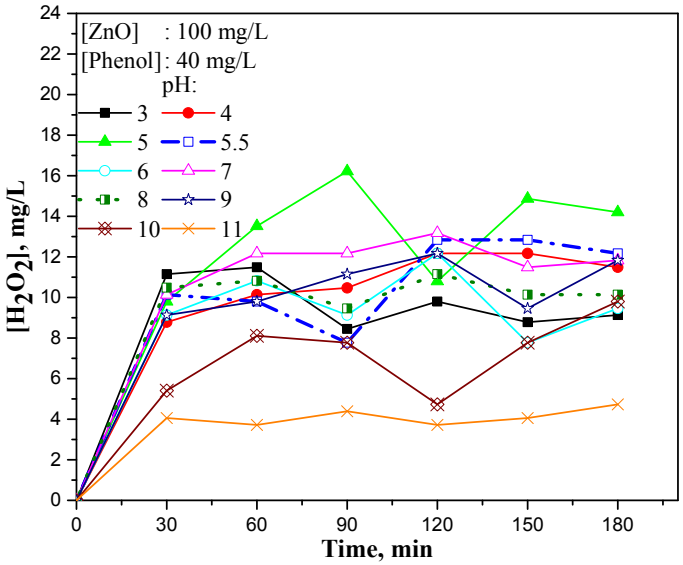

Fig. 3.13: Effect of pH on the oscillation in the concentration of insitu formed H_2O_2 under photocatalysis

The H_2O_2 concentrations, especially at the maximum of the oscillation curve are more in the pH range of 4 to 8 at which maximum phenol degradation is also observed. As explained earlier, more phenol decomposition produces more free radicals which can lead to enhanced

H_2O_2 formation resulting in higher maximum. Once the critical maximum concentration of H_2O_2 is reached, the free radicals interact more frequently with H_2O_2 resulting in decomposition until the critical minimum is reached when the formation process begins to dominate again.

The behavior of phenol as well as the nature of the catalyst ZnO is different at different pH which can influence the rate of reaction and the fate of H_2O_2 in photocatalytic systems. The phenomenon of oscillation is more pronounced in the acidic range compared to the alkaline pH with few exceptions as in other instances. In weakly acidic solution, or generally when the pH is less than the pKa of ~ 10 (at 25^0C), most of the phenol molecules remain un-dissociated. Hence maximum number of phenol molecules can be adsorbed onto the positively charged surface resulting in increased activation and subsequent degradation of phenol and correspondingly more H_2O_2. Hence the amount of H_2O_2 at the maximum of the oscillation curve is more. In the alkaline medium, especially above the PZC of ZnO, i.e. > 9, degradation of phenol is less for reasons explained earlier. The characteristics of ZnO and phenol in this pH range will also reduce the adsorption and consequent degradation of phenol and H_2O_2 formation.

The pH of the reaction medium has significant effect on the surface properties of semiconductor oxide particles, including the surface charge, size of the aggregation and the band edge position [7, 123, 124]. These can also affect the adsorption–desorption characteristics of the surface of the catalyst which in turn will influence the degradation of phenol and the formation/decomposition of H_2O_2. The pH effect on the photocatalytic

behavior of H_2O_2 in presence of phenol is further complicated by the different mechanisms by which degradation of phenol and generation of H_2O_2 take place at different pH.

The photocatalytic fate of externally added H_2O_2 in presence of ZnO and in the absence of any substrate at three typical pH, was investigated under identical conditions and the results are plotted in figure 3.14.

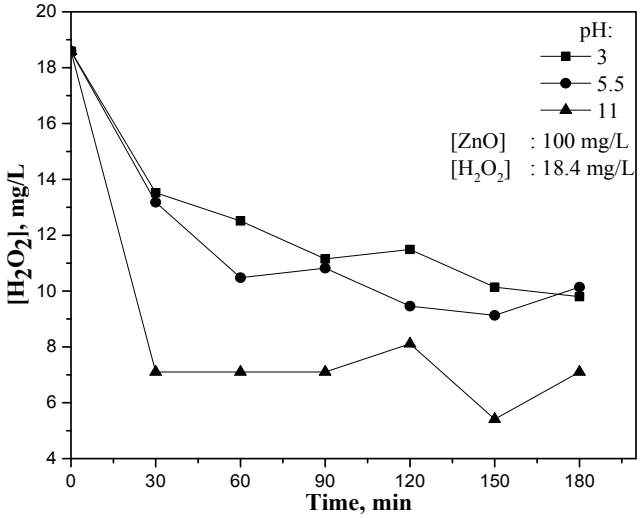

Fig. 3.14: Effect of pH on the oscillation in the concentration of H_2O_2 in the absence of phenol under photocatalysis

In this case, the concentration of H_2O_2 falls steeply at the beginning reaches a steady value and starts mild oscillation at all pH. The concentration of H_2O_2 is the least at the extreme alkaline pH=11 and the maximum at the acidic pH=3. Comparison of the results in the presence as well as in the absence of phenol shows that the oscillation is more significant in presence of phenol which in turn highlights the role of the substrate in determining the fate of H_2O_2.

3.3.5 Effect of particle size

Another important parameter to be considered in photocatalytic degradation process is surface morphology that includes particle size and agglomerate size of the catalyst. This is due to the direct relationship of the chemistry of the organic compounds and surface characteristics of the photocatalyst [125] with the rates of various processes. The influence of catalyst particles on the degradation of organic compounds in photocatalytic systems has been a subject of many studies earlier. In the current instance, the effect of particle size on the degradation of phenol is investigated in the range 6 to 60 μm. The phenol degradation is practically not affected in the range 6 to 40 μm. Beyond this range, the degradation decreases with increase in particle size (figure 3.15).

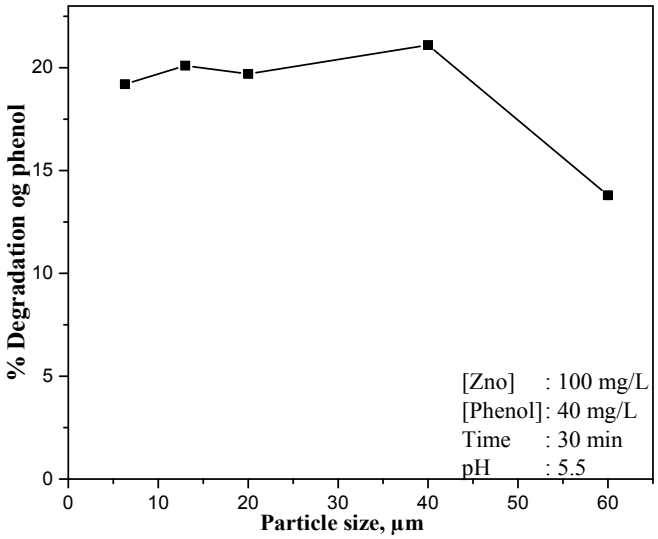

Fig. 3.15: Effect of particle size on the photocatalytic degradation of phenol

Augugliaro et al. [126] reported that there is no significant difference in the photo decomposition of H_2O_2 with or without suspended

catalyst. Jenny and Pichat [127] found that the heterogeneous photo decomposition of H_2O_2 is only twice faster than homogeneous photo decomposition. However, Ilisz et al. [128] observed that efficient photodecomposition of H_2O_2 takes place only in presence of catalysts and the initial rate of decomposition decreases with decreasing concentration of H_2O_2. The net initial rate of photocatalytic formation of H_2O_2 (after accounting for the concurrent decomposition) at different particle sizes of ZnO is shown in figure 3.16

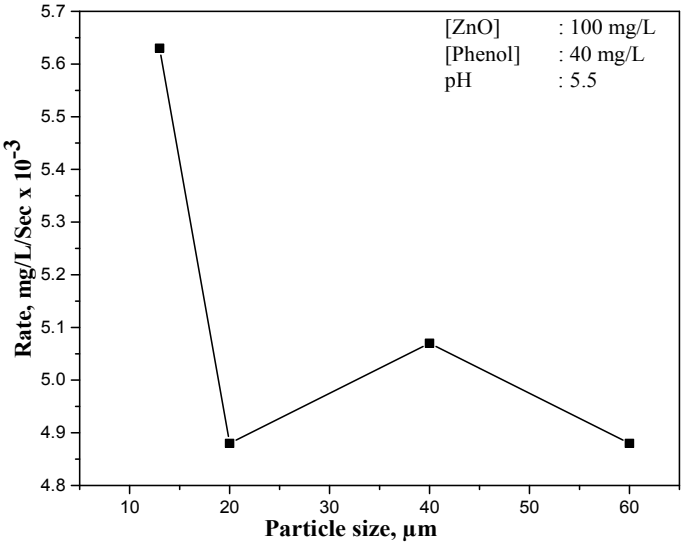

Fig. 3.16: Effect of particle size on the initial rate of H_2O_2 formation under photocatalysis

The initial rate of formation of H_2O_2 decreases steeply with particle size increase from 10 to 20 µm. The rate increases moderately when the particle size increases from 20 to 40 µm and then decreases as the particle size increases to 60 µm. In general, it may be concluded that the initial rate of formation of H_2O_2 is more or less steady when the particle size is in the range 20 to 60 µm.

As particle size of ZnO increases, the net concentration of H_2O_2 decreases at least in the initial stages. The oscillation in the concentration of H_2O_2 takes place irrespective of the size of the particles. At higher particle size, concentration of H_2O_2 becomes almost stabilized, (figure 3.17) i.e., the rates of formation and decomposition of H_2O_2 become comparable. However, any general conclusion regarding the effect of particle size on the maxima or minima in the oscillation curve is difficult due to the complexity of various free radical interactions, which can influence the formation and decomposition of H_2O_2 in a number of ways.

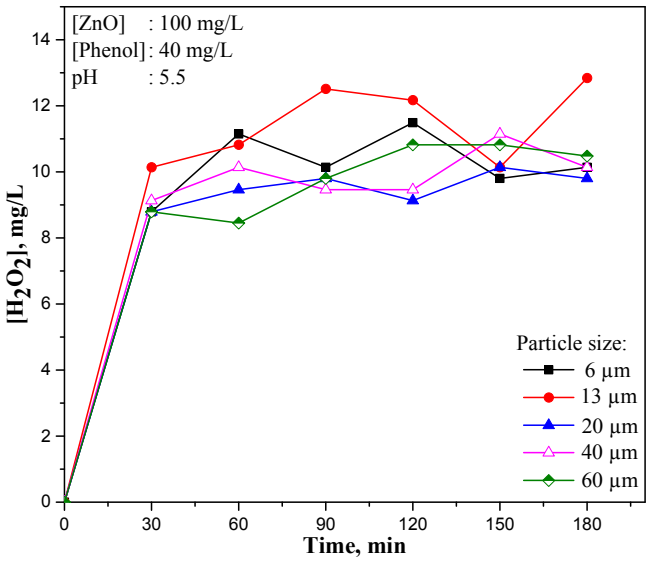

Fig. 3.17: Effect of particle size on the oscillation in the concentration of H_2O_2 under photocatalysis

3.3.6 Effect of concentration of substrate

The effect of concentration of phenol on its rate of degradation has been investigated and the results are shown in figure 3.18.

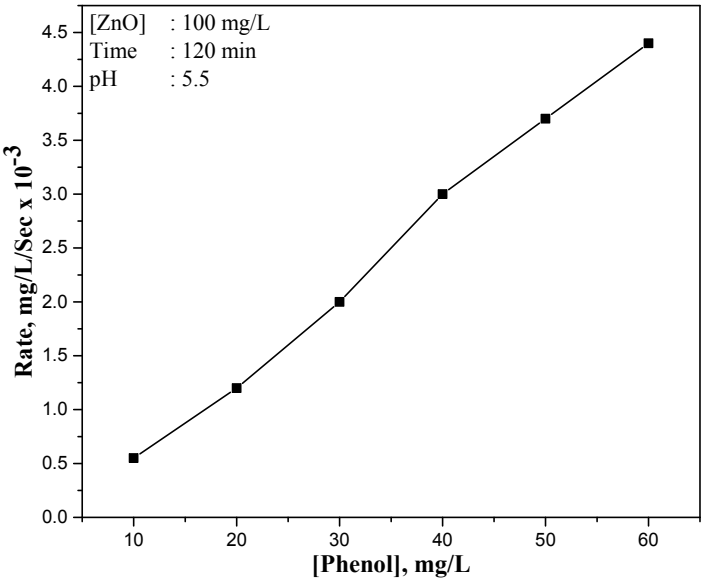

Fig. 3.18: Effect of concentration of phenol on its photocatalytic degradation rate

The rate of degradation increases with increase in the concentration of phenol in the range 10 to 60 mg/L studied here. With increase in concentration, more reactant molecules get adsorbed on to the catalyst sites, get activated and interact with correspondingly more $^{\bullet}OH$ radicals. This will continue until all the surface sites are occupied. Thereafter, increase in concentration cannot result in increased surface occupation and the phenol removal becomes more or less steady, independent of concentration. In the present instance the optimized catalyst dosage of 100 mg/L is sufficient to ensure adequate adsorption of phenol in the entire range of 10 to 60 mg/L as seen from the general uniform increase in rate. The reaction follows first order kinetics throughout. The plot of $-\ln [C/C_0]$ vs time in the concentration range 10 to 60 mg/L (figure 3.19) shows a linear dependence confirming first order kinetics.

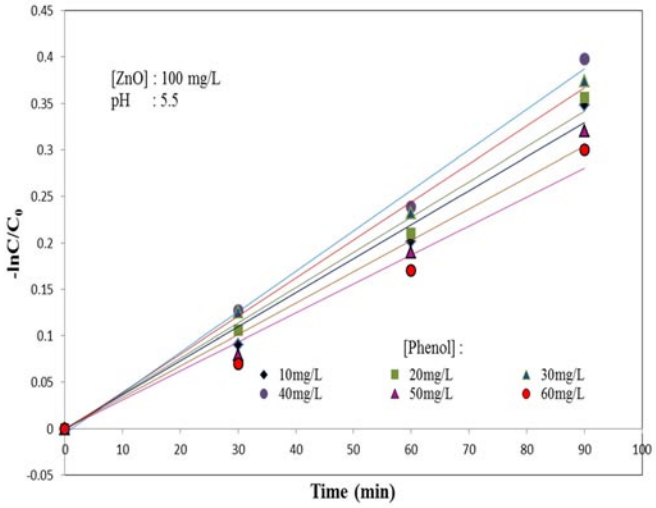

Fig. 3.19: Kinetics of ZnO mediated photocatalytic degradation of phenol

The effect of concentration of phenol on the oscillation in the concentration of H_2O_2 is shown in figure 3.20.

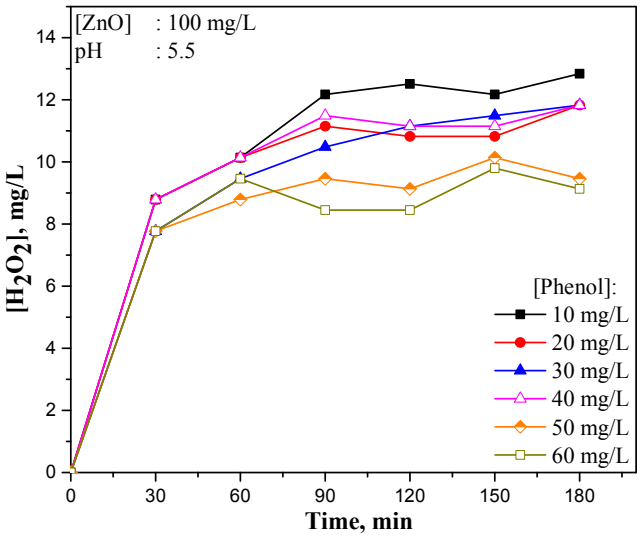

Fig. 3.20: Effect of concentration of phenol on the oscillation in the concentration of H_2O_2 under photocatalysis

The oscillation phenomenon is seen at all concentrations of phenol though the net concentration of H_2O_2 as well as the number and shape of crests and troughs vary. Eventually the concentration of H_2O_2 appears to be stabilizing at all concentrations. The net concentration of H_2O_2 decreases as the concentration of phenol increases from 10 to 60 mg/L, even though it should have been higher corresponding to the increased phenol degradation. This may be because, at higher concentration of phenol, the possibility of its interaction with the $^{\bullet}OH$ is more resulting in enhanced degradation. Consequently, the $^{\bullet}OH$ and $HO_2^{\bullet}$ radicals available for the formation of H_2O_2 by interaction between themselves as well as with other reactive species are relatively less. This results in lower net concentration of H_2O_2.

Another possibility for the formation of H_2O_2 can be the combination of hydroxyl radicals formed from water during the photocatalysis. However, in the absence of any organic substrate (phenol in the current case), the quantity of H_2O_2 formed is quite low compared to that in the presence of phenol. The effect of phenol on the quantity of H_2O_2 formed and on its formation-decomposition profile is shown in figure 3.21. Degradation of phenol leads to increased amounts of H_2O_2 in photocatalytic systems. However, there is no direct correlation between the concentration of H_2O_2 formed and that of phenol due to competitive interactions resulting in inconsistent amounts of H_2O_2.

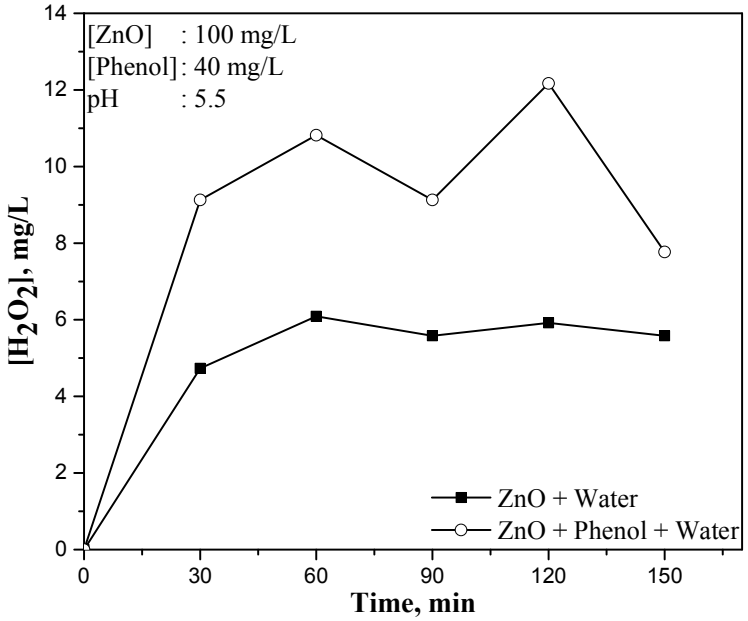

Fig. 3.21: Influence of presence of phenol on the net concentration of H_2O_2 in photocatalytic system

3.3.7 Effect of addition of phenol on the fate of H_2O_2 under photocatalysis

In order to confirm the role of phenol in the formation and fate of H_2O_2, phenol was introduced to the reaction system containing externally added H_2O_2. Initially there was only ZnO and H_2O_2 (14 mg/L) in the system. After 60 minutes of irradiation, which showed steep decrease in the concentration of H_2O_2, 40 mg/L phenol was introduced and the net concentration of H_2O_2 was analyzed. This experiment was done at three different pH (figure 3.22).

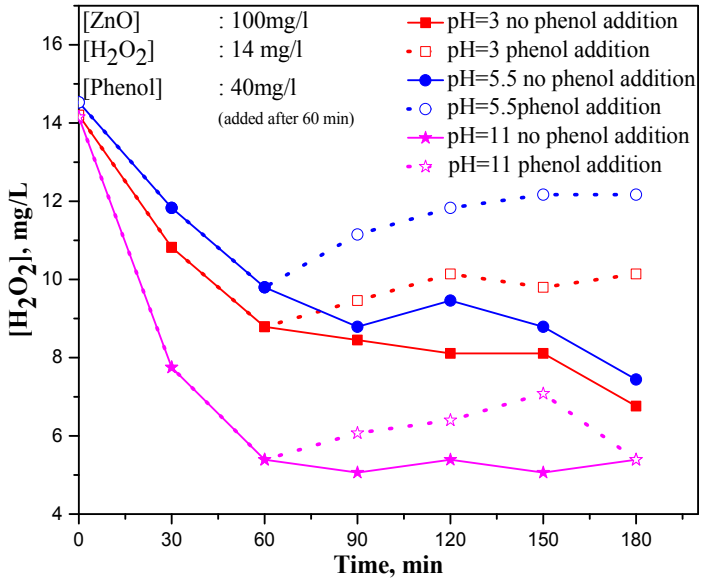

Fig. 3.22: Effect of addition of phenol (after 60 min) on the oscillation in the concentration of H_2O_2 under photocatalysis.

In all cases, addition of phenol results in enhanced formation of H_2O_2. This further reconfirms the role of substrate in the generation of H_2O_2. Hence, it is reasonable to assume that a major part of H_2O_2 present in the system is formed concurrently with the degradation of the pollutant though the minor contribution of $^{\bullet}OH$ radicals formed from water cannot be ruled out.

3.3.8 Effect of addition of extra ZnO during the course of the photocatalytic reaction on the oscillation

Effect of addition of extra amount of ZnO to the reaction system in which the H_2O_2 formation and/or decomposition have already been in progress at different pH is plotted in figures 3.23 to 3.25. Initially there was 50 mg/L of ZnO in the system and the insitu formed H_2O_2 was

analysed after 30 and 60 minutes of irradiation. After 60 minutes, the reaction suspension was divided into 2 portions. In the first case, UV irradiation continued without extra ZnO. In the second sample, extra ZnO (50 mg/L) was added and UV irradiation was continued. In both cases periodic analysis of H_2O_2 was continued upto 180 minutes. These experiments were done at 3 different pH (3, 5.5 and 11).

At pH ~ 3 (figure 3.23), when the UV irradiation continued without extra ZnO addition, H_2O_2 continued to increase with mild oscillation and stabilized thereafter. When extra ZnO was added and the irradiation was continued, H_2O_2 also increased as expected and the oscillation continued even more strongly with sharp crests and troughs.

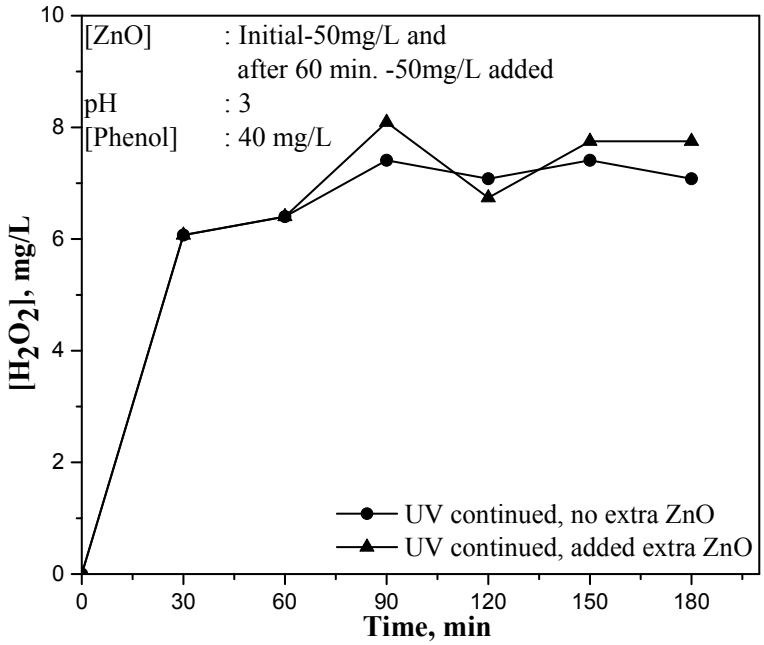

Fig. 3.23: Effect of addition of extra ZnO (after 60 min) on the oscillation in the concentration of H_2O_2 at pH=3 under photocatalysis

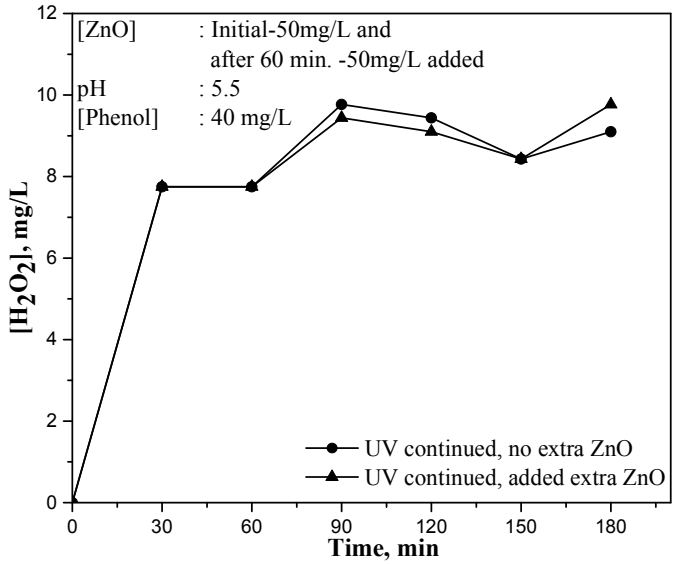

Fig. 3.24: Effect of addition of extra ZnO (after 60 min) on the oscillation in the concentration of H_2O_2 at pH=5.5 under photocatalysis

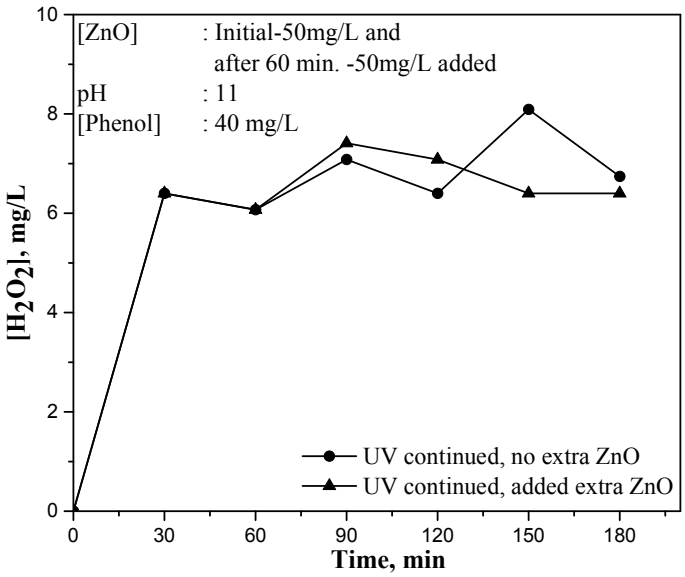

Fig. 3.25: Effect of addition of extra ZnO (after 60 min) on the oscillation in the concentration of H_2O_2 at pH= 11 under photocatalysis

At pH 5.5, when UV irradiation continued with and without extra ZnO, the H_2O_2 increased initially followed by mild oscillation (figure 3.24). The stabilized concentration of H_2O_2 is more or less same in both cases.

At pH ~ 11, when UV irradiation was continued without addition of extra ZnO, initially H_2O_2 increased and the oscillation continued vigorously (figure 3.25). However, addition of extra ZnO and continued UV radiation resulted in relatively lower increase in the net H_2O_2 concentration. The maximum in the oscillation curve was higher without extra addition of ZnO when the irradiation was continued.

Thus, it is seen that the effect of extra addition of ZnO on the oscillation in the concentration of H_2O_2 is dependent on the pH. This is understandable since pH influences the surface characteristics of ZnO, chemistry of phenol and subsequent interactions as explained earlier.

3.3.9 Effect of externally added H_2O_2

The effect of externally added H_2O_2 on the degradation of phenol as well as its own fate under photocatalytic conditions was experimentally verified. The results are shown in figure 3.26. As expected, the enhanced number of free radicals generated from the decomposition of added H_2O_2 results in enhanced phenol degradation.

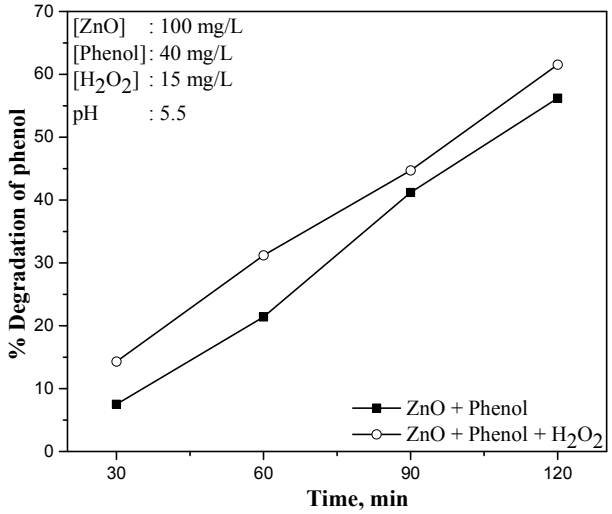

Fig. 3.26: Effect of added H_2O_2 on the photocatalytic degradation of phenol

However, corresponding increase in the concentration of H_2O_2 is not observed in the case of experiments with extra addition of H_2O_2 (figure 3.27).

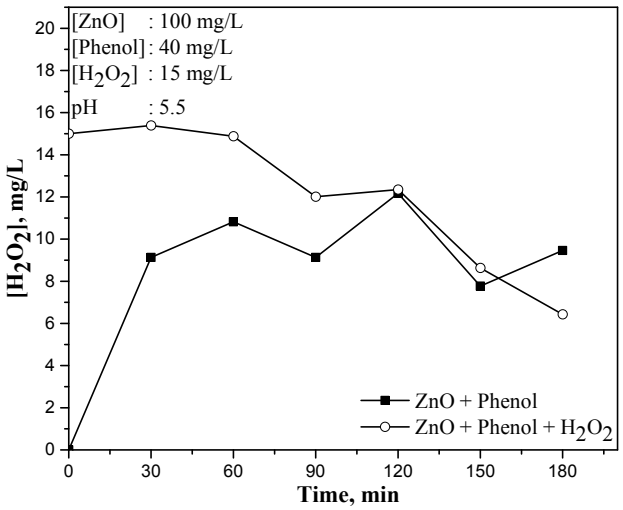

Fig. 3.27: Effect of added H_2O_2 on the net concentration of H_2O_2 under photocatalysis

In this case, the final net concentration (of H_2O_2) in the later stages of irradiation is not much different from the corresponding systems without

any added H_2O_2. Formation as well as decomposition of H_2O_2 is taking place in the system simultaneously and they compete with each other. The process is primarily concentration-dependent. At higher concentration of H_2O_2 (as in the case of external addition), the decomposition is dominant in the beginning. This may be the reason for initial drop in the net concentration of H_2O_2. Hence, in the case of externally added H_2O_2, once the more dominant decomposition has brought its concentration down to moderate level, the system behaves similar to that in which there is no externally added H_2O_2.

3.3.10 Effect of addition of H_2O_2 during the course of the photocatalytic reaction on the oscillation

Effect of 'in-between' addition of H_2O_2 after 60 minutes of reaction to the system at different pH (figure 3.28) also confirms the results in the above section.

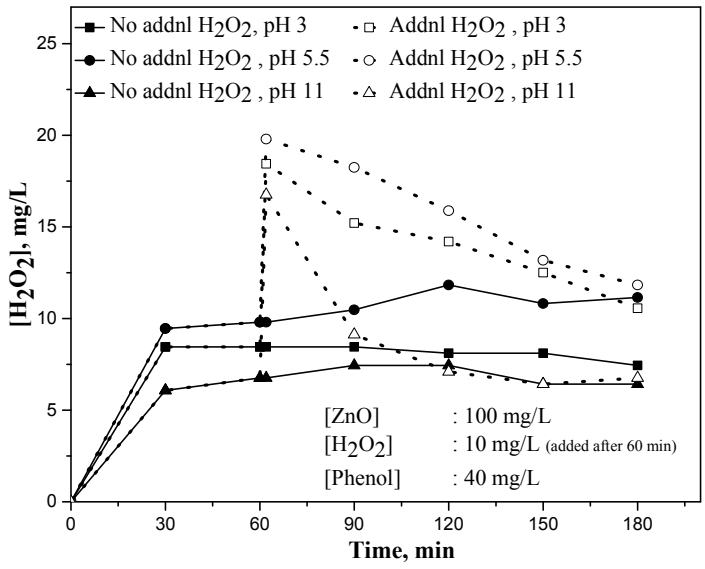

Fig. 3.28: Effect of addition of H_2O_2 (after 60 min) on the oscillation in its concentration under photocatalysis

The reaction system initially (upto 60 minutes) consisted of only insitu formed H_2O_2. After that, 10 mg/L of H_2O_2 was added extra. Fate of the total amount of H_2O_2 was analyzed at different pH.

As expected, the increased concentration of H_2O_2 in all three cases leads to domination of the decomposition process which continues for relatively longer time. At pH 3 and 5.5, the decomposition process is slow and the net concentration of H_2O_2 remains higher for longer time compared to the case with no externally added H_2O_2. The trend indicates that eventually the net concentration of H_2O_2 in the system, with or without 'in between' added H_2O_2, will be more or less the same. At pH 11, the externally added H_2O_2 decomposes faster initially, stabilizes and becomes indistinguishable from the system with no 'in between' added H_2O_2. Parallel decomposition of H_2O_2 into water and O_2 without generating reactive free radicals also makes the system with and without added H_2O_2 comparable as the reaction proceeds.

3.3.11 Role of O_2/air in photocatalysis

Oxygen plays an important role in photocatalytic degradation reactions in aqueous solutions by scavenging the electrons generated on photo activated ZnO and thereby inhibiting the recombination of electrons and holes. The electron is picked up by O_2 to generate superoxide radical anion and other reactive species. Thus both the electrons and holes will be available for the formation of free radicals and interaction with the pollutant. Hirakawa et al. [129] demonstrated the role of dissolved O_2 and superoxide ion in TiO_2 photocatalysis and even developed a method to follow photocatalytic reactions by measuring the consumption of dissolved

oxygen. In order to confirm the effect of O_2 on the photocatalytic degradation phenol, the reaction system is deaerated with N_2 and the experiments were carried out under otherwise identical conditions. The results are shown in figure 3.29.

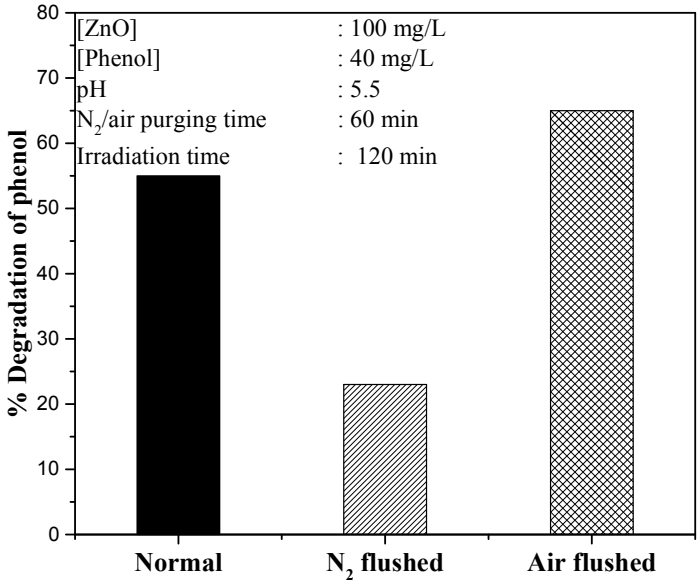

Fig. 3.29: Effect of O_2 on the photocatalytic degradation of phenol

The results showed that the photocatalytic degradation of phenol proceeds slowly in systems deaerated with N_2. When air is introduced into the system the degradation increases and even exceeds the degradation in the normal system, possibly due to the availability of more O_2. This confirms that O_2 plays an important role in the photocatalytic degradation of phenol. In order to test the role of O_2 in the formation/decomposition of H_2O_2 and the phenomenon of oscillation in the photocatalytic system experiments were carried out in the absence of O_2 by flushing the reaction system with N_2. The concentration of H_2O_2 generated is much less here (Figure 3.30).

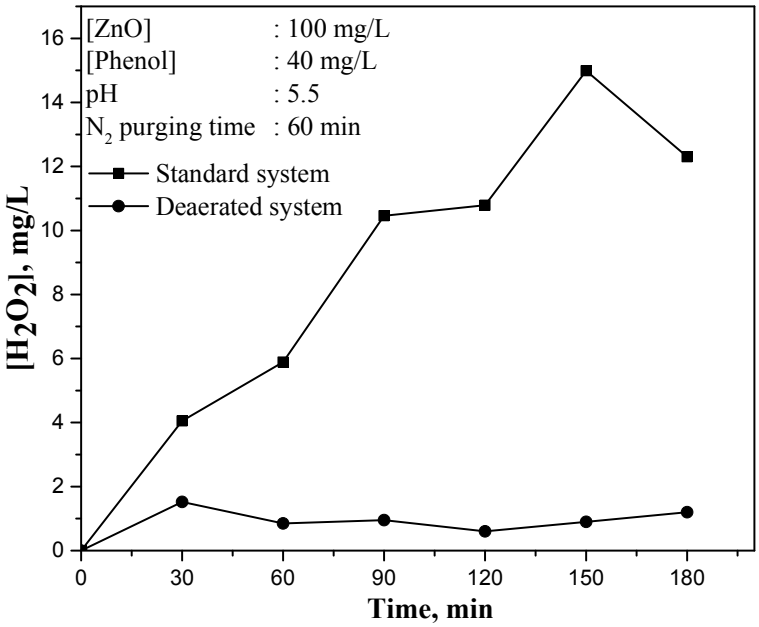

Fig. 3.30: Effect of deaeration with nitrogen on the oscillation in the concentration of H_2O_2 under photocatalysis

However, the phenomenon of oscillation is observed even in the deaerated systems, though with much reduced maxima and minima in the concentration of H_2O_2, suggesting that once H_2O_2 is formed by whatever mechanism, subsequent decomposition and formation can take place even in the absence or reduced concentration of O_2. H_2O_2 itself can act as an electron acceptor as follows:

$$H_2O_2 + e^- \rightarrow {}^{\bullet}OH + OH^- \quad \text{.....(69)}$$

H_2O_2 can also serve as a hole scavenger and decompose as in reaction (70).

$$H_2O_2 + {}^{\bullet}OH / h^+ \rightarrow HO_2^{\cdot} + H_2O/H^+ \quad \text{.....(70)}$$

Consequently, the decomposition of H_2O_2 would proceed in a unique way as H_2O_2 plays the dual role of electron and hole scavenger. The $HO_2^{\bullet}$ or $^{\bullet}OH$ thus generated may also react on the surface either to regenerate H_2O_2 or degrade or mineralize the pollutants.

3.3.12 Effect of recycling of catalyst

In order to scale up the photocatalytic process and eventual commercialization, recycling of the used catalyst is necessary. The reusability of ZnO used in the current study is tested as follows: ZnO is separated from the reaction system by simple centrifugation. It is then washed with distilled water, centrifuged again, air dried at room temperature (~ 30^0C) and then reused as such for the photocatalytic degradation of phenol. The results are presented in figure 3.31.

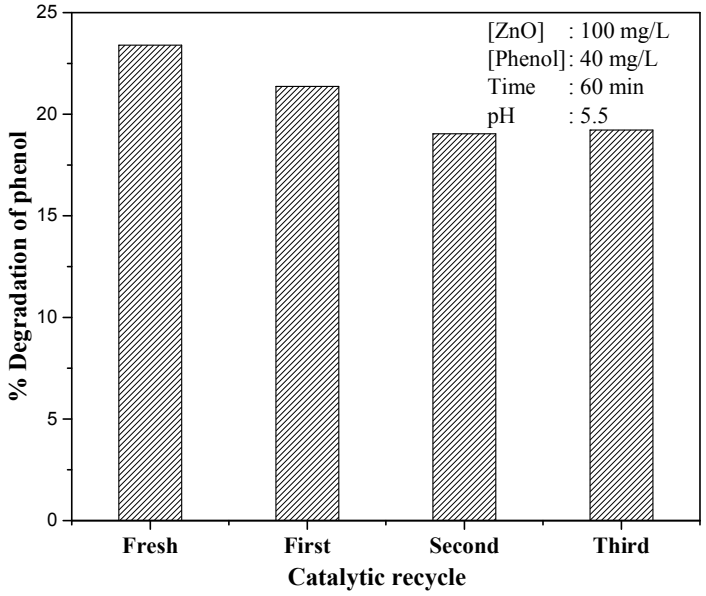

Fig. 3.31: Efficiency of recycled ZnO for the photocatalytic degradation of phenol

It is seen that the catalytic activity decreases slightly up to second recycle and then becomes steady. With increasing number of recycles at least some of the substrate and/or the intermediate molecules might be remaining strongly adsorbed or getting trapped in the cavities on ZnO, resulting in subsequent lower adsorption and hence decreased photocatalytic degradation. Formation of small amounts of photo-insensitive hydroxides (fouling) has also been reported on the surface of repeatedly used ZnO photocatalyst [130].

3.3.13 Corrosion of ZnO under photocatalysis

The possibility of corrosion under extreme acidic and alkaline conditions as well as photocorrosion, normally observed in the case of ZnO, was tested by weight loss method under the experimental conditions at different pH (figure 3.32). 50 mL of phenol solution (40 mg/L) was taken in different 250 mL beakers and the pH was adjusted as required. 1.0 g of ZnO was precisely weighed and added to each of these beakers and mixed well. The suspensions were kept for specific periods (1 hour and 4 hour). Thereafter the suspension in each beaker was centrifuged and the clear supernatant solution was transferred to dry previously weighed 250 mL beakers. The phenol solution in each beaker was evaporated. Once the evaporation is complete, weight of the dry beaker was determined. It was then dried again for 1 hour and weighed. The process was continued until the weight becomes constant. Same experiments were repeated under UV irradiation. The % corrosion of ZnO was calculated from the weight difference.

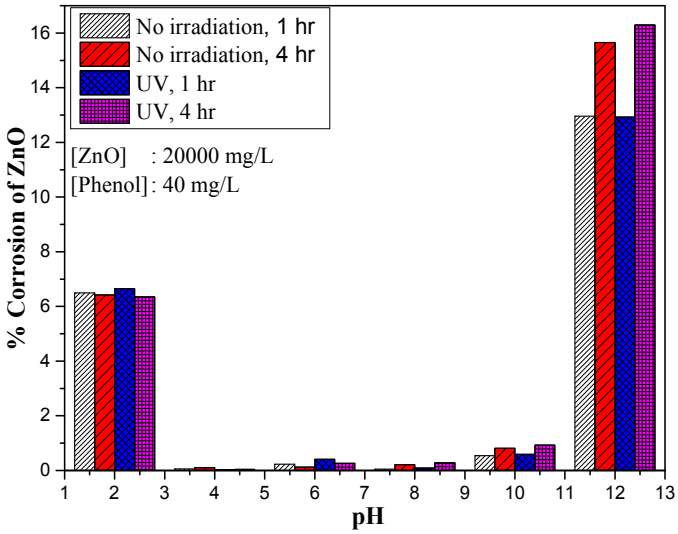

Fig. 3.32: Corrosion of ZnO at different pH in the presence and absence of UV irradiation

The corrosion is negligible in the pH range 4 to 10 with or without UV irradiation. The corrosion does not differ much after 1 hour or 4 hour irradiation at pH below 11. The corrosion is ~ 6% at pH 2 and ~ 15% at pH 12 after 4hour. Irradiation did not enhance the corrosion significantly, at least during the period of study. Since all major investigations reported in the present paper are carried out at the optimized pH of 5.5, corrosion can be considered negligible under the conditions of the study.

3.3.14 Memory effect

It has been reported that trapped electrons and holes on the surface of irradiated TiO_2 have an unusually long life time extending to hours after the irradiation source is put off [131]. The effect of this phenomenon, though not universally recognized, is examined in the case of ZnO catalyst by measuring the phenol degradation and H_2O_2 concentration after discontinuing the UV irradiation. It was observed that phenol degradation does not increase once

the irradiation source is cut off (figure 3.33). Hence, in this case, the memory effect is not strong enough to cause a major chemical reaction.

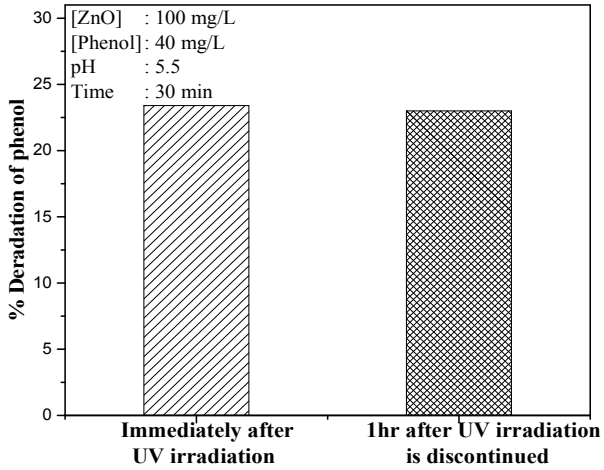

Fig. 3.33: Effect of discontinuing UV irradiation on the phenol degradation

But there is slight to moderate initial decrease in the concentration of H_2O_2 once the irradiation is discontinued, followed by stabilization (figure 3.34). The phenomenon of oscillation is also sustained for some time after the UV is cut off even though the crests and troughs are not as prominent as in the presence of UV light. Here, the free radicals which are formed even after the irradiation is put off, though at reduced rate, participate in various interactions resulting in both formation and decomposition of H_2O_2. The inconsistency in the phenomenon of oscillation is seen in the memory effect too as is evident from the nature of the oscillation curves when the irradiation is put off after different periods (30, 60, 90 minutes). Competitively these radicals interact less with phenol and more with themselves or H_2O_2. Hence, there is no phenol degradation, once the UV irradiation is discontinued.

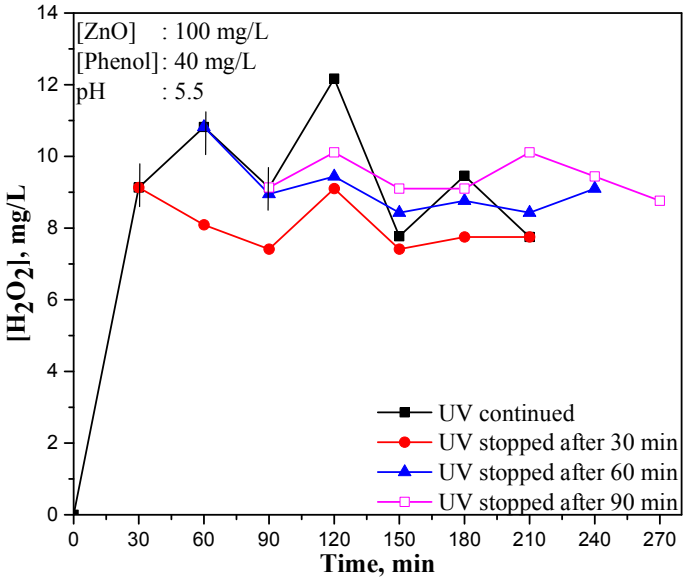

Fig. 3.34: Effect of discontinuing UV irradiation on the oscillation in the concentration of H_2O_2

The oscillation is not observed in experiments without illumination with or without the catalyst with externally added H_2O_2 at similar concentration. Irradiation in presence of catalyst is a prerequisite for the oscillation in the concentration of H_2O_2. Hence it is logical to assume that the variation in the concentration of H_2O_2 as above (when the irradiation is discontinued at different periods of time) is caused by the phenomenon of 'memory effect' in which the system can store some of the photocatalytic effects in 'memory'. The formation of the reactive free radicals and their interactions will continue, though at reduced rate, during this period. The duration of the post-irradiation activity in the dark is at least 90 minutes in the present case (figure 3.34). Hence it is not simply due to the lifetime of the radicals which is only few seconds. Similar memory effect has been reported earlier in the case of photocatalysis using ZnO and TiO_2 [130]. Although the efficiency of the dark process due to memory effect is not as

high as in the presence of illumination, the phenomenon needs in depth investigation because it has the potential for the decontamination of polluted water or other similar systems for longer duration even after the source of energy is turned off.

3.3.15 Mineralization process

Some of the intermediates formed during AOPs may be stable and hence their removal becomes difficult. In such cases the treatment may not be fully effective to make water reusable. The intermediates formed during AOPs also have to be degraded and eventually converted to harmless products such as CO_2, H_2O and salts. COD/TOC is the parameter which is used to evaluate the mineralization efficiency. In the present instance, the COD values are determined at various stages of reaction. The results are shown in figure 3.35.

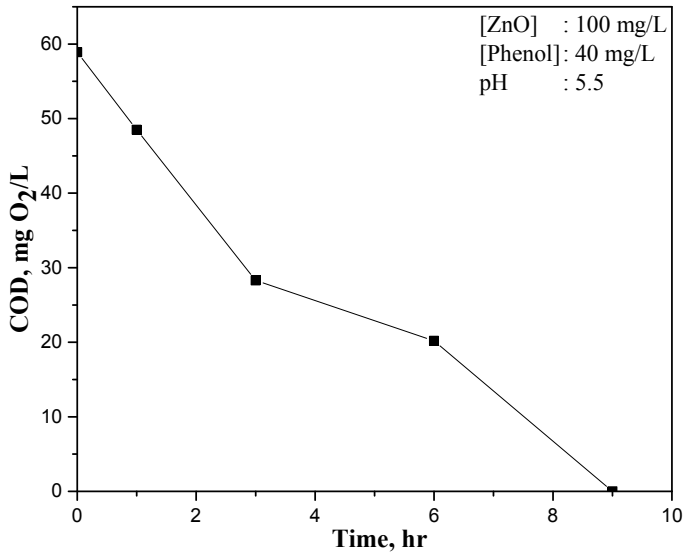

Fig. 3.35: COD of the reaction system after different periods of UV irradiation

Results show that complete mineralization of phenol takes place in 9 hour time. However, as seen in earlier results, the degradation of phenol is completed in much less time. This confirms that the mineralization of phenol proceeds through a number of intermediates which take longer time for further degradation and eventual mineralization. The reaction intermediates detected were catechol, hydroquinone and traces of benzoquinone. The concentration of the intermediates was comparatively small probably because they may be getting transformed into other products and eventually mineralized at the same rate or faster compared to parent phenol.

3.4 Mechanism of the process

In semiconductor mediated photocatalysis, when the semiconductor is irradiated with a source equal to or more of its band gap energy electron from the valence band gets promoted to the conduction band (e_{cb}^-) leaving a positively charged hole in the valence band (h_{vb}^+).

$$ZnO \rightarrow e_{cb}^- + h_{vb}^+ \quad \text{.....(71)}$$

The electrons are then free to migrate within the conduction band. The holes may be filled by migration of electrons from an adjacent molecule leaving that with a hole and the process can be repeated [5, 132]. The electrons and holes can recombine with no productive result or, they can give ROS such as $O_2^{-\bullet}$, $^\bullet OH$ and $HO_2^\bullet$ at the surface as follows:

$$O_2 + e_{cb}^- \rightarrow O_2^{-\bullet} \quad \text{.....(72)}$$

$$h_{vb}^+ + H_2O \rightarrow {}^\bullet OH + H^+ \quad \text{.....(73)}$$

$$O_2^{-\bullet} + H^+ \rightarrow HO_2^\bullet \quad \text{.....(74)}$$

The mechanism of semiconductor mediated photocatalytic degradation can be schematically presented as in figure 3.36.

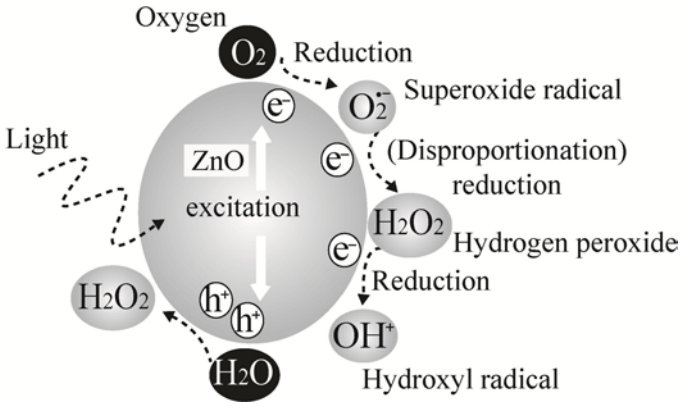

Fig. 3.36: Mechanism of semiconductor photocatalysis showing formation of ˙OH radicals and H_2O_2 [133]

3.4.1 Formation of ˙OH radicals

Formation of ˙OH radicals and other reactive oxygen species and their interaction with the substrate molecule is observed in semiconductor mediated photocatalytic degradation of organic contaminants in water [16, 21, 135-138]. In the current study also, the formation of ˙OH radicals on the surface of the UV irradiated ZnO is confirmed by the photoluminescence (PL) technique as explained earlier under section 3.2.4. Under UV irradiation ZnO–TPA system shows gradual increase in the PL intensity at 425 nm with time of irradiation, as shown in figure 3.37.

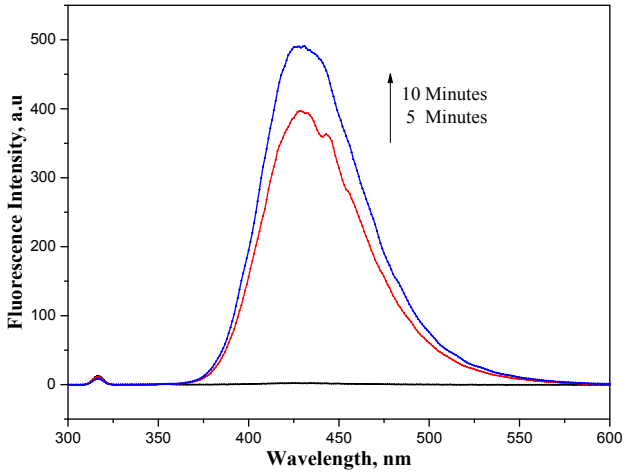

Fig. 3.37: PL spectral changes observed during the UV irradiation of ZnO with mixed solution of terephthalic acid and NaOH

This is attributed to the formation of HTPA (see section 3.2.4) by the interaction of $^{\bullet}OH$ radicals formed insitu on the surface of ZnO with TPA during UV irradiation. No PL was observed in the absence of UV and ZnO thereby confirming the role of these two components on the formation of reactive $^{\bullet}OH$ radicals. Earlier Sayed et al. [118] also demonstrated the formation of $^{\bullet}OH$ radicals on the surface of UV-illuminated TiO_2 films using this technique.

The free radicals $^{\bullet}OH$ and $HO_2^{\bullet}$ can give rise to H_2O_2 as in reactions (65) and (66). Further they can interact with phenol resulting in its degradation and eventual mineralization as in reaction (64). Since the amount of H_2O_2 generated in the absence of phenol is insignificant, it is reasonable to assume that the degradation of phenol and the formation of H_2O_2 are interrelated. However, the actual increase in the concentration of H_2O_2 after the initial period of ~ 30 minutes was less than expected compared to the degradation of phenol. After a while, the H_2O_2 levels off,

or shows periodic increase and decrease in concentration much before the degradation of phenol attains a plateau. The degradation of phenol continues even after the H_2O_2 has stabilized or the oscillation has set in. Since the concentration of H_2O_2 does not increase beyond a critical limit and its concentration is fluctuating periodically, it may be inferred that H_2O_2 formed is consumed insitu or is undergoing parallel decomposition into water and oxygen [119]. When the rate of formation and decomposition balances, the plateau is reached. When one process dominates the other cyclically, that results in oscillation. When the concentration reaches a particular maximum, the decomposition process will begin to dominate bringing its net concentration down. Similarly when the concentration reaches a critical minimum, the formation process will start dominating. This process happens many times over and hence an oscillatory pattern is obtained. H_2O_2 also participates in the degradation of phenol, which incidentally is another source of H_2O_2 generation. This also leads to stabilization or oscillation in the concentration of H_2O_2.

Formation of H_2O_2 from various ROS is shown below:

The primary step is the formation of electron and hole in the irradiated semiconductor oxide as is shown in reaction (71)

$$^{\bullet}OH + {}^{\bullet}OH \rightarrow H_2O_2 \quad \text{.....(75)}$$

$$O_2 + 2e_{cb}^- + 2H^+ \rightarrow H_2O_2 \quad \text{.....(76)}$$

$$2H_2O + 2h_{vb}^+ \rightarrow H_2O_2 + 2H^+ \quad \text{.....(77)}$$

$$O_2^{-\bullet} + H^+ \rightarrow HO_2^{\bullet} \quad \text{.....(78)}$$

$$HO_2^{\bullet} + HO_2^{\bullet} \rightarrow H_2O_2 + O_2 \quad \text{.....(79)}$$

$$O_2^{-\bullet} + HO_2^{\bullet} \rightarrow O_2 + HO_2^{\bullet-} \quad \text{.....(80)}$$

$$HO_2^{\bullet-} + H^+ \rightarrow H_2O_2 \quad \text{.....(81)}$$

Various steps involved in the decomposition of H_2O_2 may be presented as follows:

$$H_2O_2 + UV \rightarrow 2^{\bullet}OH \quad \text{.....(82)}$$

$$2h_{vb}^{+} + H_2O_2 \rightarrow O_2 + 2H^{+} \quad \text{.....(83)}$$

$$2e_{cb}^{-} + 2H^{+} + H_2O_2 \rightarrow 2H_2O \quad \text{.....(84)}$$

$$H_2O_2 + {}^{\bullet}OH \rightarrow H_2O + HO_2^{\bullet} \quad \text{.....(85)}$$

$$H_2O_2 + HO_2^{\bullet} \rightarrow H_2O + {}^{\bullet}OH + O_2 \quad \text{.....(86)}$$

$$H_2O_2 + O_2^{-\bullet} \rightarrow {}^{\bullet}OH + OH^{-} + O_2 \quad \text{.....(87)}$$

Thus, the same free radicals can contribute to the formation and decomposition of H_2O_2 depending on the conditions. At the same time, being a complex free radical system, other interactions leading to the formation and decomposition of H_2O_2 are also possible.

The ROS ($^{\bullet}OH$, $HO_2^{\bullet}$, H_2O_2, etc.) will interact with phenol on the surface of ZnO as well as in the bulk resulting in degradation and mineralization of the latter as shown in reaction (64).

Hoffmann et al. [16] and Kormann et al. [134] have shown that the quantum yield for H_2O_2 production during the oxidation of a variety of low molecular weight compounds has a Langmuir – Hinshelwood type dependence on O_2 partial pressure. By using ^{18}O isotope labeling experiments Hoffmann et al. [16] showed that all the O_2 in photochemically produced H_2O_2 arises from dioxygen reduction by conduction band electrons. No H_2O_2 is detected in the absence of O_2.

The empirical rate of formation of H_2O_2 by the heterogeneous photocatalytic surface reaction in presence of phenol may be expressed as [16]:

$$\frac{d[H_2O_2]}{dt} = \Phi_0 \frac{d[h\nu]_{abs}}{dt} = f(C_6H_5OH, O_2) = k_p \theta_{C6H5OH}.\theta_{O2} \quad .....(88)$$

where Φ_0 is the quantum yield for H_2O_2 production, k_p is the rate constant for H_2O_2 formation, θ_{C6H5OH} and θ_{O2} are the concentration of C_6H_5OH and O_2 adsorbed onto the surface respectively.

The rate of decomposition of H_2O_2 by reaction with holes may be expressed as:

$$-\frac{d[H_2O_2]}{dt} = \Phi_1[H_2O_2]\frac{d[h\nu]_{abs}}{dt} = f(C_6H_5OH, O_2, H_2O_2) \quad .....(89)$$

where Φ_1 is the quantum yield for peroxide decomposition at the illuminated surface.

Combining the equations (88) and (89), the empirical equation for the net formation of H_2O_2 can be expressed as

$$\frac{d[H_2O_2]}{dt} = (\Phi_0 - \Phi_1[H_2O_2]) \frac{d[h\nu]_{abs}}{dt} \quad .....(90)$$

During continuous irradiation by direct light a stationary state may be achieved which yields a simple steady state relationship valid for long irradiation times as follows:

$[H_2O_2]_{ss} = (\Phi_0 / \Phi_1)$ where ss refers to 'steady state' .....(91)

That is, the steady state concentration of H_2O_2 which is an intermediate as well as final product in the reaction as discussed in the foregoing sections is given by the ratio of intrinsic quantum yield for formation and decomposition of H_2O_2.

3.5 Conclusions

Semiconductor mediated photocatalysis is an environment friendly technology for the removal of trace amount of chemical pollutants from water. H_2O_2 formed during the photocatalytic degradation of phenol in water in presence of ZnO undergoes concurrent decomposition resulting in oscillation in its concentration. Various parameters such as catalyst loading, substrate concentration, particle size, pH, externally added H_2O_2, presence of air/O_2, etc. influence this unique phenomenon. The oscillation continues, though mildly, for some more time even after the energy source is switched off, indicating the presence of memory effect. A reaction mechanism based on the observations is proposed and discussed.

Chapter 4

INVESTIGATIONS ON THE SONOCATALYTIC DEGRADATION OF PHENOL AND THE FATE OF H_2O_2 FORMED INSITU

Contents

4.1 Introduction

Recently, sonocatalysis has been receiving special attention as an environment - friendly technology for the removal of hazardous organic pollutants from wastewater. However the degradation rate is slow compared to other established methods. Investigations aimed at enhancing the efficiency of ultrasound (US) promoted decontamination of water are in progress in many laboratories. These include using a variety of catalysts with different physico-chemical characteristics, modification of reactor design and reaction conditions, combining US with other AOP techniques, etc.

Basic principles of sonocatalysis were discussed already in Chapter 1. Ultrasonic irradiation results in the formation of light of a comparatively wide wavelength range of 200 to 500 nm. Light with wavelength below 375 nm can excite the semiconductor catalyst and generate highly active

•OH radicals on the surface. Thus the basic mechanism is partly that of photocatalysis. At the same time the more complex phenomenon of formation of hotspots upon implosion of some of the US irradiated bubbles on the catalyst surface also leads to the generation of electron-hole pairs and excess •OH radicals. Since the formation of electron-hole pairs is the first step in both photocatalysis and sonocatalysis, the efficiency of the process depends on the ability to prevent their recombination.

In liquids US produces cavitation which consists of nucleation, growth and collapse of bubbles. The collapse of the bubbles results in localized supercritical condition such as high temperature, pressure, electrical discharges and plasma effects. The temperature of the gaseous contents of a collapsing cavity can reach approximately 5500^0C and that of the liquid immediately surrounding the cavity reaches up to 2100^0C. The localized pressure is estimated to be around 500 atmospheres resulting in the formation of transient supercritical water. The cavities are thus capable of functioning like high energy micro reactors. The consequence of these extreme conditions is the cleavage of dissolved oxygen molecules and water molecules into radicals such as H•, •OH and O• which will react with each other as well as with H_2O and O_2 during the rapid cooling phase giving HO_2• and H_2O_2. In this highly reactive nuclear environment, organic pollutants can be decomposed and inorganic pollutants can be oxidized or reduced. This phenomenon is being explored in the emerging field of sonocatalysis for the removal of water pollutants.

Acoustic cavitation produces highly reactive primary radicals such as $^{\bullet}OH$ and $^{\bullet}H$ as in reaction (92). Recombination and a number of other reactions occur within the bubble as in reactions (93) to (97) following this primary radical generation

$$H_2O \overset{>>>}{\rightarrow} H^{\bullet} + {}^{\bullet}OH \quad \text{..... (92)}$$

$$^{\bullet}OH + H^{\bullet} \rightarrow H_2O \quad \text{..... (93)}$$

$$^{\bullet}OH + {}^{\bullet}OH \rightarrow H_2O_2 \quad \text{..... (94)}$$

$$H^{\bullet} + H_2O \rightarrow {}^{\bullet}OH + H_2 \quad \text{..... (95)}$$

$$H^{\bullet} + O_2 \rightarrow HO_2^{\bullet} \quad \text{..... (96)}$$

$$HO_2^{\bullet} + HO_2^{\bullet} \rightarrow H_2O_2 + O_2 \quad \text{..... (97)}$$

$^{\bullet}OH$ radical is a nonselective oxidant with a high redox potential (2.8 eV) which is able to oxidize most organic pollutants [139].

Similarly the photocatalytic reaction initiated by ultrasound induced sonoluminescence can be represented as follows [138]:

$$SC\ (Semiconductor) + h\upsilon \rightarrow h^+ + e^- \quad \text{..... (98)}$$

$$h^+ + e^- \rightarrow \text{Heat (Recombination)} \quad \text{..... (99)}$$

$$h^+ + OH^- \rightarrow {}^{\bullet}OH \quad \text{..... (100)}$$

$$h^+ + H_2O \rightarrow {}^{\bullet}OH + H^+ \quad \text{..... (101)}$$

Scavenging of conduction band electrons

$$e^- + O_2 \rightarrow O_2^{-\bullet} \quad \text{..... (102)}$$

Formation of multiple peroxide species

$H^+ + O_2^{-\bullet} \rightarrow HO_2^{\bullet}$ ..... (103)

$HO_2^{\bullet} + e^- + H^+ \rightarrow H_2O_2$ ..... (104)

Various reactive species produced as above react with phenol as in reaction (105) below

Phenol + Reactive oxygen species ($O_2^{-\bullet}$, $HO_2^{\bullet}$, $^{\bullet}OH$) →
Intermediates → $H_2O + CO_2$ ..... (105)

4.2 Experimental details

4.2.1 Materials used

The materials used, relevant details and their characteristics are the same as provided in Chapter 3 section 3.2.1.

4.2.2 Analytical procedures

Sampling and analysis were performed as explained in Chapter 3 section 3.2.2 to 3.2.4.

4.2.3 Sonocatalytic experimental set up

The experiments were performed using aqueous solutions of phenol of the desired concentration. Specified quantity of the catalyst was suspended in the phenol solution. Sonication provides adequate mixing of the suspension. Additional mechanical mixing did not make any notable consistent difference in the reaction rate. The ultrasonic bath (Equitron) was operated at a frequency of 53 kHz and a power of 100 W unless indicated otherwise. Water from the sonicator was continuously replaced by circulation from a thermostat maintained at the required

temperature, (29 ± 1°C). The position of the reactor in the ultrasonic bath was always kept the same. Typical reaction assembly is shown in figure 4.1.

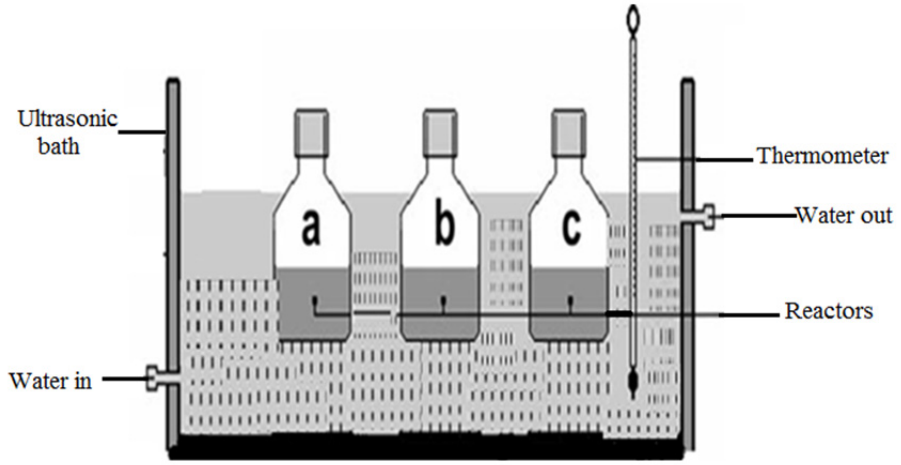

Fig. 4.1: Schematic diagram of the sonocatalytic experimental setup

4.3 Results and discussion

4.3.1 Preliminary results

Preliminary investigations on the sonocatalytic degradation of phenol using ZnO catalysts showed that no significant degradation took place in the absence of ultrasound or the catalyst suggesting that both catalyst and sound are essential to effect reasonable degradation. However, small quantity of phenol degraded under US irradiation even in the absence of catalysts (figure 4.2).

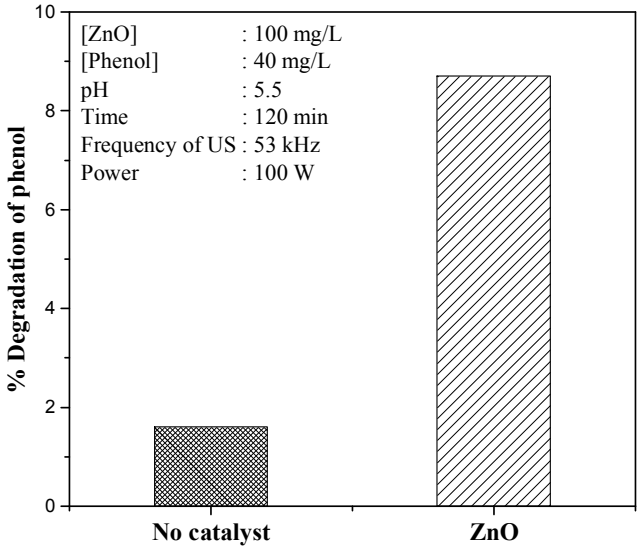

Fig. 4.2: Sonocatalytic degradation of phenol with and without ZnO

Sonolysis of water is known to produce free radicals H$^{\bullet}$ and $^{\bullet}$OH {via reaction (92)}, which are capable of attacking the organic compounds in solution [57]. When ZnO is irradiated by US, electrons get promoted from the valence band to the conduction band creating holes in the valence band. The OH^- ions that are adsorbed on the surface of the catalyst get oxidized to $^{\bullet}$OH radicals by the holes in the valence band. The electron in the conduction band is donated to oxygen generating superoxide radical anion $O_2^{-\bullet}$ which eventually gives rise to more reactive species such as $HO_2^{\bullet}$, $^{\bullet}$OH, H_2O_2, etc. as explained in Chapter 3. These species are involved in the mineralization reaction of phenol and formation of H_2O_2 as follows:

ROS ($^{\bullet}$OH, $HO_2^{\bullet}$ etc.) + phenol→ Intermediates + H_2O_2 →→ $H_2O_2 + H_2O + CO_2$ ..... (106)

$2\ ^{\bullet}OH \rightarrow H_2O_2$ ..... (107)

$HO_2^{\bullet} + HO_2^{\bullet} \rightarrow H_2O_2 + O_2$ ..... (108)

The fate of concurrently formed H_2O_2 during the sonocatalytic degradation of phenol in presence of ZnO is shown in figure 4.3

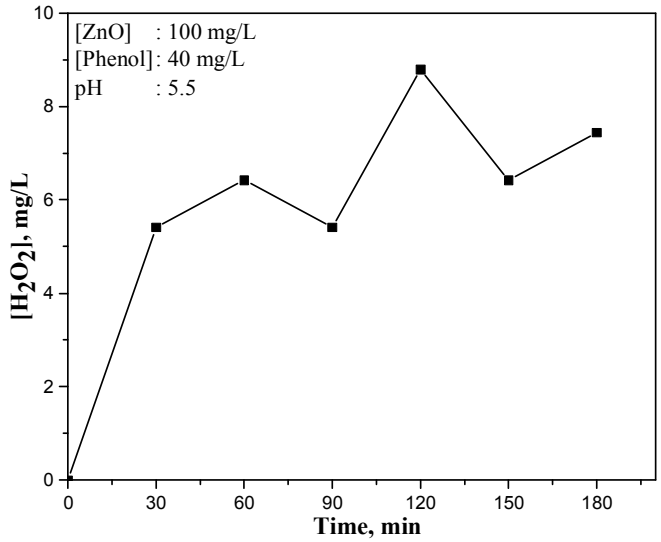

Fig. 4.3: Concentration of H_2O_2 during sonocatalytic degradation of phenol

The concentration of H_2O_2 increases and then decreases in a wave like fashion resulting in well-defined crests and troughs during the sonocatalytic degradation processes. Since H_2O_2 is an essential byproduct of phenol degradation its concentration was expected to increase and ultimately stabilize when the phenol degradation is complete. The oscillation in the concentration of H_2O_2 shows that it is generated/ decomposed/consumed simultaneously depending on the reaction conditions, in particular its concentration. When the concentration reaches a particular maximum, the decomposition dominates bringing its net concentration down. Similarly when the concentration reaches a critical minimum, the formation process gets precedence. This process happens many times over again and again.

Various parameters relevant for the efficiency of the sonocatalytic process are experimentally optimized and the results are as follows:

4.3.2 Effect of catalyst dosage

The sonocatalytic degradation of phenol in presence of ZnO at various loadings is shown in figure 4.4.

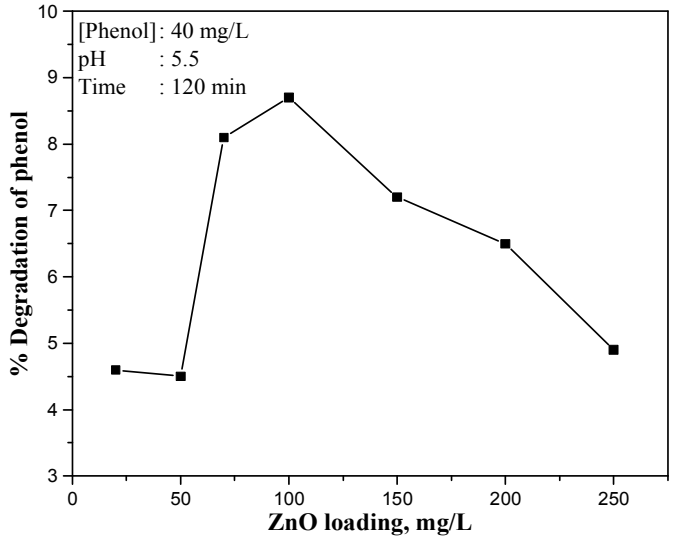

Fig. 4.4: Effect of catalyst loading on the sonocatalytic degradation of phenol

The degradation increases with increase in ZnO loading and reaches an optimum in the range of 75 to 100 mg/L. Beyond this optimum, the degradation remains more or less steady for a while and steeply decreases thereafter. The enhanced degradation efficiency with increase in the dosage is probably due to increased number of catalytic sites, higher production of $^{\bullet}OH$ radicals and more effective interaction with the substrate. It is known that the addition of particles of appropriate size in suitable amounts into the liquid system helps to break up the

microbubbles created by US into smaller ones and result in a rise in temperature of the irradiated liquid [6**].** Introduction of more catalyst particles into the solution provides more nucleation sites for cavitation bubbles at their surface. This will result in decrease in the cavitation thresholds responsible for the increase in the number of bubbles when the liquid is irradiated by US. The increase in the number of cavitation bubbles increases the pyrolysis of water and the sonocatalytic degradation of phenol. Any further increase in catalyst concentration beyond the optimum will only result in the particles coming too close to each other or aggregating thereby limiting the number of active sites on the surface. Higher concentration of the suspended particles may also disturb the transmission of ultrasound in water medium. Hence no further increase in the degradation of the pollutant is observed beyond the optimum dosage.

The fate of H_2O_2 formed under US at different ZnO loading is shown in figure 4.5. The concentration of H_2O_2 formed simultaneously with the degradation of phenol does not increase correspondingly and stabilizes or fluctuates as in photocatalysis due to concurrent formation and decomposition. Hence the optimum catalyst loading for phenol degradation need not necessarily hold good for optimum H_2O_2 at any point of time. The effect of catalyst loading on the concurrent formation and decomposition of H_2O_2 and the oscillation phenomenon is investigated and the results are presented in figure 4.5.

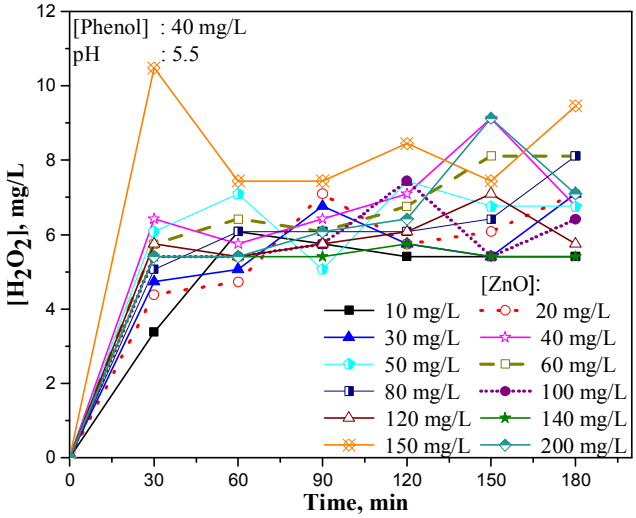

Fig. 4.5: Effect of catalyst loading on the oscillation in the concentration of H_2O_2 under sonocatalysis (*Also see Fig. 4.5.1 and 4.5.2*)

Due to complexity, the crowded figure 4.5 is further subdivided in to figure 4.5.1 and 4.5.2 for better clarity and understanding.

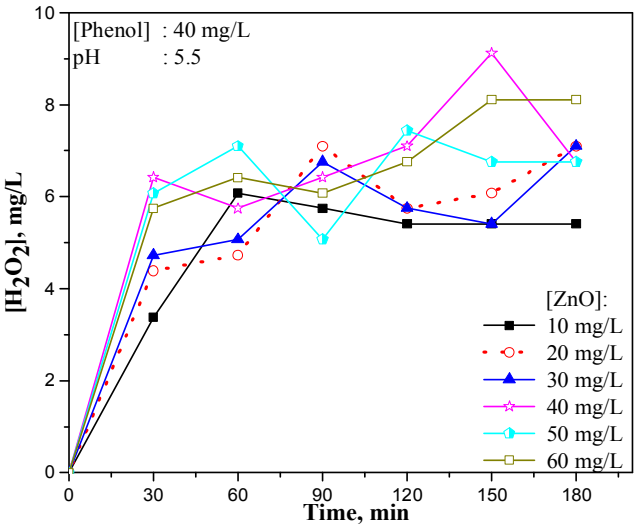

Fig. 4.5.1: Effect of catalyst loading (10 to 60 mg/L) on the oscillation in the concentration of H_2O_2 under sonocatalysis

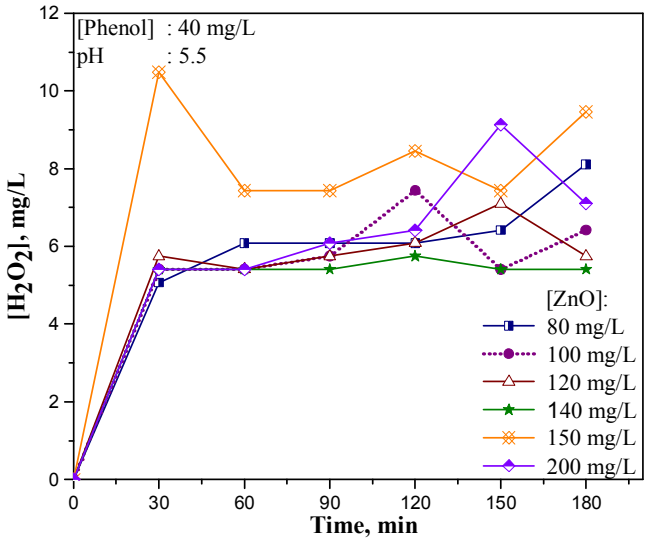

Fig. 4.5.2: Effect of catalyst loading (80 to 200 mg/L) on the oscillation in the concentration of H_2O_2 under sonocatalysis

The concentration of H_2O_2 at the maxima and minima in the oscillation curve as well as the number of maxima and minima do not follow any consistent pattern with respect to catalyst loading. Catalyst loading for highest maximum in the oscillation curve as well as highest net concentration of H_2O_2 is 150 mg/L. The lowest net concentration of H_2O_2 is not quite distinct for any specific catalyst dosage (except for one of the troughs in the oscillation curve at 50 mg/L of ZnO). The results show that there is no consistent correlation between the catalyst dosage and the amount of H_2O_2 or its oscillatory behavior. Since the formation and decomposition of H_2O_2 is occurring in parallel all the time, optimization of catalyst loading with respect to H_2O_2 concentration in the system may not be consistent or reliable. Hence the optimum loading of ZnO (100 mg/L) for phenol degradation is taken as the basis for further studies on the oscillation in the concentration of H_2O_2.

The net initial rate of formation of H_2O_2 before it reaches the first maximum in the oscillation curve may be a relatively more reliable parameter for comparison. The values are plotted in figure 4.6.

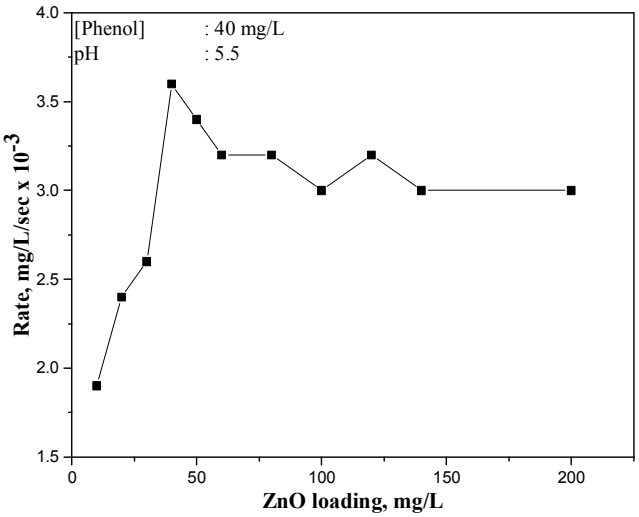

Fig. 4.6: Effect of catalyst loading on the net initial rate of formation of H_2O_2 under sonocatalysis

The rate increases initially with increase in catalyst loading up to 40 mg/L and decreases afterwards up to 100 mg/L. Later on the rate increases slightly and eventually stabilizes. This trend may be correlated at least partially with the rate of degradation of phenol, thereby confirming the role of substrate in the generation of free radicals which are precursors for H_2O_2 formation.

4.3.3 Effect of pH

The pH of the reaction medium is known to have strong influence on US or UV-induced degradation of organic pollutants. In photolysis, the effect as well as the site of bond breakage might be different at different

pH due to difference in the distribution of molecular charges. In sonocatalytic reaction, pH can alter the distribution of the pollutants in the bulk region, on the surface and at the site of the cavity collapse. The surface charge of semiconductors, the interfacial electron transfer and the photoredox processes occurring in their presence are also affected by pH. Sonocatalytic degradation of phenol at various pH is experimentally tested and shown in figure 4.7.

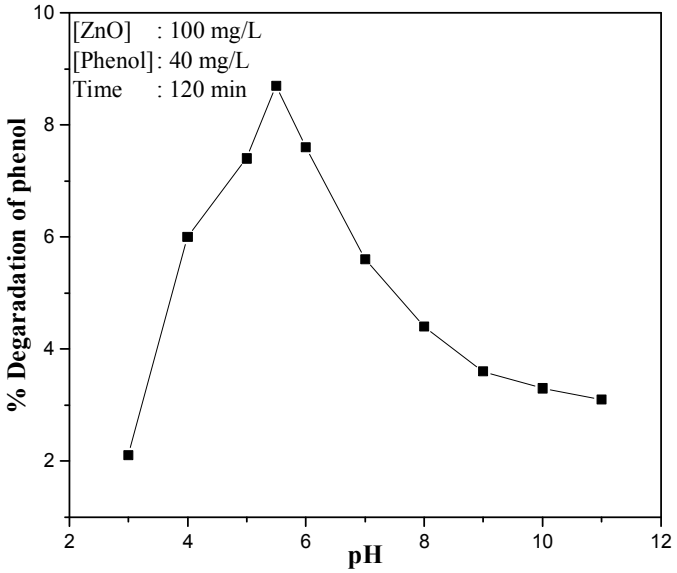

Fig. 4.7: Effect of pH on the sonocatalytic degradation of phenol

It is clear from the graph that maximum degradation is observed in the acidic pH range of 5 to 6, which peaks at pH 5.5.

Figure 4.8 shows the periodic variation in the concentration of insitu formed H_2O_2 in the system at different times and at different pH during the sonocatalytic degradation of phenol on ZnO.

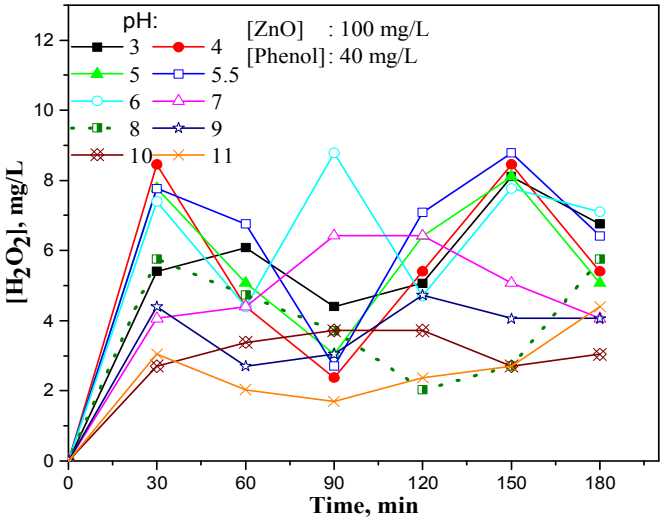

Fig. 4.8: Effect of pH on the oscillation in the concentration of insitu formed H_2O_2 under sonocatalysis

The oscillation as well as the maxima in the concentration of H_2O_2 is more pronounced in the acidic region 4 to 6. This is consistent with the observations on the sonocatalytic degradation of phenol on ZnO in which maximum degradation is observed at approximately same pH range. The relatively lower maxima and minima at pH 3 (compared to other values in the acidic range), as well as in the alkaline range of 9 to 11 is consistent with the degradation of phenol and probably because of the corrosion and dissolution of ZnO which reduces the effective surface sites for the formation of $^{\bullet}OH$ radicals and subsequent interactions. This was explained in Chapter 3 {reaction (67) and (68)}. As explained earlier, more phenol decomposition produces more free radicals which can lead to enhanced H_2O_2 concentration resulting in higher maximum in the oscillation curve. Once the critical maximum concentration of H_2O_2 is reached, the free radicals interact more frequently with H_2O_2 resulting in its decomposition until the critical minimum is reached when the formation process begins to

dominate again. The results show that the pH effect on the oscillation in the concentration of H_2O_2 under sonocatalysis is generally comparable with the results under photocatalysis.

The physical characteristics as well as the behavior of phenol and the catalyst ZnO are different at different pH which can influence the rate of reaction and the fate of H_2O_2 in sonocatalytic systems. As in the case of photocatalysis, here also the phenomenon of oscillation is more pronounced in the acidic range compared to the alkaline pH. Under alkaline conditions, during US irradiation, the phenolate ions are concentrated in the gas-water interface of the bubbles where the hydrophobicity is strong and cannot vaporize into the cavitation bubbles [90]. They can react only outside of the bubble film with the $^{\bullet}OH$ radicals cleaved from water. Hence degradation of phenol and oscillation in the concentration of H_2O_2 is less. However in the acidic range when phenol is in its molecular state, it enters the gas-water interface of bubbles and even vaporizes into cavitation bubbles. The molecules can react inside by thermal cleavage and outside with $^{\bullet}OH$ radicals. This results in higher degradation of phenol as well as enhanced formation and decomposition of H_2O_2. Hence the oscillation is quite significant in the acidic pH range.

As explained in Chapter 3, when the pH is less than the pKa of ~ 10, most of the phenol molecules will remain un-dissociated. Consequently phenol molecules can be adsorbed on or be in the close proximity of the positively charged surface resulting in increased interaction and degradation of phenol and correspondingly more H_2O_2. Hence the amount of H_2O_2 at the maximum of the oscillation curve is more. Above the PZC of ZnO, i.e. > 9, the catalyst surface is negatively charged. When the pH exceeds 10, ionic

species of phenol will be predominant and the phenolate species may get repelled away from the surface. This also leads to reduction in the adsorption and consequent decrease in degradation of phenol and H_2O_2 formation.

The pH of the reaction medium has been proven to have significant effect on the surface properties of semiconductor oxide particles such as the surface charge, size of the aggregation and the band edge position. Hence pH can affect the surface process including adsorption–desorption characteristics of the catalyst, surface initiated/promoted degradation of phenol and the formation/decomposition of H_2O_2. The mechanism of sonocatalytic degradation of phenol is different at different pH, which also complicates the pH effect on the fate of H_2O_2 in presence of phenol [7, 123, 124]. Serpone et al. [7] showed that the sonochemical degradation of phenol proceeds through different intermediates at different pH. The intermediates are (i) catechol (CC), hydroquinone (HQ) and p-benzoquinone (BQ) at pH 3, (ii) CC and HQ at pH 5.7 and (iii) no detectable intermediate at pH 12. Further, the sonication of HQ produces BQ while the sonication of BQ produces HQ and in both cases hydroxyl-p-benzoquinone is formed in traces as another intermediate. These intermediates themselves undergo sonolytic degradation, though by different mechanisms. Thus the system consists of too many constituents and variables which make it difficult to identify the influence of pH on the oscillation behavior of H_2O_2 precisely.

4.3.4 Effect of particle size

At the optimized loading for phenol degradation, the effect of particle size on the H_2O_2 formation is examined. The sonocatalytic rate of degradation of phenol is not influenced by the particle size variation (6 to 60 μm) as reported by Anju et al. [87]. This can be explained based on

the fact that US itself leads to decrease in particle size and enhanced surface area due to deaggregation [140]. The US also increases the mass transfer between the liquid phase and the catalyst surface [5], making the surface more readily available for reactants. Further, the US reduces the charge recombination and promotes the production of additional $^{\bullet}OH$ from the residual H_2O_2 [141].

$$ZnO\ (e^{-}) + H_2O_2 \rightarrow ZnO + {}^{\bullet}OH + {}^{-}OH \quad \text{..... (109)}$$

Consequent to these US effects, the negative impact of increasing particle size of the catalyst on the rate of degradation of phenol is compensated in sonocatalysis.

The effect of particle size of ZnO on the initial rate of formation of H_2O_2 is shown in figure 4.9.

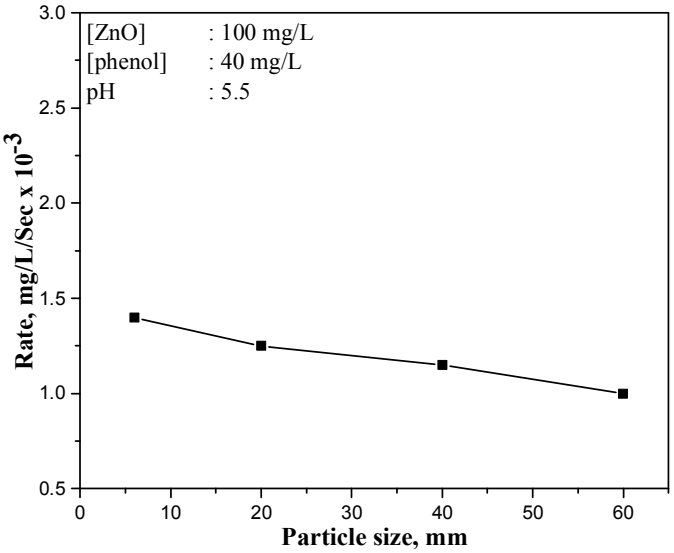

Fig. 4.9: Effect of particle size on the initial rate of H_2O_2 formation under sonocatalysis

With increase in particle size in the range of 6 to 60 µm, the initial rate of H_2O_2 formation decreases slightly from 1.4×10^{-3} to 1.1×10^{-3} mg/L/sec possibly due to lower surface area and decrease in the rate of generation of $^{\bullet}OH$ radicals. However, the nature of the oscillation curve as well as the successive maxima and minima of the curve remains qualitatively the same (figure 4.10) in all cases irrespective of the initial particle size of the catalyst. The average net concentration of H_2O_2 is the highest at the lowest particle size of 6 µm and the lowest at the highest particle size of 60 µm. However individual maxima or minima do not obey this general conclusion.

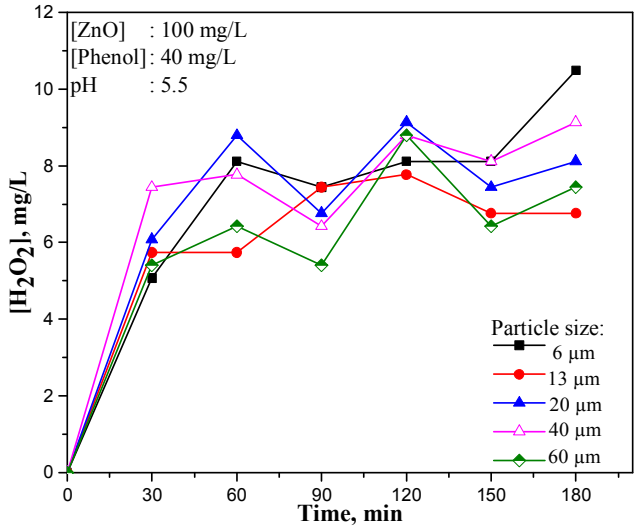

Fig. 4.10: Effect of particle size on the oscillation in the concentration of H_2O_2 under sonocatalysis

In order to see whether the effect of ZnO on the sonocatalytic degradation of phenol is simple particle effect or not, the experiments were conducted in presence of SiO_2 and Al_2O_3 particles individually in place of

ZnO, under identical condition. Simple SiO_2 or Al_2O_3 particles have very little effect on the sonochemical removal of phenol. This confirmed that it is not just the particle effect that promotes sonocatalytic degradation in the presence of semiconductor oxides such as ZnO, which act catalytically. Small amounts of H_2O_2 are formed in presence of SiO_2 and Al_2O_3 also probably due to suspended particles effect. However the H_2O_2 gets stabilized and does not undergo oscillation as vigorously as in the presence of ZnO. The initial concentration of sonochemically formed H_2O_2 in the presence of SiO_2, Al_2O_3 and ZnO in the order $SiO_2 > Al_2O_3 \geq ZnO$ (figure 4.11). This also indicates that in the presence of an active sonocatalyst like ZnO, the free radicals interact more with the activated phenol leading to its degradation and less with other free radicals to form H_2O_2. The concurrent decomposition of H_2O_2 in presence of ZnO also contributes to its lower concentration.

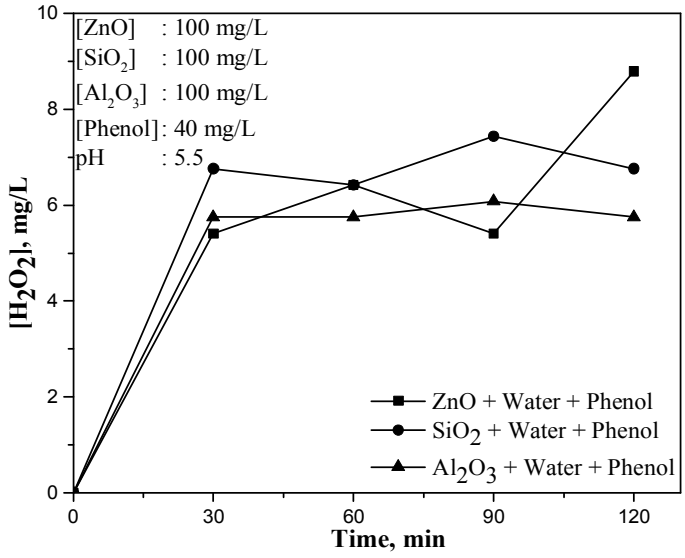

Fig. 4.11: Effect of various particles on the oscillation in the concentration of H_2O_2 under sonocatalysis

The relatively higher yield of H_2O_2 by sonolysis in presence of particles irrespective of their catalytic activity is explained by Keck et al. [143] as follows: The bubble size and collapse time are not influenced by the nature and concentrations of the particles used. But the shape of the bubbles may have changed from spherical to asymmetric. The larger surface of these asymmetric shaped bubbles will enable more radicals to escape into the bulk. This will result in the formation of more H_2O_2.

4.3.5 Effect of concentration of substrate

The effect of concentration of phenol on the rate of sonocatalytic degradation is shown in figure 4.12.

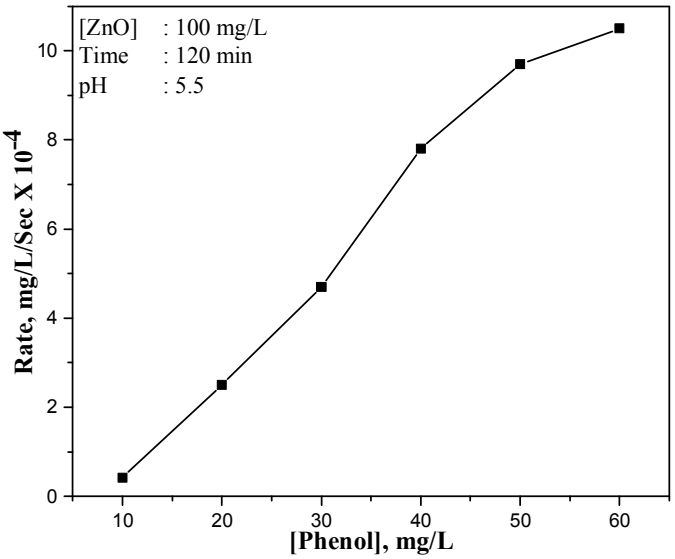

Fig. 4.12: Effect of concentration of phenol on its sonocatalytic degradation rate

The results indicate that the rate of phenol degradation increases with increase in the concentration of the substrate up to 50 mg/L beyond which it slows down, due to saturation of the catalyst surface as explained in the case of photocatalysis in Chapter 3. Kinetics of the degradation is determined from the plot of $-\ln[C/C_0]$ vs time in the concentration range of 10 to 40 mg/L (figure 4.13). The plot shows a linear dependence indicating pseudo first order kinetics. At higher concentration the kinetics changes to lower order and eventually zero order, as in the case of photocatalysis.

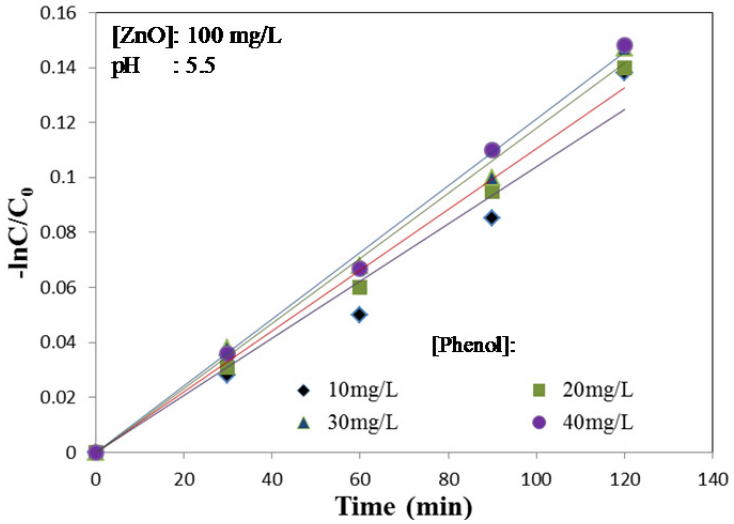

Fig. 4.13: Kinetics of ZnO mediated sonocatalytic degradation of phenol at lower concentrations

In the case of oscillation in the concentration of H_2O_2 the effect of concentration of substrate is shown in figure 4.14.

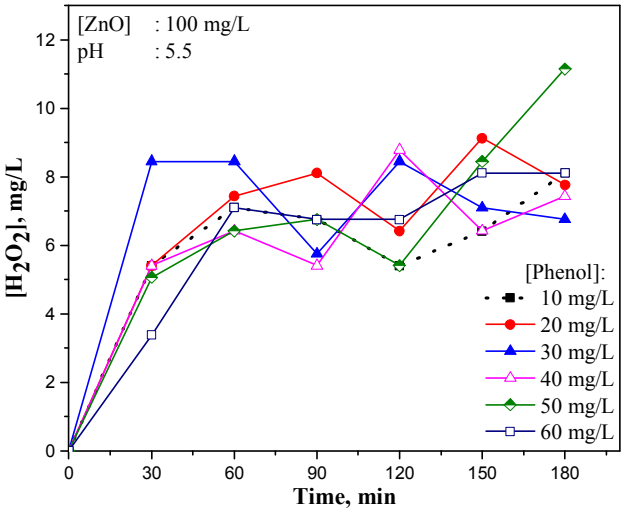

Fig. 4.14: Effect of concentration of phenol on the oscillation in the concentration of H_2O_2 under sonocatalysis

The number of maxima and minima in the oscillation curve increases and oscillation becomes steeper with increase in concentration of phenol except in the case of the lowest and highest concentration of 10 and 60 mg/L. The concentrations of H_2O_2 at the maxima of the oscillation curve are fairly the same in the case of phenol concentration in the range of 20 to 40 mg/L. However, the similarity is not strictly adhered to with respect to the minima in the oscillation curve. When phenol concentration is increased from 10 to 40 mg/L, the rate of its degradation also increases steeply. Similar increase is not seen in the case of H_2O_2 either in terms of the maxima or minima of the oscillation curve or the net concentration of H_2O_2. Thus there is clear lack of quantitative correlation between the degradation of phenol and the corresponding H_2O_2 generated insitu. At higher phenol concentrations, more number of reactive free radicals is generated and they in turn interact with phenol resulting in enhanced

degradation. Consequently the number of reactive free radicals available for the formation of H_2O_2 is less. Hence, the net concentration of H_2O_2 is not increasing corresponding to the higher degradation of phenol. The complexity of the multitude of free radical interactions, affects the consistency of the formation and decomposition of H_2O_2, possibly more than other reactions. This results in the oscillation and the unpredictable concentration of H_2O_2.

4.3.6 Role of phenol on the sonocatalytic fate of H_2O_2

In the case of US irradiation, H_2O_2 is produced even in the absence of phenol indicating the formation of free radicals $^{\bullet}OH$ and $HO_2^{\bullet}$ in liquid water (figure 4.15).

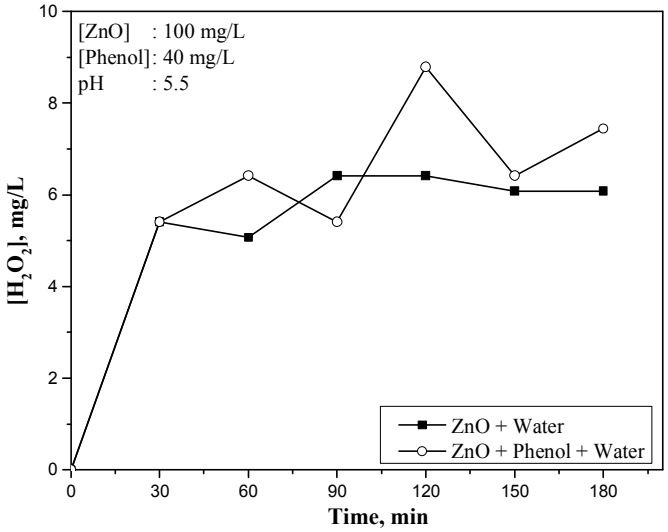

Fig. 4.15: Influence of presence of phenol on the net concentration of H_2O_2 in sonocatalytic system

From the figure it is clear that the concentration of H_2O_2 is more in presence of phenol. When phenol is present in system, some of the $^{\bullet}OH$

radicals may react with it before they could recombine to produce H_2O_2. At the same time, the degradation of phenol produces H_2O_2. Also the H_2O_2 may be decomposing producing more free radicals which also interact with and degrade phenol. Thus H_2O_2 and $^{\bullet}OH$ play multiple roles and take part in a multitude of interactions.

The sonocatalytic decomposition of H_2O_2 was investigated (in the absence of phenol) under identical conditions at different pH (figure 4.16).

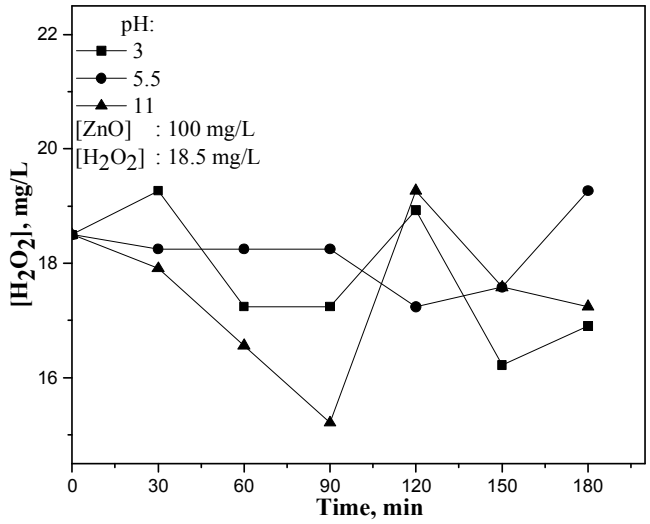

Fig. 4.16: Sonocatalytic fate of H_2O_2 at different pH in the absence of phenol

In this case also the concurrent formation and decomposition of H_2O_2 is observed at all pH. The concentration of H_2O_2 remains stable in the beginning at pH 5.5 and mild oscillation occurs thereafter. At extreme acidic as well as alkaline pH, where the surface processes become more complex, oscillation in the concentration of H_2O_2 occurs more intensely.

Comparison of the fate of added H_2O_2 in the presence as well as the absence of phenol at pH 5.5 shows that the oscillation is more significant in presence of phenol (figure 4.17).

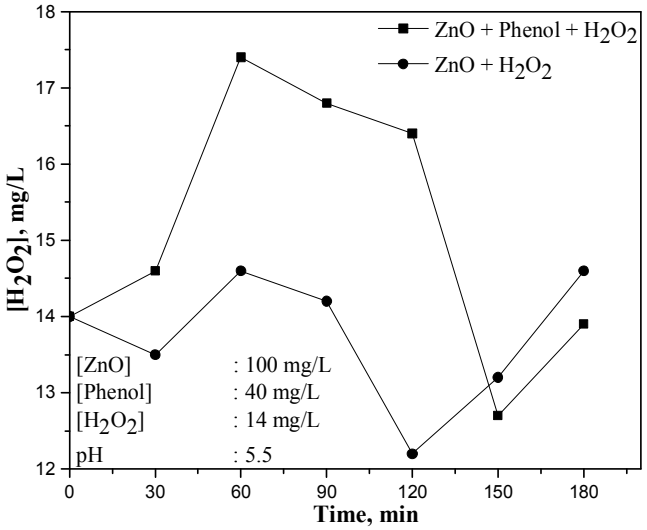

Fig. 4.17: Fate of H_2O_2 in the presence as well as absence of phenol under sonocatalysis

The net concentration of H_2O_2 is high in presence of phenol. The degradation of phenol generates more free radicals and at least some of them will be recombining or participating in interactions leading to the formation of more H_2O_2. This is further verified as follows by adding phenol to the H_2O_2/ZnO/US system in between the reaction and measuring the concentration of H_2O_2

4.3.7 Effect of addition of phenol on the fate of H_2O_2 during sonication

In order to further verify the effect of phenol on the oscillation in the concentration of H_2O_2 in detail, phenol is added to ZnO/H_2O_2 system after 60 minutes of irradiation under standard reaction conditions. Three

typical pH conditions (3, 5.5 and 11) were chosen for the study. The results are shown in figure 4.18.

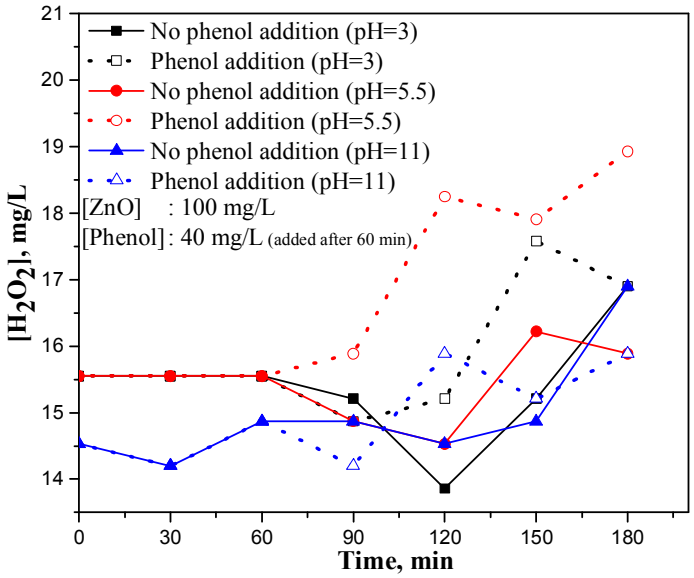

Fig. 4.18: Effect of addition of phenol (after 60 min) on the oscillation in the concentration of H_2O_2 under sonocatalysis

At pH 5.5 where the degradation of phenol is maximum, the H_2O_2 formation is accelerated by phenol addition. At pH 11 addition of phenol reduces the H_2O_2 concentration initially, followed by increase and oscillation thereafter. At pH 3 the H_2O_2 concentration decreases initially when phenol is added to the system. Shortly thereafter the trend becomes fairly similar to that at pH 5.5. As expected, at pH 3 and 11 the net amount of H_2O_2 at any point of time is less compared to than at pH 5.5, due to the lower rate of degradation of phenol. In general, the nature of the H_2O_2 curve remains similar at acidic pH of 3 and 5.5 even though the net amount remains different.

4.3.8 Effect of externally added H_2O_2

The effect of externally added H_2O_2 on the sonocatalytic degradation of phenol and the oscillation in the concentration of H_2O_2 is studied and the results are shown in figure 4.19 and 4.20.

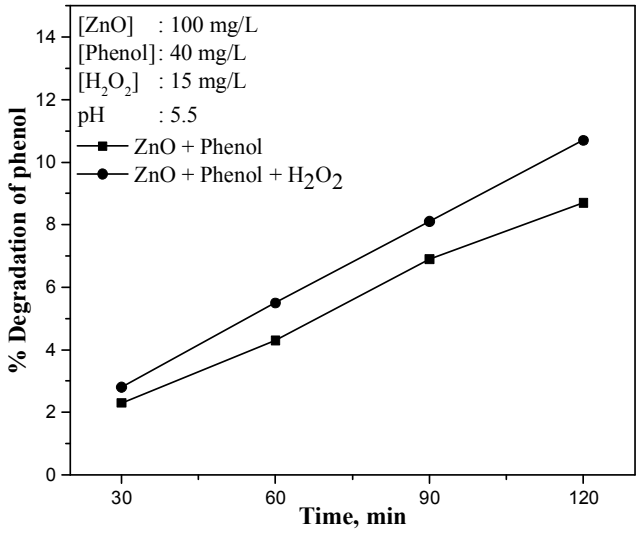

Fig. 4.19: Effect of added H_2O_2 on the sonocatalytic degradation of phenol

In the beginning, added H_2O_2 decomposes faster producing more $^{\bullet}OH$ radicals which can accelerate the degradation of phenol. However, the decomposition of H_2O_2 to water and oxygen also occurs in parallel which restricts the continued availability of the oxidizing species at the same rate for phenol degradation. At the same time, the H_2O_2 formed insitu will be compensating at least partially for the H_2O_2 decomposition. The net effect is the relatively higher availability of H_2O_2 throughout and the continued higher rate of degradation of phenol.

However, corresponding to the enhanced degradation of phenol in the presence of externally added H_2O_2, the net concentration of H_2O_2 does not increase in the beginning. It remains steady for a while, then increases for a short period and starts oscillating thereafter (figure 4.20) confirming concurrent formation and decomposition. In the absence of externally added H_2O_2, the net concentration of insitu formed H_2O_2 will continue to increase until sufficient concentration is built up. At that point, the decomposition will start dominating. Thereafter formation and decomposition process occurs simultaneously and the oscillation continues, as expected.

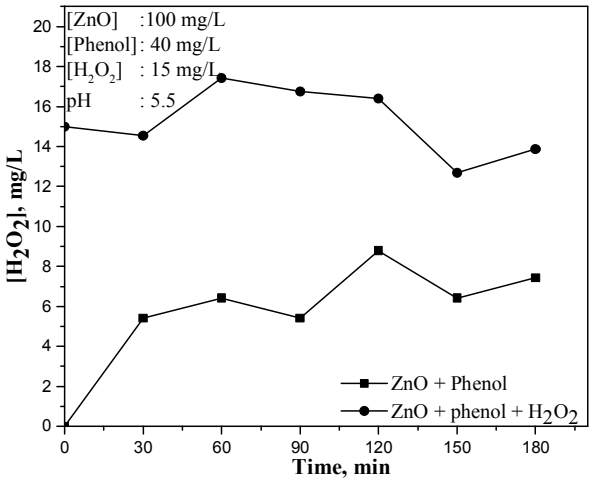

Fig. 4.20: Effect of added H_2O_2 on the net concentration of H_2O_2 under sonocatalysis

4.3.9 Effect of addition of H_2O_2 during the course of the sonocatalytic reaction on the oscillation

The effect of H_2O_2 addition to the phenol/ZnO/US system during the course of the reaction on the oscillation at pH 3, 5.5 and 11 is shown in figure 4.21.

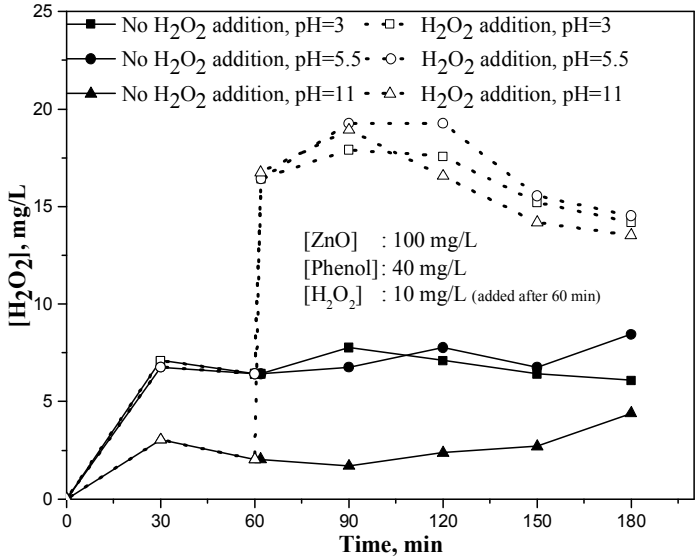

Fig. 4.21: Effect of addition of H_2O_2 (after 60 min) on the oscillation in its concentration of H_2O_2 under sonocatalysis

Here the concentration of H_2O_2 as well as the nature of the oscillation does not vary significantly at pH 3 and 5.5. As expected the concentration of H_2O_2 is less at pH 11. The higher H_2O_2 concentration after the external addition remains steady for a while and decreases thereafter. The trend is same at all pH, possibly because, addition of H_2O_2 together with the insitu formed quantity will make the system over-saturated and it is difficult to distinguish the relatively smaller increase or decrease in the total concentration. Hence the oscillation appears weak. This confirms that there is a critical range of H_2O_2 concentration above which the oscillation is weak possibly due to the balancing of formation and decomposition process.

4.3.10 Effect of addition of extra ZnO during the course of the sonocatalytic reaction on the oscillation

Since the 'in-between' addition of two major components of the reaction system, i.e., phenol and H_2O_2 is found to influence the phenomenon of oscillation in varying degrees, the effect of the third component, i.e., ZnO also is tested and the results are as follows:

Figure 4.22 to 4.24 shows the effect of addition of extra ZnO to the sonocatalytic system in which the H_2O_2 formation and/or decomposition has already been in progress at different pH, 3, 5.5 and 11. As expected, the extra addition of ZnO enhances the rate of formation of $^{\bullet}OH$ radical and hence of H_2O_2.

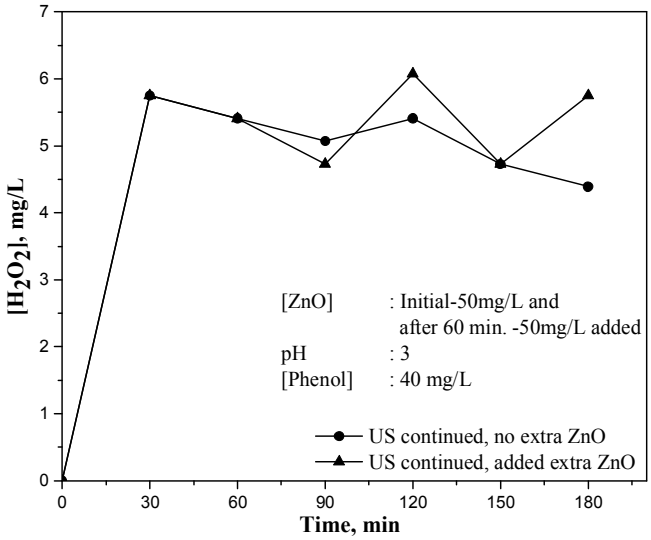

Fig. 4.22: Effect of addition of extra ZnO (after 60 min) on the oscillation in the concentration of H_2O_2 at pH= 3 under sonocatalysis

At pH 3 (figure 4.22), when the US irradiation of the system is continued as such with no extra ZnO, the net concentration of H_2O_2 is almost stable indicating that the rate of formation and decomposition are almost balanced. This continues upto 120 minutes and thereafter the concentration of H_2O_2 decreases, possibly due to domination of the decomposition process. When US irradiation continues and extra ZnO was added to the system after 60 minutes, formation and decomposition of H_2O_2 takes place more vigorously and the oscillation in the concentration of H_2O_2 becomes sharper with clear maxima and minima.

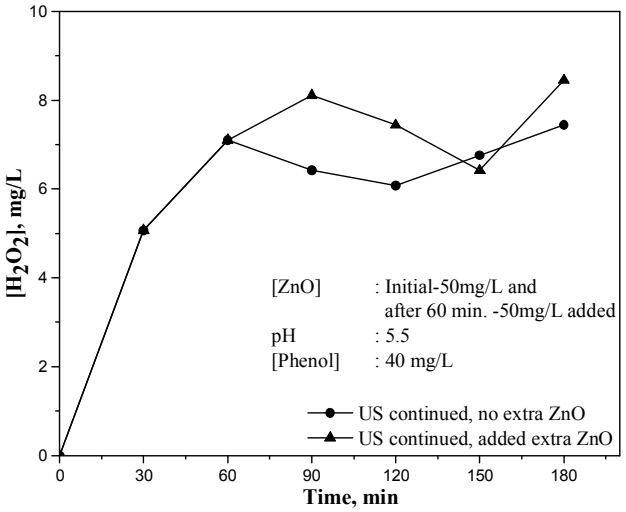

Fig. 4.23: Effect of addition of extra ZnO (after 60 min) on the oscillation in the concentration of H_2O_2 at pH= 5.5 under sonocatalysis

At pH 5.5 (figure 4.23) when the US irradiation of the system is continued as such, H_2O_2 decomposition dominates slightly upto 120 minutes and the concentration shows slight decrease. Thereafter the formation of H_2O_2 dominates, though slowly. But when US irradiation is

continued with extra ZnO, the formation of H_2O_2 is enhanced. The trend continues upto 90 minutes followed by a mild decrease. Towards later stages, at 150 minutes, the formation process dominates possibly due to assistance from extra ZnO.

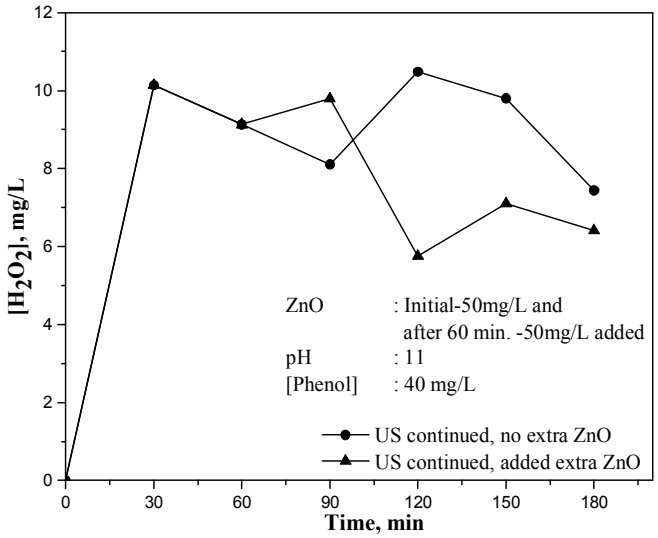

Fig. 4.24: Effect of addition of extra ZnO (after 60 min) on the oscillation in the concentration of H_2O_2 at pH= 11 under sonocatalysis

At pH 11(figure 4.24) when the US irradiation of the system is continued, oscillation of H_2O_2 occurs as usual with clear maxima and minima. As expected the effect of extra ZnO addition in between is more complex in the alkaline pH of 11. In this case addition of ZnO after 60 minutes of reaction results in initial slight increase in concentration of H_2O_2 followed by sharp decrease indicating total domination of the decomposition process. Thereafter mild oscillation continues. Extreme alkaline pH is known to have unpredictable impact on the concentration as well as behavior of H_2O_2 in sonocatalytic systems in presence of ZnO

as demonstrated earlier. Hence it may be concluded that the effect of ZnO on the oscillation in the concentration of H_2O_2 is pH dependent, even though the same cannot be quantitatively confirmed due to the simultaneous and complex formation and decomposition processes.

4.3.11 Adsorption study

In order to verify the contribution of adsorption/desorption of H_2O_2 to the change in its concentration in presence of ZnO, the adsorption of H_2O_2 on ZnO is measured in the presence as well as absence of phenol by standard techniques. The results are presented in figures 4.25 a and b.

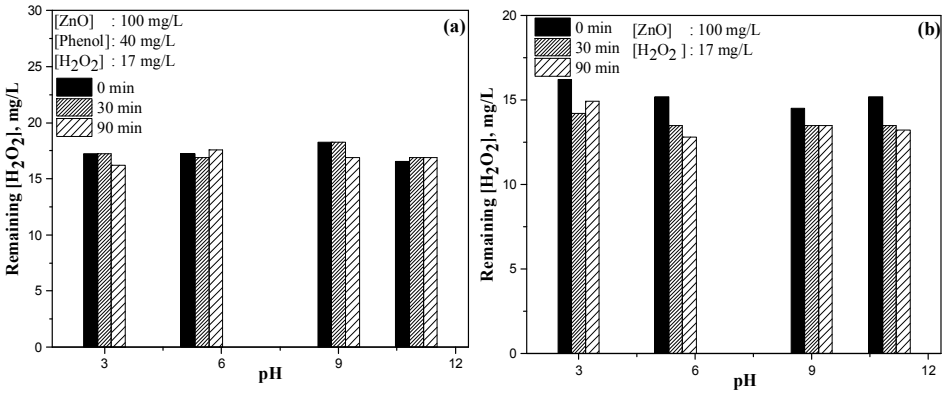

Fig. 4.25: Adsorption of H_2O_2 on ZnO (a) in the presence of phenol and (b) in the absence of phenol

The results show that adsorption of H_2O_2 on ZnO is practically negligible in presence of phenol in the pH range of 3 to 11. In the absence of phenol, very small amount of H_2O_2 is adsorbed and thereafter, the H_2O_2 concentration remains steady, irrespective of pH. This illustrates that the oscillation in the concentration of H_2O_2 is not an adsorption-

desorption process and is the result of a chemical reactions initiated by the ultrasound-generated reactive free radicals.

4.3.12 Corrosion of ZnO under sonocatalysis

One of the major criticism against ZnO as a photocatalyst is its corrosion under extreme acidic and alkaline condition as well as photocorossion. In this context, possible corrosion of ZnO at different pH was studied in detail as reported in Chapter 3 section 3.3.13. The corrosion of ZnO under similar condition is tested in presence of ultrasound with frequency 53 kHz as the irradiation source. Figure 4.26 shows the corrosion of ZnO at different pH in the presence as well as in the absence of US irradiation.

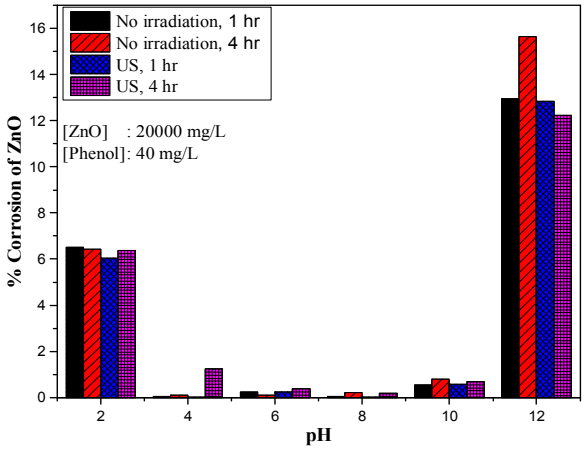

Fig. 4.26: Corrosion of ZnO at different pH in the presence and absence of US irradiation

Similar to photocatalysis, the corrosion is negligible in the pH range 4 to 10 with or without irradiation. Over a period of 4 hour, the corrosion is ~ 6% at pH 2 and ~ 14% at pH 12. Irradiation did not enhance the

corrosion significantly, at least during the period of study. Since all major investigations reported in the present study are carried out at the optimized pH of 5.5, corrosion can be considered negligible under the conditions of the study.

4.3.13 Memory effect

Semiconductors are reported to retain the memory of ultrasound irradiation and generate electron-hole pairs for some more time after the energy source is cut off [124]. The effect of this phenomenon, though not universally recognized, is examined by measuring the sonocatalytic phenol degradation and insitu H_2O_2 generation under standardized conditions after discontinuing the US. The US source was switched off after irradiating the samples for 30, 60 and 90 minutes each. Samples were then drawn at different intervals and analyzed for the concentration of phenol and H_2O_2 in the system. The degradation of phenol is insignificant after the irradiation is put off probably because the number of reactive free radicals generated is relatively small. However, the formation of H_2O_2 continues for some more time, followed by the oscillatory trend (figure 4.27) when the US irradiation is discontinued after 30 minutes,. This indicates minor memory effect resulting in the formation/reaction of $^{\bullet}OH$ radicals for some more time. When US irradiation is stopped after 60 and 90 minutes, the H_2O_2 concentration decreases showing the decomposition phase. In this case oscillation in the concentration of H_2O_2 continued with lower maxima and minima compared to the system under continued US irradiation.

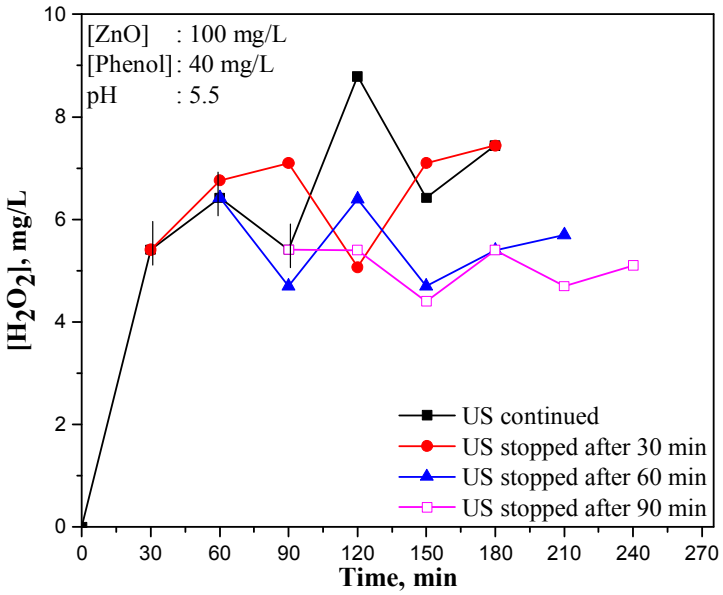

Fig. 4.27: Effect of discontinuing US irradiation on the oscillation in the concentration of H_2O_2

The variation in the concentration of H_2O_2 as above, especially the increase when the US is cutoff after 30 minutes, is caused by either the generation of reactive radicals or the combination of $^{\bullet}OH$ radicals already available in the system for some more time. However, the life time of the radicals is only few seconds. Hence it is more probable that the surface is involved in the process of generating fresh free radicals even after the US is off confirming a short memory effect. Similar memory effect has been reported earlier in the case of TiO_2 [130, 131]. Although the efficiency of the dark process due to the memory effect is not as high as in the presence of illumination, the phenomenon needs in-depth investigation since it has the potential for the decontamination of polluted water or other similar systems for longer duration even after the source of energy is turned off.

4.3.14 Role of O_2/air in sonocatalysis

Sono and photocatalytic reactions require the presence of efficient electron acceptors so that the recombination of the electrons and holes at the surface can be prevented. Fast recombination between electrons and holes inhibits the interfacial charge transfer and the reactions that follow. Dioxygen molecules are efficient electron acceptors and hence sono or photo catalytic reactions do not occur or occur very slowly in the absence of dissolved oxygen [132]**.** This was verified by measuring the sonocatalytic degradation of phenol in deaerated (N_2 flushed) and aerated (air flushed) system. The results are shown in figure 4.28.

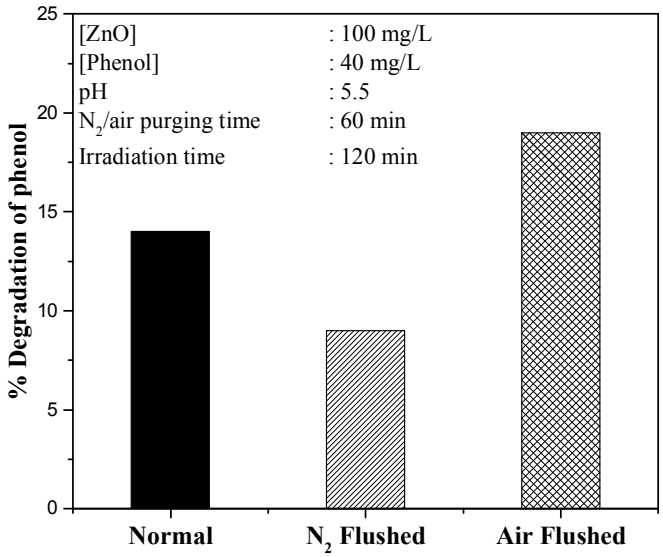

Fig. 4.28: Effect of O_2 on the sonocatalytic degradation of phenol

From the figure it is clear that the degradation of phenol is inhibited in deaerated system with little or no O_2. The degradation is enhanced when the system was bubbled with O_2/air. Presence of oxygen can

prevent the recombination of electrons and holes which in turn results in the formation of more ROS.

However deaeration by bubbling the system with nitrogen affects the oscillation in the concentration of H_2O_2 moderately (figure 4.29). The effect is seen even in system with externally added H_2O_2.

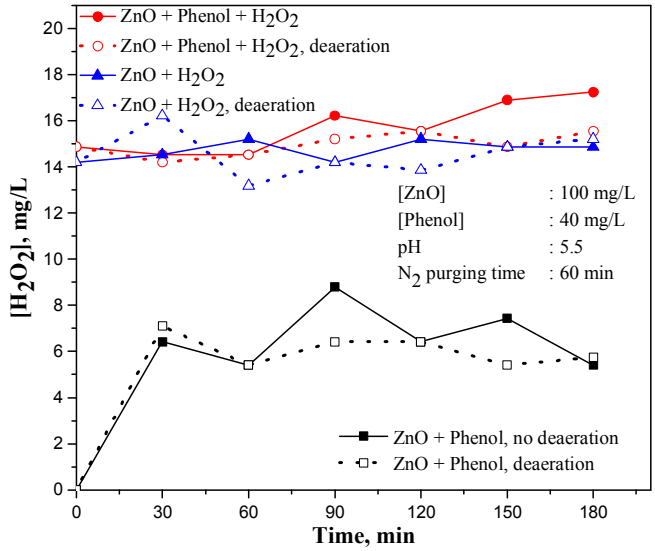

Fig. 4.29: Effect of deaeration with nitrogen on the oscillation in the concentration of H_2O_2 under sonocatalysis

The observation that the oscillation in the concentration of H_2O_2 is affected only moderately by deaeration shows that in the absence of O_2, H_2O_2 may be serving as an electron acceptor as follows:

$$H_2O_{2\,(ad)} + e^- \rightarrow {}^{\bullet}OH_{(ad)} + HO^-_{(ad)} \qquad \text{..... (110)}$$

The oscillation curve becomes more or less a straight line in the deaerated system, which indicates that the H_2O_2 formation or decomposition

is not significant in the absence of O_2. In the case of deaerated ZnO/H_2O_2 sonocatalytic system initially the H_2O_2 concentration increases slightly indicating US initiated free radical formation and their interactions to form H_2O_2. This is followed by decrease in the concentration of H_2O_2 and moderate oscillation.

According to many earlier reports H_2O_2 behaves uniquely in many AOPs by functioning as electron and/or hole scavenger in the same system as in reactions (110) and (111) [132, 143-145].

$$H_2O_{2\,(ad)} + {}^{\bullet}OH\ /h^{+} \rightarrow HO_2^{\bullet}{}_{(ad)} + H_2O/H^{+} \qquad \text{..... (111)}$$

Hence the recombination of electrons and holes is inhibited. Such behavior by H_2O_2 has been proven in the case of photocatalysis by using Cavity Ring Down Spectroscopy (CRDS) [143]. The electron or hole transfer to H_2O_2 generates $HO_2^{\bullet}$ or ${}^{\bullet}OH$ as above which may further react on the surface or get desorbed into the bulk. Such desorption of ${}^{\bullet}OH$ radicals from the TiO_2 surface has been confirmed by single molecule imaging using Fluorescence Microscopy [146] as well as Laser Induced Fluorescence Spectroscopy [147]. The desorption of $HO_2^{\bullet}$ (formed by the decomposition of H_2O_2) from the surface was confirmed by CRDS [146].

As expected the net concentration of H_2O_2 is slightly more in the presence of phenol and externally added H_2O_2 in system with no deaeration compared to the deaerated system. Hence it may be generally concluded that under sonocatalysis, where free radicals and H_2O_2 are produced from water also, O_2 does plays a major role in the degradation of phenol. However, the general phenomenon of oscillation is not affected

much though the concentration of H_2O_2 at the maximum and minimum are influenced moderately.

4.4 Mechanism of the process

The overall mechanism of sonocatalytic formation of ROS and degradation of organic pollutant is schematically presented in figure 4.30.

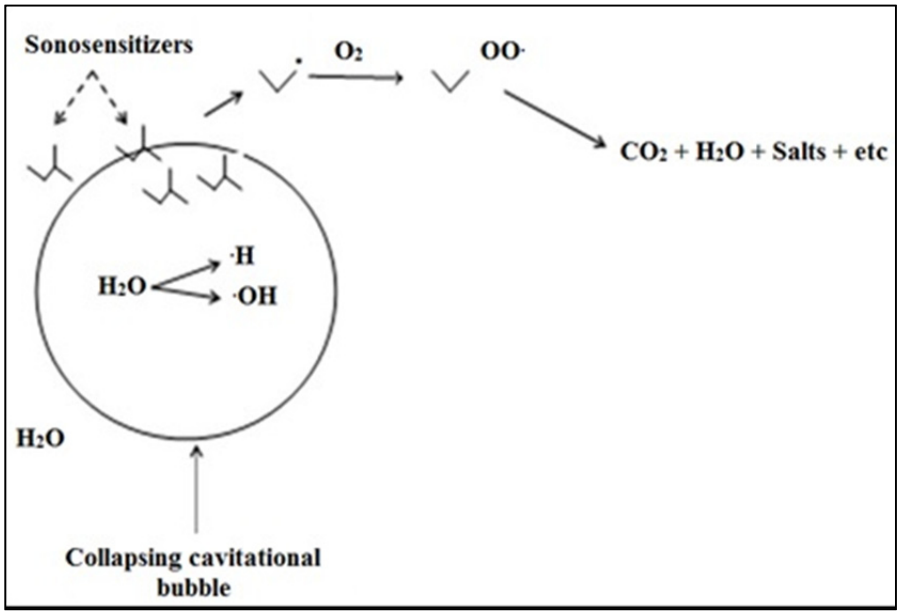

Fig. 4.30: Mechanism of the sonocatalytic degradation of organic pollutants

The basic mechanism of ZnO mediated sonocatalytic degradation of phenol is presented as follows:

$ZnO + >>> \rightarrow h^+ + e^- >>> \text{Ultrasound}$ ..... (112)

$h^+ + e^- \rightarrow \text{Heat}$ ..... (113)

$h^+ + OH^- \rightarrow {}^{\bullet}OH$ ..... (114)

$h^+ + H_2O \rightarrow {}^{\bullet}OH + H^+$ ..... (115)

$$e^- + O_2 \rightarrow O_2^{-\bullet} \quad \text{..... (116)}$$

$$H^+ + O_2^{-\bullet} \rightarrow HO_2^{\bullet} \quad \text{..... (117)}$$

$$HO_2^{\bullet} + e^- + H^+ \rightarrow H_2O \quad \text{..... (118)}$$

Phenol + Reactive species ($O_2^{-\bullet}$, $HO_2^{\bullet}$, $^{\bullet}OH$) $\rightarrow$
Intermediates $\rightarrow$ H_2O + CO_2 ..... (119)

4.4.1 Formation of $^{\bullet}OH$ radicals

Presence of $^{\bullet}OH$ radicals on the surface of the US irradiated ZnO is confirmed by the photoluminescence technique as explained in Chapter 3 under section 3.4.1. Figure 4.31 shows the PL spectrum under US irradiation. Increasing PL with time of irradiation corresponds to the formation of more $^{\bullet}OH$ as explained under 3.4.1.

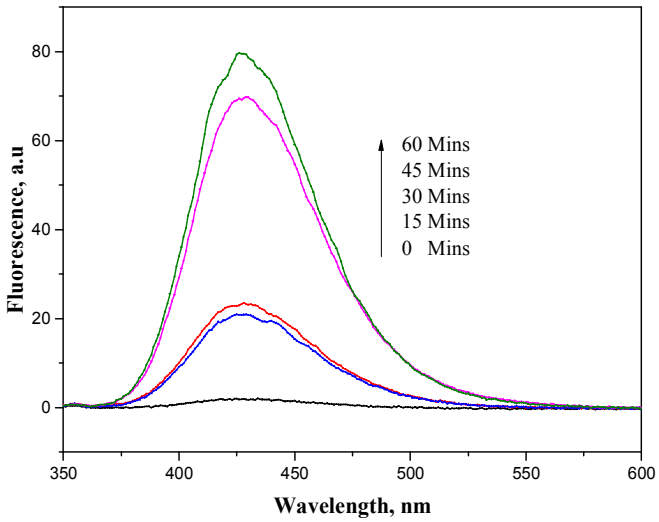

Fig. 4.31: PL spectral changes observed during the US irradiation of ZnO with mixed solution of terephthalic acid and NaOH

Possible steps involved in the concurrent formation and decomposition of H_2O_2 leading to the oscillation are similar to those given in reactions (75) to (87) in Chapter 3 section 3.4.1.

The steps are presented again in the context of US irradiation.

$$^{\bullet}OH + {}^{\bullet}OH \rightarrow H_2O_2 \quad \text{..... (120)}$$

$$2H_2O + 2h_{vb}^{+} \rightarrow H_2O_2 + 2H^{+} \quad \text{..... (121)}$$

$$O_2^{-\bullet} + H^{+} \rightarrow HO_2^{\bullet} \quad \text{..... (122)}$$

$$HO_2^{\bullet} + HO_2^{\bullet} \rightarrow H_2O_2 + O_2 \quad \text{.....123)}$$

$$O_2^{-\bullet} + HO_2^{\bullet} \rightarrow O_2 + HO_2^{-\bullet} \quad \text{..... (124)}$$

$$HO_2^{-\bullet} + H^{+} \rightarrow H_2O_2 \quad \text{..... (125)}$$

The concurrent decomposition of H_2O_2 takes place as follows:

$$H_2O_2 + >>> \rightarrow 2\ {}^{\bullet}OH \quad \text{..... (126)}$$

$$2\ h_{vb}^{+} + H_2O_2 \rightarrow O_2 + 2\ H^{+} \quad \text{..... (127)}$$

$$2\ e_{cb}^{-} + 2\ H^{+} + H_2O_2 \rightarrow 2\ H_2O \quad \text{..... (128)}$$

$$H_2O_2 + {}^{\bullet}OH \rightarrow H_2O + HO_2^{\bullet} \quad \text{..... (129)}$$

$$H_2O_2 + HO_2^{\bullet} \rightarrow H_2O + {}^{\bullet}OH + O_2 \quad \text{..... (130)}$$

Being a complex free radical system, other interactions leading to the formation and decomposition of H_2O_2 are also possible. The effect of various parameters on the phenomenon of oscillation is explained in respective sections. In many cases the effect is inconsistent due to the complex interplay of a number of factors. However, the phenomenon of oscillation in the concentration of H_2O_2, with periodic maxima and minima, is evident in all cases.

4.5 Conclusions

Sonication and sonocatalysis are potential AOPs for the removal of toxic organic pollutants from water. However the efficiency is much lower compared to photocatalysis. US induced sonoluminescence makes sonocatalysis partially photocatalytic thereby opening the possibility of the combined process i.e., sonophotocatalysis. H_2O_2 formed during the sonocatalytic degradation of phenol in water undergoes concurrent decomposition resulting in oscillation in its concentration. Various reaction parameters such as catalyst loading, substrate concentration, particle size, pH, externally added H_2O_2 and presence of air/O_2 influence the phenomenon in general and the maxima and minima in the oscillation curve in particular. H_2O_2 plays a unique role as acceptor of both electrons and holes in deaerated system. The oscillation phenomenon continues for some more time even after the source of ultrasound is switched off, thereby indicating the presence of mild memory effect in the semiconductor. A reaction mechanism based on the observations is proposed and discussed.

Chapter 5

INVESTIGATIONS ON THE SONOPHOTOCATALYTIC DEGRADATION OF PHENOL AND THE FATE OF H_2O_2 FORMED INSITU

Contents

5.1 Introduction

Sonophotocatalysis involves the use of combination of ultrasound and ultraviolet light in presence of catalysts such as semiconductor oxides. The general principle behind sonocatalysis and photocatalysis are the same viz. they both produce $^{\bullet}OH$ radicals which are powerful oxidizing agents. Hence, if the two modes of irradiation are operated in combination, more free radicals will be available for the degradation reaction, thereby increasing the rates of degradation. One of the drawbacks of photocatalysis is that, continuous operation results in blocking of UV active sites by adsorbed species which reduces the efficiency of the process. This can be overcome to some extent by continuous cleaning of catalyst surface during the photocatalytic process. Ultrasonic irradiation is one such technique which can be used simultaneously with UV irradiation. Sonication alone results in very low efficiency for the degradation of pollutants. Studies are in progress in

many laboratories for improving the efficiency of sonocatalysis. Sonophotocatalysis has been investigated in this context as a potential candidate. Another important parameter that requires in-depth analysis in this respect is the fate of H_2O_2 under sonophotocatalysis. Sonophotocatalytic degradation of phenol in presence of a typical semiconductor oxide; ZnO and the fate of concurrently formed H_2O_2 are investigated in detail and presented in this chapter.

5.2 Experimental details

5.2.1 Materials used

Materials used for the studies in this chapter are described in Chapter 3 and 4 in sections 3.2.1 and 4.2.1.

5.2.2 Analytical procedures

Sampling and analysis were performed as explained in Chapter 3 and 4 under sections 3.2.2 and 4.2.2 respectively. The mercury vapor lamp for UV light, the ultrasonic bath for US and the rest of the equipments used for the study are the same as described in Chapter 3 and 4.

5.2.3 Sonophotocatalytic experimental setup

The experiments were performed using aqueous solutions of phenol of desired concentration. Specified quantity of the catalyst is suspended in the solution. The reaction set up is a combination of those used in Chapters 3 and 4. The reactors are same as those used in photocatalysis. They are placed in an ultrasonic bath in which water from a thermostat at the required temperature was circulated. Unless otherwise mentioned, the reaction temperature was maintained at 29 ± 1^{o}C. The position of the

reactor in the ultrasonic bath was always kept the same. A high intensity UV lamp (400 W medium pressure mercury vapor quartz lamp) mounted above is used as the UV irradiation source. The ultrasonic bath was operated at a frequency of 53 kHz and a power of 100 W unless indicated otherwise. Rest of the experimental procedure, sampling and analysis methods etc. are the same as described in Chapters 3 and 4. Typical reactor set up is shown in Fig. 5.1.

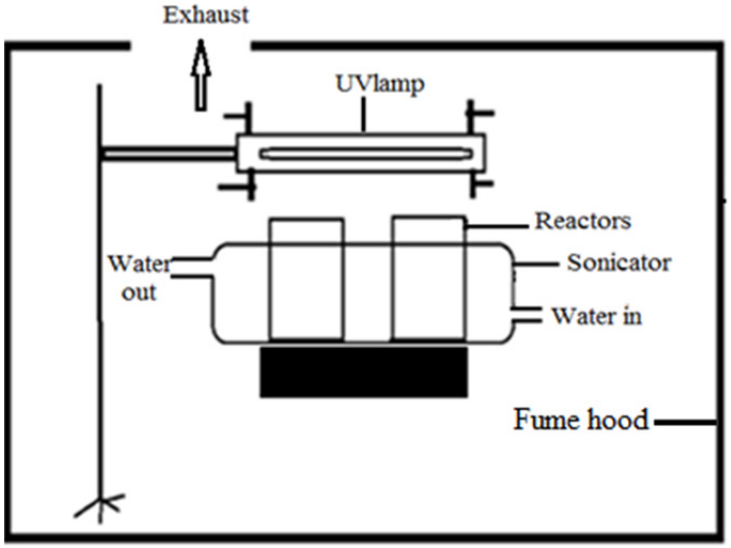

Fig. 5.1: Schematic diagram of the sonophotocatalytic experiment set up

5.3 Results and discussion

5.3.1 Preliminary results

Preliminary results on the sonophotocatalytic degradation of phenol are compared with the sono and photo catalysis under identical reaction parameters. The results are shown in figure 5.2.

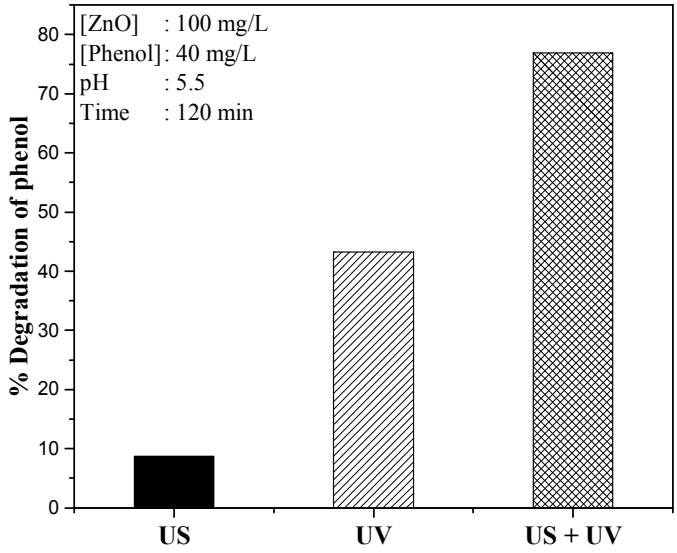

Fig. 5.2: Sono, photo and sonophoto catalytic degradation of phenol in presence of ZnO

The degradation is more facile in the presence of UV light (photocatalysis) compared to US irradiation (sonocatalysis). The sonophotocatalytic degradation in the concurrent presence of UV, US and ZnO is more than the sum of the degradation under photocatalysis and sonocatalysis, which supports the earlier reports on the synergy of the combined process [6, 87].

The percentage degradation of phenol with time under sonophoto catalysis is shown in figure 5.3. Corresponding results under sono and photocatalysis are shown in the 'inset'.

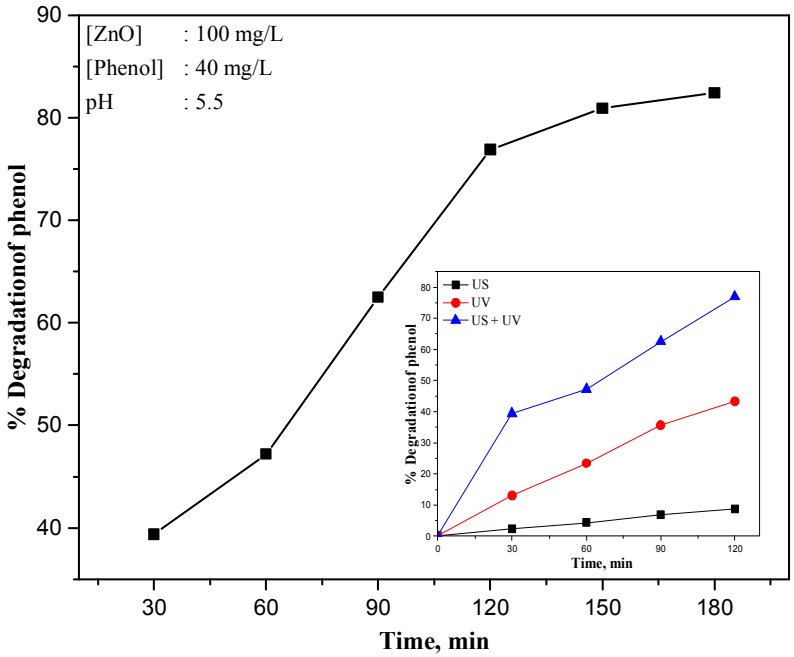

Fig. 5.3: Sonophotocatalytic degradation of phenol
Inset: Comparison of sono, photo and sonophotocatalysis

The degradation of phenol increases with time up to 120 minutes, slows down gradually and then level off.

The fate of concurrently formed H_2O_2 in sonophotocatalysis is shown in figure 5.4. Corresponding data under sono and photocatalysis are plotted in the 'inset' figure. In the case of sono and photo catalysis, the H_2O_2 formed during the degradation undergoes parallel decomposition resulting in an oscillation-like phenomenon. As a result of concurrent formation and decomposition, the net concentration of H_2O_2 remains relatively lower and may eventually level off. In the case of sonophotocatalysis, the concentration of H_2O_2 levels off initially and increases steeply again showing that, in this case, the formation process can dominate more frequently.

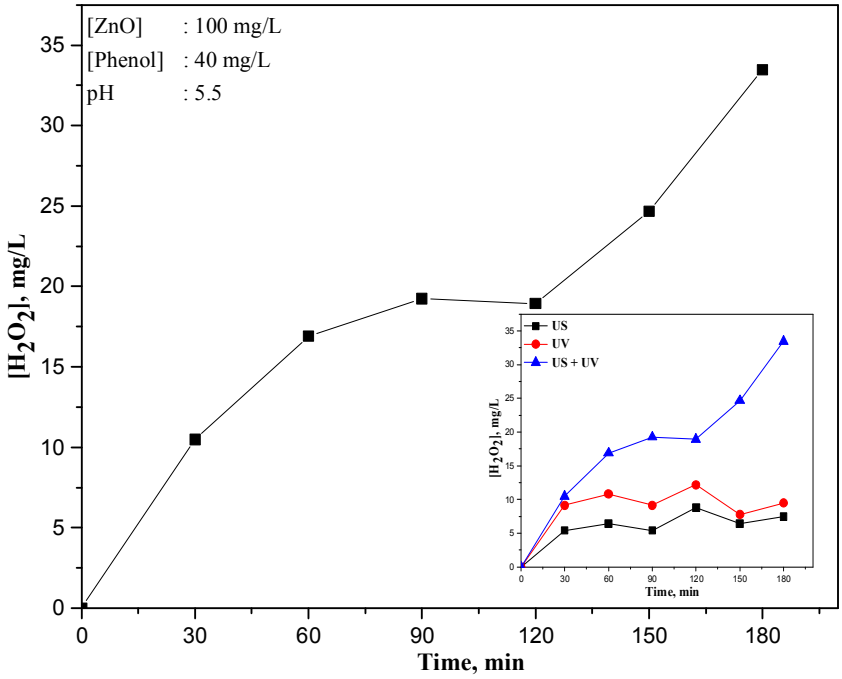

Fig. 5.4: Concentration of H_2O_2 during sonophotocatalytic degradation of phenol in presence of ZnO
Inset: Comparison of sono, photo and sonophotocatalysis

The net stabilized concentration of H_2O_2 in the system increases in the order sono < photo < sonophoto.

5.3.2 Effect of catalyst dosage

The catalyst dosage for optimum sonophotocatalytic degradation of phenol is experimentally determined and the result is shown in figure 5.5.

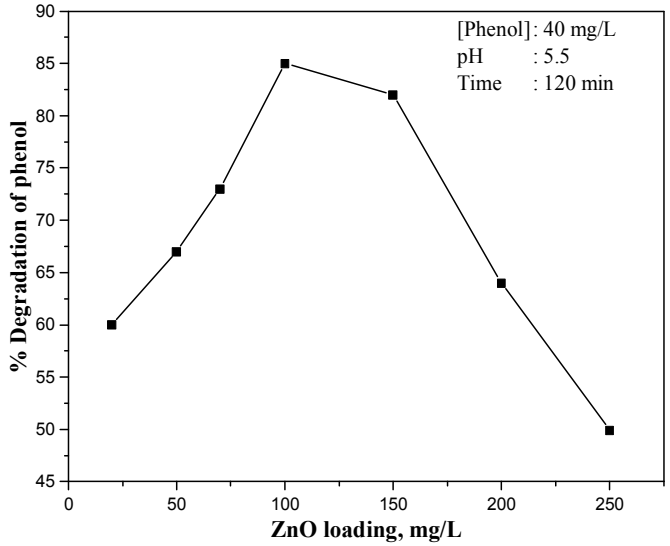

Fig. 5.5: Effect of catalyst loading on the sonophotocatalytic degradation of phenol

Phenol degradation increases with increase in catalyst loading, reaches an optimum and then decreases. Optimum loading obtained here is 100 to 150 mg/L. The enhanced degradation efficiency is probably due to increased number of adsorption sites and more effective interaction with the UV/US radiation which lead to generation of higher number of reactive hydroxyl radicals. In the case of photo and sonophoto catalysis, any further increase in catalyst concentration beyond the optimum will only result in light scattering and reduced passage of light through the sample. Hence no further increase in degradation is observed. In the case of sonophotocatalysis, the decrease in degradation with increase in catalyst loading beyond the optimum is more pronounced compared to photocatalysis. However, the optimum loading and the trend remain fairly the same suggesting that US induced increase in the rate of photocatalysis may be resulting at least partly

from the increase in light absorbed by the reaction system. This leads to higher concentration of active species. At higher catalyst loading, beyond the optimum when filtering and/or scattering of light becomes more prominent, the amount of photoproduced active species does not increase further and even decreases.

The effect of catalyst dosage on the concurrently formed H_2O_2 in sonophotocatalytic systems is shown in figure 5.6.

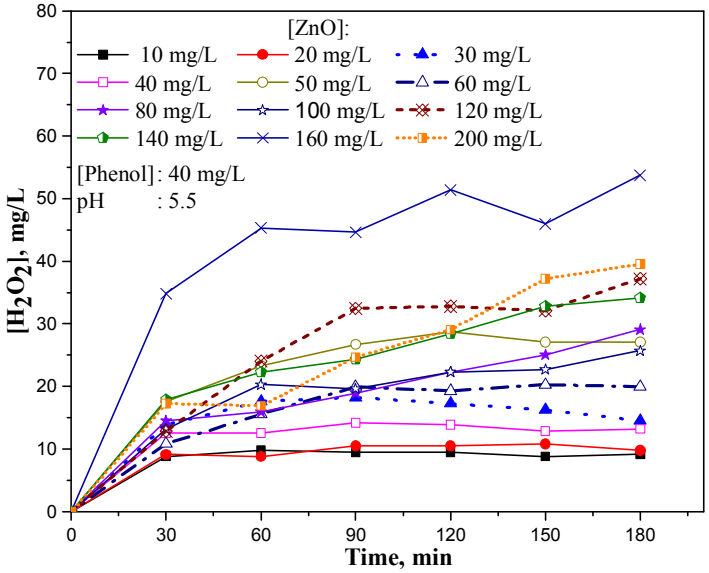

Fig. 5.6: Effect of catalyst loading on the oscillation in the concentration of H_2O_2 under sonophotocatalysis (*Also see Fig. 5.6.1 and 5.6.2*)

Similar to photo and sono catalysis described in Chapter 3 and 4, here also the data and the curves are too crowded in the figure 5.6. Hence the results are presented in two separate figures 5.6.1 and 5.6.2.

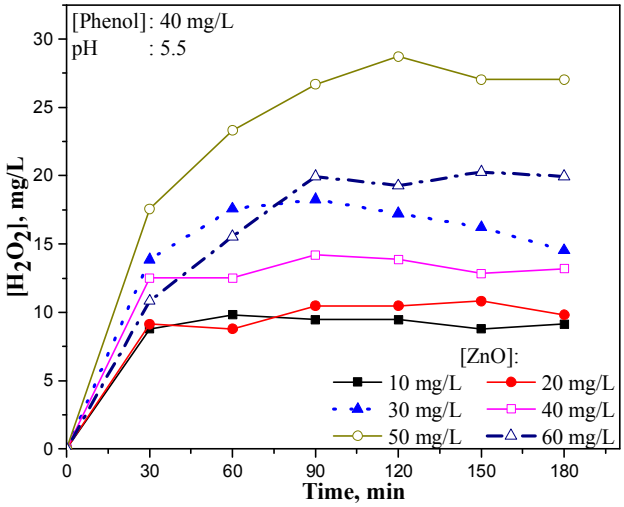

Fig. 5.6.1: Effect of catalyst loading (10 to 60 mg/L) on the oscillation in the concentration of H_2O_2 under sonophotocatalysis

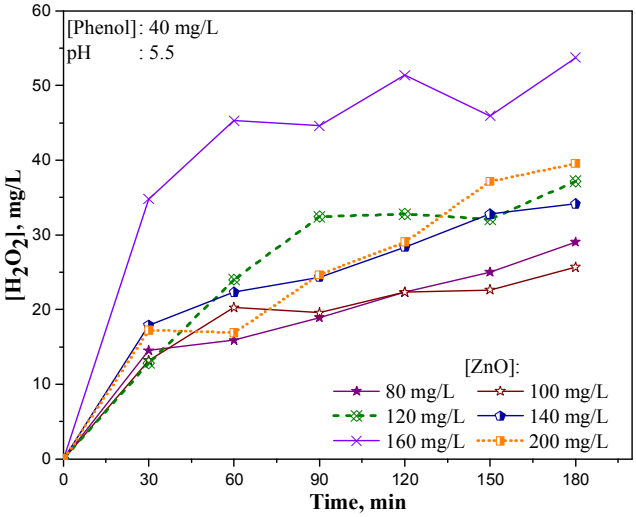

Fig. 5.6.2: Effect of catalyst loading (80 to 200 mg/L) on the oscillation in the concentration of H_2O_2 under sonophotocatalysis

As the catalyst dosage increases the net concentration of H_2O_2 in the system also increases with some exceptions as are there in the case of

sono and photo catalysis. Maximum H_2O_2 is seen at 160 mg/L. In most cases the concentration of H_2O_2 increases sharply and then stabilizes after 90 minutes. The oscillation in the concentration of H_2O_2 also is seen, though less distinct compared to sono or photo catalysis.

The net initial rate of formation of H_2O_2 at various loadings is calculated and plotted in figure 5.7.

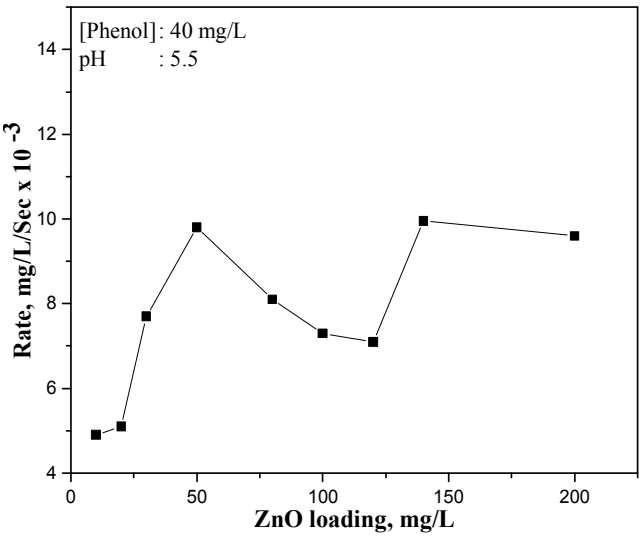

Fig. 5.7: Effect of catalyst loading on the net initial rate of formation of H_2O_2 under sonophotocatalysis

The initial rate of formation of H_2O_2 increases sharply from 10 to 50 mg/L decreases steeply thereafter and remain fairly stable in the range of 80 to 120 mg/L. From 120 to 150 mg/L there is another increase followed by stabilization. In the case of sonophotocatalysis, the rate of formation of H_2O_2 is relatively high compared to decomposition and hence H_2O_2 goes on increasing initially. This naturally results in faster accumulation of H_2O_2 and consequent decomposition. In this fast and

complex simultaneous formation-decomposition process initial rate of formation of H_2O_2 cannot remain consistently reproducible. Hence, the absolute quantitative values are not the same in repeated experiments even though the trend remain the same. Hence an oscillatory type phenomenon is seen even in the net initial rate of formation. At higher ZnO loading the formation and decomposition rate balances and the net rate is stabilized.

5.3.3 Effect of pH

The results reported in Chapter 3 and 4 show that pH of the solution influences the degradation in both UV and US-induced reactions. Hence the effect of pH on the sonophotocatalytic degradation was also studied in the pH range of 3 to 11. The pH of the solution was adjusted initially and was not controlled during the course of reaction. The results are presented in figure 5.8.

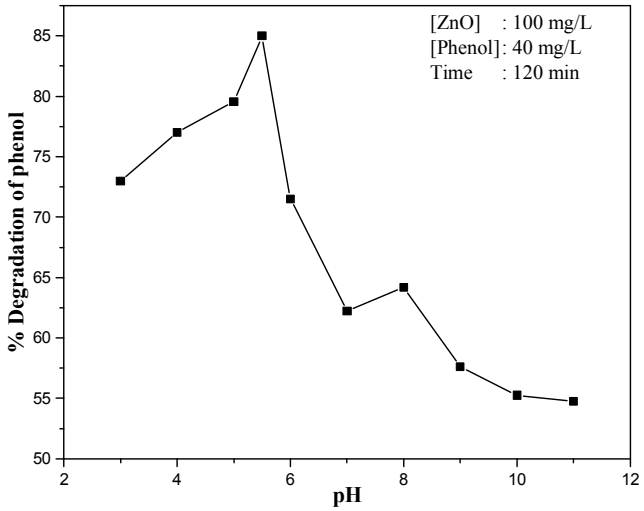

Fig. 5.8: Effect of pH on the sonophotocatalytic degradation of phenol

The degradation is more efficient in the acidic region than in the alkaline region. In the acidic pH range of 4 to 5.5, over 85% conversion is effected in 2 hours while it is around 55 to 60% in the alkaline range. The pH effect is similar to the observations in the case of photocatalytic and sonocatalytic systems. The optimum pH in all these cases is 5.5. This is similar to the observations of Wu et al. [90] who reported 98% of sonophotocatalytic degradation of phenol at pH 3 in presence of TiO_2 while under alkaline conditions it was 60%. Kaur and Sigh [148] reported that visible light induced sonocatalytic degradation of reactive red (RR) dye was maximum at operating pH of 3 and the rate constant for degradation decreased with increase in pH in the range 3 to 9. The enhanced sonophotocatalytic degradation under acidic pH can be attributed to the fact that under such conditions, both UV and US induced reactions are favored as demonstrated earlier. Castrantas and Gibilisco [149] also reported that the rate of photocatalytic degradation under acidic conditions is faster than under alkaline conditions.

Higher degradation efficiency for various types of phenol in the acidic range has been reported by other authors also [120, 150] using TiO_2 as the catalyst. The relatively lower degradation rate below pH 4 is probably because ZnO is a poor photocatalyst in this region due to change in surface properties and its corrosion in aqueous acidic media. This is consistent with the findings of other researchers as well [121, 151, 152].

Possible reasons for the enhanced degradation in the acidic range under photo and sono catalysis are discussed in detail under sections 3.3.4 and 4.3.3. In sonophotocatalysis, almost 80 % degradation was obtained

in the acidic pH range whereas it is only 55% in the alkaline range. In the region of pH 4 to 5.5, degradation under sonophotocatalysis is approximately 60% more than that under photocatalysis. However, under alkaline conditions, this enhancement is only about 20%.

The synergy index for sonophotocatalytic degradation was calculated using the equation:

$$\text{Synergy index} = \frac{R_{US+UV}}{R_{US} + R_{UV}} \quad \text{..... (131)}$$

Where R_{US} is rate of degradation under US, R_{UV} is the rate of degradation under UV and R_{US+UV} is the rate of degradation in the combined presence of US and UV. The synergy index at different pH is calculated for 2hr degradation and given in table 5.1.

Table 5.1: Synergy index at different pH

pH	Synergy Index
3	1.69
4	1.36
5	1.41
5.5	1.23
6	1.09
7	1.02
8	1.10
9	1.17
10	1.32
11	1.45

The synergy is maximum in the acidic range and the least under neutral pH conditions.

Figure 5.9 shows the fate of H_2O_2 during sonophotocatalytic degradation of phenol at different pH.

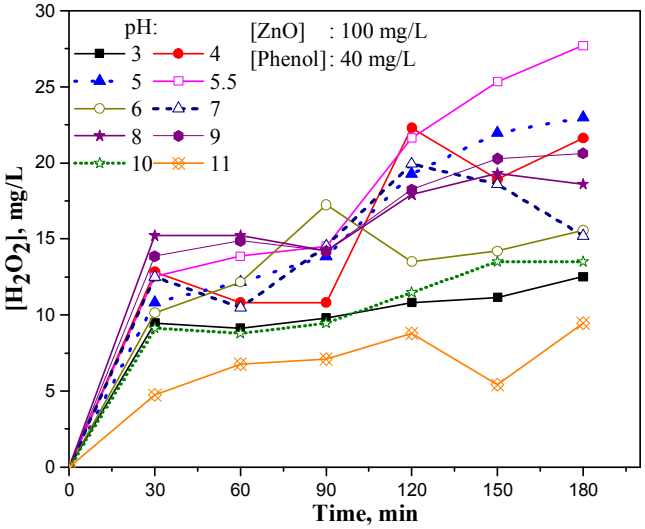

Fig. 5.9: Effect of pH on the oscillation in the concentration of insitu formed H_2O_2 under sonophotocatalysis

At extreme acidic as well as alkaline pH the net concentration of H_2O_2 in the system is low compared to other pH. Maximum H_2O_2 is obtained at pH 5.5, where the degradation of phenol also is maximum. In the pH range of 4 to 9 two stabilization periods are seen at time interval 30 to 90 and 120 to 180 minutes. In sonophotocatalysis, the rate of formation of H_2O_2 is high enough at all pH to compensate for the relatively lower rate of decomposition and maintain an increasing trend. Hence the maxima and minima in the oscillation curve is not as pronounced as in the case of sono and photo catalysis and the oscillation tends to be weaker and moves towards stabilization with time.

The pH-dependent behavior of phenol as well as of the catalyst ZnO has been shown to influence the rate of reaction and the fate of H_2O_2 in photo and sono catalytic systems as explained in Chapter 3 and 4 respectively. As expected, similar behavior is observed in the case of sonophotocatalysis also. Thus, the phenomenon of oscillation is relatively more pronounced in the acidic range compared to the alkaline pH. Under alkaline conditions, during US irradiation, the phenolate ions are concentrated in the gas–water interface of the bubbles where the hydrophobicity is strong and cannot vaporize into the cavitation bubbles [90]. They can react only outside of the bubble film with the $^{\bullet}OH$ radicals cleaved from water. Consequently degradation of phenol and oscillation in the concentration of H_2O_2 is less. However, phenol is in its molecular state in the acidic pH and enters the gas–water interface of bubbles and even vaporizes into cavitation bubbles. Hence they can react inside by thermal cleavage and outside with $^{\bullet}OH$ radicals. This leads to enhanced degradation of phenol. Correspondingly, the formation and decomposition of H_2O_2 also is higher. Hence the net concentration of H_2O_2 is more significant in the acidic pH range except at pH ~ 3.

As stated in earlier chapters, when the pH of the suspension is less than the pKa ~ 10 most of the phenol molecules will remain un-dissociated. Hence maximum number of phenol molecules gets adsorbed onto the positively charged ZnO surface leading to increased degradation of phenol and correspondingly more H_2O_2. This also results in overall higher concentration of H_2O_2 including at the maximum of the oscillation curve.

Similarly in the alkaline medium, especially above the PZC of ZnO, i.e. > 9, the catalyst surface is negatively charged and phenol is predominantly in the form of phenolate ions. The phenolate ions will get repelled away from the surface. This will also reduce the adsorption and consequent degradation of phenol and H_2O_2 formation.

The fate of externally added H_2O_2 under sonophotocatalysis in the absence of any substrate in presence of ZnO at different pH was investigated under identical conditions and the results are plotted in figure 5.10.

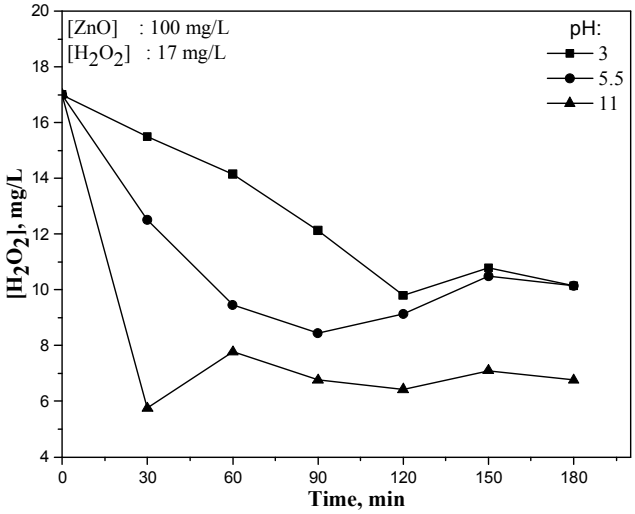

Fig. 5.10: Effect of pH on the oscillation in the concentration of H_2O_2 in the absence of phenol under sonophotocatalysis

As expected, at higher concentration of H_2O_2, the decomposition dominates and its concentration falls steeply in the beginning and reaches a steady value. Thereafter slow formation and decomposition process results in mild oscillation at all pH. The concentration of H_2O_2 is the least at the extreme alkaline pH=11 and the maximum at the acidic pH=3.

Comparison of the results with the system containing phenol, shows that even with externally added H_2O_2, the stabilized concentration (of H_2O_2) is less in the absence of phenol. This illustrates the role of free radicals generated during the degradation of phenol in the formation of H_2O_2.

5.3.4 Effect of particle size

In photo as well as sono catalysis it was observed that particle size with in a small range of 6 to 60 μm has only little effect on phenol degradation. The effect of particle size in this range on the sonophotocatalytic degradation of phenol also is studied and the results are plotted in figure 5.11.

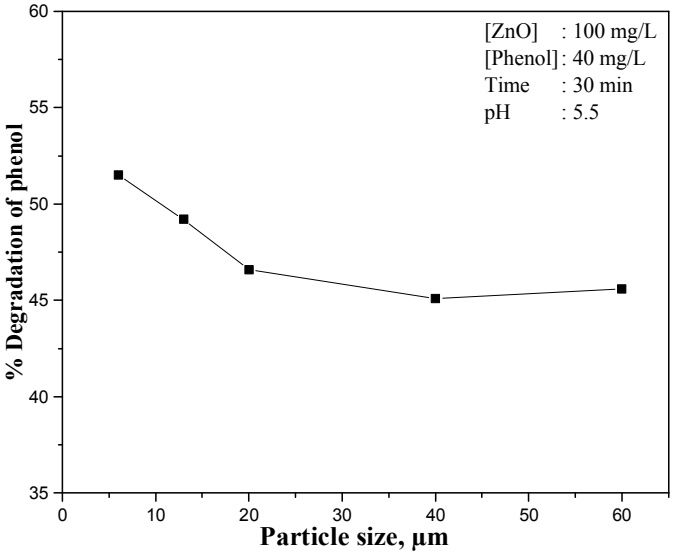

Fig. 5.11: Effect of particle size on the sonophotocatalytic degradation of phenol

As particle size increases from 6 to 20 μm, sonophotocatalytic degradation of phenol slightly decreases and then stabilizes in the range of 20 to 60 μm. This is fairly similar to the results under photocatalysis.

The inverse relationship between the particle size and phenol degradation can be explained based on the increased surface area of smaller particles. This results in more surface sites for adsorption of the pollutant, generation of more reactive free radicals and better surface promoted interaction between the reactants and consequently higher degradation.

The effect of particle size on the concurrently formed H_2O_2 is evaluated by measuring the net initial rate of formation of H_2O_2 at different particle size of ZnO and the result is shown in figure 5.12.

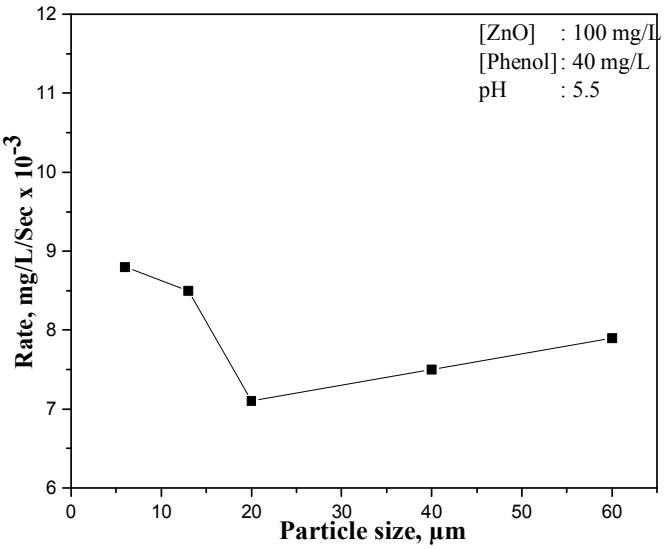

Fig. 5.12: Effect of particle size on the initial rate of H_2O_2 formation under sonophotocatalysis

The net initial rate of formation of H_2O_2 decreases steeply when the particle size increases from 6 to 20 µm. Thereafter the degradation is stabilized when particle size range is 20 to 60 µm. The net concentration of H_2O_2 at various time intervals in presence of ZnO particles in the range 6 to 60 µm is shown in figure 5.13.

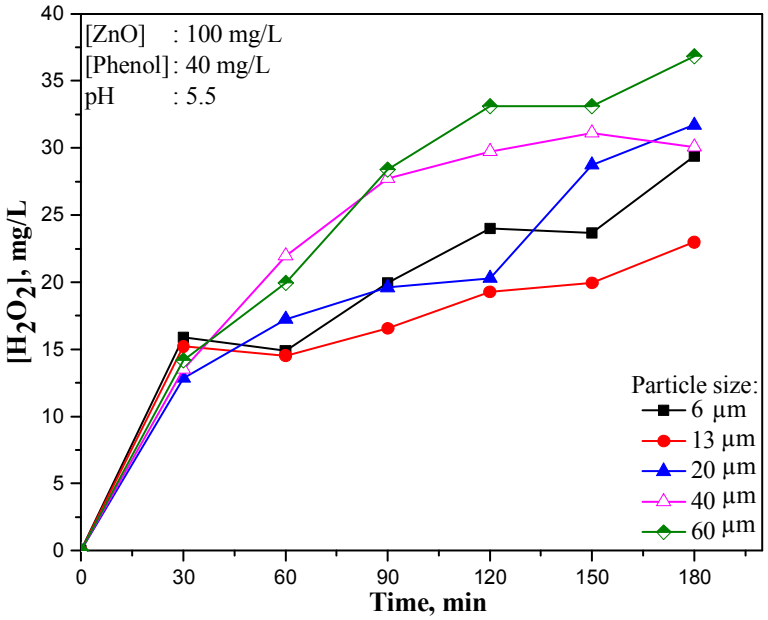

Fig. 5.13: Effect of particle size on the oscillation in the concentration of H_2O_2 under sonophotocatalysis

Maximum concentration of H_2O_2 is observed at 60 µm and minimum at 13 µm particle size. As particle size increases the net concentration of H_2O_2 in the system also increases in general, even though there are some exceptions. This indicates that at higher particle size ZnO does not favour the decomposition of H_2O_2 and as a result the formation process will be more prominent. Hence the oscillation is weak and the H_2O_2 will continue to increase. However direct correlation between particle size of ZnO and the net concentration of H_2O_2 at any point of time during the reaction is difficult because of the interplay of many known and unknown factors which influence formation and decomposition of H_2O_2.

5.3.5 Effect of concentration of substrate

The effect of initial concentration of phenol on its rate of sonophotocatalytic degradation is investigated and the results are shown in figure 5.14.

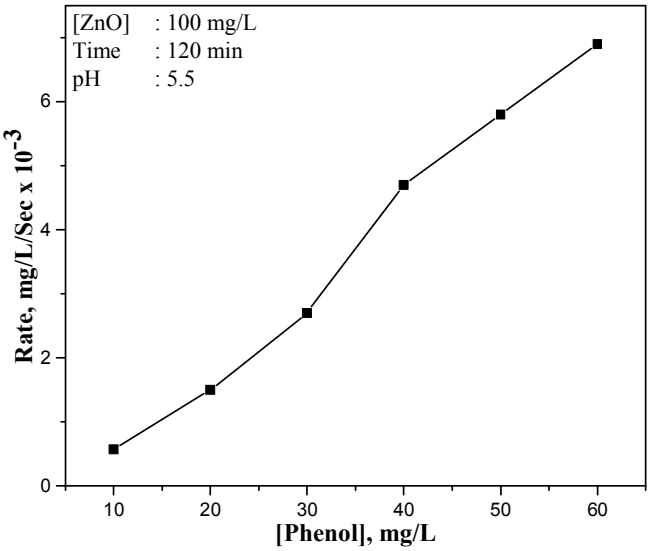

Figure 5.14 Effect of concentration of phenol on its sonophotocatalytic degradation rate

The rate of sonophotocatalytic degradation increases with increase in concentration of phenol in the range of 10 to 60 mg/L. The trend is similar in photocatalysis and sonocatalysis as explained in Chapter 3 and 4 in sections 3.3.6 and 4.3.5 respectively. The kinetics of the degradation, assuming Langmuir Hinshelwood mechanism, is determined by plotting the $-\ln[C/C_0]$ vs time for various concentration of phenol (figure 5.15). The straight line logarithmic plots indicate pseudo first order kinetics, as in the case of many AOPs under similar reaction conditions.

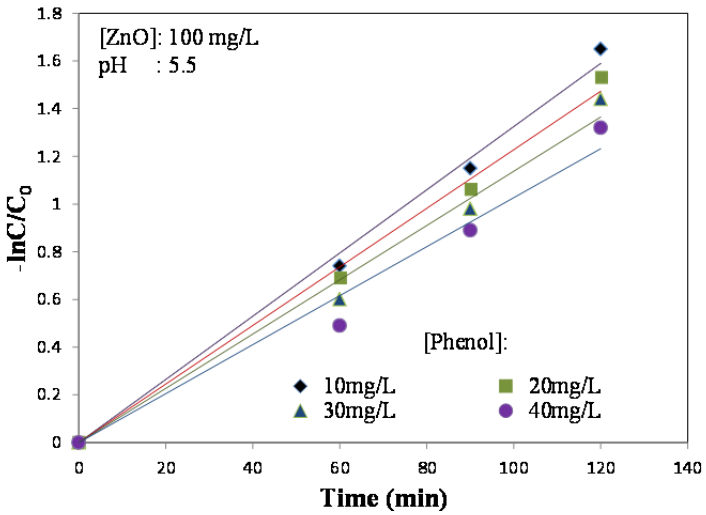

Fig. 5.15: Kinetics of ZnO mediated sonophotocatalytic degradation of phenol at lower concentrations

First order kinetics at concentrations in the range of 10 to 40 mg/L can be explained based on the same factors as in the case of sono as well as photo catalytic processes. In photocatalysis, as concentration of pollutant increases more reactant molecules get adsorbed on to the catalyst surface and can interact with more $^{\bullet}OH$ radicals. This will continue until all the surface sites are occupied. In sonocatalysis degradation reaction takes place mainly in the bulk of the solution where the concentration of $^{\bullet}OH$ radicals is relatively smaller [153]. As pollutant concentration increases it can more effectively utilize the otherwise limited $^{\bullet}OH$ radicals leading to increased degradation. This trend will continue until the phenol concentration is sufficiently high to interact with optimum number of $^{\bullet}OH$ radicals. Thereafter the rate of degradation remains the same or even decreases with increase in concentration of the substrate gradually indicating decreasing order of reaction.

The effect of concentration of phenol on the oscillation in the concentration of insitu formed H_2O_2 is shown in figure 5.16.

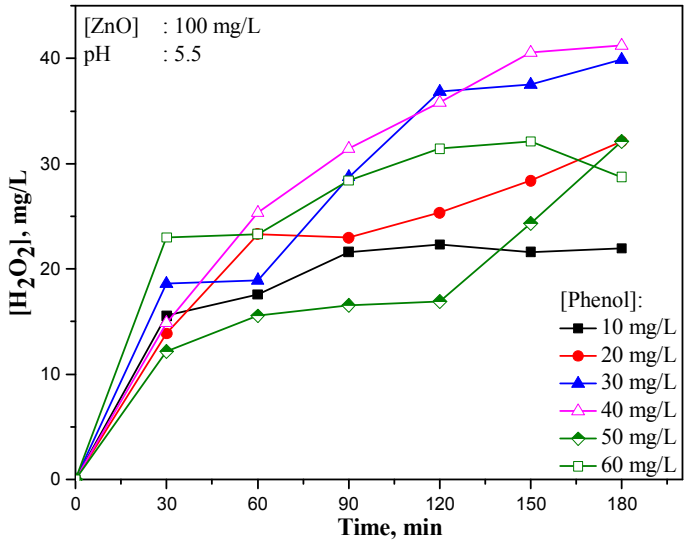

Fig. 5.16: Effect of concentration of phenol on the oscillation in the concentration of H_2O_2 under sonophotocatalysis

The net concentration of H_2O_2 increases sharply in the beginning at all phenol concentrations, stabilises for a while, increases again and stabilises thereafter. As in the case of other reaction parameters, exceptions to the trend are there in this case too. The net concentration of H_2O_2 increases with increase in concentration of phenol up to 40 mg/L. Above this concentration, the net concentration of H_2O_2 decreases as seen from the lowest concentration (of H_2O_2) at 50 mg/L of phenol. However, at 60 mg/L, the concentration of H_2O_2 is more. This confirms that in sonophotocatalysis too, there is no absolutely consistent or reproducible trend as far as the oscillation or net concentration of H_2O_2 is concerned. However a general trend is visible in most cases with few exceptions.

It was observed that small quantity of H_2O_2 is produced even in the absence of any organic substrate in sonocatalysis. The quantity of H_2O_2 formed without any substrate was measured in the sonophotocatalytic systems also and the results are plotted in figure 5.17.

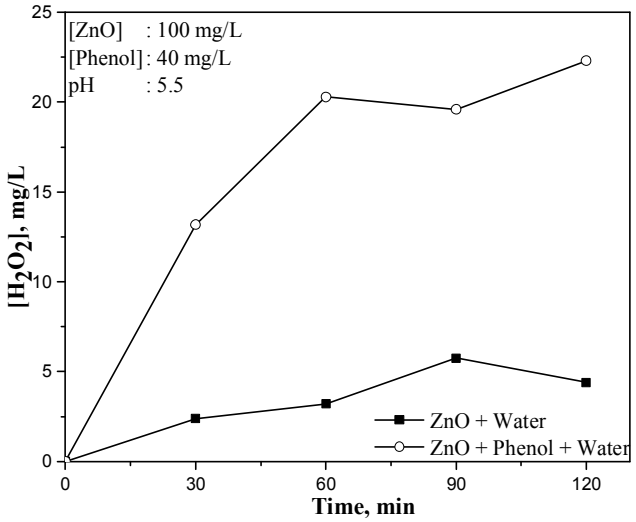

Fig. 5.17: Influence of presence of phenol on the net concentration of H_2O_2 in sonophotocatalytic system

Here also it is observed that in the absence of any organic substrate the quantity of H_2O_2 in the system is very small. When phenol is present in the system, more $^{\bullet}OH$ radicals are generated and hence the net concentration of H_2O_2 is high. This reconfirms the importance of interaction between the $^{\bullet}OH$ radicals and phenol molecules in the formation of H_2O_2.

5.3.6 Effect of addition of phenol on the fate of H_2O_2 under sonophotocatalysis

The role of phenol in the formation and fate of H_2O_2 in sonophotocatalytic systems is further verified by the addition of phenol

into a system containing only H_2O_2 in the beginning. The results are plotted in figure 5.18. Initially the system contains only irradiated ZnO and H_2O_2 (15 mg/L). After 60 minutes of reaction suspension was split into two. Phenol (40 mg/L) was introduced in to one part and the irradiation was continued in both cases. The net concentration of H_2O_2 was analyzed in both the systems i.e. with and without phenol. The experiment was done at three different pH (3, 5.5 and 11).

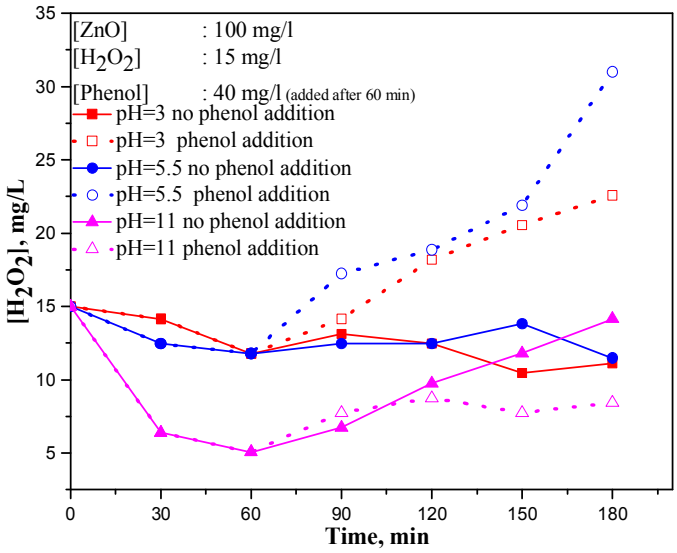

Fig. 5.18: Effect of addition of phenol (after 60 min) on the oscillation in the concentration of H_2O_2 under sonophotocatalysis

As seen in the figure, addition of phenol results in enhanced formation of H_2O_2 at pH 3 as well as 5.5. But at pH 11, where the degradation of phenol is also less, formation of $^{\bullet}OH$ radical from added phenol will be low. Hence the net concentration of H_2O_2 even after phenol addition is not much different and is even slightly less compared to the system without phenol.

5.3.7 Effect of addition of extra ZnO during the course of the sonophotocatalytic reaction on the oscillation

Effect of addition of extra amount of ZnO in to the reaction system in which the H_2O_2 formation and/or decomposition have already been in progress at different pH is investigated and the results are plotted in figure 5.19 to 5.21. Initially there was 50 mg/L of ZnO in the system and the insitu formed H_2O_2 was analyzed after 30 and 60 minutes of irradiation. After 60 minutes, the reaction solution was divided into 2 portions. In the first case irradiation (US + UV) continued without extra ZnO. In the second sample extra ZnO (50 mg/L) was added and irradiation (US + UV) continued. The analysis of H_2O_2 was done in both cases. The experiments were done at three different pH (3, 5.5 and 11).

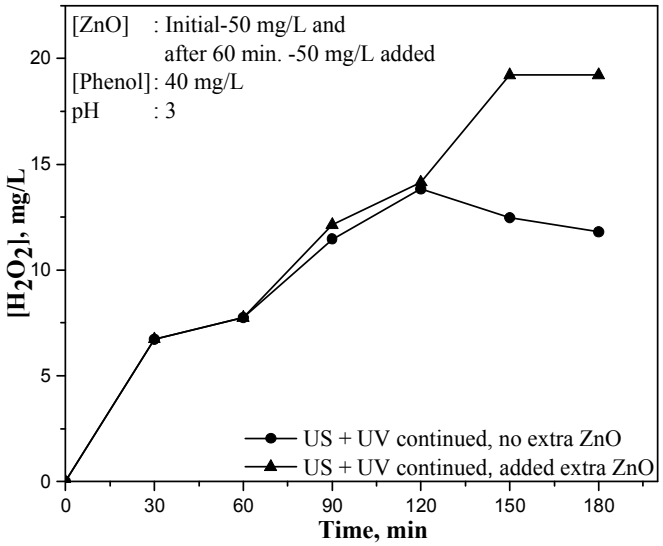

Fig. 5.19: Effect of addition of extra ZnO (after 60 min) on the oscillation in the concentration of H_2O_2 at pH=3 under sonophotocatalysis

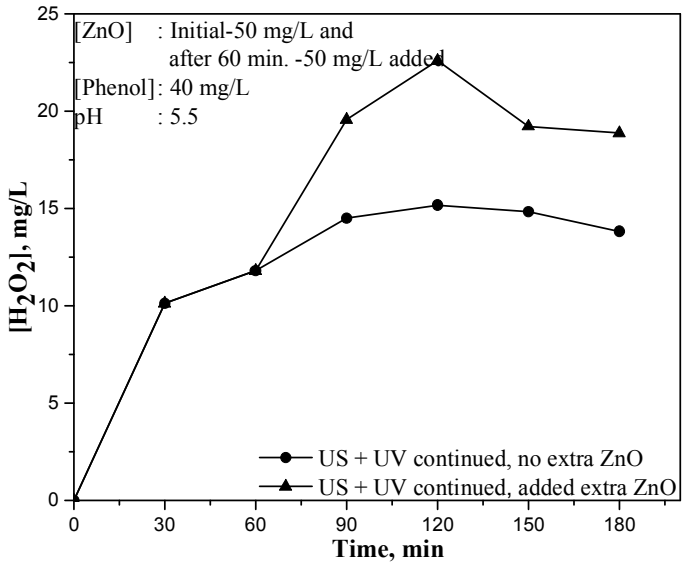

Fig. 5.20: Effect of addition of extra ZnO (after 60 min) on the oscillation in the concentration of H_2O_2 at pH= 5.5 under sonophotocatalysis

At pH 3 (figure 5.19), when irradiation was continued, H_2O_2 continued to increase for a while and then decreased gradually. When extra ZnO was added and the irradiation was continued, H_2O_2 increased sharply and then got stabilized.

At pH 5.5 (figure 5.20), when the irradiation was continued without extra ZnO, the H_2O_2 concentration initially increased and then got stabilized. When extra ZnO was added and irradiation was continued, the concentration of H_2O_2 increased sharply, then decreased slightly and got stabilized as in the case of typical oscillation.

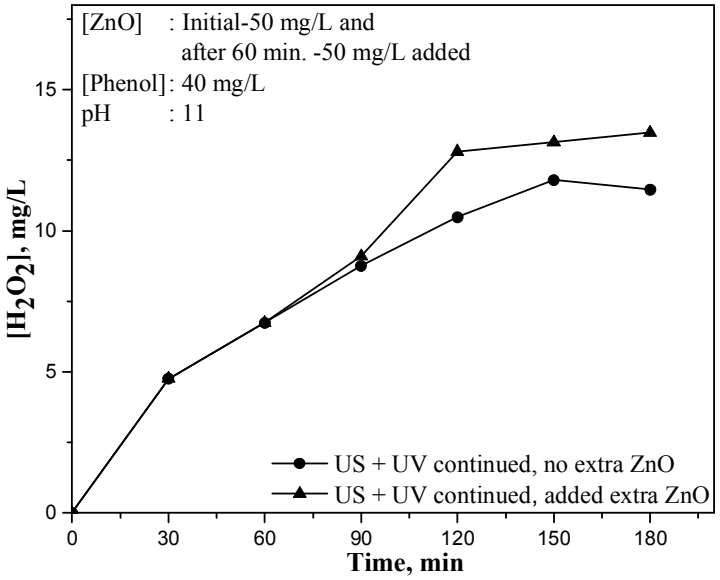

Fig. 5.21: Effect of addition of extra ZnO (after 60 min) on the oscillation in the concentration of H_2O_2 at pH= 11 under sonophotocatalysis

At pH 11 (figure 5.21), continuing the irradiation with no extra ZnO addition, results in increase in the net concentration of H_2O_2 and stabilization thereafter. But when extra ZnO was added and irradiation was continued sharp increase in the net concentration of H_2O_2 occurs with stabilization thereafter. This trend is almost same as at pH 3 and 5.5. The results also show that even at alkaline pH where the degradation of phenol is less, extra ZnO can generate more $^{\bullet}OH$ radicals and these radicals combine to form more H_2O_2.

Thus it is seen that irrespective of pH, addition of ZnO results in enhancement in the net concentration of H_2O_2 under sonophotocatalysis. This can be explained in terms of the availability of extra surface sites for the formation of more ROS and effective interaction.

5.3.8 Effect of externally added H_2O_2

Decomposition of H_2O_2, externally added or insitu formed, results in production more $^{\bullet}OH$ radicals which can accelerate the degradation of phenol. This possibility is tested by externally adding H_2O_2 in to the sonophotocatalytic reaction system. The fate of the net H_2O_2 (including the externally added) in the system also is verified. The effect of added H_2O_2 on the phenol degradation is shown in figure 5.22.

As expected, the enhanced number of free radicals generated from the decomposition of added H_2O_2 results in enhanced phenol degradation. The fate of net H_2O_2 (added + concurrently formed) is shown in figure 5.23.

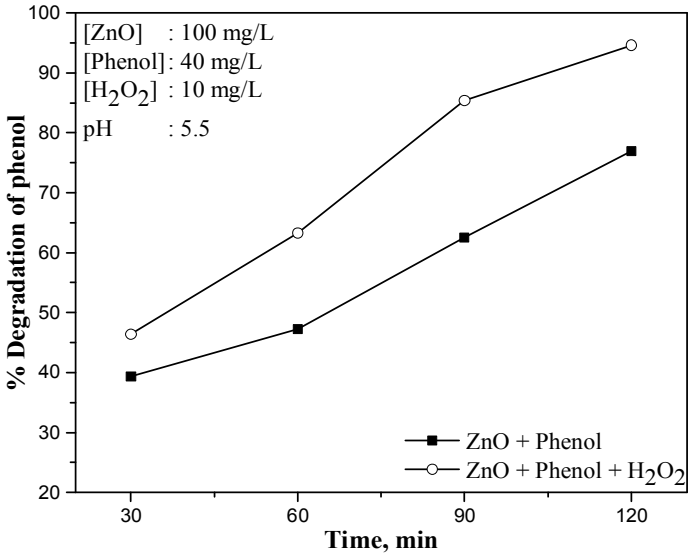

Fig. 5.22: Effect of added H_2O_2 on the sonophotocatalytic degradation of phenol

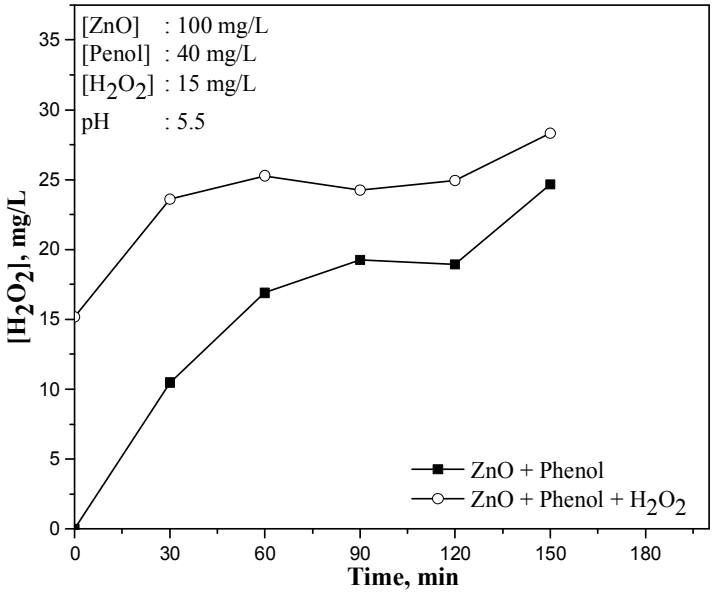

Fig. 5.23: Effect of added H_2O_2 on the net concentration of H_2O_2 under sonophotocatalysis

In sonophotocatalysis, the rates of degradation of phenol and the corresponding formation of H_2O_2 are much higher compared to sono or photo catalysis. Hence the initial decrease in the concentration of added H_2O_2 by decomposition is more than compensated by the higher formation rate. Consequently, the concentration of H_2O_2 increases fairly steeply in the beginning, stabilizes and again increases. The sharp increase in the concentration of H_2O_2 in the case of the system with no added H_2O_2 towards later stages of reaction is possibly due to the domination of the formation process at that point in time. Eventually the concentration of H_2O_2 becomes comparable in both cases as is in the case of many other similar situations reported in earlier chapters. Hence in the case of externally added H_2O_2, once the more dominant decomposition process has brought its concentration down to or stabilized at moderate

level, the system behaves similar to those cases in which there is no externally added H_2O_2. This is further verified by adding H_2O_2 in between to a reaction in progress as explained in the following sections.

5.3.9 Effect of addition of H_2O_2 during the course of the sonophotocatalytic reaction on the oscillation

Effect of addition of H_2O_2 (after 60 minutes) to the reaction in progress at different pH is shown in figure 5.24. Initially the system had only insitu formed H_2O_2. After 60 minutes, 10 mg/L of H_2O_2 was added externally. Fate of the total amount of H_2O_2 was analyzed at different pH.

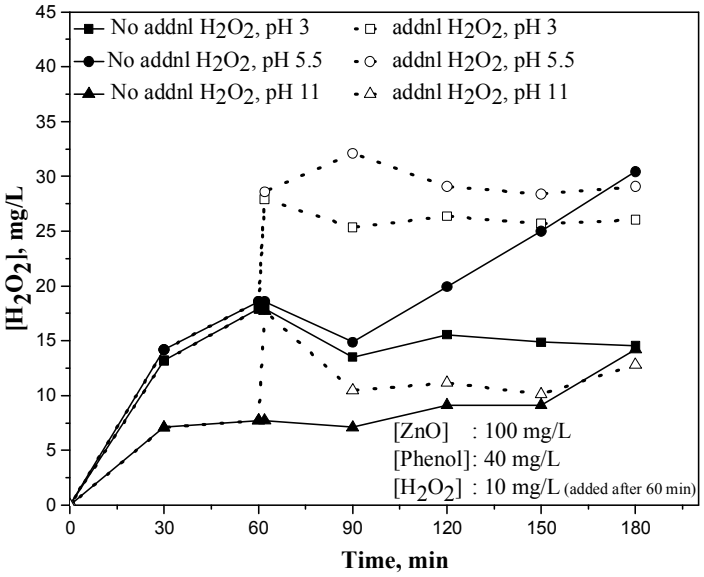

Fig. 5.24: Effect of addition of H_2O_2 (after 60 min) on the oscillation its concentration under sonophotocatalysis

With the addition of extra H_2O_2 to the system the net H_2O_2 concentration was higher. Thereafter the concentration of H_2O_2 remained fairly steady at pH 3 and 5.5 even though fresh H_2O_2 also was generated insitu in the system. At pH 11 net concentration of H_2O_2 decreases steeply indicating the domination of the decomposition process. In all three cases of added H_2O_2, the net concentration is stabilized at later stages thereby confirming that the formation and decomposition process occurs at more or less same rate. The concentration of H_2O_2 levels off (after the addition of extra H_2O_2) probably because at such high concentration, the formation and decomposition processes are balancing each other.

5.3.10 Role of O_2/air in sonophotocatalysis

It has been proven that dissolved oxygen plays an important role in photocatalysis by scavenging the electrons generated on photoactivated ZnO.

$$e^- + O_2 \rightarrow O_2^{-\bullet} \quad \text{..... (132)}$$

$$O_2 + 2e_{cb}^- + 2H^+ \rightarrow H_2O_2 \quad \text{..... (133)}$$

This will reduce the recombination of photoproduced electrons and holes and hence both will be available for the formation of free radicals and interaction with the pollutant. In order to confirm the effect of O_2/air on the sonophotocatalytic degradation of phenol, the standardized reaction system is deaerated with N_2 and subjected to simultaneous sono and photo irradiation. The results are plotted in figure 5.25.

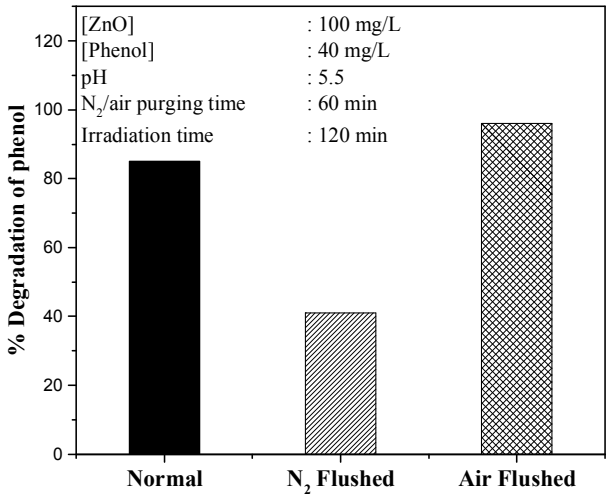

Fig. 5.25: Effect of O_2 on the sonophotocatalytic degradation of phenol

Degradation of phenol slows down in presence of nitrogen (absence of O_2) while it increases in the air flushed system. This reconfirms the role O_2 in the sonophotocatalytic degradation of phenol which can be explained as in Chapter 3 section 3.3.11. The effect of O_2 on the sonophotocatalytic formation/decomposition (oscillation) of H_2O_2 is shown in figure 5.26.

The concentration of H_2O_2 generated is much less in the N_2 flushed system, as expected due to the low rate of degradation of phenol and consequent decrease in H_2O_2 formation. The concurrent decomposition of H_2O_2 as explained earlier can reduce the concentration further. Hence the net amount of H_2O_2 is significantly less in the absence of O_2. H_2O_2 also functions as a hole scavenger and decomposes in the process as follows:

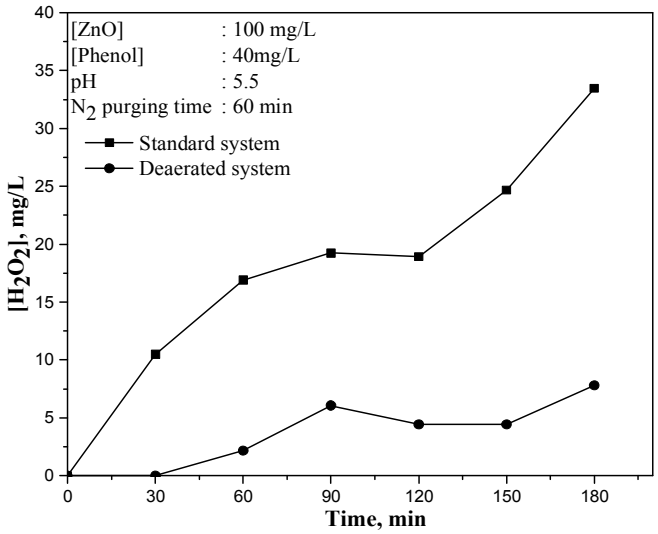

Fig. 5.26: Effect of deaeration with nitrogen on the oscillation in the concentration of H_2O_2 under sonophotocatalysis

$$H_2O_2 + {}^{\bullet}OH/h^+ \rightarrow HO_2^{\bullet} + H_2O/H^+ \quad \text{..... (134)}$$

These factors together contribute to the sharp decrease in the concentration of H_2O_2 in the absence of O_2.

5.3.11 Corrosion of ZnO under sonophotocatalysis

One of the reasons cited often for the preference given to TiO_2 over ZnO as a photocatalyst is the corrosion of the latter under acidic conditions and photo irradiation. In this context, the possible corrosion of ZnO at different pH was studied under sono and photo catalysis and the results were summarized in Chapters 3 and 4 sections 3.3.13 and 4.3.11 respectively. The corrosion of ZnO under sonophotocatalytic condition is also investigated. The experimental procedure was same as discussed

earlier. Figure 5.27 shows the corrosion of ZnO at different pH in the presence as well as in the absence of irradiation (US + UV).

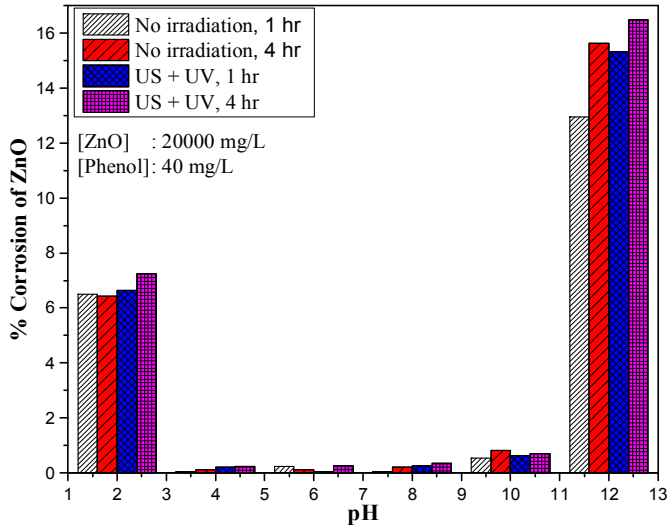

Fig. 5.27: Corrosion of ZnO at different pH in the presence and absence of (US + UV) irradiation

As in the case of sono and photocatalysis, the corrosion is negligible in the pH range 4 to 10 with or without irradiation. However, there is significant corrosion after 4 hours i.e., ~ 6% and ~ 15% at pH 2 and 12 respectively. Similar to sono and photo catalytic results irradiation did not enhance the corrosion significantly, at least during the short period of study. Since all major investigations reported here are carried out at the optimized pH of 5.5, corrosion can be considered negligible under the conditions of the study.

5.3.12 Memory effect

In sono as well as photo catalysis it was observed that semiconductors can retain the irradiation effect for some more time and continue the

formation of electron/hole pairs. This phenomenon termed as 'memory effect' is examined in sonophotocatalysis too and the results are shown in figure 5.28.

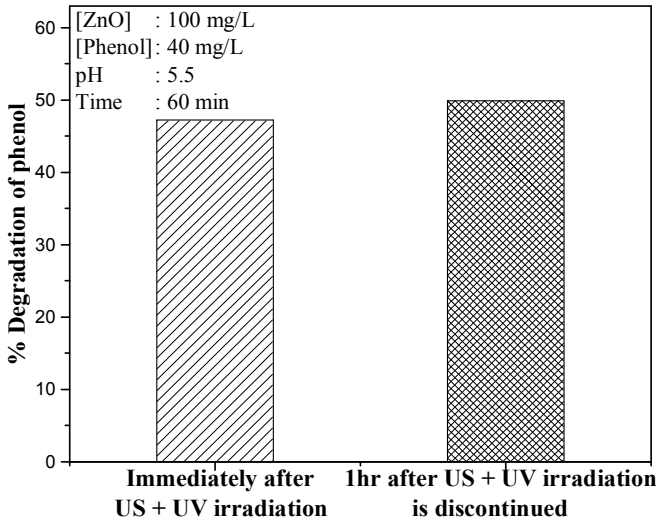

Fig. 5.28: Effect of discontinuing (US + UV) irradiation on the phenol degradation

From the figure it is clear that degradation of phenol continued for little more time when the irradiation source is cut off indicating a possible slight memory effect. Although the efficiency of the memory effect is not significant in this case, the phenomenon needs in-depth investigation because, once confirmed and optimized it has the potential for the decontamination of polluted water or other similar systems for longer duration even after the source of energy is turned off. Fate of H_2O_2 was also examined after the irradiation source was turned off and the results are shown in figure 5.29.

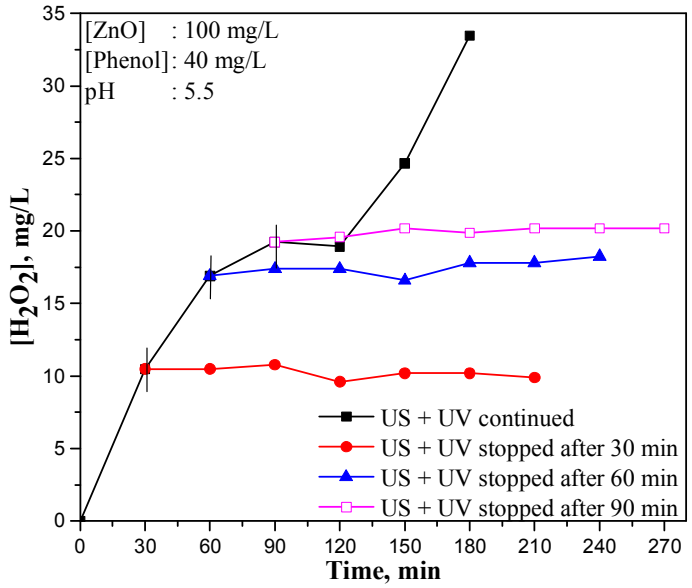

Fig. 5.29: Effect of discontinuing (US + UV) irradiation on the oscillation in the concentration of H_2O_2

The concentration of H_2O_2 remains steady once the US/UV is put off. Hence the memory effect is not seen here. Since the net concentration of H_2O_2 is relatively higher in sonophotocatalysis, it is also possible that marginal change in its concentration as a result of memory effect may not be quite distinct as in the case of sono and photo catalysis.

5.4 Mechanism of the process

Mechanism of photo and sono catalytic degradation of phenol was explained in detail in Chapters 3 and 4 respectively. The overall mechanism of sonophotocatalytic process leading to the formation of ROS and the degradation of phenol is a combination of the two processes and is schematically presented in figure 5.30.

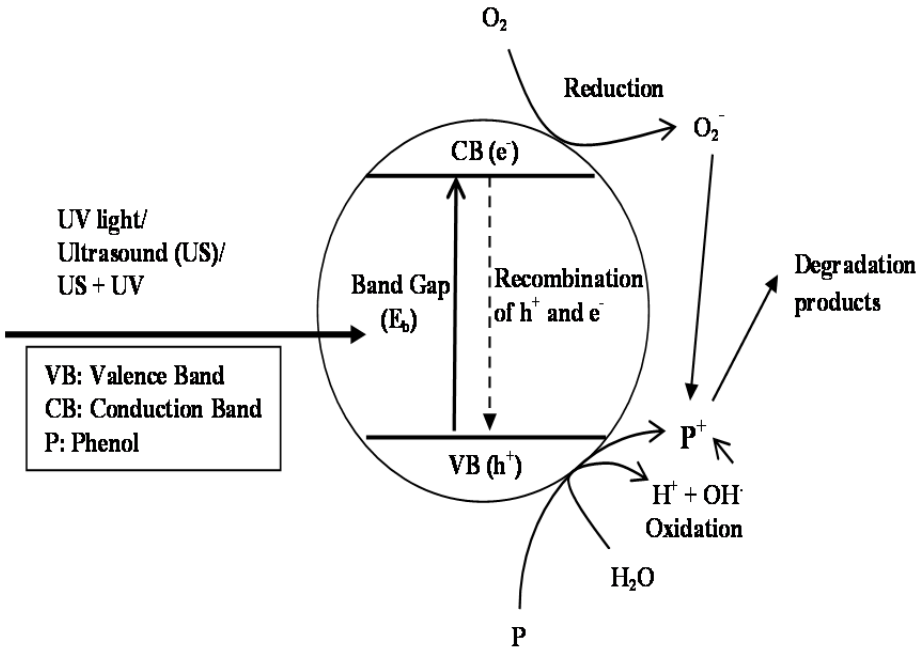

Fig. 5.30: Sonophotocatalytic activation of semiconductor oxides and the formation of ROS

The synergy of sonophotocatalysis shows the interplay of features involved in sonolysis and photolysis favoring enhanced degradation which the two processes cannot provide individually. The mechanism of synergy can be briefly explained as follows:

As already explained sonolysis of water produces active radicals $H^{\bullet}$ and $^{\bullet}OH$ via cavitation and leads to a series of chain reactions as follows [73].

$$H_2O + >>> \rightarrow H^{\bullet} + {}^{\bullet}OH \quad \text{..... (135)}$$

$$H^{\bullet} + {}^{\bullet}OH \rightarrow H_2O \quad \text{..... (136)}$$

$$^{\bullet}OH + {}^{\bullet}OH \rightarrow H_2O_2 \quad \text{..... (137)}$$

$$2{}^{\bullet}OH \rightarrow H_2O + O^{\bullet} \quad \text{..... (138)}$$

Further, the following reactions can occur in the presence of oxygen.

$O_2 \rightarrow 2^{\bullet}O$ ..... (139)

$O_2 + {}^{\bullet}O \rightarrow O_3$ ..... (140)

$O_2 + {}^{\bullet}H \rightarrow {}^{\bullet}O_2H$ (or $O + {}^{\bullet}OH$) ..... (141)

${}^{\bullet}O + {}^{\bullet}O_2H \rightarrow {}^{\bullet}OH + O_2$ ..... (142)

${}^{\bullet}O + H_2O \rightarrow 2^{\bullet}OH$ ..... (143)

$2^{\bullet}O_2H \rightarrow H_2O_2 + O_2$ ..... (144)

The free radicals thus produced can take part in the degradation of phenol as follows:

Reactive oxygen species (${}^{\bullet}OH$, $HO_2{}^{\bullet}$etc) + phenol →
Intermediates → $H_2O + CO_2$ ..... (145)

The photocatalytic degradation of phenol already explained in Chapter 3 proceeds as follows [140]:

$ZnO + UV \rightarrow e_{cb}^{-} + h_{vb}^{+}$ ..... (146)

Formation of primary reactive radicals by valence band holes

$h^{+} + OH^{-} \rightarrow {}^{\bullet}OH$ ..... (147)

$h^{+} + H_2O \rightarrow {}^{\bullet}OH + H^{+}$ ..... (148)

Scavenging of conduction band electrons

$e^{-} + O_2 \rightarrow O_2^{-\bullet}$ ..... (149)

Formation of multiple peroxide species

$H^{+} + O_2^{-\bullet} \rightarrow HO_2^{\bullet}$ ..... (150)

$$HO_2^{\bullet} + e^- + H^+ \rightarrow H_2O_2 \quad \text{..... (151)}$$

These radicals will react with phenol as in equation (145).

The ozone produced in reaction 140 can also promote the degradation of phenol in combination with UV via the direct and indirect production of hydroxyl radicals.

$$O_3 + h\nu \rightarrow O_2 + O \quad \text{..... (152)}$$

$$O + H_2O \rightarrow {}^{\bullet}OH + {}^{\bullet}OH \quad \text{..... (153)}$$

$$O + H_2O \rightarrow H_2O_2 \quad \text{..... (154)}$$

$$H_2O_2 + h\nu \rightarrow {}^{\bullet}OH + {}^{\bullet}OH \quad \text{..... (155)}$$

The major component in sonophotocatalysis is the photocatalysis. US induced sonoluminescence and consequent photocatalysis has been discussed in Chapter 4 section 4.4. However beyond an optimum dosage of the catalyst, the particles get agglomerated and light cannot penetrate into the entire catalyst surface. However in presence of US, the agglomerated particles are deagglomerated constantly, thereby exposing more and more fresh surface sites to the US and UV. The effect is equivalent to having fresh highly active catalyst surface throughout and this leads to higher activity. Hence the combination of (US + UV) provides extra activity in addition to the individual effects and this leads to synergy.

H_2O_2 is a by-product/intermediate in the degradation of phenol under sono, photo and sonophoto catalysis. The simultaneous formation and decomposition process of H_2O_2 was already discussed in Chapter 3 and 4. Various steps involved in the formation and decomposition of

H_2O_2, some of which were already discussed earlier, are summarized below:

Formation of H_2O_2:

$$^{\bullet}OH + {}^{\bullet}OH \rightarrow H_2O_2 \quad \text{.....(156)}$$

$$O_2 + 2e_{cb}^- + 2H^+ \rightarrow H_2O_2 \quad \text{.....(157)}$$

$$2H_2O + 2h_{vb}^+ \rightarrow H_2O_2 + 2H^+ \quad \text{.....(158)}$$

$$O_2^{-\bullet} + H^+ \rightarrow HO_2^{\bullet} \quad \text{.....(159)}$$

$$HO_2^{\bullet} + HO_2^{\bullet} \rightarrow H_2O_2 + O_2 \quad \text{..... (160)}$$

$$O_2^{-\bullet} + HO_2^{\bullet} \rightarrow O_2 + HO_2^{-\bullet} \quad \text{..... (161)}$$

$$HO_2^{-\bullet} + H^+ \rightarrow H_2O_2 \quad \text{..... (162)}$$

Decomposition of H_2O_2:

$$H_2O_2 + US/UV \rightarrow 2^{\bullet}OH \quad \text{..... (163)}$$

$$h_{vb}+ + H_2O_2 \rightarrow O_2 + 2\ H^+ \quad \text{..... (164)}$$

$$H_2O_2 + {}^{\bullet}OH \rightarrow H_2O + HO_2^{\bullet} \quad \text{..... (165)}$$

$$e_{cb}^- + 2\ H^+ + H_2O_2 \rightarrow 2\ H_2O \quad \text{..... (166)}$$

$$H_2O_2 + HO_2^{\bullet} \rightarrow H_2O + {}^{\cdot}OH + O_2 \quad \text{..... (167)}$$

The formation and decomposition of H_2O_2 proceeds in parallel after buildup of a critical initial concentration. The same free radicals can contribute to the formation and/or decomposition of H_2O_2 depending on the conditions. At the same time, being a complex free radical system, many other reactive species also may be possible, especially in sonophotocatalysis, resulting in more interactions leading to the formation and decomposition of H_2O_2. Depending on the concentration of the substrate and H_2O_2 at any point of time, either of the process will dominate. However, unlike in the

case of sono or photo catalysis, the oscillation in the concentration of H_2O_2 is not very sharp and the number of crests and troughs is less. This may be because, the formation process is more dominant in sonophotocatalysis due to the higher degradation of phenol. The decomposition can at best equal the formation which results in stabilization. Hence, the oscillation is not quite distinct in this case.

5.5 Conclusions

The sonophotocatalytic degradation of phenol in the concurrent presence of UV and US is more than the sum of the degradation under photocatalysis and sonocatalysis, which confirms the synergy of the process. The oscillation in the concentration of H_2O_2 observed in the case of sono and photo catalysis is less evident in sonophotocatalysis probably due to the accelerated rate of formation compared to decomposition. The net concentration of H_2O_2 in the system at any point of time is in the order; sono < photo < sonophoto. Various parameters such as catalyst loading, substrate concentration, particle size, pH, externally added H_2O_2 and presence of air/O_2 influence the concentration and behavior of H_2O_2. A suitable reaction mechanism is proposed and discussed.

Chapter 6

EFFECT OF SALTS/IONS ON THE PHOTO, SONO AND SONOPHOTO CATALYTIC DEGRADATION OF PHENOL AND OSCILLATION IN THE CONCENTRATION OF H_2O_2 FORMED INSITU

Contents

6.1 Introduction

Photo, sono and sonophoto catalytic degradation of phenol in presence of ZnO and the effect of various parameters on the same are discussed in detail in Chapter 3 to 5. The fate of insitu formed H_2O_2 also is investigated and discussed. In this context, the impact of the presence of natural and man-made contaminants in water, especially the salts, on the efficiency of the process is investigated and discussed in detail in this chapter. Some reports in literature show that the photocatalytic degradation of many organic compounds in water is inhibited by inorganic salts [22, 24, 32, 154]. The degree of inhibition depends on a number of parameters such as nature of the substrate, nature of the salt and its concentration, pH etc. Possible mechanisms for the inhibition involve competitive adsorption of the anion, scavenging of reactive $^{\bullet}OH$ free radicals, decreased irradiation

effects etc. At the same time presence of certain anions has been shown to increase the photo, sono and sonophoto catalytic degradation of water pollutants. Gogate et al. [5, 155] and Mahamuni and Pandit [65] reported that sonochemical degradation of phenol is enhanced in presence of Cl^- ions. Minero et al. [156] also demonstrated the enhancement of the sonochemical degradation of dyes by inorganic anions. Suspended particles which are known to influence the sonication effects may complicate the effect of anions. However, the effect of anions on the sono and sonophoto catalytic degradation of water pollutants and the fate of insitu formed H_2O_2 have not been investigated in detail so far. This gap is addressed in our study and reported in this chapter.

The effect of various anions such as acetate (CH_3COO^-), fluoride (F^-), chloride (Cl^-), nitrate (NO_3^-), sulphate (SO_4^{2-}), carbonate (CO_3^{2-}), bicarbonate (HCO_3^-) and phosphate (PO_4^{3-}) on the photo, sono and sonophoto catalytic degradation of phenol and insitu formed H_2O_2 is studied in detail here. The role of respective cations such as Na^+, K^+, Mg^{2+}, Ca^{2+} and Al^{3+} also is investigated. However, in the case of cations, the study is only preliminary and there is scope for further in-depth investigation on the effect.

6.2 Experimental details

6.2.1 Materials used

The sources of materials used and their characteristics are the same as provided in Chapters 3, 4 and 5 sections 3.2.1, 4.2.1 and 5.2.1. Chemicals other than those used in Chapters 3 to 5 are CH_3COONa, NaF, NaCl, Na_2SO_4, $NaNO_3$, Na_2CO_3, $NaHCO_3$, Na_3PO_4, KCl, $MgCl_2$, $CaCl_2$,

$AlCl_3$, K_2SO_4, $MgSO_4$, $CaSO_4$, $Al_2(SO_4)_3$, KNO_3, $Mg(NO_3)_2$, $Ca(NO_3)_2$ and $Al(NO_3)_3$. They were of AnalaR grade or equivalent from Merck India Ltd.

6.2.2 Analytical procedures

Equipment used and the analytical procedures are also the same as described in Chapters 3, 4 and 5 section 3.2.2, 4.2.2 and 5.2.2.

6.2.3 Experimental set up

The photo, sono and sonophoto catalytic experiments were done in the same way as described in previous chapters, under sections 3.2.5, 4.2.3 and 5.2.3 respectively. The experiments were performed using aqueous solution of phenol of desired concentration. Specified quantity of the catalyst is suspended in the solution. Required quantities of various salt solutions were added to the reaction suspension such that the concentration of various components is as desired. Rest of the experimental procedures, sampling and analysis methods, etc. are the same as described in Chapters 3, 4 and 5.

6.3 Results and discussion

6.3.1 Preliminary results

Degradation of phenol under photo, sono and sonophoto catalytic conditions was investigated in presence of anions: CH_3COO^-, F^-, Cl^-, NO_3^-, SO_4^{2-}, CO_3^{2-}, HCO_3^- and PO_4^{3-} at various concentrations (of the anion) and different times of irradiation. The cation was kept the same in all cases, i.e., Na^+. The effect of these anions at two typical concentrations, i.e. 2 and 10 mg/L on the photo, sono and sonophoto catalytic degradation of phenol is shown in figure 6.1 to 6.3.

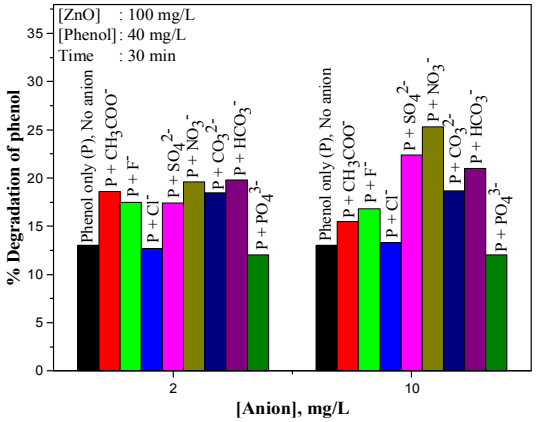

Fig. 6.1: Effect of various anions on the photocatalytic degradation of phenol

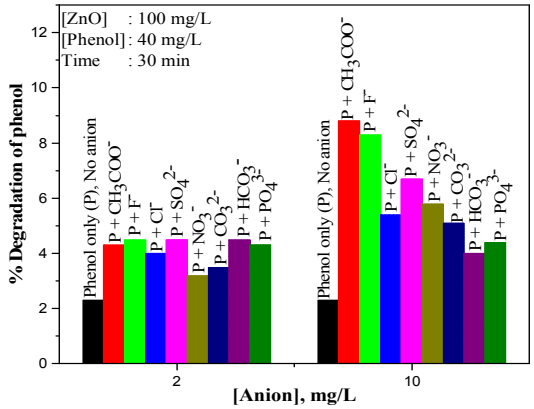

Fig. 6.2: Effect of various anions on the sonocatalytic degradation of phenol

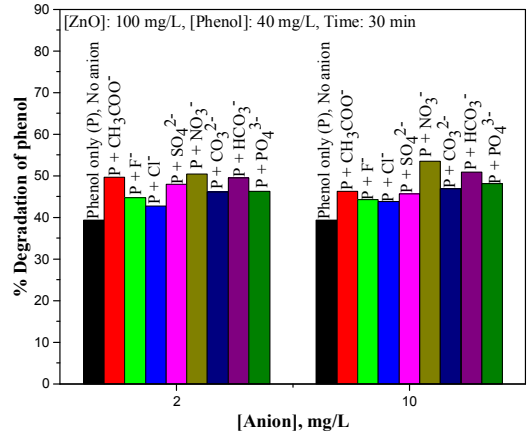

Fig. 6.3: Effect of various anions on the sonophotocatalytic degradation of phenol

In photocatalysis all ions except Cl^- and PO_4^{3-} enhance phenol degradation. Surprisingly, all the anions enhance the sonocatalytic

degradation of phenol. In sonophotocatalysis all ions slightly enhance the degradation. This is contrary to the results reported by many investigators according to which, the degradation is inhibited by anions. Such inhibition is explained based on the reduced availability of surface sites for adsorption of the substrate due to competition from the anions. The anions are also known to scavenge the ROS, especially $^{\bullet}OH$, which also could cause the inhibition of the degradation of phenol. However in the present instance, the degradation rate increased in the presence of anions. Here the effect warranted detailed investigation. The anion effect is examined in detail at different concentrations and extended reaction times and the results are as follows:

6.3.2 Effect of concentration of anions and reaction time on phenol degradation

6.3.2.1 Photocatalysis

The effect of various anions on the photocatalytic degradation of phenol is investigated in detail and the results are plotted in figures 6.4 to 6.11.

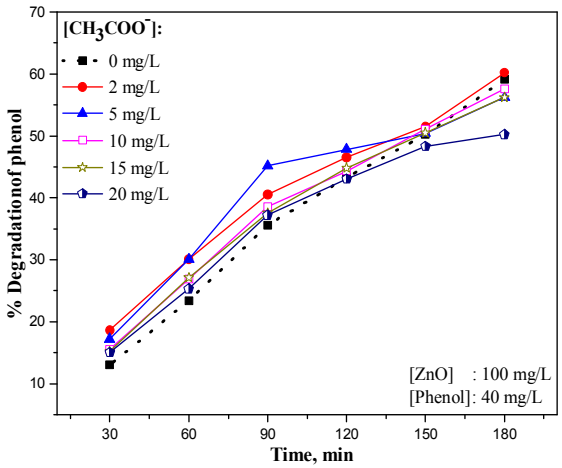

Fig. 6.4: Effect of CH_3COO^- ions on the photocatalytic degradation of phenol

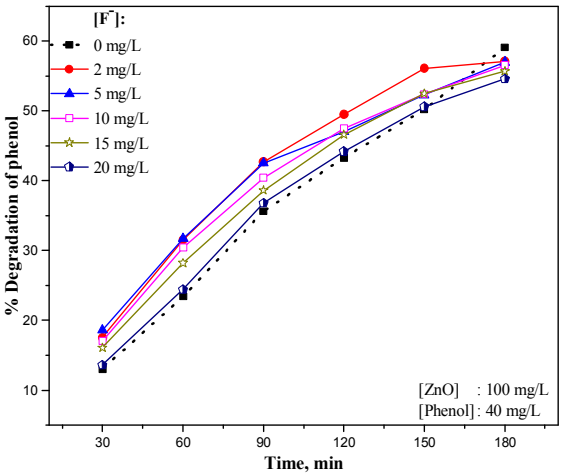

Fig. 6.5: Effect of F^- ions on the photocatalytic degradation of phenol

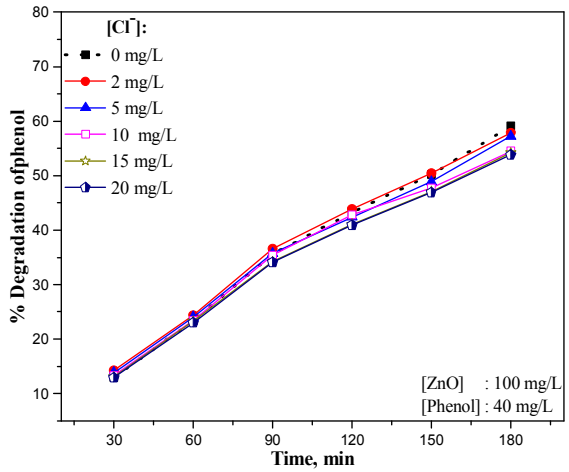

Fig. 6.6: Effect of Cl^- ions on the photocatalytic degradation of phenol

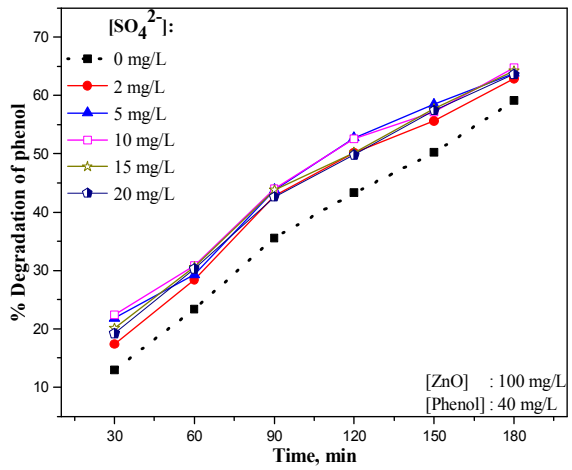

Fig. 6.7: Effect of SO_4^{2-} ions on the photocatalytic degradation of phenol

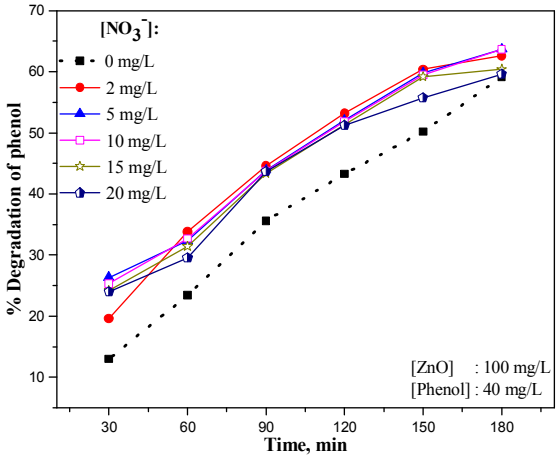

Fig. 6.8: Effect of NO_3^- ions on the photocatalytic degradation of phenol

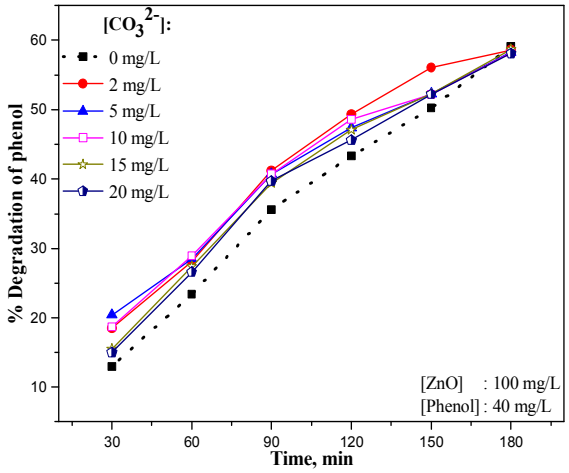

Fig. 6.9: Effect of CO_3^{2-} ions on the photocatalytic degradation of phenol

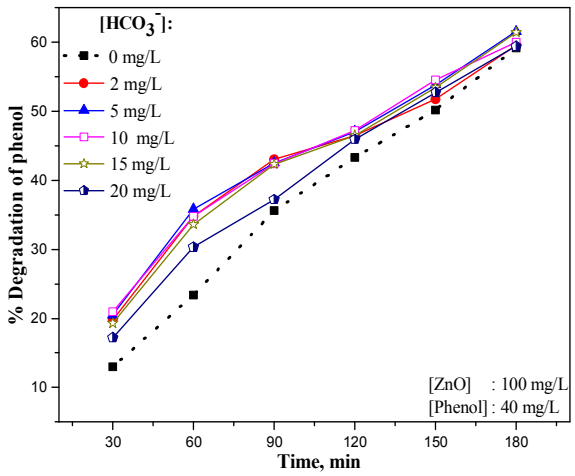

Fig. 6.10: Effect of HCO_3^- ions on the photocatalytic degradation of phenol

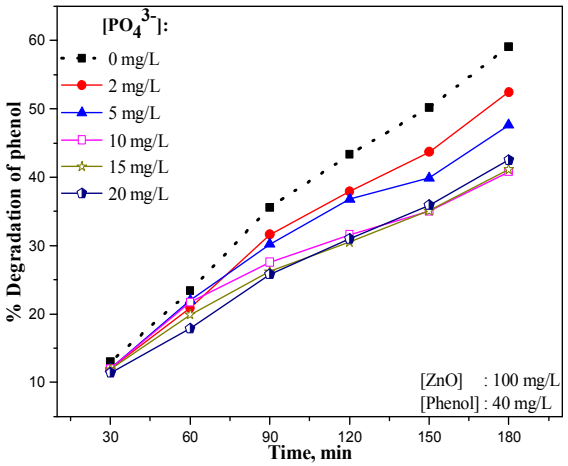

Fig. 6.11: Effect of PO_4^{3-} ions on the photocatalytic degradation of phenol

In the case of photocatalysis, the degradation of phenol increases initially with increase in concentration of the anion except in the case of PO_4^{3-}. The degree of enhancement at various concentrations and different reaction times is shown in table 6.1. The optimum enhancement is generally at ~ 5 to 10 mg/L of the anion (except for PO_4^{3-}). However as the reaction progresses the advantage of this concentration range is not sustained. After ~ 120 minutes of irradiation, the degradation of phenol is more or less the same irrespective of the concentration of the anion in many cases. In the case of Cl^- ion, in the early stages of reaction (up to 90 minutes) there is mild enhancement at lower concentration of 2 to 5 mg/L. As reaction proceeds, Cl^- shows a slight inhibitory effect at higher concentrations (10 to 20 mg/L). In the case of PO_4^{3-} ion, as concentration of ion and reaction time increases, inhibitory effect also increases.

As seen from the figures 6.4 to 6.11 as well as tables 6.1 and 6.2, the degree of enhancement slows down with time in the case of all anions. The effect of concentration of the anion on the enhancement is only moderate and follows fairly consistent pattern except in the case of Cl^- and PO_4^{3-}. However, it can be generally concluded that all anions (except Cl^- and

PO_4^{3-}) at lower concentrations and in the initial stages of reaction enhance the photocatalytic degradation of phenol in presence of ZnO.

Table 6.1: Percentage enhancement of **photocatalytic degradation** of phenol in presence of various anions. [ZnO]: 100 mg/L, [Phenol]: 40 mg/L

Anion	Conc. of the anion (mg/L)	% enhancement after					
		30 min	60 min	90 min	120 min	150 min	180 min
CH_3COO^-	2	43.1	28.6	12.1	7.4	2.6	1.9
	5	32.3	28.6	27	10.4	0.4	-4.9
	10	19.2	14.9	8.4	2.3	1.8	-2.5
	15	16.9	15.8	5.3	3.5	0.6	-4.9
	20	15.4	8.1	4.5	-0.69	-3.8	-15.1
F^-	2	34.6	34.6	19.9	14.3	11.8	-3.4
	5	43.1	35.5	19.4	8.5	4.2	-3.6
	10	30.8	29.9	13.5	8.8	4.4	-4.2
	15	23.8	20.5	8.4	7.6	4.6	-5.7
	20	4.6	4.3	3.4	3.1	0.79	-7.6
Cl^-	2	9.2	4.3	2.8	1.4	0.4	-2.0
	5	6.2	2.6	0.28	-2.07	-2.6	-3.2
	10	2.3	0.0	-0.56	-1.2	-5.0	-7.8
	15	0.77	-0.43	-3.9	-5.1	-6.2	-8.3
	20	-0.77	-1.3	-4.2	-5.5	-6.6	-8.9
SO_4^{2-}	2	33.8	21.4	20.2	15.9	10.8	6.4
	5	67.7	25.2	23.4	21.7	16.5	7.95
	10	72.3	31.6	23.6	21.5	13.9	9.6
	15	54.6	30.8	23.0	15.9	14.9	8.6
	20	47.7	29.5	19.7	15.0	14.3	7.6
NO_3^-	2	50.8	44.4	25.3	22.9	20.3	5.9
	5	102.3	38.0	23.3	20.0	19.1	7.7
	10	94.6	40.3	23.0	19.6	18.5	7.7
	15	86.2	34.2	21.9	18.5	17.9	2.2
	20	84.6	26.0	22.8	18.2	11.0	0.85
CO_3^{2-}	2	42.3	20.1	15.7	13.9	11.8	-0.84
	5	56.9	21.8	14.3	9.5	4.2	-1.4
	10	43.8	23.5	14.3	12.2	4.0	-1.5
	15	19.2	17.1	10.7	8.8	4.2	-0.67
	20	15.4	13.7	11.5	5.3	4.0	-1.7
HCO_3^-	2	52.3	48.7	20.8	7.4	3.0	0.67
	5	57.7	53.0	19.4	8.5	7.2	4.1
	10	61.5	48.7	19.1	9.0	8.6	1.5
	15	48.5	50.9	18.8	7.4	6.4	3.9
	20	32.3	29.5	4.5	6.0	5.0	0.51
PO_4^{3-}	2	-7.7	-10.7	-11.2	-12.5	-12.9	-11.3
	5	-7.7	-6.0	-15.2	-15.0	-20.5	-19.5
	10	-7.7	-7.3	-22.5	-27.0	-30.3	-31
	15	-8.5	-14.9	-26.4	-29.6	-30.1	-30.5
	20	-12.4	-23.5	-27.5	-28.4	-28.5	-28.1

Negative (-) sign indicates inhibition

The effect of varying concentration of individual anions and extended reaction time on the photocatalytic degradation of phenol is summarised in table 6.2.

Table 6.2: Effect of concentration of the anion and reaction time on the **photocatalytic degradation** of phenol. [ZnO]: 100 mg/L, [Phenol]: 40 mg/L

Anions	Effect of concentration (mg/L) on initial rate*	Effect of reaction time (min)
CH_3COO^-	Moderate enhancement at all concentrations in the early stages with optimum at 2 to 5 mg/L.	Initial enhancement. Eventually slows down with no net effect at lower concentration. Inhibition at higher concentration.
F^-	Enhancement throughout. Optimum at 2 to 5 mg/L.	Initial enhancement. Slowdown later and slight inhibition at all concentration after 180 minutes.
Cl^-	Concentration has little effect.	Mild inhibition from 90 minutes onwards.
SO_4^{2-}	Enhancement throughout. Optimum at 5 to 10 mg/L.	Enhancement throughout. Degree of enhancement slows down with time.
NO_3^-	Enhancement throughout. Varying concentration > 5 mg/L has only little effect.	Enhancement throughout. Eventually stabilizes and decreases after 180 minutes.
CO_3^{2-}	Enhancement throughout. Varying concentration has only little effect.	Initial enhancement, decreases with time towards later stages of reaction and eventually 'no effect' to slight inhibition.
HCO_3^-	Enhancement throughout. Variation in concentration has little effect upto 15 mg/L.	Enhancement throughout. Degree of enhancement decreases with time at later stages. Eventually 'no effect'.
PO_4^{3-}	Inhibition throughout.	Inhibition throughout. Degree of inhibition increases with time and stabilizes at ~ 120 minutes.

* Based on the % degradation in the initial 30 to 60 minutes

The enhancement efficiency of anions at various concentrations at various times of reaction for the photocatalytic degradation of phenol is compared and presented in table 6.3

Table 6.3: Comparative efficiency of anions at various concentrations and reaction times for the enhancement of the **photocatalytic degradation** of phenol. [ZnO]: 100 mg/L, [Phenol]: 40 mg/L

Time (min)	Conc. of anion (mg/L)	Comparative efficiency of enhancement
30	2	$HCO_3^- \approx NO_3^- > CH_3COO^- \approx CO_3^{2-} > F^- \approx SO_4^{2-} > Cl^- > PO_4^{3-}$
	5	$NO_3^- > SO_4^{2-} > HCO_3^- \approx CO_3^{2-} > F^- > CH_3COO^- > Cl^- > PO_4^{3-}$
	10	$NO_3^- > SO_4^{2-} > HCO_3^- > CO_3^{2-} > F^- > CH_3COO^- > Cl^- > PO_4^{3-}$
	15	$NO_3^- > SO_4^{2-} > HCO_3^- > F^- > CO_3^{2-} \approx CH_3COO^- > Cl^- > PO_4^{3-}$
	20	$NO_3^- > SO_4^{2-} > HCO_3^- > CH_3COO^- \approx CO_3^{2-} > F^- > Cl^- > PO_4^{3-}$
60	2	$HCO_3^- > NO_3^- > F^- > CH_3COO^- > SO_4^{2-} \approx CO_3^{2-} > Cl^- > PO_4^{3-}$
	5	$HCO_3^- > NO_3^- \approx F^- > CH_3COO^- > SO_4^{2-} > CO_3^{2-} > Cl^- > PO_4^{3-}$
	10	$HCO_3^- > NO_3^- > SO_4^{2-} \approx F^- > CO_3^{2-} > CH_3COO^- > Cl^- > PO_4^{3-}$
	15	$HCO_3^- > NO_3^- > SO_4^{2-} > F^- > CO_3^{2-} \approx CH_3COO^- > Cl^- > PO_4^{3-}$
	20	$HCO_3^- \approx SO_4^{2-} > NO_3^- > CO_3^{2-} > CH_3COO^- > F^- > Cl^- > PO_4^{3-}$
90	2	$NO_3^- > HCO_3^- \approx SO_4^{2-} \approx F^- > CO_3^{2-} > CH_3COO^- > Cl^- > PO_4^{3-}$
	5	$CH_3COO^- > NO_3^- \approx SO_4^{2-} > F^- \approx HCO_3^- > CO_3^{2-} > Cl^- > PO_4^{3-}$
	10	$SO_4^{2-} \approx NO_3^- > HCO_3^- > CO_3^{2-} \approx F^- > CH_3COO^- > Cl^- > PO_4^{3-}$
	15	$SO_4^{2-} \approx NO_3^- > HCO_3^- > CO_3^{2-} \approx F^- > CH_3COO^- > Cl^- > PO_4^{3-}$
	20	$NO_3^- \approx SO_4^{2-} > CO_3^{2-} > CH_3COO^- \approx HCO_3^- \approx F^- > Cl^- > PO_4^{3-}$
120	2	$NO_3^- > SO_4^{2-} \approx F^- \approx CO_3^{2-} > CH_3COO^- \approx HCO_3^- > Cl^- > PO_4^{3-}$
	5	$SO_4^{2-} \approx NO_3^- > CH_3COO^- \approx CO_3^{2-} \approx F^- \approx HCO_3^- > Cl^- > PO_4^{3-}$
	10	$SO_4^{2-} \approx NO_3^- > CO_3^{2-} > F^- \approx HCO_3^- > CH_3COO^- > Cl^- > PO_4^{3-}$
	15	$NO_3^- \approx SO_4^{2-} > CO_3^{2-} \approx HCO_3^- \approx F^- > CH_3COO^- > Cl^- > PO_4^{3-}$
	20	$NO_3^- > SO_4^{2-} > HCO_3^- \approx CO_3^{2-} \approx F^- > CH_3COO^- > Cl^- > PO_4^{3-}$
150	2	$NO_3^- > CO_3^{2-} \approx F^- \approx SO_4^{2-} > HCO_3^- \approx CH_3COO^- \approx Cl^- > PO_4^{3-}$
	5	$NO_3^- \approx SO_4^{2-} > HCO_3^- > CO_3^{2-} \approx F^- > CH_3COO^- \approx Cl^- > PO_4^{3-}$
	10	$NO_3^- > SO_4^{2-} > HCO_3^- > F^- \approx CO_3^{2-} > CH_3COO^- > Cl^- > PO_4^{3-}$
	15	$NO_3^- > SO_4^{2-} > HCO_3^- \approx F^- \approx CO_3^{2-} > CH_3COO^- > Cl^- > PO_4^{3-}$
	20	$SO_4^{2-} > NO_3^- > HCO_3^- \approx CO_3^{2-} > F^- > CH_3COO^- \approx Cl^- > PO_4^{3-}$
180	2	$SO_4^{2-} \approx NO_3^- > CH_3COO^- \approx HCO_3^- \approx CO_3^{2-} \approx Cl^- \approx F^- > PO_4^{3-}$
	5	$SO_4^{2-} \approx NO_3^- > HCO_3^- > CO_3^{2-} \approx F^- \approx Cl^- \approx CH_3COO^- > PO_4^{3-}$
	10	$SO_4^{2-} \approx NO_3^- > HCO_3^- \approx CO_3^{2-} \approx CH_3COO^- \approx F^- > Cl^- > PO_4^{3-}$
	15	$SO_4^{2-} > HCO_3^- \approx NO_3^- > CO_3^{2-} > CH_3COO^- \approx F^- \approx Cl^- > PO_4^{3-}$
	20	$SO_4^{2-} > NO_3^- \approx HCO_3^- \approx CO_3^{2-} > F^- \approx Cl^- > CH_3COO^- > PO_4^{3-}$

The comparative efficiency of the anions varies with their respective concentrations and reaction times. Though no general conclusions are possible, it may be stated that NO_3^- and SO_4^{2-} remains powerful enhancers throughout while Cl^-, CH_3COO^- and PO_4^{3-} are the least efficient enhancers or even inhibitors.

6.3.2.2 Sonocatalysis

The effect of varying concentration of the anion and extended reaction time on the sonocatalytic degradation of phenol is experimentally determined and is plotted in figure 6.12 to 6.19.

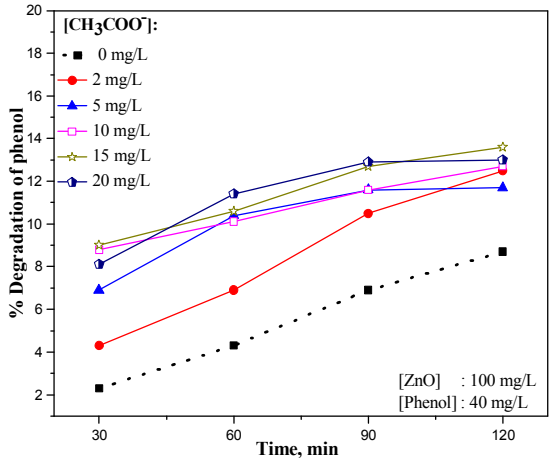

Fig. 6.12: Effect of CH_3COO^- ions on the sonocatalytic degradation of phenol

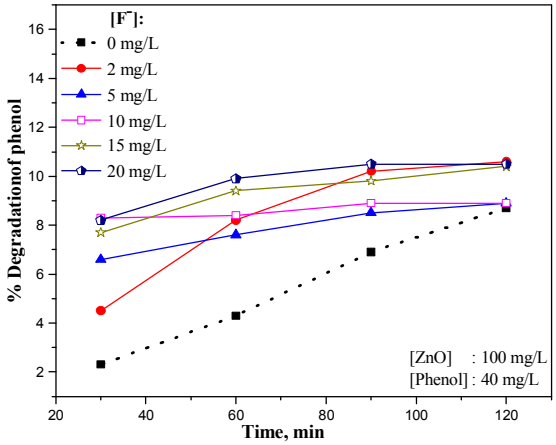

Fig. 6.13: Effect of F^- ions on the sonocatalytic degradation of phenol

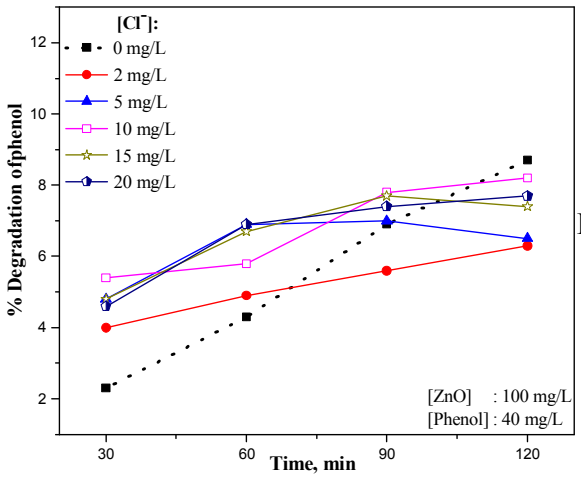

Fig. 6.14: Effect of Cl^- ions on the sonocatalytic degradation of phenol

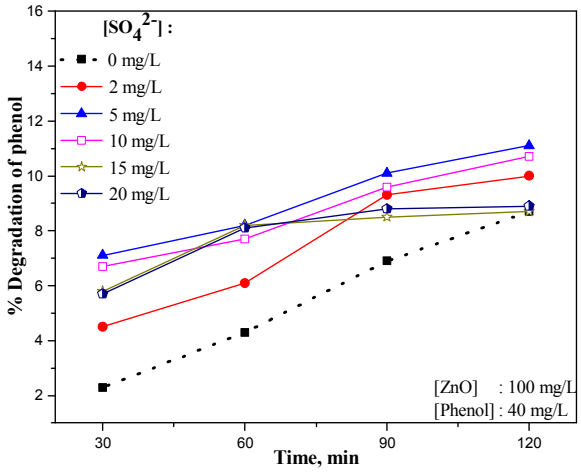

Fig. 6.15: Effect of SO_4^{2-} ions on the sonocatalytic degradation of phenol

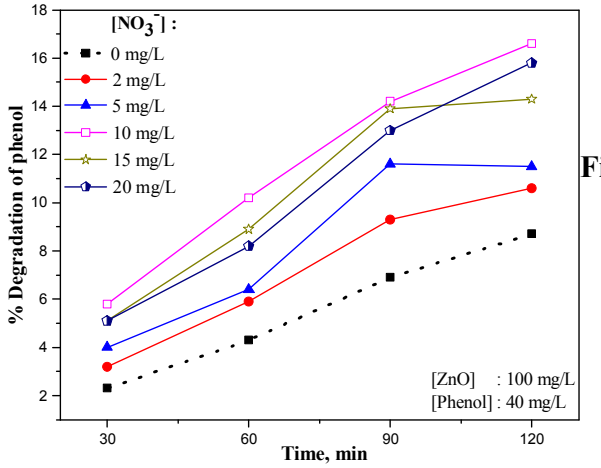

Fig. 6.16: Effect of NO_3^- ions on the sonocatalytic degradation of phenol

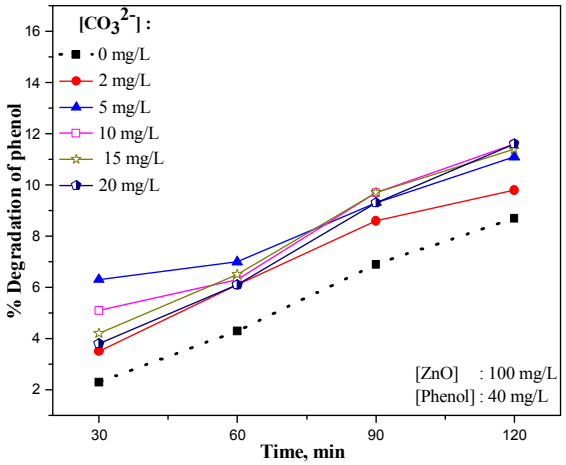

Fig. 6.17: Effect of CO_3^{2-} ions on the sonocatalytic degradation of phenol

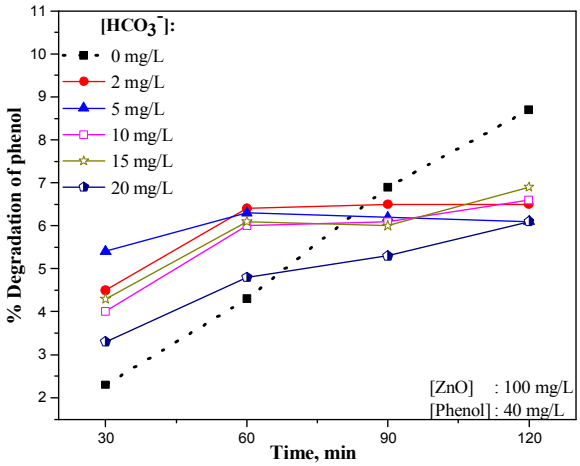

Fig. 6.18: Effect of HCO_3^- ions on the sonocatalytic degradation of phenol

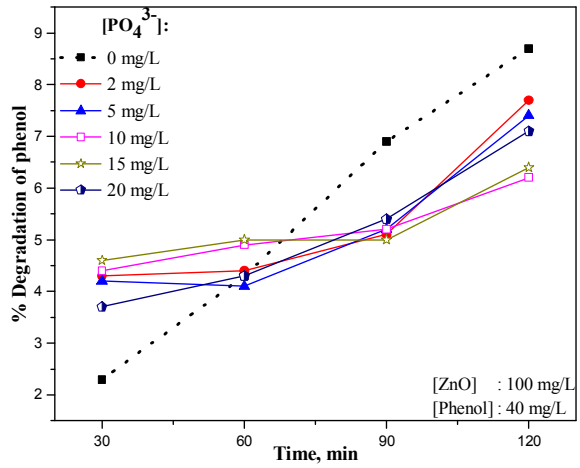

Fig. 6.19: Effect of PO_4^{3-} ions on the sonocatalytic degradation of phenol

In the case of sonocatalysis, initially the degradation of phenol increases with increase in concentration of the anions though the trend is not consistent throughout. In the case of SO_4^{2-}, CO_3^{2-} and HCO_3^- the optimum initial enhancement is seen at 5 mg/L. In the case of NO_3^-, the optimum concentration is 10 mg/L while for PO_4^{3-} it is 15 mg/L. In the case of CH_3COO^- (except for minor variations in the early and later stages) and F^-, the degradation continues to increase with increase in concentration in the range studied here with maximum ~ 20 mg/L. In the case of Cl^- the concentration effect is not consistent and fluctuates with reaction time. Beyond optimum concentration of the anion the degradation of phenol decreases/stabilizes with increase in concentration in most cases. However as the reaction progresses, the degree of enhancement slows down with time in the case of most of the anions and in the case of PO_4^{3-}, Cl^- and HCO_3^-, the enhancement gives way to inhibition towards later stages of the reaction.

The % enhancement of the sonocatalytic degradation of phenol caused by anions (over the degradation in the absence of anions under otherwise identical conditions) with increasing time of irradiation and increasing concentrations is summarized and given in table 6.4.

Table 6.4: Percentage enhancement of **sonocatalytic degradation** of phenol in presence of various anions. [ZnO]: 100 mg/L, [Phenol]: 40 mg/L

Anion	Conc. Of anion (mg/L)	% enhancement after			
		30 min	60 min	90 min	120 min
CH_3COO^-	2	86.9	60.5	52.2	43.6
	5	200	141.9	68.1	25.6
	10	282.6	106.1	68.1	25.6
	15	291.3	146.4	84.1	56.3
	20	252.2	165.1	86.9	49.4
F^-	2	95.6	90.6	47.8	21.8
	5	186.9	76.7	23.2	2.3
	10	260.9	95.3	28.9	2.3
	15	234.8	118.6	42	19.5
	20	256.5	130.2	52.2	20.7
Cl^-	2	73.9	13.9	-18.8	-27.6
	5	108.7	60.5	1.4	-25.3
	10	134.8	34.9	13.0	-5.7
	15	108.7	55.8	11.6	-14.9
	20	100.0	60.5	7.2	-11.4
SO_4^{2-}	2	95.7	41.9	34.8	14.9
	5	208.7	90.7	46.4	27.6
	10	191.3	79.1	39.1	22.9
	15	152.2	90.7	23.2	0.0
	20	147.8	88.4	27.5	2.3
NO_3^-	2	39.1	37.2	34.8	21.8
	5	73.9	48.8	34.8	32.2
	10	152.2	137.2	105.8	90.8
	15	121.7	107	101.4	64.4
	20	121.7	90.7	88.4	81.6
CO_3^{2-}	2	52.2	41.9	24.6	12.6
	5	173.9	62.8	34.8	27.6
	10	121.7	46.5	40.6	33.3
	15	82.6	51.2	40.6	31.0
	20	65.2	41.9	34.8	33.3
HCO_3^-	2	95.7	48.8	-5.8	-25.3
	5	134.8	46.5	-10.1	-29.9
	10	73.9	39.5	-11.6	-31.8
	15	86.9	41.9	-13	-20.7
	20	86.9	10.4	-23.3	-29.9
PO_4^{3-}	2	86.9	2.3	-26.1	-11.5
	5	82.6	-4.7	-24.6	-14.9
	10	91.3	13.9	-24.6	-28.7
	15	100.0	16.3	-27.5	-26.4
	20	60.9	0.0	-21.7	-18.4

Negative (-) sign indicates inhibition

The effect of varying concentration of individual anions and extended reaction time on the sonocatalytic degradation of phenol is summarised in Table 6.5

Table 6.5: Effect of concentration of the anion and reaction time on the **sonocatalytic degradation** of phenol. [ZnO]: 100 mg/L, [Phenol]: 40 mg/L

Anions	Effect of concentration (mg/L) on initial rate*	Effect of reaction time (min)
CH_3COO^-	Enhancement throughout. Degree of enhancement increases with increase in concentration. Optimum at 15 mg/L.	Enhancement throughout. Degree of enhancement slows down with time.
F^-	Enhancement throughout. Degree of enhancement increases with increase in concentration initially.	Enhancement throughout. Degree of enhancement slows down with time.
Cl^-	Initial enhancement with optimum at 10 mg/L.	Degree of enhancement slows down with time. Eventually the enhancement gives way to inhibition after ~ 90/120 minutes.
SO_4^{2-}	Enhancement throughout. Optimum at 5 mg/L.	Enhancement throughout. Degree of enhancement decreases with time at all concentrations.
NO_3^-	Enhancement throughout. Optimum at 10 mg/L.	Enhancement throughout. Degree of enhancement slows down with time.
CO_3^{2-}	Enhancement throughout. Optimum at 5 mg/L.	Enhancement throughout. Concentration effect fluctuates with time. Degree of enhancement decreases with time.
HCO_3^-	Initial enhancement with optimum at 5 mg/L.	Enhancement gives way to Inhibition by ~ 90 minutes.
PO_4^{3-}	Initial enhancement with optimum at 15 mg/L.	Enhancement gives way to Inhibition after ~ 60 minutes.

* Based on the % degradation in the initial 30 to 60 minutes

As seen from the figure 6.12 to 6.19 and table 6.4 and 6.5 almost all anions enhance sonocatalytic degradation of phenol at least in the initial stages. The effect of concentration of the anion on the enhancement does not follow any strictly consistent pattern and the optimum is varying in the range

of 5 to 15 mg/L in most of the cases. With extended reaction time the degree of enhancement decreases and the effect of Cl^-, $HCO_3^-$and PO_4^{3-} changes from enhancement to inhibition towards later stages of reaction.

Based on the data given above, the enhancement efficiency of different anions for the sonocatalytic degradation of phenol is compared and presented in table 6.6.

Table 6.6: Comparative efficiency of anions at various concentrations and reaction times for the enhancement of the **sonocatalytic degradation** of phenol. [ZnO]: 100 mg/L, [Phenol]: 40 mg/L

Time (min)	Concentration of anion (mg/L)	Comparative efficiency of enhancement
30	2	$F^- \approx SO_4^{2-} \approx HCO_3^- > CH_3COO^- \approx PO_4^{3-} > Cl^- > CO_3^{2-} > NO_3^-$
	5	$SO_4^{2-} > CH_3COO^- > F^- > CO_3^{2-} > HCO_3^- > Cl^- > PO_4^{3-} > NO_3^-$
	10	$CH_3COO^- > F^- > SO_4^{2-} > NO_3^- > Cl^- > CO_3^{2-} > PO_4^{3-} > HCO_3^-$
	15	$CH_3COO^- > F^- > SO_4^{2-} > NO_3^- > Cl^- > PO_4^{3-} > HCO_3^- > CO_3^{2-}$
	20	$F^- > CH_3COO^- > SO_4^{2-} > NO_3^- > Cl^- > HCO_3^- > CO_3^{2-} > PO_4^{3-}$
60	2	$F^- > CH_3COO^- > HCO_3^- > CO_3^{2-} \approx SO_4^{2-} > NO_3^- > Cl^- > PO_4^{3-}$
	5	$CH_3COO^- > SO_4^{2-} > F^- > CO_3^{2-} \approx Cl^- > NO_3^- \approx HCO_3^- > PO_4^{3-}$
	10	$NO_3^- > CH_3COO^- > F^- > SO_4^{2-} > CO_3^{2-} > HCO_3^- > Cl^- > PO_4^{3-}$
	15	$CH_3COO^- > F^- > NO_3^- > SO_4^{2-} > Cl^- > CO_3^{2-} > HCO_3^- > PO_4^{3-}$
	20	$CH_3COO^- > F^- > NO_3^- \approx SO_4^{2-} > Cl^- > CO_3^{2-} > HCO_3^- > PO_4^{3-}$
90	2	$CH_3COO^- > F^- > SO_4^{2-} \approx NO_3^- > CO_3^{2-} > HCO_3^- > Cl^- > PO_4^{3-}$
	5	$CH_3COO^- > SO_4^{2-} > NO_3^- \approx CO_3^{2-} > F^- > Cl^- > HCO_3^- > PO_4^{3-}$
	10	$NO_3^- > CH_3COO^- > CO_3^{2-} \approx SO_4^{2-} > F^- > Cl^- > HCO_3^- > PO_4^{3-}$
	15	$NO_3^- > CH_3COO^- > F^- \approx CO_3^{2-} > SO_4^{2-} > Cl^- > HCO_3^- > PO_4^{3-}$
	20	$NO_3^- \approx CH_3COO^- > F^- > CO_3^{2-} > SO_4^{2-} > Cl^- > PO_4^{3-} \approx HCO_3^-$
120	2	$CH_3COO^- > F^- \approx NO_3^- > SO_4^{2-} \approx CO_3^{2-} > PO_4^{3-} > HCO_3^- \approx Cl^-$
	5	$NO_3^- > CO_3^{2-} \approx SO_4^{2-} \approx CH_3COO^- > F^- > PO_4^{3-} > Cl^- > HCO_3^-$
	10	$NO_3^- > CO_3^{2-} > CH_3COO^- \approx SO_4^{2} > F^- > Cl^- > PO_4^{3-} \approx HCO_3^-$
	15	$NO_3^- > CH_3COO^- > CO_3^{2-} > F^- > SO_4^{2} > Cl^- > HCO_3^- > PO_4^{3-}$
	20	$NO_3^- > CH_3COO^- > CO_3^{2-} > F^- > SO_4^{2-} > Cl^- > PO_4^{3-} > HCO_3^-$

NO_3^-, CH_3COO^- and F^- are the most efficient enhancers while PO_4^{3-}, HCO_3^- and Cl^- are the least efficient. However, as in the case of most AOPs, there are minor exceptions in this case too.

6.3.2.3 Sonophotocatalysis

The effect of the anions on the sonophotocatalytic degradation of phenol is experimentally verified and the results are given in figures 6.20 to 6.27.

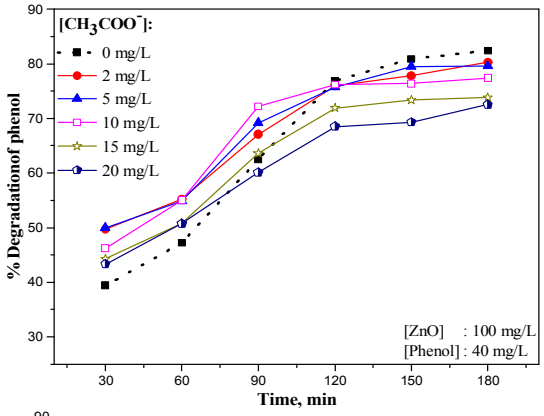

Fig. 6.20: Effect of CH_3COO^- ions on the sonophotocatalytic degradation of phenol

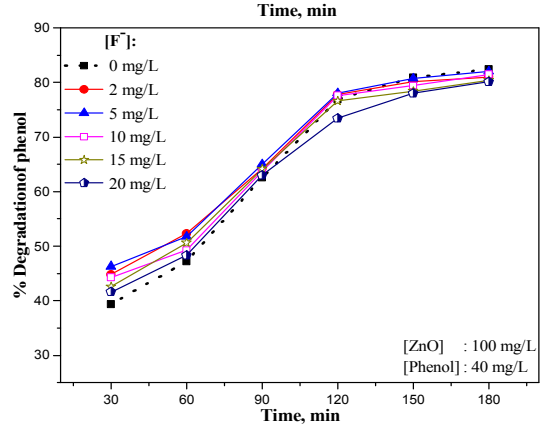

Fig. 6.21: Effect of F^- ions on the sonophotocatalytic degradation of phenol

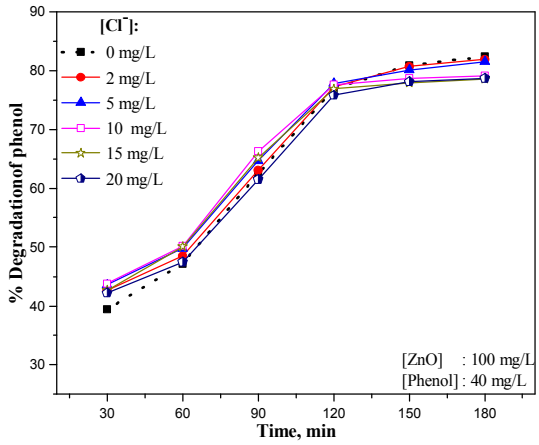

Fig. 6.22: Effect of Cl^- ions on the sonophotocatalytic degradation of phenol

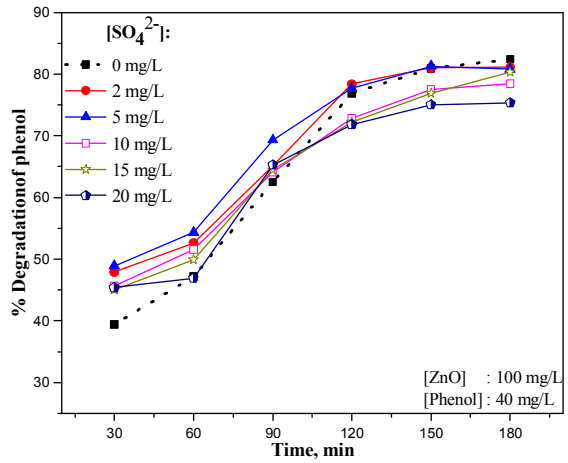

Fig. 6.23: Effect of SO_4^{2-} ions on the sonophotocatalytic degradation of phenol

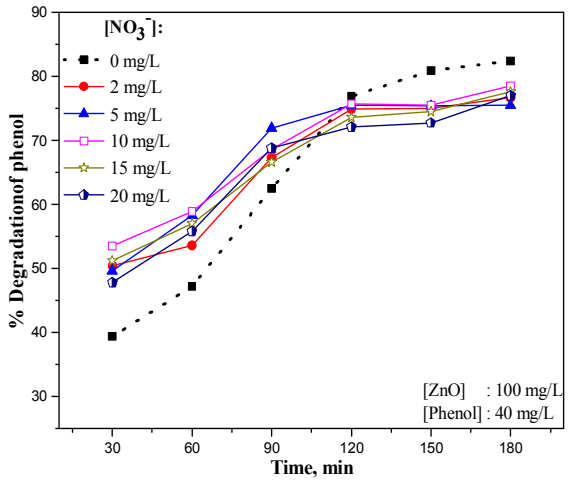

Fig. 6.24: Effect of NO_3^- ions on the sonophotocatalytic degradation of phenol

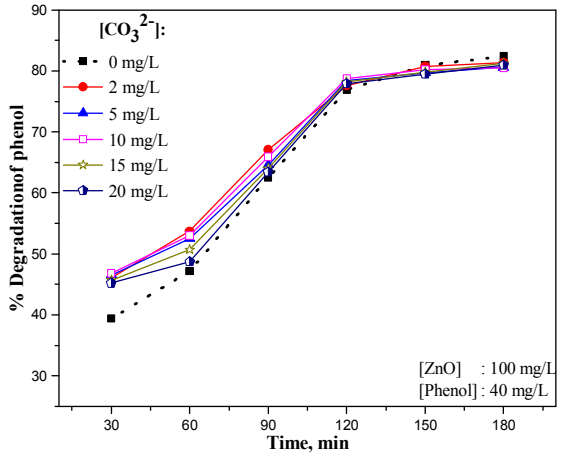

Fig. 6.25: Effect of CO_3^{2-} ions on the sonophotocatalytic degradation of phenol

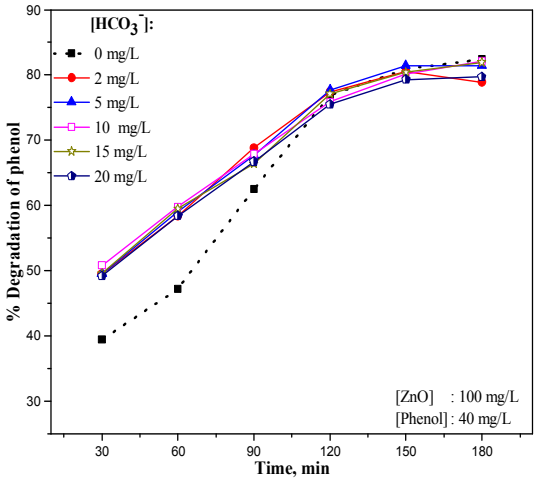

Fig. 6.26: Effect of HCO_3^- ions on the sonophotocatalytic degradation of phenol

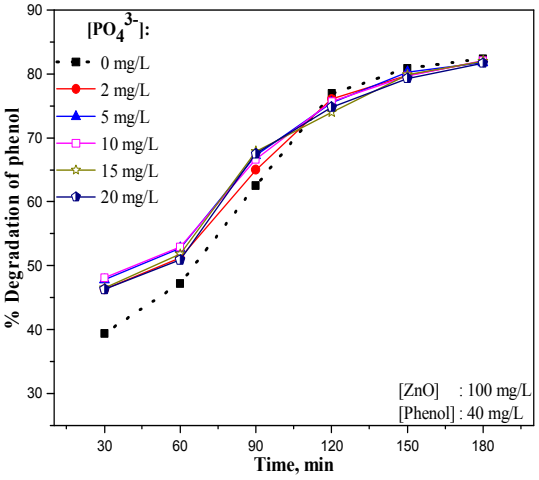

Fig. 6.27: Effect of PO_4^{3-} ions on the sonophotocatalytic degradation of phenol

In this case almost all anions enhance phenol degradation in the initial stages of reaction. Later on, the effect becomes 'nil' to inhibition. The % enhancement of the sonophotocatalytic degradation of phenol caused by the anions (over the degradation in the absence of anions under otherwise identical conditions) with increasing time of irradiation and increasing concentrations is computed and given in table 6.7.

Table 6.7: Percentage enhancement of **sonophotocatalytic degradation** of phenol in presence of various anions. [ZnO]: 100 mg/L, [Phenol]: 40 mg/L

Anion	Conc. Of the anion (mg/L)	% enhancement after					
		30 min	60 min	90 min	120 min	150 min	180 min
CH_3COO^-	2	26.1	16.9	6.9	-1.17	-3.8	-2.6
	5	26.9	16.1	10.7	-1.6	-1.7	-3.4
	10	17.3	16.5	15.5	-0.91	-5.6	-6.1
	15	12.4	7.6	1.8	-6.5	-9.3	-10.4
	20	9.9	7.4	1.6	-10.9	-14.3	-12.0
F^-	2	13.7	10.8	2.7	1.2	-0.87	-1.7
	5	17.5	9.5	4.0	1.4	-0.25	-0.49
	10	12.4	4.4	1.9	0.91	-1.9	-1.1
	15	8.1	7.2	2.6	-0.39	-3.1	-2.4
	20	5.6	2.3	0.8	-4.6	-3.6	-2.8
Cl^-	2	8.4	2.8	0.96	0.52	-0.25	-0.61
	5	10.7	5.5	3.5	1.2	-0.99	-1.1
	10	11.2	6.4	6.1	0.91	-2.7	-4.0
	15	8.4	6.1	4.3	0.0	-3.7	-4.7
	20	7.1	0.64	-1.6	-1.4	-3.5	-4.5
SO_4^{2-}	2	21.6	11.4	4.3	1.9	0.12	-1.6
	5	24.1	15.0	10.9	1.04	0.49	-1.9
	10	16.0	9.1	2.6	-5.4	-4.2	-4.9
	15	14.2	5.7	3.2	-6.1	-4.9	-2.5
	20	15.2	-0.64	-5.8	-6.6	-7.3	-8.6
NO_3^-	2	27.9	13.6	7.7	-2.6	-7.3	-6.9
	5	25.9	23.5	15.0	-1.8	-6.8	-8.4
	10	35.8	24.8	9.8	-1.6	-6.6	-4.7
	15	29.9	20.8	6.6	-4.3	-7.9	-5.8
	20	21.3	18.2	10.1	-6.2	-10.1	-6.6
CO_3^{2-}	2	17.0	13.8	7.4	0.91	-0.25	-1.2
	5	18.0	11.2	3.4	1.95	-1.5	-2.2
	10	18.8	12.3	5.4	2.3	-0.87	-2.3
	15	16.0	7.4	2.4	1.7	-1.4	-1.3
	20	14.7	3.2	1.4	1.3	-1.7	-1.7
HCO_3^-	2	25.6	23.7	10.1	0.65	-0.49	-4.2
	5	25.6	25.0	8.3	1.0	0.62	-1.2
	10	28.9	26.7	8.6	-1.3	-0.99	-0.36
	15	25.9	26.1	6.2	0.26	-0.62	-0.66
	20	24.9	23.7	6.7	-1.8	-2.0	-3.3
PO_4^{3-}	2	17.5	8.5	4.0	-1.0	-1.4	-0.49
	5	21.3	11.7	7.5	-1.8	-0.74	-0.73
	10	22.1	12.1	6.6	-1.6	-1.5	-0.36
	15	18.0	9.7	8.6	-3.8	-1.2	-0.49
	20	17.5	7.8	8.0	-2.7	-1.9	-0.85

Negative (-) sign indicates inhibition

The trend in the enhancement with concentration of the anion and time of reaction is generally comparable to that in the case of photocatalysis. The effect of varying concentration of individual anions and extended reaction time on the sonophotocatalytic degradation of phenol as shown in the figures is summarized in table 6.8.

Table 6.8: Effect of concentration of the anion and reaction time on the **sonophotocatalytic degradation** of phenol. [ZnO]: 100 mg/L, [Phenol]: 40 mg/L

Anions	Effect of concentration (mg/L) on initial rate*	Effect of reaction time (min)
CH_3COO^-	Enhancement initially with optimum in the range of 2 to 5 mg/L.	Initial enhancement. Eventually slows down to become inhibition after ~ 120 minutes.
F^-	Initial enhancement with optimum at 5 mg/L.	Initial enhancement. Eventually slows down reaching 'no effect' to mild inhibition after 120 minutes.
Cl^-	Slight initial enhancement. Little concentration effect.	Slight initial enhancement. Eventually slows down reaching 'no effect' to mild inhibition after 120 minutes.
SO_4^{2-}	Initial enhancement with optimum at 5 mg/L.	Initial enhancement. Eventually slows down reaching inhibition after 90-120 minutes.
NO_3^-	Initial enhancement with optimum at10 mg/L.	Initial enhancement. Eventually slows down. Inhibition after 120 minutes.
CO_3^{2-}	Initial enhancement at all concentrations. Little concentration effect.	Initial enhancement with no effect after 120 minutes and slight inhibition thereafter.
HCO_3^-	Initial enhancement. Concentration effect is not significant.	Initial enhancement, slows down and eventually 'no effect' to mild inhibition after 120-150 minutes.
PO_4^{3-}	Initial enhancement. Concentration has little effect.	Initial enhancement. 'No effect' to mild inhibition after 120 minutes.

* Based on the % degradation in the initial 30 to 60 minutes

From table 6.8, it is clear that all anions enhance sonophotocatalytic degradation initially. As reaction proceeds the enhancing effect by all the ions slows down and the effect becomes 'nil' to inhibition.

Based on the graph 6.20–6.27 and tables 6.7 and 6.8 the sonophotocatalytic enhancement efficiency of anions at various concentrations at various times of reaction is compared and presented in table 6.9.

Table 6.9: Comparative efficiency of anions at various concentrations and reaction times for the enhancement of the **sonophotocatalytic degradation** of phenol. [ZnO]:100 mg/L, [Phenol]:40 mg/L

Time (min)	Conc. Of anion (mg/L)	Comparative efficiency of enhancement
30	2	$NO_3^- \approx CH_3COO^- \approx HCO_3^- > SO_4^{2-} > PO_4^{3-} \approx CO_3^{2-} > F^- > Cl^-$
	5	$CH_3COO^- \approx NO_3^- \approx HCO_3^- \approx SO_4^{2-} > PO_4^{3-} > CO_3^{2-} \approx F^- > Cl^-$
	10	$NO_3^- > HCO_3^- > PO_4^{3-} > CO_3^{2-} \approx CH_3COO^- \approx SO_4^{2-} > F^- \approx Cl^-$
	15	$NO_3^- > HCO_3^- > PO_4^{3-} \approx CO_3^{2-} > SO_4^{2-} \approx CH_3COO^- > Cl^- \approx F^-$
	20	$HCO_3^- > NO_3^- > PO_4^{3-} \approx SO_4^{2-} \approx CO_3^{2-} > CH_3COO^- > Cl^- \approx F^-$
60	2	$HCO_3^- > CH_3COO^- > CO_3^{2-} \approx NO_3^- \approx SO_4^{2-} \approx F^- > PO_4^{3-} > Cl^-$
	5	$HCO_3^- \approx NO_3^- > CH_3COO^- \approx SO_4^{2-} > PO_4^{3-} \approx CO_3^{2-} \approx F^- > Cl^-$
	10	$HCO_3^- \approx NO_3^- > CH_3COO^- > CO_3^{2-} \approx PO_4^{3-} > SO_4^{2-} > Cl^- \approx F^-$
	15	$HCO_3^- > NO_3^- > PO_4^{3-} \approx CH_3COO^- \approx CO_3^{2-} \approx F^- \approx Cl^- \approx SO_4^{2-}$
	20	$HCO_3^- > NO_3^- > PO_4^{3-} \approx CH_3COO^- > CO_3^{2-} \approx F^- \approx Cl^- \approx SO_4^{2-}$
90	2	$HCO_3^- \approx NO_3^- \approx CO_3^{2-} \approx CH_3COO^- > SO_4^{2-} \approx PO_4^{3-} \approx F^- \approx Cl^-$
	5	$NO_3^- > SO_4^{2-} \approx CH_3COO^- \approx HCO_3^- \approx PO_4^{3-} > F^- \approx Cl^- \approx CO_3^{2-}$
	10	$CH_3COO^- > NO_3^- \approx HCO_3^- \approx PO_4^{3-} \approx Cl^- \approx CO_3^{2-} > SO_4^{2-} \approx F^-$
	15	$PO_4^{3-} \approx NO_3^- \approx HCO_3^- > Cl^- \approx SO_4^{2-} \approx F^- \approx CO_3^{2-} \approx CH_3COO^-$
	20	$NO_3^- > PO_4^{3-} \approx HCO_3^- > CH_3COO^- \approx CO_3^{2-} \approx F^- > Cl^- > SO_4^{2-}$
120	2	$SO_4^{2-} \approx F^- \approx CO_3^{2-} \approx HCO_3^- \approx Cl^- > PO_4^{3-} \approx CH_3COO^- \approx NO_3^-$
	5	$CO_3^{2-} \approx F^- \approx Cl^- \approx SO_4^{2-} \approx HCO_3^- > PO_4^{3-} \approx NO_3^- \approx CH_3COO^-$
	10	$CO_3^{2-} \approx F^- \approx Cl^- > CH_3COO^- \approx HCO_3^- \approx PO_4^{3-} \approx NO_3^- > SO_4^{2-}$
	15	$CO_3^{2-} \approx HCO_3^- \approx Cl^- > F^- \approx PO_4^{3-} \approx NO_3^- > SO_4^{2-} \approx CH_3COO^-$
	20	$CO_3^{2-} > HCO_3^- \approx Cl^- \approx PO_4^{3-} > F^- \approx NO_3^- \approx SO_4^{2} > CH_3COO^-$
150	2	$SO_4^{2-} > CO_3^{2-} \approx Cl^- \approx HCO_3^- \approx F^- \approx PO_4^{3-} > CH_3COO^- > NO_3^-$
	5	$HCO_3^- \approx SO_4^{2-} > F^- \approx PO_4^{3-} \approx Cl^- \approx CH_3COO^- \approx CO_3^{2-} > NO_3^-$
	10	$CO_3^{2-} \approx HCO_3^- \approx F^- \approx PO_4^{3-} \approx Cl^- > SO_4^{2-} \approx CH_3COO^- \approx NO_3^-$
	15	$HCO_3^- \approx PO_4^{3-} \approx CO_3^{2-} > F^- \approx Cl^- \approx SO_4^{2-} > NO_3^- > CH_3COO^-$
	20	$CO_3^{2-} \approx PO_4^{3-} \approx HCO_3^- > F^- \approx Cl^- > SO_4^{2-} > NO_3^- > CH_3COO^-$
180	2	$PO_4^{3-} \approx Cl^- \approx CO_3^{2-} > F^- \approx SO_4^{2-} \approx CH_3COO^- > HCO_3^- > NO_3^-$
	5	$F^- \approx PO_4^{3-} \approx HCO_3^- \approx Cl^- \approx SO_4^{2-} \approx CO_3^{2-} > CH_3COO^- > NO_3^-$
	10	$PO_4^{3-} \approx HCO_3^- \approx F^- \approx CO_3^{2-} > Cl^- > NO_3^- \approx SO_4^{2-} > CH_3COO^-$
	15	$PO_4^{3-} \approx HCO_3^- \approx CO_3^{2-} \approx F^- \approx SO_4^{2-} > Cl^- \approx NO_3^- > CH_3COO^-$
	20	$PO_4^{3-} \approx CO_3^{2-} \approx F^- \approx HCO_3^- > Cl^- > NO_3^- > SO_4^{2-} > CH_3COO^-$

The comparative efficiency of the anions for enhancement at various concentration and reaction time vary widely indicating the complexity of the anion effect under sonophotocatalysis. At early reaction time, NO_3^- and HCO_3^- are strong enhancers at all concentrations. The situation changes with time and at later stages of reaction, all anions become inhibitors. Even PO_4^{3-} which is a strong inhibitor of photo and sono catalysis is a good enhancer in the early stages of reaction. Generally it may be stated that the inconsistency of 'anion effect' is more evident in the case of sonophotocatalysis.

6.3.3 Anion induced enhancement: Slow down and eventual inhibition

The gradual decline of the anion effect from enhancement of the degradation to stabilization/inhibition with time as demonstrated earlier can be summarized as shown in figures 6.28 to 6.32 (photo), 6.33 to 6.37 (sono) and 6.38 to 6.42 (sonophoto) for quick reference. The gradual change is clear in all cases.

6.3.3.1 Photocatalysis

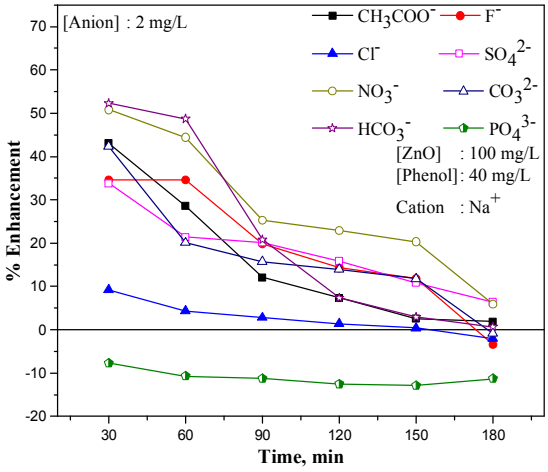

Fig. 6.28: Transition of anion effect from enhancement to inhibition in the photocatalysis: [Anion]: 2 mg/L

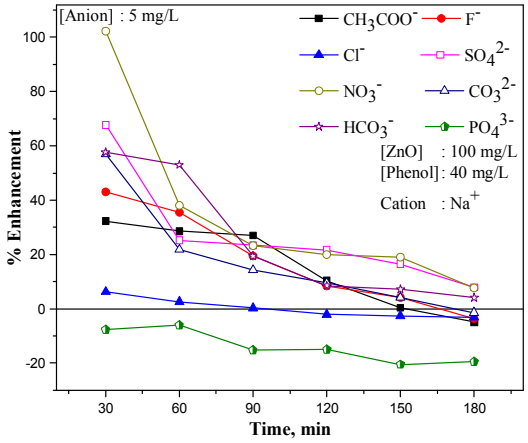

Fig. 6.29: Transition of anion effect from enhancement to inhibition in the photocatalysis: [Anion]: 5 mg/L

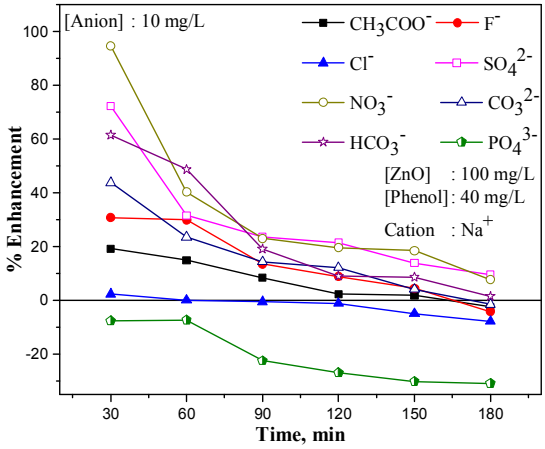

Fig. 6.30: Transition of anion effect from enhancement to inhibition in the photocatalysis: [Anion]: 10 mg/L

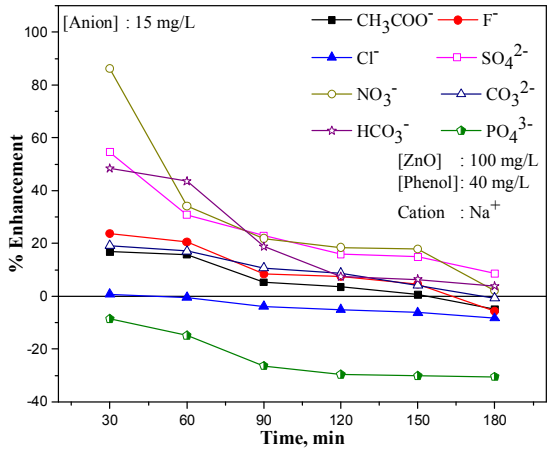

Fig. 6.31: Transition of anion effect from enhancement to inhibition in the photocatalysis: [Anion]: 15 mg/L

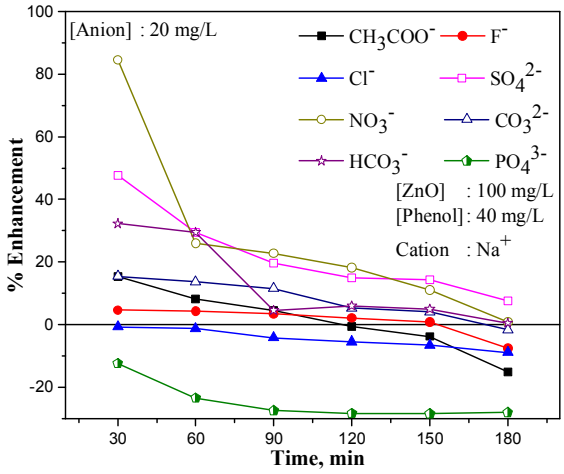

Fig. 6.32: Transition of anion effect from enhancement to inhibition in the photocatalysis: [Anion]: 20 mg/L

From the figures (6.28-32) it is clear that in photocatalysis, the % enhancement increases initially with increase in concentration of the anion, passes through an optimum and decreases at higher concentration as seen in tables 6.1 and 6.2. Similarly the % enhancement decreases with time. In this case Cl^- (except at the very early stages) and PO_4^{3-} act as inhibitor throughout.

6.3.3.2 Sonocatalysis

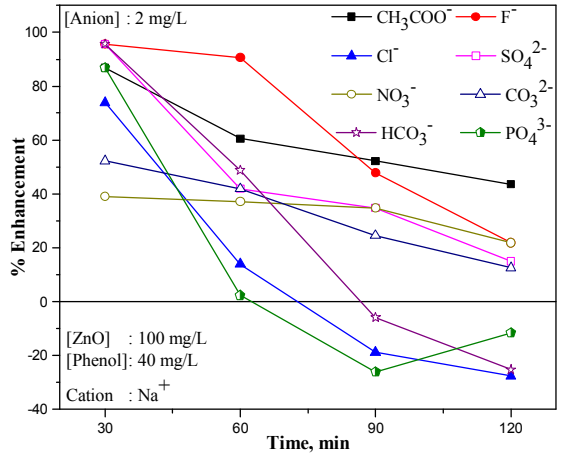

Fig. 6.33: Transition of anion effect from enhancement to inhibition in the sonocatalysis: [Anion]: 2 mg/L

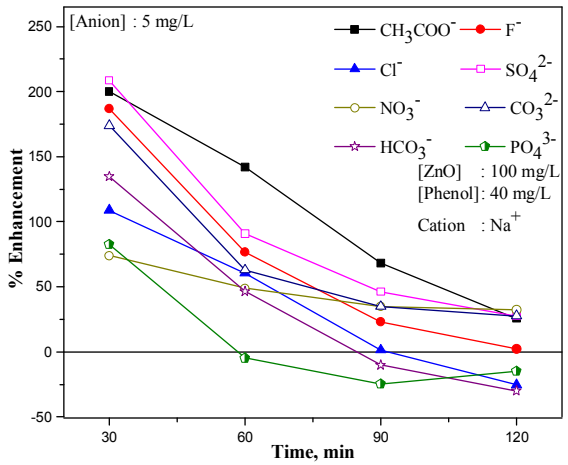

Fig. 6.34: Transition of anion effect from enhancement to inhibition in the sonocatalysis: [Anion]: 5 mg/L

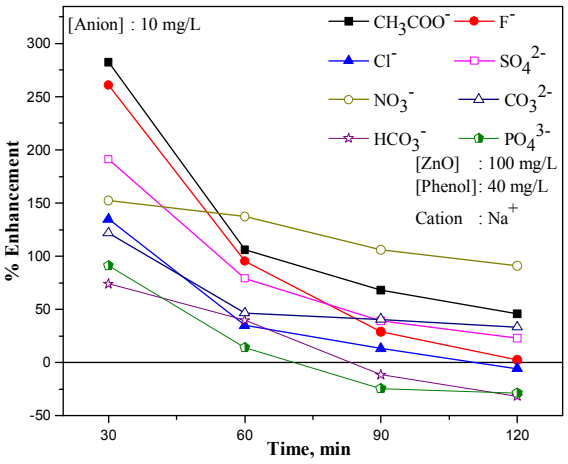

Fig. 6.35: Transition of anion effect from enhancement to inhibition in the sonocatalysis: [Anion]: 10 mg/L

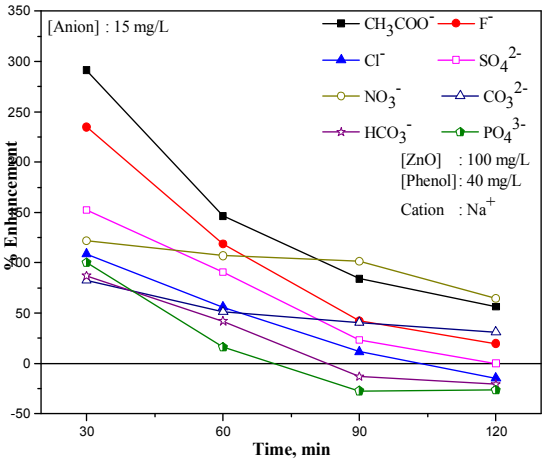

Fig. 6.36: Transition of anion effect from enhancement to inhibition in the sonocatalysis: [Anion]: 15 mg/L

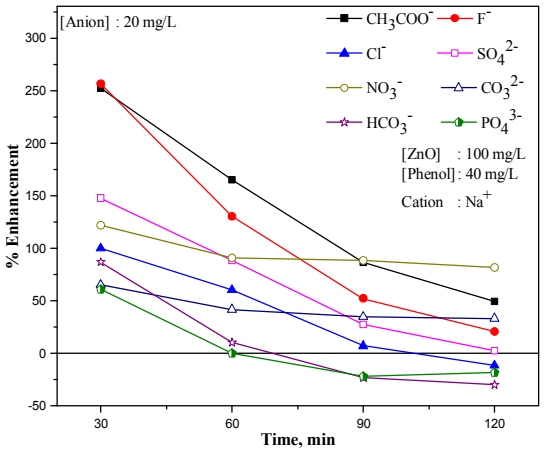

Fig. 6.37: Transition of anion effect from enhancement to inhibition in the sonocatalysis: [Anion]: 20 mg/L

These figures (6.33-37) demonstrate once again that the effect of concentration of the anion on the phenol degradation does not follow any consistent pattern in the case of sonocatalysis. All the anions studied here, at all concentrations, enhance sonocatalytic degradation of phenol in the initial stages up to 60 minutes. The degree of enhancement decreases as the reaction proceeds. In the case of PO_4^{3-}, Cl^- and HCO_3^- the initial enhancement gives way to inhibition at higher reaction time for all concentration of the anions. It can be generally concluded that all anions at lower concentrations and in the initial stages of reaction enhance the sonocatalytic degradation of phenol in presence of ZnO. The trend is similar in the case of photo and sono catalysis even though the precise effect is different in the case of individual anions.

6.3.3.3 Sonophotocatalysis

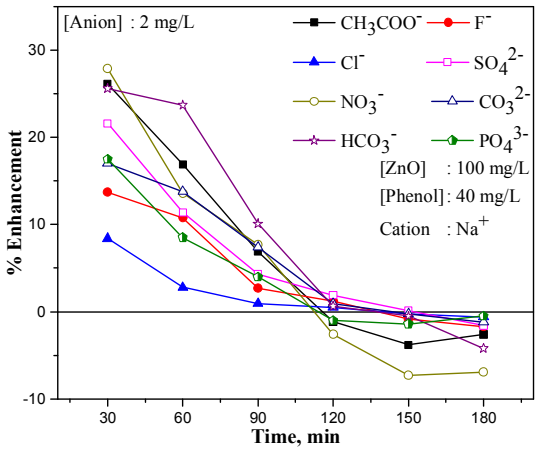

Fig. 6.38: Transition of anion effect from enhancement to inhibition in the sonophotocatalysis: [Anion]: 2 mg/L

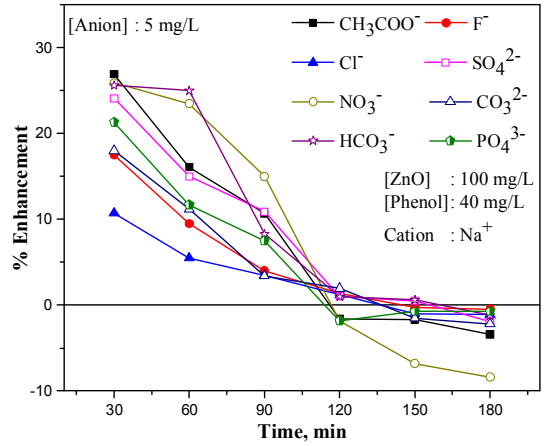

Fig. 6.39: Transition of anion effect from enhancement to inhibition in the sonophotocatalysis: [Anion]: 5 mg/L

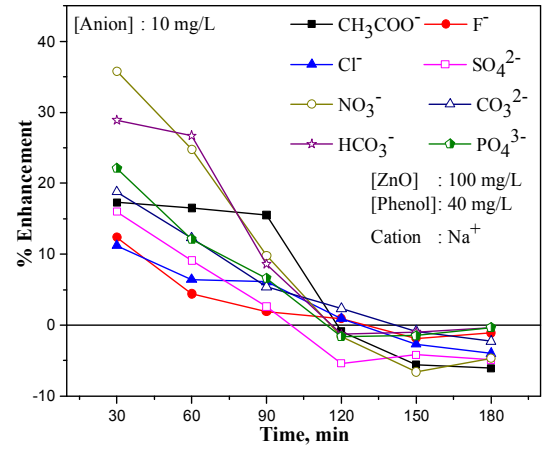

Fig. 6.40: Transition of anion effect from enhancement to inhibition in the sonophotocatalysis: [Anion]:10 mg/L

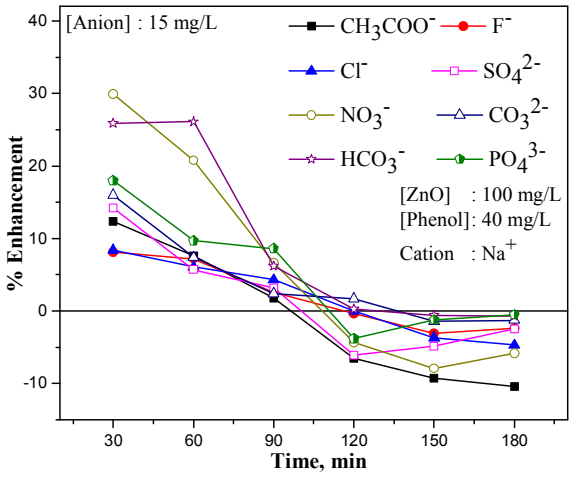

Fig. 6.41: Transition of anion effect from enhancement to inhibition in the sonophotocatalysis: [Anion]:15 mg/L

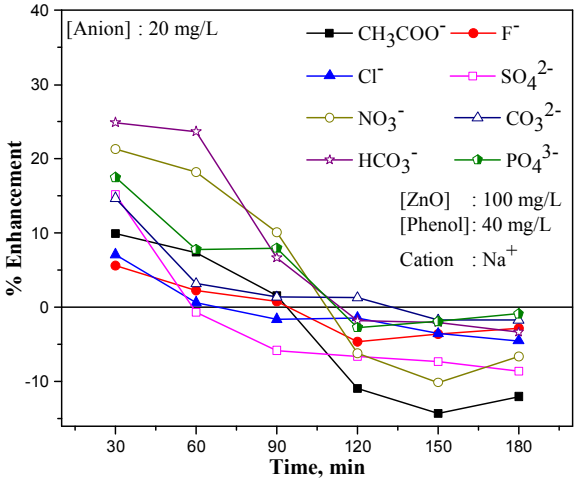

Fig. 6.42: Transition of anion effect from enhancement to inhibition in the sonophotocatalysis: [Anion]: 20 mg/L

In the case of sonophotocatalysis (figure 6.38-42) also enhancement in the degradation of phenol decreases with time of reaction. All anions including PO_4^{3-} act as enhancers, for phenol degradation up to 60 to 90 minutes of irradiation. Thereafter the enhancing effect becomes weak and all anions become either 'neutral' or inhibitors.

Thus it may be seen that, even though the anion effect is not predictably consistent in all cases, a general trend is evident. All anions, except for minor variations, enhance the degradation of phenol at lower concentrations and initial reaction times. Gradually the enhancing effect slows down and eventually some of the anions become inhibitors while others have 'no effect'. Hence it is important that the presence of anions in water and their effect, including concentration and 'time' effect on the degradation of the target pollutant is carefully monitored before selecting the appropriate AOP for any particular application.

6.3.4 Effect of anions on the synergy

The synergy in the case of sonophotocatalysis reported earlier in Chapter 5 section 5.3.3 is retained in the early stages in presence of individual ions also at all concentrations (table 6.10). The synergy remains more or less the same at most concentrations with some exceptions. The synergy also depends on the time of reaction as well as pH of the reaction medium which needs to be taken up as another detailed investigation. In the current instance, only '30 minutes data' which show enhancement at all concentrations of anions at the fixed pH of 5.5 is chosen for comparison. The trend may be different when the anions inhibit the degradation.

Table 6.10: The synergy of **sonophotocatalytic degradation** of phenol in presence of various anions. [ZnO]: 100 mg/L, [Phenol]: 40 mg/L Time: 30 minutes

Anion	Conc. Of anion (mg/L)	% Degradation of phenol			Synergy
		US	UV	US + UV	
No anion	-	2.3	13	39.4	2.58
CH_3COO^-	2	4.3	18.6	49.7	2.17
	5	6.9	17.2	50.0	2.07
	10	8.8	15.5	46.2	1.90
	15	9	15.2	44.3	1.83
	20	8.1	15.0	43.3	1.87
F^-	2	4.5	17.5	44.8	2.03
	5	6.6	18.6	46.3	1.83
	10	8.3	17.0	44.3	1.75
	15	7.7	16.1	42.6	1.78
	20	8.2	13.6	41.6	1.90
Cl^-	2	4.0	14.2	42.7	2.34
	5	4.8	13.8	43.6	2.24
	10	5.4	13.3	43.8	2.34
	15	4.8	13.1	42.7	2.38
	20	4.6	12.9	42.2	2.41
SO_4^{2-}	2	4.5	17.4	47.9	2.18
	5	7.1	21.8	48.9	1.69
	10	6.7	22.4	45.7	1.51
	15	5.8	20.1	45.0	1.73
	20	5.7	19.2	45.4	1.82
NO_3^-	2	3.2	19.6	50.4	2.21
	5	4.0	26.3	49.6	1.63
	10	5.8	25.3	53.5	1.72
	15	5.1	24.2	51.2	1.74
	20	5.1	24.0	47.8	1.64
CO_3^{2-}	2	3.5	18.5	46.1	2.09
	5	6.3	20.4	46.5	1.74
	10	5.1	18.7	46.8	1.96
	15	4.2	15.5	45.7	2.31
	20	3.8	15.0	45.2	2.40
HCO_3^-	2	4.5	19.8	49.5	2.03
	5	5.4	20.5	49.5	1.91
	10	4.0	21	50.8	2.03
	15	4.3	19.3	49.6	2.10
	20	3.3	17.2	49.2	2.40
PO_4^{3-}	2	4.3	12	46.3	2.84
	5	4.2	12	47.8	2.95
	10	4.4	12	48.1	2.93
	15	4.6	11.9	46.5	2.81
	20	3.7	11.4	46.3	3.06

6.3.5 Adsorption of anions on ZnO

In the case of most AOPs, anions are reported to inhibit the degradation of the pollutants, which is often attributed to the competitive adsorption and consequent reduction in the number of active sites on the catalyst for the substrate. However, in the present case, most anions enhance the degradation of the pollutant under photo, sono and sonophoto catalysis. Does it mean that the anions are not getting adsorbed or only weakly adsorbed on the surface of ZnO? In order to verify this, experiments were conducted on the adsorption of phenol over ZnO generally in line with the procedure adopted by Guillard et al. [32] and Chen et al. [157], using PO_4^{3-} as the test pollutant. PO_4^{3-} effect is different under photo, sono and sonophoto catalysis. Under photocatalysis, PO_4^{3-} functions as an inhibitor throughout at all concentrations of all reaction times. Under sonocatalysis, it acts as an enhancer in the beginning and as an inhibitor later on. Under sonophotocatalysis, the effect is an average of the effect under photo and sono catalysis in the early stages, i.e., mild enhancement. This is followed by 'no effect' at later stages of reaction. The adsorption experiments are conducted as follows:

a) Adsorption of phenol on ZnO from a solution containing only phenol (A)
b) Adsorption of PO_4^{3-} on ZnO from a solution containing only PO_4^{3-} (B)
c) Adsorption of phenol and PO_4^{3-} on ZnO from the solution containing both (C)
d) Pre-adsorption of phenol on ZnO and evaluation of further adsorption of phenol, if any, when 'phenol pre-adsorbed ZnO' (PPZ) is brought in contact with fresh phenol solution (D).

e) Evaluation of desorption of phenol/adsorption of PO_4^{3-}, if any, when the PPZ is brought in contact with PO_4^{3-} solution (E).

f) Evaluation of the adsorption/desorption of phenol and PO_4^{3-}, if any, when the PPZ is brought in contact with the phenol-PO_4^{3-} solution (F).

g) Pre-adsorption of anion PO_4^{3-} on ZnO and subsequent adsorption of phenol, if any, on the 'anion pre-adsorbed ZnO' (APZ) from phenol solution (G)

h) Adsorption/desorption of phenol/anion on APZ from phenol-anion solution (H)

i) Adsorption of anion on APZ from anion solution (I)

Typical adsorption/desorption data under the above conditions is given in table 6.11

Table 6.11: Adsorption/desorption of phenol/anion on ZnO under various conditions. [ZnO]: 3750 mg/L, [Phenol]: 1500 mg/L, [PO_4^{3-}]: 370 mg/L

Condition	Adsorption of phenol (%)	Adsorption of anion (%)	% variation in phenol/PO_4^{3-} adsorption from standard condition	
			Phenol	PO_4^{3-}
A	9.0	NA	NA	NA
B	NA	11.0	NA	NA
C	5.4	7.4	- 40.0	- 32.7
D	1.4	NA	+15.6	NA
E	-8.0*	5.8	NA	- 38.2
F	1.8	3.1	+20.0	-71.8
G	3.6	NA	- 60.0	NA
H	4.1	~ 0.0	- 54.4	No further adsorption
I	NA	~ 0.0	NA	No further adsorption

NA: Not applicable * Desorption

The extent of adsorption of phenol under different conditions and it's desorption from phenol-pre-adsorbed ZnO in the presence of PO_4^{3-} anion clearly shows that the adsorption (of phenol) is less in the presence of PO_4^{3-}. This also indicates that there is competition between phenol and the anion for the active surface sites.

The adsorption of PO_4^{3-} from pure PO_4^{3-} solution (B) is more than that from phenol-PO_4^{3-} solution (C) on fresh ZnO. The relatively small but significant adsorption of phenol even in the presence of PO_4^{3-} shows that the latter cannot block all the adsorption sites and phenol also can get competitively adsorbed, though less effectively. At the same time the adsorption of both phenol and PO_4^{3-} is mutually inhibited in their simultaneous presence indicating competition for the surface sites. In the case of PPZ, only very small amount of extra phenol gets adsorbed when brought in contact with fresh phenol solution (D) indicating that most of the available surface sites where phenol can get adsorbed are already occupied. When PPZ is brought in contact with PO_4^{3-} (E), the adsorbed phenol gets desorbed almost quantitatively. A good part of the sites from which phenol is displaced is occupied by PO_4^{3-}. When the PPZ is brought in contact with the solution containing both phenol and PO_4^{3-} (F), both get adsorbed only moderately, with PO_4^{3-} adsorption being slightly more. Hence the number of sites available for further adsorption of phenol and PO_4^{3-} is much less on PPZ.

The adsorption of phenol from pure phenol solution on 'anion (PO_4^{3-}) pre-adsorbed ZnO' (APZ) is at least 60% less compared to fresh ZnO (G). Adsorption of moderate amounts of phenol shows that there

may be few distinct sites not occupied by PO_4^{3-}, but are available for phenol. However, unlike in the case of PO_4^{3-} which can effectively displace adsorbed phenol, the latter cannot displace pre-adsorbed former. Hence no desorption of PO_4^{3-} is observed. This is reconfirmed from the experiment H in which phenol-PO_4^{3-} solution is brought in contact with APZ. In this case again, some phenol gets adsorbed in the vacant sites while no extra PO_4^{3-} gets adsorbed or desorbed. Experiment I also shows that the adsorption by the anion is complete in the first instance itself.

Thus it may be inferred that almost all the available surface sites are fully occupied by phenol or anion in their exclusive presence. There may be very few distinct sites of adsorption for phenol on the ZnO surface and the anion is unable to fully block them. At the same time, the anions get competitively better adsorbed and can even replace at least some of the adsorbed phenol. Hence in the presence of PO_4^{3-}, the surface initiated/ promoted degradation of phenol is inhibited at higher concentration of the former. The observation that the effect of even a strongly adsorbing anion like PO_4^{3-} on the degradation of phenol is different under different condition of concentration/time of reaction/mode of activation shows that surface promoted reaction is not the only route for the degradation of organics under the current reaction conditions. In any case, the inhibition/decrease in the enhancement of the degradation of phenol at higher concentration of most of the anions shows that the surface does play a role, though it is not the only mode of reaction initiation/propagation. This also reconfirms that the dominant mechanism of the degradation involves processes other than surface-initiated processes. It is also known that suspended particles play a role in sonocatalysis and sonophotocatalysis

which is not limited to adsorption of the substrate, anions or other reaction intermediates or products on the surface.

Even if the anions are getting competitively better adsorbed on the surface, they need not be remaining on the surface under sonication due to the phenomena of microstreaming and microbubbles eruption [156]. This type of surface cleaning can contribute to sustained long term catalytic activity of ZnO. Since there is no inhibition in presence of anions which are proven inhibitors in many other AOPs, this type of surface cleaning may indeed be happening in sonocatalysis or sonophotocatalysis. Since the degree of enhancement of phenol degradation slows down with time of reaction as well as increase in concentration of the anions, it may be inferred that with various reaction intermediates and higher number of anion molecules engaged in severe competition for adsorption sites, microstreaming and microbubbles eruption may not be adequate to fully clean the surface. The concentration of phenol decreases with time of reaction while the concentration of anions remains more or less the same. The US initiated reactive free radicals will interact more frequently with the anions in preference to the less abundant phenol or its reaction intermediates at later stages of reaction, causing further decrease in the degradation rate. Decrease in the concentration of the substrate together with competition from many of the insitu formed intermediates for the reactive free radicals and the US/UV energy also may lead to decreased rate of degradation. This results in decreasing enhancement with time or even eventual inhibition.

Adsorption of PO_4^{3-} on ZnO is confirmed from the FTIR spectrum of pure ZnO, pure Na_3PO_4, and 'ZnO brought in contact with Na_3PO_4' (figure 6.43). Characteristic bands of PO_4^{3-} are seen in the case of 'ZnO brought in contact with Na_3PO_4' showing the strong adsorption.

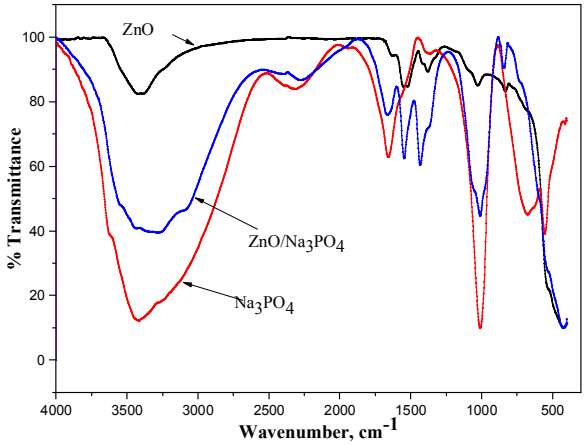

Fig. 6.43: FTIR spectrum showing adsorption of phosphate on ZnO

The adsorption of various anions and the relatively higher adsorption of PO_4^{3-} ions on semiconductor oxides such as TiO_2 have been reported earlier [158]. The Point of Zero Charge (PZC) of ZnO is ~ 9 ± 0.3 [25]. This means that ZnO surface is positively charged when the pH is lower than this value and negatively charged when the pH is higher. Solution pH influences the ionization state of ZnO surface according to the reactions (67) and (68) {Reproduced below for ready reference}:

$$---Zn - OH + H^+ \leftrightarrow ZnOH_2^+ \quad \text{..... (168)}$$

$$-- Zn - OH + OH^- \leftrightarrow Zn\text{-}O^- + H_2O \quad \text{.....(169)s}$$

Hence at the acidic pH, anion can get adsorbed strongly. Had adsorption of phenol been the only essential factor for degradation, presence of anions could have strongly inhibited the degradation at the natural pH of 5.5 of the current reaction system. However this happens only at higher concentration of the anion thereby confirming that processes other than surface initiated processes are also important in photo, sono and sonophoto catalytic degradation.

6.3.6 Solubility of anions and layer formation

Another possible reason, often cited for the effect of anions, in particular the inhibition by anions, is the formation of an inorganic layer on the catalyst surface. The efficiency of layer formation depends on the solubility of the salts [159]. Higher the solubility of the salt, lower the adsorption/layer formation. The solubility of the salts (in mg/g of water at 25^0C) tested here is in the order [160];

$$NaNO_3\ (91.2) > CH_3COONa\ (50.4) > Na_2CO_3\ (30.7) \geq Na_2SO_4\ (28.1) > NaCl\ (36.0) > Na_3PO_4\ (14.4) > NaHCO_3\ (10.3) > NaF\ (4.13) \quad \text{.....(170)}$$

Correspondingly the layer formation, if any, will be in the reverse order, i.e.,

$$F^- > HCO_3^- > PO_4^{3-} > Cl^- > SO_4^{2-} > CO_3^{2-} > CH_3COO^- > NO_3^- \quad \text{.....(171)}$$

Hence, had there been a layer formation on the surface, it should have inhibited the surface initiated degradation of phenol in the same order as in (171). In other words, if it is enhancement in place of inhibition, contribution from the surface initiated processes towards

the enhancement in the degradation of phenol, could be in the reverse order of (171), i.e. least enhancement in presence of F^-, HCO_3^-, PO_4^{3-}, etc. and maximum enhancement in presence of SO_4^{2-}, CH_3COO^-, NO_3^-, etc. However, this trend is not seen consistently in the case of photo, sono or sonophoto catalysis, though the possibility can be seen in few instances. The complexity of the system with too many homogenous and heterogeneous processes operating in parallel and the multitude of free radicals and reaction intermediates make the general correlation based on solubility of the anions difficult.

6.3.7 Ionic strength

Anions are known to increase the ionic strength of the solutions. In the case of sonicated system, presence of anions can lead to salting out of the pollutant into the cavitation bubbles where gas phase pyrolysis could take place. Presence of salts can also modify the partition coefficient and hence the distribution of aqueous and organic phases. Dissolved salts can also possibly create instabilities in the system and facilitate easy generation of cavities. Consequently, the concentration of phenol at the gas-liquid interface increases resulting in its higher concentration at the cavity implosion sites. This will result in enhanced interaction of phenol with the reactive free radicals and thus enhanced degradation. The presence of salt can also decrease the vapor pressure of the medium and increase the surface tension, both resulting in more violent collapse of the cavities. This may be an important factor contributing to the anion induced enhancement in the degradation of phenol under sono and sonophoto catalysis. However excessive salt concentration affects the US/UV penetration into the system [161] which reduces the anion-

induced enhancement of phenol degradation at higher concentration of the former.

6.3.8 Scavenging effect of anions

Many of the factors discussed above except the ionic strength effect can explain only the inhibition or reduced enhancement of the degradation by the anions. No uniform theory is able to explain the enhancement effect by the anions and the trends observed here. Another factor to be considered in this context is the scavenging effect by the anions which is reported to have both inhibitory and enhancing effects depending on the reaction conditions. Many anions are known to scavenge the reactive $^{\bullet}OH$ radicals which can cause inhibition. The scavenging rate constants of $^{\bullet}OH$ by some of the anions tested here are summarized in Table 6.12 [32, 162, 163].

Table 6.12: Scavenging rate constants of $^{\bullet}OH$ by various anions.

Anions	Scavenging rate constants ($mol^{-1}s^{-1}$)
NO_3^-	1.4×10^8
Cl^-	4.3×10^9
CO_3^{2-}	3.9×10^8
SO_4^{2-}	1×10^{10}
$H_2PO_4^-$	2×10^4
Ac^-	7.0×10^7
HCO_3^-	8.5×10^6

F^- ion, unlike in the case of other halides, cannot be oxidized by the valence band or the $^{\bullet}OH$ radicals [24].

Immediate outcome of the scavenging of reactive $^{\bullet}OH$ radicals is the formation of radical anion. These radical anions are also reactive towards organic compounds although less efficiently than $^{\bullet}OH$ [32].

For e.g.

$$^{\bullet}OH + HCO_3^- \rightarrow H_2O + CO_3^{\bullet-} \quad \text{.....(172)}$$

$$^{\bullet}OH + CO_3^{2-} \rightarrow OH^- + CO_3^{\bullet-} \quad \text{.....(173)}$$

$$^{\bullet}OH + SO_4^{2-} \rightarrow OH^- + SO_4^{\bullet-} \quad \text{.....(174)}$$

$$^{\bullet}OH + NO_3^- \rightarrow OH^- + NO_3^{\bullet} \quad \text{.....(175)}$$

$$CH_3COO^- + {}^{\bullet}OH \rightarrow OH^- + CH_3COO^{\bullet} \rightarrow OH^- + CH_3^{\bullet} + CO_2 \text{ ..(176)}$$

$$^{\bullet}OH + Cl^- \rightarrow OH^- + Cl^{\bullet} \quad \text{.....(177)}$$

$$Cl^{\bullet} + Cl^- \rightarrow Cl_2^{\bullet-} \quad \text{.....(178)}$$

etc. …..

Enhancement of the degradation of phenol by these anions can be explained based on the hypothesis that the radicals $CO_3^{\bullet-}$, $NO_3^{\bullet-}$, $Cl_2^{\bullet-}$, etc. undergo slower radical-radical recombination or deactivation compared to $^{\bullet}OH$. Hence these radical anions are more readily available for longer time than $^{\bullet}OH$ to react with substrate and effect degradation. Thus the relatively lower reactivity is compensated by the better availability for reaction with the substrate. If they are not reacting with the anions, good amount of $^{\bullet}OH$ would undergo recombination and get deactivated. Enhancement of the degradation of phenol as in the present case, is possible only when the reaction rate between added anions and $^{\bullet}OH$, forming radical anion was higher than that between substrate and $^{\bullet}OH$, although both would be much lower than radical-radical recombination.

In the case of sono process, the scavenging of the $^{\bullet}OH$ by the anions takes place at the air-water interface of the cavitation bubbles where polarizable anions can undergo accumulation. The radical anions can diffuse into the solution bulk and react there with the substrate. The $^{\bullet}OH$ radical concentration is less in the bulk and hence their recombination also is less. Consequently, the $^{\bullet}OH$ will interact with the more abundant substrate and anions, both of which can lead to enhanced degradation. Under such conditions, scavenging of $^{\bullet}OH$ radical (which could have got self-deactivated by recombination otherwise) by the anion in the bulk forming radical anion can result in enhanced degradation. Hence, it may even be said that the anions are protecting the $^{\bullet}OH$ radicals from total deactivation and keeping them available, though with slightly reduced activity, for the degradation of the substrate. However above a particular concentration of the anion, the concentration of $^{\bullet}OH$ radicals available to interact with them is relatively less. Similarly, once the reaction has progressed substantially and the concentration of substrate has come down towards the later stages of reaction, the radical anion $X^{\bullet -}$ which has only substrate as the sink, cannot have much enhancing effect. From that point onwards, the enhancement by the anions is reduced and eventually they function as inhibitors by blocking the surface site. Thus further surface-initiated $^{\bullet}OH$ radical formation and activation of the substrate are slowed down. Hence the enhancement decreases with time of reaction as well as concentration of the anion and may even become inhibition.

Minero et al. [156] reported the formation of radical species like $^{\bullet}NO_2$, $^{\bullet}Br_2$, $^{\bullet}I_2$, etc. in presence of respective anions under sonochemical conditions and their subsequent interaction with phenol to form more

harmful compounds such as nitro-, chloro-, bromo- phenol, etc. According to them sonolysis cannot be used for the mineralization of phenol pollutant from water. However in the current study, in which sonolysis is carried out in presence of catalyst ZnO the formation of substituted phenols is not noticed. The reasons may be the relatively lower concentration of salts used in the study and the presence of ZnO as an active sonocatalyst. In presence of ZnO, the US induced sonoluminescence will lead to photocatalysis which is efficient for the mineralization of phenol. Solid particles may also play a physical role in the overall degradation scheme by facilitating additional nucleation sites and surface cavitation due to surface roughness [142, 164]. The formation of crevices and the wall of particles break up the spherical symmetry of the large sized cavitation bubble into many tiny cavitation bubbles. Increase in number of cavitation bubbles increases the pyrolysis of water and the sonochemical degradation. The adsorbed anions may be enhancing the nucleation capability of the surface which reaches an optimum with full surface coverage. Hence the degree of enhancement increases with increase in concentration and eventually stabilizes. The initial enhancement, gradual slow down and eventual inhibition of the degradation of phenol in presence of the anions clearly illustrate the importance of their interaction with the surface and surface initiated free radicals. The relative concentration of the radical anions formed insitu and their reactivity play an important role in deciding the ultimate influence of the anions.

6.4 Effect of anions on the fate of insitu formed H_2O_2

As explained in Chapter 3 to 5, the H_2O_2 formed during the photo, sono and sonophoto catalytic degradation of phenol undergoes concurrent decomposition forming more reactive $^{\bullet}OH$ and $HO_2^{\bullet}$ radicals and ultimately results in oscillation in its concentration. The effect of various anions on the fate of concurrently formed H_2O_2 during the photo, sono and sonophoto catalytic degradation of phenol in presence of ZnO is investigated and presented in figure 6.44 to 6.46. The concentration of anions is selected as 5 mg/L and all parameters are kept identical.

In photocatalysis (figure 6.44), except in the case of acetate and carbonate as well as nitrate (at later stages) the concentration of H_2O_2 is less compared to the system without anion.

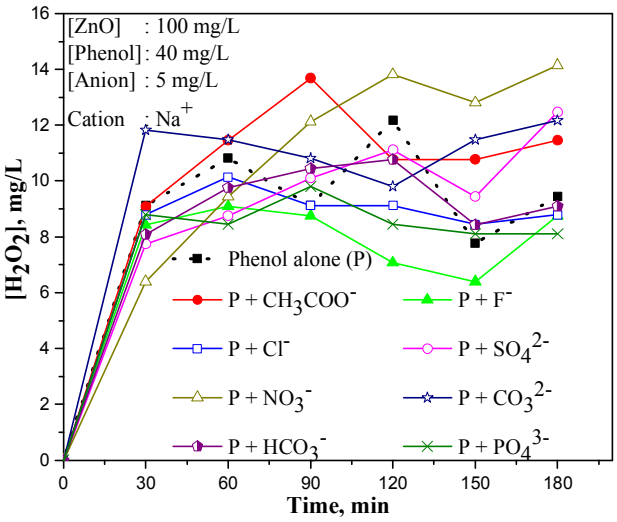

Fig. 6.44: Oscillation in the concentration of insitu formed H_2O_2 under photocatalysis in presence of various anions

However, the phenomenon of oscillation is seen in all cases. H_2O_2 at the maximum of the oscillation curve is the highest in presence of CH_3COO^- and NO_3^-. The lowest minimum of the curve happens in the

case of F^-. Even in the case of those anions which enhance the degradation of phenol, the net concentration of H_2O_2 is not always enhanced and the nature of the oscillation curve also differs from anion to anion. Many factors such as nature and concentration of anion, nature and concentration of substrate, adsorption of the substrate, nature of the catalyst, pH, etc. may influence the anion effect on the phenomenon of oscillation.

In sonocatalysis (figure 6.45), initially, the amount of H_2O_2 is more in the presence of all anions, as seen from the results in the first 30 minutes. This shows that under sonocatalysis enhancement in the degradation of phenol effected by anions also leads to enhanced H_2O_2 formation.

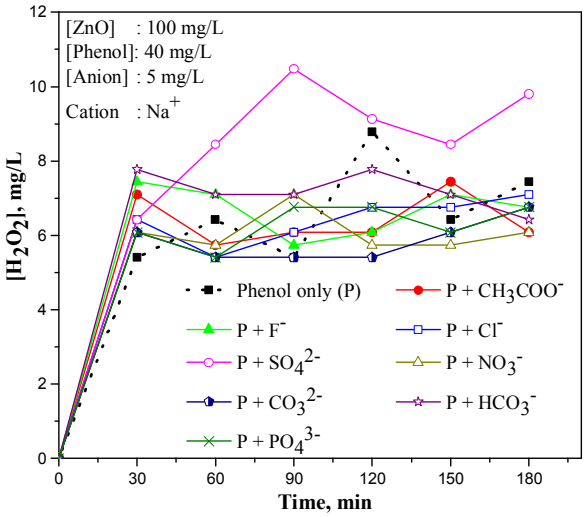

Fig. 6.45: Oscillation in the concentration of insitu formed H_2O_2 under sonocatalysis in presence of various anions

Once sufficient concentration of H_2O_2 is reached (which is dependent on a number of reaction parameters), the decomposition process dominates for a while until a certain minimum is reached and then the formation process takes over again. The almost stabilized net

concentration of H_2O_2 at later stages of reaction is less in the presence of anions in most cases. Since phenol degradation is enhanced, the concentration of insitu formed H_2O_2 also is expected to be more. However this is seen only in the beginning and not sustained, except in the presence of SO_4^{2-} which is not the best enhancer of phenol degradation among the anions studied here. As explained earlier, anions are good scavengers of $^{\bullet}OH$ radicals. Hence the availability of $^{\bullet}OH$ radicals for recombination and the formation of H_2O_2 is less resulting in decreased amounts of net H_2O_2. This also indirectly indicates that the formation of H_2O_2 happens primarily by the recombination or other reactions involving the $^{\bullet}OH$ radicals.

The higher net concentration of H_2O_2 in the presence of SO_4^{2-} ions shows that the $^{\bullet}OH$ radicals are not fully trapped by these anions and they are available for the formation of H_2O_2 throughout. This is unique among the anions studied here and has to be treated as an exception which needs to be investigated further. It is known that SO_4^{2-} ions get adsorbed on the surface and interact with the photoproduced holes [16] to generate sulphate radicals as follows:

$$h^+ + SO_4^{2-} \rightarrow SO_4^{\bullet-} \quad \text{.....(179)}$$

S is a strong oxidizing agent and hence the $SO_4^{\bullet-}$ radical can accelerate the degradation process according to reactions (180) to (182).

$$SO_4^{\bullet-} + H_2O \rightarrow SO_4^{2-} + {}^{\bullet}OH + H^+ \quad \text{.....(180)}$$

$$SO_4^{\bullet-} + \text{Pollutant} \rightarrow SO_4^{2-} + \text{Intermediate} \quad \text{.....(181)}$$

$$SO_4^{\bullet-} + \text{Intermediate} \rightarrow\rightarrow SO_4^{2-} + CO_2 + \text{Salts} \quad \text{.....(182)}$$

As seen in reaction (180), presence of $SO_4^{\bullet-}$ can lead to the formation of more $^{\bullet}OH$ radicals. The $^{\bullet}OH$ radicals can combine and form more H_2O_2. Hence, unlike in the case of other anions which scavenge the $^{\bullet}OH$, the SO_4^{2-} anions concurrently generate them. Hence the availability of $^{\bullet}OH$ and consequently the concentration of H_2O_2 is relatively more.

However, same trend in the concentration of H_2O_2 is not seen in the case of photo or sonophoto catalysis suggesting that the presence of intermediates, various free radicals and multiple interactions also are crucial in determining the ultimate fate of H_2O_2 in the system.

In sonophotocatalysis (figure 6.46), the net concentration of H_2O_2 is high in most cases indicating more facile formation process compared to decomposition.

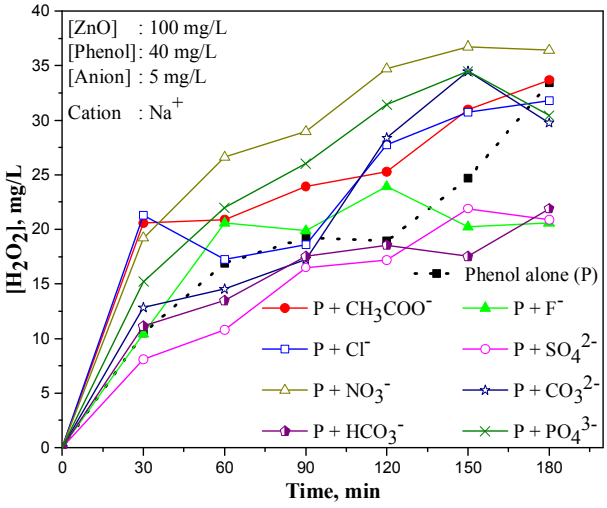

Fig. 6.46: Oscillation in the concentration of insitu formed H_2O_2 under sonophotocatalysis in presence of various anions

Only in the case of HCO_3^- and SO_4^{2-}, the net concentration of H_2O_2 is less compared to the system without anion. Maximum H_2O_2 is seen in

presence of NO_3^-. However, NO_3^- is the best enhancer anion in sonophotocatalysis only in the early stages of degradation. Hence the consistently higher concentration of H_2O_2 even after longer reaction time may be due to the lower rate of decomposition of H_2O_2 rather than higher rate of formation.

Due to simultaneous formation and decomposition, the rates of which depend on a number of factors, the concentration of H_2O_2 at any point in time during the reaction is not reproducible consistently. Hence the experiments had to be repeated many number of times under strictly identical conditions in order to get the most reliable reproducible data.

6.4.1 The effect of concentration of the anions on the insitu formed H_2O_2

It has been demonstrated earlier that the effect of anion on the degradation of phenol varies with concentration of the anion and the reaction time. In this context, the effect of varying the concentration of anions on the H_2O_2 concentration at different times of phenol degradation in sono, photo and sonophoto catalysis is investigated and is shown in figure 6.47 to 6.54 (photo), 6.55 to 6.62 (sono) and 6.63-6.70 (sonophoto).

6.4.1.1. Photocatalysis

The effect of anions on the net concentration of H_2O_2 under photocatalysis is shown in figures 6.47 to 6.54.

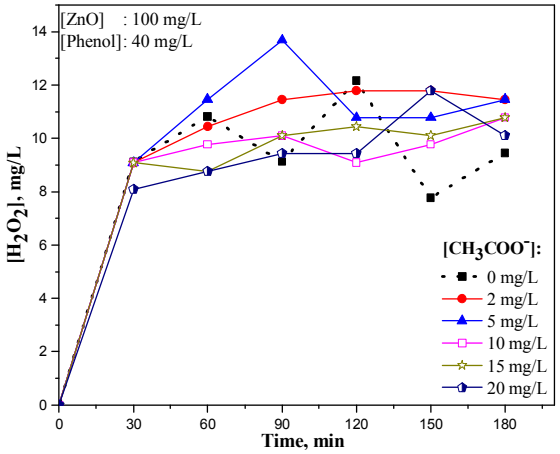

Fig. 6.47: Effect of CH_3COO^- on the oscillation in the concentration of H_2O_2 under photocatalysis

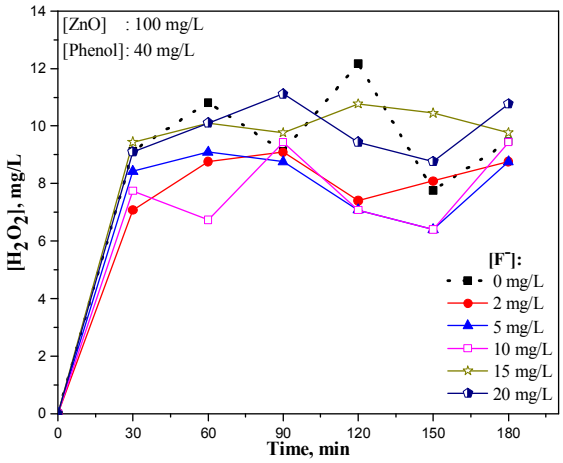

Fig. 6.48: Effect of F^- on the oscillation in the concentration of H_2O_2 under photocatalysis

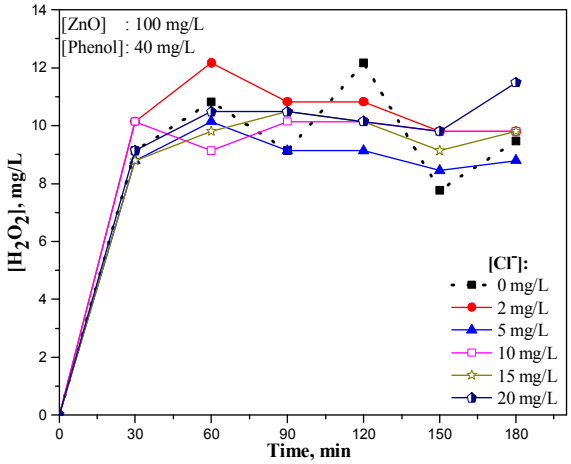

Fig. 6.49: Effect of Cl^- on the oscillation in the concentration of H_2O_2 under photocatalysis

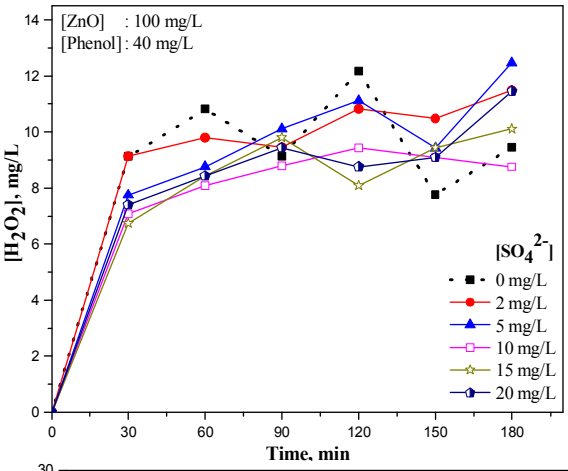

Fig. 6.50: Effect of SO_4^{2-} on the oscillation in the concentration of H_2O_2 under photocatalysis

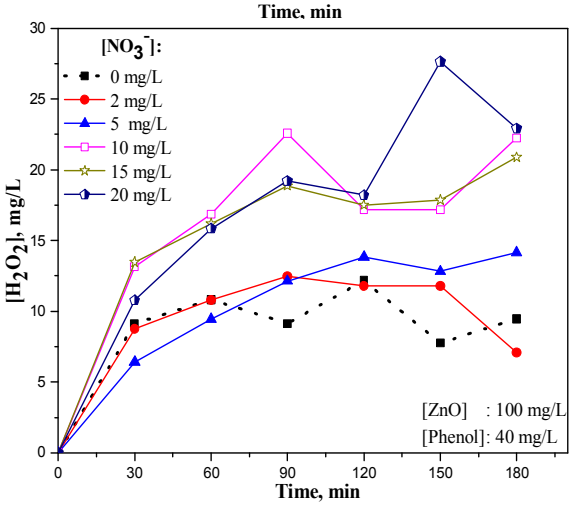

Fig. 6.51: Effect of NO_3^- on the oscillation in the concentration of H_2O_2 under photocatalysis

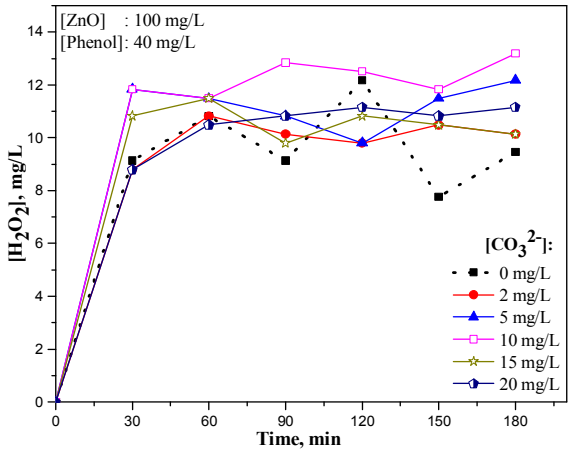

Fig. 6.52: Effect of CO_3^{2-} on the oscillation in th concentration of H_2O_2 under photocatalysis

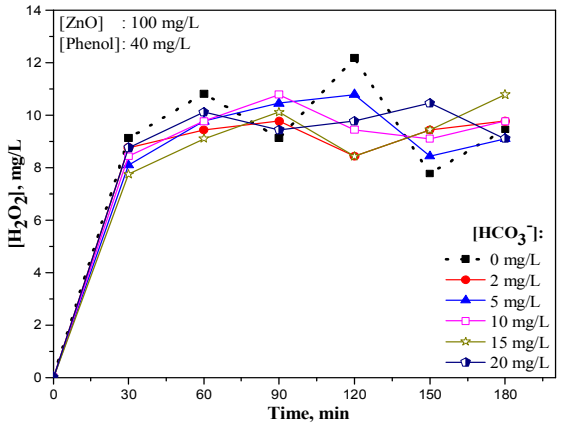

Fig. 6.53: Effect of HCO_3^- on the oscillation in the concentration of H_2O_2 under photocatalysis

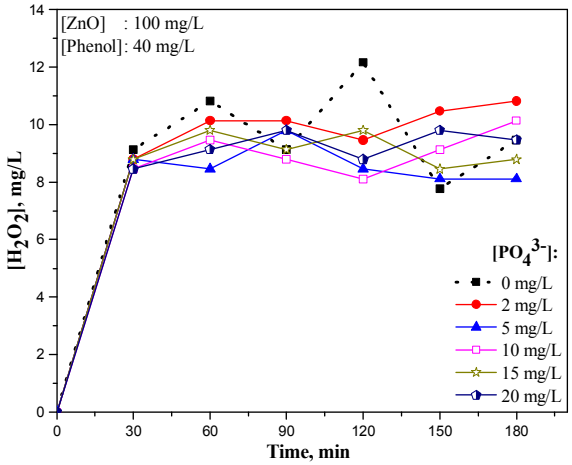

Fig. 6.54: Effect of PO_4^{3-} on the oscillation in the concentration of H_2O_2 under photocatalysis

In presence of CH_3COO^-, the net concentration of H_2O_2 is maximum at lower concentration (up to 5 mg/L). At higher concentration (> 5 mg/L) of CH_3COO^- the net concentration of H_2O_2 is lower than the reference (without anion) up to ~ 120 minutes of reaction. Thereafter the net H_2O_2 increases and remains more at all concentrations. In presence of F^- the concentration of H_2O_2 is generally lower up to 120 minutes except for a brief period at the higher concentration of 15 and 20 mg/L. In the case of Cl^-, the concentration of H_2O_2 remains generally low except at 2 mg/L of the anion up to 120 minutes. The H_2O_2 concentration remains almost stabilized with only weak oscillation at all Cl^- concentrations. In the case of

SO_4^{2-}, the net concentration of H_2O_2 is less than the reference up to 120 minutes. Thereafter H_2O_2 is more in the reaction system in presence of anion at almost all concentrations possibly due to dominating decomposition in the case of the reference and dominating formation (of H_2O_2) in the presence of the anion.

In presence of NO_3^-, except at low concentration of 2 and 5 mg/L in the beginning, the net concentration of H_2O_2 is higher throughout compared to the system without anion. The oscillation is sharper and more distinct at higher concentration of > 10 mg/L. In the presence of CO_3^{2-}, generally the net concentration of H_2O_2 is higher except at around 120 minutes where the oscillation curve in the absence of anion has a sharp maximum. In the case of HCO_3^- and PO_4^{3-} concentration of H_2O_2 is slightly less in presence of anion at all concentration, except for a brief period around 90 minutes and after 150 minutes where the reference oscillation curve is at its lower point.

Even though the oscillatory pattern in the concentration of H_2O_2 is there in presence of most of the anions, the trend varies with concentration of the anions and the time of reaction. The oscillation becomes generally weaker with time and shows stabilization trend. In this case also it is not possible to have any general quantitative conclusions on the effect of anions on the oscillation or in the concentration of H_2O_2, due to the complexity of the interactions involved.

6.4.1.2 Sonocatalysis

The effect of anions at different concentrations on the net concentration of H_2O_2 at different reaction times under sonocatalysis is shown in figures 6.55 to 6.62.

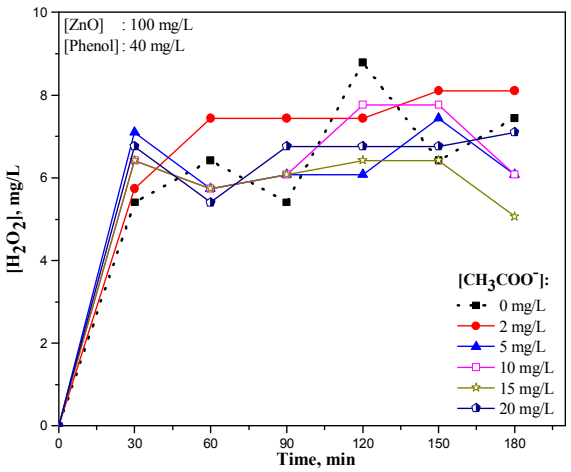

Fig. 6.55: Effect of CH_3COO^- on the oscillation in the concentration of H_2O_2 under sonocatalysis

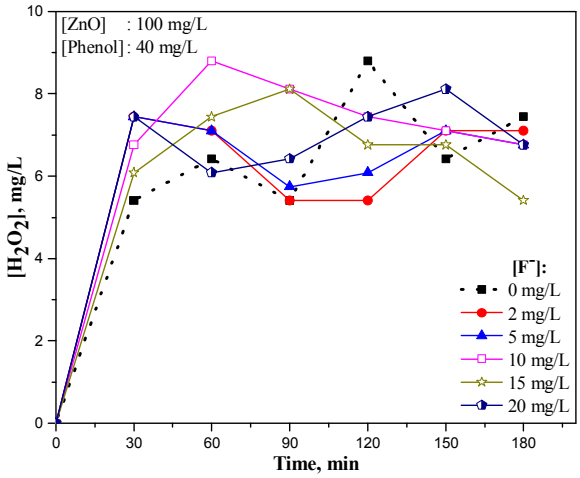

Fig. 6.56: Effect of F^- on the oscillation in the concentration of H_2O_2 under sonocatalysis

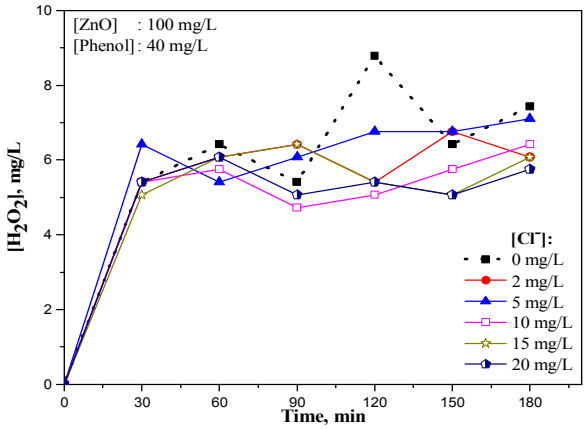

Fig. 6.57: Effect of Cl^- on the oscillation in the concentration of H_2O_2 under sonocatalysis

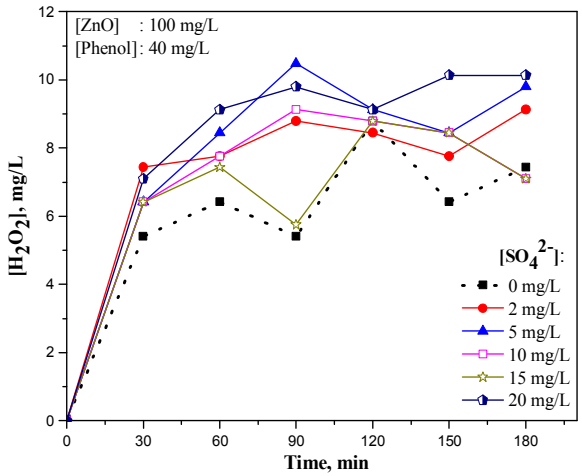

Fig. 6.58: Effect of SO_4^{2-} on the oscillation in the concentration of H_2O_2 under sonocatalysis

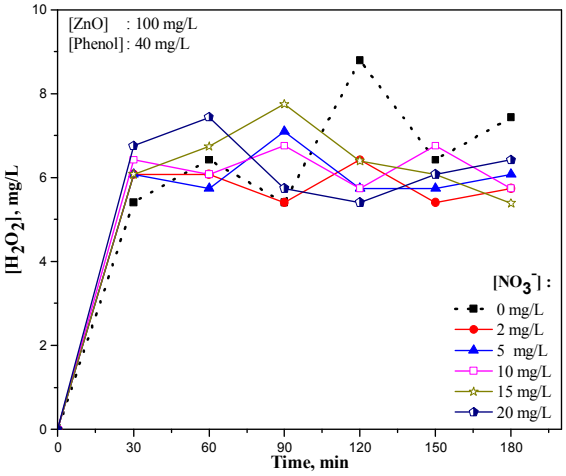

Fig. 6.59: Effect of NO_3^- on the oscillation in the concentration of H_2O_2 under sonocatalysis

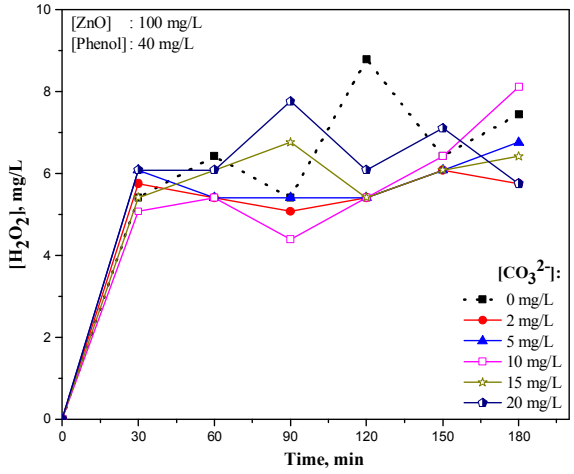

Fig. 6.60: Effect of CO_3^{2-} on the oscillation in the concentration of H_2O_2 under sonocatalysis

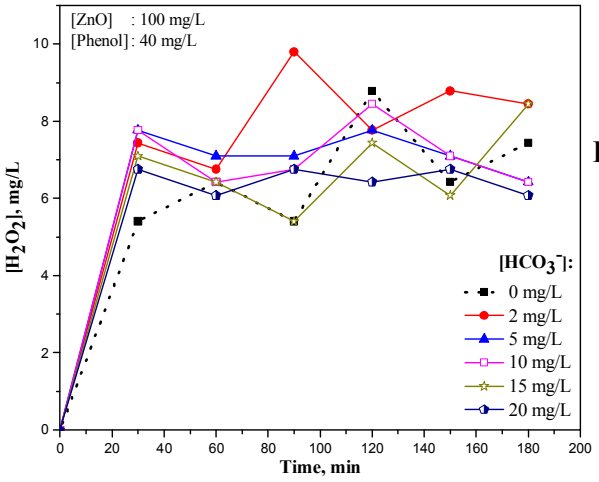

Fig. 6.61: Effect of HCO_3^- on the oscillation in the concentration of H_2O_2 under sonocatalysis

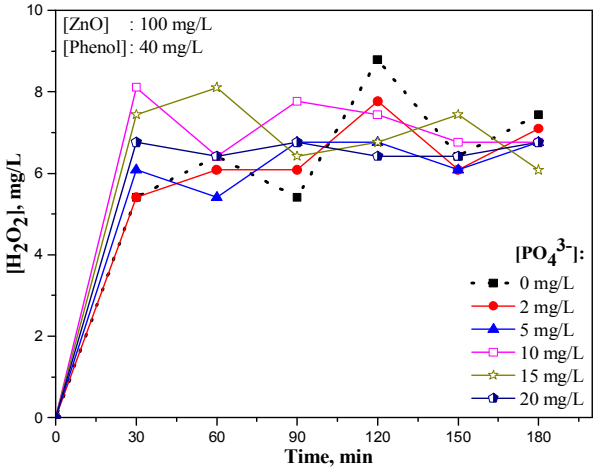

Fig. 6.62: Effect of PO_4^{3-} on the oscillation in the concentration of H_2O_2 under sonocatalysis

From the figures (6.55 to 6.62) it is seen that in sonocatalysis, in the case of most of the anions at all concentrations, the oscillation weakens with time and tends towards stabilization. However, as in other cases, there is no consistent trend that can lead to any general conclusion. In the presence of CH_3COO^-, the concentration of H_2O_2 is high initially compared to the reference. As reaction proceeds, the oscillation weakens and a stabilization trend sets in at almost all concentrations of the anion. The H_2O_2 concentration is slightly lower where the reference curve of the

oscillation (without added anions) is at its maximum. In the presence of a highly reactive anion F^-, the H_2O_2 concentration is more at all concentrations of the anion compared to the absence (of anion) up to 90 minutes. Later on the concentration of H_2O_2 becomes less compared to the reference when the reference is at its maximum, as in the case of CH_3COO^- ions. In presence of Cl^- the concentration of H_2O_2 remains slightly lower than the reference almost throughout. In this case the difference between the highest maximum and lowest minimum of H_2O_2 in the oscillation curve is relatively small indicating stabilization trend. In the presence of SO_4^{2-}, H_2O_2 is substantially more in presence of anion compared to the reference. It remains so throughout and the oscillation also is well pronounced. This is also not fully consistent with the influence of SO_4^{2-} on the degradation of phenol as explained earlier.

In the case of NO_3^- ions, the concentration of H_2O_2 is more in the initial stages followed by distinct oscillatory pattern. At later stages of reaction, when the reference has its maximum in the oscillation curve, the net concentration of H_2O_2 is less compared to that in the absence of the anion. The oscillation is well pronounced in the presence of CO_3^{2-} and HCO_3^- also with clear crests and troughs. The qualitative similarity of the oscillation curves in the case of HCO_3^- and CO_3^{2-} with respect to the net H_2O_2 concentration points to the similarity in radical interactions in the case of the two anions and possible formation of $CO_3^{\bullet-}$ from HCO_3^- as shown in reactions (172) and (173). The net concentration of H_2O_2 is more initially compared to the reference in the presence of HCO_3^- upto ~ 90 minutes. It becomes lower only when compared to the crest of the reference oscillation curve. Generally,

H_2O_2 remains lower than the reference in presence of CO_3^{2-} except at higher concentrations at the trough of the reference curve. In presence of PO_4^{3-}, initially H_2O_2 is more upto ~ 30 minutes at all concentrations. PO_4^{3-} is a good adsorbent and blocks the surface especially at higher concentrations. Hence the availability of surface activated phenol is less and the $^{\bullet}OH$ radicals in the bulk recombine and form more H_2O_2. Hence the H_2O_2 is more in the early stages and the $^{\bullet}OH$ radicals interact more frequently with them resulting in enhanced decomposition. This ultimately brings down net concentration of H_2O_2.

The results show that the phenomenon of oscillation and the effect of anions on the concentration of H_2O_2 is even more complex in sonocatalysis, making it difficult to propose a generally acceptable explanation.

6.4.1.3 Sonophotocatalysis

The effect of anions on the sonophotocatalytic generation and net concentration of H_2O_2 is given in figures 6.63 to 6.70.

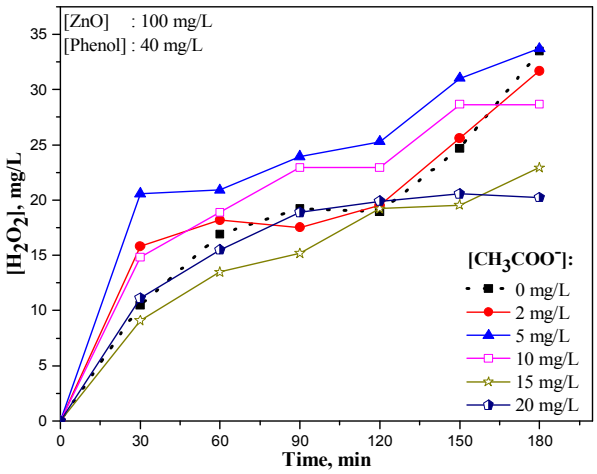

Fig. 6.63: Effect of CH_3COO^- on the oscillation in the concentration of H_2O_2 under sonophotocatalysis

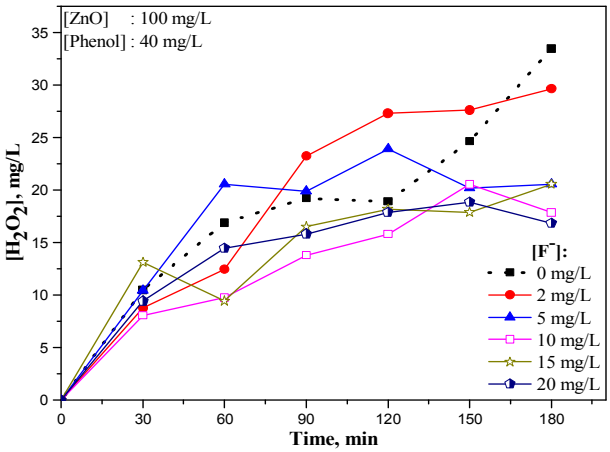

Fig. 6.64: Effect of F^- on the oscillation in the concentration of H_2O_2 under sonophotocatalysis

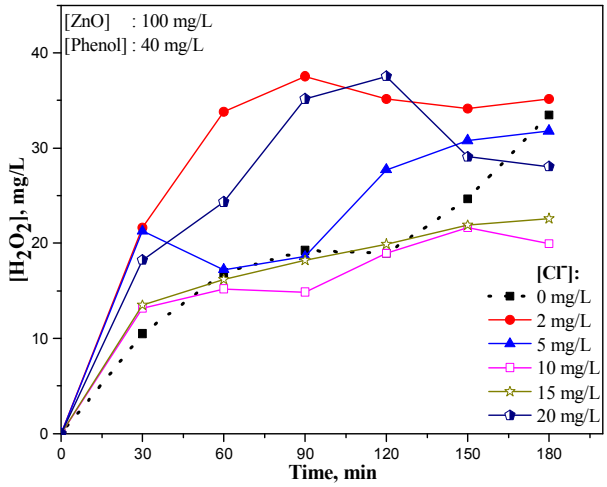

Fig. 6.65: Effect of Cl^- on the oscillation in the concentration of H_2O_2 under sonophotocatalysis

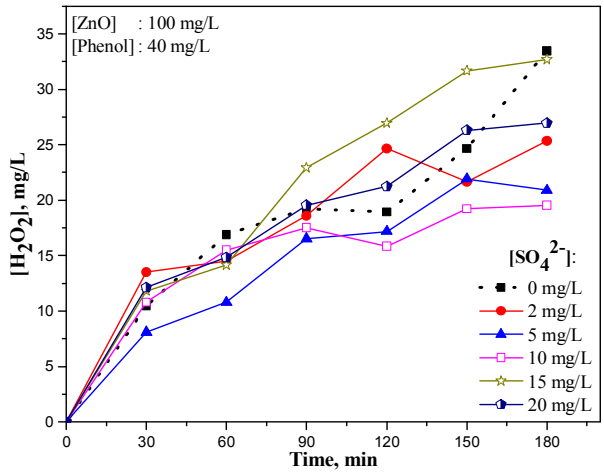

Fig. 6.66: Effect of SO_4^{2-} on the oscillation in the concentration of H_2O_2 under sonophotocatalysis

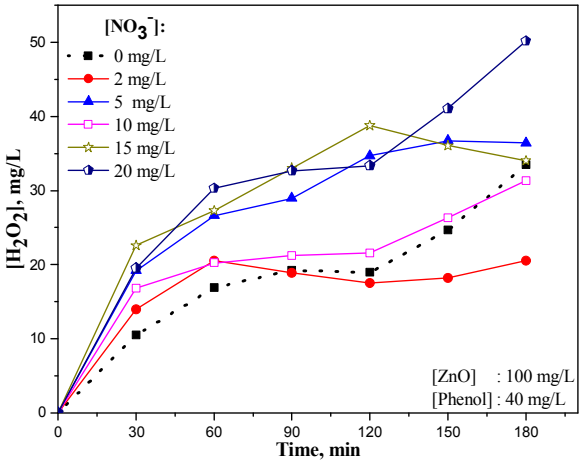

Fig. 6.67: Effect of NO_3^- on the oscillation in the concentration of H_2O_2 under sonophotocatalysis

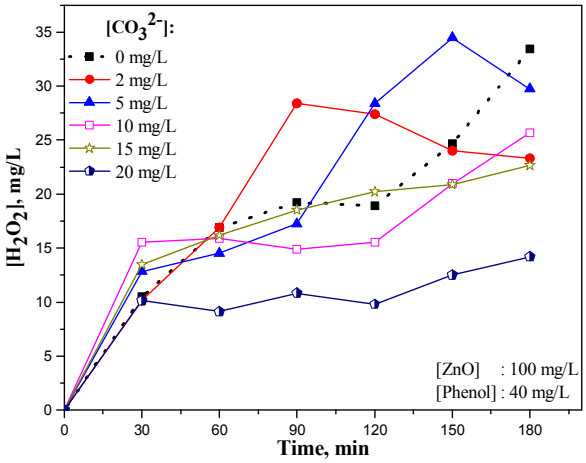

Fig. 6.68: Effect of CO_3^{2-} on the oscillation in the concentration of H_2O_2 under sonophotocatalysis

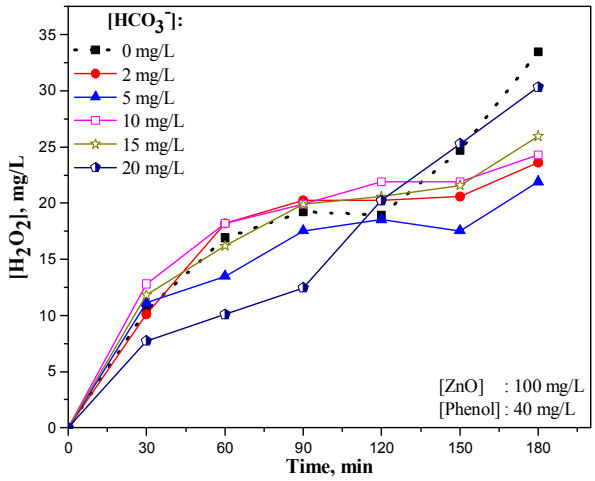

Fig. 6.69: Effect of HCO_3^- on the oscillation in the concentration of H_2O_2 under sonophotocatalysis

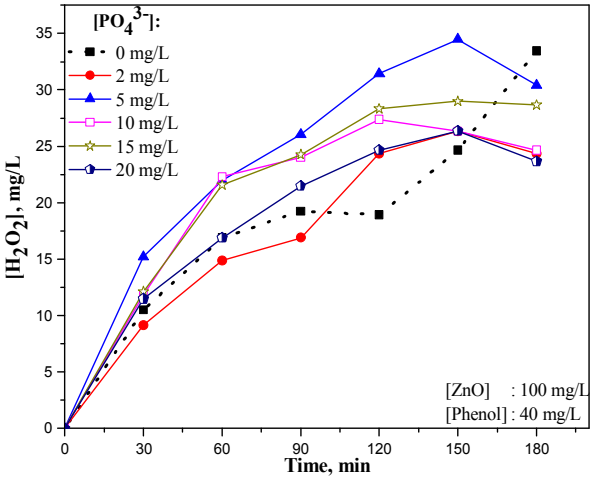

Fig. 6.70: Effect of PO_4^{3-} on the oscillation in the concentration of H_2O_2 under sonophotocatalysis

In the case of CH_3COO^-, the net concentration of H_2O_2 remains higher than that of reference at lower concentrations. At higher concentration of 15 to 20 mg/L of the anion the net concentration of H_2O_2 is less. In this case, the trend is more towards stabilization rather than oscillation. In the presence of F^-, the net concentration of H_2O_2 is less even at 10 mg/L of the anion at the early stages of reaction. The H_2O_2 starts increasing at ~ 60 minutes and the trend continues upto ~ 120 minutes. At this stage the net concentration of H_2O_2 is stabilized or decreasing. In the case of Cl^-, the net concentration of H_2O_2 is higher than that of reference initially, at all concentrations. The trend continues except at concentrations of 10 and 15 mg/L. In the case of SO_4^{2-}, the behavior of H_2O_2 is even more complex, with no consistent concentration effect even in the broad classification of range of 'low' or 'high'. This is probably because of the presence of a number of highly reactive radical anion such as $SO_4^{-\bullet}$.

In presence of NO_3^-, the net concentration of H_2O_2 is higher at all concentrations initially. As the reaction proceeds, at 2 mg/L of the anion the net concentration of H_2O_2 become slightly less than the reference after 90 minutes. In the case of CO_3^{2-}, the H_2O_2 is more initially at all concentrations. Later on H_2O_2 remains more than the reference only at lower concentrations, i.e. 2 and 5 mg/L. In the case of HCO_3^-, at almost all concentrations the net concentration of H_2O_2 is generally same or lower than that of reference. In the case of PO_4^{3-}, except for 2 mg/L, the net H_2O_2 concentration is higher than that of the reference. At later stages of reaction (after 150 minutes), for all concentrations, the net concentration of H_2O_2 become lower.

From the forgoing observations, it may be concluded that the effect of anions on the H_2O_2 formed insitu in sono, photo and sonophoto catalysis is quite complex and no consistent correlation is possible. This may be one of the reasons why the fate of H_2O_2 in these AOPs is often overlooked or not reported by fellow researchers.

6.4.2 Summary of the effect of anions on the net initial rate of formation of H_2O_2

In view of the complexity of the process involving multitude of competing reactions in presence of various anions meaningful comparison of the results or interpretations of the data is difficult. In the search for a rational parameter for comparison, the net initial rate of formation of H_2O_2 before it reaches the first maximum in the oscillation curve is examined.

The net initial rate of formation of H_2O_2 in presence of anions under photocatalysis is computed and presented in table 6.13.

Table 6.13: Effect of various anions on the initial net rate of formation of H_2O_2 in **photocatalysis.** [Phenol]: 40 mg/L [ZnO]: 100 mg/L

Concentration (mg/L)	Net Initial rate of formation of H_2O_2 (mg/L/sec x 10^3)								
	CH_3COO^-	F^-	Cl^-	SO_4^{2-}	NO_3^-	CO_3^{2-}	HCO_3^-	PO_4^{3-}	Nil
2	5.1	3.9	5.6	5.1	4.9	4.9	4.9	4.9	5.1
5	5.1	4.7	4.9	4.3	3.6	6.6	4.5	4.9	5.1
10	5.1	4.3	5.6	3.9	7.3	6.6	4.7	4.7	5.1
15	5.1	5.2	4.9	3.7	7.5	6.0	4.3	4.9	5.1
20	4.5	5.1	5.1	4.1	6.0	4.9	4.9	4.7	5.1

The table shows that the net initial rate of formation of H_2O_2 in presence of anions is slightly less compared to the system without anion except at certain random concentrations of NO_3^-, Cl^- and CO_3^{2-}. Even for this parameter, there is no consistent pattern at different concentrations of the anions.

Similarly the net initial rate in the case of sonocatalysis is computed and tabulated in table 6.14.

Table 6.14: Effect of various anions on the initial net rate of formation of H_2O_2 in **sonocatalysis.** [Phenol]: 40 mg/L [ZnO]: 100 mg/L

Concentration (mg/L)	Net Initial rate of formation of H_2O_2 (mg/L/sec x 10^3)								
	CH_3COO^-	F^-	Cl^-	SO_4^{2-}	NO_3^-	CO_3^{2-}	HCO_3^-	PO_4^{3-}	Nil
2	3.2	4.2	3.0	4.2	3.3	3.2	4.2	3.0	3.1
5	3.8	4.2	3.5	3.5	3.3	3.3	4.3	3.3	3.1
10	3.5	3.7	3.0	3.5	3.5	2.8	4.3	4.5	3.1
15	3.5	3.3	2.8	3.5	3.3	3.0	3.8	4.2	3.1
20	3.7	4.2	3.0	3.5	3.7	3.3	3.7	3.7	3.1

The table 6.14 shows that there is slight enhancement of the net initial rate of formation of H_2O_2 in presence of most of the anions at different concentrations. The enhancement in the rate is much less compared to that for corresponding degradation of phenol, possibly due to the concurrent decomposition of H_2O_2 and other reaction of the free radicals.

The net initial rate of formation of H_2O_2 before it reaches the first maximum in the oscillation curve in the case of sonophotocatalysis is shown in table 6.15.

Table 6.15: Effect of various anions on the initial net rate of formation of H_2O_2 in **sonophotocatalysis.** [Phenol]: 40 mg/L [ZnO]: 100 mg/L

Concentration (mg/L)	**Net Initial rate of formation of H_2O_2 (mg/L/sec x 10^3)**								
	CH_3COO^-	**F^-**	**Cl^-**	**SO_4^{2-}**	**NO_3^-**	**CO_3^{2-}**	**HCO_3^-**	**PO_4^{3-}**	**Nil**
2	8.8	4.9	12.0	7.5	7.8	5.6	5.6	5.1	5.8
5	11.4	5.8	11.8	4.5	10.7	7.1	6.2	8.5	5.8
10	8.2	4.5	7.3	6.0	9.4	8.6	7.1	6.6	5.8
15	5.1	7.3	7.5	6.6	12.5	7.5	6.6	6.7	5.8
20	6.2	5.2	10.1	6.7	10..9	5.6	4.3	6.4	5.8

As expected, the effect of anions is even more complex than in the case of photo and sono catalysis. Almost all anions, depending on the reaction condition behave as enhancers. Minor variations in the case of certain anions at certain concentration can be treated as exceptions which occur in complex reaction systems. The complexity of both photocatalysis and sonocatalysis got more compounded in the case of sonophotocatalysis.

6.5 Effect of cations on the photo, sono and sonophoto catalytic degradation of phenol

Anions are always associated with cations and hence the effect of various cations is also important in the design of suitable AOP system for wastewater treatment. In this context, the influence of a number of cations (Na^+, K^+, Mg^{2+}, Ca^{2+}, Al^{3+}) which are likely to be present in water on the ZnO-mediated photo, sono and sonophoto catalytic degradation of phenol is investigated. The anions selected in these cases were NO_3^-, SO_4^{2-} and Cl^-. For each anion, the effect of its cation on the degradation is investigated. The results are plotted in figures 6.71 to 6.79.

6.5.1 Photocatalysis

The effect of various cations on the photocatalytic degradation of phenol is shown in figures 6.71 to 6.73.

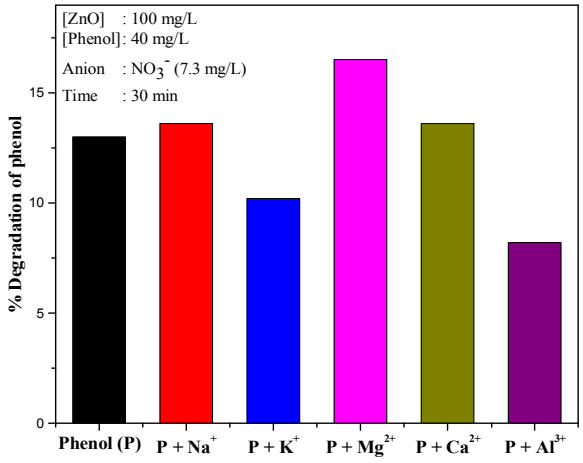

Fig. 6.71: Effect of various cations on the photocatalytic degradation of phenol: (Anion: NO_3^-)

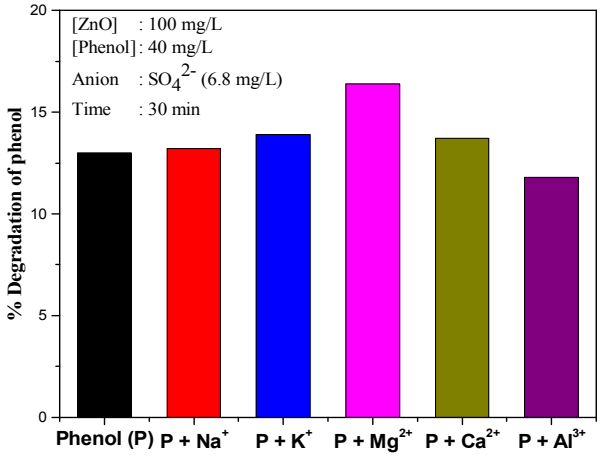

Fig.6.72: Effect of various cations on the photocatalytic degradation of phenol: (Anion: SO_4^{2-})

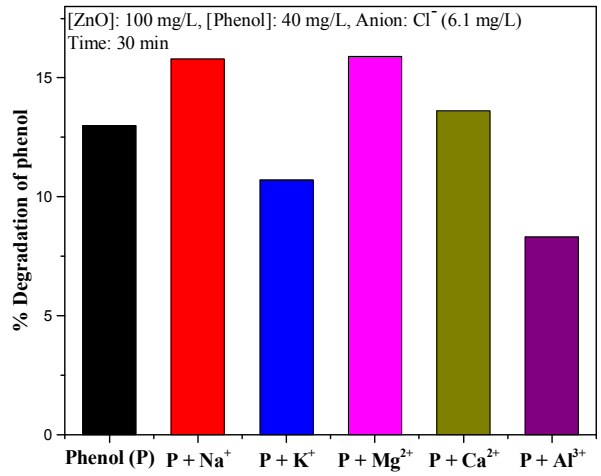

Fig.6.73: Effect of various cations on the photocatalytic degradation of phenol: (Anion: Cl^-)

In the case of photocatalysis, salts containing NO_3^- and SO_4^{2-} are the best enhancers among various anions for phenol degradation (section 6.3.2.1). However, the degree of enhancement varies significantly with change in the cation of the salt.

For all three salts, Al^{3+} cation is an inhibitor. K^+ is an inhibitor in the case of NO_3^- and Cl^- anions while it has practically no effect in the

case of SO_4^{2-} anions. Na^+ and Ca^{2+} are mild enhancers with the three anions. Mg^{2+} is an efficient enhancer in all three cases.

The trend of cation effect on the photocatalytic degradation of phenol is more or less the same qualitatively for the three anions as follows:

NO_3^-: $Mg^{2+} > Na^+ \approx Ca^{2+} \approx$ No Cation $> K^+ > Al^{3+}$

SO_4^{2-}: $Mg^{2+} > Na^+ \approx Ca^{2+} \approx K^+ \approx$ No Cation $> Al^{3+}$

Cl^-: $Mg^{2+} \approx Na^+ > Ca^{2+} \approx$ No Cation $> K^+ > Al^{3+}$

For the three anions tested here salts containing Mg^{2+} followed by Na^+ and Ca^{2+} are better for enhancing the photocatalytic degradation of pollutants in water. Thus it may be tentatively inferred that $MgSO_4/Mg(NO_3)_2/MgCl_2$ are the best among the salts tested here to enhance the degradation. However, detailed studies are needed and the parameters have to be optimized for each salt in view of the complex nature of interaction between the cation/anion, the surface of the ZnO, the substrate, various reactive species etc.

6.5.2 Sonocatalysis

The effect of various cations on the sonocatalytic degradation of phenol is shown in figures 6.74 to 6.76.

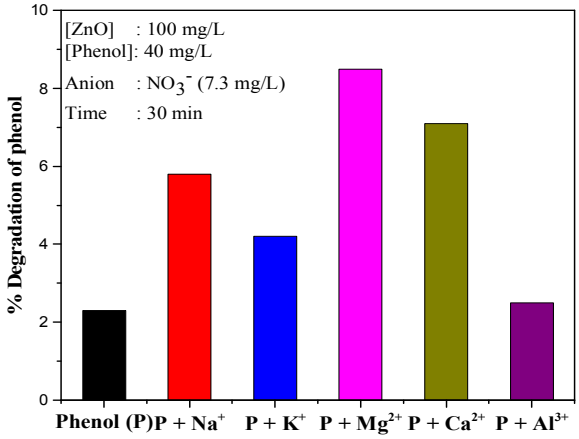

Fig. 6.74: Effect of various cations on the sonocatalytic degradation of phenol: (Anion: NO_3^-)

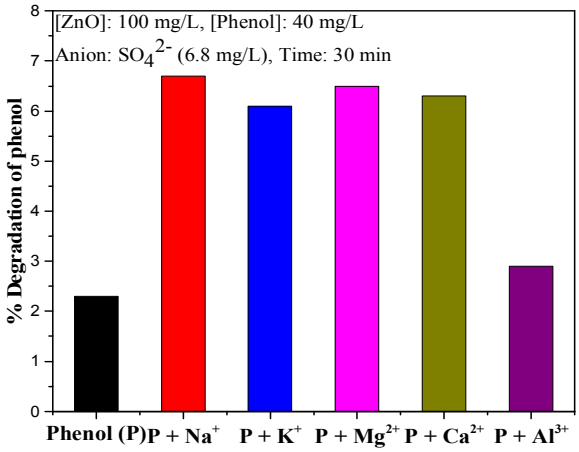

Fig. 6.75: Effect of various cations on the sonocatalytic degradation of phenol: (Anion: SO_4^{2-})

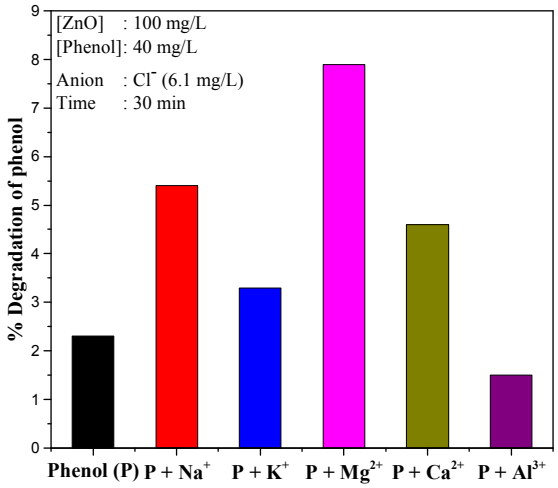

Fig.6.76: Effect of various cations on the sonocatalytic degradation of phenol: (Anion: Cl^-)

All cations except Al^{3+} enhance sonocatalytic degradation of phenol, even though the degree of enhancement varies with difference in the anions. Al^{3+} exhibits least enhancement or even 'no effect' or inhibition. Among the anions, Cl^- is not a good enhancer compared to other anions tested here (see section 6.3.2.2). Naturally it is expected that Al^{3+} as the cation and Cl^- as the corresponding anion will result in least enhancement or even inhibition. For all three anions i. e. NO_3^-, SO_4^{2-} and Cl^-, the degradation is generally enhanced irrespective of the cation. Hence it is certain that the enhancement observed for various salts is mainly due to the anion itself. However, even for same anions, the cations influence the effect of salt as seen in the figures 6.74 to 6.76. Thus the enhancing effect of the cations may be compared as follows:

NO_3^-: $Mg^{2+} > Ca^{2+} > Na^+ > K^+ > Al^{3+} \approx$ No Cation

SO_4^{2-}: $Mg^{2+} \approx Na^+ \approx Ca^{2+} > K^+ > Al^{3+} \approx$ No Cation

Cl^-: $Mg^{2+} > Na^+ > Ca^{2+} > K^+ >$ No Cation $> Al^{3+}$

Combining the results on the effect of cation and anion it is seen that NO_3^- and CH_3COO^- are the best enhancing anions (table 6.6) and Mg^{2+} and Ca^{2+} followed by Na^+ are the best cations. Hence it may be inferred that $Mg(CH_3COO)_2$ or $Mg(NO_3)_2$ may be very good salts for enhancing sonocatalytic activity. Preliminary studies showed that $Mg(NO_3)_2$ has the highest sonocatalytic activity. However, detailed studies are needed to arrive at the most promising salts based on the reaction parameters and the system composition.

6.5.3 Sonophotocatalysis

The effect of various cations on the sonophotocatalytic degradation of phenol is shown in figures 6.77 to 6.79.

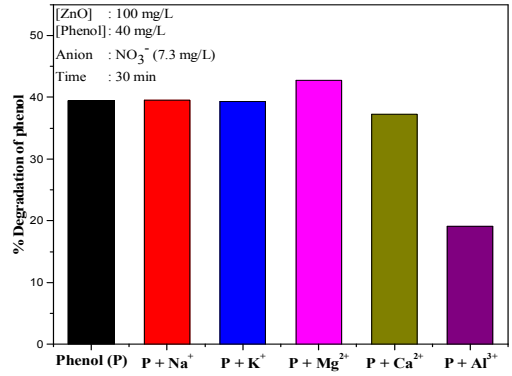

Fig. 6.77: Effect of various cations on the sonophotocatalytic degradation of phenol: (Anion: NO_3^-)

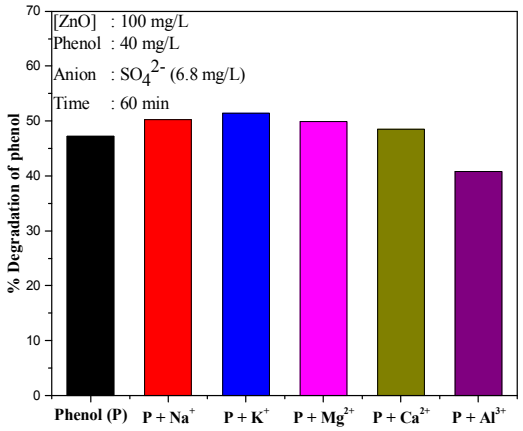

Fig. 6.78: Effect of various cations on the sonophotocatalytic degradation of phenol: (Anion: SO_4^{2-})

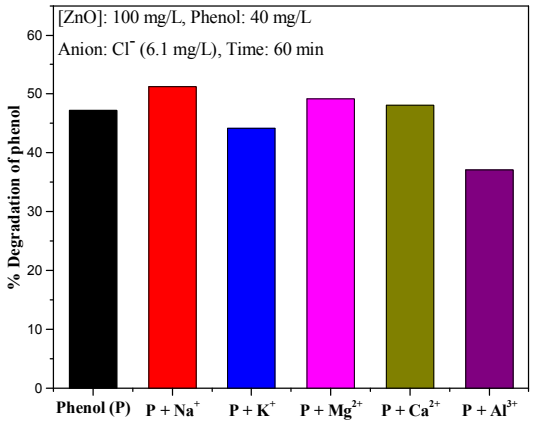

Fig. 6.79: Effect of various cations on the sonophotocatalytic degradation of phenol: (Anion: Cl^-)

In the case of sonophotocatalysis also Al^{3+} inhibits the degradation irrespective of the anion. Even with the NO_3^- anion which is a clear enhancer of sonophotocatalytic degradation of phenol, Al^{3+} cation becomes a strong inhibitor. Other cations have only negligible effect irrespective of the anion. Hence it may be inferred that the cations/salt effect, at least in the concentrations tested here, is not quite distinct at higher degradation range. The combined effect of photo and sono catalysis is capable to some extent in compensating for whatever inhibitive effect is there from the salts, as discussed in earlier chapters. The effect of cation on the degradation of phenol may be summarized as:

NO_3^-: $Mg^{2+} > Na^+ \approx Ca^{2+} \approx K^+ \approx$ No Cation $> Al^{3+}$

SO_4^{2-}: $Mg^{2+} \approx Na^+ > Ca^{2+} \approx K^+ \approx$ No Cation $> Al^{3+}$

Cl^-: $Mg^{2+} \approx Na^+ \approx Ca^{2+} \approx K^+ \approx$ No Cation $> Al^{3+}$

Just as in the case of anion effects, other parameters such as concentration of the cations, reaction time, etc. may influence the cation effect differently. In view of the complexity of the mechanism of salt effect, it may not be easy to clearly distinguish the anion and cation effect precisely by simple straight forward experiments. However certain general conclusions can be arrived at which will be helpful in identifying the optimum reaction conditions for enhanced degradation.

6.5.4 Ionic radius vs cation effect

One possible explanation for the effect of cations/salts on the rate of degradation of organics in the presence of catalysts is their adsorption/layer formation on the catalyst surface. The layer formation

may inhibit or in rare cases promote the adsorption of the substrate and subsequent activation in presence of US/UV/US+UV. In such cases, the size of the cation may have a role. Lower the size of the cation, the higher the volume and effectiveness in covering the surface and the result is more inhibition or less enhancement of the degradation of phenol. A correlation between the ionic radius of the cation and the degree of enhancement of the degradation of phenol in presence of cation is examined in tables 6.16 to 6.18.

Table 6.16: Ionic radius of cations [165] vs % enhancement in their presence in **photocatalysis.**

[ZnO]: 100 mg/L, [Phenol]: 40 mg/L, [NO_3^-]: 7.3 mg/L, [SO_4^{2-}]: 6.8 mg/L, [Cl^-]: 6.1 mg/L

Cation	Ionic radius (Å)	% Enhancement					
		In 30 min (Anion: Nitrate)	In 60 min (Anion: Nitrate)	In 30 min (Anion: Sulphate)	In 60 min (Anion: Sulphate)	In 30 min (Anion: Chloride)	In 60 min (Anion: Chloride)
Na^+	0.98	4.6	16.7	1.5	12.0	21.5	22.2
K^+	1.33	-21.5	-15.0	6.9	-6.0	-17.7	5.1
Mg^{2+}	0.65	26.9	15.8	26.2	12.4	22.3	24.4
Ca^{2+}	0.94	4.6	-1.7	5.4	-3.4	4.6	2.1
Al^{3+}	0.45	-36.9	-32.1	-9.2	-17..1	-36.2	-10.3

Table 6.17: Ionic radius [165] of cations vs % enhancement in their presence in **sonocatalysis.**

[ZnO]: 100 mg/L, [Phenol]: 40 mg/L, [NO_3^-]: 7.3 mg/L, [SO_4^{2-}]: 6.8 mg/L, [Cl^-]: 6.1 mg/L

Cation	Ionic radiusÅ)	% Enhancement					
		In 30 min (Anion: Nitrate)	In 60 min (Anion: Nitrate)	In 30 min (Anion: Sulphate)	In 60 min (Anion: Sulphate)	In 30 min (Anion: Chloride)	In 60 min (Anion: Chloride)
Na^+	0.98	152.2	60.5	191.3	79.1	134.8	34.9
K^+	1.33	82.6	34.9	165.2	81.4	43.5	13.9
Mg^{2+}	0.65	269.6	125.6	182.6	97.7	243.5	179.1
Ca^{2+}	0.94	208.7	111.6	173.9	118.6	100	39.5
Al^{3+}	0.45	8.7	11.6	26.1	-11.6	-34.8	-39.5

Table 6.18: Ionic radius [165] of cations vs % enhancement in their presence in **sonophotocatalysis.**

[ZnO]: 100 mg/L, [Phenol]: 40 mg/L, [NO_3^-]: 7.3 mg/L, [SO_4^{2-}]: 6.8 mg/L, [Cl^-]: 6.1 mg/L

Cation	Ionic radius (Å)	% Enhancement					
		In 30 min (Anion: Nitrate)	In 60 min (Anion: Nitrate)	In 30 min (Anion: Sulphate)	In 60 min (Anion: Sulphate)	In 30 min (Anion: Chloride)	In 60 min (Anion: Chloride)
Na^+	0.98	0.25	-8.9	11.9	6.4	2.3	8.7
K^+	1.33	-0.25	3.2	3.3	8.9	2.5	-6.4
Mg^{2+}	0.65	8.4	14.8	13.9	5.7	0	4.2
Ca^{2+}	0.94	-5.5	-8.3	-3.0	2.8	4.8	1.9
Al^{3+}	0.45	-51.5	-32.6	-9.2	-13.6	-26.1	-21.4

Based on the ionic radius of the cations their coverage on the surface of ZnO and consequently the inhibition of the degradation of phenol should have been in the order:

$$Al^{3+} > Mg^{2+} > Ca^{2+} \approx Na^+ > K^+$$

But this trend is not observed in the case of the cations, irrespective of the anions except in the case of Al^{3+}. In any case, as has been explained earlier the photo, sono and sonophoto catalytic degradation of phenol on ZnO is mostly taking place in the solution bulk and the contribution of surface is relatively less. Hence any correlation based on effect of cations on surface process may not be quite relevant or precise. Like the anions, the cations also may be influencing the bulk process which requires extensive investigation separately.

6.6 Effect of cations on the fate of H_2O_2 under photo, sono and sonophoto catalysis

The effect of above mentioned cations on the fate of concurrently formed H_2O_2 in photo, sono and sonophoto catalysis is investigated and the results are as follows.

6.6.1 Photocatalysis

The effect of cations on the fate of concurrently formed H_2O_2 under photocatalysis is shown in figures 6.80 to 6.82.

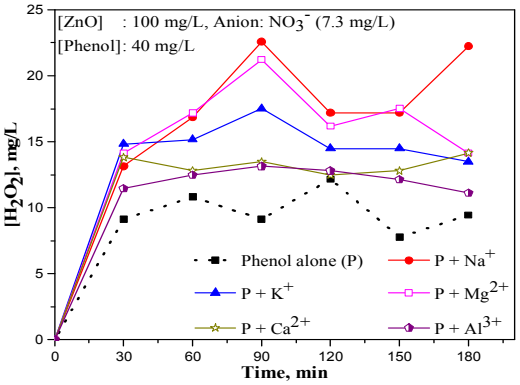

Fig. 6.80: Effect of various cations on the oscillation in the concentration of H_2O_2 under photocatalysis: (Anion: NO_3^-)

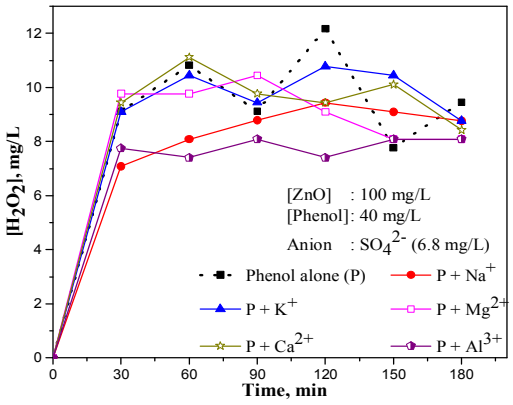

Fig. 6.81: Effect of various cations on the oscillation in the concentration of H_2O_2 under photocatalysis: (Anion: SO_4^{2-})

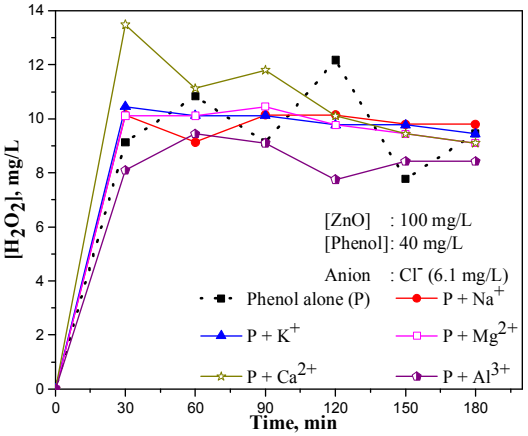

Fig. 6.82: Effect of various cations on the oscillation in the concentration of H_2O_2 under photocatalysis: (Anion: Cl^-)

With NO_3^- anion, the concentration of H_2O_2 is more in presence of all cations, compared to the reference (without cations). The effect is similar to the observation made under 'anion effect' thereby confirming the dominance of anion in determining the effect of salts on the photocatalytic process. However, presence of a dominating cation like Al^{3+} can slow down the effect of anions. In the case of SO_4^{2-} as the anion, the initial concentration of H_2O_2 is less in presence of all cations studied here. With Cl^- as the anion, except Al^{3+} and Ca^{2+}, the oscillation is weak and the net concentration of H_2O_2 is stabilized with no clear oscillation. The high concentration of H_2O_2 and the prominent crests in the beginning in presence of $CaCl_2$ unlike other salts, i.e., $Ca(NO_3)_2$ and $CaSO_4$ confirms that the effect of cations cannot be evaluated in isolation from the anions.

6.6.2 Sonocatalysis

The effect of cations on the fate of concurrently formed H_2O_2 under sonocatalysis is shown in figures 6.83 to 6.85.

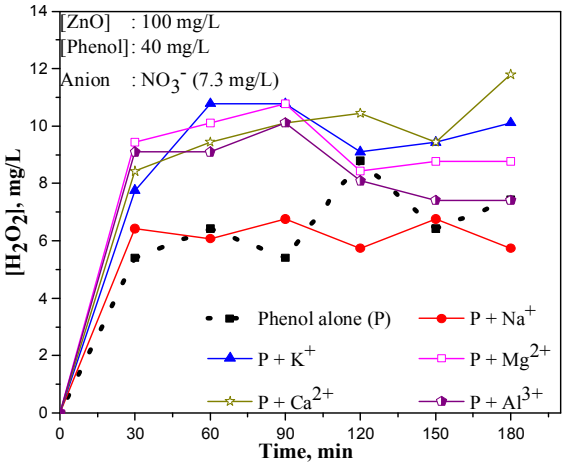

Fig. 6.83: Effect of various cations on the oscillation in the concentration of H_2O_2 under sonocatalysis: (Anion: NO_3^-)

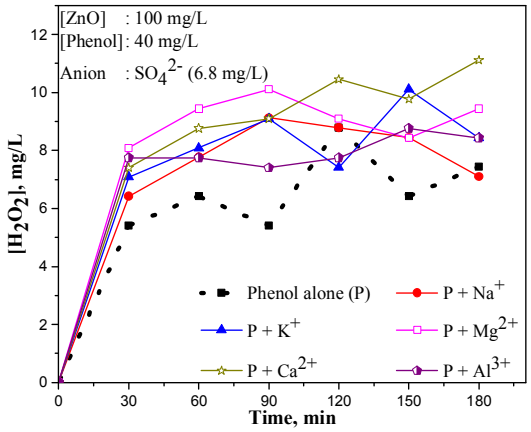

Fig. 6.84: Effect of various cations on the oscillation in the concentration of H_2O_2 under sonocatalysis: (Anion: SO_4^{2-})

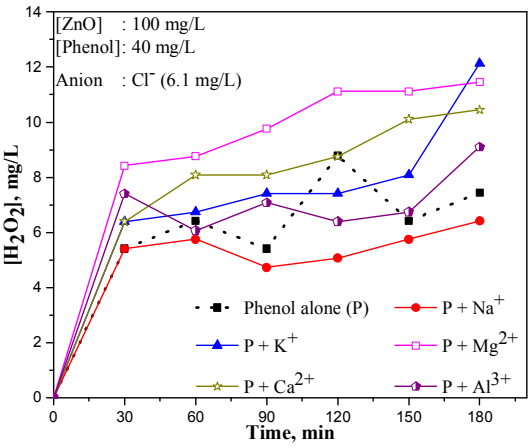

Fig. 6.85: Effect of various cations on the oscillation in the concentration of H_2O_2 under sonocatalysis: (Anion: Cl^-)

The net concentration of H_2O_2 at various times of reaction is more in the presence of all cations tested here irrespective of the nature of the anion except in the case of NaCl and $NaNO_3$ at lower concentration of 2 mg/L. While studying the anion effect it was noticed that (figure 6.57) the Cl^- ions reduce the net concentration of H_2O_2 in sonocatalytic process. Hence, in this case too the lower concentration of H_2O_2 in presence of Na^+ is a combination of the effect of Cl^- and Na^+. The net concentration of H_2O_2 is maximum in the case of Mg^{2+} cation (except minor variations)

and this is consistent with the maximum degradation of phenol in presence of this cation. The effect of Mg^{2+} on H_2O_2 is fairly similar with SO_4^{2-} and NO_3^- as the anion. Similar is the case with Ca^{2+} also. The nature of the H_2O_2 curve clearly indicates that cations also do have a role in deciding the nature of the oscillations and the net concentration of H_2O_2 though the anions have a more prominent role. However, these inferences are general with possible exceptions since even under well-defined experimental conditions, oscillation in the concentration of H_2O_2 is not amenable to any general interpretation. The complexity of the system consisting of a number of reactive free radicals, concurrent formation and decomposition of H_2O_2 and the formation of a series of intermediates, many of them competing with each other contributes to this inconsistency as explained earlier.

6.6.3 Sonophotocatalysis

The effect of cations on the fate of concurrently formed H_2O_2 under sonophotocatalysis is shown in figures 6.86 to 6.88.

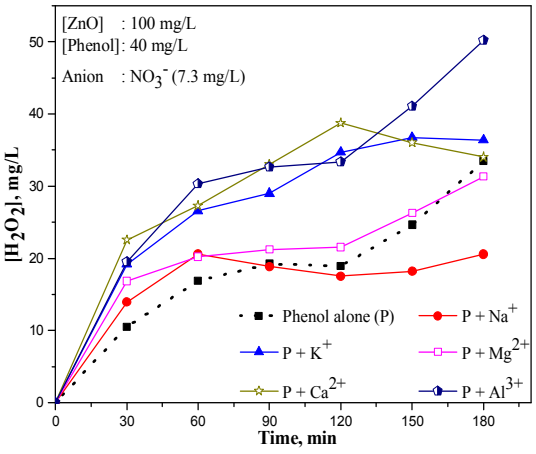

Fig. 6.86: Effect of various cations on the oscillation in the concentration of H_2O_2 under sonophotocatalysis: (Anion: NO_3^-)

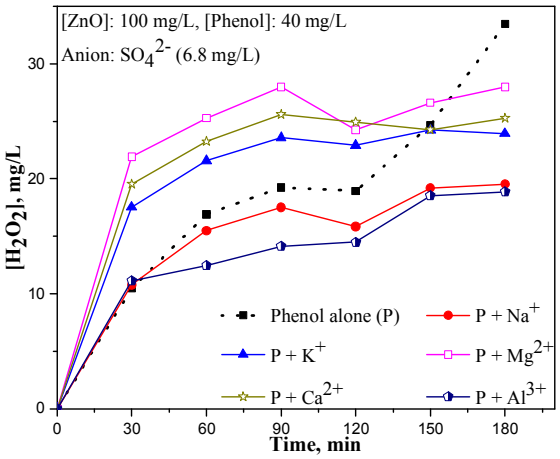

Fig. 6.87: Effect of various cations on the oscillation in the concentration of H_2O_2 under sonophotocatalysis: (Anion: SO_4^{2-})

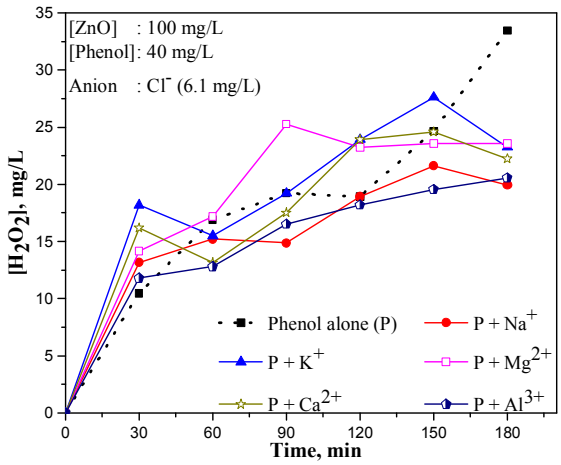

Fig. 6.88: Effect of various cations on the oscillation in the concentration of H_2O_2 under sonophotocatalysis: (Anion: Cl^-)

In the case of sonophotocatalysis, when NO_3^- is the anion, the higher concentration of H_2O_2 in presence of various cations compared to the reference (without cations) is sustained except in the case of Na^+ at later stages of reaction. In presence of SO_4^{2-} anion, the net concentration of H_2O_2 in the system is high in presence of cations K^+, Mg^{2+} and Ca^{2+}. But in presence of Na^+ and Al^{3+} the net concentration of H_2O_2 is lower compared to the system without cation. In the case of Cl^- anion, initially the net concentration of H_2O_2 is high in presence of all cations. However,

as the reaction proceeds concentration of H_2O_2 decreases and eventually goes below the reference. In the case of Mg^{2+} and K^+, the net H_2O_2 concentration remains more compared to the reference except at later stages. In the case of Ca^{2+} too, the concentration of H_2O_2 is more at the crests of the corresponding oscillation curve. As the process of oscillation has set in, the decomposition may be becoming more dominant in the presence of certain cations and consequently, the net concentration of H_2O_2 becomes less and the overall concentration profile becomes inconsistent.

6.7 Major Findings and Conclusions

The study clearly shows that presence of dissolved salts has a significant role in the photo, sono and sonophoto catalytic degradation of phenol in presence of ZnO. The effect of salts is a combination of the effect of respective cations and anions; the anion effect being more dominant. The effect is dependent on reaction time and concentration of the salt. Contrary to many earlier reports, current study shows that inorganic salts enhance the photo, sono and sonophoto catalytic degradation of phenol. The enhancement of the degradation by anions is explained based on the formation of reactive radical anions by interaction of the anion with the insitu formed $^{\bullet}OH$ radicals. The lower reactivity of the radical anion compared to highly reactive $^{\bullet}OH$ radical is compensated by the abundance of the former and better availability for the substrate. Once the concentration of the $^{\bullet}OH$ radicals became low, some of the anions which do not have the option for interaction with them will get adsorbed on the catalyst surface or block the catalytic sites. Consequently the degradation slows down and

eventual inhibition follows. However, the mechanism cannot be universally applied and the effect of every anion needs in-depth investigation and analysis, with due consideration of various reaction parameters.

The cation effect and anion effect could not be delineated precisely in the current study due to experimental limitation. However, it may be generally concluded that certain cations such as Mg^{2+} enhance the photo, sono and sonophoto catalytic degradation of phenol. Al^{3+} is clearly an inhibitor, irrespective of the nature of the anion.

With respect to the concentration and fate of concurrently formed H_2O_2, initially the anions and cations influence the same fairly in line with their effect on phenol degradation. However, after the initial period (the duration of which varies with the anion), once the concurrent formation and decomposition processes have set in, and the oscillation is in progress, the concentration of H_2O_2 at any point of time becomes inconsistent and unpredictable. The study highlights the complexity in arriving at quantitative conclusions on the effect of salts in AOPs as well as on the fate and role of insitu formed H_2O_2. The study highlights the importance of identifying cross contaminants such as salts in water quantitatively and qualitatively in designing suitable treatment methods for the decontamination (of water).

Chapter 7

SUMMARY AND CONCLUSION

AOPs such as sono, photo and sonophoto catalysis for the purification of polluted water under ambient conditions involve the formation and participation of ROS like $^{\bullet}OH$, $HO_2^{\bullet}$, $O_2^{\bullet}$, H_2O_2, etc. Among these, H_2O_2 is the most stable and is also a precursor for other reactive free radicals. The main objective of the current study was to investigate the fate of H_2O_2 formed during sono, photo and sonophoto catalytic processes. The net concentration of H_2O_2 measured in the system was not consistent with the rate of its generation. It is not reproducible either. The study is an investigation into the 'missing' of H_2O_2 from the system and its unusual behavior. The study also throws more light on the influence of naturally occurring contaminants such as various cations and anions on the efficiency of degradation of the pollutants and the fate of concurrently formed H_2O_2.

The semiconductor oxide catalyst used for the study was ZnO and the pollutant tested was phenol, which is one of the major chemical pollutants found in wastewater from petrochemical industries. The catalyst was characterized by standard wet analytical, adsorption and instrumentation techniques. The pollutant phenol was analyzed by UV-VIS spectrophotometry and the concentration of H_2O_2 was measured by standard iodometry. Various reaction parameters such as catalyst

dosage, pH, pollutant concentration, presence of contaminants, O_2, etc. were optimized for the degradation of the pollutant. The fate of H_2O_2 under each of the three AOPs is also closely monitored quantitatively.

Major findings of the study and the conclusions are as follows:

1) Semiconductor oxide mediated photocatalysis is an environment-friendly process for the removal of trace amounts of phenol from water. H_2O_2 is one of the stable intermediates formed during the degradation of phenol and it functions also as a precursor for other reactive free radicals. The concentration of H_2O_2 formed during the photocatalytic degradation of phenol cannot be quantitatively correlated with the phenol degradation. H_2O_2 undergoes concurrent decomposition resulting in 'oscillation' in its concentration. The concentration at which decomposition/formation overtakes one another is sensitive to the reaction conditions. Various parameters such as catalyst loading, substrate concentration, particle size, pH, externally added H_2O_2 and presence of air/O_2 influence this unique phenomenon of oscillation. The oscillation in the concentration of H_2O_2 continues for some more time even after the energy source is switched off, indicating the residual activity of the catalyst, i.e., 'memory effect'. A reaction mechanism for the photocatalytic degradation of phenol and the oscillation phenomenon is proposed and discussed.

2) Sonication and sonocatalysis are also potential AOPs for the removal of toxic organic pollutants from water. However the efficiency of sonocatalytic process is much lower compared to

photocatalysis. Here also the intermediate formed during the degradation process, i.e., H_2O_2, undergoes concurrent decomposition resulting in oscillation in its concentration. The oscillation is influenced by various reaction parameters such as catalyst loading, substrate concentration, particle size, pH, externally added H_2O_2, presence of air/O_2, etc. H_2O_2 plays a unique role in the process as acceptor of both electrons and holes. Suitable mechanism for the process, taking various observations into consideration is proposed and discussed.

3) The basic mechanism of sonocatalysis involves the formation of 'hotspot' and sonoluminescence. US induced sonoluminescence makes sonocatalysis partially photocatalytic thereby opening the possibility of combining the two process i.e., sonophotocatalysis for enhanced efficiency. The sonophotocatalytic degradation of phenol in the concurrent presence of UV and US is more than the sum of the degradation under photocatalysis and sonocatalysis, which confirms the synergy. The oscillatory behavior of H_2O_2 observed in the case of sono and photo catalysis is less evident in sonophotocatalysis probably due to the accelerated rate of formation compared to decomposition. The net concentration of H_2O_2 in the system at any point of time is in the order; sono < photo < sonophoto. The reaction parameters which affect the concentration of H_2O_2 in the system are catalyst loading, substrate concentration, particle size of catalyst, pH, externally added H_2O_2, presence of air/O_2, etc. A mechanism taking into account the observations is proposed and discussed.

4) The impact of the presence of natural and man-made contaminants in water on the efficiency of the degradation process is also investigated in detail. It was observed that the inorganic salts likely to be present in water influence the rate of degradation and the behavior of insitu formed H_2O_2 under sono, photo and sonophoto catalysis. The effect of salts is dependent on the reaction time and concentration of the anions. Contrary to many earlier reports, current study shows that the inorganic salts enhance the sono, photo and sonophoto catalytic degradation of phenol. Various anions interact with the reactive $^{\bullet}OH$ radicals and respective radical anions are produced which cause the enhancement effect. Oscillation in the concentration of H_2O_2 is also influenced by the salts. But in this case there is no consistent pattern for the salt effect. The cations also influence sono, photo and sonophoto catalysis. However it is the anions in the salt that has more dominant role in deciding the salt effect. In short, identification of the contaminants in water is important in the design of appropriate and efficient treatment methods.

To sum up, ZnO mediated sono, photo and sonophoto catalytic degradation of phenol in water generates H_2O_2 as an intermediate as well as final product. The H_2O_2 thus formed undergoes concurrent decomposition resulting in oscillation in its concentration in sonocatalysis, weak oscillation/stabilization in photocatalysis and stabilization in the case of sonophotocatalysis. Once the concentration of H_2O_2 reaches a particular maximum, decomposition process starts dominating. Similarly the formation will start dominating, once a critical minimum is reached. H_2O_2

is an important water soluble trace gas species in the atmosphere which can undergo various reactions in presence of photocatalytically active suspended particulate matter resulting in active free radicals. This can affect the chemistry of upper atmosphere, making the study of the fate of H_2O_2 in presence of light and sound relevant from the climate change angle as well.

References

[1] S. Devipriya, S. Yesodharan, Photocatalytic degradation of pesticide contaminants in water, Sol. Energy Mater. Sol. Cells 86 (2005) 309–348

[2] W.H. Glaze, J.W. Kang, D.H. Chapin, The chemistry of water treatment processes involving ozone, hydrogen peroxide and UV-radiation, Ozone: Sci. Eng. 9 (1987) 335–352

[3] M.N. Chong, B. Jin, C.W.K. Chow, C. Saint, New developments in photocatalytic water treatment technology: A review, Water Res. 44 (2010) 2997–3027

[4] C.G. Joseph, G.L. Puma, A. Bono, D. Krishnaiah, Sonophotocatalysis in advanced oxidation process: A short review, Ultrason. Sonochem. 16 (2009) 583–589

[5] P.R. Gogate, Treatment of wastewater streams containing phenolic compounds using hybrid techniques based on cavitation: A review of the current status and the way forward, Ultrason. Sonochem. 15 (2008) 1–15

[6] Y.C. Chen, P. Smirniotis, Enhancement of photocatalytic degradation of phenol and chlorophenols by ultrasound, Ind. Eng. Chem. Res. 41 (2002) 5958–5965

[7] N. Serpone, R. Terzian, P. Colarusso, Sonochemical oxidation of phenol and three of its intermediate products in aqueous media: Catechol, hydroquinone and benzoquinone. Kinetic and mechanistic aspects, Res. Chem. Intermed. 18 (1992) 183–202

[8] J.M. Poyatos, M.M. Muñio, M.C. Almecija, J.C. Torres, E. Hontoria, F. Osorio, Advanced oxidation processes for wastewater treatment: State of the art, Water Air Soil Pollut. 205 (2010) 187–204

[9] O. Legrini, E. Oliveros, A.M. Braun, Photochemical processes for water treatment, Chem. Rev. 93 **(**1993) 671-698

[10] E. Neyens, J. Baeyens, A review of classic fenton's peroxidation as an advanced oxidation technique, J. Hazard. Mater. 98 (2003) 33-58

[11] M. Niaounakis, C.P. Halvadakis, Olive processing waste management – Literature review and patent survey, 2nd Ed., Elsevier, Amsterdam (2006)

[12] J.E.F. Moraes, F.H. Quina, C.A.O. Nascimento, D.N. Silva, O. Chiavone-Filho, Treatment of saline wastewater contaminated with hydrocarbons by the photo-Fenton process, Environ. Sci. Technol. 38 (2004) 1183-1187

[13] J.M. Herrmann, Heterogenous photocatalysis: Fundamentals and application to the removal of various types of aqueous pollutants, Catal. Today 53 (1999) 115-129

[14] C. Kittle, Introduction to solid state physics, Wiley Eastern Limited, New Delhi (1976)

[15] A.L. Linsebigler, G. Lu, J.T. Yates, Photocatalysis on TiO_2 surfaces: Principles, mechanisms, and selected results, Chem. Rev. 95 (1995) 735-758

[16] M.R. Hoffmann, S.T. Martin, W. Choi, D.W. Bahnemann, Environmental applications of semiconductor photocatalysis, Chem. Rev. 95 (1995) 69-96

[17] J. Peral, X. Domonech, D.H. Ollis, Heterogeneous photocatalysis for purification, decontamination and deodorization of air, J. Chem. Technol. Biotechnol. 70 (1997) 117-140

[18] K. Kavita, C. Rubina, L.S. Rameshwar, Treatment of hazardous organic and inorganic compounds through aqueous-phase photocatalysis: A review, Ind. Eng. Chem. Res. 43 (2004) 7683-7696

[19] M. Gratzel, Photoelectrochemical cells, Nature 414 (2001) 338-344

[20] S. Ahmed, M.G. Rasul, W.N. Martens, R. Brown, M.A. Hashib, Heterogeneous photocatalytic degradation of phenols in wastewater: A review on current status and developments, Desalination 261 (2010) 3–18

[21] C.S. Turchi and D.F. Ollis, Photocatalytic degradation of organic water contaminants: Mechanisms involving hydroxyl radical attack, J. Catal. 122 (1990) 178-192

[22] M. Abdullah, G.K-C. Low, R.W. Mathews, Effects of common inorganic anions on rates of photocatalytic oxidation of organic carbon over illuminated titanium dioxide, J. Phys. Chem. 94 (1990) 6820-6825

[23] C. Minero, G. Mariella, V. Maurino, D. Vione, E. Pelizzetti., Photocatalytic transformation of organic compounds in the presence of inorganic ions. 2. Competitive reactions of phenol and alcohols on a titanium dioxide-fluoride system, Langmuir 16 (2000) 8964-8972

[24] P. Calza, E. Pelizzetti, Photocatalytic transformation of organic compounds in the presence of inorganic ions, Pure Appl. Chem. 73 (2001) 1839–1848

[25] S. Sakthivel, B. Neppolian, M.V. Shankar, B. Arabindoo, M. Palanichamy, V. Murugesan, Solar photocatalytic degradation of azo dye: Comparison of photocatalytic efficiency of ZnO and TiO_2, Sol. Energy Mater. Sol. Cells 77 (2003) 65–82

[26] R. Sandhya, D. Suja, Y. Suguna, Photocatalytic degradation of phosphamidon on semiconductor oxides, J. Hazard. Mater. 102 (2003) 217–229

[27] C. Hu, J.C. Yu, Z. Hao, P.K. Wong, Effects of acidity and inorganic ions on the photocatalytic degradation of different azo dyes, Appl. Catal., B: Environ. 46 (2003) 35–47

[28] G. Sivalingam, M.H. Priya, M. Giridhar, Kinetics of the photodegradation of substituted phenols by solution combustion synthesized TiO_2, Appl. Catal., B: Environ. 51 (2004) 67–76

[29] C.G. Wu, C.C. Chao, F.T. Kuo, Enhancement of the photo catalytic performance of TiO_2 catalysts via transition metal modification, Catal. Today 97 (2004) 103–112

[30] W. Han, W. Zhu, P. Zhang, Y. Zhang, L. Li, Photocatalytic degradation of phenols in aqueous solution under irradiation of 254 and 185 nm UV light, Catal. Today 90 (2004) 319–324

[31] W. Zhang, T. An, M. Cui, G. Sheng, J. Fu, Effects of anions on the photocatalytic and photoelectrocatalytic degradation of reactive dye in a packed-bed reactor, J Chem. Technol. Biotechnol. 80 (2005) 223–229

[32] C. Guillard, E. Puzenat, H. Lachheb, A. Houas, J-M. Herrmann, Why inorganic salts decrease the TiO_2 photocatalytic efficiency, Inter. J. photoenerg. 07 (2005) 1-9

[33] N. Barka, S. Qourzal, A. Assabbane, A. Nounah, Y. Ait-Ichou, Factors influencing the photocatalytic degradation of Rhodamine B by TiO_2-coated non-woven paper, J. Photochem. Photobiol., A: Chem. 195 (2008) 346–351

[34] A.D. Parag, M. Giridhar, Photocatalytic degradation of phenol by base metal-substituted orthovanadates, Chem. Eng. J. 161 (2010) 136–145

[35] F.V. Leticia, B.P. Jose, O.A. Conchi, Role of activated carbon features on the photocatalytic degradation of phenol, Appl. Surf. Sci. 256 (2010) 5254–5258

[36] P.A. Mangrulkar, S.P. Kamble, M.M. Joshi, J.S. Meshram, N.K. Labhsetwar, S.S. Rayalu, Photocatalytic degradation of phenolics by N-doped mesoporous titania under solar radiation, Inter. J. Photoenerg. Article ID 780562 (2012) 10 pages

[37] C.S. Lu, C.C. Chen, L.K. Huang, P.A. Tsai, H.F. Lai, Photocatalytic degradation of Acridine Orange over $NaBiO_3$ driven by visible light irradiation, Catalysis 3 (2013) 501-516

[38] A. Ameta, R. Ameta, M Ahuja, Photocatalytic degradation of methylene blue over ferric tungstate, Sci. Revs. Chem. Commun. 3 (2013) 172-180.

[39] H. Benhebal, M. Chaib, T. Salmon, J. Geens, A. Leonard, S.D. Lambert, M. Crine, B. Heinrichs, Photocatalytic degradation of phenol and benzoic acid using zinc oxide powders prepared by the sol–gel process, Alex. Eng. J. 52 (2013) 517–523

[40] N. Jallouli, K. Elghniji, H. Trabelsi, M. Ksibi, Photocatalytic degradation of paracetamol on TiO_2 nanoparticles and TiO_2/cellulosic fiber under UV and sunlight irradiation, Arab. J. Chem. (Available online 12th April 2014) http://dx.doi.org/10.1016/j.arabjc.2014.03.014)

[41] R.R. Dalbhanjan, N.S. Pande, B.S. Banerjee, S.P. Hinge, A.V. Mohod, P.R. Gogate, Degradation of patent blue V dye using modified photocatalytic reactor based on solar and UV irradiations, Desalin. Water Treat. 57 (2016) 18217-18228

[42] P. Rathore, R. Ameta, S. Sharma, Photocatalytic degradation of Azure A Using N-doped zinc oxide, J. Text. Sci. Technol. 1 (2015) 118-126

[43] P. Gelate, M. Hodnett, B. Zeqiri, Supporting infrastructure and early measurements. National Physical Laboratory Report. Teddington. Middlesex, UK (2000) pp- 2-11

[44] N.N. Mahamuni, Y.G. Adewuyi, Advanced oxidation processes (AOPs) involving ultrasound for waste water treatment: A review with emphasis on cost estimation, Ultrason. Sonochem. 17 (2010) 990–1003

[45] J. Weiss, Radiochemistry of aqueous solutions, Nature 155 (1944) 748–750

[46] K. Makino, M.M. Mossoba, P. Reisz, Chemical effects of ultrasound on aqueous solutions: Evidence for ·OH and ·H by spin trapping, J. Amer. Chem. Soc. 104 (1982) 3537–3539

[47] L.H. Thompson, L.K. Doraiswamy, Sonochemistry: Science and engineering, Ind. Eng. Chem. Res. 38 (1999) 1215–1249

[48] T.J. Mason, Ultrasound in synthetic organic chemistry, Chem. Soc. Rev. 26 (1997) 443-451

[49] P.R. Gogate, S. Mujumdar, A.B. Pandit, Large-scale sonochemical reactors for process intensification: Design and experimental validation, J. Chem. Technol. Biotechnol. 78 (2003) 685–693

[50] S. Vajnhandl, A. Majcen L. Marechal, Ultrasound in textile dyeing and the decolouration/mineralization of textile dyes, Dyes Pigm. 65 (2005) 89–101

[51] M.S. Al-Amoudi, S.A. Bazaid, A.M.A. Adam, A.M. Asiri, M. Salman, Sono and sonophotoctalysis for wastewater treatment, Pelagia Research Library, Der Chemica Sinica 3 (2012) 129-147

[52] A. Kotronarou, G. Mills, M.R. Hoffmann, Oxidation of hydrogen sulfide in aqueous solution by ultrasonic irradiation, Environ. Sci. Technol. 26 (1992) 2420–2428

[53] K.S. Suslick, Sonochemistry, Science 247 (1990) 1439–1445

[54] Y.G. Adewuyi, Sonochemistry: Environmental science and engineering applications, Ind. Eng. Chem. Res. 40 (2001) 4681–4715

[55] K.S. Suslick, D.A. Hammerton, R.E. Cline Jr., The sonochemical hot spot, J. Amer. Chem. Soc. 108 (1986) 5641–5642

[56] J. Rae, M. Ashokkumar, O. Eulaerts, C. Von Sonntag, J. Reisse, F. Grieser, Estimation of ultrasound induced cavitation bubble temperatures in aqueous solutions, Ultrason. Sonochem. 12 (2005) 325–329

[57] K.S. Suslick, L.A. Crum, in M.J. Crocker (Ed.), Encyclopedia of Acoustics, Wiley Interscience, New York (1997) pp 271-282

[58] H. Chen, S. Liu, J. Wang, D. Chen, Study on effect of microparticle's size on cavitation erosion in solid–liquid system, J. Appl. Phys. 101 (2007) 1-5

[59] C. Minero, M. Lucchiari, D. Vione, V. Maurino, Fe (III)-enhanced sonochemical degradation of methylene blue in aqueous solution, Environ. Sci. Technol. 39 (2005) 8936–8942

[60] Y.L. Pang, A.Z. Abdullah, S. Bhatia, Review on sonochemical methods in the presence of catalysts and chemical additives for treatment of organic pollutants in wastewater, Desalination 277 (2011) 1–14

[61] A. Kotronarou, G. Mills, M. R. Hoffmann, Ultrasonic irradiation of p-nitrophenol in aqueous solution, J. Phys. Chem. 95 (1991) 3630–3638

[62] J.-G. Lin, C.-N. Chang, J.-R. Wu, Decomposition of 2-chlorophenol in aqueous solution by ultrasound/H_2O_2 process, Water Sci. Technol. 33 (1996) 75-81

[63] Y. Jiang, C. Petrier, T. David Waite, Effect of pH on the ultrasonic degradation of ionic aromatic compounds in aqueous solution, Ultrason. Sonochem. 9 (2002) 163–168

[64] G.V. Svitelska, G.P. Gallios, A.I. Zouboulis, Sonochemical decomposition of natural polyphenolic compound (condensed tannin), Chemosphere 56 (2004) 981–987

[65] N.N. Mahamuni, A.B. Pandit, Effect of additives on ultrasonic degradation of phenol, Ultrason. Sonochem. 13 (2006) 165–174

[66] N. Shimizu, C. Ogino, M.F. Dadjour, T. Murata, Sonocatalytic degradation of methylene blue with TiO_2 pellets in water, Ultrason. Sonochem. 14 (2007) 184–190

[67] J.H. Sun, S.P. Sun, J.Y. Sun, R.X. Sun, L.P. Qiao, H.Q. Guo, M.H. Fan, Degradation of azo dye Acid black 1 using low concentration iron of Fenton process facilitated by ultrasonic irradiation, Ultrason. Sonochem. 14 (2007) 761–766

[68] S. Fındık, G. Gunduz, Sonolytic degradation of acetic acid in aqueous solutions, Ultrason. Sonochem. 14 (2007) 157–162

[69] H. Nakui, K. Okitsu, Y. Maeda, R. Nishimura, Effect of coal ash on sonochemical degradation of phenol in water, Ultrason. Sonochem. 14 (2007) 191-196

[70] J. Hartmann, P. Bartels, U. Mau, M. Witter, W.Y. Tu¨mpling, J. Hofmann, E. Nietzschmann, Degradation of the drug diclofenac in water by sonolysis in presence of catalysts, Chemosphere 70 (2008) 453–461

[71] M. Li, J-T. Li, H-W. Sun, Decolorizing of azo dye Reactive red 24 aqueous solution using exfoliated graphite and H_2O_2 under ultrasound irradiation, Ultrason. Sonochem. 15 (2008) 717–723

[72] H. Ghodbane, O. Hamdaoui, Degradation of Acid Blue 25 in aqueous media using 1700 kHz ultrasonic irradiation: Ultrasound/Fe (II) and ultrasound/H_2O_2 combinations, Ultrason. Sonochem. 16 (2009) 593–598

[73] W. Xie, Y. Qin, D. Liang, D. Song, D. He, Degradation of m-xylene solution using ultrasonic irradiation, Ultrason. Sonochem. 18 (2011) 1077–1081

[74] F. Guzman-Duque, C. Pétrier, C. Pulgarin, G. Peñuela, R.A. Torres-Palma, Effects of sonochemical parameters and inorganic ions during the sonochemical degradation of crystal violet in water, Ultrason. Sonochem. 18 (2011) 440–446

[75] O. Moumeni, O. Hamdaoui, Intensification of sonochemical degradation of malachite green by bromide ions, Ultrason. Sonochem. 19 (2012) 404–409

[76] M. Hoseini, G.H. Safari, H. Kamani, J. Jaafari, M. Ghanbarain, A.H. Mahvi, Sonocatalytic degradation of tetracycline antibiotic in aqueous solution by sonocatalysis, Toxicol. Environ. Chem. 95 (2013) 1680–1689

[77] H. Zhao, G. Zhang, Q. Zhang, MnO_2/CeO_2 for catalytic ultrasonic degradation of methyl orange, Ultrason. Sonochem. 21 (2014) 991–996

[78] M.Q. Cai, X.Q. Wei, Z.J. Song, M.C. Jin, Decolorization of azo dye Orange G by aluminum powder enhanced by ultrasonic irradiation, Ultrason. Sonochem. 22 (2015) 167–173

[79] A. Khataee, M. Sheydaei, A. Hassani, M. Taseidifar, S. Karac, Sonocatalytic removal of an organic dye using TiO_2/ Montmorillonite nanocomposite, Ultrason. Sonochem. 22 (2015) 404–411

[80] P.R. Gogate, A.B. Pandit, Sonophotocatalytic reactors for wastewater treatment: A critical review, AIChE J. 50 (2004) 1051-1079

[81] L. Davydov, E.P. Reddy, P. France, P.G. Smirniotis, Sonophotocatalytic destruction of organic contaminants in aqueous systems on TiO_2 powders, Appl. Catal., B: Environ. 32 (2001) 95-105

[82] A. Nakajima, M. Tanaka, Y. Kameshima, K. Okada, Sonophotocatalytic destruction of 1, 4-dioxane in aqueous systems by HF-treated TiO_2 powder, J. Photochem. Photobiol., A: Chem. 167 (2004) 75

[83] A.V. Vorontsov, Y-C. Chen, P.G. Smirniotis, Photocatalytic oxidation of VX simulant 2-(butylamino)ethanethiol, J. Hazard. Mater. 113 (2004) 89-95

[84] V. Ragaini, E. Selli, C.L. Bianchi, C. Pirola, Sono-photocatalytic degradation of 2-chlorophenol in water: Kinetic and energetic comparison with other techniques, Ultrason. Sonochem. 8 (2001) 251-258

[85] M. Mrowetz, C. Pirola, E. Selli, Degradation of organic water pollutants through sonophotocatalysis in the presence of TiO_2 Ultrason. Sonochem. 10 (2003) 247–254

[86] E. Selli, C.L. Bianchi, C. Pirola, M. Bertelli, Degradation of methyl tert-butyl ether in water: Effects of the combined use of sonolysis and photocatalysis, Ultrason. Sonochem. 12 (2005) 395–400

[87] S.G. Anju, S. Yesodharan, E.P. Yesodharan, Zinc oxide mediated sonophotocatalytic degradation of phenol in water, Chem. Eng. J. 189-190 (2012) 84-93

[88] C. Wu, X. Liu, D. Wei, J. Fan, L. Wang, Photosonochemical degradation of phenol in water, Wat. Res. 35 (2001) 3927–3933

[89] H. Harada, Sonophotocatalytic decomposition of water using TiO_2 photocatalyst, Ultrason. Sonochem. 8 (2001) 55-58

[90] Y.C. Chen, A.V. Vorontsov, P.G. Smirniotis, Enhanced photocatalytic degradation of dimethyl methylphosphonate in the presence of low-frequency ultrasound, Photochem. Photobiol. Sci. 2 (2003) 694–698

[91] A.M.T. Silva, E. Nouli, A.C. Carmo-Apolina´rio, N.P. Xekoukoulotakis, D. Mantzavinos, Sonophotocatalytic/H_2O_2 degradation of phenolic compounds in agro-industrial effluents, Catal. Today 124 (2007) 232–239

[92] R. Vinu, M. Giridhar, Kinetics of sonophotocatalytic degradation of anionic dyes with nano-TiO_2, Environ. Sci. Technol. 43 (2009) 473–479

[93] J-H. Park, Photochemical degradation and toxicity reduction of methyl 1-[(butylamino)carbonyl]-1H-benzimidazol-2-ylcarbamate in agricultural wastewater: Comparative study of photocatalysis and sonophotocatalysis, Desalination 249 (2009) 480–485

[94] J. Madhavan, P.S. Sathish Kumar, S. Anandan, F. Grieser, M. Ashokkumar, Sonophotocatalytic degradation of monocrotophos using TiO_2 and Fe^{3+}, J. Hazard. Mater. 177 (2010) 944–949

[95] K. Sekiguchi, C. Sasaki, K. Sakamoto, Synergistic effects of high-frequency ultrasound on photocatalytic degradation of aldehydes and their intermediates using TiO_2 suspension in water, Ultrason. Sonochem. 18 (2011) 158–163

[96] S.K. Kavitha, P.N. Palanisamy, Photocatalytic and sonophotocatalytic degradation of Reactive red 120 using dye sensitized TiO_2 under visible light, Inter. J. Civil Environ. Eng. 3 (2011) 6 pages

[97] V. Anoop, K. Harmanpreet, D. Divya, Photocatalytic, sonolytic and sonophotocatalytic degradation of 4-chloro-2-nitro phenol, Archives of Environmental Protection 39 (2013) 17 - 28

[98] A. Durán, J.M. Monteagudo, I. Sanmartín, A. García-Díaz, Sonophotocatalytic mineralization of antipyrine in aqueous solution, Appl. Catal., B: Environ. 138– 139 (2013) 318– 325.

[99] N. Talebian, M.R. Nilforoushan, F.J. Mogaddas, Comparative study on the sonophotocatalytic degradation of hazardous waste, Ceram. Int. 39 (2013) 4913–4921

[100] B.B. Nileema, D.B. Snehal, R.D. Rachana, D.M. Deepika, P.H. Shruti, S.B. Barnali, V.M. Ashish, P.R. Gogate, Sonocatalytic and sonophotocatalytic degradation of rhodamine 6G containing wastewaters, Ultrason. Sonochem. 21 (2014) 1797–1804

[101] M. Ahmad, E. Ahmed, Z.L. Hong, W. Ahmed, A. Elhissi, N.R. Khalid, Photocatalytic, sonocatalytic and sonophotocatalytic degradation of Rhodamine B using ZnO/CNTs composites photocatalysts, Ultrason. Sonochem. 21 (2014) 761–773

[102] F. Zaviska, P. Drogui, E.M. El Hachemi, E. Naffrechoux, Effect of nitrate ions on the efficiency of sonophotochemical phenol degradation, Ultrason. Sonochem. 21 (2014) 69–75.

[103] S-M. Lam, J.C. Sin, A.Z. Abdullah, A.R. Mohamed, Degradation of wastewaters containing organic dyes photocatalysed by ZnO: A review. Desalin. Water Treat. 41 (2012) 131–169

[104] N. Hariprasad, S.G. Anju, E.P. Yesodharan, S. Yesodharan, Sunlight induced removal of Rhodamine B from water through semiconductor photocatalysis, Res. J. Mater. Sci. 1 (2013) 9-17.

[105] N. Daneshvar, D. Salari, A.R. Khataee, Photocatalytic degradation of azo dye acid red 14 in water on ZnO as an alternative catalyst to TiO_2, J. Photochem. Photobiol., A 162 (2004)317–322.

[106] S.K. Kansal, M. Singh, D. Sud, Studies on the photodegradation of two commercial dyes in aqueous phase using different photocatalysts, J. Hazard. Mater. 141 (2007) 581–590.

[107] Ü. Özgür, Ya.I. Alivov, C. Liu, A. Teke, M.A. Reshchikov, S. Doğan, V. Avrutin, S.-J. Cho, H. Morkoç, A comprehensive review of ZnO materials and devices, J. Appl. Phys. 98 (2005) 1-103

[108] V.A. Coleman, C. Jagadish, Basic properties and applications of ZnO, zinc oxide bulk, thin films & nano structures, Elseiver (2006)

[109] F. Tamaddon, M.A. Amrollahi, L. Sharafat, A green protocal for chemo selective O-acylation in the presence of zinc oxide as a heterogeneous, reusable and ecofriendly catalyst, Tetrahedron Lett. 46 (2005) 7841-7844

[110] T. Chungui, Q. Zhang, A. Wu. M. Jiang, Z. Liang, B. Jiang, H. Fu, Cost effective lardge-scale synthesis of ZnO photocatalyst with excellent performance for dye photodegradation, Chem. Commun. 48 (2012) 2858-2860

[111] A.S. Shriwas, D. Aparna, M. Sonali, M.E. Wankhede, C. Jayashree, P. Renu, J. Urban, S.K. Haram, S.W. Gosawi, S.K. Kulkarni, Synthesis and analysis of ZnO and CdSe nanoparticles, Parmana J. Phy. 65 (2005) 615-620

[112] R.B.H. Tahar, Boron-doped zinc oxide thin films prepared by sol-gel technique, J. Mater. Sci. 40 (2005) 5285-5289

[113] J. Yu, X. Yu, Hydrothermal synthesis and photocatalytic activity of zinc oxide hollow spheres, Environ. Sci. Technol. 42 (2008) 4902-4907

[114] K.M. Parida, S.S. Dash, D.P. Das, Physico-chemical characterization and photocatalytic activity of zinc oxide prepared by various methods, J. Colloid Interface Sci. 298 (2006) 787-793

[115] A.D. Eaton, L.S. Clesceri, E.W. Rice, A.E. Greenberg, Standard methods for the examination of water and waste water, American public health association, Washington (2005) pp 515-516

[116] A.D. Eaton, L.S. Clesceri, E.W. Rice, A.E. Greenberg, Standard methods for the examination of water and waste water, American public health association, Washington (2005) pp 4153-4154

[117] J. Yu, W. Wang, B. Cheng, B.-L. Su, Enhancement of photocatalytic activity of mesoporous TiO_2 powders by hydrothermal surface fluorination treatment, J. Phys. Chem. C 113 (2009) 6743–6750

[118] M. Sayed, F. Pingfeng, H.M. Khan, P. Zhang, Effect of isopropanol on microstructure and activity of TiO_2 films with dominant {110} facets for photocatalytic degradation of Bezafibrate, Int. J. Photoenerg. 2014 (2014) 1–11

[119] T.J. Mason, J.L. Luche, Chemistry under extreme or nonclassical conditions, John Wiley & Sons, New York (1997)

[120] P.N. Vijayalaxmi, P. Saritha, N. Rambabu, V. Himabindu, Y. Anjaneyulu, Sonochemical degradation of 2 chloro-5methyl phenol assisted by TiO_2 and H_2O_2, J. Hazard. Mater. 174 (2010) 151–155

[121] A.K. Khodja, T. Sehili, J.F. Pilichowski, P. Boule, Photocatalytic degradation of 2-phenyl phenol on TiO_2 and ZnO in aqueous suspensions, J. Photochem. Photobiol. 141 (2001) 231–239

[122] J. Saien, A.R. Soleymani, Degradation and mineralization of Direct blue 71 in a circulating up-flow reactor by UV/TiO_2 process and employing a new method in kinetic study, J. Hazard. Mater. 14 (2007) 507–512

[123] S.K. Pardeshi, A.B. Patil, A simple route for photocatalytic degradation of phenol in aqueous zinc oxide suspension using solar energy, Sol. Energy 82 (2008) 700–705

[124] S.H. Szczepankiewicz, J.A. Moss, M.R. Hoffmann, Slow surface charge trapping on irradiated TiO_2, J. Phys. Chem. B 106 (2002) 2922–2927

[125] C. Guillard, H. Lachheb, A. Houas, E. Elaloui, J-M. Hermann, Influence of chemical structure of dyes, of pH and of inorganic salts on their photocatalytic degradation by TiO_2. Comparison of the efficiency of powder and supported TiO_2, J. Photochem. Photobiol. A: Chem. 158 (2003) 27-36

[126] V. Augugliaro, V. Loddo, L. Palmisano, M. Schiavello, Heterogeneous photocatalytic systems: Influence of some operational variables on actual photons absorbed by aqueous dispersions of TiO_2, Sol. Energy Mater. Sol. Cells 38 (1995) 411–419

[127] B. Jenny, P. Pichat, Determination of the actual photocatalytic rate of H_2O_2 decomposition over suspended TiO_2. Fitting to the Langmuir–Hinshelwood form, Langmuir 7 (1991) 947–954

[128] I. Ilisz, K. Foglein, A. Dombi, Photochemical behavior of H_2O_2 in near UV – irradiated aqueous TiO_2 suspensions, J. Mol. Catal., A: Chem. 135 (1998) 55–61

[129] T. Hirakawa, T. Daimon, M. Kitazawa, N. Ohguri, C. Koga, N. Negishi, S. Matsuzawa, Y. Nosaka, An approach to estimating photocatalytic activity of TiO_2 suspension by monitoring dissolved oxygen and superoxide ion on decomposing organic compounds, J. Photochem. Photobiol., A: Chem. 190 (2007) 58–68

[130] S. Anandan, A. Vinu, N. Venkatachalam, B. Arabindoo, V. Murugesan, Photocatalytic activity of ZnO impregnated Hβ and mechanical mix of ZnO/Hβ in the degradation of monocrotophos in aqueous solution, J. Mol. Catal., A: Chem. 256 (2006) 312–320

[131] Q. Li, Y. Wai, P Wu, R. Xie, J.K. Shang, Palladium oxide nanoparticles on nitrogen-doped titanium oxide: Accelerated photocatalytic disinfection and post –illumination catalytic memory, Adv. Mater. 20 (2008) 3717–3723

[132] H. Gerischer, A. Heller, The role of oxygen in photo oxidation of organic molecules on semiconductor surfaces, J. Phys. Chem. 95 (1991) 5261–5267

[133] Y. Nosaka, A. Nosaka in P. Pichat. (Ed.) Photocatalysis and Water Purification, 1st Ed., Wiley- VCH Verlag GmbH, Weinheim, Germany (2013) pp 1-24

[134] C. Kormann, D.W. Bahnemann, M.R. Hoffmann, Photocatalytic production of hydrogen peroxide and organic peroxides in aqueous suspensions of titanium dioxide, zinc oxide and desert sand, Environ. Sci. Technol. 22 (1988) 798–806

[135] D. Ollis, P. Pichat, N. Serpone, TiO_2 photocatalysis-25 years, Appl. Catal., B: Environ. 99 (2010) 377–387

[136] P. Pichat, Photocatalysis and Water Purification: From fundamentals to recent applications, Wiley-VCH Verlag GmbH, Weinheim, Germany 2013

[137] R.W. Matthews, Photooxidation of organic material in aqueous suspensions of titanium dioxide, Water Res. 20 (1986) 569–578

[138] L. Davydov, P.G. Smirniotis, Quantification of the primary processes in aqueous heterogeneous photocatalysis using single stage oxidation reactions, J. Catal. 191 (2000) 105–115

[139] B. Neppolian, L. Ciceri, C.L. Bianchi, F. Grieser, M. Ashok kumar, Sonophotocatalytic degradation of 4-chlorophenol using Bi_2O_3/$TiZrO_4$ as a visible light responsive photocatalyst, Ultrason. Sonochem. 18 (2011) 135-139

[140] T. Tuziuti, K. Yasui, M. Sivakumar, Y. Iida, Correlation between acoustic cavitation noise and yield enhancement of sonochemical reaction by particle addition, J Phys Chem., A 109 (2005) 4869-4872

[141] G. Heit, A.M. Braun, UV photolysis of aqueous systems: spatial differentiation between volumes of primary and secondary reactions, Water Sci. Technol. 35 (1997) 25–30

[142] A. Keck, E. Gilbert, R. Koster, Influence of particles on sonochemical reactions in aqueous solutions, Ultrasonics 40 (2002) 661-665

[143] J. Yi, C. Bahrini, C. Schoemaecker, C. Fittschen, W. Choi, Photocatalytic decomposition of H_2O_2 on different TiO_2 surfaces along with the concurrent generation of HO_2 radicals monitored using cavity ring down spectroscopy, J. Phys. Chem. C 116 (2012) 10090-10097

[144] T. Tachikawa, T. Majima, Single molecule fluorescence imaging of TiO_2 photocatalytic reactions, Langmuir 25 (2009) 7791-7802

[145] Y. Murakami, L. Ohta, T. Hirakawa, Y. Nosaka, Direct detection of OH radicals in the gas phase diffused from the Pt/TiO_2 and WO_3/ TiO_2 photocatalysts, Chem. Phys. Lett. 493 (2010) 292-295

[146] C. Bahrini, A. Parker, C. Schoemaecker, C. Fittschen , Direct detection of HO_2 radicals in the vicinity of TiO_2 photocatalytic surfaces using CW-CRDS, Appl. Catal., B: Environ. 99 (2010) 413-419

[147] I. Poulios, A. Avranas, E. Rekliti, A. Zouboulis, Photocatalytic oxidation of auramine O in the presence of semiconducting oxides, J. Chem. Technol. Biotechnol. 75 (2000) 205–212

[148] S. Kaur, V. Singh, Visible light induced sonophotocatalytic degradation of Reactive Red dye 198 using dye sensitized TiO_2, Ultrason. Sonochem. 14 (2007) 531-537

[149] H.M. Castrantas, R.D. Gibilisco, UV destruction of phenolic compounds under alkaline conditions, ACS Symp. Series 422 (1990) 77-99

[150] J.G. Lin, C.N. Chang, J.R. Wu, Decomposition of 2-chlorophenol in aqueous solution by ultrasound/H_2O_2 process, Water Science Technol. 33 (1996) 75-81

[151] H-H. Ou, S-L. Lo, C-H. Wu, Exploring the interparticle electron transfer process in the photocatalytic oxidation of 4-chlorophenol, J. Hazard. Mater. 137 (2006) 1362-1370

[152] I.M. Khokhawala, P.R. Gogate, Degradation of phenol using a combination of ultrasonic and UV irradiations at pilot scale operation, Ultrason. Sonochem. 17 (2010) 833-838

[153] M. Goel, H. Hongqiang, A.S. Majumdar, M.B. Ray, Sonochemical decomposition of volatile and nonvolatile organic compounds: A comparative study, Water Res. 38 (2004) 4247–4261.

[154] P. Pichat, C. Guillard, C. Mallard, L. Almaric, J.C. D'Oliveira, in D.F Ollis and H. Al-Ekabi (Eds.), Photocatalytic purification and treatment of water and air, Elsevier, Amsterdam (1993) p 207

[155] P.R. Gogate, S. Majumdar, J. Thampi, A.M. Wilhelm, A.B. Pandit, Destruction of phenol using sonochemical reactors: Scale up aspects and comparison of novel configuration with conventional reactors, Sep. Purif. Technol. 34 (2004) 25-34

[156] C. Minero, P. Pellizzari, V. Maurino, E. Pelizzetti, D. Vione, Enhancement of dye sonochemical degradation by some inorganic anions present in natural waters, Appl. Catal., B: Environ. 77 (2008) 308-316

[157] H.Y. Chen, O. Zahraa, M. Bouchy, Inhibition of the adsorption and photocatalytic degradation of an organic contaminant in an aqueous suspension of TiO_2 by inorganic ions, J. Photochem. Photobiol., A: Chem. 108 (1997) 37-44

[158] H.P. Boehm, Acidic and basic properties of hydroxylated metal oxide surfaces, Discuss Faraday Soc. 52 (1971) 264-275

[159] L. Amalric, C. Guillard, E. Blanc-Brude, P. Pichat, Correlation between the photocatalytic degradability over TiO_2 in water of meta and para substituted methoxybenzenes and their electron density, hydrophobicity and polarizability properties, Water Res. 30 (1996) 1137-1142

[160] R.L. David. Hand book of chemistry. 84th Ed. , CRC Press, Boca Raton, Florida (2004), pp779-782

[161] A.B. Pandit, P.R. Gogate, S. Majumdar, Ultrasonic degradation of 2:4:6 trichloro phenol in presence of TiO_2 catalyst, Ultrason. Sonochem. 8 (2001) 227-231

[162] A. Tauber, G. Mark, H-P. Schuchmann, C. von Sonntag, Sonolysis of tert-butyl alcohol in aqueous solution, J. Chem. Soc., Perkin Trans. 2 (1999) 1129–1135

[163] C. Minero, V. Maurino, E. Pelizzetti, D. Vione, An empirical, quantitative approach to predict the reactivity of some substituted aromatic compounds towards reactive radical species ($Cl_2^{-\bullet}$, $Br_2^{-\bullet}$, $^{\bullet}NO_2$, $SO_3^{-\bullet}$, $SO_4^{-\bullet}$) in aqueous solution, Environ. Sci. Pollut. Res. 13 (2006) 212-214

[164] O. Hamdaoui, E. Naffrechoux, Adsorption kinetics of 4-chlorophenol onto granular activated carbon in the presence of high frequency ultrasound, Ultrason. Sonochem. 16 (2009) 15-22

[165] B.R. Puri, L.R. Sharma, K.C. Kalia, Principles of inorganic chemistry, 28th Ed., Vallabh publications, New Delhi (2003) p 80

.....ൠ.....

ANNEXURES

Annexure I

List of Abbreviations and Symbols

AB 1	Acid Blue 1
AB1	Acid Black 1
AB25	Acid Blue 25
AO	Acridine Orange
AOP	Advanced Oxidation Processes
BB3	Basic Blue 3
BET	Brunauer-Emmett Teller
BOD	Biological Oxygen Demand
CB	Conduction Band
CNTs	Carbon Nano Tubes
COD	Chemical Oxygen Demand
DMMP	Di Methyl Phosphonate
DMSO	Di Methyl Sulphoxide
eV	Electron Volt
FAS	Ferrous Ammonium Sulphate
GAC	Granulated Activated Carbon
h	Plank's Constant
H_2O_2	Hydrogen Peroxide
HPLC	High Performance Liquid Chromatography
HTPA	2-hydroxy terephthalic acid
KHz	Kilo Hertz
M	Molar
MB	Methylene Blue
MG	Malachite Green
MHz	Mega Hertz
mM	Milli Molar

MMT	Montmorillonite K10
MTBE	Methyl Tertiary Butyl Ether
nm	Nano Meter
O_3	Ozone
OP	Organophosphorus
PL	Photoluminescence
ppb	Parts per billion
ppm	Parts per million
Rh6G	Rhodamine 6G
RhB	Rhodamine B
ROS	Reactive Oxygen Species
rpm	Rotations per minute
SEM	Scanning Electron Microscopy
TC	Tetracycline
TEM	Transmission Electron Microscopy
TOC	Total Organic Carbon
TPA	Terephthalic acid
TSS	Total Suspended Solids
US	Ultrasound
UV	Ultraviolet
V	Volt
VB	Valence Band
XRD	X-ray diffractogram
µm	Micro meter
µmol/L	Micro mols/Liter
4C2NP	4 – Chloro – 2 – Nitro Phenol

List of Publications

A. Published in peer reviewed journals: 8

[1] Anju S G, **Jyothi K P**, Sindhu Joseph, Suguna Yesodharan and Yesodharan E P, "**Ultrasound assisted semiconductor mediated catalytic degradation of organic pollutants in water: Comparative efficacy of ZnO, TiO_2 and ZnO-TiO_2**", ***Res. J. Rec. Sci***., Vol. 1 (ISC-2011), 191-201 (**2012**)

[2] **Jyothi K P**, Sindhu Joseph, Suguna Yesodharan and Yesodharan E P, "**Periodic change in the concentration of hydrogen peroxide formed during the semiconductor mediated sonocatalytic treatment of wastewater: Investigations on pH effect and other operational variables**, ***Res. J. Rec. Sci.,*** Vol. 2 (ISC-2012), 136-149 (**2013**)

[3] Sindhu Joseph, **Jyothi K P**, Suja P Devipriya, Suguna Yesodharan and Yesodharan E P, "**Influence of reaction intermediates on the oscillation in the concentration of insitu formed hydrogen peroxide during the photocatalytic degradation of phenol pollutant in water on semiconductor oxides**", ***Res. J. Rec. Sci.,*** Vol. 2 (ISC-2012), 82-89 (**2013**)

[4] **Jyothi K P**, Suguna Yesodharan, Yesodharan E P, "**Ultrasound (US), Ultraviolet light (UV) and combination (US + UV) assisted semiconductor catalysed degradation of organic pollutants in water: Oscillation in the concentration of hydrogen peroxide formed in situ**", ***Ultrason. Sonochem.,*** Vol. 21, 1787–1796 (**2014**)

[5] Sindhu Joseph, **Jyothi K P**, Suguna Yesodharan, Yesodharan E P, "**Oscillation in the concentration of H_2O_2 during advance oxidation processes: TiO_2 mediated sonocatalytic degradation of phenol**", ***IOSR-JAC,*** 21-28 (**2014**)

[6] Phonsy P D, Anju S G, **Jyothi K P**, Suguna Yesodharan, Yesodharan E P, "**Semiconductor mediated photocatalytic degradation of plastics and recalcitrant organic pollutants in water: Effect of additives and fate of insitu formed H_2O_2**", ***J. Adv. Oxid. Technol.,*** Vol.18, No.1, 85-97 (**2015**)

[7] **Jyothi K P**, Suguna Yesodharan, Yesodharan E P, "**Sono, photo and sonophotocatalytic decontamination of organic pollutants in water : Studies on the lack of correlation between pollutant degradation and concurrently formed H_2O_2**", ***Current Science***, *109*, 189–195 (**2015)**

[8] **Jyothi K P**, Suguna Yesodharan, Yesodharan E P, "**Influence of commonly occurring cations on the sono, photo and sonophoto catalytic decontamination of water**", ***IOSR-JAC***, 15-24 (**2016**)

B. Presented in conferences: 13

i) National

[1] **Jyothi K P**, Sindhu Joseph, Anju S G, Suguna Yesodharan, Yesodharan E P, "Role and fate of hydrogen peroxide in the sono and photocatalytic transformation of organic pollutants in water" in **National Conference On Climate Change: Challenges and Strategies**, Feb. **2012**; Proceedings page no-19

[2] **Jyothi K P**, Suguna Yesodharan, Yesodharan E P, "Unusual behavior of insitu formed H_2O_2 during the sono, photo and sonophotocatalytic transformation of organic pollutants in water" in **25th Kerala Science Congress**, Jan. **2013**; Proceeding page no-306

[3] **Jyothi K P,** Suguna Yesodharan, Yesodharan E P, "Sono, photo and sonophotocatalytic decontamination of organic pollutants in water: Investigations on the lack of correlation between the pollutant degradation and concurrently formed H_2O_2, in **First National Conference on Advanced Oxidation Process**, Nov. 2013; Proceeding page no-41

[4] **Jyothi K P**, Suguna Yesodharan, Yesodharan E P, "What happens to the H_2O_2 formed during the photo catalytic degradation of organic pollutants in water? An investigation" in **26th Kerala Science Congress,** Jan. **2014**; Proceedings page no-128

[5] **Jyothi K P**, Suguna Yesodharan, Yesodharan E P, **"**Investigations on resolving the inconsistency in insitu formed H_2O_2 during advanced oxidation processes: Clear evidence for the phenomenon of oscillation" in **27th Kerala Science Congress,** Jan. **2015**; Proceeding page no-49

[6] **Jyothi K P**, Yesodharan E P, "Natural contaminants as facilitators in wastewater treatment: Reversal of role from inhibition to enhancement in photocatalysis" in **28th Kerala Science Congress,** Jan.2016; Proceedings page no-2661

ii) International

[1] **Jyothi K P**, Sindhu Joseph, Suguna Yesodharan and Yesodharan E P, "Periodic change in the concentration of hydrogen peroxide formed during the semiconductor mediated sonocatalytic treatment of wastewater: Investigations on pH effect and other operational variables" in **2nd International Science Congress**, Dec. 2012; Proceedings page no-71

[2] Phonsy P D, Anju S G, **Jyothi K P**, Suguna Yesodharan, Yesodharan E P, "Semiconductor mediated photocatalytic degradation of plastics and recalcitrant organic pollutants in water: Effect of additives and fate of insitu formed H_2O_2" in **18th International conference on semiconductor photocatalysis and solar energy conversion (SPASEC-18), San Diego, USA,** Nov. **2013**; Proceedings page no-172

[3] **Jyothi K P**, Suguna Yesodharan, Yesodharan E P, "Investigations on the influence of reaction parameters on the phenomenon of oscillation of H_2O_2 concentration in AOPs" in **3rd International Science Congress,** Dec. **2013**; Proceedings page no-117

[4] **Jyothi K P**, Suguna Yesodharan, Yesodharan E P, "Effect of anionic contaminants on the sonocatalytic degradation of phenol and concurrently formed H_2O_2" in **3rd International Conferences on Advanced Oxidation Process,** Sept. 2014; Proceedings page no-47

[5] Sindhu Joseph, **Jyothi K P**, Suguna Yesodharan, Yesodharan E P, "Oscillation in the concentration of H_2O_2 during advance oxidation processes: TiO_2 mediated sonocatalytic degradation of phenol" in **International Conference on Emerging Trends in Engineering and Management**, Dec. 2014; Proceedings Page no-21

[6] **Jyothi K P**, Suguna Yesodharan, Yesodharan E P, "Effect of anions on the oscillation in the concentration of hydrogen peroxide formed insitu in sonocatalytic systems" in **2nd Asia-Oceania Sonochemical Society Conference (AOSS-2),** July **2015** at **Kuala Lumpur, Malaysia**; Proceedings page no-60

[7] **Jyothi K P**, Suguna Yesodharan, Yesodharan E P, "Influence of commonly occurring cations on the sono, photo and sonophoto catalytic decontamination of water" in **International Conference on Emerging Trends in Engineering and Management (ICETEM 16),** Jan. **2016**; Proceedings page no-15.

Annexure III

Reprints of Paper published

Research Journal of Recent Sciences ISSN 2277-2502
Vol. 1 (ISC-2011), 191-201 (2012) Res.J.Recent Sci.

Ultrasound assisted semiconductor mediated catalytic degradation of organic pollutants in water: Comparative efficacy of ZnO, TiO_2 and ZnO-TiO_2

Anju S.G., Jyothi K.P., Sindhu Joseph, Suguna Y. and Yesodharan E.P.*
School of Environmental Studies, Cochin University of Science and Technology, Kochi-682022 INDIA

Available online at: www.isca.in
(Received 26th November 2011, revised 6th January 2012, accepted 25th January 2012)

Abstract

Sonocatalytic degradation of organic pollutants in water is investigated using ZnO, TiO_2 and combination of ZnO and TiO_2 (ZnO-TiO_2) as catalysts, with phenol as the test substrate. The efficacy of the catalysts is in the order ZnO-TiO_2 > ZnO > TiO_2. The degradation in presence of ZnO-TiO_2 is more than the sum of the degradation achieved in presence of the individual oxides under identical conditions, thereby demonstrating a synergistic effect. The ratio of the components in the mixed oxide is optimized. The kinetics of the degradation as well as the influence of various parameters such as catalyst loading, concentration of the pollutant and pH on the degradation efficiency is evaluated. Maximum degradation is observed in the acidic pH for all catalysts. H_2O_2 is formed in the reaction and it undergoes simultaneous decomposition resulting in periodic increase and decrease in its concentration. This observation of the phenomenon of oscillation in the concentration of H_2O_2 is the first of its kind in sonocatalytic systems. A mechanism for the degradation of phenol is proposed based on the observations as well as the concurrent formation and decomposition of H_2O_2.

Keywords: Zinc oxide, titanium dioxide, sonocatalysis, phenol, hydrogen peroxide.

Introduction

Advanced Oxidation Processes (AOP) involving Ultraviolet light, Fenton reagents, Ozone, Ultrasound etc have been tested individually as well as in combination, in the presence and absence of catalysts for the treatment of wastewater containing pesticides, phenols, chlorophenols, dyes and other pollutants [1-5]. The mechanism in all these cases involves the formation of active ·OH radicals which mineralize the pollutants into carbon dioxide, phosphates, sulphates etc.

Recently, Ultrasonic (US) irradiation mediated by suitable catalysts (sonocatalysis) has been receiving special attention as an environment - friendly technique for the treatment of hazardous organic pollutants in wastewater[6]. However the degradation rate is slow compared to other established methods. Investigations aimed at enhancing the efficiency of US promoted decontamination of water are in progress in many laboratories. These include testing a variety of catalysts with different physico-chemical characteristics, modification of reactor design and reaction conditions, combining US with other AOP techniques etc[6-9]. Coupling US with Ultraviolet (UV) irradiation enhances the efficiency of semiconductor mediated degradation of aqueous pollutants synergistically[6,7,10,11].

In liquids US produces cavitation which consists of nucleation, growth and collapse of bubbles. The collapse of the bubbles results in localized supercritical condition such as high temperature, pressure, electrical discharges and plasma effects[10]. The temperature of the gaseous contents of a collapsing cavity can reach approximately 5500^0C and that of the liquid immediately surrounding the cavity reaches up to 2100^0C. The localized pressure is estimated to be around 500 atmospheres resulting in the formation of transient supercritical water[12]. The cavities are thus capable of functioning like high energy micro reactors. The consequence of these extreme conditions is the cleavage of dissolved oxygen molecules and water molecules into radicals such as H·, OH· and O· which will react with each other as well as with H_2O and O_2 during the rapid cooling phase giving HO_2· and H_2O_2. In this highly reactive nuclear environment, organic pollutants can be decomposed and inorganic pollutants can be oxidised or reduced. This phenomenon is being explored in the emerging field of sonocatalysis for the removal of water pollutants.

Most of the studies on the sonocatalytic degradation of water pollutants are made using TiO_2 catalyst, mainly due to its wide availability, stability, non-toxicity and reactivity. Another similar semiconductor oxide ZnO has received relatively less attention possibly due to its corrosive nature under extreme pH conditions. At the same time ZnO is reported to be more efficient than TiO_2 for the visible light induced photocatalytic degradation of organic pollutants because the former can absorb a larger fraction of solar spectrum compared to the latter [13,14]. Earlier studies in our laboratory showed that ZnO is very efficient as a sono catalyst and sonophotocatalyst for the degradation of trace pollutants in water[15]. Comparative study of the catalytic

Research Journal of Recent Sciences ISSN 2277-2502
Vol. 1 (ISC-2011), 191-201 (2012) Res. J. Recent Sci.

activity of nano-sized TiO_2, ZnO and composite TiO_2/ZnO powders for the sonocatalytic degradation of dyestuffs showed that the composite powder is more effective[16]. Similarly Tb_7O_{12}/TiO_2 composite was reported to perform better as sonocatalyst compared to the individual oxides for the degradation of amaranth[17]. In spite of the multitude of research papers on the sonocatalytic activity of TiO_2 and its modified forms, not many reports are available on the use of ZnO or coupled ZnO-TiO_2 as sonocatalysts for the removal of water pollutants. In this paper we report the comparative assessment of the sonocatalytic activity of ZnO, TiO_2 and ZnO-TiO_2 for the removal of trace amounts of phenol in water and the factors influencing their performance.

Material and Methods

ZnO and TiO_2 used in the study were supplied by Merck India Limited. In both cases the particles were approximately spherical and nonporous with over 99% purity. The surface areas of TiO_2 and ZnO, as determined by the BET method are 15 and 12 m^2/g respectively. ZnO-TiO_2 catalysts were prepared by physically mixing respective components in required weight ratios and thoroughly mixing for 30 minutes using mechanical shaker. Phenol AnalaR Grade (99.5% purity) from Qualigen (India) was used as such without further purification. Doubly distilled water was used in all the experiments. All other chemicals were of AnalaR Grade or equivalent. The average particle size of both ZnO and TiO_2 was 10 µm, unless mentioned otherwise.

The experiments were performed using aqueous solutions of phenol of the desired concentration. Specified quantity of the catalyst is suspended in the solution. In the case of US irradiation experiments, sonication was sufficient to ensure adequate mixing of the suspension. Additional mechanical mixing did not make any notable consistent difference in the US reaction rate. The reactor was a cylindrical Pyrex vessel of 250 ml capacity. In the case of sonocatalytic experiments, ultrasonic bath was used as the source of US. The ultrasonic bath operated at 40 kHz and power of 100 W. Water from the sonicator was continuously replaced by circulation from a thermostat maintained at the required temperature. Unless otherwise mentioned, the reaction temperature was maintained at 27 ± 1^0C. The position of the reactor in the ultrasonic bath was always kept the same. At periodic intervals samples were drawn, the suspended catalyst particles were removed by centrifugation and the concentration of phenol left behind was analyzed by Spectrophotometry at 500 nm. H_2O_2 is determined by standard iodometry. Degradation and mineralization were identified by the evolution of CO_2. Adsorption studies were performed as follows[18]:

A fixed amount (0.1 g) of the catalyst was introduced to 100 ml of phenol solution of required concentration in a 250 ml beaker and the pH was adjusted as required. The suspension was agitated continuously at constant temperature of 27 ± 1^0C for 2 hrs to achieve equilibrium. This was then centrifuged at 3000 rpm for 10 min. After centrifugation the concentration of phenol in the supernatant was determined colorimetrically. The adsorbate uptake was calculated from the relation : $q_e = (C_0 - C_e)V / W$

where C_0 is the initial adsorbate concentration (mg/L), C_e is the equilibrium adsorbate concentration in solution (mg/L), V is the volume of the solution in liter, W is the mass of the adsorbent in gram and q_e is the amount adsorbed in mg per gram of the adsorbent.

Results and Discussion

Preliminary investigations on the sonocatalytic degradation of phenol were made using ZnO and TiO_2 catalysts under identical conditions. The results show that ZnO with 14% degradation of phenol is more efficient as sonocatalyst than TiO_2 with 7% degradation in 2 hr time under otherwise identical conditions.

No significant degradation of phenol took place in the absence of US or the catalyst suggesting that both catalyst and sound are essential to effect degradation. Small quantity of phenol degraded under US irradiation even in the absence of the catalyst. This is understandable since sonolysis of water is known to produce free radicals $H^{\cdot}$ and $OH^{\cdot}$ (via reaction 1), which are capable of attacking the organic compounds in solution.

$H_2O \xrightarrow{>>>} H^{\cdot} + {}^{\cdot}OH$ (1) >>> refers to sonication

The process is facilitated in a heterogeneous environment such as the presence of ZnO or TiO_2. The presence of the particles helps to break up the microbubbles created by US into smaller ones, thus increasing the number of regions of high temperature and pressure[10]. This leads to increase in the number of OH radicals which will interact with the phenol present in water and oxidise it, resulting in eventual mineralization.

Coupling of ZnO and TiO_2 in the weight ratio 1:1 results in 13.5% phenol degradation which is same as in the case of ZnO of same mass. This is more than the sum of degradation achieved in the presence of individual ZnO and TiO_2 at loadings equivalent to their concentration in the combination, thereby showing synergistic effect. The % degradation varies with the composition of ZnO-TiO_2 with maximum degradation of 14% in presence of ZnO/TiO_2 at 4:6 as shown in figure 1. Hence further studies with the ZnO-TiO_2 combination were carried out using this ratio.

The synergy index can be calculated from the rate of degradation using the following equation: Synergy index = $R_{(Z-T)} / (R_Z + R_T)$

Research Journal of Recent Sciences ISSN 2277-2502
Vol. **1 (ISC-2011),** 191-201 **(2012)** *Res. J. Recent Sci.*

where R_Z, R_T and $R_{(Z-T)}$ are sono catalytic degradation rates in presence of ZnO, TiO_2 and ZnO-TiO_2 respectively. The maximum synergy index thus calculated is approx. 1.30 for ZnO concentration of 10% (by mass) in the coupled ZnO-TiO_2. With increase in the concentration of ZnO in the couple, the synergy index drops slowly. Beyond 40% concentration of ZnO, the couple behaves more like pure ZnO as a sonocatalyst.

The effect of various parameters on the efficiency of the catalysts is investigated in detail in order to optimize the conditions of degradation of phenol in presence of each of them.

Effect of catalyst dosage: The effect of catalyst dosage on the sonocatalytic degradation of phenol is studied at different loadings of ZnO, TiO_2 and ZnO-TiO_2. The results are plotted in figure 2.

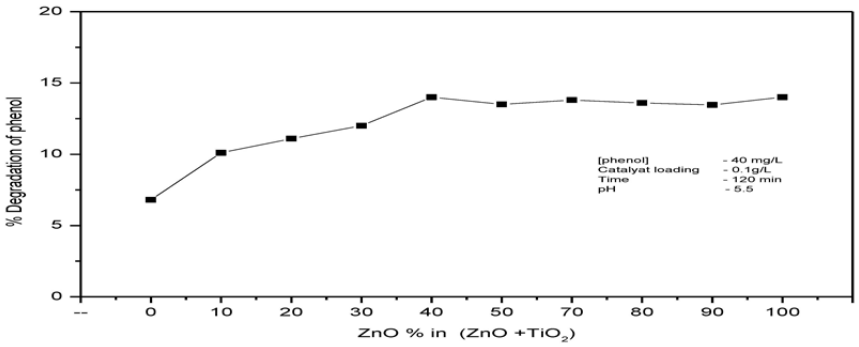

Figure-1
Effect of ZnO/TiO2 ratio on the sonocatalytic activity

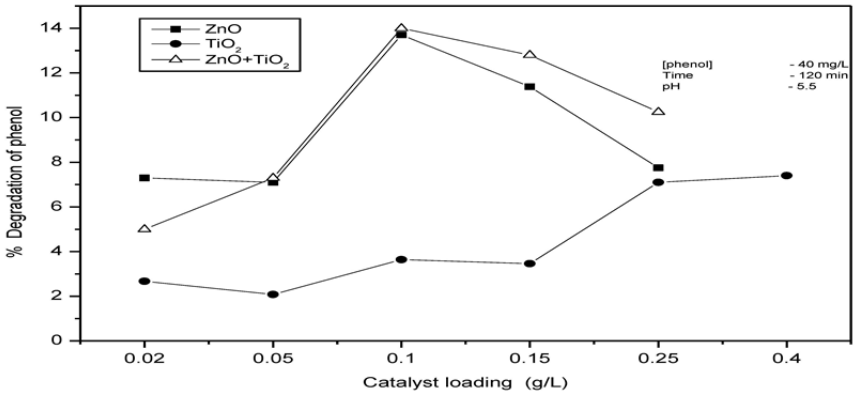

Figure-2
Effect of catalyst dosage on the sonocatalytic activity of ZnO, TiO_2 and ZnO+TiO_2

Research Journal of Recent Sciences ISSN 2277-2502
Vol. 1 (ISC-2011), 191-201 (2012) Res. J. Recent Sci.

In all three cases the degradation increases with increase in catalyst loading and reaches an optimum range. Beyond this optimum, the degradation slows down and thereafter remains more or less steady or even decreases. The enhanced degradation efficiency with increase in the dosage is probably due to increased number of catalytic sites, higher production of OH radicals and more effective interaction with the substrate. It is known that the addition of particles of appropriate amount and size into the liquid system results in increase in the acoustic noise and a rise in temperature in the irradiated liquid[19]. Introduction of more catalyst particles in the solution provide more nucleation sites for cavitation bubbles at their surface. This will result in decrease in the cavitation thresholds responsible for the increase in the number of bubbles when the liquid is irradiated by US. The increase in the number of cavitation bubbles increases the pyrolysis of water and the sonocatalytic degradation of phenol. Any further increase in catalyst concentration beyond the optimum will only result in the particles coming too close to each other or aggregating thereby limiting the number of active sites on the surface. Higher concentration of the suspended particles may also disturb the transmission of ultrasound in water medium. Hence no further increase in the degradation of the pollutant is observed beyond the optimum dosage. However the number of particles alone or the effect of ultrasound on them is not the only factor leading to increased degradation with increase in catalyst dosage, as seen in the difference in the optimum amount of ZnO , TiO_2 or ZnO-TiO_2 with comparable particle size and surface area. Surface and bulk interactions of the reactant molecules play an important role in the sonocatalytic degradation of organics in suspended systems.

The increase in the degradation of phenol with increase in catalyst dosage as observed here is inconsistent with the report that adsorption of the pollutant molecules on the surface may protect them from ultrasonic degradation [20]. The adsorption of phenol on the catalysts is determined at the optimum degradation dosages and the values are 24, 16 and 19 mg/g of the catalyst for TiO_2, ZnO and ZnO-TiO_2 respectively. TiO_2 is a better adsorber compared to the other two catalysts. However, the sonocatalytic activity is less compared to ZnO thereby confirming that adsorption is not the major factor in sonocatalysis. At the same time increase in the degradation rate with increase in catalyst loading, as observed in the current study shows that adsorption does not inhibit the degradation altogether. Adsorption helps the surface initiated degradation on the one hand and protects at least partly, the adsorbed species from cavitation effects. At the same time cavitation is known to alter the adsorption/desorption/degradation rates [21].

The current study shows that ZnO is more efficient than TiO_2 for the degradation of phenol. Appropriate combination of ZnO -TiO_2 is having the same activity as ZnO. This also shows that the effect of particles is not limited to cavitation or its consequences alone. Irradiation of aqueous solution by ultrasound is known to produce ultraviolet light by sonoluminescence[22]. Since ZnO is known to be a better harvester of light[14], the higher sonocatalytic activity can be at least partly attributed to the photocatalysis occurring during US irradiation. The presence of suspended particles lead to better propagation of the ultrasonic wave in the suspended medium resulting in the production of cavitation bubbles and emission of light throughout the reactor. This light can activate ZnO leading to the production of OH radicals which can either react with phenol and degrade it or recombine to produce H_2O_2. Higher adsorption of the pollutant on the surface of the catalysts is known to retard the absorption of light resulting in lower degradation. At the same time lower adsorption can result in decreased reaction rate, prolonged degradation time and even incomplete degradation. Hence reasonable degree of adsorption combined with good absorption of light resulting from sonoluminescence lead to good sonocatalytic activity of semiconductor oxides. The higher activity of ZnO-TiO_2 indicates that the better adsorption capability of TiO_2 and the light absorption capability of ZnO can be suitably exploited to achieve maximum degradation of the pollutant in water by sonocatalysis.

H_2O_2 formation and decomposition: Formation of H_2O_2 is observed in the case of sonocatalytic and photocatalytic degradation of phenol in presence of ZnO, TiO_2 and ZnO-TiO_2. Hydrogen peroxide is produced even in the absence of phenol indicating the formation of free radicals OH and HO_2 in liquid water by US/UV. The results are shown in figures 3 and 4.

The results indicate that H_2O_2 formation is more in presence of UV than US in the case of ZnO and ZnO-TiO_2. In the case of TiO_2, the H_2O_2 formed is more in presence of US compared to UV, at least in the initial stages. In the case of US, the concentration of H_2O_2 is less in the presence of phenol probably because some of the ·OH radicals formed may be reacting with phenol before they could recombine to produce H_2O_2. Also in this case, thermal decomposition of H_2O_2 to water and oxygen rather than to reactive radical species may be occurring[23]. In the case of TiO_2 the difference in H_2O_2 concentration in the reaction system, between in the presence and absence of phenol is not significant. In this case, the degradation of phenol is also less. The concentration of H_2O_2 is increasing and decreasing periodically showing that it is undergoing simultaneous formation and decomposition. At the same time, the degradation of phenol continues without break, though the rate of degradation slows down with time.

The decomposition and consequent decrease in the concentration of H_2O_2 is more evident even in the initial stages in the case of TiO_2. It is also pertinent to note that the maxima and minima attained in the case of respective

Research Journal of Recent Sciences ISSN 2277-2502
Vol. 1 (ISC-2011), 191-201 (2012) Res. J. Recent Sci.

catalysts remain more or less in the same range, irrespective of the number of crests and valleys. This suggests that there is some kind of an equilibrium concentration for H_2O_2 in each system, at which the rate of decomposition and formation balances each other. The maximum concentration of H_2O_2 reached is different for different catalysts indicating that it is dependent on the catalyst. Similar oscillatory behavior in the concentration of H_2O_2 during photocatalysis [24] and sonophotocatalysis[15] has been reported earlier. It is known[25] that H_2O_2 decomposes and produces OH radicals during, sono, photo and sonophotocatalysis. These radicals can accelerate the degradation of phenol. This is tested by adding H_2O_2 in the beginning of the experiments. The results are shown in table 1.

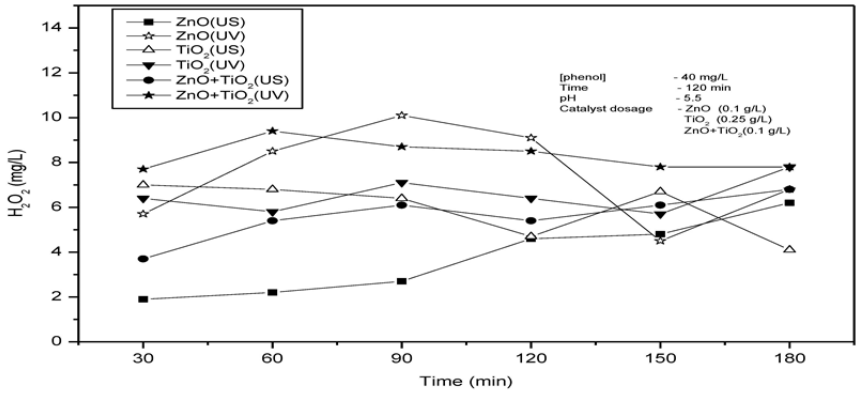

Figure-3
Oscillation in the concentration of H_2O_2 in the presence of phenol under sono and photo catalytic condition on various catalysts

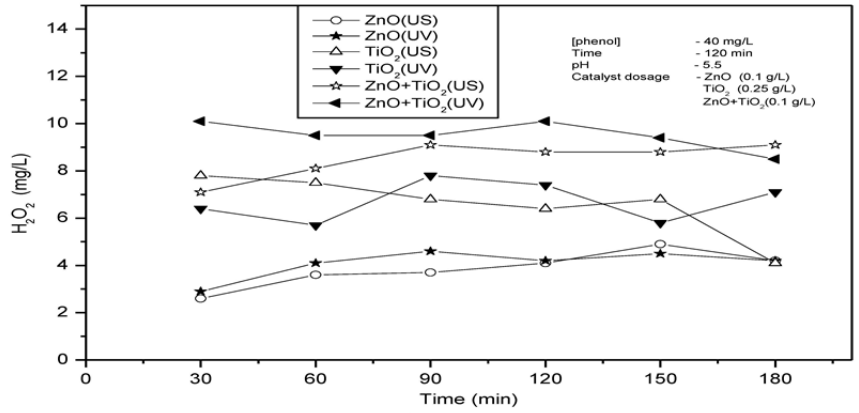

Figure-4
Oscillation in the concentration of H_2O_2 in the absence of phenol under sono and photo catalytic condition on various catalysts

Research Journal of Recent Sciences ISSN 2277-2502
Vol. 1 (ISC-2011), 191-201 (2012) Res. J. Recent Sci.

Table 1
Effect of added H_2O_2 on the degradation of phenol under US, UV and (US + UV)
[Catalyst]: 0.1g/L pH: 5.5 Reaction Volume: 50 ml [Phenol]: 40 mg/L

Reaction Condition	% Degradation of phenol without added H_2O_2			% Degradation of phenol with added H_2O_2			% enhancement by added H_2O_2		
	30 min	60 min	90 min	30 min	60 min	90 min	30 min	60 min	90 min
US (ZnO)	1.1	6.0	9.5	3.0	7.1	11.2	172.7	18.3	17.9
UV (ZnO)	7.0	17.5	33.2	14.3	31.2	44.7	104.3	78.3	34.6
US (TiO_2)	0.8	3.7	5.2	1.8	4.7	5.8	125.0	27.0	11.5
UV (TiO_2)	5.8	14.6	26.3	10.5	24.8	34.6	81.0	70.0	31.6
US (ZnO-TiO_2)	1.1	6.2	10.1	2.7	7.4	11.4	145.5	19.4	12.9
UV (ZnO-TiO_2)	9.2	18.3	36.6	16.1	29.5	45.8	75.0	61.2	25.1

H_2O_2 enhances the degradation of phenol significantly in the beginning. However this high rate of enhancement is not sustained later on. This can be explained as follows:

In the beginning, added H_2O_2 decomposes faster in presence of UV and US producing maximum OH radicals which can degrade phenol. However, the decomposition of H_2O_2 to water and oxygen also occurs in parallel which restricts the continued availability of the oxidizing species for phenol degradation. Further, even in those experiments without externally added H_2O_2, the H_2O_2 formed insitu will be accelerating the reaction rate. Hence the effect of initially added H_2O_2 is not that prominent in the later stages of the reaction. The decrease in the enhancement of degradation with time is relatively less in the case of UV. Here the decomposition of H_2O_2 is occurring slowly thereby making the OH radicals available for degradation reaction for extended period. The thermal decomposition of H_2O_2 into inactive H_2O and O_2 also is lower in the case of UV irradiation compared to US.

H_2O_2 accelerates the degradation in all cases following a fairly uniform pattern. The enhancement effect is comparable in the case of ZnO and ZnO-TiO_2. This shows that in the case of the coupled catalyst, the mechanism of degradation of phenol as well as the formation and decomposition of H_2O_2 is more or less dictated by ZnO since it has higher sono and photocatalytic activity compared to TiO_2.

Concentration Effect: The effect of concentration of phenol on the rate of degradation is investigated. The results are plotted in figure 5.

In the case of ZnO, TiO_2 as well as ZnO-TiO_2 the rate increases linearly with increase in concentration at lower concentration range of 10-40 mg/L. At higher concentrations, the rate slows down as the concentration increases. Thus the degradation follows first order kinetics at lower concentration which changes to lower order at higher concentration. Decrease in the rate of degradation and hence in the order of the reaction at higher concentration of the reactant has been reported in the case of photocatalysis[26,27], sonocatalysis[28] as well as sonophotocatalysis[15]. In the present study the kinetics observed in the case of all three catalysts is similar indicating that the mechanism of degradation may be the same. However, the change of reaction order takes place at slightly lower concentration ranges in the case of TiO_2 showing the role of surface characteristics and adsorption on the rate of reaction.

Sonocatalytic reactions occur at the surface, in the bulk as well as at the interface of the cavitation bubble. At the surface of the collapsed bubble, the concentration of the OH radicals is relatively high. At low concentration, when the amount of phenol at the surface or in the bulk is low, a considerable part of the OH radicals will recombine yielding H_2O_2. Only about 10% of the OH radicals generated in the bubble can diffuse into the bulk solution[29]. These factors result in lower degradation of phenol. With increase in concentration, the probability of interaction of OH radicals with phenol increases on the surface as well as in the bulk resulting in increased rate of degradation. The degradation rate slows down and reaches almost a constant level when the concentration of phenol on the catalyst surface as well as at the bubble surface reach a saturation limit during the persistence of the bubble. This is in agreement with earlier findings[30].

The general mechanism of sonocatalytic degradation in aqueous medium involves the formation of OH radicals and their attack on the organic substrate. This can also explain the decrease in the recombination of OH radicals resulting in lower concentration of H_2O_2 at higher concentration of phenol[31]. At higher concentration of the substrate, the surface is fully covered as a result of which it cannot effectively absorb the light produced by ultrasound, resulting in decreases photocatalytic effect and eventual stabilization. Also at higher concentrations, the phenol molecules can act as mutual screens thereby preventing effective interaction of all molecules with the ultrasound [32].

Research Journal of Recent Sciences ISSN 2277-2502
Vol. **1 (ISC-2011),** 191-201 **(2012)** *Res. J. Recent Sci.*

Effect of pH: The pH of the reaction medium is known to have strong influence on US or UV-induced degradation of organic pollutants. In photolysis, the possibility of bond breakage and the site might be different at different pH due to difference in the distribution of molecular charges. In sonocatalytic reaction, pH can alter the distribution of the pollutants in the bulk region, on the surface and at the site of the cavity collapse. The surface charge of semiconductors and the interfacial electron transfer and the photoredox processes occurring in their presence are also affected by pH. Hence the effect of pH on sonocatalytic degradation of phenol was investigated in the range 3-11. The pH of the suspension was adjusted initially and it was not controlled during the irradiation. The results are presented in figure 6.

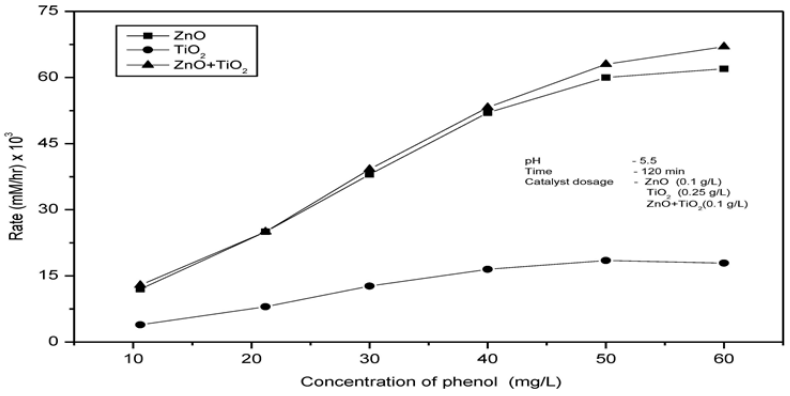

Figure-5
Effect of concentration of phenol on the intial rate of sonocatalytic degradation on various catalysts

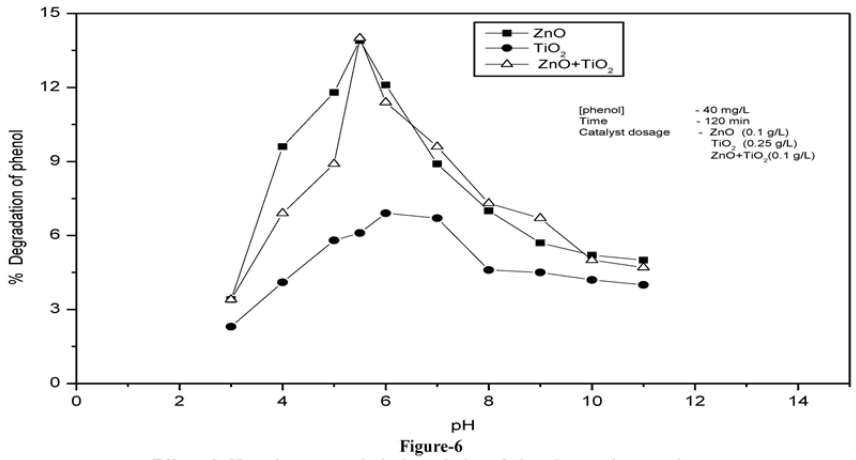

Figure-6
Effect of pH on the sonocatalytic degradation of phenol on various catalysts

Research Journal of Recent Sciences ISSN 2277-2502
Vol. **1 (ISC-2011),** 191-201 **(2012)** *Res. J. Recent Sci.*

The degradation is more efficient in the acidic region than in the alkaline region in the case of the three catalysts tested here. In the case of ZnO, maximum degradation is observed in the acidic pH range of 4-6, which peaks at pH 5.5. In the case of TiO_2 also similar trend follows with the maximum at pH 6. For ZnO-TiO_2, the pH effect is quite similar to that of ZnO as expected. The optimum pH in all these cases is 5.5-6. Higher degradation efficiency in the acidic range has been reported by other authors also [33-35] with different types of phenol using TiO_2 as the catalyst. The steep fall in degradation rate below pH 4 in the case of ZnO and ZnO-TiO_2 can be attributed to the corrosion of ZnO under acidic conditions.

The pH of the reaction medium has significant effect on the surface properties of semiconductor oxide particles, including the surface charge, size of the aggregation and the band edge position[36]. Hence pH can affect the adsorption – desorption characteristics of the surface of the catalyst. However, in the case of sonocatalysis, adsorption is not the only factor leading to the degradation for reasons explained earlier.

The acid-base property of metal oxides can influence their photocatalytic activity significantly. The Point of Zero Charge (PZC) of ZnO and TiO_2 are 9.3 and 6.8 approximately[14]. This means that the catalyst surface is positively charged when the pH is lower than respective PZC value and negatively charged when the pH is higher. Solution pH influences the ionization state of ZnO surface according to the reaction:

$$---Zn-OH + H^+ \leftrightarrow ZnOH_2^+ \quad (2)$$
$$--Zn-OH + OH^- \leftrightarrow Zn\text{-}O^- + H_2O \quad (3)$$

In the alkaline pH range, where phenol is expected to be in the ionized form, the adsorption on ZnO will be weaker. Hence the surface mediated degradation will be less. However under acidic conditions, phenol which remains mainly in the neutral form can get adsorbed or come closer to the catalyst surface, resulting in its degradation via active surface species or bulk hydroxyl radicals produced in the aqueous media. Further, the presence of more protons can facilitate the formation of reactive OH radicals from the available OH ions. Significant enhancement in the degradation can also be attributed to the effect of US in reducing the distance between the substrate molecule and the surface of the catalyst particles. This is not feasible in the alkaline range where repulsion between like charges of the substrate and the catalyst particles is much greater [16].

Similarly in the case of TiO_2, solution pH influences the ionization state of TiO_2 surface according to the reaction[11]

$$>Ti-OH + H^+ \leftrightarrow >Ti\text{-}OH_2^+ \quad (4)$$
$$>Ti-OH + OH^- \leftrightarrow >Ti\text{-}O^- + H_2O \quad (5)$$

At pH less than ~7, when the TiO_2 surface is positively charged, phenol which is in neutral form can get closer to the surface or weakly adsorbed. At pH > 7, when the surface is negatively charged, phenol in neutral or ionized form will keep away from the surface. In the case of ZnO, weak adsorption or al least phenol coming closer to the surface is possible upto pH 9. Hence the surface promoted sonocatalytic degradation is more in the case of ZnO than TiO_2. As expected, the pH effect on the ZnO-TiO_2 is more or less similar to that on ZnO. The results clearly indicate that there is no well defined correlation between PZC of the semiconductor oxide catalyst and the sonocatalytic degradation rate.

Possible mechanism: Sonocatalytic degradation is generally explained based on sonoluminescence and hot spot theory. Ultrasonic irradiation results in the formation of light of a comparatively wide wavelength range of 200 -500 nm. Those lights with wavelength below 375 nm can excite the semiconductor catalyst and generate highly active OH radicals on the surface. Thus the basic mechanism is partly that of photocatalysis. At the same time the more complex phenomenon of formation of hotspots upon implosion of some bubbles on the catalyst surface also leads to the formation of electron-hole pairs and excess OH radicals[14]. Since the formation of electron-hole pairs is the first step in both photocatalysis and sonocatalysis, the efficiency of the process depends on the ability to prevent their recombination. This is achieved to some extent by combining the semiconductor oxides ZnO and TiO_2 which is one of the reasons for the observed synergy here. Under ultrasonic irradiation, a series of thermal and photochemical reactions take place on the surface of composite TiO_2/ZnO particles[16]. Because of the difference in adsorption capacity, the TiO_2 part is inclined to the hole oxidation and ZnO tends towards radical oxidation. The electron transport in the TiO_2/ZnO prevents the electron – hole recombination and increases the sonocatalytic activity. Because the TiO_2 and ZnO possesses similar energy band gap (3.2 eV) the electrons can transfer easily from TiO_2 to ZnO through the crystal interface between the two which results in complete separation of electrons and holes. Such electron transport through the crystal interface of composite oxides has been reported earlier also[17].

The overall mechanism of H_2O_2 formation and the decomposition of phenol under sonocatalytic conditions can be explained as follows:

Acoustic cavitation produces highly reactive primary radicals such as OH and H as in reaction (6). Recombination and a number of other reactions occur within the bubble as in reactions (7) to (11) following this primary radical generation

$$H_2O \xrightarrow{>>>} H^{\cdot} + {}^{\cdot}OH \quad (6)$$
$${}^{\cdot}OH + H^{\cdot} \rightarrow H_2O \quad (7)$$

Research Journal of Recent Sciences ISSN 2277-2502
Vol. 1 (ISC-2011), 191-201 (2012) Res. J. Recent Sci.

$^{\cdot}OH + {}^{\cdot}OH \rightarrow H_2O_2$ (8)
$H^{\cdot} + H_2O \rightarrow {}^{\cdot}OH + H_2$ (9)
$H^{\cdot} + O_2 \rightarrow HO_2^{\cdot}$ (10)
$HO_2^{\cdot} + HO_2^{\cdot} \rightarrow H_2O_2$ (11)

OH radical is a nonselective oxidant with a high redox potential (2.8 eV) which is able to oxidise most organic pollutants [37].

Similarly the photocatalytic reaction initiated by ultrasound can be represented as follows[38]:

SC (Semiconductor) + hυ → $h^+ + e^-$ (12)
$h^+ + e^- \rightarrow$ Heat (Recombination) (13)
$h^+ + OH^- \rightarrow OH^{\cdot}$ (14)
$h^+ + H_2O \rightarrow OH^{\cdot} + H^+$ (15)

Scavenging of conduction band electrons

$e^- + O_2 \rightarrow {}^{\cdot}O_2^-$ (16)

Formation of multiple peroxide species

$H^+ + {}^{\cdot}O_2^- \rightarrow HO_2^{\cdot}$ (17)
$HO_2^{\cdot} + e^- + H^+ \rightarrow H_2O_2$ (18)

Various reactive species produced as above react with phenol as in reaction (19) below

Phenol + Reactive species ($^{\cdot}O_2^-$, $HO_2^{\cdot}$, OH^-) → Intermediates → $H_2O + CO_2$ (19)

Once sufficient concentration of H_2O_2 is reached, its decomposition also sets in as follows:

$H_2O_2 + {}^{\cdot}OH \rightarrow HO_2^{\cdot} + H_2O$ (20)
$HO_2^{\cdot} + {}^{\cdot}OH \rightarrow H_2O + O_2$ (21)

H_2O_2 can also lead to reduction in charge recombination by taking up the electron

$SC(e^-) + H_2O_2 \rightarrow SC + HO^{\cdot} + OH^-$ (22)

H_2O_2 can also produce OH radicals directly or reaction with superoxide anion

$H_2O_2 \xrightarrow{h\upsilon} 2\ {}^{\cdot}OH$ (23)
$H_2O_2 + {}^{\cdot}O_2^- \rightarrow 2\ {}^{\cdot}OH + O_2$ (24)

Conclusion

The sonocatalytic activity of ZnO, TiO_2 and ZnO-TiO_2 for the degradation of phenol pollutant in water is investigated. The efficacy of the catalysts for the degradation is in the order ZnO-TiO_2 > ZnO > TiO_2. At lower concentrations of ZnO, the percentage degradation in the presence of coupled ZnO-TiO_2 is more than the sum of the degradation achieved in the presence of individual oxides under identical conditions, implying a synergistic effect. The catalyst loading, irradiation time, initial pH and concentration of the substrate have profound effect on the rate of degradation. H_2O_2 formed during the degradation of phenol undergoes simultaneous decomposition as well. After initial accumulation upto certain concentration, decomposition of H_2O_2 also sets in resulting in oscillation in its concentration. Possible mechanism for the sonocatalytic degradation of phenol, formation and decomposition of H_2O_2 and the enhanced activity of coupled ZnO-TiO_2 is discussed.

Acknowledgement

ASG acknowledges the financial support from the Cochin University of S &T, Kochi, India. JKP and SJ acknowledge the financial support from the CSIR, New Delhi, India.

References

1. Ying-Shih M, Chi-Fanga S, Jih-Gaw L, Degradation of carbofuran in aqueous solution by ultrasound and Fenton processes: Effect of system parameters and kinetic study, *J Hazardous Mater.,* **178,** 320-325 **(2010)**
2. Zouaghi R, David B. Suptil J, Djebbar K, Boutiti A, Guittonneau S, Sonochemical and sonocatalytic degradation of monolinuron in water, *Ultrason.Sonochem.* **18**, 1107-1112 **(2011)**
3. Torres R.A, Abdelmalek F, Combet E, Petrier C,Pulgarin C, A comparative study of ultrasonic cavitation and Fenton's reagent for bisphenol A: Degradation in deionised and natural waters, *J Hazard. Mater* **146,** 546-555 **(2007)**
4. Devipriya S, Yesodharan S, Photocatalytic degradation of pesticide pollutants in water, *Solar Energy Mater and Solar Cells,* **86**, 309-348 **(2005)**
5. Malato S, Blanco J, Alarcon D.C, Maldonado M.I, , Fernandez-Ibanez P, Gernjak W, Photocatalytic decontamination and disinfection of water with solar collectors, *Catalysis Today* **122**, 137-149 **(2007)**
6. Joseph C.G, Puma G.L, Bono A, Krishniah D, Sonophotocatalysis in advanced oxidation process: A short review, *Ultrason., Sonochem.* **16**, 583-589 **(2009)**
7. Gogate P.R, Treatment of wastewater streams containing phenolic compounds using hybrid techniques based on cavitation: a review of the current status and the way forward, *Ultrason. Sonochem.***15**, 1-15 **(2008)**
8. Torres-Palma R.A, Nieto J.I, Combet E, Petrier C, Pulgarin C, An innovative ultrasaound, Fe^{2+} and TiO_2 photo assisted process for bisphenol a mineralization, *Water Res.* **44**, 2245-2252 **(2010)**
9. Davydov L, Reddy E.P, France P, Smirniotis P, Sonophotocatalytic destruction of organic contaminants in aqueous systems on TiO_2 powders, Appl. Catal.B: Environmental **32**, 95-105 **(2001)**
10. Chen Y.C, Smirniotis P, Enhancement of photocatalytic degradation of phenol and chlorophenols by ultrasound, Ind. Eng. Chem. Res. **41**,5958- 5965 **(2002)**

Research Journal of Recent Sciences ISSN 2277-2502
Vol. **1 (ISC-2011),** 191-201 **(2012)** *Res. J. Recent Sci.*

11. Kritikos D.E, Xekoukoulotakis N.P, Psillakis E, Mantzavinos D, Photocatalytic degradation of reactive black 5 in aqueous solutionds: Effect of operating conditions and coupling with ultrasound irradiation, Water Res. **41**, 2236-2246 **(2007)**

12. Nepiras E.A, Acoustic cavitation: An introduction, *Ultrasonics,* **22**, 25-40 **(1984)**

13. Poulios I, Avranas A, Rekliti E, Zouboulis A, Photocatalytic oxidation of Auramine O in the presence of semiconducting oxides, *J Chem Technol. Biotechnol.* **75**, 205-212 **(2000)**

14. Sakthivel S, Neppolian B, Shankar M V, Arabindoo B, Palanichamy M, Murugesan V, Solar photocatalytic degradation of azodye: Comparison of photocatalytic efficiency of ZnO and TiO_2, *Solar Energy Mater. and Solar Cells.* **77**, 65-82 **(2003)**

15. Anju S.G, Yesodharan S, Yesodharan E.P, Semiconductor mediated sonophotocatalytic degradation of organic pollutants in water, Proc. 23rd Kerala Science Congress, Trivandrum 156-157 **(2011)**

16. Wang J, Jiang Z, Zhang L, Kang P, Xie Y, Lv Y, Xu R, Zhang X, Sonocatalytic degradation of some dyestuffs and comparison of catalytic activities of nanosized TiO2, nano-sized ZnO and composite TiO_2/ZnO powders under ultrasonic irradiation, *Ultrasonics Sonochem.* **16**, 225-231 **(2009)**

17. Song L, Chen C, Zhang S, Sonocatalytic performance of Tb_7O_{12}/TiO_2 composite under ultrasonic irradiation, *Ultrason. Sonochem.* **18**, 713-717 **(2011)**

18. Jain S, Yamgar R, Jayram R.V, Photolytic and photocatalytic degradation of atrazine in the presence of activated carbon, *Chem. Eng. Journal,* **148**, 342-347 **(2009)**

19. Tuziuti T, Yasui K, Sivakumar M, Iida Y, Correlation between acoustic cavitation nopise and yiel enhancement of sonochemical reaction by particle addition, *J Phys Chem. A* **109**. 4869-4872 **(2005)**

20. Pandit A.B, Gogate P.R, Majumdar S, Ultrasonic degradation of 2.4.6 trichlorophenol in presence of TiO_2 catalyst, *Ultrason.Sonochem.* **8**, 227-231**(2001)**

21. Hamdaoui O, Naffrechoux E, Adsorption kinetics of 4-chlorophenol on granulated activated carbon in the presence of high frequency ultrasound, *Ultrason.Sonochem* **16**, 15-22 **(2009)**

22. Beckett M.A, Hua I, Impact of ultrasonic frequency on aqueous sonoluminescence and sonochemistry, *J.Phys.Chem A* **105**, 3796-3802 **(2001)**

23. Chand R, Ince N.H, Gogate P.R, Bremner D.H, Phenol degradation using 20,300 and 520 kHz ultrasonic reactors with hydrogen peroxide, ozone and zerovalent metals, Separation and Purification Technology **67**, 103-109 **(2009)**

24. Kuriacose J.C, Ramakrishnan V, Yesodharan E.P, Photoinduced catalytic reactions of alcohols on ZnO suspensions in cyclohexane: Oscillation in the concentration of H_2O_2 formed, Indian J. Chem. **19A**, 254-256 **(1978)**

25. Hoffmann A.J, Carraway E.R, Hoffmann M.R, Photocatalytic production of H_2O_2 and Organic peroxides` on quantum sized semiconductor colloids, Environ. Sci. Technol. **28**, 776-785 **(1994)**

26. Rabindranathan S, Devipriya S,Yesodharan S, Photocatalytic degradation of phosphamidon on semiconductor oxides, J Hazard. Mater. **102**, 217-229 **(2003)**

27. Daneshvar N, Aber S, Dorraji M.S.S, Khataee A.R, Rasoulifard, Preparation and investigation of photocatalytic properties of ZnO nanocrystals: Effect of operational parameters and kinetic study, *World Acad of Sci. Eng. And Technol.* **29**, 267-272 **(2007)**

28. Zheng W, Maurin M, Tarr M A, Enhancement of sonochemical degradation of phenol using hydrogen atom scavengers, *Ultrason.Sonochem* **12**, 313-317 **(2005)**

29. Goel M, Hongqiang H, Majumdar A.S, Ray M.B, Sonochemical decomposition of volatile and nonvolatile organic compound: A comparative study, *Water Res.* **38**, 4247-4261 **(2004)**

30. Marouani S, Hamdaoui O, Saoudi F, Chiha M, Sonochemical degradation of Rhodamine B in aqueous phase: effect of additives, *Chem. Eng. J.* **158**, 550-557 **(2010)**

31. Madhavan J, Grieser F, Ashokkumar M, Combined advanced oxidation processes for the synergistic degradation of ibuprofen in aqueous environments, *J Hazardous Mater* **178**, 202-208 **(2010)**

32. Wang J, Jiang Y, Zhang Z, Zhao G, Zhang G, Ma T, Sun W, Investigations on the sonocatalytic degradation of Congo red catalysed by nanometer rutile powder and

Research Journal of Recent Sciences ISSN 2277-2502
Vol. **1 (ISC-2011),** 191-201 **(2012)** *Res. J. Recent Sci.*

various influencing factors, *Desalination* **216**, 196-208 **(2007)**

33. Kaur S, Singh V, Visible light induced sonocatalytic degradation of Reactive Red dye 198 using dye sensitized TiO_2, *Ultrason. Sonochem*. **14**, 531-537 **(2007)**

34. Vijaya laxmi P.N, Saritha Rambabu P.N, Himabindu V, Anjaneyulu Y, Sonochemical degradation of 2 chloro-5methyl phenol assisted by TiO_2 and H_2O_2, *J Hazard Mater*. **174**, 151-155 **(2010)**

35. Ou X.H, Lo S.L, Wu C. H, Exploring the interparticular electron transfer process in the photocatalytic oxidation of 4-chlorophenol, *J Hazardous Mater*. **137**, 1362-1370 **(2006)**

36. Zhow S, Ray A.K, Kinetic studies for photocatalytic degradation of Eosin B on a thin film of Titanium dioxide; *Ind. Eng. Chem. Res.* **42**, 6020-6033**(2003)**

37. Neppolian B, Ciceri L, Bianchi C L, Grieser F, Ashok kumar M, Sonophotocatalytic degradation of 4-chlorophenol using $Bi_2O_3/TiZrO_4$ as a visible light responsive photocatalyst, *Ultrason. Sonochem* **18**, 135-139 **(2011)**

38. Davydov L, Smirniotis P.G, Quantification of the primary processes in aqueous heterogeneous photocatalysis using single stage oxidation reactions, J Catal. **191**, 105-112 **(2000)**

Research Journal of Recent Sciences ISSN 2277-2502
Vol. 2(ISC-2012), 136-149 (2013) Res.J.Recent.Sci.

Periodic Change in the Concentration of Hydrogen peroxide Formed during the Semiconductor Mediated Sonocatalytic treatment of Wastewater: Investigations on pH Effect and Other Operational Variables

Jyothi K. P, Sindhu Joseph, Suguna Yesodharan and Yesodharan E.P.
School of Environmental Studies, Cochin University of Science and Technology, Kochi, INDIA

Available online at: www.isca.in
Received 31st July 2012, revised 29th December 2012, accepted 22nd January 2013

Abstract

Hydrogen peroxide, formed in situ or externally added, is an important Reactive Oxygen Species (ROS) involved in Advanced Oxidation Processes (AOP) such as sono, photo and sonophoto catalysis being investigated as environment friendly technologies for the treatment of wastewater under ambient conditions. Among the various ROS such as ·OH, $HO_2^·$, $O_2^{·-}$, H_2O_2, O_2 etc, H_2O_2 is the most stable and it serves as a reservoir of other ROS. Current investigations on the ZnO and TiO_2 mediated sonocatalytic degradation of phenol pollutant in water reveal that, H_2O_2 formed cannot be quantitatively correlated with the degradation of the pollutant. The concentration of H_2O_2 varies in a wavelike fashion (oscillation) with well defined crests and troughs, indicating concurrent formation and decomposition. Both processes are sensitive to the reaction conditions and depending on the externally forced or in situ situation, either of them can predominate. The degradation of H_2O_2 continues for some more time even after the sonication has been put off showing that the catalyst has some residual activity. This further confirms that trapped electrons and holes have unusually longer life even after the irradiation is off. Concentration of H_2O_2, catalyst loading, dissolved gases, concentration of the organic pollutant, pH etc influence the oscillation. The degradation of phenol is favored in the acidic range with maximum at pH 5.5. The successive maxima and the minima in the oscillation of H_2O_2 concentration also are higher in the acidic range. The influence of pH on various factors leading to the oscillation in the concentration of H_2O_2 is unequivocally established from a number of experiments, for the first time in this paper. An appropriate mechanism to explain the complex phenomenon is also proposed.

Keywords: Sonocatalysis, zinc oxide, titanium dioxide, hydrogen peroxide, oscillation, pH effect.

Introduction

Considerable interest has been shown in the application of sonocatalysis, photocatalysis and its combination sonophotocatalysis using suspended semiconductor oxide particles for the environment–friendly destruction of organic pollutants in water[1-6]. Major advantages of these Advanced Oxidation Processes (AOP) include relatively mild reaction conditions and their proven ability to degrade several toxic refractory pollutants. Of these, photocatalysis has been investigated extensively with semiconductors such as TiO_2 and ZnO as catalysts for the removal of a variety of pollutants. However, many of these catalysts are active only in the UV range, which make them unattractive for solar energy harvesting. Several efforts are being made to make visible light active photocatalysts. These include dye sensitization, semiconductor coupling, impurity doping, use of coordination metal complexes and metal deposition[7-11]. Composites such as TiO_2/carbon have also been reported[12,13]. Deposition of noble metals such as Pt, Pd, Au, Ag etc on TiO_2 enhances the catalytic oxidation of organic pollutants[14,15].

Recently, Ultrasonic (US) irradiation mediated by suitable catalysts (sonocatalysis) has been receiving special attention as an environment - friendly technique for the treatment of hazardous organic pollutants in wastewater[16,17]. However the degradation rate is slow compared to other established methods. Investigations aimed at enhancing the efficiency of US promoted decontamination of water are in progress in many laboratories. These include testing a variety of catalysts with different physico-chemical characteristics, modification of reactor design and reaction conditions, combining US with other AOP techniques etc[18-22]. Coupling US with Ultraviolet (UV) irradiation enhances the efficiency of semiconductor mediated degradation of aqueous pollutants synergistically[5,19].

In liquids US produces cavitation which consists of nucleation, growth and collapse of bubbles. The collapse of the bubbles results in localized supercritical condition such as high temperature, pressure, electrical discharges and plasma effects [16,22-24]. The temperature of the gaseous contents of a collapsing cavity can reach approximately 5500^0C and that of the liquid immediately surrounding the cavity reaches up to 2100^0C. The localized pressure is estimated to be around 500 atmospheres resulting in the formation of transient supercritical water. The cavities are thus capable of functioning like high energy micro reactors. The consequence of these extreme conditions is the cleavage of dissolved oxygen molecules and water molecules

Research Journal of Recent Sciences ISSN 2277-2502
Vol. **2(ISC-2012),** 136-149 **(2013)** *Res.J.Recent.Sci.*

into radicals such as $H^{\cdot}$, $OH^{\cdot}$ and $O^{\cdot}$ which will react with each other as well as with H_2O and O_2 during the rapid cooling phase giving $HO_2^{\cdot}$ and H_2O_2. In this highly reactive nuclear environment, organic pollutants can be decomposed and inorganic pollutants can be oxidised or reduced. This phenomenon is being explored in the emerging field of sonocatalysis for the removal of water pollutants.

Studies in our laboratory have shown that H_2O_2, one of the major products of sonocatalytic degradation of organic pollutants in water, undergoes simultaneous formation and decomposition during the degradation process[5,23]. This results in oscillation in the concentration of H_2O_2. The rate of degradation of the pollutants and the oscillation phenomenon are influenced by various reaction parameters such as catalyst loading, substrate concentration, reaction volume, presence of anions, reaction intermediates, pH etc. The effect of pH on sonocatalytic degradation of pollutants in water is more complex. In this study the effect of pH on sonocatalytically formed H_2O_2 in presence of ZnO is investigated in detail.

Materials and Methods

ZnO and TiO_2 used in the study were supplied by Merck India Limited. In both cases the purity was over 99%. The surface areas of TiO_2 and ZnO, as determined by the BET method are approximately15 and 12 m^2/g respectively. The average particle size of both ZnO and TiO_2 was 10 µm. Phenol AnalaR Grade (99% purity) from Qualigen (India) was used as such without further purification. All other chemicals were of AnalaR Grade or equivalent. The sonocatalytic reactions were performed as reported earlier[5]. The concentration of phenol left behind was analyzed periodically by Spectrophotometry at 500 nm. H_2O_2 is determined by iodometry[23]. Mineralization was identified by the evolution of CO_2.

Results and Discussion

Investigations on the sonocatalytic degradation of phenol using ZnO catalysts showed that no significant degradation took place in the absence of ultrasound or the catalyst suggesting that both catalyst and sound are essential to effect reasonable degradation. However, small quantity of phenol degraded under US irradiation even in the absence of catalysts (see figure 1).

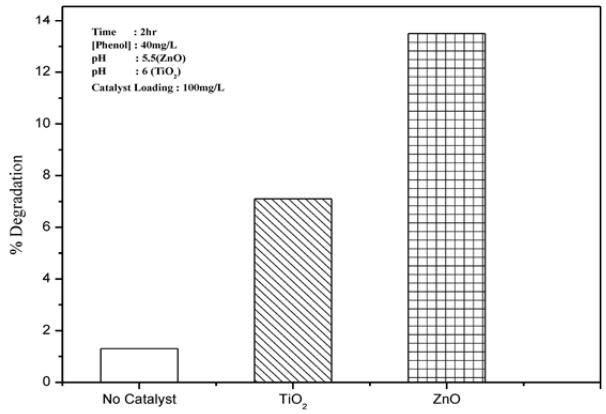

Fig 1.Sonocatalytic degradation of phenol

Research Journal of Recent Sciences ISSN 2277-2502
Vol. **2(ISC-2012),** 136-149 **(2013)** *Res.J.Recent.Sci.*

This is understandable since sonolysis of water is known to produce free radicals H· and OH· (via reaction 1), which are capable of attacking the organic compounds in solution[25].

$H_2O \xrightarrow{>>>} H^{\cdot} + {}^{\cdot}OH$ (1)

The free radicals thus produced can lead to the formation of H_2O_2 and degradation of phenol as follows:

$H^{\cdot} + O_2 \rightarrow HO_2^{\cdot}$ (2)

$HO_2^{\cdot} + HO_2^{\cdot} \rightarrow H_2O_2$ (3)

$2\ {}^{\cdot}OH \rightarrow H_2O_2$ (4)

Reactive oxygen species ($^{\cdot}OH$, $HO_2^{\cdot}$ etc) + phenol → Intermediates → $H_2O + CO_2$ (5)

However, there was no continuous increase in the concentration of H_2O_2 after the initial period possibly due to its parallel decomposition into water and oxygen as well as participation in the degradation of phenol[5,16,23]. At the same time the removal of phenol continued, though at a very slow rate.

The sonocatalytic degradation of phenol in presence of ZnO and TiO_2 at respective optimized loadings is shown in figure 2a. The fate of H_2O_2 formed in presence of these catalysts is shown in figure 2b.

Sonochemical processes in aqueous media are facilitated in a heterogeneous environment such as the presence of suspended particles[24,25]. The presence of the particles help to break up the microbubbles created by US into smaller ones, thus increasing the number of regions of high temperature and pressure This leads to increase in the number of reactive OH radicals which will interact with the organic pollutants present in water and oxidise them, resulting in eventual mineralization. The increase in the optimum concentration of H_2O_2 in presence of particles was reported by Keck etal[26]. Instances of decrease in the concentration of H_2O_2 in presence of particles have also been reported[19]. Our studies presented in this report as well as in earlier papers show that both increase and decrease in the concentration of H_2O_2 is possible in the same system depending on the relative concentration of H_2O_2 and the substrate as well as other reaction parameters[5,23].

The effect of ZnO loading on the sonocatalytic formation of H_2O_2 is shown in figure 3a. Catalyst loading for highest maximum in the oscillation curve of H_2O_2 is 50 mg/L. Optimum loading for the degradation of phenol is 100 mg/L (fig 3b).

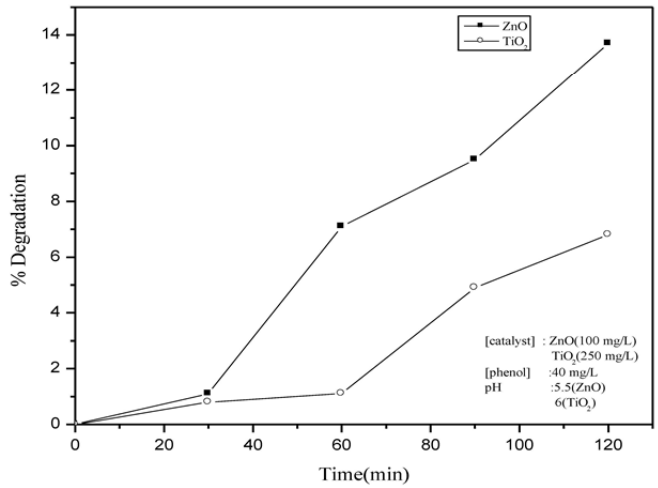

Fig 2(a): Sonocatalytic degradation of phenol in presence of ZnO and TiO_2

Research Journal of Recent Sciences ISSN 2277-2502
Vol. **2(ISC-2012),** 136-149 **(2013)** *Res.J.Recent.Sci.*

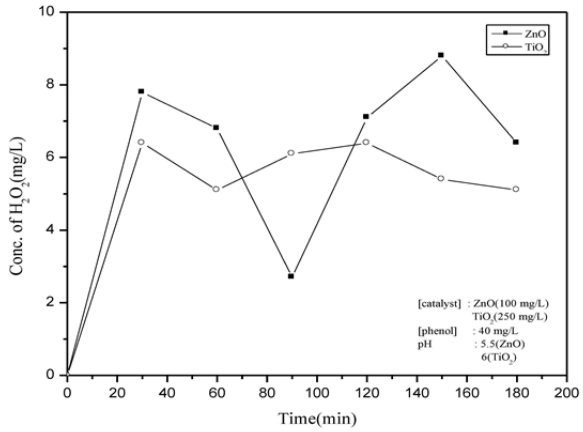

Fig 2(b): Fate of H_2O_2 during the sonocatalytic degradation of phenol in presence of ZnO and TiO_2

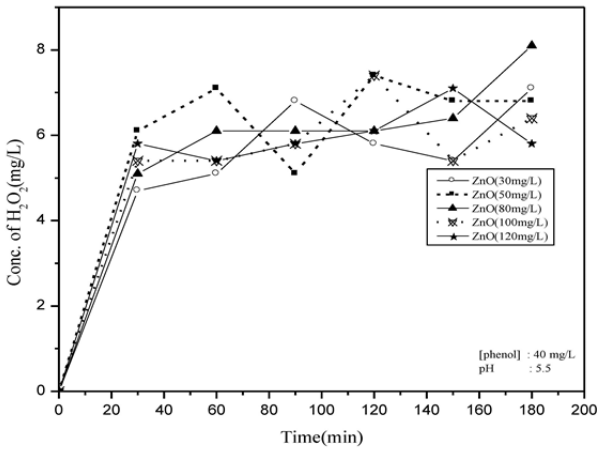

Fig 3(a): Effect of catalyst loading on the oscillation in the concentration of H_2O_2

Research Journal of Recent Sciences ISSN 2277-2502
Vol. 2(ISC-2012), 136-149 (2013) Res.J.Recent.Sci.

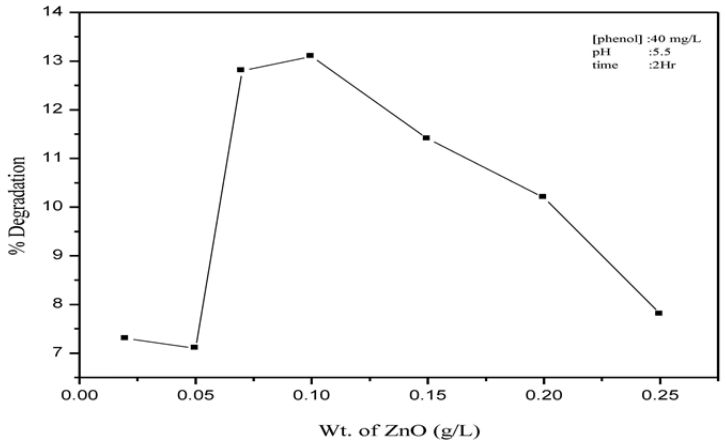

Fig 3(b): Effect of catalyst loading on the degradation of phenol

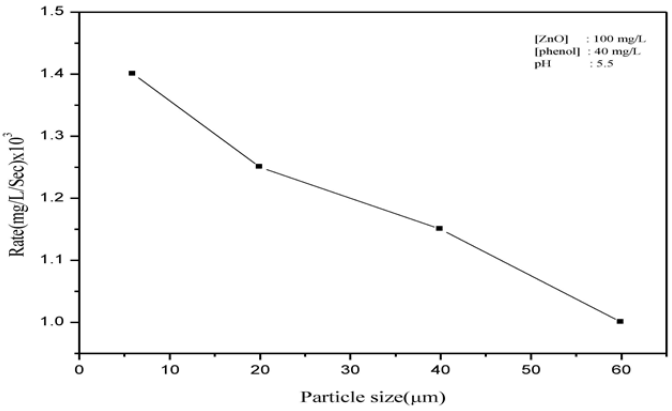

Fig 4: Effect of particle size on the initial rate of H_2O_2 formation

Research Journal of Recent Sciences ISSN 2277-2502
Vol. **2(ISC-2012),** 136-149 **(2013)** *Res.J.Recent.Sci.*

Since the formation and decomposition of H_2O_2 is occurring in parallel all the time, optimization of catalyst loading with respect to H_2O_2 formation may not be reliable. Hence the optimum loading of ZnO for phenol degradation is taken as the basis for further studies on the oscillation in the concentration of H_2O_2.

At the optimized loading for phenol degradation, the effect of particle size on the H_2O_2 formation is examined. The sonocatalytic rate of degradation of phenol increases with decrease in the particle size upto an optimum value[5]. The effect of particle size of ZnO on the H_2O_2 formed in the system is shown in figure-4.

With increase in particle size in the range of 6-60 micron, the initial rate of H_2O_2 formation decreases slightly from $1.4x\ 10^{-3}$ to $1.1\ x\ 10^{-3}$ mg/L/sec possibly due to lower surface area and decrease in the rate of generation of OH radicals. However, the nature of the oscillation curve remains the same in all cases even though the maxima of H_2O_2 concentration in the oscillation curve are higher at lower particle sizes. The successive maxima and minima of the oscillation curve remain more or less identical irrespective of the particle size of the catalyst. This confirms our earlier observation that the single most important factor that determines the rate of formation or decomposition of H_2O_2 is its concentration and either of them will predominate once a critical lower or upper concentration is reached respectively[5,21].

Simple quartz or alumina particles have very little effect on the sonochemical removal of phenol thereby indicating that it is not just the particle effect that promotes sonocatalytic degradation of phenol in the case of semiconductor oxides such as ZnO, which can act catalytically. However the concentration of sonochemically formed H_2O_2 increases initially in the presence of quartz, Al_2O_3 and ZnO in the order ZnO > quartz > alumina > no particles.

The higher yield of H_2O_2 by sonolysis in presence of particles is explained by Keck etal[26] on the assumption that the bubble size and collapse time are not influenced by the nature and concentrations of the particles used. But the shape of the bubbles may have changed from spherical to asymmetric. The larger surface of these bubbles enable more radicals to escape into the bulk forming more H_2O_2 or react with more organic molecules in the bulk.

Effect of Phenol on H_2O_2: Formation of H_2O_2 is reported in the case of sonocatalytic and photocatalytic degradation of phenol in presence of ZnO, TiO_2 and ZnO-TiO_2 catalysts[23]. In the case of US irradiation, H_2O_2 is produced even in the absence of phenol indicating the formation of free radicals OH and HO_2 in liquid water by US. The concentration of H_2O_2 is less in the presence of phenol probably because some of the ·OH radicals formed may be reacting with phenol before they could recombine to produce H_2O_2. This is confirmed by experiments with added H_2O_2 which show that H_2O_2 enhances the degradation of phenol significantly in the beginning [Table 1].

However this high rate of enhancement is not sustained later on, probably because thermal decomposition of H_2O_2 to water and oxygen rather than to reactive radical species may be occurring in presence of US[19]. The decomposition and consequent decrease in the concentration of H_2O_2 is more evident in the initial stages in the case of TiO_2[27]. The maximum concentration of H_2O_2 reached is different for different catalysts under otherwise identical conditions, indicating that it is dependent on the nature of the catalyst. It also implies that the role of the semiconductor oxide is not limited to just particle effect. In the beginning, added H_2O_2 decomposes faster producing maximum OH radicals which can degrade phenol. However, the decomposition of H_2O_2 to water and oxygen also occurs in parallel which restricts the continued availability of the oxidizing species for phenol degradation. Further, even in those experiments without externally added H_2O_2, the H_2O_2 formed insitu will be accelerating the reaction rate. Hence the effect of initially added H_2O_2 is not that prominent in the later stages of the reaction.

The effect of concentration of phenol on the rate of degradation has been investigated earlier[23]. The degradation increases with increase in the concentration of phenol upto 40 mg/L beyond which it levels off or decreases slightly, due to saturation of the catalyst surface. In the case of oscillation of H_2O_2 also the effect of concentration is fairly similar. At the optimum concentration for phenol degradation (30-40 mg/L) (figure 5), the maxima in H_2O_2 concentration in the oscillation curve also are the highest indicating a direct correlation between the rate of phenol degradation and the oscillation.

Effect of pH: The pH of the reaction medium is known to have strong influence on US or UV-induced degradation of organic pollutants. In photolysis, the possibility of bond breakage and the site might be different at different pH due to difference in the distribution of molecular charges. In sonocatalytic reaction, pH can alter the distribution of the pollutants in the bulk region, on the surface and at the site of the cavity collapse. The surface charge of semiconductors and the interfacial electron transfer and the photoredox processes occurring in their presence are also affected by pH. Previous studies[3] have shown that the degradation is more efficient in the acidic region than in the alkaline region and in the case of ZnO, maximum degradation is observed in the acidic pH range of 4-6, which peaks at pH 5.5. In the case of TiO_2 also similar trend follows with the maximum at pH 6. The effect of pH on the fate of H_2O_2, especially the oscillation in its concentration resulting from simultaneous formation and decomposition has not been investigated so far. Fig 6 shows the concentration of H_2O_2 in the system at different times during the sonocatalytic degradation of phenol on ZnO at different pH.

Research Journal of Recent Sciences ISSN 2277-2502
Vol. **2(ISC-2012),** 136-149 **(2013)** *Res.J.Recent.Sci.*

Table-1
Effect of added H_2O_2 on the sonocatalytic degradation of phenol in presence of ZnO and TiO_2

Reaction Condition	% Degradation of phenol without added H_2O_2			% Degradation of phenol with added H_2O_2			% enhancement by added H_2O_2		
	30 min	60 min	90 min	30 min	60 min	90 min	30 min	60 min	90 min
US (ZnO)	1.1	6.0	9.5	3.0	7.1	11.2	172.7	18.3	17.9
US (TiO_2)	0.8	3.7	5.2	1.8	4.7	5.8	125.0	27.0	11.5

[Catalyst]: 0.1g/L pH: 5.5 Reaction Volume: 50 ml [Phenol]: 40 mg/L

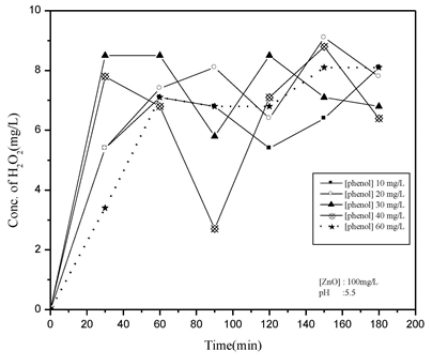

Fig 5: Effect of concentration of phenol on the oscillation in the concentration of H_2O_2 formed during the sonocatalytic degradation of phenol

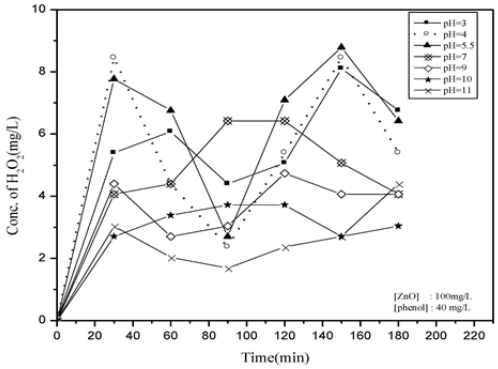

Fig 6: Effect of pH on the oscillation in the concentration of H_2O_2 during the sonocatalytic degradation of phenol

Research Journal of Recent Sciences ISSN 2277-2502
Vol. **2(ISC-2012),** 136-149 **(2013)** *Res.J.Recent.Sci.*

The oscillation as well as the maxima in the concentration of H_2O_2 is more pronounced in the acidic region. This is consistent with the observations on the sonocatalytic degradation of phenol on ZnO in which maximum degradation is observed at in the range of pH 5.5 to 6. The relatively lower maxima and minima at pH 3 are probably because of the corrosion of ZnO which reduces the effective surface sites for the formation of OH radicals and subsequent interactions. In order to decipher the effect of phenol on the oscillation, the sonocatalytic decomposition of H_2O_2 on ZnO was investigated (in the absence of phenol) under identical conditions (Figure 7)

In this case also the concurrent formation and decomposition of H_2O_2 is seen at all pH. Comparison of the results in the presence as well as the absence of phenol shows that the oscillation is more significant in presence of phenol. This illustrates the importance of interaction between the free radicals generated and phenol. This is further verified by adding phenol in between to the sonocatalytic system containing only H_2O_2 (see Figure 8)

At pH5.5 where the adsorption and degradation of phenol is maximum, the H_2O_2 formation is accelerated by phenol addition. At pH 3 and 11 where the degradation of phenol is relatively less, addition of phenol in between does not influence the oscillation as much as at pH 5.5. This reiterates the influence of phenol on the phenomenon of oscillation. Addition of H_2O_2 into the phenol-ZnO sonocatalytic system in between the reaction does not alter the course of oscillation significantly at pH 3, 5.5 or 11. This indicates that there is a critical range of H_2O_2 concentration in which the oscillation is quite facile. Beyond this, any addition of H_2O_2 will make the system over-saturated and it is difficult to distinguish the relatively smaller increase or decrease in the concentration of insitu formed H_2O_2. Addition of extra amounts of ZnO in between to an oscillating system containing phenol enhances the maxima in the oscillation curve. This suggests that the formation of OH radicals is accelerated, which in turn can result in enhanced degradation of phenol and production of more H_2O_2. Thereafter the oscillation continues with a higher maxima and minima (figure 9).

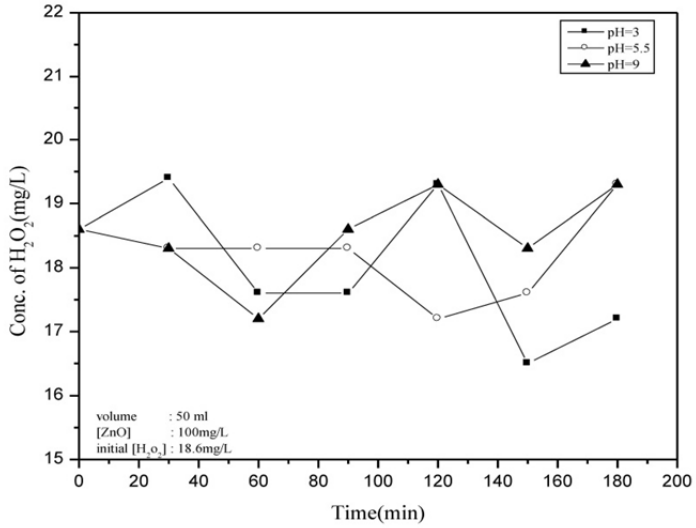

Fig 7: Effect of pH on the fate of added H_2O_2 during sonication in presence of ZnO

Research Journal of Recent Sciences ISSN 2277-2502
Vol. **2(ISC-2012),** 136-149 **(2013)** *Res.J.Recent.Sci.*

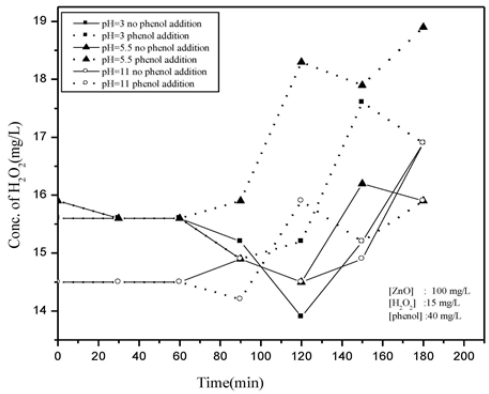

Fig 8: Effect of in between addition of phenol (after 60 min) at various pH on the oscillation in the concentration of H_2O_2

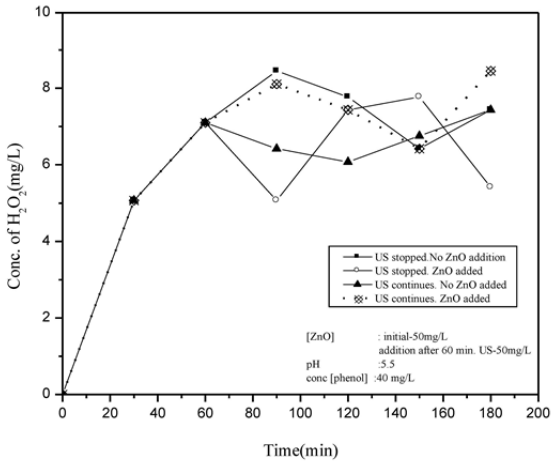

Fig 9: Effect of in between addition of ZnO (after 60 min) on the oscillation in the concentration of H_2O_2

Research Journal of Recent Sciences ISSN 2277-2502
Vol. **2(ISC-2012),** 136-149 **(2013)** *Res.J.Recent.Sci.*

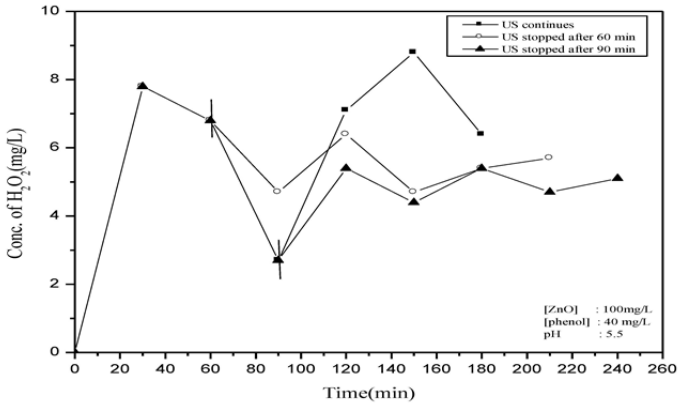

Fig 10: Memory effect of ZnO on the oscillation in the concentration of H_2O_2

Figure 10

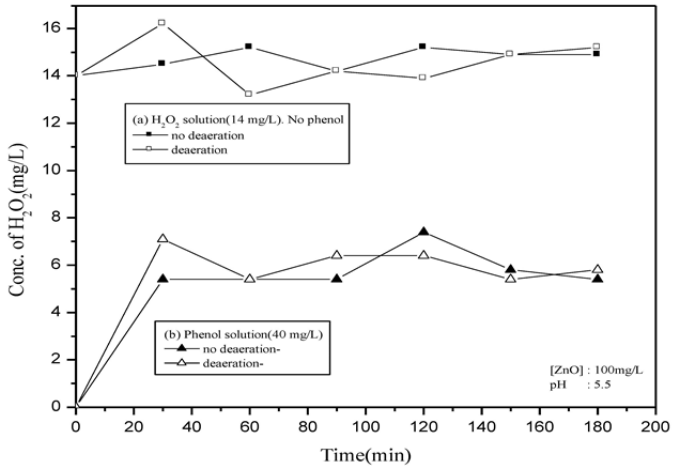

Fig 11: Effect of deaeration on the oscillation in the concentration of H_2O_2

Research Journal of Recent Sciences ISSN 2277-2502
Vol. 2(ISC-2012), 136-149 (2013) Res.J.Recent.Sci.

It has been reported that trapped electrons and holes on the surface of TiO_2 have an unusually long life time extending to hours after the irradiation source is put off [28]. Such long lived electrons and holes can react with H_2O_2 resulting in minor change in its concentration even after the US is off. However, the results are not exactly reproducible and the memory effect does not seem to be significant enough to merit any detailed investigation at this stage. Deaeration by bubbling the system with nitrogen does not affect the oscillation significantly (see figure 11).

Sono and photocatalytic reactions are known to require the presence of efficient electron acceptors so that the recombination of the electrons and holes at the surface can be prevented. Fast recombination between electrons and holes inhibits the interfacial charge transfer and the reactions that follow. Dioxygen molecules are efficient electron acceptors and hence sono or photocatalytic reactions do not occur in the absence of oxygen[29]. The observation that the oscillation in the concentration of H_2O_2 is not affected by deaeration shows that in the absence of O_2, H_2O_2 will serve as an electron acceptor as follows: $H_2O_{2\,(ad)} + e^- \rightarrow OH_{(ad)} + HO^-_{(ad)}$ (6)

The minimum in the oscillation curve is lower in the case of deaerated system which indicates that the H_2O_2 decomposition is proceeding even in the absence of oxygen. Hence the recombination of electrons and holes is not taking place. That means H_2O_2 behaves uniquely by playing the role of electron and hole scavenger in the same system as in reactions 6 and 7. $H_2O_{2\,(ad)} + .OH/h+ \rightarrow HO_{2(ad)} + H_2O/H^+$ (7)

Such behavior by H_2O_2 has been proven in the case of photocatalysis by using Cavity Ring Down Spectroscopy (CRDS)[30].

The electron or hole transfer to H_2O_2 generates $HO_2^{\cdot}$ or $^{\cdot}OH$ as above which may further react on the surface or get desorbed into the bulk. Such desorption of OH radicals from the TiO_2 surface has been confirmed by single molecule imaging using Fluorescence Microscopy[31] as well as Laser Induced Fluorescence Spectroscopy[32]. The desorption of $HO_2^{\cdot}$ (formed by the decomposition of H_2O_2) from the surface was confirmed by CRDS[33]. Once the concentration of H_2O_2 has fallen below a critical point, O_2 can compete effectively as an electron acceptor and the cycle of oscillation continues.

The behavior of phenol is different at different pH. This can influence the fate of H_2O_2 also at respective pH. In weakly acidic solution, most of the phenol molecules remain un-dissociated. Hence maximum number of phenol molecules can be adsorbed onto the surface resulting in increased degradation and correspondingly more H_2O_2. Hence the amount of H_2O_2 at the maximum of the curve is more. In the alkaline medium, the surface of TiO_2 is negatively charged and the phenolate intermediate may be repelled away from the surface[34]. Further, sonication effects also favor higher degradation in the acidic pH. When the pH exceeds 10 (pK_a value of phenol at 25^{0}C), ionic species of phenol will be predominant. When the pH is less than the pK_a, molecular species will dominate. Under sonication, the phenolate ions are concentrated in the gas-water interface of the bubbles where the hydrophobicity is strong and cannot vaporize into the cavitation bubbles[35]. They can react only outside of the bubble film with the OH radicals cleaved from water. However in the molecular state, phenol enters the gas-water interface of bubbles and even vaporizes into cavitation bubbles. They can react both inside by thermal cleavage and outside with OH radicals. This results in higher degradation of phenol as well as enhanced formation and decomposition of H_2O_2. Hence the concentration of H_2O_2 is more at the maxima and minima under acidic conditions.

The pH of the reaction medium has significant effect on the surface properties of semiconductor oxide particles, including the surface charge, size of the aggregation and the band edge position[23]. Hence pH can affect the adsorption – desorption characteristics of the surface of the catalyst. However, in the case of sonocatalysis, adsorption is not the only factor leading to the degradation for reasons explained earlier.

The complex behavior of H_2O_2 is further aggravated by the different mechanisms of sonodegradation of phenol at different pH. Sonochemical degradation of phenol proceeds through catechol (CC), hydroquinone (HQ) and p-benzoquinone (BQ) intermediates at pH 3, CC and HQ at pH 5.7and no detectable intermediate at pH 12. Further the sonication of HQ produces BQ while the sonication of BQ produces HQ and in both cases hydroxyl-p-benzoquinone is formed in traces as another intermediate[36]. In this complex system consisting of too many intermediates, the exact influence of pH on the oscillatory behavior cannot be deciphered precisely.

Our results show that H_2O_2 decomposition is negligible in the dark or by photolysis or sonolysis in the absence of a catalyst. This is in contrast with the findings of Augugliaro etal[37] as well as Jenny and Pichat[38]. Jenny and Pichat reported that the heterogeneous H_2O_2 decomposition is only twice faster than homogeneous decomposition while Augugliaro etal did not find any significant difference in the decomposition with or without suspended catalyst. However Ilisz etal[39] observed that efficient degradation of H_2O_2 takes place only in presence of catalysts in photochemical systems. Their observation that the initial rate of decomposition of H_2O_2 decreases with decreasing concentration is reconfirmed by the current findings that in the oscillation curve of H_2O_2 the decomposition of H_2O_2 begins only when a critical maximum concentration is reached and the formation process takes over when a critical lower concentration is reached.

The overall mechanism depicting the formation of ROS and degradation of phenol is schematically presented in scheme 1. Possible steps involved in the concurrent formation and decomposition of H_2O_2 are given in reactions 8 to 19.

Research Journal of Recent Sciences ISSN 2277-2502
Vol. 2(ISC-2012), 136-149 (2013) Res.J.Recent.Sci.

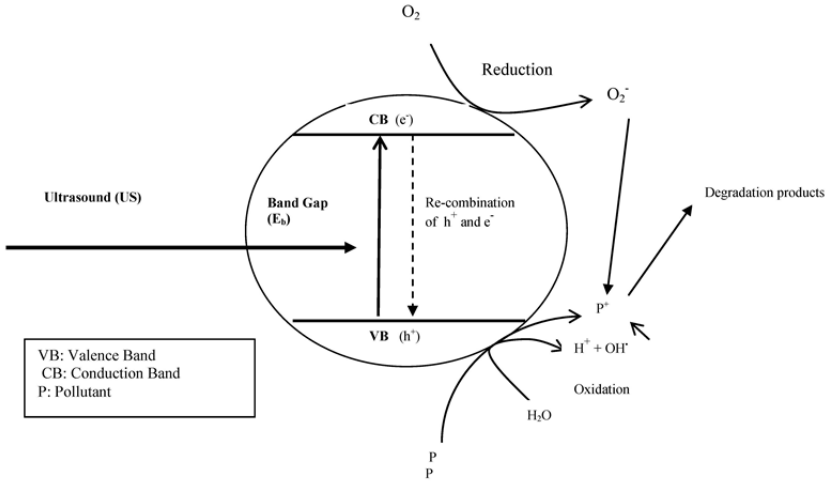

Scheme-1 Sono catalytic activation of semiconductor oxides and the formation of ROS

The formation of H_2O_2 from various ROS takes place as follows:

$OH + {}^{\cdot}OH \rightarrow H_2O_2$ (8)

$O_2 + 2e_{cb}^- + 2H^+ \rightarrow H_2O_2$ (9)

$2H_2O + 2h_{vb}^+ \rightarrow H_2O_2 + 2H^+$ (10)

$O_2^{\cdot-} + H^+ \rightarrow HO_2^{\cdot}$ (11)

$HO_2^{\cdot} + HO_2^{\cdot} \rightarrow H_2O_2$ (12)

$O_2^{\cdot-} + HO_2^{\cdot} \rightarrow O_2 + HO_2^{\cdot-}$ (13)

$HO_2^{\cdot-} + H^+ \rightarrow H_2O_2$ (14)

The concurrent decomposition of H_2O_2 takes place as follows:

$H_2O_2 + hv\ (\lambda<380\ nm) \rightarrow 2\ {}^{\cdot}OH$ (15)

$2\ h_{vb}^+ + H_2O_2 \rightarrow O_2 + 2\ H^+$ (16)

$2\ e_{cb}^- + 2\ H^+ + H_2O_2 \rightarrow 2\ H_2O$ (17)

$H_2O_2 + {}^{\cdot}OH \rightarrow H_2O + HO_2^{\cdot}$ (18)

$H_2O_2 + HO_2^{\cdot} \rightarrow H_2O + {}^{\cdot}OH + O_2$ (19)

Being a complex free radical system, other interactions leading to the formation and decomposition of H_2O_2 are also possible.

Conclusion

Hydrogen peroxide formed during the sonocatalytic degradation of phenol in water in presence of semiconductor oxides such as ZnO and TiO_2 undergoes concurrent formation and decomposition resulting in oscillation in its concentration. Various reaction parameters such as catalyst loading, substrate concentration, particle size, pH, externally added H_2O_2 and presence of air/O_2 influence the phenomenon in general and the maxima and minima in the oscillation curve in particular. H_2O_2 plays a unique role in the process as acceptor of both electrons and holes. The oscillation phenomenon continues for some more time even after the sono source is switched off, indicating the presence of memory effect in the semiconductor. A reaction mechanism based on the observations is proposed and discussed.

Acknowledgement

The authors wish to acknowledge the financial support to JKP and SJ from the University Grants Commission, India by way of Junior Research Fellowships.

References

1. Ying-Shih M., Chi-Fanga S. and Jih-Gaw L., Degradation of carbofuran in aqueous solution by ultrasound and Fenton processes: Effect of system parameters and kinetic study, *J Hazardous Mater.*, **178,** 320-325 **(2010)**

2. Entewrzari M.H., Masoud M. and Ali S.Y., A combination of ultrasound and biocatalyst: Removal of 2-chlorophenol from aqueous solution, *Ultrason. Sonochem.*, **13,** 37-41**(2006)**

Research Journal of Recent Sciences ISSN 2277-2502
Vol. **2(ISC-2012),** 136-149 **(2013)** *Res.J.Recent.Sci.*

3. Devipriya S., Yesodharan S, Photocatalytic degradation of pesticide pollutants in water, *Solar Energy Mater and Solar Cells,* **86**, 309-348 **(2005)**

4. Chong M.N., Jin B., Chow C.W.K. and Saint C., New developments in photocatalytic water treatment technology: A review, *Water Res.,* **44,** 2997-3027 **(2010)**

5. Anju S.G., Suguna Yesodharan and Yesodharan E.P. Zinc oxide mediated sonophotocatalytic degradation of phenol in water, Chem. Eng. J. **189-190**, 84-93 **(2012)**

6. Joseph C.G, Puma G.L, Bono A and Krishniah D, Sonophotocatalysis in advanced oxidation process: A short review, *Ultrason., Sonochem.* **16**, 583-589 **(2009)**

7. Moon J, Yun C.Y, Chung K.W, Kang M.S and Yi J, Photocatalytic activation of TiO_2 under visible light using Acid red, *Catal. Today*, **87**, 77-86 **(2003)**

8. Pei D, and Luan J, Development of visible light-responsive sensitized photocatalyst, *Int. J. of Photoenergy*, **2012**, article id 262831, 13 pages **(2012)**

9. Wu C.G, Chao C.C. and Kuo F.T., Enhancement of the photocatalytic performance of TiO_2 catalysts via transition metal modification, *Catal. Today,* **97**, 103-112 **(2004)**

10. Pellegrin Y., Le Pleux L., Blart E., Renaud A., Chavilion B., Szuwarski N, Boujitita M, Cario L, Jobic S, Jacquemin D and Odobel F, Ruthenium polypyridine complexes as sensitisers in NiO based p-type dye-sensitized solar cells: Effects of the anchoring groups, *J Photochem. Photobiol. A-Chem.*, **219**, 235-242 **(2011)**

11. Youngblood J, Lee S.H.A, Maeda K and Mallouk T.E., Visible light water splitting using dye sensitized oxide semiconductors, *Acc. Chem. Res*., **42**, 1966-1973 **(2009)**

12. Lee D.K., Kim S.C., Cho I.C., Kim S.J. and Kim S.W., Photocatalytic oxidation of microcystine LR in a fluidized bed reactor having TiO_2 coated activated carbon, *Purification Technology,* **34,** 59-66 **(2004)**

13. Li Y., Sun S., Ma M., Ouyang Y. and Yan W., Kinetic study and model of the photocatalytic degradation of Rhodamine B by a TiO_2-coated activated carbon catalyst: Effects of initial RhB content, light intensity and TiO_2 content in the catalyst, *Chemical Eng. J.,* **142**, 147-155 **(2008)**

14. Sakthivel S, Shankar M.V, Palanichamy M, Arabindoo A, Bahnemann D.M and Murugesan B.V, Enhancement of photocatalytic activity by metal deposition: characterization and photonic efficiency of Pt, Au, and Pd deposited on TiO_2 catalyst, *Wat. Res.,* **38**, 3001-3008 **(2004)**

15. Li F.B. and Li X.Z., Enhancement of photodegradation efficiency using Pt/TiO_2 catalyst, *Chemosphere,* **48** 1103-1111 **(2002)**

16. Kotronatou A., Mills G., Hoffmann M.R., Ultrasonic irradiation of p-nitrophenol in aqueous solution, Phys. Chem., **95**, 3630-3638 **(1991)**

17. Hartmann J., Bartels P., Mau U., Witter M., Tumpling W.V., Hofmann J., and Nietzschmann E., Degradation of the drug diclofenac in water by sonolysis in presence of catalysts, *Chemosphere,* **70**, 453-461 **(2008)**

18. Gogate P.R., Treatment of wastewater streams containing phenolic compounds using hybrid techniques based on cavitation: a review of the current status and the way forward, *Ultrason. Sonochem.,* **15**, 1-15 **(2008)**

19. Torres-Palma R.A., Nieto J.I., Combet E., Petrier C. and Pulgarin C., An innovative ultrasaound, Fe^{2+} and TiO_2 photo assisted process for bisphenol a mineralization, *Water Res.* **44**, 2245-2252 **(2010)**

20. Davydov L., Reddy E.P., France P. and Smirniotis P., Sonophotocatalytic destruction of organic contaminants in aqueous systems on TiO_2 powders, *Appl. Catal.B: Environmental* **32**, 95-105 **(2001)**

21. Chen Y.C. and Smirniotis P., Enhancement of photocatalytic degradation of phenol and chlorophenols by ultrasound, *Ind. Eng. Chem. Res.,* **41**,5958- 5965 **(2002)**

22. Kritikos D.E., Xekoukoulotakis N.P., Psillakis E., Mantzavinos D., Photocatalytic degradation of reactive black 5 in aqueous solutionds: Effect of operating conditions and coupling with ultrasound irradiation, *Water Res.* **41**, 2236-2246 **(2007)**

23. Anju S.G., Jyothi K.P., Sindhu Joseph, Suguna Yesodharan and Yesodharan E.P., Ultrasound assisted semiconductor mediated catalytic degradation of organic pollutants in water: Comarative efficacy of ZnO, TiO_2 and ZnO-TiO_2, *Res. J. Recent Sci.* **1**, 191-201 **(2012)**

24. Nepiras E.A., Acoustic cavitation: An introduction, *Ultrasonics,* **22**, 25-40 **(1984)**

25. Suslick K.S., Crum L.A., in Crocker M.J (Ed.), *Encyclopedia of Acoustics,* **1,** *Wiley Inter5science, New York,* 271-282 **(1997)**

26. Keck A., Gilbert E. and Koster R., Influence of particles on sonochemical reactions in aqueous solutions, *Ultrasonics* **40**, 661-665 **(2002)**

27. Pulgarin C., Kiwi J., Overview on photocatalytic and electro catalytic pretreatment of industrial non-biodegradable pollutants and pesticides, *Chimia,* **50**, 50-55 **(1996)**

28. Szczepankiewicz S., Moss J.A. and Hoffmann M.R., Slow surface charge trapping on irradiated TiO_2, *J Phys Chem. B*., **106**, 2922-2927 **(2002)**

Research Journal of Recent Sciences ISSN 2277-2502
Vol. **2(ISC-2012),** 136-149 **(2013)** *Res.J.Recent.Sci.*

29. Gerischer H and Heller A, The role of oxygen in photooxidation of organic molecules on semiconductor particles, *J Phys Chem,* **95(13),** 5261-5267 **(1991)**

30. Yi J., Bahrini C., Schoemaecker C., Fittschen C., Choi W, Photocatalytic decomposition of H_2O_2 on different TiO_2 surfaces along with the concurrent generation of HO_2 radicals monitored using cavity ring down spectroscopy, *J Phys Chem. C,* **116**, 10090-10097 **(2012)**

31. Tachikawa T. and Majima T., Single molecule fluorescence imaging of TiO_2 photocatalytic reactions, *Langmuir*, **25**, 7791-7802 **(2009)**

32. Murakami Y., Ohta L., Hirakawa T. and Nosaka Y., Direct detection of OH radicals in the gas phase diffused from the Pt/TiO_2 and WO_3/TiO_2 photocatalysts, *Chem. Phys. Lett*., **493**, 292-295 **(2010)**

33. Bahrini C., Parker A., schoemaecker C. and Fittschen C., Direct detection of HO_2 radicals in the vicinity of TiO_2 photocatalytic surfaces using CW-CRDS, *Appl. Catal. B, Environ.,* **99**, 413-419 **(2010)**

34. Pardeshi S.K. and Patil A.B., A simple route for photocatalytic degradation of phenol in aqueous zinc ioxide suspension using solar energy, *Solar Energy,* **82**, 700-705 **(2008)**

35. Wu C., Liu X., Wei D., Fan J. and Wang L., Photosonochemical degradation of phenol in water, *Wat. Res*., **35** 3927-3933 **(2001)**

36. Serpone N., Terzian R. and Colarusso P., Sonochemical oxidation of phenol and three of its intermediate products in aqueous media: Catechol, hydroquinone and benzoquinone. Kinetic and mechanistic aspects, *Res Chem Intermed.* **18**, 183-202 **(1992)**

37. Augugliaro V., Davi E., Palmisano L., Schiavello M. and Sclafani A., Influence of hydrogen peroxide on the kinetics of phenol photodegradation in aqueous titanium dioxide dispersions, *Appl. Catal*., **65**, 101-109 **(1990)**

38. Jenny B. and Pichat P., Determination of the actual photocatalytic rate of hydrogen peroxide decomposition over suspended titania. Fitting to the Langmuir-Hinshelwood form, *Langmuir,* **7,** 947-949 **(1991)**

39. Ilisz I., Foglein K. and Dombi A., The photochemical behavior of H_2O_2 in near UV-irradiated aqueous TiO_2 suspensions, *J Mol Catal. A:Chem,* **135**, 55-61 **(1998)**

Research Journal of Recent Sciences ISSN 2277-2502
Vol. 2(ISC-2012), 82-89 (2013) Res. J. Recent. Sci.

Influence of Reaction Intermediates on the Oscillation in the Concentration of insitu formed Hydrogen peroxide during the Photocatalytic Degradation of Phenol Pollutant in Water on Semiconductor Oxides

Sindhu Joseph, Jyothi K.P., Suja P. Devipriya, Suguna Yesodharan and Yesodharan E.P.
School of Environmental Studies, Cochin University of Science and Technology, Kochi 682022, INDIA

Available online at: www.isca.in
Received 31th July 2012, revised 29th December 2012, accepted 22nd January 2013

Abstract

Phenols are common pollutants in many petrochemical industry wastewaters. Due to the stability of the aromatic ring their destruction requires extreme conditions. Photocatalysis using semiconductor oxides as catalysts is found to be an effective Advanced Oxidation Process (AOP) for the mineralisation of phenol. The degradation proceeds through the formation of various intermediates which eventually get mineralized to yield CO_2 and H_2O. The intermediates identified are hydroquinone, catechol, and benzoquinone which are formed by the interaction of photogenerated OH radicals with phenol. These intermediates do not accumulate beyond a particular concentration even though the phenol degradation continues unabated. The insitu formed H_2O_2 concentration increases and decreases periodically in a wave like fashion indicating concurrent formation and decomposition. Externally added H_2O_2 enhances the degradation rate of phenol initially due to the generation of more reactive OH radicals by inhibiting the recombination of photogenerated electrons and holes as well as by its own self decomposition. Externally added catechol and hydroquinone inhibit the degradation of phenol initially. However their influence on the fate of H_2O_2 is not quite significant. The study also shows that the formation/decomposition of H_2O_2 is concentration dependent and after the initial build up, the formation or decomposition takes precedence depending on the concentration and composition of the reaction system. Possible reasons for the observed phenomenon are analysed and a mechanism is proposed.

Keywords: Photocatalysis, zinc oxide, titanium dioxide, hydrogen peroxide, phenol, oscillation.

Introduction

Heterogeneous photocatalysis is an Advanced Oxidation Process (AOP), widely investigated for the degradation of organic pollutants in water and air[1-6]. The basic mechanism of photocatalysis involving hydroxyl radicals has also been well established[6]. Some of the major industrial pollutants in water degraded by photocatalysis include dyes, pesticides, petrochemicals etc. Semiconductor oxides such as TiO_2 and ZnO and their modifications by doping, immobilizing, metal deposition etc. are the most widely tested photocatalysts[7-9]. The process involves illumination of the catalyst particles either dispersed as slurry in the contaminated aqueous solution or in immobilized form. Combination of sonolysis and photocatalysis, referred to as sonophotocatalysis is emerging as another AOP in water purification[10]. It is also reported that the sonophotocatalytic degradation of phenol pollutant in water is more than the sum of individual sono and photocatalysed degradation, implying synergy in the combined process[11].

Phenols are common pollutants in many petrochemical industry wastewaters. Photocatalytic degradation of phenols in water has been investigated extensively[2,12-14]. The degradation mechanism involves complexation of OH radicals with the pi (π) system of the aromatic ring forming a pi complex in which the OH groups do not have a specific position in the molecule. The second step corresponds to the formation of a sigma complex between the carbon atom of the aromatic ring and the radical OH. The formation of the sigma complex is usually the rate determining step of the reaction[2,13].

One of the reaction products in all these processes is H_2O_2. However, the concentration of H_2O_2 does not increase beyond a limit, even though the degradation of the pollutant proceeds unhindered. It has been reported from our laboratories that the concentration of insitu formed H_2O_2 undergoes an oscillatory type of behavior resulting in periodic increase and decrease, possibly due to concurrent formation and decomposition[15,16]. Externally added H_2O_2 enhances the degradation rate significantly by inhibiting the rate of recombination of photogenerated electrons and holes, thereby increasing formation of reactive oxygen species and the degradation rate of pollutants[17,18]. However, the attention of researchers was always focused on achieving optimum mineralisation of the pollutant and consequently the fate of concurrently formed H_2O_2 has received much less attention. In the case of phenol, the eventual mineralisation proceeds through a number of intermediates, of which some are fairly stable. These intermediates can influence the overall photocatalytic degradation rate of phenol including the fate of insitu formed H_2O_2. In this paper, we are reporting our findings on the influence of reaction intermediates on the photocatalytic degradation of phenol and the oscillatory behavior of insitu formed and externally added H_2O_2.

Research Journal of Recent Sciences ISSN 2277-2502
Vol. 2(ISC-2012), 82-89 (2013) Res. J. Recent. Sci

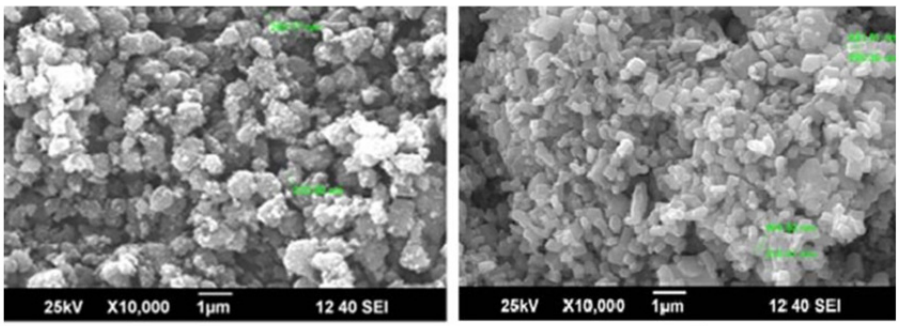

a b

Figure-1
Typical SEM image of (a) TiO_2 and (b) ZnO

Material and Methods

ZnO and TiO_2 used in the study were supplied by Merck India Limited. In both cases the purity was over 99%. The surface areas of TiO_2 and ZnO, as determined by the BET method were 15 and 12 m^2/g respectively. The average particle size of both ZnO and TiO_2 was approx.10 µm, as determined by Scanning Electron Microscopy (SEM). Typical SEM of ZnO and TiO_2 are shown in figure 1.

Phenol AnalaR Grade (99% purity) from Qualigen (India) was used as such without further purification. All other chemicals were of AnalaR Grade or equivalent. The catalytic reactions were performed as reported earlier[19]. The concentration of phenol left behind was analyzed periodically by Spectrophotometry at 500 nm. The intermediates catechol (CC), hydroquinone (HQ) and benzoquinone (BQ) were monitored by HPLC using UV detector. H_2O_2 was determined by iodometry[16]. Mineralization was identified by the evolution of CO_2.

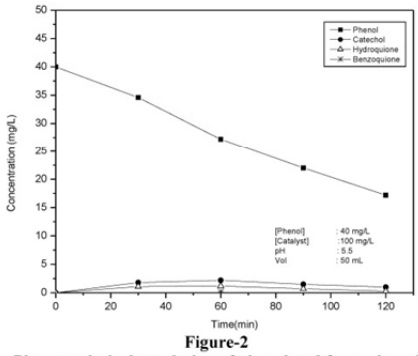

Figure-2
Photocatalytic degradation of phenol and formation of intermediates on ZnO

Results and Discussion

Investigations on the photocatalytic degradation of phenol using ZnO and TiO_2 catalysts under identical conditions showed that no significant degradation took place in the absence of UV light or the catalyst suggesting that both catalyst and light are essential to effect degradation. ZnO is slightly more efficient as a photocatalyst compared to TiO_2. The ultimate reaction products are CO_2 and H_2O formed by the mineralisation of phenol. H_2O_2 is an end- product as well as intermediate which participate in further reactions with phenol and reactive oxygen species resulting in the formation of H_2O and O_2. The reaction intermediates detected are CC, HQ and traces of BQ. The concentration of the intermediates is comparatively small probably because they may be getting transformed into other products and eventually mineralized at the same rate or faster compared to parent phenol (figure 2).

While there is a clear increase and later stabilization in the degradation of phenol, the concentration of intermediates does not increase correspondingly. The intermediates detected are the same in the case of both ZnO and TiO_2 even though the quantities are slightly different. BQ is not detected in the case of TiO_2 while a very small quantity is detected in one instance in the case of ZnO. Intermediates such as pyrogallol, 2-hydroxy benzoquinone and 1,2,4 benzene triol reported by other authors[2] are not detected in our experiments. The H_2O_2 formed insitu increases initially. However, after reaching a maximum its concentration decreases and reaches a minimum where it starts rising again. This periodic increase and decrease in the concentration of H_2O_2 in a wavelike fashion indicates concurrent formation and decomposition (figure-3).

Research Journal of Recent Sciences ISSN 2277-2502
Vol. **2(ISC-2012),** 82-89 **(2013)** *Res. J. Recent. Sci*

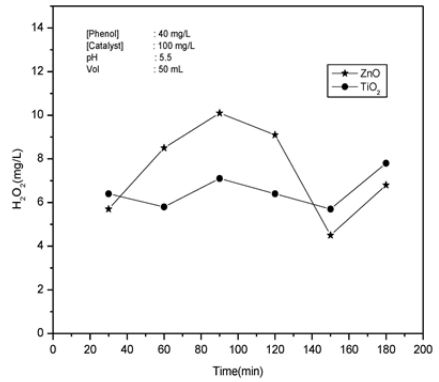

Figure-3
Formation and decomposition of H_2O_2 during the photocatalytic degradation of Phenol

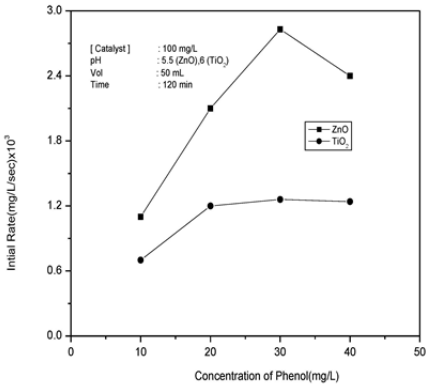

Figure-4
Effect of concentration of Phenol on its photocatalytic degradation on ZnO and TiO_2

One of the most important operating parameters in the photocatalytic degradation of phenol in presence of semiconductors is the pH of the medium because it affects the surface charge or the isoelectric point of the catalyst particles, size of the catalyst aggregates and the positions of the valence and conduction bands. In the case of ZnO and TiO_2, the effect of pH is often correlated with their respective Point of Zero Charge (PZC). When the pH of the medium is less than the PZC of the catalyst the surface of the catalyst becomes positively charged and the neutral or negatively charged contaminant ions can get adsorbed onto the activated catalyst surface leading to enhanced degradation. In the case o both ZnO and TiO_2 acidic pH favours such a situation. The natural pH of water containing small quantities of phenol contaminant is in the acidic range, approx. 5.5 and 6 in ZnO and TiO_2 suspension respectively. Hence all studies in presence of ZnO and TiO_2 were conducted in the natural pH of phenol solution which also happens to be the optimum pH for degradation of phenol[11].

Similarly, the optimum catalyst loading of ZnO and TiO_2 for phenol degradation has been determined experimentally and the values are100 and 250 mg/L respectively. Beyond the optimum loading the light photon absorption coefficient decreases radially. However such a light attenuation over the radial distance does not obey the Beer-Lambert law due to the strong absorption and scattering of light photons by the catalyst particles[20]. Excess catalyst particles lead to screening of light which reduces the effective surface area of the semiconductor being exposed to illumination leading to decreased photocatalytic efficiency. Investigations on the effect of concentration of phenol on its photocatalytic degradation show that the rate of degradation is optimum at 30 mg/L in presence of both ZnO and TiO_2 (figure 4)

All further investigations in this report were carried out using the optimized parameters as above, unless mentioned otherwise.

The effect of addition of major intermediates catechol and hydroquinone at different concentrations on the rate of phenol degradation in presence of ZnO are shown in figures 5 and 6 respectively.

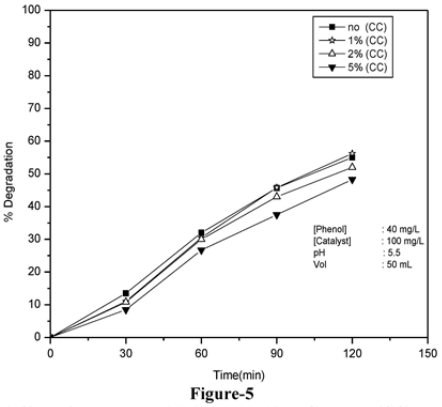

Figure-5
Effect of externally added intermediate Catechol (CC) on the photocatalytic degradation of phenol on ZnO

Research Journal of Recent Sciences ISSN 2277-2502
Vol. **2(ISC-2012),** 82-89 **(2013)** *Res. J. Recent. Sci*

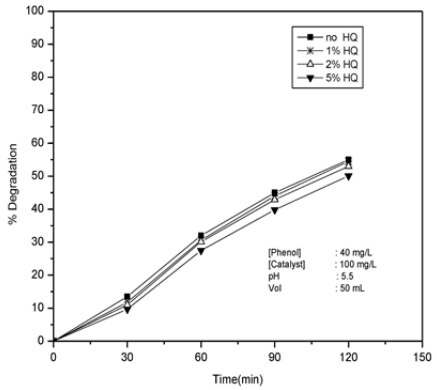

Figure-6
Effect of externally added intermediate Hydroquinone (HQ) on the photocatalytic degradation of phenol on ZnO

The rate of degradation of phenol is retarded slightly, probably because the intermediates are also getting adsorbed on the surface, thereby reducing the surface concentration and consequent activation of phenol molecules. The intermediates are also getting degraded at comparable or even faster rate. Once they are completely removed from the surface, majority of the vacated sites will be occupied by phenol and its degradation proceeds smoothly without any hindrance. The behavior is identical in the case of TiO_2 also. Evaluation of comparative adsorption of phenol, catechol and hydroquinone in equimolar concentrations on ZnO and TiO_2 show that the extent of adsorption is approximately the same. The inhibition of phenol degradation by CC as well as HQ is increasing with increase in their concentration. At higher concentrations the intermediates occupy more surface sites and because of the concentration advantage, at least part of the surface sites vacated by mineralized intermediates will be occupied by fresh molecules of the same. In the absence of externally added intermediates, the concentration of insitu formed intermediates is very small and because they degrade concurrently, the relative concentration of phenol will always be more. Hence the surface will always be preferentially occupied by phenol and influence of the intermediates on the degradation will be negligible.

The effect of the intermediates on the fate of H_2O_2 is plotted in figure 7.

In presence of the added intermediates also the oscillation is sustained. However, the H_2O_2 at the maxima as well as the minima in the oscillation curve is more in presence of the added intermediate. This implies that the rate of formation is enhanced by the intermediate while the rate of decomposition is inhibited. This can be attributed to the relatively faster rate of degradation of catechol or hydroquinone which produces more OH radicals compared to phenol only. This is further verified by investigating the effect of concentration of the intermediates on the oscillation in the concentration of H_2O_2 (figures 8 a,b) in presence of ZnO. The results show that the maxima and minima of H_2O_2 in the oscillation curve are increasing with increase in the concentration of the intermediate.

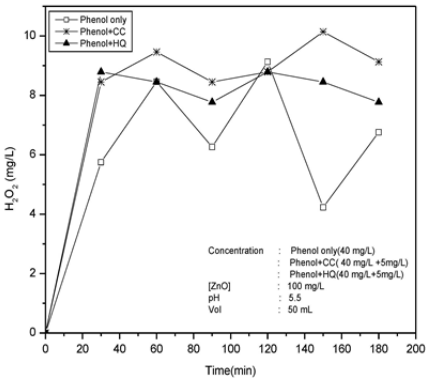

Figure-7
Effect of added intermediate CC and HQ on H_2O_2 formed during the photocatalytic degradation of phenol

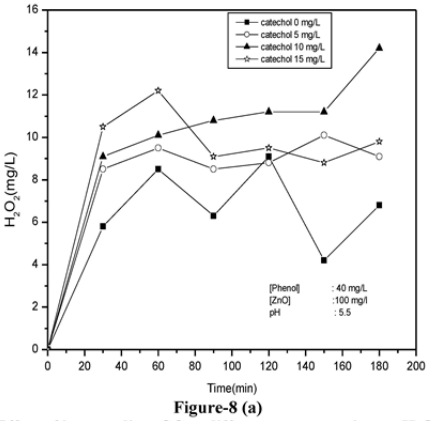

Figure-8 (a)
Effect of intermediate CC at different concentration on H_2O_2 the photocatalytic degradation of phenol in presence of ZnO

Research Journal of Recent Sciences ISSN 2277-2502
Vol. **2(ISC-2012),** 82-89 **(2013)** *Res. J. Recent. Sci*

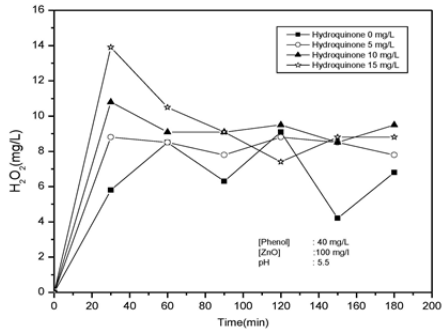

Figure-8 (b)
Effect of added intermediate HQ on H_2O_2 formed during the photocatalytic degradation of phenol in presence of ZnO

The influence of concentration of the intermediate is less pronounced in the case of TiO_2 catalysts (not shown here). The surface composition as well as the composition of the catalyst-bulk interface is more or less the same in presence of the intermediate.

The basic mechanism of the photocatalytic degradation of phenol involves the formation of OH radicals initiated by the activated catalyst surface followed by their interaction with the substrate as well as various intermediates such as catechol, hydroquinone and p-benzoquinone as follows: [2].

Semiconductor + h ν → $h^+ + e^-$ (1)
$h^+ + e^- \rightarrow$ Heat (2)
$h^+ + H_2O \rightarrow H^+ + {}^{\cdot}OH$ (3)
$OH + {}^{\cdot}OH \rightarrow H_2O_2$ (4)
$O_2 + e^- \rightarrow O_2^{\cdot-}$ (5)
$O_2^{\cdot-} + H_2O \rightarrow HO_2^{\cdot} + {}^{\cdot}OH$ (6)
$h^+ + {}^{\cdot}OH \rightarrow {}^{\cdot}OH$ (7)
$HO_2^{\cdot} + HO_2^{\cdot} \rightarrow H_2O_2$ (8)

Various reactive oxygen species formed as above will interact with phenol as shown in scheme 1.

Reactive oxygen species + phenol → Intermediates → H_2O + CO_2 (9)

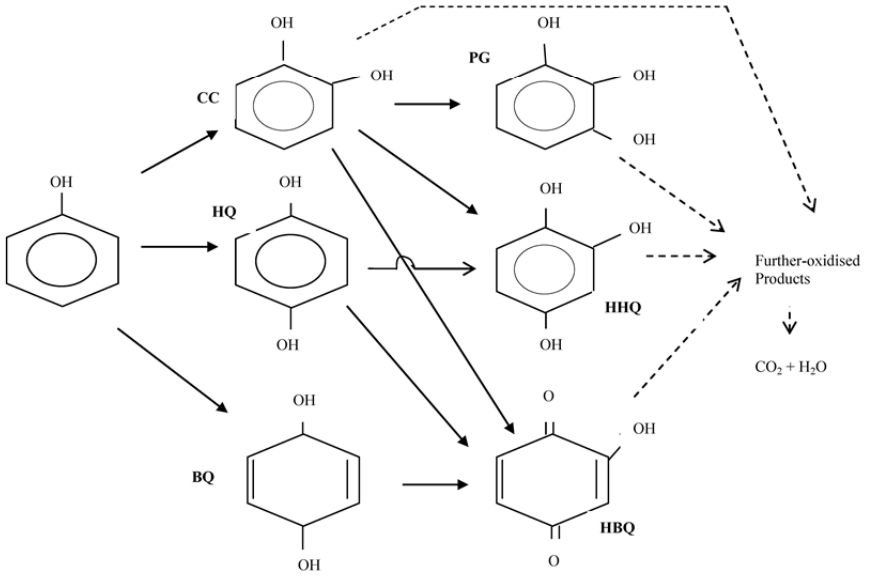

Scheme-1
Mechanism of the photocatalytic mineralisation of phenol on ZnO

Research Journal of Recent Sciences ISSN 2277-2502
Vol. **2(ISC-2012),** 82-89 **(2013)** *Res. J. Recent. Sci*

It is also possible for the photogenerated holes to react with adsorbed phenol to yield dihydroxycyclohexadienyl radicals via phenol radical cation[2,21]. The energy of holes in the valence band of TiO_2 is approx. -7.5eV which is high enough for the holes to react with H_2O and organic compounds. This would happen if phenol is strongly adsorbed onto the surface. Adsorption studies of very dilute solution of phenol in water (< 30 mg/L) on ZnO and TiO_2 shows that phenol does get adsorbed on to the surface under our reaction conditions, though not very significantly. Hence the possibility of scheme 2 cannot be ruled out.

Based on the observations from the direct photosonochemical degradation of phenol in water, Wu etal[13] suggested that reaction of hydroxyl radical with phenol in presence of oxygen leads to the formation of peroxyl radicals, which form hydroquinone and catechol after eliminating superoxide radicals and rearranging the aromatic system. These compounds degrade to carboxylic acids and eventually to CO_2. However, in the present study carboxylic acid intermediate is not detected probably because of its shorter lifetime or a different mechanism of degradation altogether.

Under mild oxidizing conditions provided by H_2O, direct conversion of phenol to CO_2 and H_2O is not probable. But water can take part in the reaction along with the dissolved oxygen present in the medium to yield hydroxylated intermediates and then the final product[22]. The intermediates formed during the degradation depend on the reaction conditions and the reagents used. Velasco etal[23] reported the presence of hydroquinone and benzoquinone during the photocatalytic degradation of phenol in presence of carbon/titania composite. In the presence of Fenton's reagent, more intermediates such as catechol resorcinol, hydroquinone, p-benzoquinone and o-benzoquinone have been detected[24]. When the degradation was carried out with Fe(II)-Fe(III) green rust, only non-aromatic intermediates were detected[25]. Sivalingam etal[14] reported formation of catechol and hydroquinone when the degradation was carried out in presence of Degussa P-25. Pyrogallol also has been detected during the photocatalytic degradation of phenol by base metal-substituted vanadates[25]. In the present study we could detect the presence of only three intermediates; catechol, hydroquinone and traces of benzoquinone which also disappeared eventually. This indicates that the intermediates also get degraded fast and as time progresses, as the phenol concentration decreases, the rate of degradation of the intermediate becomes even faster. The rates of degradation of phenol, catechol and hydroquinone under identical conditions on ZnO and TiO_2 are given in figure 9 which shows that the rates are comparable.

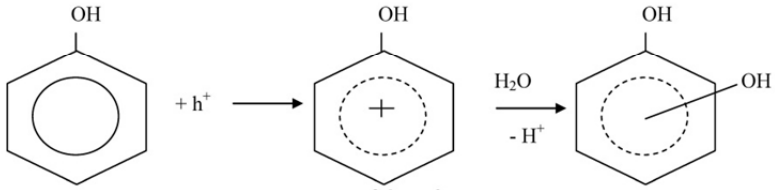

Scheme-2
Reaction of photogenerated hole with H_2O and phenol

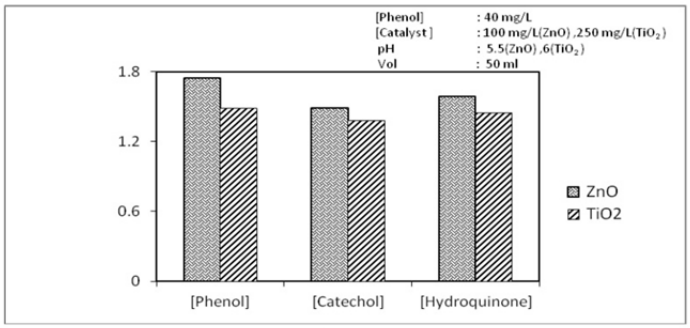

Figure-9
Comparative initial rate of degradation of Phenol, Catechol and Hydroquinone

Research Journal of Recent Sciences ISSN 2277-2502
Vol. **2(ISC-2012),** 82-89 **(2013)** *Res. J. Recent. Sci*

The present study was carried out at the natural pH of the phenol solution-catalyst suspension, ie 5.6-5.7. Serpone etal [26] have reported that the intermediates depend on the pH conditions in the case of ultrasonic removal of phenol. They reported that the principal intermediates at pH 3 are catechol, hydroquinone and p-benzoquinone while only catechol and hydroquinone were detected at pH 5.4-5.7. No intermediates were observed at pH 12. In the current study, the intermediates are the same in case of both ZnO and TiO_2 indicating that in the case of photocatalysis, pH is the prime factor that determines the mechanism of the reaction.

The periodic change in the concentration of H_2O_2 and the oscillatory behavior suggest that its formation and decomposition takes place simultaneously. The decrease in concentration can be either due to its parallel decomposition into water and oxygen and/or its participation in the degradation of phenol[15,27,28]. At the same time the removal of phenol continues. H_2O_2 formed consequent to reactions (1) to (8) decomposes simultaneously as follows:

$H_2O_2 + hv\ (\lambda<380\ nm) \rightarrow 2\ {}^{\cdot}OH$ (10)

$2\ h_{vb}^{+} + H_2O_2 \rightarrow O_2 + 2\ H^{+}$ (11)

$2\ e_{cb}^{-} + 2\ H^{+} + H_2O_2 \rightarrow 2\ H_2O$ (12)

$H_2O_2 + {}^{\cdot}OH \rightarrow H_2O + HO_2^{\cdot}$ (13)

$H_2O_2 + HO_2^{-} \rightarrow H_2O + {}^{\cdot}OH + O_2$ (14)

Being a complex free radical system, other interactions leading to the formation and decomposition of H_2O_2 are also possible.

Since both the formation and decomposition are initiated by free radicals and reactive oxygen species, the surface plays an important role. Phenol and various intermediates formed have similarity in the adsorption and photocatalytic behavior. Hence the intermediates are not expected to influence the oscillatory behavior of H_2O_2 significantly, at least in the concentration range of insitu formation. However, the concentrations of H_2O_2 at the maxima and minima of the curve increase in the presence of the added intermediates. This indicates that the intermediates enhance the formation of H_2O_2 and inhibits its decomposition, though slightly. The formation and decomposition of H_2O_2 proceeds in parallel after build up of a critical initial concentration. Depending on the concentration of the substrate and H_2O_2 at any point of time, either of the process will predominate.

Conclusion

Photocatalytic degradation of phenol proceeds through two major intermediates; catechol and hydroquinone. The intermediates do not influence the rate of degradation significantly as they themselves undergo degradation and eventual mineralisation under the experimental conditions. H_2O_2 formed in the process undergoes simultaneous formation and decomposition resulting in oscillation in its concentration. Depending on the relative concentration of the substrate, stable intermediates and H_2O_2, the formation or decomposition will predominate. The degradation of phenol as well as the formation and decomposition of H_2O_2 is initiated by ·OH radicals generated at the photo-activated semiconductor oxide surface. The degradation ultimately leads to complete mineralization of phenol. The study provides convincing experimental evidence for the concurrent formation and decomposition of H_2O_2 in photocatalytic systems. Further, it demonstrates that semiconductor mediated photocatalysis can be developed into a viable route for the removal of organic water pollutants.

Acknowledgement

The authors gratefully acknowledge the financial support from the University Grants Commission (UGC)/Dept of Science and Technology (DST), Government of India to SJ (UGC JRF), JKP (UGC JRF) and SPD (DST WOS-A).

References

1. Herrmann J.M., Heterogeneous Photocatalysis: fundamentals and applications to the removal of various types of aqueous pollutants, *Catal. Today,* **53**, 115-129 **(1999)**
2. Okamoto K., Yamamoto Y., Tanaka H., Tanaka M. and Itaya A., Heterogeneous photocatalytic degradation of phenol over TiO_2 powder, *Bull Chem Soc. Jpn,* **58,** 2015-2022 **(1985)**
3. Devipriya S. and Yesodharan S., Photocatalytic degradation of pesticide pollutants in water, *Solar Energy Mater and Solar Cells,* **86**, 309-348 **(2005)**
4. Sakthivel S., Neppolean B., Shankar M.V., Arabindoo B., Palanichamy M. and Murugesan V., Solar photocatalytic degradation of azo dye: Comparison of photocatalytic efficiency of ZnO and TiO_2, *Solar Energy Materials and Solar Cells*, **77(1),** 65-82 **(2003)**
5. Uchida H., Itoh S. and Yoneyama H., Photocatalytic decomposition of propyzamide using TiO_2supported on activated carbon, *Chemistry Letters*, **22**, 1995-1998 **(1993)**
6. Turchi C.S. and Ollis D.F., Photocatalytic degradation of organic water contaminants: mechanisms involving hydroxyl radical attacks, *J. Catal,* **122**, 178-192 **(1990)**
7. Wu C.G., Chao C.C. and Kuo F.T., Enhancement of the photocatalytic performance of TiO_2 catalysts via transition metal modification, *Catal. Today,* **97(23),** 103-112 **(2004)**
8. Sakthivel S., Shankar M.V., Palanichamy M., Arabindoo A., Bahnemann D. M. and Murugesan B.V., Enhancement of photocatalytic activity by metal deposition: characterization and photonic efficiency of Pt, Au, and Pd deposited on TiO_2 catalyst, *Wat. Res.,* **38 (130),** 3001-3008 **(2004)**
9. Pellegrin J.Y., Le Pleux L, Blart L.E., Renaud A., Chavilion B., Szuwarski N., Boujitita M., Cario L., Jobic

Research Journal of Recent Sciences ISSN 2277-2502
Vol. **2(ISC-2012),** 82-89 **(2013)** *Res. J. Recent. Sci*

S., Jacquemin D. and Odobel F., Ruthenium polypyridine complexes as sensitisers in NiO based p-type dye-sensitized solar cells: Effects of the anchoring groups, *J Photochem. Photobiol. A-Chem.*, **219(2)**, 235-242 **(2011)**

10. Joseph C.G., Puma G.L., Bono A., Krishniah D., Sonophotocatalysis in advanced oxidation process: A short review, *Ultrason., Sonochem.* **16**, 583-589 **(2009)**

11. Anju S.G., Suguna Yesodharan and Yesodharan E.P., Sonophotocatalytic degradation of phenol over semiconductor oxides, *Chem Eng. J.,* **189-190(1),** 84-93 **(2012)**

12. Kim S. and Choi W., Visible light induced photocatalytic degradation of 4-chlorophenol and phenolic compounds in aqueous suspension of pure titania: demonstrating the existence of surface complex-mediated path, *Journal of Phys. Chem. B*, **109(11),** 5143-5149 **(2005)**

13. Wu C., Liu X., Wei D., Fan J., Wang L., Photosonochemical degradation of phenol in water, *Wat. Res.* **35(16)** 3927-3933 **(2001)**

14. Sivalingam G., Priya M.H. and Madras G., Effect of substitution on the photocatalytic degradation of phenol using combustion synthesized TiO_2: Mechanism and kinetics, *Appl. Catal. B: Environ*., **51,** 67-76 **(2004)**

15. Anju S.G., Jyothi K.P., Sindhu Joseph, Suguna Yesodharan and Yesodharan E.P., Ultrasound assisted semiconductor mediated catalytic degradation of organic pollutants in water: Comarative efficacy of ZnO, TiO_2 and ZnO-TiO_2, *Res J Rec Sci.,* **1**, 191-201 **(2012)**

16. Kuriacose J.C., Ramakrishnan V. and Yesodharan E.P., Photoinduced catalytic reactions of alcohols on ZnO suspensions in cyclohexane: Oscillation in the concentration of H_2O_2 formed, *Indian J. Chem*., **19A**, 254-256 **(1978)**

17. Pignatello J.J. and Sun Y., Complete oxidation of metolachlor and methyl parathion in water by photoassisted fenton reaction, *Wat Res*., **29**, 1837-1844 **(1995)**

18. Han W., Zhu W., Zhang P., Zhang Y. and Li L., Photocatalytic degradation of phenols in aqueous solutions under irradiation of 254 and 185 nm UV light, Catal. Today, **90**, 319-324 **(2004)**

19. Rabindranathan S., Devipriya S. and SugunaYesodharan, Photocatalytic degradation of phosphamidon on semiconductor oxides, *J. Hazard. Mater.,* **102**, 217-229 **(2003)**

20. Chen C.C., Lu, C.S., Chung and Y.C., Jan, J.L., UV light induced photodegradation of malachite green on TiO_2 nanoparticles, *J. Hazard.Mater.*, **141**, 520-528 **(2007)**

21. Hashimoto K., Kawai T. and Sakata T., *Photocatalytic reactions of hydrocarbons and fossil fuels with water-Hydrogen production and oxidation, J Phys Chem* , **88**, 4083 **(1984)**

22. Desahpande P.A., Madras G., Photocatalytic degradation of phenol by base metal substituted orthovanadates, *Chem. Eng. J.,* **161,** 136-145 **(2010)**

23. Velasco L.F., Parra J.B. and Ania C.O., Role of activated carbon features on the photocatalytic degradation of phenol, *Applied Surf. Sci.* **256,** 5254-5258 **(2010)**

24. Yalfani M.S., Contreras S., Medina F. and Suegras J., Phenol degradation by Fenton's process using catalytic insitu generated hydrogen peroxide, *Appl. Catal. B:Environ,* **89**, 519-526 **(2009)**

25. Hanna K., Kone K. and Ruby T.C., Fenton-like oxidation and mineralization of phenol using synthetic Fe(II)-Fe(III) green rust, *Environ Sci. Poll. Res*., **17**, 124-134 **(2010)**

26. Serpone N., Terzian R., Colarusso P., Minero C., PelizettiE and Hidaka H., *Res. Chem. Int.* **18(2-3),** 183-190 **(1992)**

27. Anju S.G., Jyothi K.P., Sindhu Joseph, Suguna Y.esodharan and Yesodharan E.P., Ultrasound assisted semiconductor mediated catalytic degradation of organic pollutants in water: Comparative efficacy of ZnO, TiO_2 and ZnO-TiO_2, *Res. J. Recent Sci.,* **1**, 191-201 **(2012)**

28. Hartmann J., Bartels P., Mau U., Witter M., Tumpling W.V., Hofmann J., Nietzschmann E., Degradation of the drug diclofenac in water by sonolysis in presence of catalysts, *Chemosphere,* **70**, 453-461 **(2008)**

Ultrasonics Sonochemistry 21 (2014) 1787–1796

Contents lists available at ScienceDirect

Ultrasonics Sonochemistry

journal homepage: www.elsevier.com/locate/ultson

Ultrasound (US), Ultraviolet light (UV) and combination (US + UV) assisted semiconductor catalysed degradation of organic pollutants in water: Oscillation in the concentration of hydrogen peroxide formed in situ

K.P. Jyothi, Suguna Yesodharan, E.P. Yesodharan *

School of Environmental Studies, Cochin University of Science and Technology, Kochi 682022, India

ARTICLE INFO

Article history:
Received 9 January 2014
Received in revised form 17 March 2014
Accepted 18 March 2014
Available online 28 March 2014

Keywords:
Ultrasound
UV light
Sonocatalysis
Semiconductors
Hydrogen peroxide
Oscillation

ABSTRACT

Application of Advanced Oxidation Processes (AOP) such as sono, photo and sonophoto catalysis in the purification of polluted water under ambient conditions involve the formation and participation of Reactive Oxygen Species (ROS) like $^{\bullet}OH$, $HO_2^{\bullet}$, $O_2^{\bullet-}$, H_2O_2 etc. Among these, H_2O_2 is the most stable and is also a precursor for the reactive free radicals. Current investigations on the ZnO mediated sono, photo and sonophoto catalytic degradation of phenol pollutant in water reveal that H_2O_2 formed in situ cannot be quantitatively correlated with the degradation of the pollutant. The concentration of H_2O_2 formed does not increase corresponding to phenol degradation and reaches a plateau or varies in a wave-like fashion (oscillation) with well defined crests and troughs, indicating concurrent formation and decomposition. The concentration at which decomposition overtakes formation or formation overtakes decomposition is sensitive to the reaction conditions. Direct photolysis of H_2O_2 in the absence of catalyst or the presence of pre-equilibrated (with the adsorption of H_2O_2) catalyst in the absence of light does not lead to the oscillation. The phenomenon is more pronounced in sonocatalysis, the intensity of oscillation being in the order sonocatalysis > photocatalysis ⩾ sonophotocatalysis while the degradation of phenol follows the order sonophotocatalysis > photocatalysis > sonocatalysis > sonolysis > photolysis. In the case of sonocatalysis, the oscillation continues for some more time after discontinuing the US irradiation indicating that the reactive free radicals as well as the trapped electrons and holes which interact with H_2O_2 have longer life time (memory effect).

1. Introduction

Advanced Oxidation Processes (AOP) such as sonocatalysis, photocatalysis and their combination sonophotocatalysis using semiconductor oxide catalysts have been extensively investigated as environment-friendly technologies for the removal of chemical and bacterial pollutants from water [1–6]. Relatively mild reaction conditions and proven ability to degrade several toxic refractory pollutants make these AOPs attractive as viable techniques. Most widely used catalyst in this context is TiO_2 which is active only in the UV range and hence unattractive for solar energy harvesting. Another semiconductor being investigated is ZnO which has mild photocatalytic activity in visible light. Several efforts are being made to extend the light absorption of these materials to the visible range of solar spectrum. These include dye sensitization, semiconductor coupling, impurity doping, use of coordination metal complexes, metal deposition etc [7–12].

Recently, Ultrasound (US) irradiation mediated by suitable catalysts (sonocatalysis) has been receiving special attention as an environment-friendly technique for the treatment of hazardous organic pollutants in wastewater [2,5,6]. However the degradation rate is slow compared to other established methods. Investigations on enhancing the efficiency of sonocatalysis by combination with other AOP techniques is in progress in many laboratories [5,6,13–15]. Coupling US with Ultraviolet (UV) irradiation enhances the efficiency of semiconductor mediated degradation of aqueous pollutants synergistically [5,6,13,15].

One of the major products of the AOP degradation of organic pollutants in water is H_2O_2 which functions as a reactant, intermediate and the end product. However, the fate of H_2O_2 has not received due attention since the focus has always been on removal of the pollutant and purification of water. In the present study the role and fate of H_2O_2 formed during the sono, photo and

* Corresponding author. Tel.: +91 9847193695; fax: +91 484 2577311.
E-mail address: epyesodharan@gmail.com (E.P. Yesodharan).

http://dx.doi.org/10.1016/j.ultsonch.2014.03.019
1350-4177/

sonophotocatalytic decontamination of phenol in water is investigated in detail. The study is especially important in view of the fact that H_2O_2 is an important water soluble trace gas species in the atmosphere which can act as a precursor for highly reactive free radicals ·OH and HO_2. In the presence of suspended particulate matter including solar active materials, this can lead to the formation of variety of chemical species with short and long term impact on atmospheric chemistry and climate change.

2. Materials and methods

ZnO (99.5%) used in the study was supplied by Merck India Limited. The surface area, as determined by the BET method is ~12 m^2/g. The consistency of the physicochemical characteristics of ZnO used in the study with those reported in literature was confirmed by X-ray diffractogram (XRD) and Scanning Electron Microscopy (SEM) measurements.

The average particle size, determined by SEM was 10×10^{-2} μm, unless mentioned otherwise. Phenol AnalaR Grade (99.5% purity) and H_2O_2 (30.0% w/v) from Qualigen (India) were used as such without further purification. All other chemicals were of AnalaR Grade or equivalent. Water distilled twice was used in all the experiments. The sonocatalytic, photocatalytic and sonophotocatalytic experiments were performed as reported earlier [5].

The experiments were conducted using aqueous solutions of phenol of the desired concentration. Specified quantity of the catalyst was suspended in the solution and kept under agitation using a magnetic stirrer. In the case of US irradiation experiments, sonication was sufficient to ensure adequate mixing of the suspension. Additional mechanical mixing did not make any notable consistent difference in the US reaction rate. Hence mixing by sonication alone was chosen for all US and (US + UV) experiments. The reactor used in all experiments was a cylindrical Pyrex vessel of 250 ml capacity. In photocatalytic experiments, the reactor was placed in a glass vessel of 500 ml capacity through which water from a thermostat at the required temperature was circulated. A high intensity UV lamp (400 W medium pressure mercury vapor quartz lamp) mounted above is used as the UV irradiation source. In the case of sonocatalytic and sonophotocatalytic experiments, ultrasonic bath was used as the source of US. The ultrasonic bath operated at 40 kHz and power of 100 W. Water from the sonicator was continuously replaced by circulation from a thermostat maintained at the required temperature. The position of the reactor in the ultrasonic bath was always kept the same. Unless otherwise mentioned, the reaction temperature was maintained at 29 ± 1C. At periodic intervals samples were drawn, the suspended catalyst particles were removed by centrifugation and the concentration of phenol left behind was analyzed by Spectrophotometry at 500 nm. Sample from reaction system kept in the dark under exactly identical conditions but without UV or US irradiation was used as the reference. H_2O_2 is determined by iodometry after removing the suspended particles from the sample by centrifugation. The actual analysis takes place approximately 5 min (sample preparation time) after the sample is drawn from the irradiated system and hence the possibility of any reactive short lived free radical interfering with the estimation of H_2O_2 can be ruled out. Mineralization of phenol was identified by confirming the evolution of CO_2 and determination of the Total Organic Carbon Content (TOC) using TOC analyzer model Elementar Analysensysteme GmbH.

3. Results and discussion

The degradation of phenol in water was investigated in presence of ZnO, UV and US individually as well as in combination. No significant degradation took place in the absence of either UV and catalyst or US and catalyst indicating that the catalyst and an energy source are essential to effect reasonable degradation. The degradation is more facile in photocatalysis compared to sonocatalysis. The degradation of ~90% achieved in the concurrent presence of UV, US and ZnO (sonophotocatalysis) is more than the sum of the degradation under photocatalysis (~55%) and sonocatalysis (~13%) which confirms the synergy reported in similar experiments earlier [5,16]. Small quantity of phenol degraded in the presence of US as well as (US + UV) even in the absence of catalysts; i.e. ~0.3% in 2 h and ~0.5% in 8 h time even though no degradation was observed under identical conditions in presence of UV. This is possible since sonolysis of water is known to produce extreme temperature (>3000 °C) and pressure (>300 atm.) conditions capable of generating free radicals H· and OH· via reaction (1) [17]:

$$H_2O \xrightarrow{\gg} H^{\cdot} + {}^{\cdot}OH \quad \gg \text{refers to ultrasound} \tag{1}$$

More Reactive Oxygen Species (ROS) such as $HO_2^{\cdot}$ will be formed in presence of O_2 as in reaction (2):

$$H^{\cdot} + O_2 \longrightarrow HO_2^{\cdot} \tag{2}$$

When semiconductor oxides such as TiO_2, ZnO etc. are irradiated by UV, US or their combination (UV + US), electrons get promoted from the valence band to the conduction band creating holes in the valence band. The OH^- ions that are adsorbed on the surface of the catalyst get oxidized to ·OH radicals by the holes in the valence band. The electron in the conduction band is donated to oxygen generating superoxide radical anion $O_2^{-\cdot}$ which eventually gives rise to more reactive species such as $HO_2^{\cdot}$, ·OH, H_2O_2 etc. These species are involved in photooxidation reactions resulting in the mineralization of phenol and formation of H_2O_2 as follows:

$$\text{ROS } ({}^{\cdot}OH,\ HO_2^{\cdot} \text{ etc.}) + \text{phenol} \longrightarrow \text{Intermediates} + H_2O_2 \rightarrow\rightarrow H_2O_2 + H_2O + CO_2 \tag{3}$$

$$HO_2^{\cdot} + HO_2^{\cdot} \longrightarrow H_2O_2 + O_2 \tag{4}$$

$$2\,{}^{\cdot}OH \longrightarrow H_2O_2 \tag{5}$$

The fate of concurrently formed H_2O_2 during the degradation of phenol in presence of ZnO is shown in Fig. 1. The concentration of H_2O_2 increases and then decreases in a wave like fashion resulting in well defined crests and troughs in the case of sonocatalysis and photocatalysis. In the case of sonophotocatalysis, the concentration of H_2O_2 tends to stabilize rather than oscillating. Since H_2O_2 is an

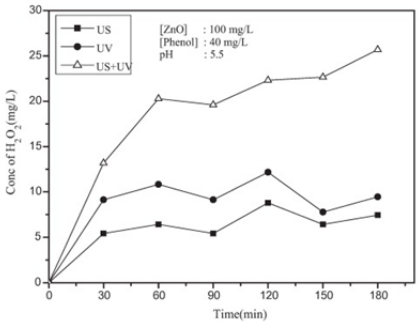

Fig. 1. Concentration of H_2O_2 during the sono, photo and sonophotocatalytic degradation of phenol in presence of ZnO.

essential byproduct of phenol degradation its concentration was expected to increase and ultimately stabilize when the phenol degradation is complete. The oscillation/stabilization in the concentration shows that H_2O_2 is generated/decomposed/consumed simultaneously depending on the reaction conditions, in particular its concentration. When the concentration reaches a particular maximum, the decomposition dominates bringing its net concentration down. Similarly when the concentration reaches a critical minimum, the formation process gets precedence. This process happens many times over again and again. The degradation of phenol continues unabated even when the concurrently formed H_2O_2 shows stabilization in the case of sonophotocatalysis or oscillation in the case of sono and photocatalysis. The decomposition of H_2O_2 is known to take place as follows:

$$ZnO \xrightarrow{UV/US/(US+UV)} e_{cb} + h_{vb} \quad (6)$$

$$H_2O_2 + UV/US/(US + UV) \longrightarrow 2{\cdot}OH \quad (7)$$

$$2h^+_{vb} + H_2O_2 \longrightarrow O_2 + 2H^+ \quad (8)$$

$$2e^-_{cb} + 2H^+ + H_2O_2 \longrightarrow 2H_2O \quad (9)$$

$$H_2O_2 + {\cdot}OH \longrightarrow H_2O + HO^{\cdot}_2 \quad (10)$$

$$H_2O_2 + HO^{\cdot}_2 \longrightarrow H_2O + {\cdot}OH + O_2 \quad (11)$$

$$H_2O_2 + O^{-\cdot}_2 \rightarrow {\cdot}OH + OH^- + O_2 \quad (12)$$

Thus, the same free radicals can contribute to the formation and decomposition of H_2O_2 depending on the conditions. At the same time, being a complex free radical system, other interactions leading to the formation and decomposition of H_2O_2 are also possible.

The degradation of phenol in presence of semiconductor oxides under sono, photo and sonophotocatalytic conditions has been investigated extensively by many researchers including our group. In the current study also, the findings are similar to those reported earlier and hence not discussed in detail. However, the fate of H_2O_2, in particular its stabilization and/or the phenomenon of oscillation in its concentration is not subjected to detailed study so far. Hence the current study is focused on the effect of various reaction parameters on the fate of H_2O_2 formed in situ during the sono, photo and sonophotocatalytic degradation of phenol.

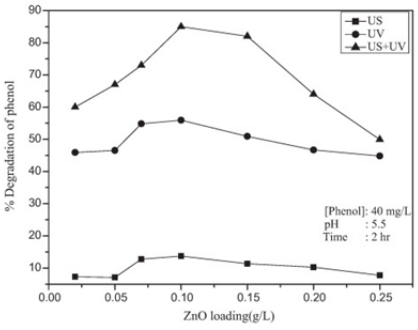

Fig. 2. Effect of catalyst loading on the sono, photo and sonophotocatalytic degradation of phenol in presence of ZnO.

3.1. Effect of catalyst dosage

The catalyst loading for optimum degradation of phenol has been experimentally determined for sono, photo and sonophotocatalysis as shown in Fig. 2. The degradation increases with increase in loading and then stabilizes in all cases. The enhanced degradation efficiency can be attributed to the increased availability of catalyst sites for adsorption of the reactant molecules, better absorption of radiations and generation of reactive free radicals and their interactions. However, beyond the optimum, increased catalyst concentration can result in light scattering and reduced passage of light through the sample resulting in shrinkage of photoactivated volume of the suspension. Another reason may be the aggregation of the catalyst particles causing decrease in the number of exposed active surface sites. The particles cannot be fully and effectively suspended beyond a particular loading in a particular reactor which also causes suboptimal penetration of light and reduced adsorption of substrates on the surface. The optimum range of ZnO is in the order sonophotocatalysis (0.10–0.15 g/L) ⩾ sonocatalysis (0.10–0.15 g/L) > photocatalysis (0.075–0.10 g/L). This difference may be due to the deagglomeration of the aggregate catalyst particles by US which can bring more surface sites in contact with the irradiation as well as the pollutant molecules. This is not possible in photocatalysis where light cannot penetrate into the agglomerated optically dense medium of concentrated ZnO suspensions. The concentration of H_2O_2 formed simultaneously with the degradation of phenol does not increase correspondingly and stabilises or fluctuates due to concurrent formation and decomposition. Hence the optimum catalyst loading for phenol degradation need not necessarily hold good for optimum H_2O_2 at any point of time. Hence the effect of catalyst loading on the concurrent formation and decomposition of H_2O_2 and the oscillation phenomenon is investigated at the optimized loading as above and two other loadings on either side of this optimum under sono, photo and sonophotocatalytic conditions. Typical results are shown in Fig. 3a–c. Due to simultaneous formation and decomposition, the concentration of H_2O_2 at any point in time during the reaction is not reproducible consistently. Hence the experiments had to be repeated many number of times under strictly identical conditions in order to get the most reliable reproducible data. As seen from the graphs, in the case of sonocatalysis, the concentration of H_2O_2 is relatively lower and shows distinct oscillations with well defined crests and troughs indicating periodic domination of formation and decomposition process. The concentration of H_2O_2 at the maxima and minima in the oscillation curve as well as the number of maxima and minima do not follow any consistent pattern with respect to catalyst loading. In the case of photocatalysis the rate of formation and hence concentration of H_2O_2 are higher compared to sonocatalysis. Here the decomposition may dominate only for shorter period and hence the trough of the curve also is at a higher concentration at higher loadings. In the case of sonophotocatalysis the oscillation is less pronounced with the formation rate and net concentration of H_2O_2 remaining high always. In this case, the trend is towards stabilization of the concentration of H_2O_2 indicating comparable formation and decomposition rate with former having slight edge over the latter. The stabilised concentration of H_2O_2 is higher at higher loadings.

The effect of catalyst loading is further confirmed by adding ZnO in between the reaction into sono, photo and sonophotocatalytic system when the H_2O_2formation and/or decomposition have already been in progress. As expected, the extra addition of ZnO enhances the rate of OH radical and hence H_2O_2 formation resulting in oscillation/stabilization at higher concentration in sonocatalysis (Fig. 4). In the case of photocatalysis, the extra addition does not result in significant change indicating comparable formation and decomposition rates (of H_2O_2). In sonophotocatalysis, where

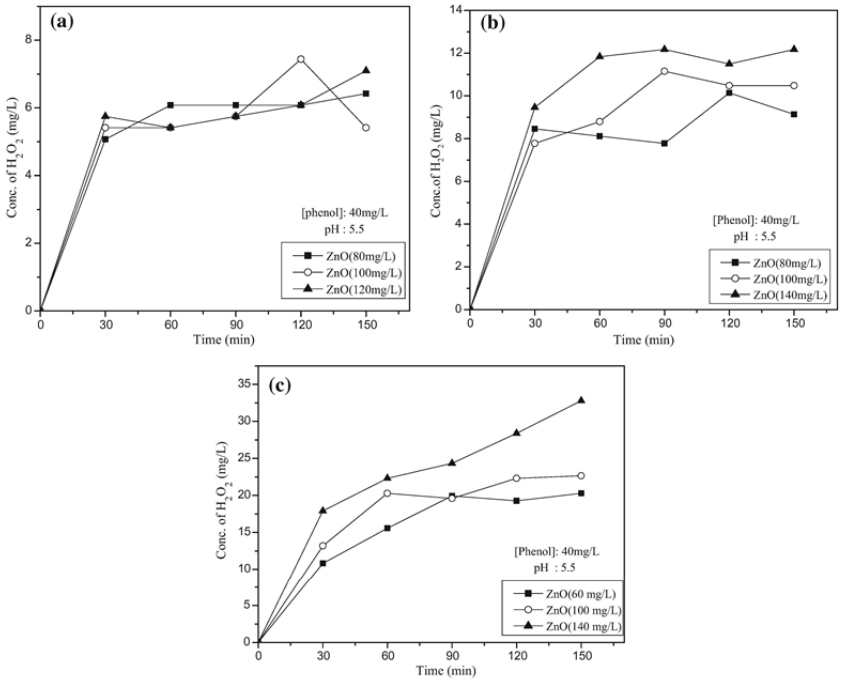

Fig. 3. (a) Effect of catalyst loading on the oscillation in the concentration of H_2O_2 under sonocatalysis. (b) Effect of catalyst loading on the oscillation in the concentration of H_2O_2 under photocatalysis. (c) Effect of catalyst loading on the oscillation in the concentration of H_2O_2 under sonophotocatalysis.

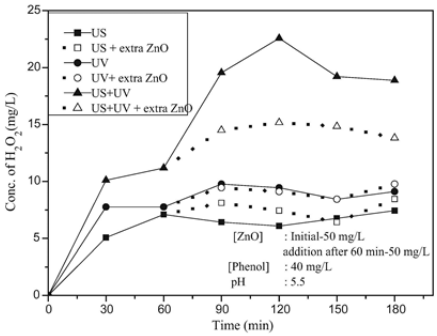

Fig. 4. Effect of in between addition of ZnO (after 60 min) on the oscillation in the concentration of H_2O_2.

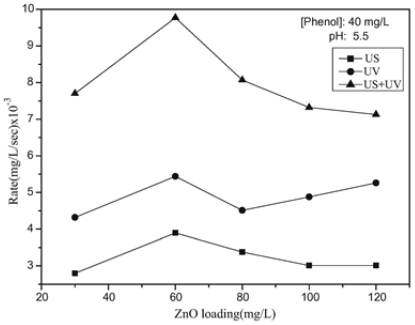

Fig. 5. Effect of catalyst loading on the initial rate of formation of H_2O_2 under sono, photo and sonophotocatalysis.

the net concentration of H_2O_2 is much higher, extra addition of ZnO leads to decreased concentration of H_2O_2 probably because the extra generated free radicals interact more with the more abundant H_2O_2 leading to decomposition and eventual stabilization. In any case, a general correlation between H_2O_2 build up at any point of time and catalyst loading is not appropriate, since H_2O_2 is undergoing concurrent formation and decomposition during the reaction through a number of routes as in reactions (7)–(12). The net initial rate of formation of H_2O_2 before it reaches the first maximum in the oscillation curve, at various loadings which may be more appropriate for comparison, is plotted in Fig. 5. The rate increases initially with dosage in sono, photo and sonophotocatalysis. Later on the rate decreases and eventually stabilizes probably because the decomposition becomes more prominent.

The influence of particles on the decomposition of H_2O_2 in photocatalytic systems has been a subject of many studies. Augugliaro et al. [18] reported that there is no significant difference in the decomposition of H_2O_2 with or without suspended catalyst in photocatalytic systems. Jenny and Pichat [19] found that the heterogeneous H_2O_2 decomposition is only twice faster than homogeneous decomposition. However, Ilisz et al. [20] observed that efficient photodegradation of H_2O_2 takes place only in presence of catalysts and the initial rate of decomposition decreases with decreasing concentration. Current study shows that H_2O_2 decomposition is negligible in the dark or by photolysis or sonolysis in the absence of a catalyst. Further we observed that in sonocatalytic systems the decomposition of H_2O_2 begins when a critical maximum concentration is reached and the formation process dominates when a critical lower concentration is reached. This is in line with the findings of Ilisz et al.

3.2. Effect of concentration of substrate

The effect of phenol concentration on the rate of degradation showed that it follows first order kinetics in sono, photo and sonophotocatalysis at lower concentrations [5]. At higher concentrations of >30 ppm the reaction order decreases and tends to become zero order. In the case of sonocatalysis with distinct oscillation in the concentration of H_2O_2, the number of maximum and minimum in the curve increases with increase in concentration (Fig. 6) even though this cannot be strictly generalized at higher concentrations (50 mg/L). Similarly the concentration of H_2O_2 at the maximum and minimum are also higher as the concentration of phenol increases, even though the trend is not strictly adhered to with respect to the minima at higher concentration. When phenol concentration is increased from 10 to 20 mg/L, the rate of degradation is almost doubled. At the same time the maxima and minima in the H_2O_2 oscillation curve also increased indicating its correlation with phenol degradation. However at very higher concentration of phenol (50 ppm) where its degradation is much faster, the correlation is not maintained. This is probably because, with too many reactive free radicals generated at higher phenol concentration, the recombination as well as other interactions competes with phenol degradation resulting in multitude of unpredictable reactions leading to many intermediates. In the case of photocatalysis, the effect of concentration of phenol on the oscillation is not significant in the range 20–40 mg/L and the concentration of H_2O_2 is eventually stabilised (Fig. 7). In the case of sonophotocatalysis, H_2O_2 increases sharply in the beginning at all phenol concentrations (Fig. 7), stabilises for a brief period, increases again and stabilises thereafter. In this case also the stabilised concentration of H_2O_2 is higher at higher concentration of phenol. The finding is further confirmed by in between addition of phenol to ZnO/H_2O_2 system after 60 min of irradiation at standard reaction conditions. The result is enhanced formation of H_2O_2 in sono, photo and sonophotocatalysis (Fig. 8).

The formation of H_2O_2 in water, observed in the case of ultrasound even in the absence of catalyst particles, is not seen in the case of UV irradiation. Even in the case of US + UV in the absence of the catalyst, the H_2O_2 concentration and behavior remains more or less same as in the case of sonolysis, indicating that light alone does not contribute to the formation or decomposition of H_2O_2. In the case of sonolysis, it has been reported that presence of suspended particles such as quartz or alumina can enhance the

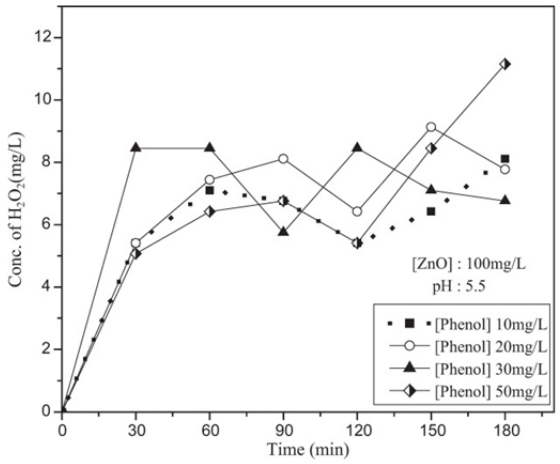

Fig. 6. Effect of concentration of phenol on the oscillation in the net concentration of H_2O_2 under sonocatalysis.

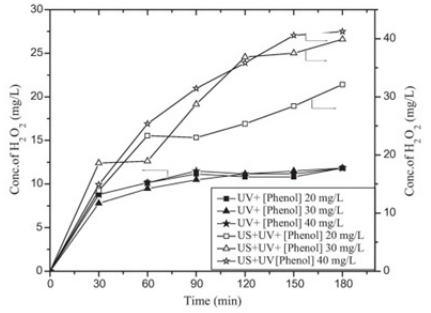

Fig. 7. Effect of concentration of phenol on the oscillation in the net concentration of H_2O_2 under photo and sonophotocatalysis.

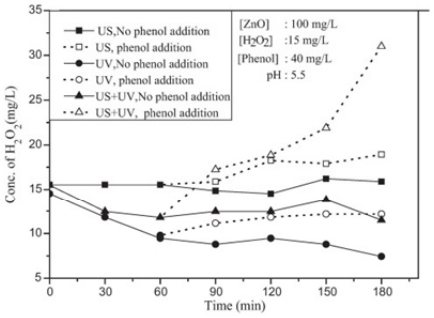

Fig. 8. Effect of in between addition of phenol (after 60 min) on the oscillation in the concentration of H_2O_2 under sono, photo and sonophotocatalysis.

formation of H_2O_2 [21]. However, such enhancement was not seen in the current study. This may be either due to the inability of the particles to enhance the formation of H_2O_2 or the balancing of concurrent formation and decomposition resulting in insignificant net increase. Further, the sonolytic degradation of phenol also is negligible in the presence of quartz or alumina particles. Hence the suspended particles can promote sonocatalytic degradation of phenol or the formation of H_2O_2 only when they are catalytically active like in the case of semiconductor oxides such as ZnO. Once the free radical formation and the resultant degradation of phenol or formation of H_2O_2 sets in, the process may be aided by ZnO particles in sono and sonophotocatalytic systems possibly by the transfer of sonolytic or photolytic energy created by the US or UV or US + UV throughout the system. Heterogeneous nucleation of bubbles in presence of particles is known to enhance the cavitation power [22]. This in turn may increase the pyrolysis of H_2O molecules and the formation of OH radicals which are highly reactive and hence short-lived. It is also known that flashes of Single Bubble Sonoluminescence (SBSL) caused by implosion of bubbles involve intense UV light which can activate semiconductor oxides and cause the degradation of organic pollutants [23]. However this component contributed by the particles in addition to their catalytic effect cannot be delineated in the presence of a highly active catalyst like ZnO.

The enhancement in sonolytic formation of H_2O_2 in presence of particles is explained by Keck et al. [21] on the assumption that the shape of the bubbles may have changed from spherical to asymmetric though the nature and concentrations of the particles used are not expected to influence the bubble size and collapse time. This change of shape may result in larger surface area of the bubbles enabling accelerated free radical formation which may escape into the bulk leading to more H_2O_2 formation and phenol degradation. However, current results show that the initial build up of reasonable quantity of free radicals is prerequisite for the particle effect if any to happen which is possible only in the presence of a sono or photocatalytically active material.

3.3. Effect of added H_2O_2

The current results indicate that oscillation in the concentration of H_2O_2 begins only after certain minimum quantity of H_2O_2 is built up in the system. Thereafter the periodic increase and decrease in its concentration occurs. This is further verified by following the net concentration of H_2O_2 in sono, photo and sonophotocatalytic system in which H_2O_2 has been added initially before the irradiation starts. As expected, added H_2O_2 leads to increased number of reactive free radicals, increased interaction with phenol molecules and correspondingly more degradation in all cases (Table 1).

Once sufficient concentration of H_2O_2 is formed in situ in the system, the role of externally added H_2O_2 becomes less significant as seen from the relative increase in the degradation of phenol after 30 min and 120 min.

However, corresponding to this enhanced degradation of phenol in the presence of initially added H_2O_2, the net concentration of H_2O_2 does not increase in the beginning. It remains steady for a while and starts oscillating thereafter (Fig. 9). Thus it is reconfirmed that H_2O_2 undergoes concurrent formation and decomposition and their rates are more or less identical in the beginning in presence of added H_2O_2 in sono, photo and sonophotocatalytic systems. Slowly the rate of decomposition starts dominating in the case of photocatalysis and the net concentration of H_2O_2 decreases. In the case of sono and sonophotocatalysis, the rate of formation of H_2O_2 dominates initially after the steady state. Eventually the rates of formation and decomposition balance and the concentration of H_2O_2 levels off or decreases slightly.

Once sufficient concentration of H_2O_2 is formed in situ in the system, the effect, if any, of externally added H_2O_2 on the oscillation in its concentration or the degradation of phenol becomes indistinguishable. Parallel decomposition of H_2O_2 into water and O_2 without generating reactive free radicals and the concentration-dependent oscillation also make the system with and without added H_2O_2 comparable as the reaction proceeds.

3.4. Effect of pH

The pH of the reaction medium is known to have strong influence on US or UV-induced degradation of organic pollutants. In photolysis or photocatalysis, the ease of bond breakage and the site of attack might be different at different pH due to difference in the distribution of molecular charges. The surface charge of semiconductors, the interfacial electron transfer and the photoredox processes occurring in their presence are also affected by pH. In sonocatalysis, pH can further alter the distribution of the pollutants in the bulk region, on the surface and at the site of the cavity collapse. Previous studies on the sono, photo and sonophotocatalytic degradation on ZnO showed that the degradation is more favored in the acidic region with maximum in the acidic pH range of 4–6, which peaks at pH 5.5 [5]. However, the effect of pH on the fate of H_2O_2, especially the oscillation resulting from simultaneous

Table 1
Effect of externally added H_2O_2 on the sono, photo and sonophotocatalytic degradation of phenol over ZnO. [ZnO]: 100 mg/L, [phenol]: 40 mg/L, added [H_2O_2]: 15 mg/L, pH: 5.5. ~Percentage increase within brackets.

Irradiation condition	% Degradation of phenol at different irradiation time (time in minutes)			
	30	60	90	120
US	1.1	7.0	9.5	13.7
US + H_2O_2	3.0 (170%)	7.0	11.2	16.9 (23%)
UV	7.5	21.4	41.2	56.2
UV + H_2O_2	14.3 (90%)	31.2	44.7	61.5 (9%)
US + UV	26.1	54.7	62.5	87.9
US + UV + H_2O_2	46.4 (78%)	63.3	85.4	94.6 (8%)

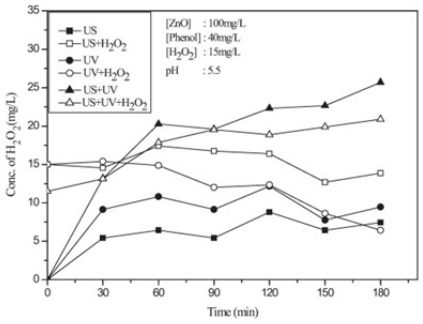

Fig. 9. Effect of added H_2O_2 on the net concentration of H_2O_2 under sono, photo and sonophotocatalysis.

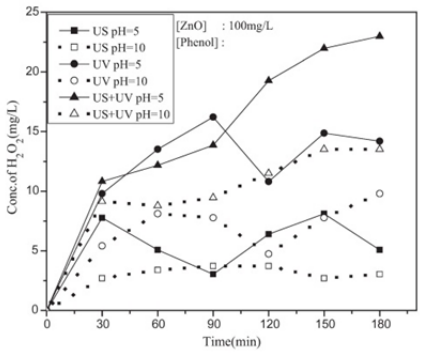

Fig. 10. Effect of pH on the oscillation in the concentration of H_2O_2 during sono, photo and sonophotocatalysis.

formation and decomposition, has not received due attention so far.

Fig. 10 shows the concentration of H_2O_2 in the system at different times during the sono, photo and sonophotocatalytic degradation of phenol on ZnO at two typical pH values; acidic and alkaline. In all three instances, the oscillation is more significant in the acidic pH of ~5 at which maximum phenol degradation is also observed. The maximum in the oscillation curve also is higher in this range confirming its relation with phenol degradation. As explained earlier, more phenol decomposition produces more free radicals which can lead to enhanced H_2O_2 concentration resulting in higher maximum. Once the critical maximum concentration of H_2O_2 is reached, the free radicals interact more frequently with H_2O_2 resulting in degradation until the critical minimum is reached when the formation process begins to dominate again. In the case of sonophotocatalysis, the formation of H_2O_2 is high enough at both pH to cover up the relatively lower decomposition. Hence the oscillation tends to be weaker and moves towards stabilization though pH effect is quite visible on phenol degradation [5].

The behavior of phenol as well as the catalyst ZnO is different at different pH which can influence the rate of reaction and the fate of H_2O_2 in sono, photo and sonophotocatalytic systems. The phenomenon of oscillation is more pronounced in the acidic range compared to the alkaline pH. Under alkaline conditions, during US irradiation, the phenolate ions are concentrated in the gas–water interface of the bubbles where the hydrophobicity is strong and cannot vaporize into the cavitation bubbles [24]. They can react only outside of the bubble film with the OH radicals cleaved from water. Hence degradation of phenol and oscillation in the concentration of H_2O_2 is less. However in the acidic range when it is in its molecular state, phenol enters the gas–water interface of bubbles and even vaporizes into cavitation bubbles. They can react inside by thermal cleavage and outside with OH radicals. This results in higher degradation of phenol as well as enhanced formation and decomposition of H_2O_2. Hence the oscillation is quite significant in the acidic pH range.

In weakly acidic solution, or when the pH is less than the pK_a, (pK_a value of phenol at 25 °C is 10) most of the phenol molecules remain un-dissociated. Hence maximum number of phenol molecules can be adsorbed onto the surface resulting in increased degradation of phenol and correspondingly more H_2O_2. Hence the amount of H_2O_2 at the maximum of the oscillation curve is more. In the alkaline medium, especially above the PZC of ZnO, i.e. >9, the catalyst surface is negatively charged. When the pH exceeds 10 ionic species of phenol will be predominant and the phenolate intermediates may get repelled away from the surface. This will also reduce the adsorption and consequent degradation of phenol and H_2O_2 formation.

The pH of the reaction medium has significant effect on the surface properties of semiconductor oxide particles, including the surface charge, size of the aggregation and the band edge position [25,26]. Hence pH can affect the adsorption–desorption characteristics of the surface of the catalyst. This will also influence the degradation of phenol and the formation/decomposition of H_2O_2. The pH effect on the behavior of H_2O_2 in presence of phenol is further complicated by the different mechanisms by which degradation of phenol takes place at different pH. Serpone et al. [27] showed that the sonochemical degradation of phenol proceeds through different intermediates at different pH. These intermediates themselves

undergo sonolytic degradation, though by different mechanisms. Thus the system consists of too many constituents and variables which make it difficult to identify the influence of pH on the oscillation behavior precisely.

In this context, the corrosion under extreme acidic and alkaline conditions as well as photocorrosion, normally observed in the case of ZnO, was tested by weight loss method under the experimental conditions at different pH. The corrosion is negligible in the pH range 4–10 with or without irradiation in 4 h time. During the same period, there is slight corrosion (<2%) at pH 3 and significant corrosion (~8%) at pH ⩾ 2. Irradiation did not enhance the corrosion significantly, probably because the period of study was short. Since all major investigations reported in the present paper are carried out at the optimized pH of 5.5, corrosion is considered negligible at least during the period of the study.

3.5. Role of O_2 in the fate of H_2O_2

Most photocatalytic reactions do not occur in the absence of O_2 since dioxygen molecules usually serve as electron acceptor thereby preventing/retarding electron–hole recombination [28]. Our studies also showed that the sono, photo and sonophotocatalytic degradation of phenol proceeds slowly in deaerated systems [5]. In order to test the role of O_2 in the formation/ decomposition of H_2O_2 and the phenomenon of oscillation in these three systems, experiments were carried out in the absence of O_2 by flushing the reaction system with N_2. The concentration of H_2O_2 generated is much less in the case of photo and sonophotocatalysis (Fig. 11). In the case of sonocatalysis, the difference is not that significant probably because of the sonolytic effect on water which generates free radicals even in the absence of O_2. However, the phenomenon of oscillation is observed even in the deaerated systems, though with reduced maxima and minima in the concentration of H_2O_2, suggesting that once H_2O_2 is formed by whatever mechanism, subsequent decomposition and formation can take place even in the absence/reduced concentration of O_2. Hence H_2O_2 itself can act as an electron acceptor as follows:

$$H_2O_2 + e^- \longrightarrow {}^{\cdot}OH + OH^- \quad (13)$$

H_2O_2 can also serve as a hole scavenger and decompose as in reaction (14):

$$H_2O_2 + {}^{\cdot}OH/h^+ \longrightarrow HO_2^{\cdot} + H_2O/H^+ \quad (14)$$

Consequently, the decomposition of H_2O_2would proceed in a unique way as H_2O_2 plays the dual role of electron and hole scavenger. The $HO_2^{\cdot}$ or ${}^{\cdot}OH$ thus generated may also react on the surface either to regenerate H_2O_2 or degrade or mineralize the pollutants.

It is possible that reactive nitrogen species also may be produced in the sono, photo and sonophotocatalytic systems in presence of air or added N_2. However, the effect of such species on the fate of H_2O_2 and the oscillation in its concentration requires further in-depth investigations, which is beyond the scope of the current study.

3.6. Memory effect

The fate of H_2O_2 after the irradiation source is turned off is followed in sono, photo and sonophotocatalysis under otherwise identical reaction conditions. The oscillation in the concentration of H_2O_2 continues for some more time in sonocatalysis (Fig. 12). The effect is not seen in sonophotocatalysis in which the concentration of H_2O_2 is relatively more and remains stable. In the case of photocatalysis, there is slight initial decrease followed by stabilization in the concentration of H_2O_2. Since the behavior of H_2O_2 is different in sono, photo and sonophotocatalytic experiments, it may not be due to any inherent characteristic of H_2O_2 formed and remaining in the system. The oscillation is not observed in experiments with externally added H_2O_2 at similar concentration without illumination with or without the catalyst. Irradiation in presence of catalyst is a prerequisite for the continued oscillation in the concentration of H_2O_2 (after the irradiation is turned off).

Hence it is logical to assume that the variation in the concentration of H_2O_2 as above is caused by the phenomenon of 'memory effect' in which the catalyst can store some of the photo/sono/sonophoto catalytic activity in 'memory'. Thus the catalyst can remain active for an extended period of time once the irradiation source is turned off. The formation of the reactive free radicals will continue, though at reduced rate, during this period. The degradation of phenol is insignificant during the period probably because the number of reactive free radicals is relatively small. The duration of the post-irradiation activity in the dark is at least 90 min in the present case (as seen in Fig. 12). Hence it is not due to the lifetime of the radicals which is only few seconds. Similar memory effect has been reported earlier in the case of ZnO [29] and TiO_2 [26,30]. Although the efficiency of the dark process is not as high

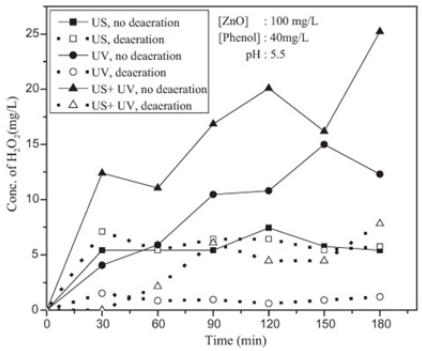

Fig. 11. Effect of deaeration with nitrogen on the oscillation in the concentration of H_2O_2 under sono, photo and sonophotocatalysis.

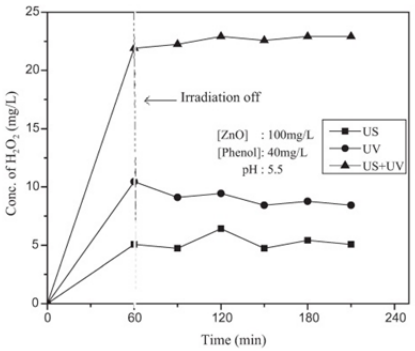

Fig. 12. Memory effect of ZnO on the oscillation in the concentration of H_2O_2 under sono, photo and sonophotocatalysis.

as in the presence of illumination, the phenomenon needs in depth investigation because it has the potential for the decontamination of polluted water or other similar systems for longer duration even after the source of energy is turned off.

3.7. Mechanism of the process

In semiconductor mediated sono, photo and sonophotocatalysis, electron from the valence band gets promoted to the conduction band (e_{cb}^-) leaving a positively charged hole in the valence band (h_{vb}^+) (reaction (6)). The electrons are then free to migrate within the conduction band. The holes may be filled by migration of electrons from an adjacent molecule leaving that with a hole and the process can be repeated [13,28]. The electrons and holes can recombine with no productive result or, they can give ROS such as $O_2^{\cdot-}$and $^{\cdot}OH$ and $HO_2^{\cdot}$ at the surface as follows:

$$O_2 + e_{cb} \longrightarrow O_2^{\cdot-} \quad (15)$$

$$H_{vb}^+ + H_2O \longrightarrow {}^{\cdot}OH + H_{aq}^+ \quad (16)$$

$$O_2^{\cdot-} + H^+ \longrightarrow HO_2^{\cdot} \quad (17)$$

The free radicals $^{\cdot}OH$ and $HO_2^{\cdot}$ can give rise to H_2O_2 as in (4) and (5). Further they can interact with phenol resulting in its degradation and eventual mineralization (as in reaction (3)). Since the amount of H_2O_2 generated in the absence of phenol is insignificant, it is reasonable to assume that the degradation of phenol and the formation of H_2O_2 are interrelated. However, the actual increase in the concentration of H_2O_2 after the initial period of approx. 30 min was less than expected compared to the degradation of phenol. After a while, the H_2O_2 levels off, much earlier than the degradation of phenol attains a plateau in photo and sonophotocatalysis. In the case of sonocatalysis, the concentration of H_2O_2 starts decreasing after reaching an initial maximum, then increases and again decreases in a periodic fashion. In all these cases, the degradation of phenol continues even after the H_2O_2 has stabilised or the oscillation has set in.

Since the concentration of H_2O_2 does not increase beyond a critical limit and its concentration is fluctuating periodically, it may be inferred that H_2O_2 formed is consumed in situ or is undergoing parallel decomposition into water and oxygen [5]. When the rate of formation and decomposition balances, the plateau is reached. When one process dominates the other cyclically, that results in oscillation. When the concentration reaches a particular maximum, the decomposition dominates bringing its net concentration down. Similarly when the concentration reaches a critical minimum, the formation process dominates. This process happens many times over in sonocatalysis in which the formation process is slower compared to photo and sonophotocatalysis. H_2O_2 also participates in the degradation of phenol, which incidentally is another source of H_2O_2 generation. This also leads to stabilization or oscillation in the concentration of H_2O_2.

In addition to the US initiated sonoluminescence effect which makes ZnO behave like a photocatalyst, sonolysis of water by itself is known to produce active radicals $H^{\cdot}$ and $OH^{\cdot}$ via cavitation (reaction (1)) which attack organic compounds in solution (reaction (3)). The microbubbles generated by US tend to break up into smaller ones in presence of particles thus increasing the total number of regions of high temperature and pressure [17,31]. However this can result in enhancement of the photodegradation of the pollutant or formation of H_2O_2 only if the particles are catalytically active as in the case of ZnO, since no such enhancement was seen in the presence of alumina which s not a photocatalyst. Dissolved oxygen serves as a source for nucleus cavitation which leads to the generation of more reactive species as follows [31]:

$$O_2 \longrightarrow 2{}^{\cdot}O \quad (18)$$

$$O_2 + {}^{\cdot}O \longrightarrow O_3 \quad (19)$$

$$O_2 + {}^{\cdot}H \longrightarrow {}^{\cdot}O_2H (\text{or } O + {}^{\cdot}OH) \quad (20)$$

$${}^{\cdot}O + {}^{\cdot}O_2H \longrightarrow {}^{\cdot}OH + O_2 \quad (21)$$

$${}^{\cdot}O + H_2O \longrightarrow 2{}^{\cdot}OH \quad (22)$$

Various active species produced as above react with phenol in the bulk solution or at the interface between the bubbles and the liquid phase. The ozone produced as above can decompose as in reaction (23) and produce more ROS as in reactions (18), (22), and (24):

$$O_3 + h\upsilon \longrightarrow O_2 + O \quad (23)$$

$$O + H_2O \longrightarrow H_2O_2 \quad (24)$$

Hoffmann et al. [32] and Kormann et al. [33] have shown that the quantum yield for H_2O_2 production during the oxidation of a variety of low molecular weight compounds has a Langmuir–Hinshelwood type dependence on O_2 partial pressure. By using ^{18}O isotope labeling experiments Hoffmann et al. showed that all the O_2 in photochemically produced H_2O_2 arises from dioxygen reduction by conduction band electrons. No H_2O_2 detected in the absence of O_2.

The empirical rate of formation of H_2O_2 by the heterogeneous photocatalytic surface reaction in presence of phenol may be expressed as [32]:

$$\frac{d[H_2O_2]}{dt} = \Phi_0 \frac{d[h\nu]_{abs}}{dt} = f(C_6H_5OH, O_2) = k_p \theta_{C_6H_5OH} \cdot \theta_{O_2} \quad (25)$$

where Φ_0 is the quantum yield for H_2O_2 production, k_p is the rate constant for H_2O_2 formation, $\theta_{C_6H_5OH}$ and θ_{O_2} are the concentration of C_6H_5OH and O_2 adsorbed onto the surface respectively.

The rate of decomposition of H_2O_2 by reaction with holes may be expressed as:

$$-\frac{d[H_2O_2]}{dt} = \Phi_1[H_2O_2]\frac{d[h\nu]_{abs}}{dt} = f(C_6H_5OH, O_2, H_2O_2) \quad (26)$$

where Φ_1 is the quantum yield for peroxide decomposition at the illuminated surface.

Combining the Eqs. (25) and (26), the empirical equation for the net formation of H_2O_2 can be expressed as:

$$\frac{d[H_2O_2]}{dt} = (\Phi_0 - \Phi_1[H_2O_2])\frac{d[h\nu]_{abs}}{dt} \quad (27)$$

During continuous irradiation by direct light or from the photochemical component of US irradiation a stationary state may be achieved which yields a simple steady state relationship valid for long irradiation times in the case of photocatalysis as follows:

$$[H_2O_2]_{ss} = (\Phi_0/\Phi_1) \quad (28)$$

That is, the steady state concentration of H_2O_2 which is an intermediate as well as final product in the reaction as discussed in the foregoing sections is given by the ratio of intrinsic quantum yield for formation and decomposition of H_2O_2.

4. Conclusion

Hydrogen peroxide formed during the sono-, photo- and sonophoto-catalytic degradation of phenol in water in presence of ZnO is an intermediate as well as end product. H_2O_2 undergoes concurrent formation and decomposition resulting in oscillation in its concentration in sonocatalysis and stabilization in the case of photo and sonophotocatalysis. Various reaction parameters such

as catalyst loading, substrate concentration, pH, presence of air/O_2 etc. influence the maxima and minima in the oscillation curve. In the absence or at lower concentration of O_2, H_2O_2 itself functions as an electron acceptor and plays a significant role in the formation and decomposition of H_2O_2. Suspended particles which are not capable of functioning as sono, photo or sonophoto catalysts do not influence the oscillation process significantly. A mechanism taking into account the observations is proposed and discussed. H_2O_2 is an important water soluble trace gas species in the atmosphere which can undergo various reactions in presence of photocatalytically active suspended particulate matter resulting in active free radicals. This can affect the chemistry of upper atmosphere, making the study of the fate of H_2O_2 in presence of light and sound relevant from the climate change angle as well.

Acknowledgements

The authors wish to acknowledge financial support to J.K.P. from the University Grants Commission (India) by way of Junior Research Fellowship.

References

[1] M. Ying-Shih, S. Chi-Fanga, L. Jih-Gaw, Degradation of carbofuran in aqueous solution by ultrasound and Fenton processes: effect of system parameters and kinetic study, J Hazard. Mater. 178 (2010) 320–325.
[2] R.A. Torres, F. Abdelmalek, E. Combet, C. Petrier, C. Pulgarin, A comparative study of ultrasonic cavitation and Fenton's reagent for bisphenol A degradation in deionised and natural waters, J. Hazard. Mater. 146 (2007) 546–555.
[3] S.P. Devipriya, Suguna Yesodharan, Photocatalytic degradation of pesticide pollutants in water, Sol. Energy Mater. Sol. Cells 86 (2005) 309–348.
[4] M.N. Chong, B. Jin, C.W.K. Chow, C. Saint, New developments in photocatalytic water treatment technology: a review, Water Res. 44 (2010) 2997–3027.
[5] S.G. Anju, Suguna Yesodharan, E.P. Yesodharan, Zinc oxide mediated sonophotocatalytic degradation of phenol in water, Chem. Eng. J. 189–190 (2012) 84–93.
[6] C.G. Joseph, G.L. Puma, A. Bono, D. Krishniah, Sonophotocatalysis in advanced oxidation process: a short review, Ultrason. Sonochem. 16 (2009) 583–589.
[7] P. Ji, M. Takeuchi, T.-M. Cuong, J. Zhang, M. Matsuoka, M. Anpo, Recent advances in visible light-responsive titanium oxide-based photocatalysis, Res. Chem. Intermed. 36 (2010) 327–347.
[8] D. Pei, J. Luan, Development of visible light-responsive sensitized photocatalysts, Int. J. Photoenergy 2012 (2012) 1–13 (Article ID 262831).
[9] C.G. Wu, C.C. Chao, F.T. Kuo, Enhancement of the photocatalytic performance of TiO_2 catalysts via transition metal modification, Catal. Today 97 (2004) 103–112.
[10] T. Hada, A. Hattori, Y. Tokihisa, A patterned TiO_2/SnO_2 bilayer type photocatalyst, J. Phys. Chem. 104 (2000) 4587–4592.
[11] S. Sakthivel, M.V. Shankar, M. Palanichamy, A. Arabindoo, D.M. Bahnemann, B.V. Murugesan, Enhancement of photocatalytic activity by metal deposition: characterization and photonic efficiency of Pt, Au, and Pd deposited on TiO_2 catalyst, Water Res. 38 (2004) 3001–3008.
[12] S.P. Suja, Suguna Yesodharan, E.P. Yesodharan, Solar photocatalytic removal of chemical and bacterial pollutants from water using Pt/TiO_2 coated ceramic tiles, Int. J. Photoenergy 2012 (2012) 1–8 (Article ID 970474).
[13] P.R. Gogate, Treatment of wastewater streams containing phenolic compounds using hybrid techniques based on cavitation: a review of the current status and the way forward, Ultrason. Sonochem. 15 (2008) 1–15.
[14] R.A. Torres-Palma, J.I. Nieto, E. Combet, C. Petrier, C. Pulgarin, An innovative ultrasound, Fe^{2+} and TiO_2 photo assisted process for bisphenol a mineralization, Water Res. 44 (2010) 2245–2252.
[15] Y.C. Chen, P. Smirniotis, Enhancement of photocatalytic degradation of phenol and chlorophenols by ultrasound, Ind. Eng. Chem. Res. 41 (2002) 5958–5965.
[16] J. Madhavan, P.S. Sathish Kumar, S. Anandan, F. Grieser, M. Ashok Kumar, Sonophotocatalytic degradation of monocrotophos using TiO_2 and Fe^{3+}, J. Hazard. Mater. 177 (2010) 944–949.
[17] K.S. Suslick, L.A. Crum, in: M.J. Crocker (Ed.), Encyclopedia of Acoustics, vol. 1, Wiley Interscience, New York, 1997, pp. 271–282.
[18] V. Augugliaro, V. Loddo, L. Palmisano, M. Schiavello, Heterogeneous photocatalytic systems: influence of some operational variables on actual photons absorbed by aqueous dispersions of TiO_2, Sol. Energy Mater. Sol. Cells 38 (1995) 411–419.
[19] B. Jenny, P. Pichat, Determination of the actual photocatalytic rate of H_2O_2 decomposition over suspended TiO_2. Fitting to the Langmuir–Hinshelwood form, Langmuir 7 (1991) 947–954.
[20] I. Ilisz, K. Foglein, A. Dombi, Photochemical behavior of H_2O_2 in near UV – irradiated aqueous TiO_2 suspensions, J. Mol. Catal. A 135 (1998) 55–61.
[21] A. Keck, E. Gilbert, R. Koster, Influence of particles on sonochemical reactions in aqueous solutions, Ultrasonics 40 (2002) 661–665.
[22] H.B. Marschall, K.A. Morch, A.P. Keller, M. Kjeldsen, Cavitation inception by almost spherical particles in water, Phys. Fluids 15 (2003) 545–553.
[23] H. Ogi, M. Horoa, M. Shimoyama, Activation of TiO_2 photocatalysis by single bubble sonoluminescence for water treatment, Ultrasonics 40 (2002) 649–650.
[24] C. Wu, X. Liu, D. Wei, J. Fan, L. Wang, Photosonochemical degradation of phenol in water, Water Res. 35 (2001) 3927–3933.
[25] S.K. Pardeshi, A.B. Patil, A simple route for photocatalytic degradation of phenol in aqueous zinc oxide suspension using solar energy, Sol. Energy 82 (2008) 700–705.
[26] S.H. Szczepankiewicz, J.A. Moss, M.R. Hoffmann, Slow surface charge trapping on irradiated TiO_2, J. Phys. Chem. B 106 (2002) 2922–2927.
[27] N. Serpone, R. Terzian, P. Colarusso, Sonochemical oxidation of phenol and three of its intermediate products in aqueous media: catechol, hydroquinone and benzoquinone. Kinetic and mechanistic aspects, Res. Chem. Intermed. 18 (1992) 183–202.
[28] H. Gerischer, A. Heller, The role of oxygen in photooxidation of organic molecules on semiconductor surfaces, J. Phys. Chem. 95 (1991) 5261–5267.
[29] K.P. Jyothi, Sindhu Joseph, Suguna Yesodharan, E.P. Yesodharan, Periodic change in the concentration of H_2O_2 formed during the semiconductor mediated sonocatalytic treatment of waste water; investigations on pH effect and other operational variables, Res. J. Rec. Sci. 2 (2012) 1–14.
[30] Q. Li, Y. Wai, P. Wu, R. Xie, J.K. Shang, Palladium oxide nanoparticles on notrogen-doped titanium oxide: accelerated photocatalytic disinfection and post –illumination catalytic memory, Adv. Mater. 20 (2008) 3717–3723.
[31] K. Sekiguchi, C. Sesaki, K. Sakamoto, Synergistic effect of high frequency ultrasound on photocatalytic degradation of aldehydes and their intermediates using TiO_2 suspension in water, Ultrason. Sonochem. 18 (2011) 757–764.
[32] M.R. Hoffmann, S.T. Martin, W. Choi, D.F. Bahnemann, Environmental applications of semiconductor photocatalysis, Chem. Rev. 95 (1995). 69-06.
[33] C. Kormann, D.W. Bahnemann, M.R. Hoffmann, Photocatalytic production of hydrogen peroxide and organic peroxides in aqueous suspensions of titanium dioxide, zinc oxide and desert sand, Environ. Sci. Technol. 22 (1988) 798–806.

IOSR Journal of Applied Chemistry (IOSR-JAC)
ISSN: 2278-5736
PP 21-28
www.iosrjournals.org

Oscillation in the Concentration of H_2O_2 during Advanced Oxidation Processes: TiO_2 Mediated Sonocatalytic Degradation of Phenol

Sindhu Joseph[1],K. P. Jyothi[2], SugunaYesodharan[3], E. P. Yesodharan[4*]
[1,2,3,4]*School of Environmental Studies*
Cochin University of Science and Technology, Kochi 682022, India

Abstract: *Sono, photo and sonophotocatalysis are major Advanced Oxidation Processes (AOP) under intensive investigation as potential technologies for the removal of trace pollutants from water. The techniques involve the formation and participation of Reactive Oxygen Species (ROS) like ·OH, HO_2·, O_2^{-}·, H_2O_2 etc. Among these, H_2O_2 is the most stable and is also a precursor for the reactive free radicals. Current investigations on the TiO_2 mediated sonocatalytic degradation of phenol pollutant in water confirm our earlier findings using ZnO catalyst that H_2O_2 formed insitu cannot be quantitatively correlated with the degradation of the pollutant. The concentration of H_2O_2 formed does not increase corresponding to phenol degradation and reaches a plateau or varies in a wave-like fashion (oscillation) with well defined crests and troughs, indicating concurrent formation and decomposition. The number of maxima and minima or their precise occurrence at any point in time is unpredictable and inconsistent, indicating the complexity of the free radical process. The influence of various reaction parameters on the oscillation are identified and investigated in detail.*

Keywords: *Hydrogen peroxide, oscillation, sonocatalysis, titanium dioxide.*

I. INTRODUCTION

Advanced oxidation processes (AOPs) are generally used to degrade hazardous and non-biodegradable organic materials and convert them into carbon dioxide by producing •OH radicals during the oxidation process. Several kinds of AOPs (e.g. ultrasound, fenton, ozone and ultraviolet light) have been effectively used in the treatment of wastewater containing pesticides, phenols and azo dyes [1-5]. Major advantages of these AOPs include relatively mild reaction conditions and proven ability to degrade several toxic refractory pollutants.

Recently, Ultrasonic (US) irradiation mediated by suitable catalysts (sonocatalysis) has been receiving special attention as an environment - friendly technique for the treatment of hazardous organic pollutants in wastewater. However the degradation rate is slow compared to other established methods. Investigations aimed at enhancing the efficiency of US promoted decontamination of water are in progress in many laboratories. These include testing a variety of catalysts with different physico-chemical characteristics, modification of reactor design and reaction conditions, combining US with other AOP techniques etc [2-5]. Coupling US with Ultraviolet (UV) irradiation enhances the efficiency of semiconductor mediated degradation of aqueous pollutants synergistically [2, 6-8].

In liquids US produces cavitation which consists of nucleation, growth and collapse of bubbles. The collapse of the bubbles results in localized supercritical condition such as high temperature, pressure, electrical discharges and plasma effects [9]. The temperature of the gaseous contents of a collapsing cavity can reach approximately 5500^0C and that of the liquid immediately surrounding the cavity reaches up to 2100^0C. The localized pressure is estimated to be around 500 atmospheres resulting in the formation of transient supercritical water [10]. The cavities are thus capable of functioning like high energy micro reactors. The consequence of these extreme conditions is the cleavage of dissolved oxygen and water molecules into radicals such as H·, OH· and O· which will react with each other as well as with H_2O and O_2 during the rapid cooling phase giving HO_2· and H_2O_2. In this highly reactive nuclear environment, organic pollutants can be decomposed and inorganic pollutants can be oxidised or reduced. This phenomenon is being explored in the emerging field of sonocatalysis for the removal of water pollutants. Most of the studies on the sonocatalytic degradation of water pollutants are made using TiO_2 catalyst, mainly due to its wide availability, stability, non-toxicity and reactivity. Studies in our laboratory have shown that H_2O_2, one of the major products of sonocatalytic degradation of organic pollutants in water, undergoes simultaneous formation and decomposition during the degradation process [11-14]. This

results in oscillation in the concentration of H_2O_2. In this study the influence of various operational parameters on the oscillation of H_2O_2 in presence of TiO_2 under sonocatalysis is investigated in detail.

II. MATERIALS AND METHODS

Degussa P-25 TiO_2 (99% pure) consisting of approx. 70% anatase and 30% rutile is used as such without further purification. The average particle size was around 15-20 μm and the BET surface area was ~15 m^2/g. Phenol AnalaR Grade (99% purity) from Qualigen (India) was used as such without further purification. All other chemicals were of AnalaR Grade or equivalent. The sonocatalytic reactions were performed as reported earlier [11]. The concentration of phenol left behind was analyzed periodically by Spectrophotometry at 500 nm. H_2O_2 is determined by iodometry [12]. Mineralization was identified by the evolution of CO_2.

III. RESULTS AND DISCUSSION

Investigations on the sonocatalytic degradation of phenol using TiO_2 catalysts showed that no significant degradation took place in the absence of ultrasound or the catalyst suggesting that both catalyst and sound are essential to effect reasonable degradation. However, small quantity of phenol degraded under US irradiation even in the absence of catalysts (Fig.1).

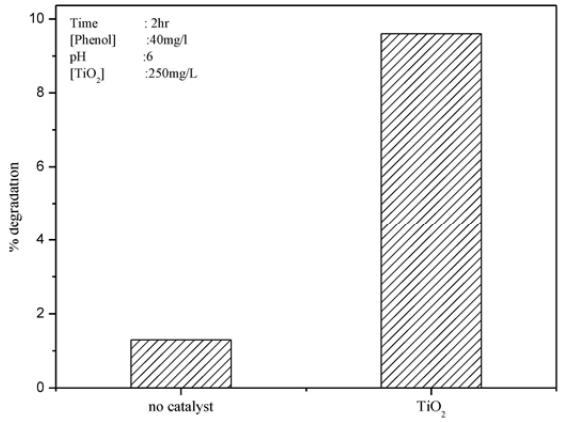

Figure 1: Sonocatalytic degradation of phenol

This is understandable since sonolysis of water is known to produce free radicals H· and OH· (via reaction 1), which are capable of attacking the organic compounds in solution [13].

H_2O >>> H· + ·OH (1) >>> indicates US

The free radicals thus produced can lead to the formation of H_2O_2 and degradation of phenol as follows:

$H· + O_2 \rightarrow HO_2·$ (2)
$HO_2· + HO_2· \rightarrow H_2O_2 + O_2$ (3)
$2\ ·OH \rightarrow H_2O_2$ (4)
Reactive oxygen species (·OH, HO_2· etc) + phenol → Intermediates → $H_2O + CO_2$(5)

However, there was no continuous increase in the concentration of H_2O_2 after the initial period possibly due to its parallel decomposition into water and oxygen as well as participation in the degradation of phenol [11, 12, 15]. At the same time the removal of phenol continued, though at a very slow rate. The sonocatalytic degradation of phenol as well as the fate of H_2O_2 formed in presence of TiO_2 at the optimized loadings is shown in Fig. 2a and b.

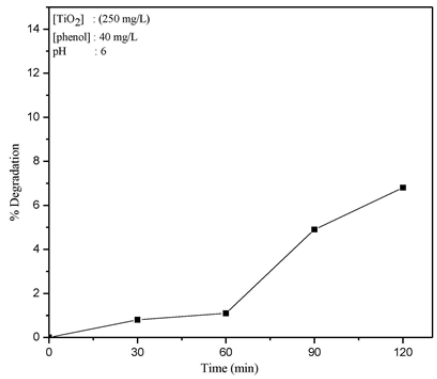

Figure 2a: Sonocatalytic degradation of phenol in presence TiO_2

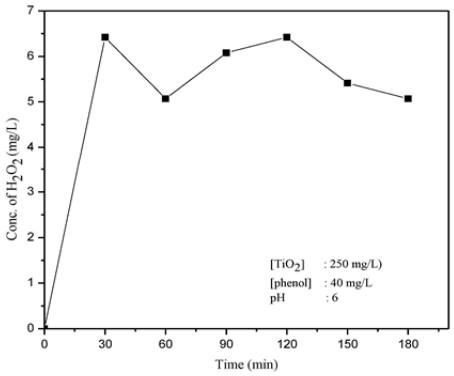

Figure 2b: Fate of H_2O_2 during the sonocatalytic degradation of phenol in presence of TiO_2

Sonochemical processes in aqueous media are facilitated in a heterogeneous environment such as the presence of suspended particles [9,10]. The presence of the particles helps to break up the microbubbles created by US into smaller ones, thus increasing the number of regions of high temperature and pressure. This leads to increase in the number of reactive OH radicals which will interact with the organic pollutants present in water and oxidise them, resulting in eventual mineralization. The increase in the optimum concentration of H_2O_2 in presence of particles was reported by Keck etal [16]. Instances of decrease in the concentration of H_2O_2 in presence of particles have also been reported [7]. Our studies presented in this report as well as in earlier papers show that both increase and decrease in the concentration of H_2O_2 is possible in the same system depending on the relative concentration of H_2O_2 and the substrate as well as other reaction parameters [12-14].

3.1 Effect of catalyst dosage

The effect of TiO_2 loading on the sonocatalytic degradation of phenol is shown in Fig. 3a. Optimum loading for the degradation of phenol is 0.25g/L. However, no such optimum is distinct in the case of the coproduct H_2O_2 as can be seen in Fig. 3b.

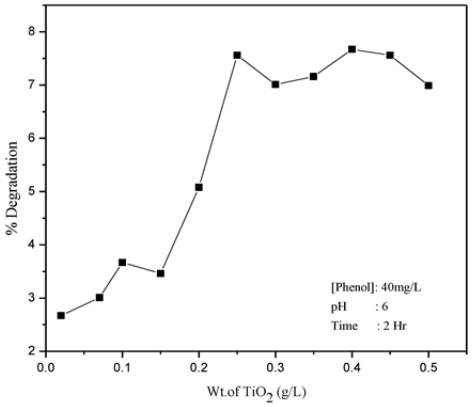

Figure 3a: Effect of catalyst loading on the degradation of phenol

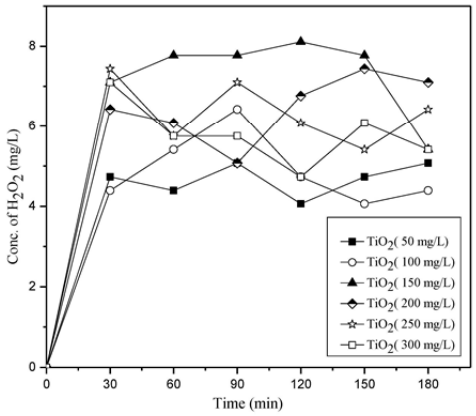

Figure3b: Effect of catalyst loading on the oscillation in the concentration of H_2O_2

Since the formation and decomposition of H_2O_2 are occurring in parallel all the time, optimization of catalyst loading with respect to H_2O_2 formation may not be reliable. In any case the maximum in the oscillation curve is high at higher loading of 0.20 and 0.25g/L. At catalyst dosage of 0.15 g/L, the H_2O_2 concentration remains steady for longer time and starts decreasing only after150 min. In this case the oscillation may set in later. This is consistent with earlier reported results on the unpredictability of H_2O_2 concentration at any point in the sono or photocatalysis. For these reasons the optimum loading of TiO_2 for phenol degradation is taken as the basis for further studies on the oscillation in the concentration of H_2O_2 also.

3.2 Effect of concentration of substrate

The effect of concentration of phenol on the rate of photocatalytic degradation has been investigated earlier [12-14]. The degradation increases with increase in the concentration of phenol up to an optimum level beyond which it levels off or decreases slightly, due to saturation of the catalyst surface. The degradation

follows pseudo first order kinetics at lower concentration and zero order at later stage. However the effect of varying concentration of phenol on the fate of H_2O_2 in TiO_2 sonocatalysis has not been investigated so far. Hence this aspect is examined here. As the concentration of phenol increases the maximum in the oscillation curve of H_2O_2 also increases (Fig. 4). The minimum also is relatively higher possibly because the rate of formation dominates rate of decomposition more frequently. This may be due to the formation of more ·OH radicals from phenol.

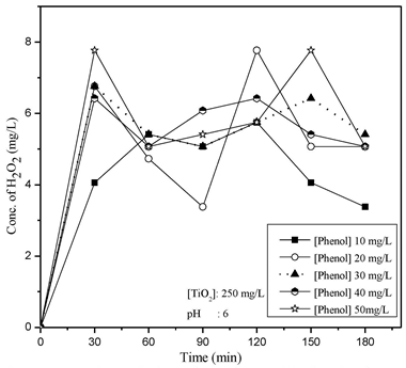

Figure 4: Effect of concentration of phenol on the oscillation in the concentration of H_2O_2

3.3 Effect of PH

The pH of the reaction medium is known to have strong influence on US or UV-induced degradation of organic pollutants. In photolysis, the possibility of bond breakage and the site might be different at different pH due to difference in the distribution of molecular charges. In sonocatalytic reaction, pH can alter the distribution of the pollutants in the bulk region, on the surface and at the site of the cavity collapse. The surface charge of semiconductors and the interfacial electron transfer and the photoredox processes occurring in their presence are also affected by pH. Previous studies [11] have shown that the degradation is more efficient in the acidic region than in the alkaline region. In the case of TiO_2 maximum degradation of phenol is observed at pH 6. The degradation continues to increase with time and eventually slows down at all pH. The pH effect is explained based on the point of zero charge (PZC) of TiO_2 and corresponding change in the absorption characteristics. The effect of pH on the fate of H_2O_2 is investigated and is shown in Fig. 5.

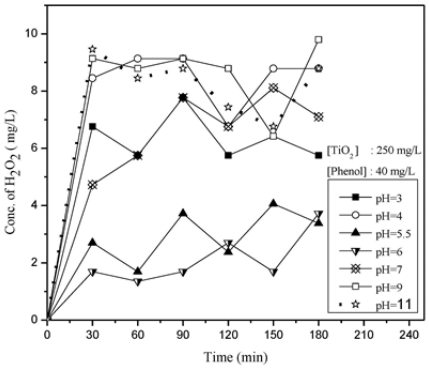

Figure 5: Effect of pH on the oscillation in the concentration of H_2O_2

At lower pH where the degradation of phenol is more, the net amount of H_2O_2 is relatively less. The oscillation occurs more frequently with lower concentration at both maxima as well as minima. This is probably because of the competition between phenol, various intermediates and H_2O_2 itself for the reactive free radicals, resulting in increased degradation of phenol and decreased accumulation of H_2O_2. At higher pH, the interaction with phenol is less and the free radicals can interact among themselves to form more H_2O_2. This result in higher net concentration of H_2O_2.In order to decipher the effect of phenol and its decomposition products on the oscillation, the sonocatalytic decomposition of H_2O_2 on TiO_2 was investigated in the absence of phenol under identical conditions (Fig. 6). In this case also the concurrent formation and decomposition of H_2O_2 is seen at all pH. Comparison of the results in the presence as well as the absence of phenol shows that the oscillation is more significant in presence of phenol. This illustrates the importance of interaction between the free radicals generated and phenol.

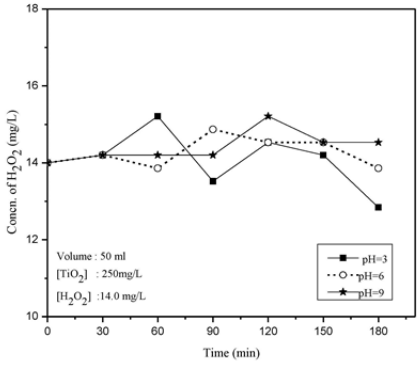

Figure6: Effect of pH on the fate of H_2O_2 during sonication in presence of TiO_2

3.4 Role of O_2 in the fate of H_2O_2

Presence of O_2 is essential for all AOPs which depend on the Reactive Oxygen Species. The degradation of phenol under sono and photocatalysis also has been proven to be inhibited in the absence of air/ O_2. The necessity of O_2 for the occurrence/propagation of oscillation is tested by deaerating the reaction system with N_2. The results are shown in Fig. 7.

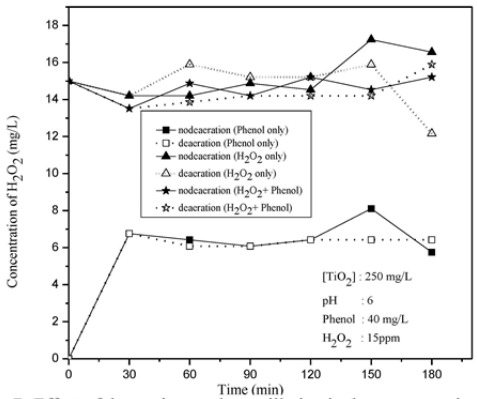

Figure7: Effect of deaeration on the oscillation in the concentration of H_2O_2

As stated earlier, small amount of $H_2O_2$is formed in sonocatalysis even in the absence of catalyst or phenol, possibly from sonolytic effect on water. The phenomenon of oscillation is observed even in the deaerated systems, though with much reduced maxima and minima in the concentration of H_2O_2, suggesting that once H_2O_2 is formed by whatever mechanism, subsequent decomposition and formation can take place even in the absence/reduced concentration of O_2. Here H_2O_2 itself can act as an electron acceptor and hole scavenger as follows:

$H_2O_2 + e^- \rightarrow {}^{\cdot}OH + OH^-$ (6)
$H_2O_2 + {}^{\cdot}OH/h^+ \rightarrow HO_2^{\cdot} + H_2O/H^+$ (7)

The $HO_2^{\cdot}$ or ${}^{\cdot}OH$ thus generated may also react on the surface either to regenerate H_2O_2 or degrade or mineralize the pollutants.

3.5 General mechanism

Sonocatalytic degradation is generally explained based on sonoluminescence and hot spot theory. Ultrasonic irradiation results in the formation of light of a comparatively wide wavelength range of 200 -500 nm. Those lights with wavelength below 375 nm can excite the semiconductor catalyst and generate highly active OH radicals on the surface. Thus the basic mechanism is partly that of photocatalysis. At the same time the more complex phenomenon of formation of hotspots upon implosion of some bubbles on the catalyst surface also leads to the formation of electron-hole pairs and excess OH radicals [17]. Since the formation of electron-hole pairs is the first step in both photocatalysis and sonocatalysis, the efficiency of the process depends on the ability to prevent their recombination. Under ultrasonic irradiation, a series of thermal and photochemical reactions take place on the surface of composite TiO_2 particles. The electron transport in the TiO_2 prevents the electron – hole recombination and increases the sonocatalytic activity.

The overall mechanism of H_2O_2 formation and decomposition under sonocatalytic conditions can be explained based on the formation and subsequent interaction of ${}^{\cdot}OH$ [13]. Recombination and a number of other reactions occur within the bubble as in reactions (8) and (9) following this primary radical generation as above.

${}^{\cdot}OH + {}^{\cdot}OH \rightarrow H_2O_2$ (8)
$H^{\cdot} + H_2O \rightarrow {}^{\cdot}OH + H_2$ (9)

Subsequently H_2O_2 is formed as in reactions (2) – (4). The H_2O_2 thus formed decompose concurrently as in reactions (6) and (7) above.

IV. CONCLUSION

Hydrogen peroxide formed during the sonocatalytic degradation of phenol in water in presence of semiconductor oxide TiO_2 undergoes concurrent formation and decomposition resulting in oscillation in its concentration. Various reaction parameters such as catalyst loading, substrate concentration, pH and presence of air/O_2 influence the phenomenon in general and the maxima and minima in the oscillation curve in particular. H_2O_2 plays a unique role in the process as acceptor of both electrons and holes. A general mechanism based on the observations is proposed and discussed.

V. Acknowledgement

The authors wish to acknowledge the financial support to KPJ from the University Grants Commission, India by way of Senior Research Fellowship.

REFERENCES

[1] M Ying-Shih M, S Chi-Fangaand L Jih-Gaw, Degradation of carbofuran in aqueous solution by ultrasound and Fenton processes: Effect of system parameters and kinetic study, *J Hazardous Mater, 178*, 2010, 320-325

[2] C.G Joseph, G.L Puma, A Bono and D Krishniah, Sonophotocatalysis in advanced oxidation process: A short review, *Ultrason.,Sonochem, 16*, 2009, 583-589

[3] J Moon, C.Y Yun, K.W Chung, M.S Kang and J Yi, Photocatalytic activation of TiO_2 under visible light using Acid red, *Catal. Today,87*, 2003, 77-86

[4] D Pei and J Luan, Development of visible light-responsive sensitized photocatalyst, *Int. J. of Photoenergy, article id262831*, 2012, 13 pages

[5] C.G Wu, C.C Chao and F.T Kuo, Enhancement of the photocatalytic performance of TiO_2 catalysts via transition metal modification, *Catal. Today, 97*, 2004, 103-112

[6] P.R Gogate , Treatment of wastewater streams containing phenolic compounds using hybrid techniques based on cavitation: a review of the current status and the way forward, *Ultrason., Sonochem, 15*, 2008, 1-15

[7] R.A Torres-Palma, J.I Nieto, E Combet, C Petrierand C Pulgarin, An innovative ultrasound, Fe^{2+} and TiO_2 photo assisted process for bisphenol a mineralization, *Water Res, 44*, 2010, 2245-2252

[8] Y.C Chenand P Smirniotis, Enhancement of photocatalytic degradation of phenol and chlorophenols by ultrasound, *Ind. Eng. Chem. Res, 41*, 2002, 5958-5965

[9] K.S Suslick and L.A Crum, Sonochemistry and sonoluminescence in Crocker M.J (Ed.), Encyclopedia of Acoustics,1 (New York: Wiley Interscience,1997)271-282

[10] E.A Nepiras, Acoustic cavitation: An introduction, *Ultrasonics, 22*, 1984, 25-40

[11] S.G Anju, Suguna Yesodharan and E.P Yesodharan, Zinc oxide mediated sonophotocatalytic degradation of phenol in water, *Chem. Eng. J. 189-190*, 2012, 84-93

[12] S.G Anju, K.P Jyothi, Sindhu Joseph, Suguna Yesodharan and E.P Yesodharan, Ultrasound assisted semiconductor mediated catalytic degradation of organic pollutants in water: Comparative efficacy of ZnO, TiO_2 and ZnO-TiO_2, *Res. J. Recent Sci. 1*, 2012, 191-201

[13] K.P Jyothi, SugunaYesodharan and E.P Yesodharan, Ultrasound (US), Ultraviolet light (UV) and combination (US + UV) assisted semiconductor catalysed degradation of organic pollutants in water: Oscillation in the concentration of hydrogen peroxide formed in situ *Ultrason. Sonochem, 21*, 2014, 1787–1796

[14] K.P Jyothi, Sindhu Joseph, Suguna Yesodharan and E.P Yesodharan, Periodic Change in the concentration of hydrogen peroxide formed during the semiconductor mediated sonocatalytic treatment of wastewater: Investigations on pH effect and other operational variables, *Res. J. Recent Sci.2*, 2013, 136-149

[15] A Kotronatou,G Mills and M.R Hoffmann, Ultrasonic irradiation of p-nitrophenol in aqueous solution, *Phys. Chem,95*, 1991, 3630-3638

[16] A Keck, E Gilbert and R Koster, Influence of particles on sonochemical reactions in aqueous solutions, *Ultrasonics, 40*, 2002, 661-665

[17] J Wang, Z Jiang, L Zhang, P Kang, Y Xie, Y Lv, R Xu and X Zhang, Sonocatalytic degradation of some dyestuffs and comparison of catalytic activities of nanosized TiO_2, nanosized ZnO and composite TiO_2/ZnO powders under ultrasonic irradiation, *Ultrason.Sonochem, 16*, 2009, 225-231

Semiconductor Mediated Photocatalytic Degradation of Plastics and Recalcitrant Organic Pollutants in Water: Effect of Additives and Fate of Insitu Formed H_2O_2

Phonsy P. D., Anju S. G., Jyothi K. P., Suguna Yesodharan, Yesodharan E. P.*

School of Environmental studies, Cochin University of Science and Technology, Kochi 682022, India

Abstract:
Contamination of water by chemical and bacterial pollutants as well as 'white pollution' caused by carelessly discarded waste plastics are major environmental problems. In the current study, the possibility of using semiconductor photocatalysis for the removal of last traces of organic water pollutants of different types is investigated. Semiconductors ZnO and TiO_2 were characterized by standard techniques and evaluated as photocatalysts. The pollutants tested include low density polyethylene plastics (PEP), phenol, catechol and organophosphorous pesticides such as phosphamidon, monocrotophos and dichlorvos. Hydrogen peroxide (H_2O_2) and peroxydisulphate (PDS) enhance the TiO_2 catalysed photomineralization rate. More than 10% of PEP could be irreversibly degraded in presence of UV-TiO_2-PDS in 300 hr time. The degradation is pH dependent in all cases though no thumb rule can be applied. H_2O_2 formed insitu during the degradation undergoes parallel decomposition resulting in stabilization or oscillation in its concentration depending on the equilibration or domination of the formation/ decomposition process. Anions naturally present in water such as NO_3^-, Cl^- and CO_3^{2-} inhibit the degradation while SO_4^{2-} enhances the same. However, this effect depends on a number of factors and no generalized conclusions are possible. The results and the probable mechanism for the degradation of the pollutants are discussed.

Keywords: Photocatalysis, Semiconductor, Monocrotophos, Phosphamidon, Dichlorvos, Phenol, Plastics

Introduction

Advanced Oxidation Processes (AOP) such as photocatalysis, sonolysis, fenton and photo-fenton, ozonation, radiolysis, UV/H_2O_2 etc are emerging as viable tools for the removal of chemical and bacterial pollutants from water. Photocatalysis is one of the most promising AOPs in view of its potential to harness solar energy as alternative natural resource under appropriate conditions (1-10). Semiconductor oxides such as TiO_2, ZnO, CdS, GaP etc have been extensively investigated as potential photocatalysts for the removal of toxic chemical and bacterial pollutants from water. Of these, ZnO and TiO_2 are the two most widely investigated photocatalysts for the purification of chemical- contaminated water. The advantages of TiO_2 include abundance, non toxic nature, stability and relatively lower cost. However, it absorbs mostly the UV region of solar spectrum, making it a poor candidate for harnessing solar energy. On the other hand, ZnO has been proven to have absorption over a wider range (8-10) though it suffers from the disadvantages of photocorrosion in acidic aqueous suspensions and incongruous dissolution to yield $Zn(OH)_2$ on ZnO particles leading to catalyst inactivation over time. Earlier studies have shown that by suitably modifying the reaction conditions, in particular the pH of the medium, this problem of corrosion/dissolution can be overcome to a great extent and optimum reaction parameters to take advantage of the wider solar absorption spectrum of ZnO can be identified (11, 12).

When a semiconductor is irradiated with photons of energy equal or greater than its band gap energy (3.2 eV in the case of TiO_2 as well as ZnO) the photons are absorbed and electron-hole pairs are created. These electrons and holes can either recombine or migrate towards the surface participating in several redox reactions eventually leading to the formation of Reactive Oxygen Species (ROS) such as OH radicals and H_2O_2 (1, 7). These transitory ROS can initiate and promote a number of reactions which end up in complete mineralisation of the pollutants into harmless products such as CO_2, water and salts as follows (2):

Semiconductor Semiconductor $\rightarrow$ $h^+ + e^-$ (1)
$h^+ + e^-$ $\rightarrow$ Heat (2)

*Corresponding author; E-mail: epyesodharan@gmail.com

ISSN 1203-8407

$O_2 + e^- \rightarrow O_2^{\cdot-}$ (3)

$O_2^{\cdot-} + 2\,H^+ + e^- \rightarrow H_2O_2$ (4)

$h^+_{VB} + H_2O \rightarrow H^+ + {}^{\cdot}OH$ (5)

${}^{\cdot}OH + {}^{\cdot}OH \rightarrow H_2O_2$ (6)

$h^+_{VB} + OH^- \rightarrow {}^{\cdot}OH$ (7)

Pollutant + ROS (H_2O_2, ${}^{\cdot}O_2^-$, $HO_2^{\cdot}$, $OH^{\cdot}$ etc) $\rightarrow$
Intermediates $\rightarrow H_2O + CO_2 +$ Salts (8)

The H_2O_2 formed does not increase corresponding to its formation since it is concurrently decomposing by a series of reactions taking place on the surface and in the bulk (11) resulting in the formation of more free radicals as follows:

$H_2O_2 + H^+ + e^- \rightarrow {}^{\cdot}OH + H_2O$ (9)

$H_2O_2 + {}^{\cdot}OH \rightarrow HO_2^{\cdot} + H_2O$ (10)

$H_2O_2 + 2h^+_{VB} \rightarrow O_2 + 2H^+$ (11)

$H_2O_2 + .OH/h^+_{VB} \rightarrow HO_2^{\cdot} + H_2O/H^+$ (12)

$HO_2^{\cdot} + .OH/h^+_{VB} \rightarrow O_2 + H_2O/H^+$ (13)

This simultaneous formation and decomposition of H_2O_2 leads to oscillation in its concentration as established in the case of sono, photo and sonophoto-catalytic degradation of organic pollutants in water (12). The fundamental mechanism of semiconductor photocatalysis (TiO_2 in this case) can be represented as in Figure 1 (6).

In the present paper we are reporting some of our findings on the ZnO and TiO_2 mediated photocatalytic degradation of a variety of environmental/water pollutants i.e. phenol and catechol (petrochemical pollutants), monocrotophos, phosphamidon and dichlorvos (organophosphorous pesticides) and polyethylene (PE) plastics. Some of these molecules were investigated earlier for their degradation under photocatalysis in presence of TiO_2 (13-18). However, to the best of our knowledge, there has been no systematic study on the photocatalytic degradation of these diverse water contaminants under identical conditions which is important in the design of multi-purpose photocatalytic reaction systems. Further, the fate of concurrently formed H_2O_2 also has not been investigated in detail as the focus was always on improving the efficiency of degradation of the pollutants. This study is intended to fill the gap, to a limited extent.

Experimental

Commercial ZnO and TiO_2 from Merck India Limited were used in the study. In both cases the particles were spherical and nonporous with >99% purity. The BET surface area of ZnO and TiO_2 were 12 and 15 m^2/g respectively. The average particle size in both cases was 10 x10^{-2} µm. Typical Scanning Electron Microscopy (SEM) images of ZnO and TiO_2 are shown in Figure 2a, b. TiO_2 consisted of approximately 70% anatase and 30% rutile. All reagents used were of AnalaR Grade or equivalent unless indicated otherwise. Dichlorvos, Phosphamidon and Monocrotophos (Technical grade) samples were from HIL, India. Phenol and catechol were from Qualigen India. All substrates were used as such without any extra purification. The solutions were prepared in doubly distilled water.

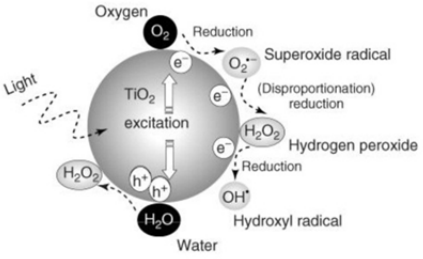

Figure 1. Mechanism of TiO_2 photocatalysis showing formation of OH free radicals and H_2O_2. (Ref. 6).

Photocatalytic experiments were conducted as explained earlier (12) using a high intensity UV lamp (400 W medium pressure mercury vapor quartz lamp). The reactor was a cylindrical pyrex vessel of 250 ml capacity. This was placed in a glass vessel of 1 litre capacity through which water from a thermostat at the required temperature was circulated. Unless mentioned otherwise, the reaction temperature was maintained at 29±1^{0}C. The irradiation was done from above. The pH of the reaction system was kept at the natural value for each pollutant suspension i.e. 5.5-6. The pollutant concentration at various intervals of irradiation was determined by drawing samples at desired intervals, centrifugation to remove suspended particles and analysis using UV-VIS spectroscopy (Phenol, 500 nm), Gas Chromatography (GC) with Flame Ionization Detector (Phosphamidon, Catechol), GC with Electron Capture Detector (Dichlorvos) and High Performance Liquid Chromatography with UV detector (Mono-crotophos). Mineralisation was confirmed by verifying that the total organic carbon (TOC) content (measured using TOC analyzer model Elementar analysensysteme GmbH.) and Chemical Oxygen Demand (measured by standard methods) are 'nil' and by qualitatively measuring CO_2 evolution during the irradiation. H_2O_2 was determined iodometrically.

For experiments with plastics, widely used PE plastic bags of approximately 30 µm size abandoned

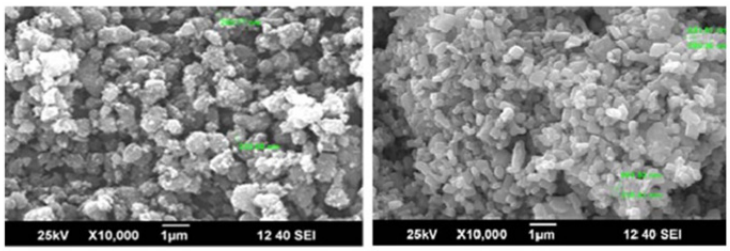

Figure 2. Typical SEM image of (a) TiO_2 (b) ZnO.

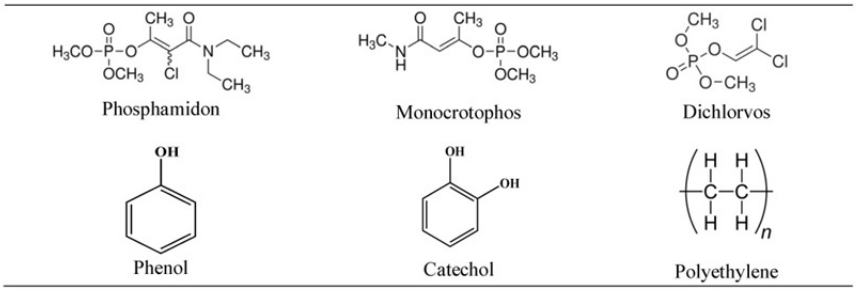

Figure 3. Chemical structures of various water pollutants subjected to the study.

in the open were collected, washed, dried, sorted and cut into small thin strips of approximately 6 cm length and 1 cm width. They were immersed in catalyst suspension in water and irradiated by UV light as done in the case of regular photocatalytic experiments. The degradation was monitored by weight loss at regular intervals, SEM, decrease in tensile strength and physical appearance. The chemical structures of the molecules are given in Figure 3.

Results and Discussion

Control experiments showed that both light and catalyst are essential for the degradation of all pollutants. The degradation was negligible in all cases in the absence of UV light in presence of catalyst or in the presence of catalyst in the absence of light. The decrease in concentration of the substrate in these cases is from 0.5 to 2% which may be due to adsorption on the catalyst. This is treated as insignificant when compared with the degradation under photocatalytic conditions.

As expected, UV light is more efficient than visible light to effect the degradation. The degradation in presence of TiO_2 and ZnO is fairly comparable in presence of UV light in the case of all pollutants tested here (Figure 4). In the case of phenol (PH) and catechol (CC), the degradation is slightly more in presence of ZnO. In the case of the three organophosphorous pesticides, i.e. phosphamidon (PPM), monocrotophos (MCP) and dichlorvos (DC), TiO_2 is more efficient. Similarity in the extent of degradation of structurally similar phenol and catechol as well as monocrotophos and phosphamidon shows that, in addition to the characteristics of the catalyst and the irradiation source, the substrate structure and hence the substrate-surface interaction are also important in the degradation process. In fact catechol is formed as an intermediate in the photocatalytic degradation of phenol along with many other products (19, 20). The intermediate is equally vulnerable to photocatalytic oxidation as the original compound. Adsorption studies of the two compounds independently and in combination also showed that these two get adsorbed on ZnO and TiO_2 at comparable rates and quantities (20). Hence the concentration of catechol detected as an intermediate during the photocatalytic degradation of phenol is often negligible.

Of the two catalysts, TiO_2 is often rated as superior from the commercial application angle because of its higher chemical stability over wide pH range,

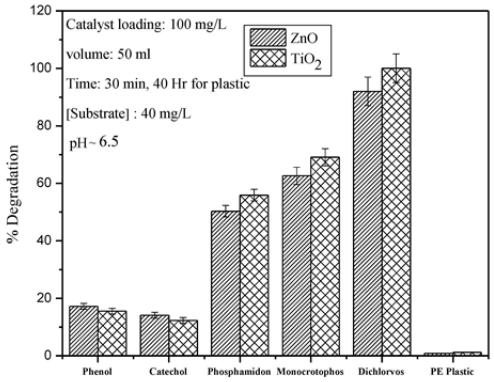

Figure 4. Comparison of ZnO and TiO_2 as photocatalysts for the degradation of various pollutants.

availability and economy. Hence further studies were carried out using TiO_2 as the catalyst.

Effect of Catalyst Loading

The effect of catalyst loading on the degradation of each of the pollutant (excluding the plastic, which is dealt with separately in the later part of this paper) is shown in Figure 5. Since it is more reliable to compare the effect of loading in the early stages of reaction before the influence of intermediates or reaction products set in, the results after 30 minutes of irradiation are considered here. The optimum loading is more or less the same, i.e. 0.1 g/L for all pollutants except in the case of the relatively more complex-structured phosphamidon for which the value is 0.15 g/L. This indicates that the major factors influencing the optimum catalyst loading are the catalyst itself and to a limited extent the structure of the reactant as long as the irradiation source and reactor geometry are kept constant. Increase in the number of effective surface sites with increase in concentration of the catalyst result in enhanced production of reactive free radicals. The number of pollutant molecules adsorbed on the surface also increases due to increased availability of catalyst particles. Stabilization or decrease in the rate of degradation beyond the optimum catalyst loading may be due to the screening effect of excess catalyst particles in the solution. Agglomeration and sedimentation of the particles also occur at higher loading leading to ineffective absorption of light and light scattering resulting in decreased catalyst activation.

Kinetics

The kinetics of degradation of each of the pollutant is determined by varying the concentration keeping all

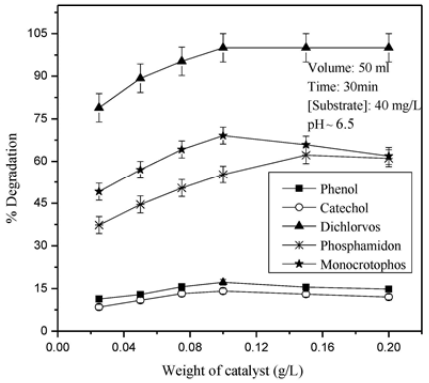

Figure 5. Effect of catalyst concentration on the degradation of various pollutants.

other parameters constant. In most cases, the photocatalytic degradation of organic compounds in water is known to follow pseudo-first order kinetics which is rationalized in terms of the Langmuir-Hinshelwood model modified to accommodate reactions occurring at solid-liquid interface (21-24). Assuming that there is no competition with reaction intermediates/ byproducts, the simplest representation for the rate of degradation of the pollutant is as follows (25):

$$-dC/dt = r_0 = k_r K C_0/ (1 + K C_0) \quad (14)$$

where r_0 is the initial rate of disappearance (mgL^{-1} min^{-1}) of the pollutant, C_0 (mgL^{-1}) its initial concentration, K the equilibrium adsorption constant and k_r,

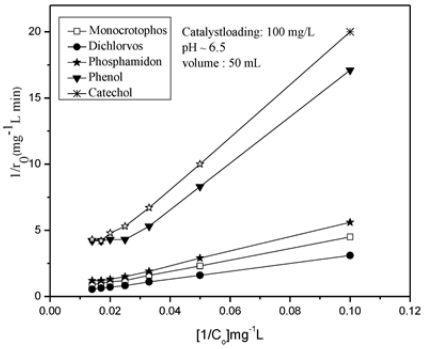

Figure 6. Reciprocal kinetic plot for the photocatalytic degradation of various pollutants.

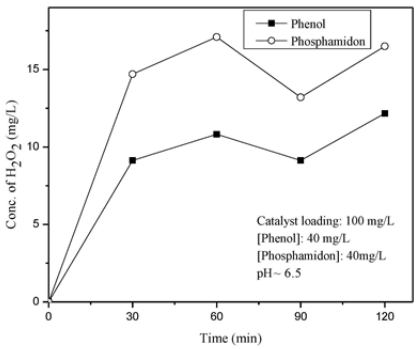

Figure 7. Fate of H_2O_2 formed during the photocatalytic degradation of phenol and Phosphamidon.

the limiting reaction rate constant at maximum coverage for the experimental conditions. Equation 14 can be rewritten as

$$1/r_0 = 1/k_r + 1/k_rK * 1/C_0 \quad (15)$$

A plot of $1/r_0$ vs $1/C_0$ will yield a straight line if the degradation follows apparent first order kinetics. Figure 6 shows that in the case of the pollutants investigated here, this relation holds good, especially in the lower concentration range. However in the case of phenol and catechol, and to limited extent in the case of monocrotophos and phosphamidon, the rate of degradation slows down at higher substrate concentration and stabilises eventually thereby decreasing the order of the reaction and reaching zero order. In the concentration range studied here the degradation of dichlorvos was always higher and the reaction followed apparent first order kinetics throughout. At higher concentration of the substrates at least a part of the UV light may be absorbed by them blocking the availability of light to the catalyst (26). Another reason for the decrease in degradation at higher concentration of the substrate may be that the intensity of radiation may not be reaching all the molecules, especially those on the other side of the reactor, away from the reaction zone due to retardation of the penetration of light (27). At low substrate concentrations, the number of catalytically active sites will not be a limiting factor and the rate of degradation is proportional to the substrate concentration in accordance with apparent first order kinetics. At high substrate concentration, the adsorbed reactant molecules and/or the respective intermediates may occupy all or most of the catalytically active sites and this leads to zero order kinetics. But the intensity of light, illumination time and catalyst concentration are constant. The concentration of active electron-hole pair generated and the reactive species formed i.e. $^{\cdot}OH$, $HO_2^{\cdot}$, H_2O_2, $O_2^{\cdot-}$ etc. also are at the maximum. Thus at higher concentrations of the substrate, the relative ratio of the reactive species available for interacting with the pollutant molecules is less. Similarity in the kinetics of degradation of different pollutants on the same catalyst indicates that the mechanism of surface-initiated processes also may be similar.

Fate of H_2O_2

One of the major products of photocatalytic degradation of organic pollutants in water is H_2O_2 which functions as a reactant, intermediate and end product. However, the concentration of H_2O_2 does not increase corresponding to the degradation and often stabilises or undergoes oscillation with periodic increase and decrease (12). Similar results have been reported in the case of sonocatalytic degradation of organic pollutants in water (28). In the present study also formation of H_2O_2 is detected during the photocatalytic degradation of all five substrates. The fate of H_2O_2 is followed in the case of two typical substrates i.e. phenol and phosphamidon under optimized reaction conditions. The results are plotted in Figure 7. As seen from the figure, the concentration of H_2O_2 is smaller than expected from the decomposition of phenol or phosphamidon indicating that H_2O_2 formed may itself be decomposing or participating in other reactions. H_2O_2 is known to decompose under photocatalytic conditions to $^{\cdot}OH$ and $HO_2^{\cdot}$ radicals as in reactions 9 and 10. Further H_2O_2 itself is a good electron acceptor capable of preventing the recombination of photogenerated electrons and holes on the surface. This

Table 1. Effect of anions on the photocatalytic degradation of water pollutants
[Pollutant]: 40 mgL^{-1}, [TiO_2]: 100 mgL^{-1}, pH: ~5.5-6, Time: 30 min, [Anion]: $4x10^{-1}$ mg L^{-1}

	% Degradation of the pollutant				
Anion	DC	MCP	PPM	PH	CC
None	90.5	61.7	50.0	16.5	12.0
Cl^-	78.0 (-13.8)	42.5 (-31.1)	42.2 (-15.6)	11.2 (-26.1)	9.8 (-22.4)
SO_4^{2-}	85.9 (-5.1)	64.3 (+4.2)	53.6 (+7.2)	16.9 (+2.4)	14.1 (+17.5)
CO_3^{2-}	81.2 (-10.3)	56.5 (-8.4)	44.8 (-10.4)	14.0 (-15.2)	9.9 (-17.5)
NO_3^-	84.5 (-6.6)	55.4 (-10.2)	48.5 (-3.0)	14.9 (-9.7)	11.5 (-4.2)
	(% change within brackets)				

concurrent formation and decomposition of H_2O_2 result in oscillation. In the beginning of the pollutant degradation, when the concentration of H_2O_2 is smaller, the formation process dominates. Once a critical maximum is reached, the free radicals generated in the system interacts with H_2O_2 more frequently resulting in its decomposition. This continues until the critical minimum is reached when the formation process picks up again. The reactive free radicals generated insitu in the system, including those formed by the decomposition of H_2O_2, participate in a series of reactions which result in further formation as well as decomposition of H_2O_2. Hence it will be difficult to correlate the amount of H_2O_2 at any point in time during the photocatalytic reaction with the substrate degradation or other surface initiated processes. Yi et al (29) showed using Cavity Ring Down Spectroscopy (CRDS) that even the $HO_2^{\cdot}$ radicals formed by decomposition of H_2O_2 cannot be correlated with the latter. This illustrates the complex nature of free radicals and their interactions in photocatalytic systems, which influences the role and fate of H_2O_2. The surface initiated free radical interactions eventually continue in the bulk as well until the degradation of the pollutant is completed, various active free radicals are deactivated by interactions and/or the system is stabilized. Various steps involved in the formation and decomposition of H_2O_2 and related interactions, in addition those listed in steps 9-13 may be summarized as follows:

$$H_2O_2 + h\nu \rightarrow 2^{\cdot}OH \quad (16)$$

$$H_2O_2\,(bulk) \rightarrow H_2O_2\,(ad) \quad (17)$$

$$HO_2^{\cdot}\,(ad) + HO_2^{\cdot}\,(ad) \rightarrow H_2O_2\,(ad) + O_2\,(ad) \quad (18)$$

$$O_2(ad) + e^- + H_2O \rightarrow HO_2^{\cdot}\,(ad) + HO^-\,(ad) \quad (19)$$

$$HO_2^{\cdot}\,(ad) + e^- + H^+ \rightarrow H_2O_2\,(ad) \quad (20)$$

$$H_2O_2\,(ad) + e^- \rightarrow .OH\,(ad) + HO^-\,(ad) \quad (21)$$

$$HO_2^{\cdot}\,(ad) \rightarrow HO_2^{\cdot}\,(bulk) \quad (22)$$

$$HO^-\,(ad) \rightarrow HO^-\,(bulk) \quad (23)$$

$$H_2O_2\,(ad) \rightarrow H_2O_2\,(bulk) \quad (24)$$

$$O_2\,(ad) \rightarrow O_2\,(bulk, gas) \quad (25)$$

Yi et al (29) demonstrated that photocatalytic decomposition of H_2O_2 proceeds in a unique way as it plays simultaneously the role of electron and hole scavenger. The initial electron or hole transfer to H_2O_2 generate $HO_2^{\cdot}$ or $^{\cdot}OH$ which may further react on the surface or desorb into the bulk. The desorption of OH radicals from the surface of TiO_2 to the bulk has been proven by single molecule imaging using fluorescence spectroscopy (30).

Effect of Anions

Wastewater contains different salts which are either naturally present or introduced from industrial and other human activities. The salts will normally remain in ionized form in water and can influence the photocatalytic degradation of trace organic pollutants. Accordingly we have investigated the effects of four typical anions commonly found in water, i.e. chloride, sulphate, carbonate and nitrate. Preliminary results are shown in Table 1.

Chloride ion shows maximum inhibition in all cases followed by Carbonate ion except in the case of monocrotophos where inhibition by Nitrate is slightly more than that by Carbonate. Sulphate ion enhances the degradation in all cases except in the case of dichlorvos where the degradation as such in the absence of any additive is very high (>90%). In the case of chloride ions, the inhibition is expected as it can get better adsorbed on the TiO_2 surface under the reaction conditions, thereby depriving the substrate molecules from interacting with the surface and getting activated. Cl^- ions also act as a scavenger of the photoproduced OH radical (31) as follows:

$$^{\cdot}OH + Cl^- \rightarrow Cl^{\cdot} + OH^- \quad (26)$$

Though the $Cl^{\cdot}$ radicals are also capable of oxidizing the pollutants, the rate will be lower than that of $^{\cdot}OH$ radicals due to the lower oxidation power of the former (32). The inhibition caused by carbonate ion also may be explained by their reaction with the reactive OH radicals (33).

$$CO_3^{2-} + {}^{\cdot}OH \rightarrow CO_3^{\cdot-} + HO^{\cdot-} \quad (27)$$

The effect of NO_3^- ions on the degradation seems to depend more on the substrates. In the case of phosphamidon and catechol, the effect, though slightly negative, can be treated as negligible. In the case of other substrates, the degradation is inhibited probably due to the competitive adsorption by NO_3^- and reduction in the number of sites available for the substrate and consequent depletion of reactive species. The lower inhibition compared to other anions tested here can be explained based on the weak adsorption of NO_3^- ions on TiO_2 (34). The enhancement of photocatalysed degradation by SO_4^{2-} ions has been observed by many authors and the most consistent explanation offered is as follows (31, 35, 36):

SO_4^{2-} gets adsorbed on the surface and interacts with the photoproduced holes

$$h^+ + SO_4^{2-} \rightarrow SO_4^{\cdot-} \quad (28)$$

Since S is a strong oxidizing agent, the sulphate radical can accelerate the degradation process according to the reaction (36):

$$SO_4^{\cdot-} + H_2O \rightarrow SO_4^{2-} + {}^{\cdot}OH + H^+ \quad (29)$$

$$SO_4^{\cdot-} + \text{Pollutant} \rightarrow SO_4^{2-} + \text{Intermediate 1} \quad (30)$$

$$SO_4^{\cdot-} + \text{Intermediate1} \rightarrow \cdots\cdots \rightarrow SO_4^{2-} + CO_2 + \text{Salts} \quad (31)$$

Intermediate 1 represents first reaction intermediate, which may go through many reactions before eventual mineralization. As seen in reaction 29, presence of SO_4^{2-} can lead to the formation of extra ${}^{\cdot}OH$ radicals which can enhance the degradation. Further SO_4^{2-} radicals are also strong oxidizing agents. The two highly reactive free radical species together can more than compensate for the inhibition caused by the depletion of surface sites taken up by the sulphate ions. However, this need not be true for all substrates as seen in the inhibition caused by SO_4^{2-} in the case of dichlorvos. In this case, since the conversion of dichlorvos is quite facile, the net concentration of the substrate will be relatively less in the early stage of the reaction itself. Hence the adsorption by SO_4^{2-} can dominate resulting in decreased adsorption and degradation of dichlorvos at later stages. Our ongoing studies show that in the case of certain anions, the initial trend gets reversed at later stages of reaction and this is being investigated in detail. Hence the effect of anions on the photocatalytic degradation of organic pollutants on any particular catalyst cannot be generalized. This is evident from the contradicting results on this aspect from different research groups. The structure of the substrate, characteristics of the catalyst, concentration of the anion, pH of the medium, reaction time etc can influence the behavior of the anion which needs to be investigated in detail in each case.

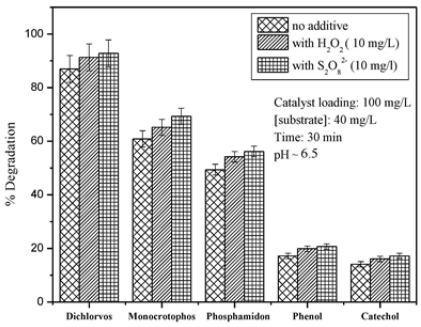

Figure 8. Effect of H_2O_2 and $S_2O_8^{2-}$ on the photocatalytic degradation of various pollutants.

Effect of Oxidizing Agents

H_2O_2 and peroxydisulphate (PDS) are two oxidants known to enhance the photocatalytic degradation of organic pollutants in water (25, 37-40). In order to confirm this in the present context, the effect of these two oxidants on the degradation of the pollutants being investigated here is examined and the results are shown in Figure 8. The oxidants alone at concentrations of < 20 mg/L, in the absence of any catalyst, do not cause any significant degradation (1-2.5% only) under standardized experimental conditions. In typical photocatalytic experiments the degradation increases moderately with the addition of 10 mg/L of H_2O_2 or PDS. The effect is dependent on the H_2O_2 /substrate ratio (25, 39, 41) and hence study of the concentration effect of H_2O_2 is important which is underway currently. The results will be reported later. H_2O_2 is known to function as an electron acceptor which can prevent the recombination of electrons and holes thus enhancing the degradation (24, 27, 39). H_2O_2 can also produce ${}^{\cdot}OH$ radicals by insitu decomposition. The Concurrent formation and decomposition of H_2O_2 in photocatalytic systems leading to its oscillation is reported in many cases (11, 12, 20) as well as earlier in this paper. The reaction between the hydroxyl radicals generated in the system and the substrate is expected to occur at or near the surface of the semiconductor as no OH radicals are produced by direct photolysis without the catalyst. However, once the surface initiated reaction has begun the OH radicals generated can propagate the decomposition of H_2O_2 in liquid phase as well as on

the catalyst surface. This will result in the formation of more reactive OH radicals for interaction with the pollutant. However at higher concentration of H_2O_2, the OH radicals will interact more with the former than with the pollutant molecule and hence the effect may be negative. Since the precise concentration of H_2O_2 is unpredictable at any point of time due to these competing reactions, generalized conclusions or predictions on the exact effect of added H_2O_2 on the degradation of different pollutants may not be desirable. For each pollutant, the concentration of H_2O_2 to be added to achieve maximum degradation/ mineralisation needs to be optimized. Various reactions in this respect leading to the formation of reactive free radicals from H_2O_2 and subsequent rinteractions are listed in equations 9-13 and 16-25.

Hydroxyl radical has 2.05 times more oxidation power than chlorine, 1.58 times the oxidation power of H_2O_2 and 1.35 times the oxidation power of ozone (42). This implies that H_2O_2 formed insitu should also enhance the degradation, though the efficiency is much lower compared to its decomposition product $^{\bullet}OH$. Since the effect is similar in all cases, irrespective of the characteristics of the substrate, it may be inferred that the catalyst and the surface-initiated free radical processes are more important determinants of the H_2O_2 effect.

The enhancement is slightly more in presence of PDS than H_2O_2 under identical conditions, as seen in the figure. This may be because, the persulphate in addition to trapping the electrons and preventing their recombination with the holes also produces sulphate radical which itself is a very strong oxidizing agent whose reduction potential E_0 is 2.6V (25). The reactions leading to the formation of reactive sulphate radical is:

$$S_2O_8^{2-} + e^- \rightarrow SO_4^{2-} + SO_4^{\bullet-} \quad (32)$$

Further reactions which result in enhanced degradation of the pollutant is shown earlier in reactions 28-31.

The inhibition caused by SO_4^{2-} in the degradation of dichlorvos is not seen in the presence of PDS. Hence, it may be presumed that the inhibition contributed by the occupation of active surface sites by the former is more than compensated by the trapping of photogenerated electrons by the latter which prevent the recombination of electrons and holes. This, in turn facilitates the formation of various ROS that is responsible for the enhancing effect by PDS.

pH Effect

Solution pH has profound influence on the oxidation potential and surface charge of semi-

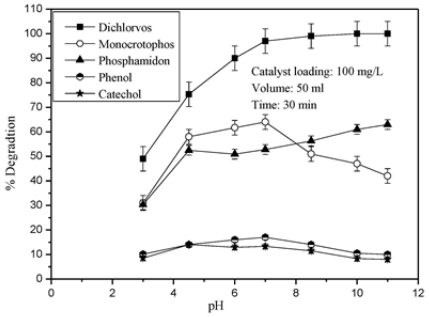

Figure 9. Effect of pH on the photocatalytic degradation of various pollutants.

conductor oxides. Consequently adsorption and degradation of the pollutant also may be affected (26). In the current study, the effect of pH on the degradation of the pollutants is studied in the range 3-11. The results are presented in Figure 9. The results show that there is no clear pattern or predictability in the effect of pH on the photocatalytic degradation of pollutants. As the figure shows, in all cases except in the case of dichlorvos and phosphamidon, the degradation increases with increase in pH, reaches a maximum around the neutral range of 6-7 and decreases again. The effect of pH is usually attributed to the surface charge of the semiconductor and its relation with the ionic form of the organic compound (25). Electrostatic attraction or repulsion between the catalyst surface and the organic molecule takes place which in turn can enhance or reduce the photocatalytic degradation rate. In the case of TiO_2 its point of zero charge (pzc) is ~ 6.8 below which the surface is positively charged. In the alkaline condition, the surface is negatively charged. The ionization state of the surface of TiO_2 under acidic and alkaline conditions is as shown below.

$$\equiv Ti^{iv}\text{-}OH + H^+ \leftrightarrow \equiv Ti^{iv}\text{-}OH_2^+ \quad (33)$$

positively charged below pH ~ 6.8

$$\equiv Ti^{iv}\text{-}OH + OH^- \leftrightarrow \equiv Ti^{iv}\text{-}O^- + H_2O \quad (34)$$

negatively charged above pH ~ 6.8

In the case of monocrotophos, it is observed that the degradation is maximum at around the pzc of TiO_2. The pKa value of monocrotophos is 4.4. The protonated form predominates in the extreme acidic pH while it exists in the anionic form at higher pH. Hence monocrotophos will not get adsorbed on the catalyst surface in the acidic range, especially below pH 4.5 which explains the lower degradation. Above pH 4.5, monocrotophos gets deprotonated. Hence the

repulsion is not there and the monocrotophos molecules may get adsorbed or come closer to the surface at least upto pH 6.8. This is consistent with the optimum degradation in the pH range of 6-7. However, there is still good amount of degradation in the alkaline range where the adsorption is expected to be minimal. Hence more than the adsorption, other factors favor the degradation of monocrotophos in alkaline pH. Similar results are reported by Sankar et al (43).

In the case of dichlorvos, the degradation increases steadily and reached 100% above pH 8.5, i.e. the degradation doubled as the pH varied from 3 to ~ 9. Dichlorvos is known to hydrolyze in alkaline media which also may have contributed to the higher degradation at least marginally in the presence of the faster photocatalytic process. Since dichlorvos is an unionizable compound, the increase in degradation in the alkaline range can be attributed to the high hydroxylation of the catalysts surface due to the presence of large quantity of OH^- ions. Consequently more OH radicals are formed and the overall rate is increased. The degradation of phosphamidon also follows similar trend as dichlorvos and the degradation is more in the alkaline pH (23). In the case of phenol the degradation increases as the pH is increased from 3 to 7. The degradation remained fairly stable in the neutral pH range and decreased again. In the case of catechol, maximum degradation is seen in the pH range of 4.5-7, remains fairly steady in this range and decreases thereafter. Higher degradation of phenol and catechol in the acidic range is understandable since they remain mainly in the neutral form and can get adsorbed onto the positively charged surface. In the alkaline region, the surface is negatively charged and the phenolate anions get repelled resulting in lower degradation. However Yang et al (44) reports that the photoelectrocatalytic degradation of 4-chlorophenol at TiO_2 electrode is higher at pH 10 contrary to what might be expected from the repulsive forces between the phenolate anions and the surface. This is explained based on the enhanced formation of OH radicals at the alkaline pH (45).

The results thus clearly show that the point of zero charge of the semiconductor catalyst and consequent adsorption of the substrate are important factors that determine the pH effect on photocatalysis. At the same time, these are not the only critical factors as is evidenced by the fair amount of degradation in the alkaline range. There cannot be any thumb rule for predicting or interpreting the effect of pH on the photocatalytic degradation of organic pollutants on semiconductor oxides. For e.g. the three organo-phosphorous pesticides considered here behave differently with respect to the optimum degradation and corresponding pH irrespective of structural similarities. In the case of phenol and catechol the trend remains fairly similar even though the pH at which maximum degradation occurred varies. Multiple factors such as variation in the surface characteristics of the semiconductor oxide, electrostatic interactions between the substrates, intermediates, solvent molecules, charged radicals, reactive oxygen species etc. may be influencing the pH effect. Similar inferences were made by other researchers also (46).

In general, the change of surface charge of the catalyst with pH can be exploited to favor adsorption of the active species. Adsorption of anionic substrates on TiO_2 and hence their degradation is favored in the lower pH range where the surface is positively charged. Similarly the degradation of some phenols decreases with increasing pH because they can dissociate and can be repelled by a negatively charged surface (47). From the observations it may be inferred that the total photocatalytic degradation is not just a surface phenomenon. At the same time the activated surface is essential for the generation of various reactive species and free radicals. Once this initiating step is executed, close neighborhood of the surface as well as the bulk of the system can also host the subsequent degradation reaction steps. When the structural orientation of the molecules favor, respective reactive species under acidic or alkaline conditions may interact with the surface and result in degradation and eventual mineralisation. The results points to the need for conducting experiments at different pH values for each substrate on each catalyst in order to identify the most efficient degradation conditions.

Photocatalytic Degradation of Plastics

Since TiO_2 mediated photocatalysis has been found to be an efficient method for the degradation of a variety of water pollutants the technique was explored for the mineralisation of extremely recalcitrant environment pollutant of the day, i.e. low density PE plastics (PEP). Comparative degradation of samples of carelessly thrown away plastics in presence of UV irradiation mediated by ZnO and TiO_2 is shown in figure 4. Accordingly TiO_2 is found to be a better catalyst and is hence chosen for detailed studies. Total Organic Carbon determination in water in which the plastic strip was suspended and irradiated in presence of TiO_2 reveal that there is no carbon left behind in solution thus confirming that the degradation does not lead to the formation of any stable intermediate and it results in complete mineralisation. The intermediates may be getting degraded faster than the plastic itself.

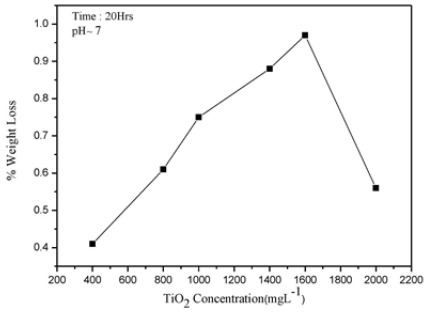

Figure 10. Effect of catalyst loading on the photocatalytic degradation of PE plastics.

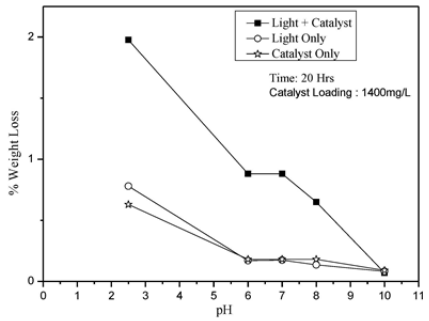

Figure 11. Effect of pH on the photocatalytic degradation of PE plastics on TiO_2.

The effect of catalyst loading on the degradation of the plastic is shown in Figure 10. As in the case of other substrates, in this case also there is an optimum catalyst dosage. Accordingly ~1400 mg/L is the optimum catalyst weight under the reaction conditions and this quantity is chosen for further studies. The effect of pH on the TiO_2 photocatalysed degradation of plastic is determined and the result is shown in Figure 11. Acidic pH favours slight degradation of plastic even in the absence of catalyst or light. However from pH 6 onwards, it does not have any effect on the degradation of the plastic in the presence of light in the absence of TiO_2 or in the presence of TiO_2 in the dark. Extreme acidic conditions may not be feasible from the environmental or economical angle in view of the need for subsequent neutralization and other processes. Hence all further investigations are made in TiO_2-natural water suspension whose pH is 6.5-7.

As in the case of photocatalytic degradation of organic pollutants, H_2O_2 is detected in the case of PEP degradation also. However, its concentration is much smaller (< 2 mg/L) and is hence not followed up. The effect of added H_2O_2 and PDS on the photocatalytic degradation of PEP in presence of TiO_2 is investigated and the results are plotted in Figure 12. The degradation is enhanced significantly by both oxidants. The effect is concentration-dependent and has an optimum in both cases (Figure 13). H_2O_2 enhances the degradation up to 1500 mg/L concentration. Above this concentration the degradation of plastics is stabilised or slightly decreased. This may be because at higher concentration of H_2O_2 the reactive free radicals as well as the electrons and holes interact more with it and less with the pollutant. H_2O_2 may also be acting as a hole or $^{\cdot}OH$ scavenger as stated earlier. The observation by Malato et al (39) and Evgenidou et al (25) that the effect of H_2O_2 depends on the H_2O_2/ Contaminant molar ratio is not relevant in the context since the pollutant is not dissolved in water.

Many reports including the current study suggest that PDS is a much better accelerator of photocatalysed degradation of organic pollutants in water (24, 25, 48, 49). Relatively faster mineralization of the pollutants and lower consumption of the oxidant make the process commercially attractive. The degradation is accelerated by the addition of sulphate anion also (Figure 12). This confirms the mechanism proposed earlier suggesting that the sulphate anions and the sulphate radical formed from the persulphate are at least partially responsible for the enhanced degradation. The TiO_2 catalysed photodegradation of PPE is almost doubled in the presence of even smaller concentration of PDS (5% of TiO_2) as in figure 12. At the optimized concentrations (Figure 13) of the oxidants, PDS is at least three times more efficient than H_2O_2 in enhancing the TiO_2 catalysed photodegradation of PPE plastic. In addition to preventing the electron-hole recombination, the oxidants accelerate the degradation by acting as sensitizers through the production of $^{\cdot}OH$ and $SO_4^{\cdot}$ radicals. The general mechanism of the acceleration is shown in equations 32 and 28-31.

SEM images of typical plastic strips before and after photocatalytic treatment shown in Figure 14 clearly illustrate that the surface morphology of plastic is severely changed and the technique is effective for the degradation of recalcitrant plastics. As irradiation progresses, the plastic sheet becomes thinner, crumbles and breaks. It is logical to assume that the cavities inside the plastic film also expand with irradiation and the photocatalytic degradation happens both on the surface and inside the film simultaneously.

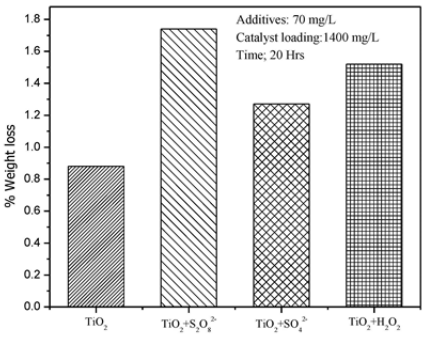

Figure 12. Effect of additives on the photocatalytic degradation of PE plastics on TiO_2.

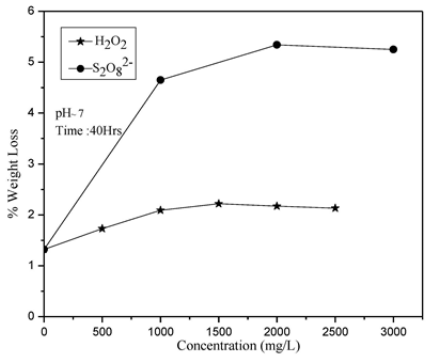

Figure 13. Effect of concentration of H_2O_2 and $S_2O_8^{2-}$ on the photocatalytic degradation of PE plastics on TiO_2.

The holes generated and the O_2^- participate in the degradation directly as well as through various radicals generated as follows:

$$h^+ + \text{-}(CH_2CH_2)\text{-} \rightarrow \text{-}(CH_2CH_2)\text{-}^+ \quad (35)$$

$$\text{-}(CH_2CH_2)\text{-}^+ + O_2^- \rightarrow \text{-}(^{\cdot}CHCH_2)\text{-} + HO_2^{\cdot} \quad (36)$$

$HO_2^{\cdot}$ radicals combine to form H_2O_2 as in reaction 18 which in turn can photodecompose as in reaction 16 to yield $^{\cdot}OH$ radicals.

The degradation is faster in the beginning and it slows down with time. This is similar to the observations by Shang et al (50) who demonstrated that photocatalytic degradation of polystyrene plastic and evolution of CO_2 and volatile organic compounds under fluorescent light deteriorate gradually. The initial faster rate can be ascribed to the interaction of reactive oxygen species with adjacent polymer chains. These molecules have to be etched away so that the catalyst surface is available for interaction with more molecules and generation of reactive free radicals. It is also possible that the degradation is initiated by photons attacking the polymer to create excited state followed by chain scission, branching, cross linking and oxidation (51). During the irradiation, the OH radicals can attack the polymer as follows:

$$\text{-}(CH_2CH_2)\text{-} + {}^{\cdot}OH \rightarrow \text{-}(CH_2{}^{\cdot}CH)\text{-} + H_2O \quad (37)$$

$$\text{-}(CH_2{}^{\cdot}CH)\text{-} + {}^{\cdot}OH \rightarrow \text{-}(^{\cdot}CH{}^{\cdot}CH)\text{-} + H_2O \quad (38)$$

The carbon centered radicals thus formed react with more O_2 leading to chain cleavage and production of new reactive radicals (50, 53).

$$\text{-}(CH_2{}^{\cdot}CH)\text{-} + O_2 \rightarrow \text{-}(CH_2(OO^{\cdot})CH)\text{-} \quad (39)$$

$$\text{-}(^{\cdot}CH{}^{\cdot}CH)\text{-} + O_2 \rightarrow \text{-}(CH(OO^{\cdot})CH)\text{-} \quad (40)$$

$$\text{-}(CH_2(OO^{\cdot})CH)\text{-} + \text{-}(CH_2CH_2)\text{-} \rightarrow \text{-}(CH_2(OOH)CH)\text{-} + \text{-}(CH_2{}^{\cdot}CH)\text{-} \quad (41)$$

$$\text{-}(CH_2(OOH)CH)\text{-} \rightarrow \text{-}(CH_2OCH)\text{-} + {}^{\cdot}OH \quad (42)$$

$$\text{-}(CH_2OCH)\text{-} + O_2 \xrightarrow{\text{Catalyst + hv}} \text{Intermediates such as HCHO, HCOOH etc.} \xrightarrow{\text{Catalyst + hv}} CO_2 + H_2O \quad (43)$$

The intermediates are not detected in water indicating that they are getting degraded faster than the plastic. Absence of any TOC in water in which the plastic strip was suspended also confirms this.

Conclusion

Semiconductor photocatalysis mediated by TiO_2 is found to be an efficient method for the removal of trace organic pollutants from water. Organophosphorous pesticides such as phosphamidon, monocrotophos and dichlorvos, phenol, catechol and even recalcitrant polyethylene plastic can be mineralized into harmless end products by this method. The degradation follows first order kinetics in most cases, even though variable kinetics with reaction order of <1 is observed at higher concentration of certain slow-degrading substrates. The influence of pH on the degradation is complex and no generalized mechanism can explain the process. The point of zero charge of the semiconductor and substrate-surface interaction are major factors that determine the pH effect. H_2O_2 and peroxydisulphate enhance the pollutant mineralization. H_2O_2 formed insitu during the degradation undergoes parallel decomposition resulting in stabilization or oscillation in its concentration depending on the equilibration or domination of the formation/

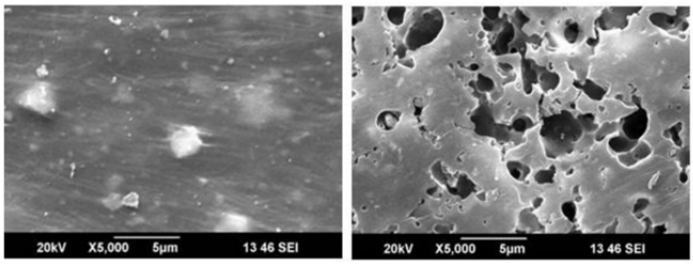

Figure 14. SEM images of polyethylene plastic (a) before and (b) after photocatalytic treatment using TiO_2 (1400mg/L) and $S_2O_8^{2-}$ (2000mg/L), Time: 300 hours.

decomposition process taking place at respective critical concentrations. Anions such as Cl^-, CO_3^{2-} and NO_3^- inhibit the degradation while SO_4^{2-} enhances the same. Critical parameters for optimum efficiency for the removal of each of the pollutant are identified and optimized.

Acknowledgement

Financial support to KPJ (Junior Research Fellowship from UGC, India) and to SGA (Senior Research Fellowship from Cochin University of Science and Technology) is gratefully acknowledged.

References

(1) Fujishima, A; Zhang, X; Tryk, D.A. *Surf. Sci. Rep.* **2008**, *63*, 515-582.

(2) Chong, M.N; Jin, B; Chow, C.W.K; Saint, C. *Water Res.* **2010**, *44*, 2997-3027.

(3) Chen, C.C; Ma, W.H.; Zhao, J.C. *Chem. Soc Rev.* **2010**, *39*, 4206-4219.

(4) Pelaez, M.; Nolan, N.T.; Pillai, S.C.; Seery, M.K.; Falaras, P.; Kontos, A.G.; Dunlop, P.S.M.; Hamilton, J.W.J.; Byrne, J.A.; O'Shea, K.; Entezari, M.H.; Dionysiou , D.D. Appl. Catal B: Environ. **2012**, *125*, 331-349.

(5) Ollis, D.F; Pichat. P; Serpone, N. *Applied Catal. B: Environ.* **2010**, *99*, 377-387.

(6) Nosaka. Y; Nosaka. A, In *Photocatalysis and Water Purification*; First Edition, Pichat. P. Ed., Wiley-VCH Verlag GmbH and Co.: 2013, pp 1-24.

(7) Herrmann, J. M. *Catal. Today* **1999**, *53*, 115-129.

(8) Hoffmann, M.; Martin, S.; Choi, W.; Bahnemann, D. *Chem. Rev.* **1995**, *95*, 69-96.

(9) Ollis, D.F; Pelizzetti, E.; Serpone, N. In *Photocatalysis: Fundamentals and Applications*; Serpone, N; Pelizzetti E, Eds., John Wiley and Sons Inc.: New York, 1989, p 603.

(10) Ollis, D.F; Al-Ekabi, H. *Photocatalytic purification and treatment of water and air*; Elsevier Amsterdam, 1993.

(11) Jyothi, K.P; Joseph, S.; Yesodharan, S.; Yesodharan, E.P. *Res. J. Recent. Sci.* **2013**, *2*, 136-149.

(12) Anju, S.G; Yesodharan, S.; Yesodharan, E.P. *Chem. Eng. J.* **2012**, *189-190*, 84-93.

(13) Devipriya, S.P; Yesodharan, S. *Solar Energy Mater. and Solar Cells* **2005**, *86*, 309-348.

(14) Madhavan, J.; Sathish kumar, P.S; Anandan, S.; Grieser, F.; Ashok kumar, M. *J. Hazard. Mater.* **2010**, *177*, 944-949.

(15) Konstantinou, I.K; Albanis, T.A. *Appl. Catal. B: Environ.* **2003**, *42*, 319-335.

(16) Wang, K.H.; Hseih, Y.H.; Chou, M.Y.; Chang C.Y. *Appl. Catal. B: Environ.* **1999**, *21*, 1-8.

(17) Burrows, H.D; Caule, L.M; Santaballa, J.A; Steenken, S. *J. Photochem. Photobiol.* **2002**, *67*, 71-108.

(18) Lu, M-C.; Roam, G-D.; Chen, J-N.; Huang, C.P., *J. Photochem. Photobiol. Chem.* **1993**, *76*, 103-110.

(19) Okamoto, K.; Yamamoto, Y.; Tanaka, H.; Tanaka, M.; Itaya, A. *Bull. Chem. Soc. Japan* **1985**, *58*, 2015-2022.

(20) Joseph, S.; Jyothi, K.P.; Devipriya, S.P.; Yesodharan, S.; Yesodharan, E.P. Res. J. Recent. *Sci.* **2013**, *2*, 82-89.

(21) Turchi, C.S; Ollis, D.F. *J. Catal.* **1990**, *122*, 178-192.

(22) Poulios, I.; Avranas, A.; Rekliti, E.; Zouboulis, A. *J. Chem. Technol. Biotechnol.* **2000**, *75*, 205-212.

(23) Rabindranathan, S.; Devipriya, S.P.; Suguna Yesodharan. *J. Hazard. Mater.* **2003**, *B102*, 217-229.

(24) Al-Ekabi, H.; Serpone, N. *J. Phys. Chem.* **1988**, *92*, 5726-5731.

(25) Evegenidou, E.; Fytianos, K.; Poulios, I. *Appl. Catal B: Environ.* **2005**, *59*, 81-89 .

(26) Anandan, S.; Vinu, A.; Venkatachalam, N.; Arabindoo, B.; Murugesan V. *J. Mol. Catal. A. Chem.* **2006**, *256*, 313-320.

(27) Yatmaz, H.C; Akyol, A.; Bayramoglu, M. *Ind. Eng. Chem. Res.* **2004**, *43*, 6035-6042.

(28) Jyothi, K.P.; Yesodharan, S.; Yesodharan, E.P. *Ultrason. Sonochem*. **2014**, *21*, 1787-1796.
(29) Yi, J.; Bahrini, C.; Shoemaecker, C.; Fittschen, C.; Choi, W. *J. Phys. Chem*. **2012**, *116*, 10090-10097.
(30) Tachikawa, T.; Majima, T. *Langmuir* **2009**, *25*, 76791-7802.
(31) Barka, N.; Quorzal, S.; Assabane, A.; Nounah, A.; Ait-Ichou, Y. *J. Photochem. Photobio. A: Chem*. **2008**, *195*, 346-351.
(32) Kiwi, J.; Lopez A.; Nadrochenko V. *Environ Sci Technol*. **2000**, *34*, 2162-2168.
(33) Haarstrick, A.; Kut, O.M.; Heinzle, E. *Environ Sci Technol*. **1996**, *30*, 817-824.
(34) Guillard, C.; Puzenat, E.; Lachheb, H.; Houas, A.; Herrmann, J.M. *Int. J. Photoenergy* **2005**, *7*, 1-9.
(35) Low, G.K.C.; McEvoy, S.R.; Matthews, R.W. *Environ Sci. Technol*. **1991**, *25*, 460-467.
(36) Kositzi, M.; Antoniadis, A.; Poulis, I.; Kiridis, I.; Malato, S. *Solar Energy* **2004**, *77*, 591-600.
(37) Evgenidou, E.; Fytianos, K.; Poulios, I. *J. Photochem. Photobiol. A: Chem.* **2005**, *175*, 29-38.
(38) Muneer, M.; Bahnemann, D. *Appl. Catal B: Environ.* **2002**, *36*, 95-111.
(39) Malato, S.; Blanco, J.; Maldonado, M.I.; Fernandez-Ibanez, P.; Campos, A. *Appl. Catal B: Environ*. **2000**, *28*, 163-174.
(40) Poulios, I.; Kositzi, M.; Kouras, A. *J. Photochem. Photobiol. A: Chem*. **1998**, *115*,175-183.
(41) Hua, Z.; Manping, Z.; Zongfeng X.; Low, G. K-C. *Water Res*. **1995**, *29*, 2681-2688.
(42) Fujihira, M.; Satoh, Y.; Osa, T. *Bull. Chem. Soc. Japan* **1982**, *55*, 666-673.
(43) Shankar, M.V.; Anandan, S.; Venkatachalam, N.; Arabindoo, B.; Murugesan, V. *J. Chem. Technol. Biotechnol.* **2004**, *79*, 1279-1285.
(44) Yang, J.; Dai, J.; Chen, C.; Zhao, J. *J. Photochem. Photobiol. A: Chem*. **2009**, *208*, 66-77.
(45) Sakthivel, S.; Neppolian, B.; Shankar, M.V.; Arabindoo, B.; Palanichamy, B.; Murugesan, V. *Solar Energy Mater. Solar Cells* **2003**, *77*, 65-82.
(46) Umar, K.; Haque, M.M; Mir, N.A.; Muneer, M.; Farooqi, I.H. *J. Adv. Oxid. Technol*. **2013**, *16*, 252-260.
(47) Brugnera, M.F.; Rajeshwar, K.; Cardoso, J.C.; Boldrin Zanoni, M.V. *Chemosphere* **2010**, *78*, 569-575.
(48) Al-Ekabi, H; Butters, B.; Delany, D.; Ireland, J.; Lewis, N.; Powell, T.; Story, J. In *Proceedings of the first international conference on TiO_2 photocatalytic purification and treatment of water and air*; London, Canada, Ollis, D.F; Al-Ekabi, H. (Eds.), Elsevier: Amsterdam 1993, p 321.
(49) Pelizzetti, E.; Carlin, V.; Minero, C.; Gratzel, M. *New J. Chem*. **1991**, *15*, 351-357.
(50) Shang, J.; Chai, M.; Zhu, Y. *Environ Sci. Technol.* **2003**, *37*, 4494-4499.
(51) Crawford, K.D.; Hughes, K.D. *J. Phys. Chem*. **1997**, *B 101*, 864-869.
(52) Wells, R.K.; Royston, A.; Badyal, J.P.S., *Macromolecules* **1994**, *27*, 7465-7468.

Received for review November 9, 2013. Revised manuscript received August 21, 2014. Accepted November 15, 2014.

31. Ashcroft, M. B., French, K. O. and Chisholm, L. A., An evaluation of environmental factors affecting species distribution. *Ecol. Model.*, 2011, **222**, 524–531.
32. Sakai, A. and Weiser, C. J., Freezing resistance of trees in North America with reference to tree regions. *Ecology*, 1973, **54**, 118–126.
33. Prentice, I. C., Cramer, W., Harrison, S. P., Leemans, R., Monserud, R. A. and Solomon, A. M., A global biome model based on plant physiology and dominance, soil properties and climate. *J. Biogeogr.*, 1992, **19**, 117–134.
34. Neilson, R. P. *et al.*, In *Sensitivity of Ecological Landscape and Regions to Global Climate Change*, US Environmental Protection Agency, Corvallis, 1989.
35. Václavík, T. and Meentemeyer, R. K., Equilibrium or not? Modelling potential distribution of invasive species in different stages of invasion. *Divers. Distrib.*, 2012, **18**, 73–83.
36. Thuiller, W., Richardson, D. M., Rouget, M., Proches, S. and Wilson, J. R., Interactions between environment, species traits, and human uses describe patterns of plant invasions. *Ecology*, 2006, **87**, 1755–1769.
37. Seabloom, E. W., Williams, J. W., Slayback, D., Stoms, D. M., Viers, J. H. and Dobson, A. P., Human impacts, plant invasion, and imperiled plant species in California. *Ecol. Appl.*, 2006, **16**, 1338–1350.
38. Wisz, M. S. *et al.*, The role of biotic interactions in shaping distributions and realised assemblages of species: implications for species distribution modelling. *Biol. Rev.*, 2013, **88**, 15–30.
39. Mangiacotti, M., Scali, S., Sacchi, R., Bassu, L., Nulchis, V. and Corti, C., Assessing the spatial scale effect of anthropogenic factors on species distribution. *PLoS ONE*, 2013, **8**, e67573.
40. Guisan, A. and Thuiller, W., Predicting species distribution: offering more than simple habitat models. *Ecol. Lett.*, 2005, **8**, 993–1009.
41. Gadagkar, R., Reproduction: the almost forgotten currency of fitness. *Curr. Sci.*, 2011, **101**, 725–726.
42. Gallien, L., Douzet, R., Pratte, S., Zimmermann, N. E. and Thuiller, W., Invasive species distribution models – how violating the equilibrium assumption can create new insights. *Global Ecol. Biogeogr.*, 2012, **21**, 1126–1136.

ACKNOWLEDGEMENTS. We thank the two anonymous reviewers for providing constructive comments that helped improve the manuscript. This project was supported by National Nature Science Foundation of China (No. U1203281, No. 41361098, No. 51269030, No. 51104127, No. 41161033), Key Research Fund for Universities at Xinjiang (No. XJDX2012113) and Open Fund of the Key Laboratory of Oasis Ecology of the Ministry of Education (No. XJDX0206-2011-04).

Received 28 April 2014; revised accepted 29 March 2015

Sono-, photo- and sonophotocatalytic decontamination of organic pollutants in water: studies on the lack of correlation between pollutant degradation and concurrently formed H_2O_2

K. P. Jyothi, Suguna Yesodharan and E. P. Yesodharan*

School of Environmental Studies, Cochin University of Science and Technology, Kochi 682 022, India

The degradation of trace amounts of phenol in water is studied under sono-, photo- and sonophotocatalytic conditions using ZnO as a catalyst. Sonophotocatalytic degradation is more than the sum of the respective sono- and photocatalytic degradation under otherwise identical conditions, indicating synergistic effect. The degradation proceeds through many intermediates and ultimately the parent compound is mineralized. The concentration of concurrently formed H_2O_2 increases and decreases periodically resulting in an oscillatory behaviour. The oscillation is more pronounced in sonocatalysis in which the degradation of phenol and corresponding formation of H_2O_2 are slower. In photocatalysis and sonophotocatalysis, where the degradation is faster, the amount of H_2O_2 is relatively more and the oscillation becomes weaker and tends towards stabilization. However, in all cases the degradation of phenol continues unabated until the mineralization is complete. The stabilized concentration of H_2O_2 is much less than the expected amount based on the degradation of the organic pollutant. Probable causes for the phenomena are discussed.

Keywords: Hydrogen peroxide, phenol, photocatalysis, sonocatalysis, zinc oxide.

ADVANCED oxidation processes (AOPs) based on the generation of highly reactive $^{\bullet}OH$ radicals which can attack the target molecules and mineralize them eventually to harmless CO_2, water and salts have been widely studied as viable candidates for the removal of chemical and bacterial pollutants from water. Some of these AOPs include wet-air oxidation, radiolysis, cavitation, photolysis, photocatalysis, fenton chemistry and electrochemical oxidation. They can be used either independently or in combination with other techniques in order to enhance the efficacy, economy and safety. In this context semiconductor-mediated sonocatalysis, photocatalysis and sonophotocatalysis have been promising with relatively higher rates of degradation for a variety of molecules[1–12]. The expected advantage of sonophotocatalysis is the

*For correspondence. (e-mail: epyesodharan@gmail.com)

synergy between photocatalysis and sonochemistry resulting in enhanced efficiency of the combined process. Relatively mild reaction conditions and proven ability to degrade several toxic refractory pollutants also make the process attractive. But large-scale application of this hybrid technique is hampered at least partially due to high cost and lack of suitable design strategies associated with the sonochemical reactors[10]. The status of sono-photocatalytic reactors and potential development needs were discussed in detail by Gogate and coworkers[8,10–12].

The most widely studied catalyst in sono-, photo- and sonophotocatalysis is TiO_2 in view of its favourable physico-chemical properties, low cost, easy availability, high stability with respect to photocorrosion and chemical corrosion, and low toxicity. However, TiO_2 has a wide band gap (~3.2 eV) and can absorb light only below 400 nm, which is in the UV range that constitutes less than 5% of sunlight. Many studies on improving the photocatalytic efficiency of TiO_2 by techniques such as dye sensitization, semiconductor coupling, impurity doping, use of coordination metal complexes, noble metal (Pt, Pd, Au, Ag, etc.) deposition, use of Fenton reagent and H_2O_2 have been reported[6–9]. The enhancement is attributed partially to the increased light absorption and inhibition of the recombination of electron–hole pair[13,14]. Another semiconductor with potential sono/photo catalytic applications is ZnO with properties comparable to those of TiO_2. Though both of them have comparable band-gap energy (~3.2 eV), in practice, ZnO is capable of absorbing a larger fraction of the solar spectrum[15] and hence is more active in the visible region for the photocatalytic decontamination of water[16–19]. The comparatively lower light-scattering effect of ZnO due to its lower refractive index (ZnO: 2.0, TiO_2: 2.5–2.7) also favours better photocatalytic efficiency. In spite of these advantages, ZnO has not received due attention as an effective environmental photocatalyst which may be due to its instability or photocorrosion under acidic conditions.

Our earlier studies revealed that ZnO can be used as an effective catalyst for the degradation of certain organic pollutants in water using sunlight as the source of energy[17,20]. We have also studied the sono-, photo- and sonophotocatalytic degradation of phenol on ZnO and the synergy of the hybrid technique was demonstrated[4]. In the present communication the study is extended and the fate of H_2O_2 formed in ZnO-mediated sono-, photo- and sonophotocatalytic systems is examined using phenol as the test pollutant. Phenol is chosen as the candidate pollutant because it is rated as one of the most common and at the same time toxic organic pollutants in wastewater. The treatment of phenol-contaminated wastewater by hybrid techniques has been the subject of many studies and the findings are discussed exhaustively in recent reviews[5,8,9,11,12]. Addition of H_2O_2 enhances the efficacy of the process which is attributed to the increased availability of hydroxyl radicals formed by its dissociation[5,12]. At the same time, the H_2O_2 itself is formed primarily from the $^{\bullet}OH$ radicals which are generated in AOPs such as sono-, photo- and sonophotocatalysis[21–24]. Thus H_2O_2 functions as a reactant, intermediate and/or the end-product and the $^{\bullet}OH$ radicals serve at least partially as the creator and destroyer of H_2O_2. However, the fate of H_2O_2 in sono-, photo- or sonophotocatalytic systems has not received due attention since the focus has always been on the removal of the pollutant and purification of water. In the present work, the role and fate of H_2O_2 formed during the sono-, photo- and sonophotocatalytic degradation of phenol in water is studied in detail.

ZnO (99.5% purity, BET surface area 12 m^2/g) used in the study (Merck India Limited) was characterized by particle size, scanning electron microscopy (SEM), X-ray diffraction (XRD) and reflectance spectroscopy. Phenol AnalaR Grade (99.5% purity) from Qualigen (India) was used as such without further purification. All other chemicals were of AnalaR Grade or equivalent. Doubly distilled water was used in all experiments. The sono-, photo- and sonophotocatalytic experiments were performed as follows[4,25].

Specified quantity of the catalyst was suspended in phenol solution of desired concentration and kept under agitation using a magnetic stirrer. In the case of ultrasound (US) irradiation experiments, sonication was sufficient to ensure adequate mixing of the suspension. Additional mechanical mixing did not make any notable consistent difference in the US reaction rate. Hence mixing by sonication alone was chosen for all US and (US + UV) experiments. The reactor used in all experiments was a cylindrical Pyrex vessel of 250 ml capacity. In photocatalytic experiments, the reactor was placed in a glass vessel of 500 ml capacity through which water from a thermostat at the required temperature was circulated. A high-intensity UV lamp (400 W medium pressure mercury vapour quartz lamp) mounted above was used as the UV irradiation source. In the case of sonocatalytic and sonophotocatalytic experiments, ultrasonic bath was used as the source of US. The ultrasonic bath was operated at 40 kHz and power of 100 W. Water from the sonicator was continuously replaced by circulation from a thermostat maintained at the required temperature. The position of the reactor in the ultrasonic bath was always kept the same. Unless otherwise mentioned, the reaction temperature was maintained at 29 ± 1°C. At periodic intervals samples were drawn, the suspended catalyst particles were removed by centrifugation and the concentration of phenol left behind was analysed by spectrophotometry. The phenol was converted into coloured antipyrene dye by reaction with 4-amino antipyrene in the presence of potassium ferricyanide at pH 7.9 ± 0.1. The concentration of the dye was measured at 500 nm and correlated to the concentration of phenol. Sample from reaction system kept in the dark under exactly identical conditions but without UV or US irradiation was used as the reference.

H_2O_2 was determined by iodometry after removing the suspended particles from the sample by centrifugation. Mineralization of phenol was identified by confirming the evolution of CO_2 and determination of the total organic carbon (TOC) content using TOC analyzer (model Elementar Analysensysteme GmbH).

Preliminary studies on the degradation of phenol in water in the presence of ZnO showed that the catalyst and an energy source are essential to effect reasonable degradation. The degradation is more facile in the presence of UV light (photocatalysis) compared to US irradiation (sonocatalysis). The sonophotocatalytic degradation in the concurrent presence of UV, US and ZnO is more than the sum of the degradation under photocatalysis and sonocatalysis (Figure 1), which confirms the synergy reported in similar experiments earlier[4,9].

Small quantity of phenol degraded in the presence of US even in the absence of catalysts. Sonolysis of water produces extreme temperature and pressure conditions capable of generating free radicals $H^\bullet$ and $OH^\bullet$, which can lead to other reactive oxygen species (ROS)[26]. They interact with phenol resulting in eventual mineralization and formation of H_2O_2 as follows

$$H_2O \xrightarrow{>>>} H^\bullet + {}^\bullet OH, \qquad >>> \text{refers to US} \qquad (1)$$

$$H^\bullet + O_2 \rightarrow HO_2^\bullet, \qquad (2)$$

$$\text{ROS } ({}^\bullet OH, HO_2^\bullet, \text{etc.}) + \text{phenol} \rightarrow \text{intermediates} + H_2O_2 \rightarrow H_2O_2 + H_2O + CO_2, \qquad (3)$$

$$HO_2^\bullet + HO_2^\bullet \rightarrow H_2O_2 + O_2, \qquad (4)$$

$$2\,{}^\bullet OH \rightarrow H_2O_2. \qquad (5)$$

The mineralization of phenol in photo- and sonophotocatalysis is verified by the absence of TOC after phenol was completely degraded and disappeared from the system. However, in sonocatalytic experiments the degradation took much longer periods and hence the mineralization could not be confirmed by TOC measurements. In this case also, it is logical to assume that the phenol disappearing from the system is eventually getting mineralized. The net TOC present in the system under identical conditions in sono-, photo- and sonophotocatalysis after 2 h of irradiation follows the order (US + UV) < UV << US, thereby reiterating the comparative mineralization efficiency of the three processes. The fate of concurrently formed H_2O_2 is shown in Figure 2.

The catalyst loading for optimum degradation of phenol has been experimentally determined for sono-, photo- and sonophotocatalysis respectively, as shown in Figure 3. The optimum loading is slightly higher at 100 mg/l in sonophotocatalysis compared to sono- and photocatalysis. In all three cases, the degradation increases with increase in catalyst loading and reaches an optimum range.

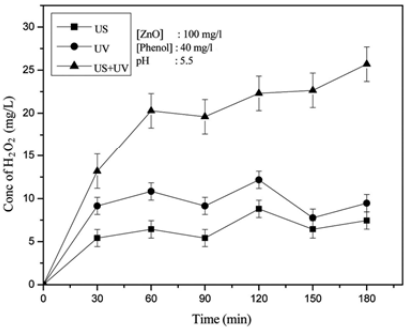

Figure 2. Concentration of H_2O_2 during sono-, photo- and sonophotocatalytic degradation of phenol in the presence of ZnO.

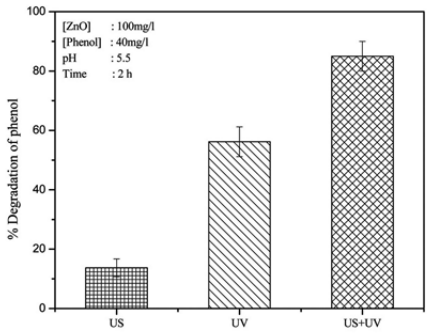

Figure 1. Sono-, photo- and sonophotocatalytic degradation of phenol in the presence of ZnO.

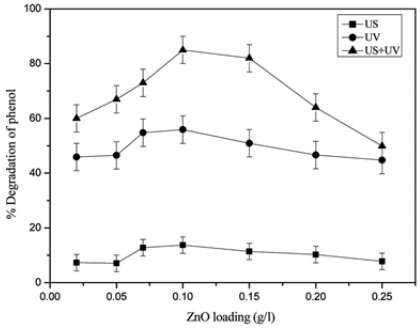

Figure 3. Effect of catalyst loading on sono-, photo- and sonophotocatalytic degradation of phenol in the presence of ZnO.

Beyond this optimum, the degradation slows down and thereafter remains more or less steady or even decreases. The enhanced degradation efficiency is probably due to increased number of adsorption sites and more effective interaction with the irradiation which lead to higher number of reactive hydroxyl radicals. In the case of photo- and sonophotocatalysis, any further increase in catalyst concentration beyond the optimum will only result in light scattering and reduced passage of light through the sample. Hence no further increase in degradation is observed. Another reason may be the aggregation of catalyst particles causing decrease in the number of available active surface sites. The particles cannot be fully and effectively suspended beyond a particular loading in a particular reactor, which also leads to suboptimal penetration of irradiation and reduced adsorption of the substrate on the surface. This can also result in stabilization or even decrease in the degradation after the optimum catalyst dosage. In the case of sonophotocatalysis, the decrease in degradation with increase in catalyst loading beyond the optimum is more pronounced compared to photocatalysis. However, the optimum loading and the trend remain fairly the same suggesting that US-induced increase in the rate of photocatalysis results at least partly from the increase in light absorbed by the reaction system. This leads to higher concentration of active species. At higher catalyst loading when filtering and/or scattering of light becomes more prominent, the amount of photoproduced active species does not increase further.

The optimum quantity of ZnO is in the order sonophotocatalysis > sonocatalysis ≥ photocatalysis. The higher optimum loading in sono- and sonophotocatalysis may be due to the deagglomeration of the aggregate catalyst particles by US, which can bring more surface sites in contact with the irradiation as well as the pollutant molecules. However, at higher ZnO concentrated suspension, the working volume of the slurry becomes low and light cannot penetrate into the optically dense medium[27]. Consequently, deagglomeration may not lead to any extra absorption of light as the zone of action of light can be different from the zone of action of US. Hence any further enhancement in degradation in sonophotocatalysis beyond the optimum catalyst loading for photocatalysis is due to the production of hydroxyl radicals predominantly by US only and not due to the photo or combined sono–photo effect. Since US-promoted OH radical generation is relatively less, the rate of degradation under sonophotocatalytic conditions at higher catalyst loadings will slow down, level-off or even decrease slightly. This is consistent with the findings of Davydov *et al.*[28], who also reported that once the optimum catalyst loading is reached in sonophotocatalytic systems, higher US power has to be used to achieve further enhancement in activity.

Contrary to the progressive decrease in the concentration of phenol due to degradation, the concentration of H_2O_2 stabilizes or fluctuates due to concurrent formation and decomposition in an irreproducible manner. Hence the optimum catalyst loading for phenol degradation need not necessarily hold good for optimum H_2O_2 at any point of time.

One possibility for the formation of H_2O_2 can be the combination of hydroxyl radicals formed from water during the sono-, photo- or sonophotocatalysis. However, in the absence of any organic substrate (phenol in the current case), the quantity of H_2O_2 formed is quite low compared to that in the presence of phenol. Degradation of phenol leads to increased amounts of H_2O_2 in sono-, photo- and sonophotocatalytic systems as seen in Figure 4. This is consistent with the earlier report[25] according to which 'in-between' introduction of extra phenol to a ZnO–phenol–H_2O system under sono-, photo- or sonophoto irradiation enhances the formation of H_2O_2. This further reconfirms the role of substrate in the generation of H_2O_2. Hence it is reasonable to assume that a major part of H_2O_2 present in the system is formed concurrently with the degradation of the pollutant though the contribution of OH radicals formed from water cannot be ruled out.

The sono-, photo- and sonophotocatalytic degradation of phenol follow variable kinetics depending on the concentration of the substrate[4]. However, the effect of concentration of phenol on the oscillation does not show any consistent trend and the precise time of reaction or concentration of H_2O_2 for the occurrence of maxima and minima is not predictable as seen from the repeated experimental results (not shown here). This may be because, with too many reactive free radicals formed in the system, the recombination as well as other competing interactions may result in multiple reactions with as many intermediates. These intermediates themselves will undergo further degradation leading to even more complex combination of free radicals and eventual mineralization. Similar inconsistency is also seen in the effect of

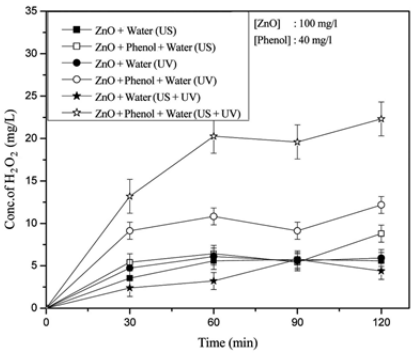

Figure 4. Influence of presence of phenol on net concentration of H_2O_2 in the sono-, photo- and sonophotocatalytic system.

pH on the phenomenon of oscillation. Repeated experiments showed that the effect of pH on the behaviour of H_2O_2 in the presence of phenol is extremely complicated possibly due to the interplay of a number of factors. The maxima and minima in the oscillation curve are present at all pH values, though the results are not consistently reproducible. H_2O_2 itself can serve as an electron acceptor or hole scavenger as follows and form free radicals required to sustain the oscillation.

$$H_2O_2 + e^- \rightarrow {}^{\bullet}OH + OH^-, \quad (6)$$

$$H_2O_2 + {}^{\bullet}OH/h^+ \rightarrow HO_2^{\bullet} + H_2O/H^+. \quad (7)$$

Serpone *et al.*[29] demonstrated that the kinetics and mechanism of photo/sono/sonophotocatalytic degradation of phenol is different at different pH values with different types of intermediates which themselves undergo different kinds of reactions. This also adds to the difficulty in delineating the effect of pH on the concentration of H_2O_2.

The current study shows that H_2O_2 decomposition is negligible in the dark or by photolysis or sonolysis in the absence of a catalyst. The formation or decomposition of H_2O_2 does not happen in the presence of alumina particles, comparable in size and surface area to ZnO. Naturally, no oscillation is observed in this case. Hence the concurrent formation and decomposition of H_2O_2 is essentially a catalytically active surface-initiated process, though it may be propagated in the homogeneous bulk as well. This is in line with the findings of Ilisz *et al.*[30].

The effect of externally added H_2O_2 on the degradation of phenol as well as its own fate under sono-, photo- and/or sonophotocatalytic conditions was experimentally verified. As expected, the enhanced number of free radicals generated from the decomposition of added H_2O_2 results in enhanced phenol degradation (Figure 5). However, corresponding increase is not detected in the case of H_2O_2 (Figure 6). In the case of photo- and sonophotocatalytic systems in which H_2O_2 is added externally, the net concentration (of H_2O_2) is not much different from the corresponding systems without any added H_2O_2 in the later stages of irradiation. In the case of the relatively slower sonocatalytic degradation of phenol, the formation as well as decomposition of H_2O_2 are also slower resulting in the net concentration of H_2O_2 (including the externally added quantity) remaining practically unchanged. This reiterates earlier inference that in sono-, photo- and sonophotocatalytic systems both the formation and decomposition of H_2O_2 compete with each other. The process is primarily concentration-dependent. At higher concentration of H_2O_2 (as in the case of external addition), the decomposition is dominant in the beginning in the case of sono- and photocatalysis and matches with the formation. This may be the reason for initial drop/stabilization in the net H_2O_2 concentration in sono- and photocatalysis. However, in sonophotocatalysis, the rates of degradation of phenol and the corresponding formation of H_2O_2 are much higher compared to sono- or photocatalysis. Hence the initial decrease in the concentration of added H_2O_2 is more than compensated by the higher formation rate. Consequently, the concentration of H_2O_2 increases fairly steeply in the beginning and slowly thereafter. Hence in the case of externally added H_2O_2, once the more dominant decomposition has brought its concentration down to moderate level, the system behaves similar to those cases in which there is no externally added H_2O_2.

In semiconductor-mediated sono-, photo- and sonophotocatalysis, the primary step involves the promotion of electron from the valence band to the conduction band (e_{cb}^-), leaving a positively charged hole in the valence band (h_{vb}^+). The electrons are then free to migrate within the conduction band. The holes may be neutralized by migration of electrons from an adjacent molecule. In the

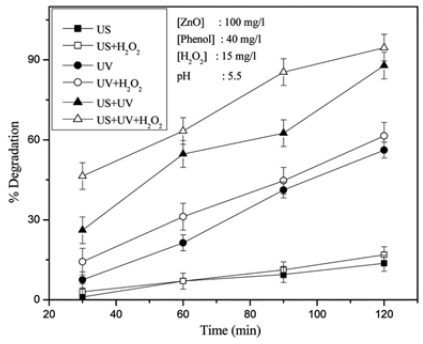

Figure 5. Effect of added H_2O_2 on the degradation of phenol under sono-, photo- and sonophotocatalysis.

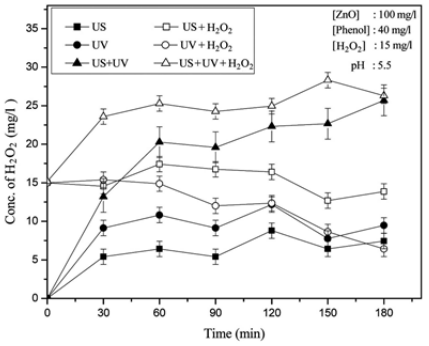

Figure 6. Effect of added H_2O_2 on net concentration of H_2O_2 under sono-, photo- and sonophotocatalysis.

process, the molecule (in the current case, phenol) gets oxidized and the process can be repeated[8]. The electrons and holes can recombine with no productive result and the efficiency of the system depends on its ability to retard the recombination. Various reactions leading to the formation of ROS such as $O_2^{-\bullet}$, $^{\bullet}OH$ and $HO_2^{\bullet}$ at the surface and their interactions have been illustrated in a number of reviews[1,8]. The free radicals $^{\bullet}OH$ and $HO_2^{\bullet}$ can give rise to H_2O_2 as in reactions (4) and (5). Further, they can interact with phenol resulting in its degradation and eventual mineralization as in reaction (3). Since the amount of H_2O_2 generated in the absence of phenol is insignificant, it is reasonable to assume that the degradation of phenol and the formation of H_2O_2 are at least partially related.

H_2O_2 is a by-product/intermediate in the degradation of phenol under sono-, photo- and sonophotocatalysis and hence its concentration is expected to increase and ultimately stabilize when the phenol degradation is complete. The oscillation/stabilization in the concentration shows that H_2O_2 is generated and decomposed/consumed simultaneously depending on the reaction conditions. When the concentration reaches a particular maximum, the decomposition dominates bringing its net concentration down. Similarly, when the concentration reaches a critical minimum, the formation process gets precedence. This process happens many times over. The degradation of phenol continues unabated even when the concurrently formed H_2O_2 shows stabilization/oscillation. The decomposition of H_2O_2 is known to take place as follows[8,24]

$$ZnO \xrightarrow{UV/US/(US+UV)} e_{cb} + h_{vb}, \quad (8)$$

$$H_2O_2 + UV/US/(US + UV) \rightarrow 2\ ^{\bullet}OH, \quad (9)$$

$$2\ h_{vb}^{+} + H_2O_2 \rightarrow O_2 + 2\ H^{+}, \quad (10)$$

$$2\ e_{cb}^{-} + 2\ H^{+} + H_2O_2 \rightarrow 2\ H_2O, \quad (11)$$

$$H_2O_2 + {}^{\bullet}OH \rightarrow H_2O + HO_2^{\bullet}, \quad (12)$$

$$H_2O_2 + HO_2^{\bullet} \rightarrow H_2O + {}^{\bullet}OH + O_2, \quad (13)$$

$$H_2O_2 + O_2^{-\bullet} \rightarrow {}^{\bullet}OH + OH^{-} + O_2. \quad (14)$$

Thus, the same free radicals can contribute to the formation and decomposition of H_2O_2 depending on the conditions. At the same time, being a complex free radical system, many other reactive species also may be possible, especially in sonophotocatalysis, resulting in more interactions leading to the formation and decomposition of H_2O_2.

Sono-, photo- and sonophotocatalytic degradation of phenol in water in presence of ZnO generates H_2O_2 as an intermediate as well as final product. The H_2O_2 thus formed undergoes concurrent decomposition resulting in oscillation in its concentration in sonocatalysis, weak oscillation/stabilization in photocatalysis and stabilization in the case of sonophotocatalysis. The oscillation is concentration-dependent, with formation or decomposition dominating at any point in time leading to increase or decrease in its concentration. H_2O_2 itself can function as an electron acceptor and hole scavenger, and thus play a significant role in the oscillation as well as in the overall phenol degradation process.

1. Nosaka, Y. and Nosaka, A. Y., Identification and roles of the active species generated on various photocatalysts. In *Photocatalysis and Water Purification* (ed. Pichat, P.), Wiley-VCH, Weinheim, Germany, 2013, pp. 3–24.
2. Devipriya, S. and Yesodharan, S., Photocatalytic degradation of pesticide pollutants in water. *Sol. Energy Mater. Sol. Cells*, 2005, **86**, 309–348.
3. Chong, M. N., Jin, B., Chow, C. W. K. and Saint, C., New developments in photocatalytic water treatment technology: a review. *Water Res.*, 2010, **44**, 2997–3027.
4. Anju, S. G., Yesodharan, S. and Yesodharan, E. P., Zinc oxide mediated sonophotocatalytic degradation of phenol in water. *Chem. Eng. J.*, 2012, **189–190**, 84–93.
5. Joseph, C. G., Puma, G. L., Bono, A. and Krishniah, D., Sonophotocatalysis in advanced oxidation process: a short review. *Ultrason. Sonochem.*, 2009, **16**, 583–589.
6. Ji, P., Takeuchi, M., Cuong, T. M., Zhang, J., Matsuoka, M. and Anpo, M., Recent advances in visible light-responsive titanium oxide-based photocatalysis. *Res. Chem. Intermed.*, 2010, **36**, 327–347.
7. Sakthivel, S., Shankar, M. V., Palanichamy, M., Arabindoo, A., Bahnemann, D. M. and Murugesan, B. V., Enhancement of photocatalytic activity by metal deposition: characterization and photonic efficiency of Pt, Au, and Pd deposited on TiO_2 catalyst. *Water Res.*, 2004, **38**, 3001–3008.
8. Gogate, P. R., Treatment of wastewater streams containing phenolic compounds using hybrid techniques based on cavitation: a review of the current status and the way forward. *Ultrason. Sonochem.*, 2008, **15**, 1–15.
9. Chen, Y. C. and Smirniotis, P., Enhancement of photocatalytic degradation of phenol and chlorophenols by ultrasound. *Ind. Eng. Chem. Res.*, 2002, **41**, 5958–5965.
10. Gogate, P. R. and Pandit, A. B., Sonophotocatalytic reactors for wastewater treatment: a critical review. *AIChE J.*, 2004, **50**, 1051-1-79.
11. Gogate, P. R., Majumdar, J., Thampi, Wilhelm, A. M. and Pandit, A. B., Destruction of phenol using sonochemical reactors: scale up aspects and comparison of novel configuration with conventional reactors. *Sep. Purif. Technol.*, 2004, **34**, 25–34.
12. Khokhawala, I. M. and Gogate, P. R., Degradation of phenol using a combination of ultrasonic and UV irradiations at pilot scale operatrion. *Ultrason. Sonochem.*, 2010, **17**, 833–838.
13. Devipriya, S. P., Yesodharan, S. and Yesodharan, E. P., Solar photocatalytic removal of chemical and bacterial pollutants from water using Pt/TiO_2 coated ceramic tiles. *Int. J. Photoenergy*, 2012, Article Id 970474, 8.
14. Pelaez, M. *et al.*, A review on the visible light active titanium dioxide photocatalysts for environmental applications. *Appl. Catal. B*, 2012, **125**, 331–349.
15. Sakthivel, S., Neppolian, B., Shankar, M. V., Arabindoo, B., Palanichamy, M. and Murugesan, V., Solar photocatalytic degradation of azo dye: comparison of photocatalytic efficiency of ZnO and TiO_2. *Sol. Energy Mater. Sol. Cells*, 2003, **77**, 65–82.

16. Lam, S.-M., Sin, J. C., Abdullah, A. Z. and Mohamed, A. R., Degradation of wastewaters containing organic dyes photocatalysed by ZnO: a review. *Desalination and Water Treatment*, 2012, **41**, 131–169.
17. Hariprasad, N., Anju, S. G., Yesodharan, E. P. and Yesodharan, S., Sunlight induced removal of Rhodamine B from water through semiconductor photocatalysis. *Res. J. Mater. Sci.*, 2013, **1**, 9–17.
18. Daneshvar, N., Salari, D. and Khataee, A. R., Photocatalytic degradation of azo dye acid red 14 in water on ZnO as an alternative catalyst to TiO_2. *J. Photochem. Photobiol. A*, 2004, **162**, 317–322.
19. Kansal, S. K., Singh, M. and Sud, D., Studies on the photodegradation of two commercial dyes in aqueous phase using different photocatalysts. *J. Hazard. Mater.*, 2007, **141**, 581–590.
20. Shibin, O. M., Rajeev, B., Veena, V., Yesodharan, E. P. and Yesodharan, S., ZnO photocatalysis using solar energy for the removal of trace amounts of alfa-methyl styrene, diquat and indigo carmine from water. *J. Adv. Oxid. Technol.*, 2014, **17**, 297–304.
21. Hoffmann, A. J., Carraway, E. R. and Hoffmann, M. R., Photocatalytic production of H_2O_2 and organic peroxides on quantum sized semiconductor colloids. *Environ. Sci. Technol.*, 1994, **28**, 776–785.
22. Wu, T., Liu, G., Zhao, J., Hidaka, H. and Serpone, N., Evidence of H_2O_2 generation during the TiO_2 assisted photodegradation of dyes in aqueous dispersions under visible light illumination. *J. Phys. Chem. B*, 1999, **103**, 4862–4867.
23. Kuriacose, J. C., Ramakrishnan, V. and Yesodharan, E. P., Photoinduced catalytic reactions of alcohols on ZnO suspensions in cyclohexane: oscillation in the concentration of H_2O_2 formed. *Indian J. Chem. A*, 1978, **19**, 254–256.
24. Jyothi, K. P., Yesodharan, S. and Yesodharan, E. P., Ultrasound, ultraviolet light and combination assisted semiconductor catalysed degradation of organic pollutants in water: oscillation in the concentration of hydrogen peroxide formed *in situ*. *Ultrason. Sonochem.*, 2014, **21**, 1787–1796.
25. Anju, S. G., Jyothi, K. P., Joseph, S., Yesodharan, S. and Yesodharan, E. P., Ultrasound assisted semiconductor mediated catalytic degradation of organic pollutants in water: comparative efficacy of ZnO, TiO_2 and ZnO–TiO_2. *Res. J. Rec. Sci.*, 2012, **1**, 191–201
26. Suslick, K. S. and Crum, L. A., *Encyclopedia of Acoustics* (ed. Crocker, M. J.), Wiley Interscience, New York, 1997, pp. 271–282.
27. Poulios, I., Avranas, A., Rekliti, E. and Zouboulis, A., Photocatalytic oxidation of auramine O in the presence of semiconducting oxides. *J. Chem. Technol. Biotechnol.*, 2000, **75**, 205–212.
28. Davydov, L., Reddy, E. P., France, P. and Smirniotis, P. P., Sonophotocatalytic destruction of organic contaminants in aqueous systems on TiO_2 powders. *Appl. Catal. B*, 2001, **32**, 95–105.
29. Serpone, N., Terzian, R. and Colarusso, P., Sonochemical oxidation of phenol and three of its intermediate products in aqueous media: catechol, hydroquinone and benzoquinone. Kinetic and mechanistic aspects. *Res. Chem. Intermed.*, 1992, **18**, 183–202.
30. Ilisz, I., Foglein, K. and Dombi, A., The photochemical behavior of H_2O_2 in near UV-irradiated aqueous TiO_2 suspensions. *J. Mol. Catal. A*, 1998, **135**, 55–61.

ACKNOWLEDGEMENTS. S.Y. thanks the Organization for the Prohibition of Chemical Weapons, The Hague, The Netherlands and K.P.J. thanks University Grants Commission, New Delhi for financial support.

Received 23 September 2014; revised accepted 6 April 2015

Tafoni along the east coast, Chennai to Mamallapuram, Tamil Nadu

Malarvizhi Arjunan and Hema Achyuthan*

Department of Geology, Anna University, Chennai 600 025, India

A study on weathering pits called tafoni was carried out on rock surfaces that age from a few hundreds to millions of years along the east coast between Chennai and Mamallapuram. Tafoni of varying sizes and shapes such as simple circular dots to oblate to prolate, hemispherical to spherical are formed on the granite, granite gneiss, charnockites (acid and mafic) and sandstone both on exposed and inner wall surfaces. In this study, their formation is related to not only tropical weathering processes, but also to sea salt water splays causing salt mineral etching, weathering processes, besides microbial activity, algal and lichen growth accentuating their formation.

Keywords: Bedrock surface, mafic minerals, tafoni, weathering processes.

WEATHERING starts generally on the rock surfaces or from their inner walls by the formation of pits[1–3]. Tafoni are pits, ellipsoidal, flat pan-like to bowl-shaped, occurring as natural rock cavities[3–9]. These cavernous weathering features include tiny pits, chemically dissolved pits, softball-sized cavities, caves and cellular honeycomb forms often lined by thin layers of dark black algae or microbial mat. Typically tafoni develop on inclined or vertical surfaces and occur in groups or clusters, and in all types of bedrocks. These cavernous weathering landforms are present on the surfaces of many different kinds of rocks located in a multitude of geographic regions around the world[1,9]. However, tafoni development and evolution are puzzling and continue to arouse curiosity[5,8–11]. Very little work has been carried out on tafoni and weathering along the east coast of Tamil Nadu from Chennai to Mamallapuram[6]. In the present communication, we describe tafoni as an important weathering type along the east coast extending from Chennai to Mamallapuram. The purpose of the study was to examine the various types and sizes of tafoni weathering features on rock surfaces of different ages, on similar/different rock types, from coastal and inland sites. Tafoni were observed over rock surfaces of different ages from a few hundred to several million years old, including on colonial grave tombstones, temple walls, sculptures (of historical periods), menhirs (ancient monumental standing stones), exposed rock outcrops, etc. Hence this study is aimed to understand the plausible causes for tafoni formation along the east coast between Chennai and Mamallapuram.

*For correspondence. (e-mail: hachyuthan@yahoo.com)

IOSR Journal of Applied Chemistry (IOSR-JAC)
e-ISSN: 2278-5736.
PP 15-24
www.iosrjournals.org

Influence of commonly occurring cations on the sono, photo and sonophoto catalytic decontamination of water

K. P. Jyothi, Suguna Yesodharan, E. P. Yesodharan*
School of Environmental Studies Cochin University of Science and Technology, Kochi 682022, India

Abstract: *Sono, photo and sonophotocatalysis mediated by ZnO catalyst have been proven to be efficient methods for the removal of chemical and bacterial pollutants from water. Combination methods are often more efficient as in the case of sonophotocatalysis which is synergic. In this case, the efficiency is more than the sum of the respective sono- and photo- catalytic processes under otherwise identical conditions. The concentration of concurrently formed H_2O_2 increases and decreases periodically resulting in oscillatory behavior. Inorganic salts likely to be present in water influence the rate of degradation of the pollutant and the behavior of H_2O_2. The effect of anions on the sono, photo and sonophotocatalytic degradation of phenol is dependent on the concentration of respective salts. Contrary to many earlier reports, current study shows that the anions and certain cations, enhance the sono, photo and sonophotocatalytic degradation of phenol. The rate of enhancement decreases with time and eventually becomes comparable to the rate without the presence of salts. The influence of various cations on the degradation of phenol and the fate of H_2O_2 is investigated under sono, photo and sonophotocatalysis. Almost all cations except Al^{3+}, irrespective of the nature of anions, enhance phenol degradation under sonocatalysis. In the case of photo and sonophotocatalysis, the effect of cations is relatively less to negligible. The effect of cations on the concurrently formed H_2O_2 as well as the oscillation phenomenon is inconsistent and unpredictable. The results are discussed and a tentative mechanism for the observation is proposed.*

Keywords: *Sonocatalysis, Photocatalysis, Sonophotocatalysis, Synergy, hydrogen peroxide, cations*

I. Introduction

Advanced Oxidation Processes (AOPs) are efficient, environment-friendly techniques for the removal of chemical and bacterial pollutants from water. Relatively mild reaction conditions and proven ability to degrade several toxic refractory pollutants make them very attractive. Some of these AOPs include wet-air oxidation, radiolysis, cavitation, photolysis, photocatalysis, fenton chemistry, microwave degradation and electrochemical oxidation. They can be used either independently or in combination with other techniques in order to enhance the efficacy, economy and safety. Semiconductor-mediated sonocatalysis, photocatalysis and sonophotocatalysis have been promising with relatively higher rates of degradation for a variety of molecules [1-4]. Earlier studies from our laboratory [2] showed that sonophotocatalysis is synergic and the efficiency of the combination for the degradation of pollutants is more than the sum of individual photocatalysis and sonocatalysis.

The chemical effects of US in liquid include cavitation which consists of nucleation, growth and collapse of bubbles, resulting in localized supercritical condition such as high temperature, pressure, electrical discharges and plasma effects [5,6]. The gaseous contents of a collapsing cavity reach temperatures of approximately 5500°C and the liquid immediately surrounding the cavity reaches up to 2100°C. The cavities thus serve the purpose of high energy micro reactors. The consequence of these extreme conditions is the cleavage of dissolved oxygen molecules and water molecules. The $H^{\bullet}$, $OH^{\bullet}$ and $O^{\bullet}$ radicals formed in the process will react with each other as well as with H_2O and O_2 during the rapid cooling phase giving $HO_2^{\bullet}$ and H_2O_2. In this highly reactive nuclear environment, organic pollutants can be decomposed and inorganic pollutants can be oxidised or reduced. This phenomenon is being explored in the emerging field of sonocatalysis for the removal of pollutants.

In photocatalysis, photo excitation of the semiconductor oxide promotes valence band electrons to the conduction band thereby creating electron deficiency or hole in the valence band. Dioxygen provides a sink for conduction band electron forming superoxide $^{\bullet}O_2^-$ which leads to the formation of hydroperoxide $HO_2^{-\bullet}$. Holes in the valence band can react with water molecules or hydroxide anion to form OH radicals. These reactive species can interact with the pollutants leading to their degradation and possibly mineralization. The mechanisms of photocatalytic and sonocatalytic reactions are similar and this has opened up opened up the possibility of combining the techniques for enhancing the degradation of organic pollutants in water.

IOSR Journal of Applied Chemistry (IOSR-JAC)
e-ISSN: 2278-5736.
PP 15-24
www.iosrjournals.org

The most widely studied catalyst in sono-, photo- and sonophotocatalysis is TiO_2 in view of its favorable physico-chemical properties, low cost, easy availability, high stability with respect to photocorrosion and chemical corrosion, and low toxicity. Another semiconductor oxide ZnO with band-gap energy of ~3.2 eV has properties comparable to those of TiO_2 and is capable of absorbing a larger fraction of the solar spectrum [7]. Hence it is more active in the visible region for the photocatalytic decontamination of water [8, 9]. The comparatively lower light-scattering effect of ZnO due to its lower refractive index (ZnO: 2.0, TiO_2: 2.5–2.7) also favours better photocatalytic efficiency. In spite of these advantages, ZnO has not received due attention as an effective environmental photocatalyst, probably due to its instability or photocorrosion under acidic conditions.

We have earlier reported the sono, photo and sonophotocatalytic degradation of water pollutants in presence of semiconductor oxides and the fate of concurrently formed H_2O_2 [2, 10]. Unlike in the case of the pollutants which undergo progressive degradation with time and eventual mineralization, H_2O_2 formed during the process does not increase correspondingly and is undergoing concurrent formation and decomposition resulting in oscillation in its concentration. Various reaction parameters influence the oscillatory behavior though the same cannot be quantitatively correlated. Further to our earlier investigations on the effect of various anions in AOPs, the influence of a number of cations (Na^+, K^+, Ca^{2+}, Mg^{2+}, Al^{3+}) which are likely to be present in water on the ZnO mediated sono, photo and sonophotocatalytic degradation of phenol and the oscillation in the concentration of simultaneously formed H_2O_2 is undertaken in the current study.

II. Materials and methods

ZnO (99.5%) used in the study was supplied by Merck India Limited. The surface area, as determined by the BET method is ~ 12 m^2/g. The consistency of the physicochemical characteristics of ZnO used in the study with those reported in literature was confirmed by X-ray diffractogram (XRD) and Scanning Electron Microscopy (SEM) measurements. Phenol AnalaR Grade (99.5% purity) and H_2O_2 (30.0% w/v) from Qualigen (India) were used as such without further purification. All other chemicals were of AnalaR Grade or equivalent. Water distilled twice was used in all the experiments. The sonocatalytic, photocatalytic and sonophotocatalytic experiments were performed as reported earlier [2]. The phenol degradation was followed by periodic sampling and analyzing by UV-VIS spectroscopy (500 nm). Adsorption and mineralisation studies were made using standard techniques. Concentration of H_2O_2 was determined by iodometry [10].

III. Results and discussion

Preliminary studies on the degradation of phenol in water in the presence of ZnO showed that the catalyst and an energy source are essential to effect reasonable degradation. The degradation is more facile in the presence of UV light (photocatalysis) compared to US irradiation (sonocatalysis). The sonophotocatalytic degradation of phenol in the concurrent presence of UV, US and ZnO is more than the sum of the degradation under photocatalysis and sonocatalysis (Figure 1), which confirms the synergy reported in similar instances earlier [3,5]. The synergy index is calculated using equation (1) [11]:

$$\text{Synergy index} = R_{US+UV} / (R_{US} + R_{UV}) \quad (1)$$

where R_{US}, R_{UV} and R_{US+UV} are the sono, photo and sonophoto catalytic degradation rates respectively. The synergy index thus calculated for ZnO is 1.25.

IOSR Journal of Applied Chemistry (IOSR-JAC)
e-ISSN: 2278-5736.
PP 15-24
www.iosrjournals.org

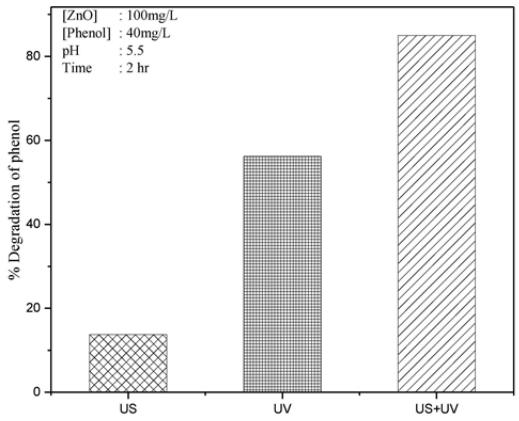

Figure 1. Sono-, photo- and sonophotocatalytic degradation of phenol in the presence of ZnO.

The optimum catalyst loading, as determined in the case of sono, photo and sonophotocatalysis from a series of experiments, is 100 mg/L. The degradation follows concentration-dependent variable kinetics, with pseudo first order at lower concentration and zero order at higher concentration. At the optimized catalyst dosage, optimum reaction rate was achieved at phenol concentration of 40 mg/L. pH studies showed that the natural pH of the reaction suspension, i.e. 5.5 is the optimum for sono, photo and sonophotocatalysis. Hence all further studies on the influence of various ions on the sono, photo and sonophotocatalytic degradation of phenol and the concurrently formed H_2O_2 were carried out using these optimized reaction conditions.

The effect of various anions on the degradation of phenol under sono, photo and sonophotocatalysis is shown in figure. 2

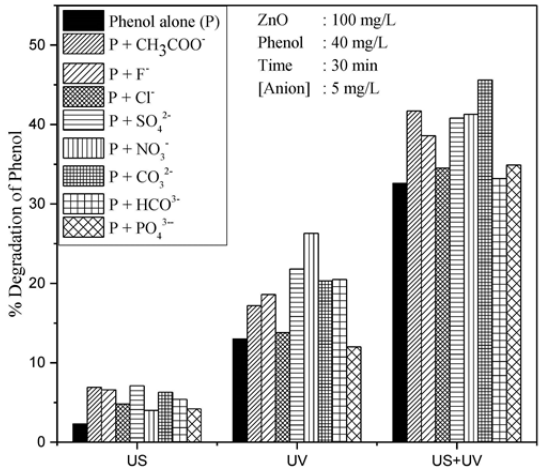

Figure 2. Effect of anions on the sono, photo and sonophotocatalytic degradation of phenol

IOSR Journal of Applied Chemistry (IOSR-JAC)
e-ISSN: 2278-5736.
PP 15-24
www.iosrjournals.org

Surprisingly, all the anions enhance the sonocatalytic degradation of phenol in the beginning of the reaction and at lower concentration. In photocatalysis, except PO_4^{3-} all other anions enhance the degradation by varying degrees. But in the case of sonophotocatalysis, the anions Cl^-, HCO_3^- and PO_4^{3-} have practically no effect while others enhance the degradation. This is contrary to the inhibition to photocatalytic degradation of organics caused by anions, as reported by many research groups [12, 13]. Reduced availability of catalytic surface sites for adsorption of the substrate due to competition from the anions is often cited as the reason for the inhibition. The anions are also known to scavenge the ROS, especially $^{\cdot}OH$, which also could have caused the inhibition. However in the present instance, the role is reversed and at least some of the anions are accelerating the degradation of phenol. The enhancement in the case of sono/photo/sonophoto catalysis is explained partially based on the formation of reactive radical species such as $F^{\cdot}$,$CO_3^{\cdot-}$, $SO_4^{\cdot-}$ etc from respective anions by interaction with the $^{\cdot}OH$ on the surface of cavitation bubbles, on the surface of the catalyst or in the bulk, individually or in suitable combination [14]. These species, though less reactive than the $^{\cdot}OH$, are more abundant and do not get deactivated easily as in the case of $^{\cdot}OH$ radicals.

The results of the investigations on the anion effect in various AOPs are being reported separately from our research group. In all these cases the cation was the same, i.e. Na^+. At the same time, understanding the specific effect by the cation also is important in the design of suitable AOP system for wastewater treatment. In this context, the effect of various cations such as Na^+, K^+, Mg^{2+}, Ca^{2+} and Al^{3+} on the sono, photo and sonophotocatalytic degradation of phenol is carried out. The anions in these cases were NO_3^-, SO_4^{2-} and Cl^-. For each anion, the effect of various cations on the degradation is investigated. The results are plotted in figures 3 (Nitrate), 4 (Sulphate) and 5 (Chloride) respectively.

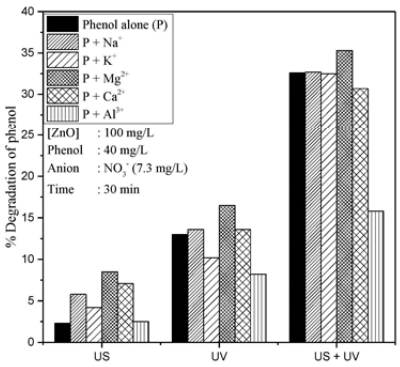

Figure 3. Effect of various cations (anion: nitrate) on the sono, photo and sonophotocatalytic degradation of phenol

IOSR Journal of Applied Chemistry (IOSR-JAC)
e-ISSN: 2278-5736.
PP 15-24
www.iosrjournals.org

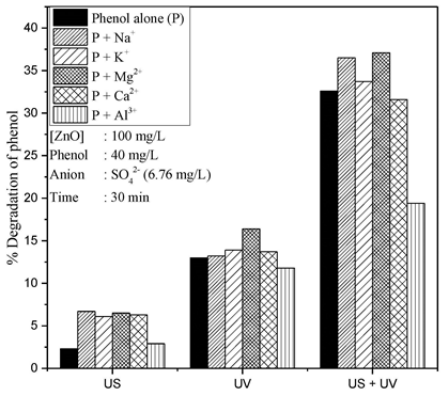

Figure 4. Effect of various cations (anion: sulphate) on the sono, photo and sonophotocatalytic degradation of phenol

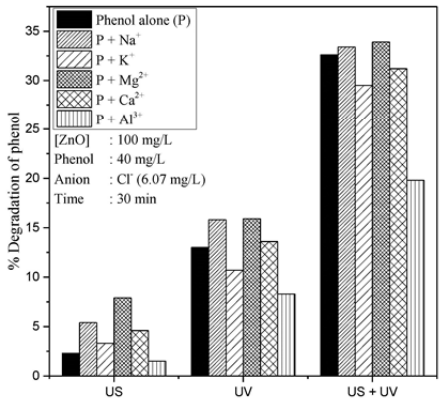

Figure 5. Effect of various cations (anion: chloride) on the sono, photo and sonophotocatalytic degradation of phenol

In the case of sonocatalysis all cations except Al^{3+} enhances phenol degradation, even though the degree of enhancement varies with different anions. In the case of NO_3^- anion, the order of enhancement for various cations is $Al^{3+} < K^+ < Ca^{2+} < Na^+ < Mg^{2+}$. In the case of sulphate as the anion, the enhancement in presence of cations except Al^{3+} remains more or less same in all cases. Incidentally sulphate anions exhibit maximum enhancement for the degradation of phenol. In this case the enhancement is in the order $Al^{3+} < K^+ \approx Ca^{2+} \approx Na^+ \approx Mg^{2+}$. When the anion is chloride, the enhancement in presence of cations still holds, though the order of efficiency is different, i.e. $Al^{3+} < K^+ < Ca^{2+} < Na^+ < Mg^{2+}$. The identical trend in presence of the cations irrespective of the difference in the anions, in the case of NO_3^- and Cl^-, and the significantly different trend when SO_4^{2-} is the anion indicate that it is difficult to isolate and compare the effect of cations when the anions are different.

In photocatalysis, in presence of Al^{3+} and K^+ the phenol degradation is inhibited when the anion is Cl^- or NO_3^-. Maximum enhancement is obtained in the case of Mg^{2+} and Na^+. In this case also, the trend is different

IOSR Journal of Applied Chemistry (IOSR-JAC)
e-ISSN: 2278-5736.
PP 15-24
www.iosrjournals.org

in presence of sulphate anion. In this case Mg^{2+} has clear enhancing effect while all other cations have only negligible effect. Even the inhibitory effect of Al^{3+} and K^{+} also is insignificant in this case.
In sonophotocatalysis the synergistic effect is not affected in presence of various cations. Except for Al^{3+} other cations have no significant effect on the degradation. The trend remains more or less the same as in the case of photocatalysis, including the consistent enhancing effect by Mg^{2+}.

Our earlier studies have shown that the effect of various salts on the AOP degradation of pollutants depends on the reaction time. Hence the influence of cation effect at another reaction time, i.e. 60 minutes, on the degradation is tested, keeping SO_4^{2-} as the anion. The results are presented in figure.6. The results show that unlike in the case of anions, extended reaction time does not modify the initial effect by cations on the degradation.

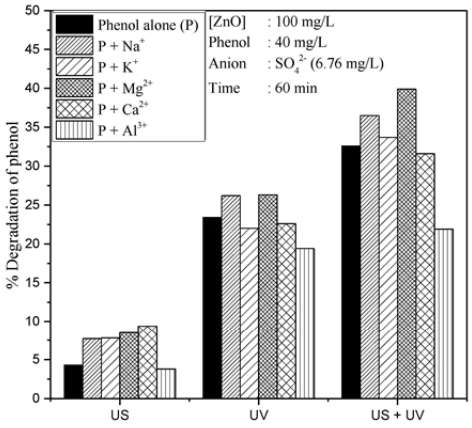

Figure 6. Effect of various cationic sulphates on the sono, photo and sonophotocatalytic degradation of phenol

One possible explanation for the effect of cations on the rate of degradation of organics in the presence of catalysts is their adsorption/layer formation on the surface. The layer formation may inhibit or promote the adsorption of the substrate and subsequent activation in presence of UV/US/(US+UV). In this case, the size of the cation may have a role, higher the size, greater the surface coverage and less the degradation of the substrate. However, the results do not show any specific trend based on the cationic size suggesting that the effect of cations is not that simple or straightforward.

In order to verify whether the effect of cations is related to their blocking the active surface sites, the adsorption of phenol in presence of these cations was measured. The results are plotted in Figure 7.
From the figure it is clear that phenol adsorption is the least in presence of Al^{3+} cations when the anion is SO_4^{2-}. The adsorption is inhibited to the maximum by $Al_2(SO_4)_3$ followed by NaCl, KCl and $MgSO_4$. However, the adsorption is enhanced by $NaNO_3$, $Ca(NO_3)_2$ and $Mg(NO_3)_2$ while $Al(NO_3)_3$ and KNO_3 do not affect. $CaSO_4$ enhances the adsorption significantly. Once again there is no direct or consistent correlation between the nature of the cation and the adsorption of phenol. If at all there is some kind of correlation, it is between the nature of the anions and the adsorption/degradation.

Previous studies have reported that sonocatalytic and photocatalytic reactions are sensitive to the presence of anions [15, 16]. Seymour and Gupta [15] observed NaCl induced enhancement in sonocatalytic degradation of organics using 20 kHz US. It is also reported that the presence of massive amounts of Cl− ions inhibit photocatalytic degradation [17]. The addition of salt increases the ionic strength of the aqueous phase. In the case of sonocatalysis,

IOSR Journal of Applied Chemistry (IOSR-JAC)
e-ISSN: 2278-5736.
PP 15-24
www.iosrjournals.org

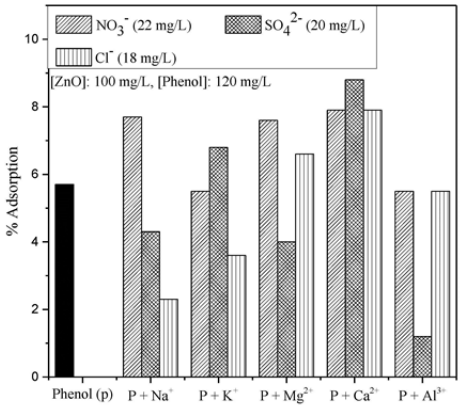

Figure 7. Effect of cations on the adsorption of phenol in presence of Nitrate, Sulphate and Chloride anions

this is expected to drive the organic pollutants towards the bubble-bulk interface where the majority of the sonodegradation takes place [18]. The increase in surface tension can affect the nucleation process and the cavitational threshold. The presence of salt will also increase the partitioning of the organic species upon cavitation implosion. Thus it was expected that the interfacial concentration of the pollutants would increase which could enhance the overall degradation rate. However, these explanations have to be selectively applied and cannot be generalized. Also it may not be quite appropriate to isolate the effects as anionic or cationic since both cations and anions do influence the degradation of the pollutant, either complimentarily or conversely.

The effect of the above cations on the concurrently formed H_2O_2 under sono, photo and sonophotocatalysis is also examined keeping nitrate as the typical anion (figures 8-10). In particular, the effect on the phenomenon of oscillation is critically examined. There is no consistent trend in this case as well. However, the net concentration of H_2O_2 is more in all cases, thereby demonstrating a correlation with the enhanced rate of phenol degradation. The amount of H_2O_2 is relatively less in presence of Al^{3+} cation which inhibits phenol degradation. In the case of sonophotocatalysis the trend is not strictly followed probably due to the interplay of a number of factors and formation of multitude of free radicals which interact in a variety of ways. Hence it may be tentatively inferred that the cations tested here inhibits the competitive decomposition of H_2O_2.resulting in higher amounts of the peroxide. Hence the simultaneous formation process in the oscillation phenomenon dominates and the net H_2O_2 is more. Even under well defined experimental conditions, oscillation is not amenable to any clear interpretation due to the complexity of the system consisting of a number of reactive free radicals, concurrent formation and decomposition of H_2O_2 and the creation of a series of intermediates, many of them competing with each other. However, the enhancing effect of the cations, except Al^{3+}, on the sono, photo and sonophotocatalytic degradation of phenol is evident in the case of H_2O_2 also.

IOSR Journal of Applied Chemistry (IOSR-JAC)
e-ISSN: 2278-5736.
PP 15-24
www.iosrjournals.org

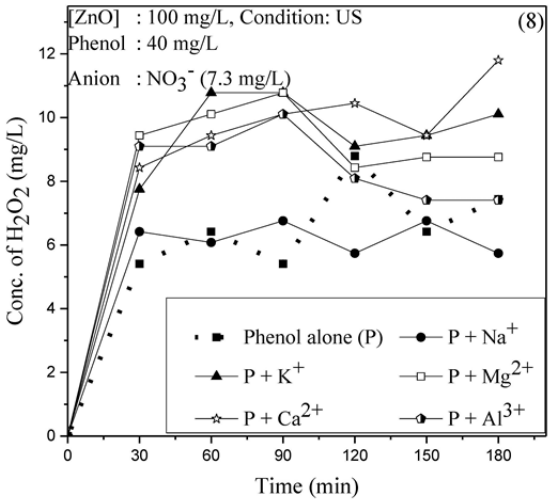

Figure 8. Effect of various cations on the oscillation in the concentration of H_2O_2 under sono catalysis (Anion: nitrate)

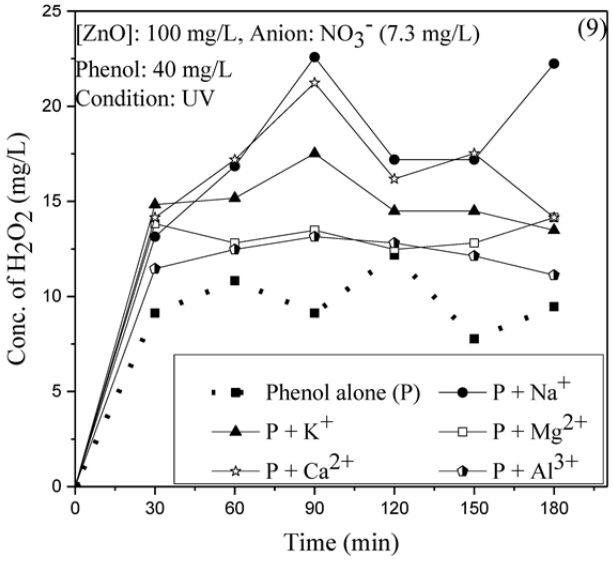

Figure 9. Effect of various cations on the oscillation in the concentration of H_2O_2 under photo catalysis (Anion: nitrate)

IOSR Journal of Applied Chemistry (IOSR-JAC)
e-ISSN: 2278-5736.
PP 15-24
www.iosrjournals.org

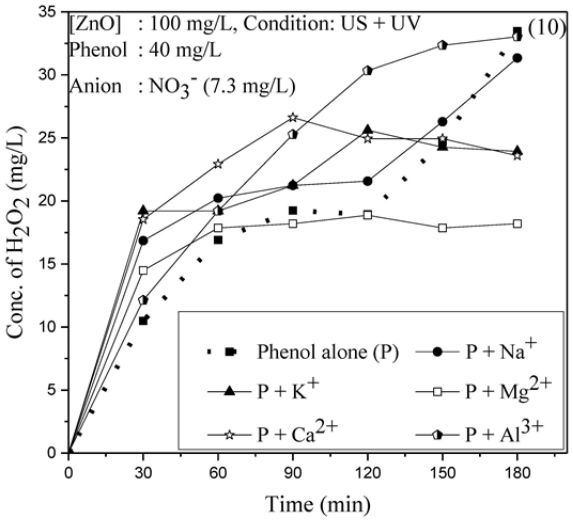

Figure 10. Effect of various cations on the oscillation in the concentration of H_2O_2 under sonophoto catalysis (Anion: nitrate)

IV. General mechanism

The basic mechanism of ZnO mediated sono, photo and sonophotocatalytic degradation of phenol is as follows:

$ZnO + h\upsilon \rightarrow h^+ + e^-$ (2)
$h^+ + e^- \rightarrow$ Heat (3)
$h^+ + OH^- \rightarrow {}^{\cdot}OH$ (4)
$h^+ + H_2O \rightarrow {}^{\cdot}OH + H^+$ (5)
$e^- + O_2 \rightarrow O_2^{\cdot-}$ (6)
$H^+ + O_2^{\cdot-} \rightarrow HO_2^{\cdot}$ (7)
$HO_2^{\cdot} + e^- + H^+ \rightarrow H_2O_2$ (8)

Phenol + Reactive species ($O_2^{\cdot-}$, $HO_2^{\cdot}$,${}^{\cdot}OH$) $\rightarrow$Intermediates $\rightarrow$ H_2O + CO_2 (9)

The H_2O_2 thus formed undergoes concurrent decomposition by a series of interactions as follows:

$H_2O_2 + UV \rightarrow 2\ {}^{\cdot}OH$ (10)
$2\ h_{vb}^+ + H_2O_2 \rightarrow O_2 + 2\ H^+$ (11)
$2\ e_{cb}^- + 2H^+ + H_2O_2 \rightarrow 2\ H_2O$ (12)
$H_2O_2 + {}^{\cdot}OH \rightarrow H_2O + HO_2^{\cdot}$ (13)
$H_2O_2 + HO_2^{\cdot} \rightarrow H_2O + {}^{\cdot}OH + O_2$ (14)
$H_2O_2 + O_2^{\cdot-} \rightarrow {}^{\cdot}OH + OH^- + O_2$ (15)

Thus, the same free radicals can contribute to the formation and decomposition of H_2O_2 depending on the conditions.

Anions act as radical scavengers and thus in the presence of anions, the relative abundance of OH radicals is decreasing very fast. But the radical anions produced as a result of interaction between ${}^{\cdot}OH$ radical and anions can also effect the degradation of organics. Unlike in the case of ${}^{\cdot}OH$ radicals which get deactivated by a number of competing reactions, the radical anions are available only for the degradation of the anions. This leads to enhancement in the degradation. The effect of cations is even more complex and cannot be explained in general. Hence the reaction parameters have to be optimized for every type of effluent water depending on the nature of salt contaminants for optimum efficiency in sono, photo and sonophotocatalysis.

IOSR Journal of Applied Chemistry (IOSR-JAC)
e-ISSN: 2278-5736.
PP 15-24
www.iosrjournals.org

V. Conclusion

Sono, photo and sonophotocatalysis mediated by ZnO catalyst have been proven to be efficient methods for the removal of chemical and bacterial pollutants from water. Combination methods are often more efficient as in the case of sonophotocatalytic degradation of phenol which is synergic. In this case, the efficiency is more than the sum of the respective sono- and photocatalytic processes under otherwise identical conditions. The concentration of concurrently formed H_2O_2 increases and decreases periodically, resulting in oscillatory behavior. Inorganic salts likely to be present in water influence the rate of degradation of the pollutant and the behavior of H_2O_2. The effect of anions on the sono, photo and sonophotocatalytic degradation of organic pollutants like phenol is dependent on the concentration of respective salts. Contrary to many earlier reports, current study shows that the anions and certain cations, enhance the sono, photo and sonophotocatalytic degradation of phenol. The rate of enhancement decreases and eventually it becomes comparable to the rate without the presence of salts. The influence of various cations on the degradation of phenol and the fate of H_2O_2 is investigated under sono, photo and sonophotocatalysis. Almost all cations except Al^{3+}, irrespective of the nature of anions, enhance phenol degradation under sonocatalysis. In the case of photo and sonophotocatalysis, the effect of cations is negligible. The effect of cations on the concurrently formed H_2O_2 as well as the oscillation phenomenon is inconsistent and unpredictable. The results are discussed and a tentative mechanism for the observation is proposed.

Acknowledgement

The authors wish to acknowledge financial support to J.K.P.from the University Grants Commission (India) by way of Senior Research Fellowship.

References

[1]. M. N Chong, B Jin, C. W. K Chow andC Saint, New developments in photocatalytic water treatment technology: a review, Water Res,44, 2010,2997–3027.
[2]. S. G Anju, S Yesodharan and E. P Yesodharan, Zinc oxide mediated sonophotocatalytic degradation of phenol in water, Chem. Eng. J, 189-190, 2012, 84–93
[3]. C. G Joseph, G. L Puma, A Bonoand D Krishniah,Sonophotocatalysis in advanced oxidation process: a short review, Ultrason. Sonochem, 16, 2009, 583–589.
[4]. P. R Gogateand A. B Pandit, Sonophotocatalytic reactors for wastewater treatment: a critical review,AIChE J, 50, 2004,1051- 1-79.
[5]. Y.C Chen, P Smirniotis, Enhancement of photocatalytic degradation of phenol and chlorophenols by ultrasound, Ind. Eng. Chem. Res, 41, 2002, 5958–5965
[6]. E.A. Nepiras, Acoustic cavitation: an introduction, Ultrasonics, 22, 1984, 25–40
[7]. S. Sakthivel, B. Neppolian, M. V Shankar, B Arabindoo, M Palanichamyand V Murugesan, Solar photocatalytic degradation of azo dye: comparison of photocatalytic efficiency of ZnO and TiO_2, Sol. Energy Mater. Sol. Cells, 77, 2003,65–82
[8]. S-M Lam, J. C Sin, A. Z Abdullahand A. R Mohamed, Degradation of wastewaters containing organic dyes photocatalysedby ZnO: a review, Desalination and Water Treatment, 41, 2012,131–169
[9]. N Hariprasad S. G Anju, E. P Yesodharan and S Yesodharan, Sunlight induced removal of Rhodamine B from water through semiconductor photocatalysis, Res. J. Mater. Sci, 1, 2013,9–17
[10]. K. P Jyothi, S. Yesodharanand E. P Yesodharan, Ultrasound, ultraviolet light and combination assisted semiconductor catalyzed degradation of organic pollutants in water: oscillation in the concentration of hydrogen peroxide formed in situ, Ultrason. Sonochem,21, 2014, 1787–1796
[11]. J. Madhavan, P. S Sathish Kumar, S Anandan, F Grieser and M Ashok Kumar, Sonophotocatalytic degradation of monocrotophos using TiO_2 and Fe^{3+}, J. Hazard. Mater, 177, 2010, 944–949
[12]. C. HuJimmy, C Yu, Z Hao and P.K Wong, Effects of acidity and inorganic ions on the photocatalytic degradation of different azo dyes, Applied Catalysis B: Environmental, 46, 2003, 35–47
[13]. N Barka, S Qourzal, A Assabbane, A Nounah and YhyaAit-Ichou, Factors influencing the photocatalytic degradation of Rhodamine B by TiO_2-coated non-woven paper, J. Photochem. Photobio. A: chemistry, 195, 2008, 346–351
[14]. C Minero, P Pellizari, V Maurino, E Pelizzetti and D Vione, Enhancement of dye sonochemical degradation by some inorganic anions present in natural waters, Appl. Catal B:Environ, 77, **2008,** 308-316
[15]. J. D Seymour, R. B Gupta, Oxidation of aqueous pollutants using ultrasound: salt induced enhancement, Ind. Eng. Chem. Res, 36 1997, 3453–3459
[16]. P Calza and E Pelizzetti, Photocatalytic transformation of organic compounds in the presence of inorganic ions, Pure Appl. Chem, 73 2001, 1839–1848
[17]. V Augugliaro, L Palmisano, A Sclafani, C Minero and E Pelizzetti, Photocatalytic degradation of phenol in aqueous TiO_2 suspensions, Toxicol. Environ. Chem, 16 1988, 89–95
[18]. A Henglein and C Kormann, Scavenging of OH radicals produced in the sonolysis of water, Int. J. Radiat. Biol, 48 1985, 251–258.

Annexure IV

Awards/Recognitions conferred based on the current study

[1]. **Best Paper Award**, First National Conference on Advanced Oxidation Process, Thapar University, Patiala, Punjab, 2013

[2]. **Best Paper Award**, International Conference on Emerging Trends in Engineering and Management (ICETEM 14), Sree Narayana Gurukulam College of Engineering, Kolenchery, Ernakulam, Kerala, 2014

[3]. **Award of Excellence** (Research Students Category), Cochin University of Science and Technology (CUSAT) 2014-15

[4]. **Best Paper Award**, International Conference on Emerging Trends in Engineering and Management (ICETEM 16), Sree Narayana Gurukulam College of Engineering, Kolenchery, Ernakulam, Kerala, 2016

.....ꕥ.....